



Università
Ca' Foscari
Venezia

**Scuola Dottorale di Ateneo
Graduate School**

**Dottorato di ricerca
in Scienze Chimiche
Cycle 28th
Dissertation year 2015**

Supramolecular Approaches to Homogeneous Catalysis

SETTORE SCIENTIFICO DISCIPLINARE DI AFFERENZA: CHIM-04

Ph.D.Thesis of **GIORGIO LA SORELLA, number 811174**

PhD Coordinator

Prof. Maurizio Selva

Tutor

Dott. Alessandro Scarso

Co-tutor

Prof. Giorgio Strukul

Ai miei genitori

SUMMARY

1.	INTRODUCTION.....	1
1.1.	“The world of Catalysis”	1
1.2.	Learning from enzymes.....	3
2.	AIM OF THE THESIS	5
3.	CATALYSIS WITHIN A SUPRAMOLECULAR H-BONDED CAPSULE	7
3.1.	State of the art.....	7
3.1.1.	Self-assembled Supramolecular Capsules and Catalysis	7
3.1.2.	The Resorcin[4]arene Capsule	16
3.2.	Results and Discussion.....	20
3.2.1.	Interaction between Capsule and formally neutral compounds	20
3.2.1.1.	Isocyanides: a class of compound with interesting features.....	20
3.2.1.2.	Hydration of Isocyanides within the cavity.....	21
3.2.1.3.	Addition of trimethylsilyl azide on isocyanides mediated by the capsule.....	26
3.2.1.4.	From Isocyanides to Diazoacetate esters	31
3.2.1.5.	Diazoacetate esters encapsulation	32
3.2.1.6.	Dipolar cycloaddition reaction between diazoacetate esters and electron-poor alkenes mediated by the resorcin[4]arene capsule.....	35
3.2.1.7.	Conclusions	41
3.2.2.	Capsule and Dipolar Compounds	42
3.2.2.1.	N-oxides properties.....	42
3.2.2.2.	Interaction between N-oxides and the resorcin[4]arene capsule.....	43
3.2.2.3.	Reaction between N-oxides and isocyanates	48
3.2.2.4.	Effect of the hexameric capsule in the reaction between N-methyl-morpholine and p-methoxyphenyl isocyanate.....	56
3.2.2.5.	Conclusions	61
3.2.3.	Capsule effect on the activation energy of reactions with encapsulable intermediates.....	62
3.2.3.1.	Sulfoxidation with hydrogen peroxide as oxidizing agent.....	62
3.2.3.2.	Sulfoxidation within the capsule cavity	62
3.2.3.3.	Hydration of alkynes	69
3.2.3.4.	Conclusions	78

4.	<i>CATALYSIS IN WATER BY MEANS OF MICELLAR MEDIA</i>	81
4.1.	<i>State of the art</i>	81
4.1.1.	Green Chemistry	81
4.1.2.	Surfactants	83
4.2.	<i>Results and Discussion</i>	89
4.2.1.	Palladium Nanoparticles and Commercial Sulfonate Anionic Surfactants	89
4.2.1.1.	Metal nanoparticles and micelles	89
4.2.1.2.	Synthesis and characterization of the Pd NPs in the presence of surfactants	90
4.2.1.3.	Study of the Pd-NPs catalytic activity	94
4.2.1.4.	Conclusions	107
4.2.2.	Multi-component synthesis of 1,2,3-triazoles promoted by micelles	108
4.2.2.1.	Two steps in one through micelles	108
4.2.2.2.	Micellar media for each step	111
4.2.2.3.	Scope of the reaction	117
4.2.2.4.	Conclusions	121
5.	<i>SUBSTRATE SELECTIVITY</i>	122
5.1.	<i>State of the art</i>	122
5.1.1.	Learning from enzymes	122
5.1.2.	Artificial substrate selectivity	123
5.2.	<i>Results and Discussion</i>	130
5.2.1.	Substrate selective amide coupling driven by self-assembled resorcin[4]arene capsule	130
5.2.1.1.	Carbodiimides as amide coupling agents	130
5.2.1.2.	Interactions with the capsule	133
5.2.1.3.	Amide coupling within the cavity	138
5.2.1.4.	Conclusions	144
5.2.2.	Substrate selectivity due to hydrophobic effect in micellar media	145
5.2.2.1.	Substrate selective Cross-Coupling Heck reactions in water	145
5.2.2.2.	Substrate selective hydrogenation of α,β -unsaturated aldehydes	150
5.2.2.3.	Conclusions	154
6.	<i>GENERAL CONCLUSIONS</i>	155
7.	<i>EXPERIMENTAL</i>	168
7.1.	<i>Compounds and Analyses</i>	168
7.2.	<i>Reactions</i>	172
7.2.1.	Hydration reaction of isocyanides capsule-catalysed	172

7.2.2. Addition of trimethylsilyl azide on isocyanides.....	175
7.2.3. Diazoacetate esters and Resorcin[4]arene capsule.....	184
7.2.4. Sulfoxidation.....	193
7.2.5. Alkynes hydration mediated by the capsule.....	206
7.2.6. N-oxides and capsule.....	215
7.2.7. Hydrogenation mediated by Pd-NPs in aqueous anionic micellar media.....	222
7.2.8. Multi-component synthesis of 1,2,3-triazoles promoted by micelles.....	252
7.2.9. Substrate selective amide coupling.....	266
7.2.10. Substrate selective Cross-Coupling Heck reactions.....	273
7.2.11. Competitive hydrogenation reaction of α,β -unsaturated aldehydes.....	283
8. <i>ACKNOWLEDGEMENTS</i>	292
9. <i>BIBLIOGRAPHY</i>	293

1. INTRODUCTION

1.1. “The world of Catalysis”

Catalysis is one of the fundamental topics of chemistry because many chemical processes require the presence of a catalyst in order to be effective. A catalyst is a chemical species that increases the rate of a reaction by lowering the activation energy barrier without changing the thermodynamic properties.

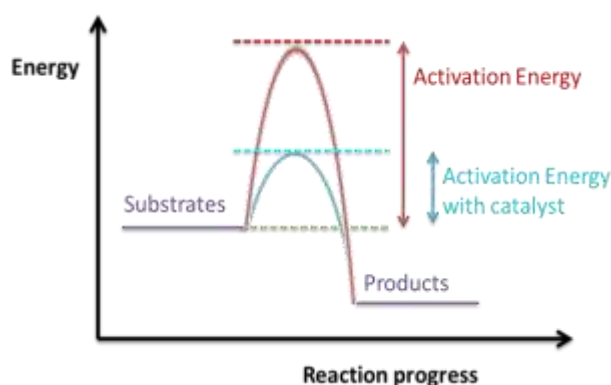


Figure 1. Effect of a catalyst on the activation energy of a reaction

Usually the catalyst is not consumed during the reaction and only small amounts are required to efficiently accelerate the conversion of substrate, because its activity is maintained for several cycles. Moreover some catalysts can change the product selectivity of a reaction and sometimes the formation of novel products can be achieved when a completely new reaction pathway is caused by the presence of the catalyst.¹ The parameters that describe the properties of a catalyst are three:

- The *activity* that provides the rate of the substrate conversion due to the catalyst;
- The *selectivity* that can be mathematically represented as the molar ratio between the amount of desired product and the amount of converted substrate;
- The *stability* that expresses how long the catalyst retains its properties without decomposition/deactivation.

The catalysts can be divided into two categories: heterogeneous catalysts, when the reaction takes place on or near to an interface between phases, and homogeneous catalysts, which require only one phase.

An heterogeneous catalyst is usually composed of an inert support where the active phase, often composed of metal particles, is dispersed. However only the catalytic sites able to interact with substrate molecules can accelerate the conversion of substrates. The porosity of the support is an important feature that confers many properties to the heterogeneous catalyst. Indeed the distribution of the catalytic sites, the reaction rate, the product- and the substrate-selectivity may depend on the support framework.² Moreover, heterogeneous catalyst are heat-resistant, recyclable, regenerable and easily recoverable from the reaction mixture.³

The term “homogeneous catalyst” includes various types of catalysts. Examples of homogeneous systems that can show catalytic activity are:

- Acid and base molecules;
- Lewis acid and Lewis base compounds;
- Organic molecules with particular properties;
- Organometallic complexes.

Organometallic complexes are widespread as homogeneous catalysts particularly for the synthesis of fine chemicals. They are composed of metal atoms or ions surrounded and bound by molecules called ligands. Ligands not only impart stability and solubility to the metal complex, but they are also extremely effective in driving the catalytic properties of the complex. Indeed, different products can be obtained using the same metal centre simply changing the ligands.^{4,5} Usually homogeneous systems show higher catalytic activity and selectivity compared to heterogeneous ones and all their reactive sites are potentially involved in interactions with substrates in the same way. In contrast heterogeneous systems allow such an extensive control of the catalyst only with single site catalyst⁶ or in specific cases where very orderly structures are used as supports. Consequently porosity of the support, size of the nanoparticles and geometrical differences of the catalytic sites cause rather diversified interactions between catalyst and substrate molecules. Unfortunately the separation of homogeneous catalysts from the reaction mixture can be very complex and their recycle difficult.

1.2. Learning from enzymes

A particular and very interesting class of catalysts is composed by enzymes, often termed hybrid catalysts. Enzymes are highly specialized proteins that catalyze reactions in biological systems showing excellent properties such as high activity, chemo-, regio-, and/or enantioselectivity and specificity.⁷ These properties are due to the presence of an active site lying in a cavity often placed in the enzyme internal surface where substrate molecules can bind and be selectively transformed into other compounds through several interactions. The affinity between the active site and the substrate molecules has been extensively investigated to explain the remarkable catalytic activity of enzymes. Their large size and shape complementarity allow the very high specificity of the enzyme's activity, while supramolecular interactions cause continuous variations in the cavity shape catalyzing the substrate conversion.⁸ When the substrate is converted, the product is released and the enzyme can recover its original conformation capable to start a new catalytic cycle. As one can easily understand, the particular microenvironment in the active site is the cause of the many effects that take place during the enzyme-substrate recognition, the substrate pre-organization, the desolvation and the stabilization of the transition state of the reaction.⁹

The fascinating properties that characterize enzymes are still unrivalled by artificial catalysts.¹⁰ For this reason an increasing number of research groups are focusing their activity in order to develop systems that can mimic the action of these natural catalyst. As one of the most obvious causes of the particular functioning of enzymes is the presence of a very large surface area compared to the substrate size, their objective became the creation of homogeneous catalytic systems capable of providing a large contact surface. This led to the use of supramolecular chemistry applied to catalysis.

During the last thirty years "Supramolecular Chemistry" has become an intensively studied topic. As early as 2005, the word 'supramolecular' was used either in the title, in the abstract or in the keywords of 2532 scientific papers.¹¹ In 2014 the number of such papers reached 4105.¹² Nevertheless the use of supramolecular chemistry in catalysis is still a moderately explored field. In this respect the use of "supramolecular containers" to carry out catalysis is an innovative and challenging topic to obtain systems capable of imitating what nature does through enzymes. In order to achieve this result, supramolecular assemblies involving weak interactions such as hydrogen bonding, π -stacking, charge transfer, hydrophilic-hydrophobic effect, and chelation of metal cations can be exploited with the aim of getting new, easy to synthesize catalytic systems.

2. AIM OF THE THESIS

The aims of this thesis were manifold and all linked by the common idea to study in depth the catalytic potential of self-assembling supramolecular systems capable to mimic the catalytic properties of enzymes.

In this respect a fundamental objective of this thesis was to demonstrate the capability of some organic capsules based on resorcin[4]arenes, that are able to host cationic guests, to act as a real catalyst even in the presence of formally neutral substrates. In fact it was suggested that the cation- π interactions developed by the capsule to accommodate cationic guests could allow the encapsulation of compounds characterized by isomerization with either zwitterionic form or predominantly carbenic electronic structure. The cavity of the capsule could provide a particular environment capable to increase the reactivity of these compounds and these effects were tested in hydration reactions, in the addition of trimethylsilyl azide to isocyanides and in the dipolar cycloaddition reaction between diazoacetate esters and electron-poor alkenes.

Alternatively, we considered the possibility that the catalytic activity could be due to the interactions between the cavity and the reaction intermediates. Therefore the oxidation of thioethers by H_2O_2 and the hydration of alkynes in the presence of acids were carried out using the resorcin[4]arene based capsule as catalyst.

The idea to investigate the interaction between the resorcin[4]arene capsule and zwitterionic compounds was further considered during a six-months stay in the research group of prof. Pablo Ballester at the Institut Català d'Investigació Química (ICIQ) of Tarragona. N-oxides were utilized as a class of compounds capable to interact with the capsule through H-bond with the hydroxyl groups of the resorcin[4]arene and to this purpose an intensive investigation of the never previously reported reaction between isocyanates and N-oxides was carried out.

Another important objective of the thesis was to show the advantages coming from the use of aqueous micellar media in several reactions. Even here supramolecular chemistry played a key role in developing catalytic systems that proved active in environmentally friendly media.

The first reaction considered was hydrogenation. The possibility to synthesize palladium nanoparticles in the presence of commercial sulfonated anionic surfactant in a facile and economic way was demonstrated. These nanoparticles operate under mild conditions and their catalytic properties proved to be highly dependent on the structure of the surfactant employed. Therefore it

was possible to synthesize different catalytic systems suitable for different reactions simply by changing the surfactant.

The synthesis of 1,2,3-triazoles was also investigated as it is an industrially significant reaction where micellar media could be used as more eco-friendly systems improving also the efficiency with respect to traditional organic solvents. The synthetic process that leads to the selective formation of 1,4-disubstituted 1,2,3-triazoles in the presence of alkynes, organic halides and NaN_3 as starting materials, is usually split in two steps. In the first step the organic azide is obtained through the reaction between organic halide and NaN_3 while in the second step the triazole formation is mediated by Cu(I) catalyst. During this thesis a catalytic system capable of condensing these two steps into one through the use of low cost commercial surfactant in water was developed.

Finally the employment of supramolecular structures was used to obtain substrate selective catalytic systems. This property is virtually unknown with traditional homogeneous catalysts but it is essential in enzyme functioning. Interesting examples of substrate selectivity were observed both with the supramolecular resorcin[4]arene capsule and with micellar media.

The steric hindrance due to the confined space within the cavity of the capsule was exploited in the substrate selective amide synthesis. With this purpose 1-ethyl-3-(3-dimethylaminopropyl) carbodiimide hydrochloride was employed as amide coupling agent. The positive charge in the molecular structure of this compound made it a good guest for the resorcin[4]arene capsule, forcing the coupling reaction to take place within the supramolecular cavity. Therefore the competitive reaction between amines and carboxylic acids with different length could be used to obtain the specific conversion of substrate characterized by proper shape and size.

The property of the micelles to host lipophilic compounds could be used in order to prepare catalytic systems able to preferably interact with the more hydrophobic substrates in a reaction mixture. This entropic effect was employed with the aim to obtain substrate selective catalytic systems in cross-coupling Heck reactions in aqueous cationic micellar medium observing interesting results. Furthermore, the high activity of the palladium nanoparticles systems obtained in the anionic micellar media was employed to achieve the chemo-selective hydrogenation of α,β -unsaturated aldehydes with very high substrate selectivity.

3. CATALYSIS WITHIN A SUPRAMOLECULAR H-BONDED CAPSULE

3.1. State of the art

3.1.1. Self-assembled Supramolecular Capsules and Catalysis

The obtainment of homogeneous catalytic systems capable to mimic the enzymes properties is one of the main pillars of the scientific research in the field of catalysis. A strategy that is proving to be promising in homogeneous catalysis is the use of especially designed three-dimensional structures that behave similarly to the catalytic sites of enzymes. In the past thirty years several methodologies have been devised to achieve structures capable to contain catalytic sites within their cavities. A first idea was to apply supramolecular structures to transition-metal complexes coordinating ligands with particular structures and steric hindrances to the metal centers.¹³ Afterwards an even more innovative step was carried out and molecular containers were employed in homogeneous catalysis. Molecular containers are three-dimensional vessels obtained from one or more subunits that are covalently bound or spontaneously assembled through weak interactions (such as hydrogen bond interactions, coordination bonds or other reversible interactions). The cavity of these containers is able to accommodate guest molecules with appropriate size, shape and electronic properties¹⁴ through prearranged and prolonged interactions. These capsules can either exhibit catalytic activity themselves facilitating the conversion of encapsulated molecules or they can be combined with catalytic centers with suitable shape and charge encapsulated within their cavities. The employment of a supramolecular structure can bring many advantages to a homogeneous catalytic system:

- The encapsulation of substrate molecules within the cavity causes an increase of their effective concentration and a possible unusual proximity that would change the bulk kinetics and thermodynamics (regio- and stereoselectivity).^{15,16}
- In some cases the cavity can stabilize the transition state of reactions reducing the activation energy of the reaction.¹⁷

- The limited space within the cavity can accommodate only finite combinations of molecules with appropriate size and shape and in the presence of a mixture of substrates only those with compatible steric hindrance can interact with the supramolecular catalytic system allowing to achieve different degrees of substrate selectivity.¹⁸

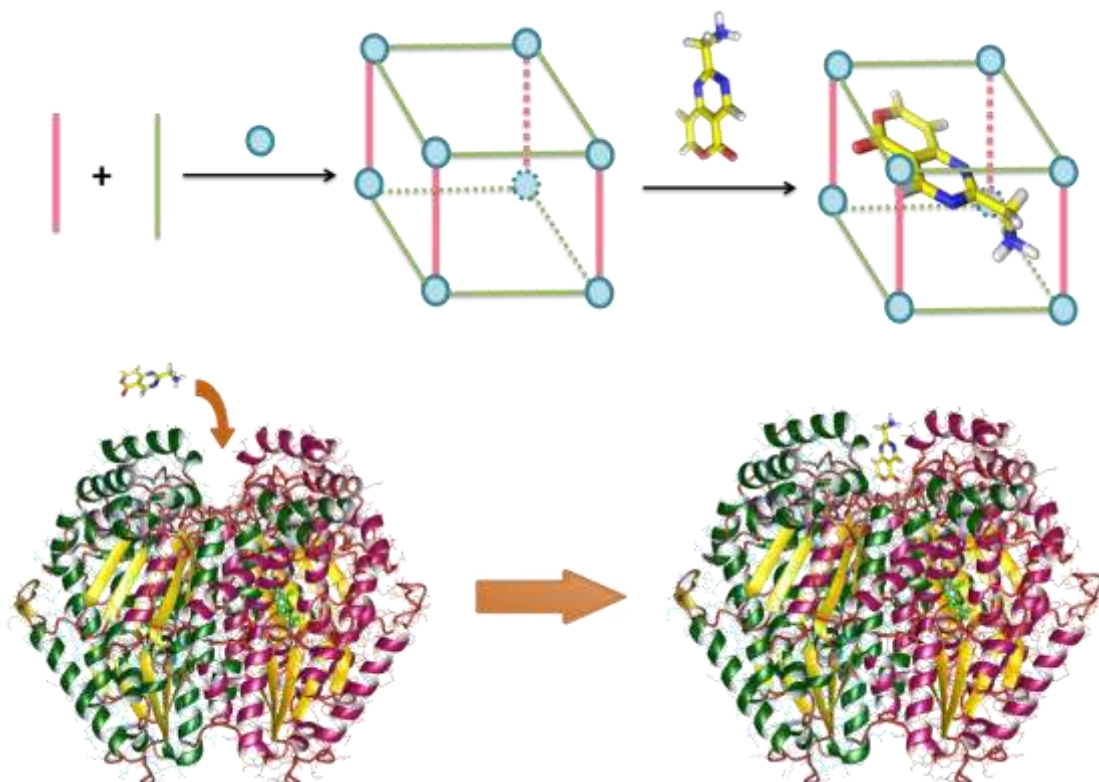


Figure 2. The supramolecular structures (above) mimicking the ability of the enzymes (bottom) to provide an elevated interaction area to substrate molecules.

As mentioned before the molecular hosts can be obtained through covalent bond between smaller molecules or they can be formed by spontaneous aggregation of the monomers by mutual weak interactions. Cases of containers obtained through covalent bonds that found application in homogeneous catalysis are uncommon. Cyclodextrins are a widespread class of molecular containers with numerous applications in various fields. Basically their structure is composed by a ring-shaped oligosaccharide usually consisting of 6 (α), 7 (β) or 8 (γ) glucopyranose units. This family of compounds attracted the attention of numerous research groups since the 1960s when the opportunity to increase strongly their solubility in water through suitable substitutions at the 2-, 3-, and 6-hydroxyl sites was discovered. Hydrophobic molecules with appropriate size can be accommodated within the cyclodextrins cavity when dissolved in aqueous media.¹⁹ For this reason the cavity size is a fundamental parameter to determine the host properties of cyclodextrins, in fact α -Cyclodextrins cannot accommodate several kinds of molecules because of their small cavities.

The cavity of γ -Cyclodextrins is quite large, while β -cyclodextrins have a size that enables to bind several organic molecules. A reaction occurring on a substrate accommodated in the cavity of cyclodextrins can experience unusual regio- and stereo-selectivity due to the steric hindrance of the cyclodextrin that controls the conformation and orientation of the reagents.²⁰ The chlorination reaction of anisole catalyzed by α -Cyclodextrins provides an example of supramolecular systems with catalytic activity even higher than enzymes. The dual action of hypochlorous acid that replace a hydroxyl group with a chlorine atom on the cyclodextrin structure and the cavity that accommodate the anisole causes an increase in the rate and selectivity for the formation of p-chloro anisole.²¹

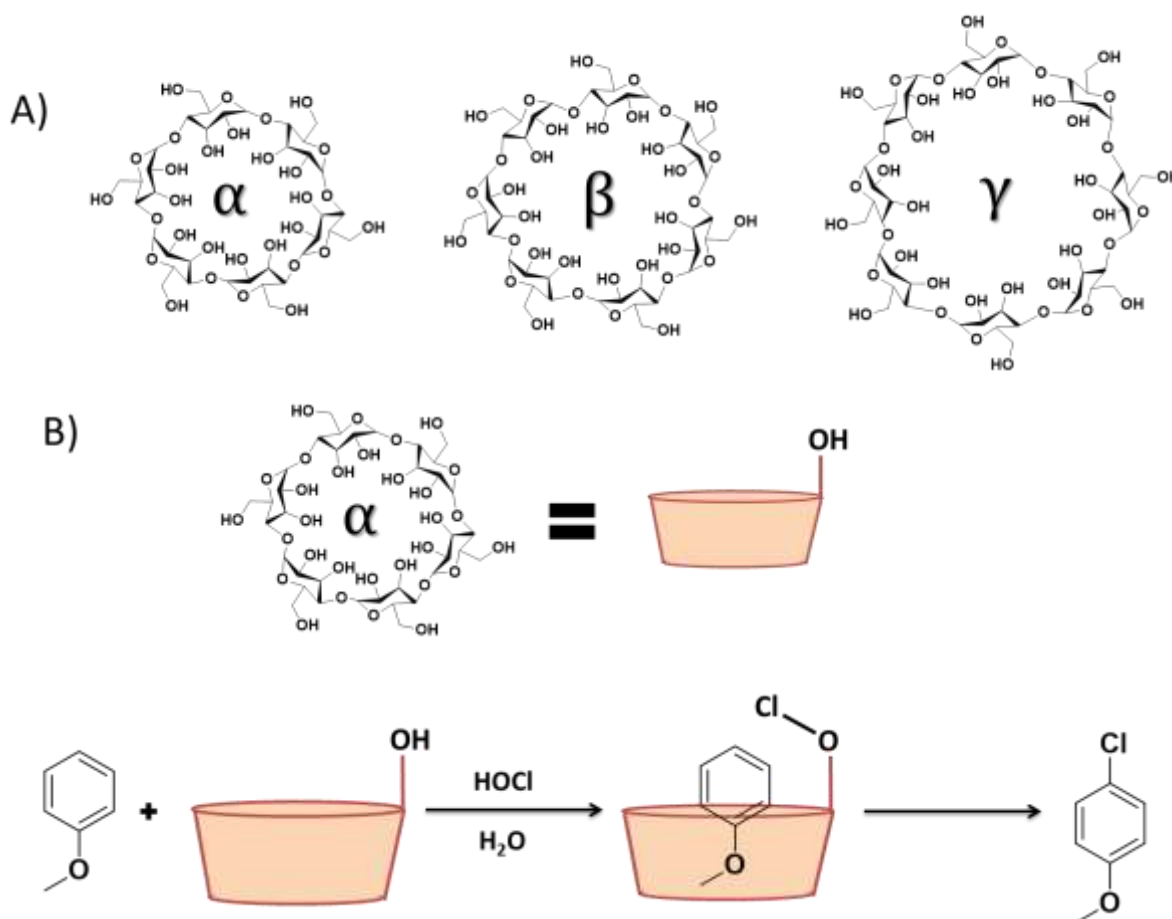


Figure 3. Molecular structures of the α -, β -, γ -cyclodextrins (A) and chlorination reaction of anisole mediated by α -cyclodextrins (B).

Another family of ring-shaped hosts is represented by crown ethers that are two-dimensional cyclic compounds containing several ether groups. Contrary to cyclodextrins, these compounds are able to solvate cations of appropriate dimensions dissolving them in organic solvents.²² In 1987 the Nobel Prize in Chemistry was awarded to Lehn, Cram and Pedersen "for their development and use of molecules with structure-specific interactions of high selectivity". These molecules are the crown ethers and the cryptands: three-dimensional compounds that behave as bi- and polycyclic

multidentate ligands. The structure of these new hosts arises from crown ethers in which two oxygen atoms are replaced by two nitrogen atoms that allow the presence of additional polyether chains.²³ This class of molecular containers has found only a marginal use in catalysis as phase-transfer catalysts.²⁴

Calixarenes are another example of cyclic oligomers whose particular shape makes them members of the cavitands class. Their structure is obtained by the hydroxyalkylation reaction of phenols and aldehydes while the name derives both from the Greek word "calix" indicating the shape cup and the chemical nomenclature "arene" that is typical of the aromatic compounds.²⁵ Several kinds of calixarenes have been developed both changing the aromatic part that can be constituted by resorcinol or pyrogallol molecules and choosing aldehydes with variable length and branches. In this manner it was possible to develop cavitands with a different number of components therefore a special nomenclature has been decided using the terminology of C-alkylcalix[n]arenes. The presence of particular aromatic groups makes calixarenes capable to accommodate cationic molecules through cation- π interactions.²⁶ Karakhanov and co-workers reported the interesting application of a series of water soluble calixarene-based systems in combination with Pd-complex as catalyst in the biphasic Wacker-oxidation of several linear alkenes and styrenes. The reaction showed different activity and substrate selectivity depending on the molecular recognition abilities of the employed calixarene due to the interactions of calixarene with the two phases and the orientation imparted to the substrate molecules.²⁷

Another interesting example of cavitands employment in catalysis was shown by Rebek and co-workers who reported the use of a deep water-soluble cavitand substituted with a carboxylic acid imidazole group. The hydrophobic effect allows the solubilization in aqueous solution of several N-substituted maleimides and the cavity acts as a phase-transfer catalyst in the reaction of these molecules with water-soluble thiols.²⁸

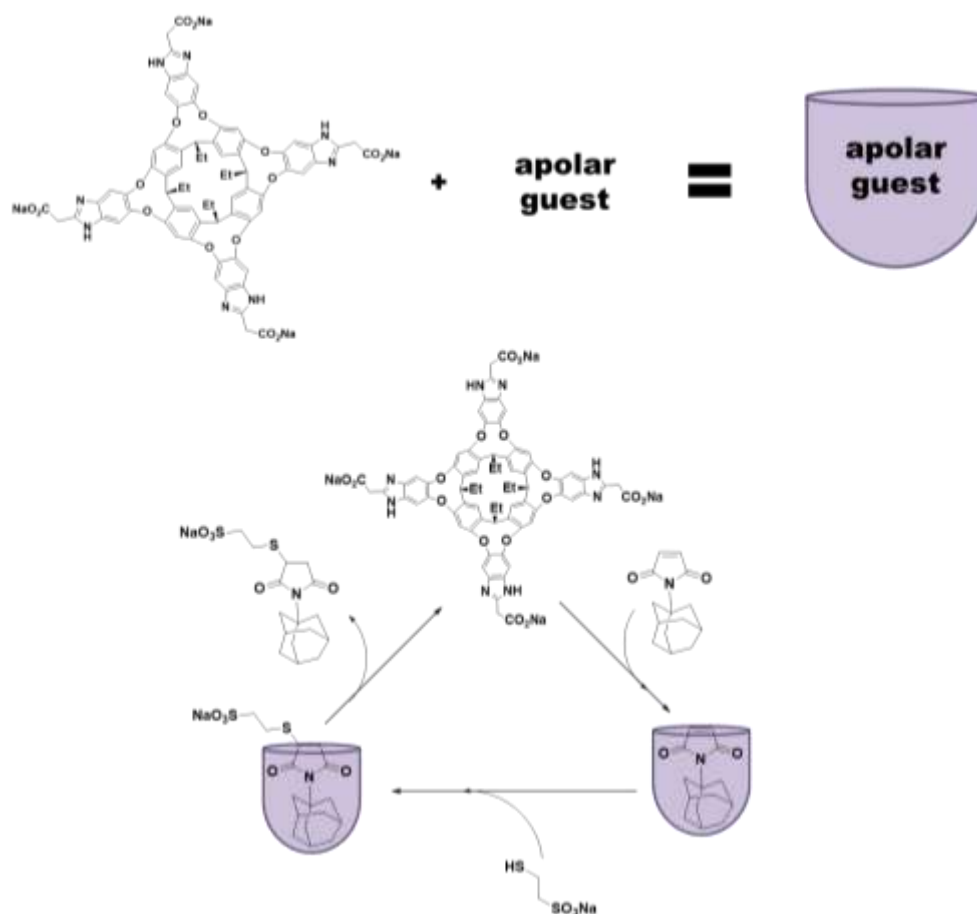


Figure 4. Cavitand used by Rebek and co-workers as a phase-transfer catalyst in the reaction between *N*-substituted maleimides and water-soluble thiols

Most research groups that study the applications of supramolecular systems in catalysis use self-assembling systems. Indeed the synthesis of macromolecular cages capable of selectively hosting guest molecules can be quite complicated and time consuming. The development of self-assembled nanostructures from highly directive and pre-designed spontaneous interactions of low molecular weight compounds is therefore highly desirable. The use of self-assembled capsules in chemical transformations represents a viable method for the creation of systems that mimic some of the peculiar features of enzymes. This led to the idea of creating self-assembled nanoreactors that are obtained by spontaneous association of low molecular weight compounds under equilibrium conditions into higher molecular weight aggregates both in water and in organic media.²⁹

The first example of self-assembled capsule is the “tennis ball” that was reported by Rebek and co-workers. This capsule is a reversible supramolecular dimer obtained through 8 hydrogen bonds³⁰ between two subunits in which two glycoluril moieties are linked through an aromatic ring. The cavity has a volume of 50 \AA^3 that is sufficient to accommodate only extremely small molecules

as methane, ethane, ethylene and noble gases.³¹ Obviously such a small capsule could never be used in catalysis, but its structure was the basis for the development of other self-assembled cages that on the contrary gave very interesting results. Initially the use of enlarged monomers through appropriate spacer allowed the synthesis of the "softball". The cavity within this capsule has a volume between 240 and 320 Å³ capable to accommodate up to two guests of the dimensions of a benzene molecule. The larger internal space allowed to use the "softball" as supramolecular catalyst for the bimolecular Diels-Alder reaction between benzoquinone and cyclohexadiene. In fact the fast encapsulation of the two substrate within the "softball" causes the formation of the endo Diels-Alder adduct with a rate increased of about two orders of magnitude with respect to the same reaction carried out in *p*-xylene in the absence of the supramolecular vessel. Unfortunately the product proved to be an excellent guest for the capsule so the system was unable to perform more than one catalytic cycle.³² In order to enable this supramolecular system to perform catalytic cycles, Rebek and coworkers tried to use substrates inducing the formation of products with low affinity for the "softball" cavity. For this purpose the cyclohexadiene was replaced by 2,5-dimethylthiophene dioxide and the Diels-Alder reaction was carried out in the presence of a catalytic amount of "softball" (10% with respect to each substrate). Interestingly the reaction rate was increased by the "softball" observing a 75% yield after 4 days at 40°C, while under the same condition only 17% yield was achieved in the absence of the supramolecular vessel.³³

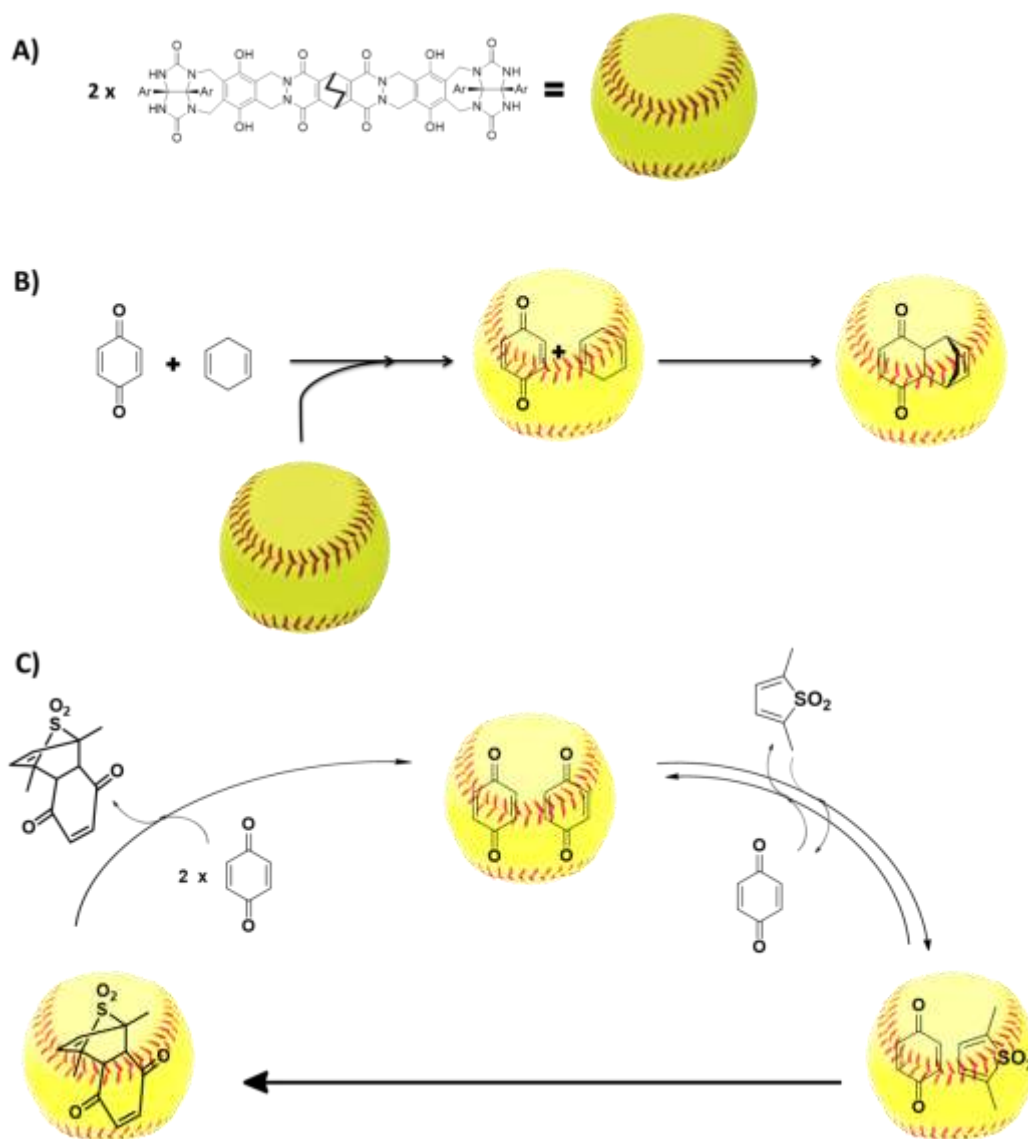


Figure 5. Molecular structure of the “softball” (A), Diels-Alder reaction between benzoquinone and cyclohexadiene mediated by the “softball” (B) and the catalytic cycle of the “softball” in the Diels-Alder reaction between 2,5-dimethylthiophene dioxide and benzoquinone.

Other molecular containers were generated using monomers that interact through hydrogen bonds. For example dimeric vessels can be obtained through an appropriate derivatization of cavitand molecules with residues having functional groups that can generate hydrogen bonds.³⁴

The hydrogen bond is not the only interaction that allows the formation of supramolecular capsules, indeed there are several examples of self-assembling cages obtained through metal-ligand bonds. The cavities within these structures are so large to allow the encapsulation of organometallic catalytic complexes and substrates with appropriate size and shape. Raymond and co-workers discovered a tetrahedral supramolecular capsule $[M_4L_6]^{12-}$ that self-assembles in water. The structure of this vessel is composed by four metal atoms ($M = Ga^{3+}, Al^{3+}, In^{3+},$ or Fe^{3+}) that are placed at the tetrahedron corners and six naphthalene-based bis-bidentate catechol ligands (L) that

compose the faces. The arrangement of these elements causes the exclusive formation of homochiral stereoisomer ($\Delta,\Delta,\Delta,\Delta$ or $\Lambda,\Lambda,\Lambda,\Lambda$)^{35,36} with a cavity of 300–350 Å³³⁷ that can accommodate several organic monocationic and neutral molecules with appropriate shape and size in water as the solvent.^{38,39,40,41} The encapsulation of the guest molecules occurs through a C₃-symmetric aperture of the host structure without rupture of the metal–ligand bonds.⁴²

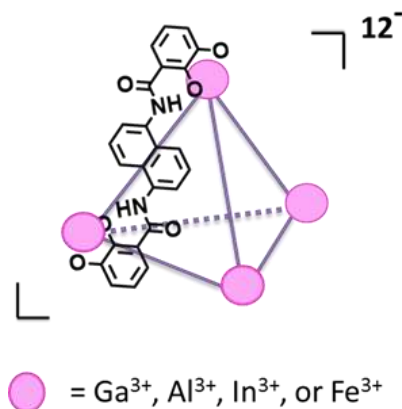


Figure 6. Raymond's tetrahedral supramolecular capsule [M₄L₆]¹²⁻ that self-assembles in water.

This capsule showed catalytic activity comparable with those of enzymatic systems in the carbon-carbon bond-forming Nazarov cyclization of 1,4-pentadien-3-ols in a water/DMSO medium under mild conditions achieving a rate enhancement of over a million times with respect to the uncatalyzed reaction. This acceleration is the result of the combination of three factors within the cavity: (i) the pre-organization of the substrate molecule, (ii) the stabilization of the cationic transition state and (iii) a higher basicity of the alcohol group.⁴³ Moreover Raymond and co-workers demonstrated the opportunity to encapsulate chemically reactive monocationic organometallic species.⁴⁴ A cationic half-sandwich iridium species Cp*(PMe₃)Ir(Me)(C₂H₄)⁺, a [RuCp(PMe₃)(D₂O)₂]⁺ obtained from the water unstable [RuCp(PMe₃)(MeCN)₂][PF₆] complex and Me₃PAu(H₂O)⁺ species demonstrated catalytic activity within the Raymond capsule and they were respectively used in the substrate selective C-H bond activation of aldehydes,^{45,46} in the isomerization of α,β -unsaturated alcohols without product inhibition⁴⁷ and in the hydroalkoxylation reaction of the 6-methylhepta-4,5-dien-1-ol. The encapsulation “isolates” the organometallic complex from the rest of the solution preventing the interaction with elements without appropriate size and shape. This property proved to be essential to obtain two interesting examples of tandem catalytic process in which the Au- or Ru-organometallic complexes and enzymes work together without any deactivation.⁴⁸

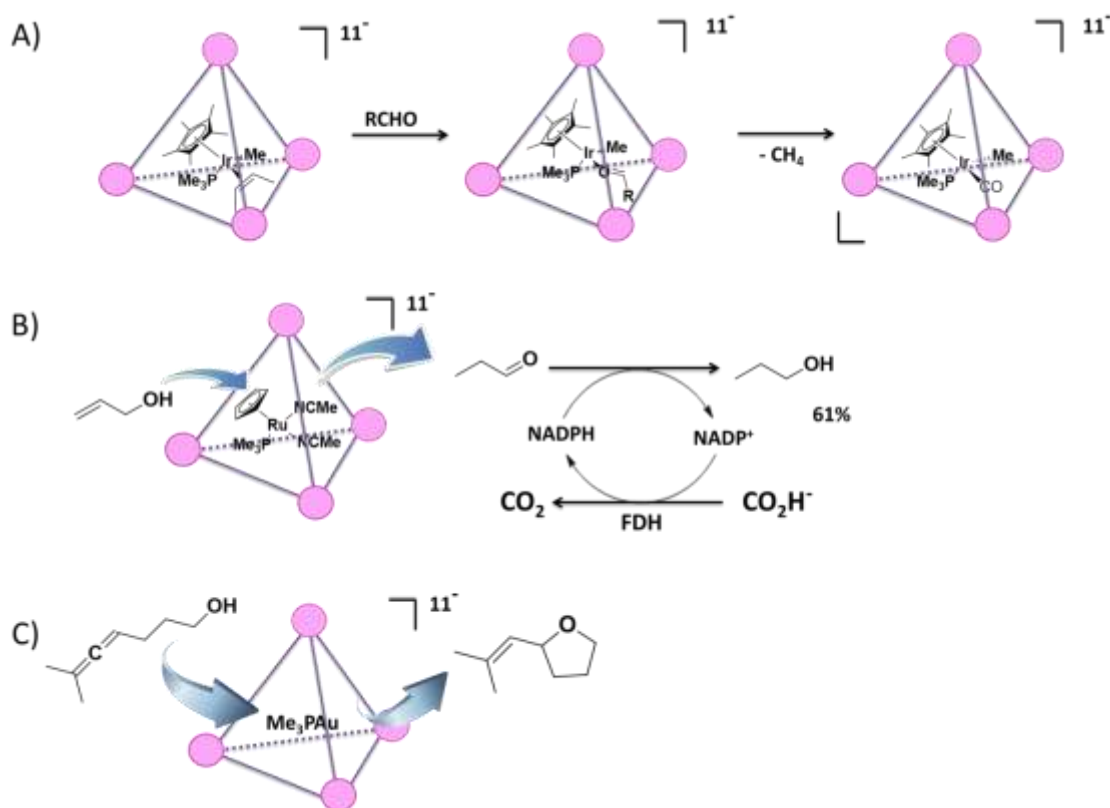


Figure 7. (A) C-H bond activation of aldehydes mediated by Ir-complex within the cavity, (B) isomerization of α,β -unsaturated alcohols catalyzed by Ru-complex working together with reduction enzyme and (C) hydroalkoxylation reaction of the 6-methylhepta-4,5-dien-1ol catalyzed by Au-complex.

Fujita and co-workers realized another example of self-assembling capsule based on metal-ligand interaction: a water-soluble octahedral supramolecular container with a general structure M_6L_4 ($M = Pd^{2+}$, $L =$ pyridine-based bridging exo-tridentate ligands)⁴⁹ with a ≈ 2 -5 nm diameter hydrophobic cavity⁵⁰ in which organic molecules are strongly retained.⁵¹ The capsule strongly absorbs light at < 370 nm⁵² and the cage can transfer the absorbed energy to the guest molecule facilitating some photodimerization⁵³ and photooxidation⁵² reactions. The cationic environment of the cavity stabilizes negatively charged molecules and facilitates reactions with anionic intermediates. An example of the M_6L_4 catalytic activity is the Knoevenagel condensation of aromatic aldehydes in which the great affinity of the substrate molecules for the cavity and the formation of bulky products allow to obtain a system capable of many catalytic cycles.⁵⁴

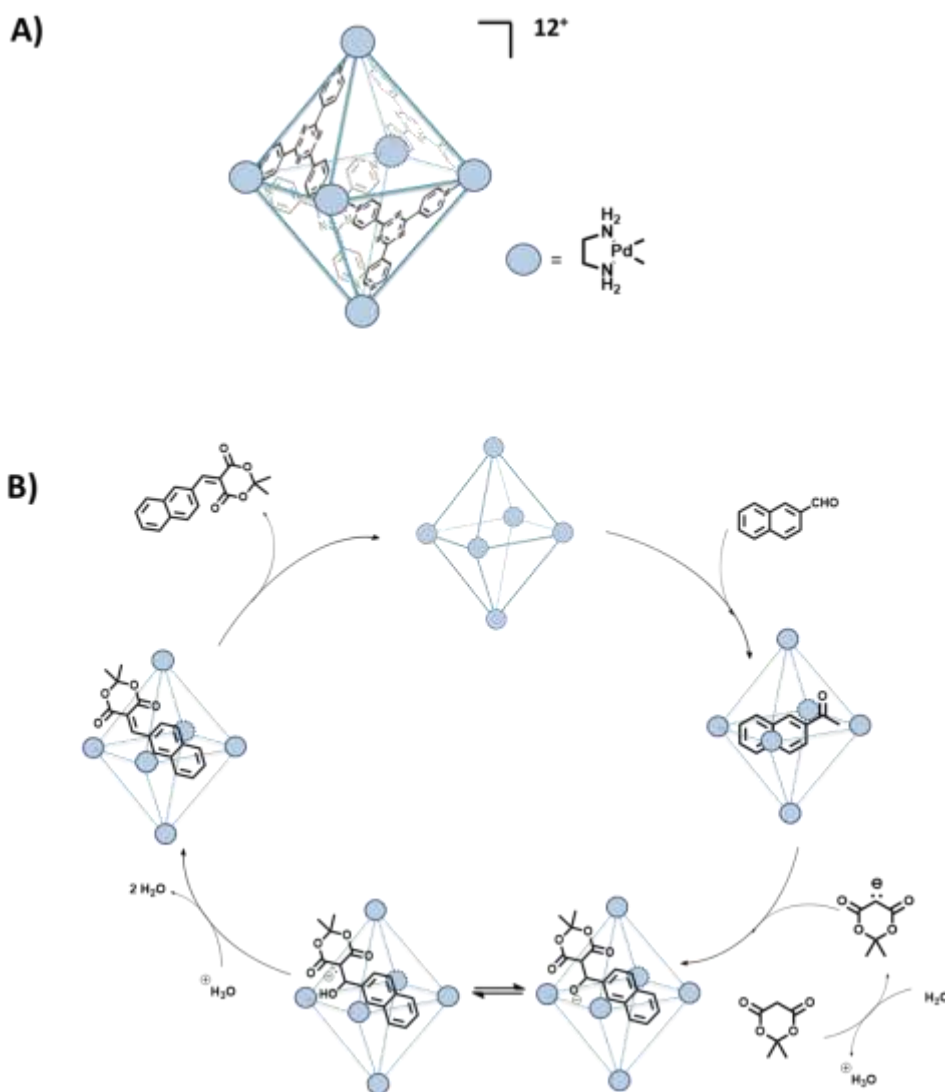


Figure 8. (A) Fujita's octahedral supramolecular capsule M_6L_4 and (B) its catalytic activity in the Knoevenagel condensation of aromatic aldehydes.

3.1.2. The Resorcin[4]arene Capsule

In 1997 MacGillivray and Atwood demonstrated the peculiar behavior of six calix[4]resorcinarenes and eight water molecules to self-assemble forming a spherical hexamer through 60 O–H...O hydrogen bonds in appropriate apolar organic solvents such as $CHCl_3$ and benzene. Each water molecule develops three hydrogen bonds with the OH groups of three neighboring resorcin[4]arene molecules, while each monomer interacts through four intramolecular hydrogen bonds with other neighboring resorcin[4]arene causing a 3D structure with a cavity of

about 1375 \AA^3 .⁵⁵ Avram and Cohen reported the C-undecylcalix[4]resorcinarene self-assembles in water-saturated CDCl_3 without any guest showing that eight solvent molecules fill the cavity.⁵⁶ Rebek and Shivanyuk showed that positively charged guest with appropriate shape and size as quaternary ammonium compounds can be accommodated⁵⁷ through an extended cation- π interaction⁵⁸ due to the high number of electron-rich aromatic rings on the surface of the capsule. The OH groups of the resorcin[4]arene molecules of the capsule allow the encapsulation of neutral species capable of H-bonding like carboxylic acids, aminoacids and polyols.⁵⁹ Moreover, Tiefenbacher and co-workers reported the encapsulation of tertiary amines that are neutral guests incapable of developing hydrogen bonds. They studied the encapsulation of amines with different basicity hypothesizing that the protonation of the amines was the cause of the encapsulation. The results showed that the delocalization of the negative charge along the entire structure of the self-assembling hexamer causes an acidity much higher than the single molecule of resorcin[4]arene reaching a $\text{p}K_a$ of about 5.5–6 and this value can be further increased through ammonium salts encapsulation.⁶⁰

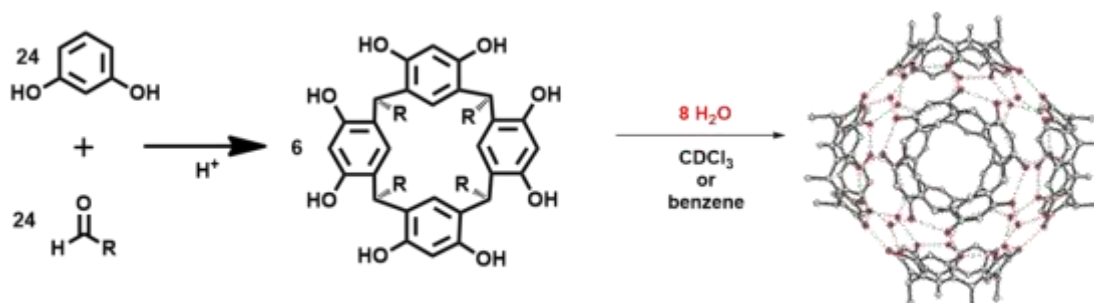


Figure 9. Resorcin[4]arene self-assembling into the hexameric capsule.

The resorcin[4]arene capsule is an ideal supramolecular structure for several applications in homogeneous catalysis. Indeed the simplicity and un-expensiveness of the monomers are combined with a very large cavity that is a feature more commonly found in self-assembling capsules based on metal-ligand interactions. For several years Strukul and Scarso have been studying the possible applications of the hexameric capsule in homogeneous catalysis. They demonstrated the possibility to entrap an organometallic complex of Au(I) within the cavity showing the effect of constrain in a confined space on the product selectivity in the hydration of 4-phenyl-1-butyne (Figure 10, A). Indeed the free Au-complex catalyzes the exclusive conversion to the corresponding ketone while the supramolecular catalytic system also causes the formation of the corresponding aldehyde and the intramolecular cyclization product.⁶¹ Moreover when the Au-complex is encapsulated the

limited residual space offers also the possibility to obtain substrate selectivity in the presence of a series of reagents with different steric hindrance (Figure 10,B).⁶²

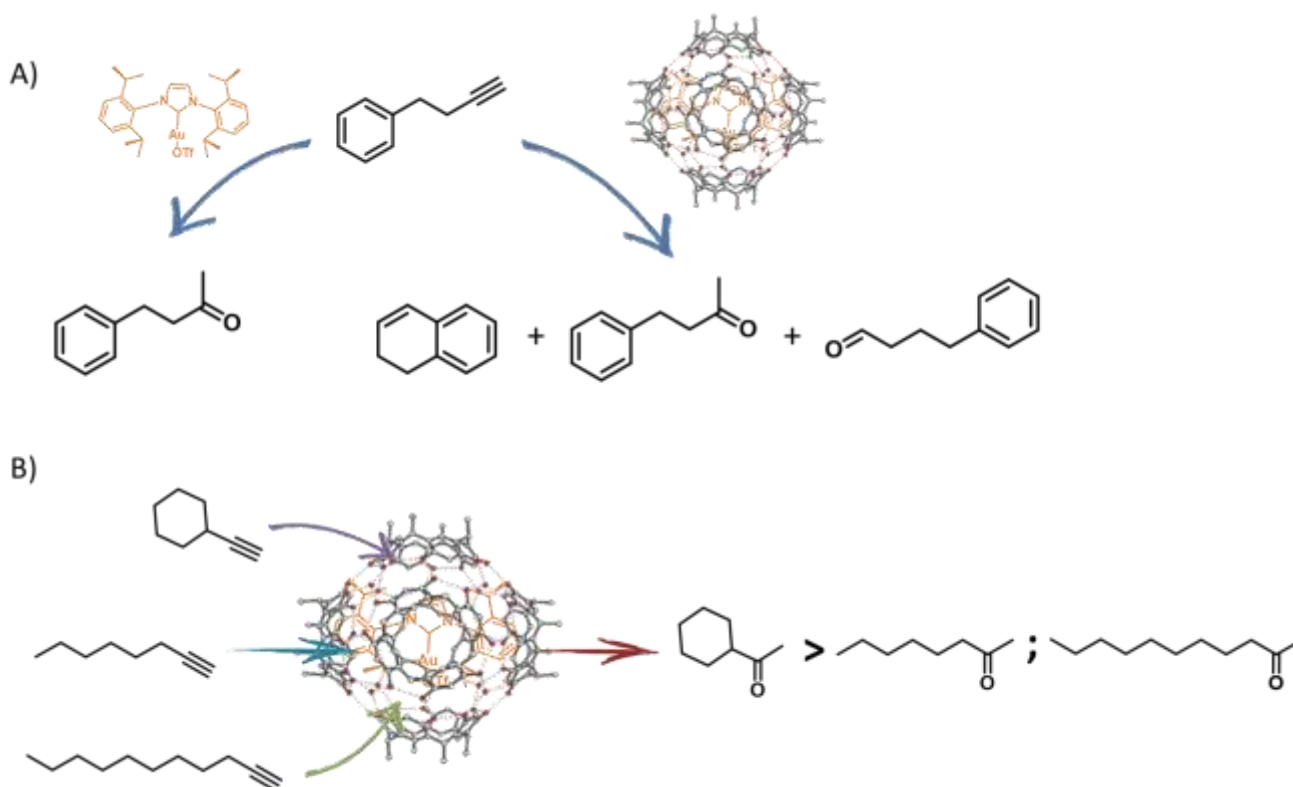


Figure 10. Encapsulated organometallic complex of Au(I) within the cavity of the resorcin[4]arene capsule showed: (A) peculiar product selectivity in the hydration reaction of 4-phenyl-1-butyne, (B) substrate selectivity in the presence of a series of reagents with different steric hindrance

My collaboration with the research group of Scarso and Strukul began with the study of the encapsulation in the resorcin[4]arene of the $[\text{Ru}(\text{bpy})_3]^{2+}$ complex in the photo-catalytic aerobic oxidation of dibutyl sulfide to sulfoxide and sulfone. $[\text{Ru}(\text{bpy})_3]^{2+}$, as a pseudo-spherical cationic complex whose shape and size perfectly fit the cavity of the hexameric capsule, experienced a modulated catalytic activity through a reversible encapsulation. The possibility of modulating the catalytic activity of $[\text{Ru}(\text{bpy})_3]^{2+}$ was exploited to obtain a circuit breaker-like system capable to switch off and on the reaction simply adding alternately a sufficient amount of capsule to cause the complex encapsulation and tetraethyl ammonium as competitive guest respectively (Figure 11).⁶³

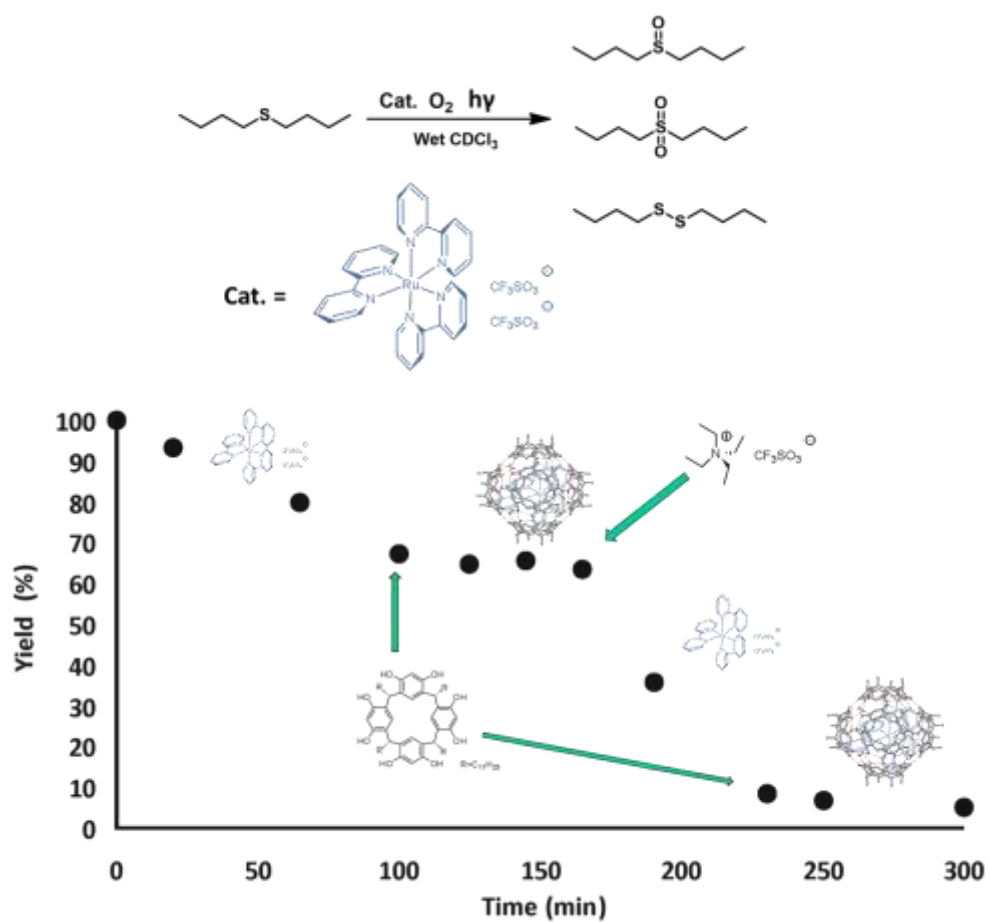


Figure 11. Variation of the residual butyl sulfide during reversible switch of the photoredox catalytic activity of $[\text{Ru}(\text{bpy})_3]^{2+}$ through sequential additions of resorcin[4]arene, competitive guest $\text{N}(\text{Et})_4^+$, and resorcin[4]arene again.

3.2. Results and Discussion

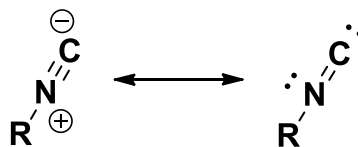
3.2.1. Interaction between Capsule and formally neutral compounds

The results presented in this chapter were published in:

- G. Bianchini, G. La Sorella, N. Canever, A. Scarso, G. Strukul, "Efficient isonitrile hydration through encapsulation within a hexameric self-assembled capsule and selective inhibition by a photo-controllable competitive guest", *Chem. Commun.*, 2013, **49**, 5322-5324;
- S. Giust, G. La Sorella, L. Sporni, F. Fabris, G. Strukul, A. Scarso, "Supramolecular Catalysis in the Synthesis of Substituted 1 H-Tetrazoles from Isonitriles by a Self-Assembled Hexameric Capsule", *Asian J. Org. Chem.*, 2015, **4**, 217-220;
- G. La Sorella, L. Sporni, G. Strukul, A. Scarso, "Supramolecular Encapsulation of Neutral Diazoacetate Esters and Catalyzed 1,3-Dipolar Cycloaddition Reaction by a Self-Assembled Hexameric Capsule", *ChemCatChem*, 2015, **7**, 291-296.

3.2.1.1. Isocyanides: a class of compound with interesting features

Isocyanides (also known as *isonitriles* or *carbylamines*) are organic compounds whose potential interest due to their unique reactivity have not been sufficiently investigated because of their limited commercial availability and the repulsive odour that discourages their employment. Isocyanides are characterized by a R-N≡C functional group that can be described with either the zwitterionic form with positive N and negative C, or the predominantly carbenic electronic structure as reported in scheme 1.⁶⁴ The linear geometry of the NC bond is due to the π lone pair of the nitrogen atom that is also responsible of the zwitterionic structure.⁶⁵



Scheme 1. Resonance structure of the isocyanide group: zwitterionic form (left) and carbenic form (right).

The carbon atom of the isocyanate functional group can behave either as an electrophile⁶⁶ or as a nucleophile⁶⁷ allowing the use of these molecules in several multi-component reactions.⁶⁸ Even if several isocyanides are natural products, specific syntheses were developed for the most part of them. Traditionally isocyanide synthesis makes use of primary amines⁶⁹ or N-formyl secondary amides⁷⁰ as starting material. More recently new methods of isocyanide synthesis have been discovered making use of alcohols as starting material.⁷¹

3.2.1.2. Hydration of Isocyanides within the cavity

Since the beginning of the studies on the use of the resorcinarene capsule in catalysis we have been interested in the opportunity to encapsulate neutral, non hydrogen bonding species. We wondered if electron poor molecules could behave as guests for the cavity taking advantage of its the electron rich surface. The particular electronic properties of the isocyanides N≡C bond spurred our interest and we decided to verify the interaction between the resorcin[4]arene capsule and isonitriles. The cyclohexyl isonitrile **I1** was chosen as the reference substrate for the preliminary studies. This substrate proved to interact with the capsule. The addition of ten equivalents of **I1** to a solution of the self-assembled hexamer in a water saturated chloroform-d led to the encapsulation of the neutral guest. The ¹H NMR analysis of the solution showed new up-field shifted broad resonances in the range 0.1 to -0.7 ppm that are diagnostic of the encapsulated species (Figure 12). The encapsulation of isocyanides is not straightforward since they are neutral molecules with minimal hydrogen bonding properties. We thought that the mainly carbenic character⁶⁵ of these species could cause their encapsulation. In fact the high electron-density provided by the concave aromatic surface of the capsule could stabilize the carbenic-like structure of the substrate. Moreover, we observed that **I1** was stable in water saturated chloroform-d at 60 °C for more than 18 hours, while under the same conditions, its complete conversion into the corresponding N-formylamide **F1** was achieved by simply adding 10 mol% of capsule as a supramolecular catalyst (Table 1, entry 2, Fig 13). The presence of **F1** was confirmed by GC-MS analysis and by the appearance of a new resonance at 8.09 ppm typical of the formyl proton.

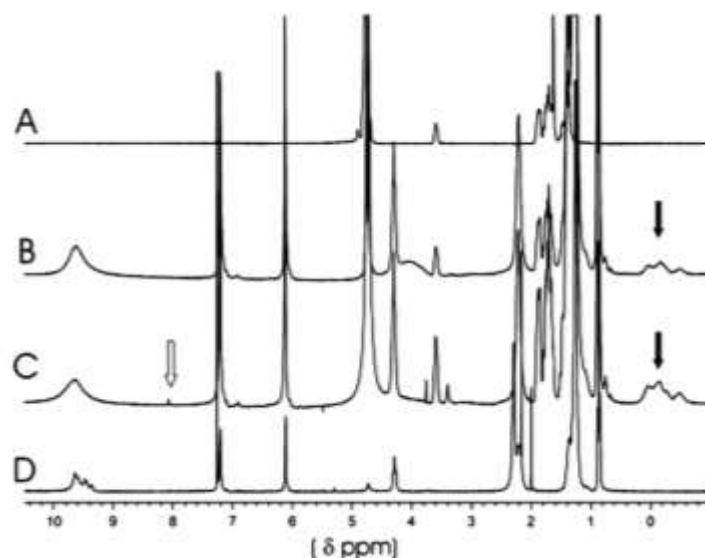


Figure 12. ^1H NMR spectra in water saturated chloroform-d: (A) **I1** (60 mM); (B) **I1** (60 mM) and resorcin[4]arene (36 mM); (C) **I1** (120 mM) and resorcin[4]arene (36 mM); (D) resorcin[4]arene (36 mM). encapsulated substrate, N-formylamide product.

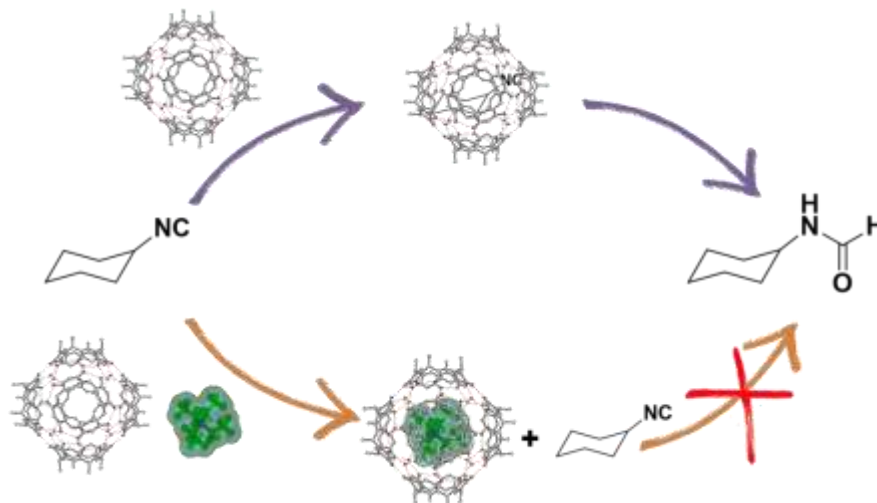


Figure 13. Hydration reaction of **I1** to **F1** catalysed only by the empty capsule.

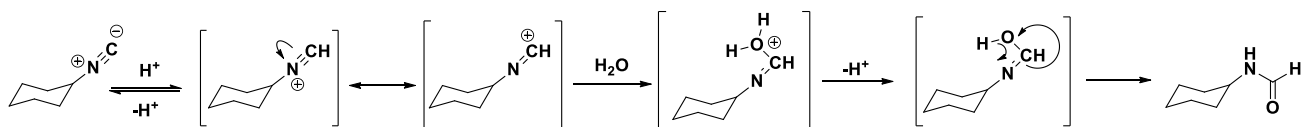
If the encapsulation of isocyanides was not completely surprising, the formation of **F1** was completely unexpected. In the literature it was reported that the N-formyl amides are obtained through the α -addition of water to the corresponding isocyanides. The accepted mechanism of this reaction occurs via protonation of the carbenic like C atom followed by water addition.⁷² Therefore isocyanide hydration has been usually catalysed by acids⁷³ even in aqueous media, paying attention to avoid possible polymerization products. Acetic⁷⁴ or trifluoroacetic acid,⁷⁵ hydrochloric acid,⁷⁶ and polymer-supported *p*-toluenesulfonic acid⁷⁷ could be used as catalyst in order to maximize the N-formyl amides formation. The reaction is usually carried out at low concentrations and high temperatures.⁷⁸ Since no acids were intentionally introduced in the reaction, we initially thought that the catalytic effect imparted by the capsule was due to the stabilization of the cationic intermediate by means of interaction with the electron rich, concave internal surfaces of the resorcin[4]arene units. The presence of a supramolecular structure that makes the intermediate more stable could favour the addition of water. In order to prove the catalytic properties of the cavity we performed control experiments repeating the hydration of **I1** under the same conditions but in the presence of an excess of tetraethylammonium trifluoromethanesulfonate (NEt_4)(OTf) (60 mM) as a competitive cationic guest (Table 1, entry 3).

#	Capsule	(NEt ₄)(OTf)	F1(%) ^a
1	-	-	0
2	+	-	>98
3	+	+	<5
4	-	+	0
5 ^b	-	-	<5

Table 1. Catalytic tests for the hydration reaction of **II** catalysed by resorcin[4]arene. Reaction conditions: [**II**]= 60 mM, [resorcinarene]= 36 mM, [(NEt₄)(OTf)]= 60 mM (10 eq. with respect to the capsule), water saturated chloroform-d 0.5 mL, T=60°C, time 18h. +: presence; -: absence; a) Determined by GC; b) [resorcinol] = 144 mM (4 eq. with respect to resorcin[4]arene).

The presence of ammonium within the capsule completely inhibited the reaction and almost no product was formed (Figure 13). Furthermore the ineffectiveness in catalyzing the reaction by the hydroxyl groups present in resorcinarene and involved in hydrogen bonding was demonstrated by repeating the reaction in the presence of resorcinol as H-bonding molecular mimic (Table 1, entry 5). Even in this case no formation of product N-formylamide was obtained emphasizing the importance of the presence of the cavity in isocyanide hydration.

After these findings, Tiefenbacher and coworkers demonstrated that the hexamer behaves as a weak acid assembly with a pKa of about 5.5, while the resorcinol moiety has a pKa of 9.15.⁶⁰ This could only partially explain the catalytic properties of the capsule in the hydration reaction of isocyanides. In fact, as discussed by Tiefenbacher himself,⁶⁰ the acidity of the capsule is increased in the presence of an ammonium guest, therefore the reaction would have given higher conversions when the cavity was occupied by **TEA**. The presence of a cavity capable to solvate compounds involved in the reaction and to develop cation- π interactions with reagents and intermediates turned out pivotal to promote the reaction. Probably the cavity was able to stabilize the protonated isocyanate and favour the water molecule attack (Scheme 2).



Scheme 2. Proposed mechanism for the acid catalysed hydration of **II**, highlighting the series of intermediate cationic species whose formation may be favoured by the presence of the capsule.

The catalytic activity of the supramolecular capsule was tested also in the presence of substrates with different steric hindrance and electronic properties. For this reason other smaller aliphatic isonitriles like isopropyl isonitrile **I2**, t-butyl isonitrile **I3** and larger aromatic ones such as benzyl isonitrile **I4** and 2,6-dimethylphenyl isonitrile **I5** were used as substrates (Table 2). The ^1H -NMR analyses of these compounds in the presence of the hexameric capsule confirmed the encapsulation of all of them giving different results. The aliphatic compound **I2** showed several new resonances in the range -0.3 to -0.7 ppm, while **I3** showed a major single and relatively sharp resonance at -0.62 ppm ($\Delta\delta$ -2.07 ppm). In the presence of benzyl substrate **I4** the aromatic resonance shielding was observed achieving $\Delta\delta$ values between -0.8 and -1.2 ppm. Similar behaviour was observed with **I5** obtaining the corresponding shielded aromatic resonances shifted upfield with a $\Delta\delta$ of about -1.6 ppm, while the methyl groups were shifted by about -2.0 ppm.

#	Substrate	Product	Yield ^a (%)
1			>98 ^a
	I2	F2	0 ^{b,c} 93 ^{c,d}
2			20
	I3	F3	0 ^b <5 ^d
3			>98
	I1	F1	0 ^b 85 ^d
4			>98 ^a
	I4	F4	0 ^b >98 ^d
5			65 ^a
	I5	F5	0 ^b 48 ^d

Table 2. Hydration reaction of isocyanides **I1**–**I5** catalyzed by the capsule in water saturated chloroform-d. Reaction conditions: [substrate] = 60 mM, [resorcinarene] = 36 mM, water saturated chloroform-d 0.5 mL, T = 60°C, time 18 h. a) Determined by GC; b) No resorcinarene added; c) Determined by ¹H NMR; d) [substrate] = 120 mM.

As can be seen from the data reported in Table 2, the catalytic activity of the supramolecular capsule was highly dependent on size, shape and electronic properties of the isocyanides. Observing the results obtained with aliphatic compounds (Table 2, entries 1-3) we noticed that the smaller substrate **I2** with an *i*-propyl residue led to higher reactivity compared to **I1** that was characterized by higher steric hindrance. Nevertheless, in the case of *t*-butyl isocyanide **I3** a low conversion to the corresponding N-formylamide **F3** was curiously observed. In the case of aromatic compounds (Table 2, entries 4, 5) the hydration reaction of benzylisocyanide **I4** gave a quantitative conversion

of the substrate into **F4** in 18 hours. However, the employment of a sterically encumbered substrate such as **I5** caused a decreasing in the catalytic activity of the capsule. In fact the conversion of this isonitrile to the corresponding N-formyl amide **F5** was one of the lowest obtained, highlighting the dependence of the catalytic activity on the presence of substrates with different size and shape.

3.2.1.3. Addition of trimethylsilyl azide on isocyanides mediated by the capsule

The results obtained in the hydration reaction of isocyanides suggested that the capsule could catalyze the addition of other molecules to these compounds. The ability of the capsule to stabilize cationic intermediates could be used to favour the addition of nucleophilic compound more reactive than water to the isocyanide functionality. As *IH*-tetrazoles with substituents in 5 position can be obtained through reaction involving trimethylsilyl azide (TMSN₃) and isocyanides,⁷⁹ TMSN₃ was chosen as substrate to verify the catalytic activity of the capsule.

As already done for the hydration reactions, **I1** was used as reference substrate. The reaction between this substrate and the TMSN₃ was investigated both in the presence and in the absence of the hexameric capsule in water saturated chloroform-d. No conversion was observed after 5 hours at 60°C in the absence of resorcin[4]arene, while a 10 mol% of capsule was sufficient to obtain the quantitative formation of *IH*-tetrazole **T1** after 6.5 hours (Table 3, entry 2).

#	Capsule	Acetic acid	Resorcinol	Ammonium	t (h)	F1 (%) ^a
1	-	-	-	-	5	0
2	+	-	-	-	6.5	>98
3^b	-	+	-	-	6	2
4^c	-	-	+	-	6	10
5^d	+	-	-	+	6.5	33

Table 3. Catalytic tests for *IH*-tetrazole **T1** synthesis by reaction of *c*-hexyl isocyanide **I1** and TMSN₃. Reaction conditions: [**T1**] = 133 mM; [TMSN₃] = 133 mM; [resorcinarene] = 80 mM; water saturated chloroform-d 0.5 mL; t = Reaction time; T = 60°C; +: presence; -: absence. a) Yield determined by ¹H-NMR; b) [Acetic acid] = 13.3 mM (1 eq. with respect to the capsule); c) [Resorcinol] = 318 mM (24 eq. with respect to the capsule); d) [N(CH₂CH₃)₄BF₄] = 133 mM (10 eq. with respect to the capsule).

Historically the methods used to synthesize tetrazoles are based on the fundamental work of Finnegan and co-workers that reported the formation of tetrazoles from nitriles and sodium azide in

the presence of ammonium chloride.⁸⁰ Regrettably a large part of these methods require harsh conditions and the use of Lewis⁸¹ or Brønsted⁸² acids as catalysts. Therefore we investigated whether the catalytic activity of the capsule was simply due to its acidic character. Initially we repeated the reaction replacing the capsule with an equivalent amount of acetic acid, whose pKa (= 4.76) was very similar to that of the resorcin[4]arene hexameric structure.⁶⁰ Under these conditions a very low conversion was obtained confirming that the capsule effect was not to behave merely as a weak Brønsted acid (Table 3, entry 3). Then we checked the catalytic properties of the hydroxyl groups of the capsule carrying out the reaction in the presence of 24 equivalents of resorcinol with respect capsule (Table 3, entry 4). This experiment showed an increase in tetrazole formation, but the activation effect was much smaller compared to that obtained in the presence of the capsule. Finally we performed the reaction in the presence of the capsule and 10 equivalents of tetraethylammonium tetrafluoroborate (NEt₄)(BF₄) as a competitive guest, preventing the entry of isocyanide molecules within the cavity (Table 3, entry 5). Under these conditions the catalytic activity of the supramolecular system decreased, confirming the key role of the cavity to promote the reaction.

¹H-NMR spectra of the capsule alone (Figure 14, A) and in the presence of 10 equivalents of **II** and TMSN₃ (Figure 14, B) were acquired. Even in this case the typical upfield-shifted signals of the hosted isocyanide were visible as it occurred during the hydration reactions. Conversely, no evidence of the preferential encapsulation of TMSN₃ was observed as reported with spectrum B in Figure 14. The spectra of the reaction after 6 hours at 60°C either without (Figure 14, C) or with (NEt₄)(BF₄)(Figure 3, D) were acquired. These analyses showed that the cycloaddition reaction in the presence of a competitive guest for the capsule gave lower conversions, demonstrating the importance of the empty cavity in order to obtain high catalytic activity, even though TMSN₃ did not macroscopically show affinity for the capsule.

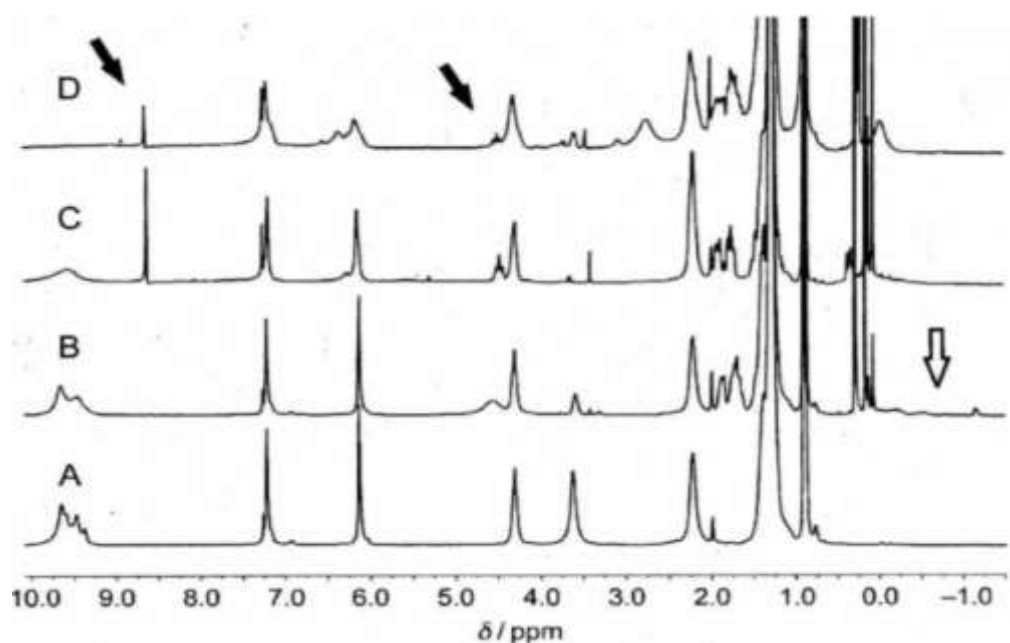


Figure 14. ^1H -NMR spectra in 0.5 mL of water-saturated CDCl_3 ; A) [Capsule] = 13.3 mM; B) [**II**] = 133 mM; [TMSN_3] = 133 mM; [Capsule] = 13.3 mM after mixing; C) [**II**] = 133 mM; [TMSN_3] = 133 mM; [Capsule] = 13.3 mM after 6.5 h at 60°C ; D) [$(\text{NET}_4)(\text{BF}_4)$] = 133 mM; [**II**] = 133 mM; [TMSN_3] = 133 mM; [Capsule] = 13.3 mM after 6.5 h at 60°C ; \blacktriangledown = *1H*-tetrazole product; \Downarrow = encapsulated isocyanide.

Interestingly, despite the high reactivity of **II** in the hydration reaction mediated by the capsule, only traces of the corresponding formylamide **F1** were observed. As it was known that 1-substituted aromatic *1H*-tetrazoles could be obtained from the corresponding formylamides,⁸³ we decided to use the capsule to catalyse the hydration reaction of **II** as reported above and once obtained the corresponding formyl-amide **F1**, add TMSN_3 to verify if **T1** was formed at 60°C for 18 h. Under these conditions no formation of *1H*-tetrazoles was observed, allowing us to exclude the formation of **F1** as a reaction intermediate and confirming the high chemo-selective synthesis of **T1** directly from **II**. These results further demonstrated that the capsule was able to stabilize cationic intermediate species through the cation- π interaction catalysing the nucleophilic attack on the isocyanide group (Figure 15).

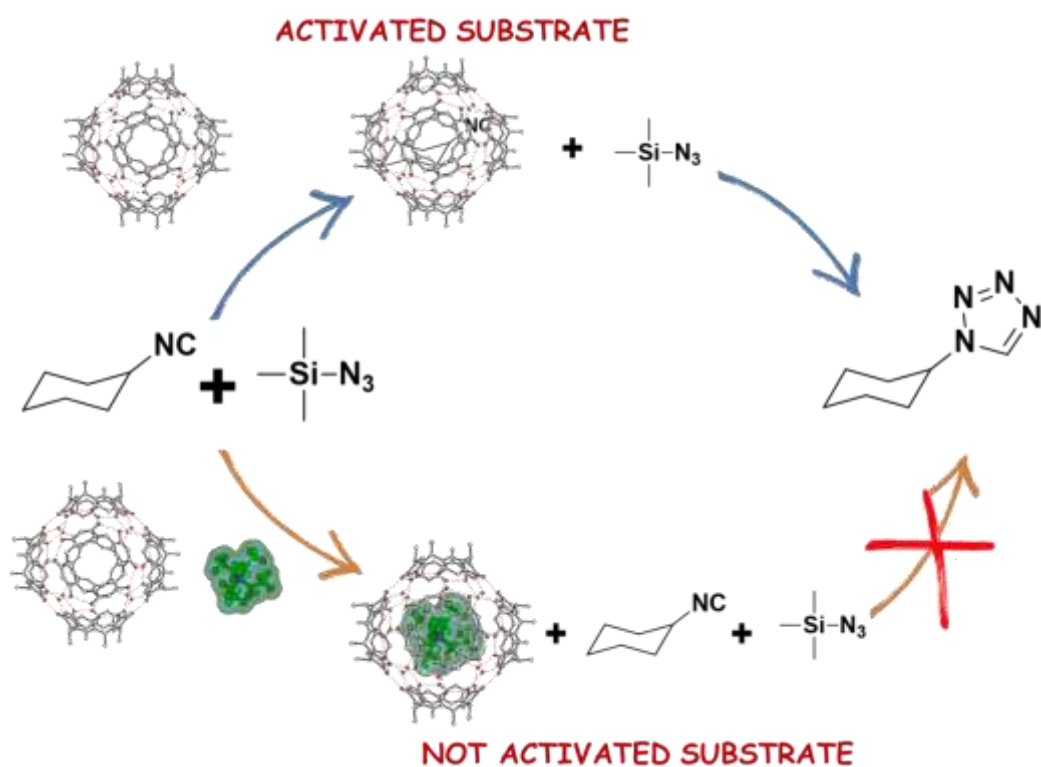


Figure 15. Cycloaddition reaction between **I1** and TMSN_3 to **T1** catalyzed only by the empty capsule through the activation of the substrate.

The catalytic activity of the supramolecular capsule was investigated in this cycloaddition reaction exploring the use of different aliphatic and aromatic isocyanides as substrates. All aliphatic substrates, except **I3**, showed slightly higher yields in the presence of the empty capsule compared to the values observed in the presence of a competitive guest such as $(\text{NEt}_4)(\text{BF}_4)$ (Table 4, entries 1-3). The low difference in catalytic activity observed with the either empty or filled capsule could be due to the non-complete filling of the space within the cavity by the ammonium salt. In fact this small space left free could be enough to allow the entrance of small substrates that could still react.

The catalytic effect of the empty capsule was much more evident in the presence of substrates with aromatic moieties in their molecular structure. In particular benzyl isocyanide **I4** and naphthyl isocyanide **I8** allowed to obtain the corresponding *1H*-tetrazoles derivatives with high yields in a relative short time in the presence of the empty cavity while low amounts of **T4** and **T8** were achieved with the capsule occupied by $(\text{NEt}_4)(\text{BF}_4)$ under the same conditions (Table 4, entries 4,7). Analogous substrates **I5** and **I7** with higher steric hindrance near the isocyanide group showed the same trend, but their reactivity was evidently lower (Table 4, entries 5,6).

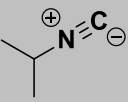
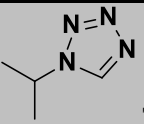
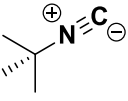
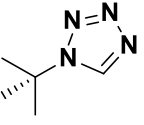
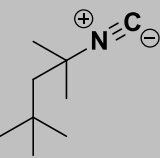
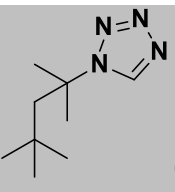
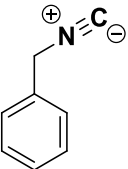
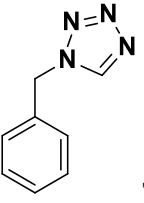
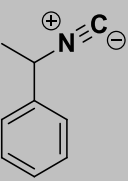
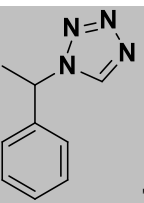
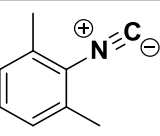
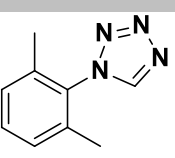
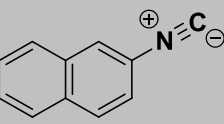
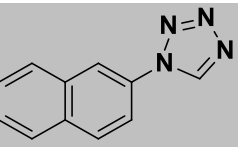
#	Substrates	Products	t (h)	Yield (%)
1	 I2	 T2	6.5	87 24 ^b
2	 I3	 T3	6	36 41 ^b
3	 I6	 T6	20	94 66 ^b
4	 I4	 T4	5.5	93 6 ^b
5	 I7	 T7	20	>98 19 ^b
6	 I5	 T5	6	40 2 ^b
7	 I8	 T8	6	81 4 ^b

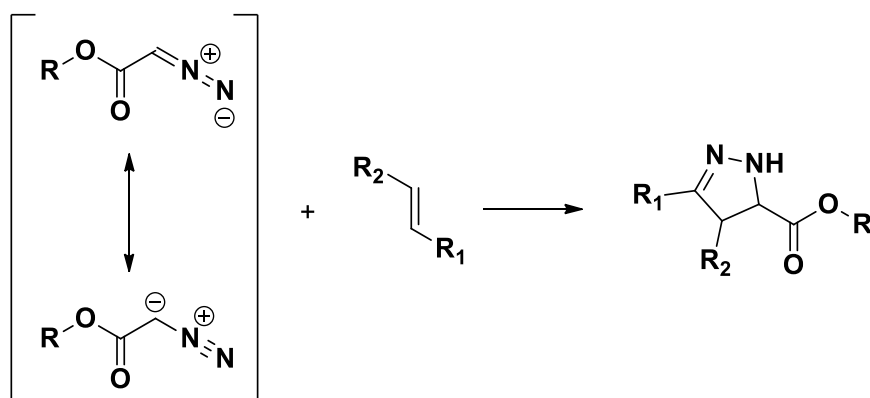
Table 4. 1H-Tetrazoles **T2-T8** syntheses from the corresponding isocyanides **I2-I8** and TMSN₃ catalyzed by the supramolecular hexameric capsule. Reaction conditions: [substrate] = 133 mM, [resorcinarene] = 80 mM, water saturated CDCl₃ 0.5 mL, T = 60°C. a) Determined by 1H-NMR. b) In the presence of (NEt₄)(BF₄) (133 mM, 10 equivalents with respect to the capsule).

Finally we investigated the capability of the supramolecular catalytic system to discriminate between pairs of substrates through competitive test in which two isocyanides were introduced in

the reaction in equimolar amounts. In order to observe the substrates intrinsic reactivity, reactions were initially carried out in the presence of methanesulfonic acid (20 mol% with respect to each substrate) as a strong Brønsted acid catalyst. When 25% conversion was achieved, the competitive reaction between 1,1,3,3-tetramethylbutyl isocyanide **I6** and (*S*)-(-)- α -methyl-bezyl isocyanide **I7** caused the formation of the corresponding *1H*-tetrazoles **T6** and **T7** in a **T6/T7** ratio = 0.3 emphasizing a three-fold higher reactivity of the aromatic substrate. Replacing the Brønsted acid with the hexameric capsule the same reaction gave a **T6/T7** ratio value of approximately 1.1 converting the aliphatic substrate at the same rate of the aromatic one. The same procedure was applied to the competitive cycloaddition reaction with cyclohexyl isocyanide **I1** and benzyl isocyanide **I4** respectively to **T1** and **T4**. In this case the competitive reaction catalysed by methanesulfonic acid showed the higher reactivity of the aromatic compound giving a product **T1/T4** ratio value of 0.4, while the capsule allowed to reverse the substrate selectivity achieving a **T1/T4** = 2.2. Unfortunately in none of the two cases the obtained values of substrate selectivity were striking, probably because of the large space within the hexameric capsule that does not provide a selection rule for molecules with such similar dimensions.

3.2.1.4. From Isocyanides to Diazoacetate esters

After the discovering that formally neutral molecules like isonitriles could be encapsulated within the hexamer of resorcin[4]arene due to a partial carbene-like electron poor character, we decided to seek for other classes of compounds with similar characteristics and study their interactions with the capsule. Diazo compounds turned out to be feasible guest molecules. In fact these are a family of organic compounds bearing a nitrogen molecule as a terminal functional group (general formula $R_2C=N_2$, Scheme 3), forming an electronic structure with a positively charged central nitrogen atom and negative charge spread between the terminal nitrogen and the carbon.⁸⁴ Besides, these compounds are well-known carbene-precursors simply through the loss of a neutral di-nitrogen molecule.⁸⁵ More specifically we focused our attention on diazoacetate esters that can be involved in the 1,3-dipolar cycloaddition reactions with electron-poor alkenes leading to 4,5-dihydro-1H-pyrazole derivatives.



Scheme 3. General 1,3-dipolar cycloaddition reaction of diazoacetate esters with electron-poor alkenes leading to 4,5-dihydro-1H-pyrazole derivatives.

3.2.1.5. Diazoacetate esters encapsulation

Ethyl-diazoacetate (**ED**) was used as the reference substrate in order to verify the opportunity to encapsulate this class of formally neutral compounds within the hexameric capsule. When 10 equivalents of **ED** were added to a solution of self-assembled capsule in water-saturated CDCl_3 , new upfield-shifted broad resonances were obtained in the $^1\text{H-NMR}$ spectrum in the $\delta = -0.86$ to -1.06 ppm range, attributed to the encapsulated ethyl moiety of the **ED** showing a $\Delta\delta \approx -2.1$ ppm (Figure 16, A and B). The shielding effect provided by the encapsulation confirmed the entrapment of the diazoacetate within the cavity. Similar results were obtained in the presence of *tert*-butyl-diazoacetate (***t*-BD**) and benzyl-diazoacetate (**BD**) as guest molecules. In fact ***t*-BD** showed a pair of major slightly broaden singlet signals at $\delta = -0.50$ and -0.52 ppm with a corresponding upfield shift of $\Delta\delta \approx -2.0$ ppm (Figure 16, C and D) while **BD** displayed a series of overlapped resonances at $\delta \approx 6.4$ ppm for the aromatic moiety and at $\delta = 3.8$ ppm for the benzyl moiety (Figure 16, E and F). Therefore the partial carbene-like character was sufficient to promote an effective encapsulation of these formally neutral compounds, confirming the hypothesis formulated.

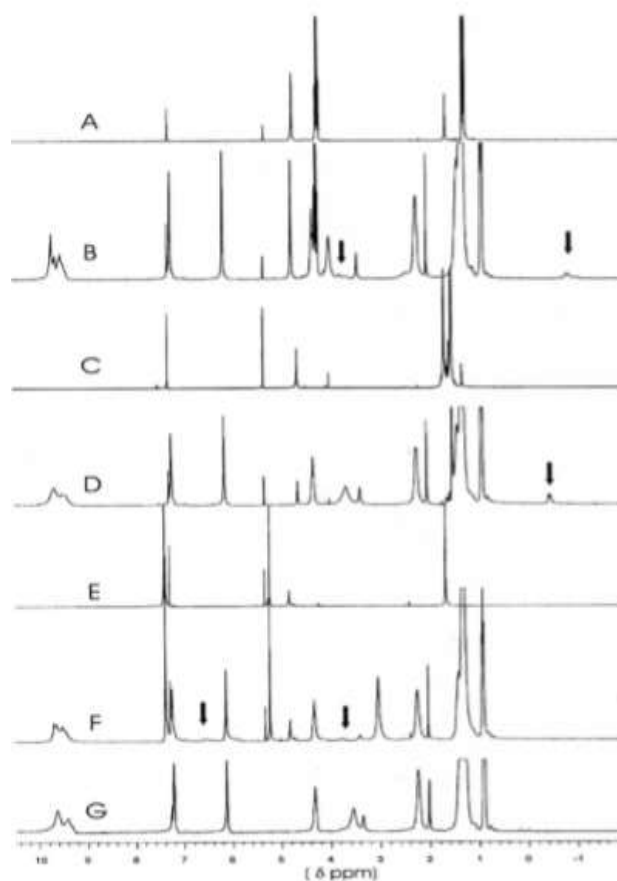


Figure 16. $^1\text{H-NMR}$ spectra in water saturated CDCl_3 of A) ethyl-diazoacetate (**ED**, 60 mM); B) **ED** (60 mM) and resorcin[4]arene (36 mM); C) tert-butyl-diazoacetate (***t*-BD**, 60 mM); D) ***t*-BD** (60 mM) and resorcin[4]arene (36 mM); E) benzyl-diazoacetate (**BD**, 60 mM); F) **BD** (60 mM) and resorcin[4]arene (36 mM). **I**: encapsulated substrate. The utilized diazoacetate esters contained small amount (5-15%) of CH_2Cl_2 as a stabilizer.

The different affinity for the cavity showed by **ED** and ***t*-BD** was estimated through the integration of the upfield-shifted resonances of the encapsulated molecules at different molar ratios with respect to the capsule. When 10 equivalents of these diazoacetate esters were added to a solution with 1 equivalent of capsule, the quantitative formation of one-to-one host-guest complex was obtained with both compounds. Further increase of the **ED** and ***t*-BD** amounts caused the further encapsulation of diazoacetate molecules. Indeed the $^1\text{H-NMR}$ of the sample with 20 equivalents of **ED** showed the encapsulation of 1.6 molecules per capsule, while this value reached 1.8 molecules per capsule in the case of ***t*-BD**. The *tert*-butyl-substituted diazoacetate exhibited slightly higher affinity for the capsule with respect to the **ED** probably because of better $\text{CH}-\pi$ interactions. Unluckily, the **BD** proved unsuitable for this methodology as the signals of the encapsulated species overlapped with the resorcin[4]arene resonances.

A study of the stability of these adducts allowed us to observe that **ED**, ***t*-BD** and **BD** remained stable both in the presence and in the absence of the capsule even at 50°C for 20 hours in water saturated CDCl₃. In fact no significant formation of the typical decomposition byproducts such as fumarate and maleate esters⁸⁶ were obtained.

The interaction between ***t*-BD** and the capsule was further investigated through 2D-NMR experiments. DOSY experiments showed a drastic decrease of the diffusion coefficient for the upfield-shifted resonances of ***t*-BD** in the presence of the resorcin[4]arene capsule assuming values in line with those of the capsule (Figure 17). Moreover NOESY experiments showed cross-peaks between the tert-butyl moiety of the diazoacetate compound and the aromatic CH group between the hydroxyl groups of resorcin[4]arene at $\delta = 6.1$ ppm (Figure 18).

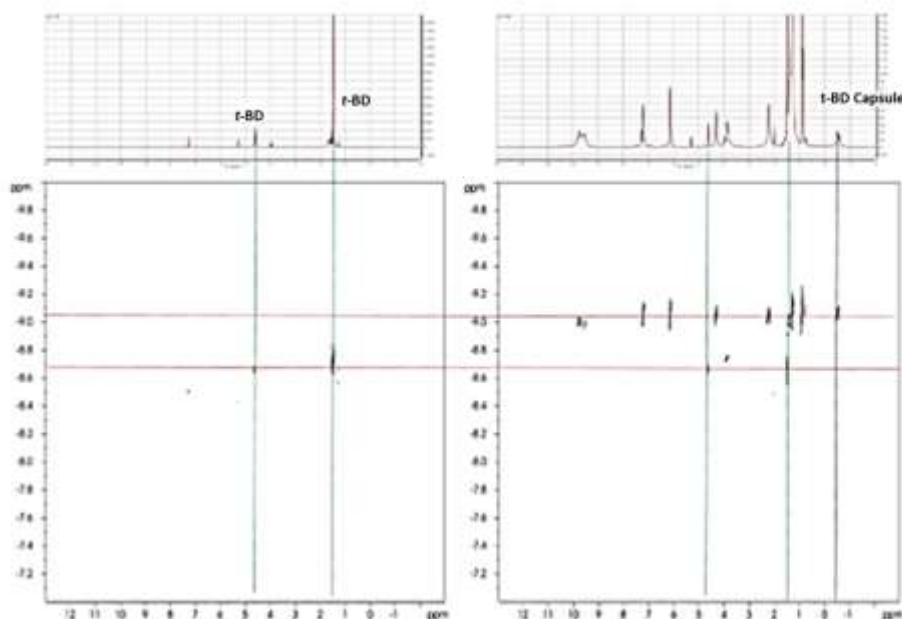


Figure 17. DOSY spectra of ***t*-BD** (on the left) and ***t*-BD** with the capsule (on the right) in water saturated CDCl₃.

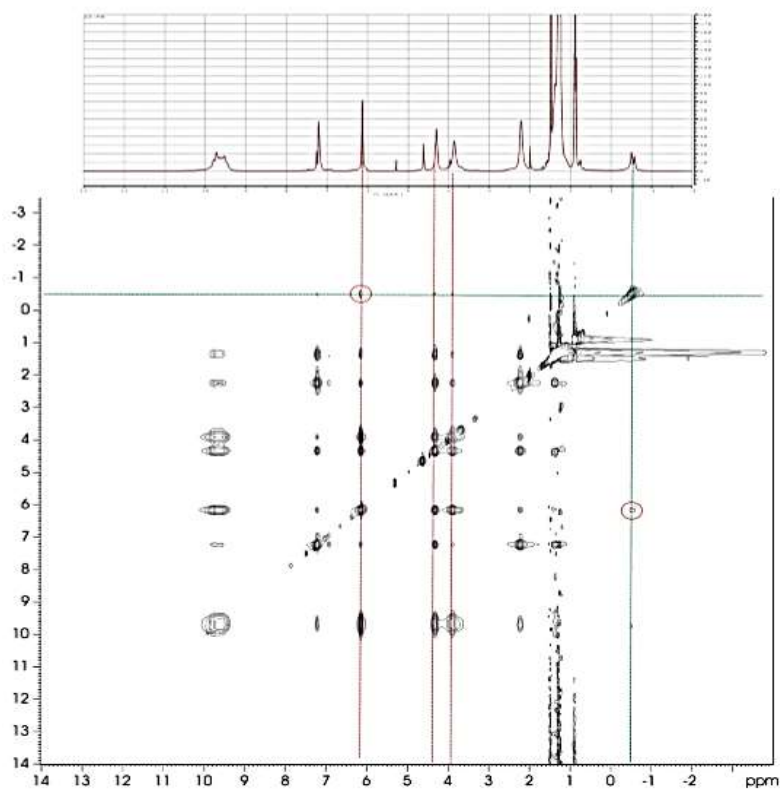


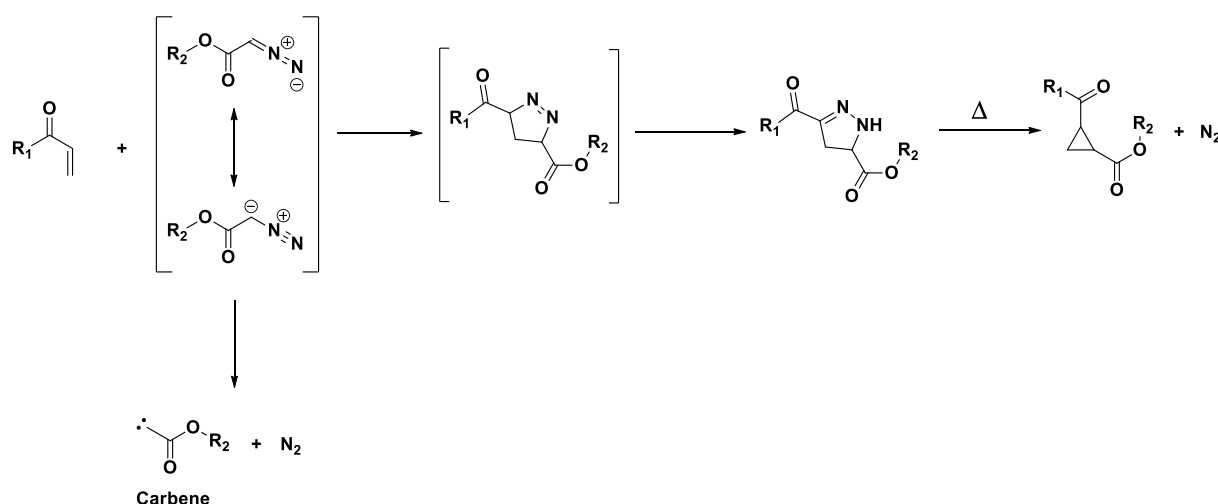
Figure 18. NOESY experiment of *t*-BD with the capsule in water saturated CDCl₃.

3.2.1.6. Dipolar cycloaddition reaction between diazoacetate esters and electron-poor alkenes mediated by the resorcin[4]arene capsule

Bimolecular reactions such as cycloadditions and in particular Diels–Alder reactions are among the most investigated chemical transformations in order to study the effects of supramolecular nanoreactors. In fact, cycloaddition reactions have been extensively investigated in both water and organic solvents in the presence of different unimolecular or self-assembled supramolecular hosts such as cyclodextrins,⁸⁷ cavitands and capsules.⁸⁸ Moreover, diazoacetate compounds are efficient substrates in the 1,3-dipolar cycloaddition reactions with a large series of dipolarophiles.⁸⁹ This reaction is spontaneous at very high concentration or it can be catalyzed by Lewis acids and bases as well as by Brønsted acids causing the initial formation of 4,5-dihydro-3*H*-pyrazoles that are unstable intermediates and tautomerize to the corresponding 4,5-dihydro-1*H*-pyrazole isomers.⁹⁰ The nature of the alkene employed can change the stability of these products and cause their spontaneous decomposition with dinitrogen loss, leading to the formation of the corresponding cyclopropyl derivatives (Scheme 4); similar results can be promoted using acids or bases.⁹¹ Stable 4,5-dihydro-1*H*-pyrazoles are formed from ethyl diazoacetate with α,β -unsaturated

aldehydes in the presence of acid catalyst⁹² or with other electron-deficient alkenes with metal Lewis acids.⁹³ Another way to synthesize the heterocyclic products consists in carrying out the reaction under Baylis-Hillman conditions with Lewis acid and/or Lewis base capable to catalyse [3+2] cycloaddition reactions.⁹⁴ The enantioselective version of the cycloaddition reaction of diazoacetate esters to electron-poor alkenes was described in the presence of α,β -unsaturated acrolein derivatives.⁹⁵

In order to study the catalytic effects of the capsule in the cycloaddition reactions, we investigated the reaction between diazoacetates with unsaturated aldehydes and acrylates used as electron-poor alkenes. The interaction of acrolein (**Ac**) and methyl acrylate (**MA**) with the capsule was investigated for possible-encapsulation. As expected, these compounds showed no effects of encapsulation on the resonances in the ¹H-NMR spectrum, even in the absence of **ED**.



Scheme 4. 1,3-Dipolar cycloaddition reaction between diazoacetate esters and electron-poor alkenes to form 4,5-dihydro-3H-pyrazoles that undergo through tautomerization to corresponding 4,5-dihydro-1H-pyrazoles. In some cases these products lead to loss of nitrogen molecules generating the corresponding cyclopropyl derivatives.

Initially the reaction of **Ac** and **ED** was tested at room temperature in CDCl₃ (Table 5, entries 1-4) achieving only 12% yield of 4,5-dihydro-1H-pyrazole **P_{AcED}** after 20 hours. When the reaction was carried out in the presence of the capsule, the yield reached 47%, emphasizing the catalytic effect of resorcin[4]arene. In order to demonstrate that the reaction was catalyzed only within the cavity, a large excess (10 equivalents with respect to the hexamer) of tetraethylammonium tetrafluoroborate (**TEA**) was introduced as competitive guest. Under these conditions the reaction conversion markedly decreased and only 8% yield of **P_{AcED}** was observed. Reducing the amount of **TEA** in the solution to 5 equivalents, no evident increase in the conversion

was observed achieving 10% yield. However a further reduction of the **TEA** amount in solution to 1 equivalent with respect to the capsule led to 28% yield of **P_{AcED}**, showing that the partially empty cavity is still able to provide a moderate catalytic effect.

Subsequently the reaction with **Ac** was studied in the presence of other diazoacetate esters such as ***t*-BD** and **BD**. Even with these substrates the presence of the empty capsule allowed to obtain high conversions, achieving 97% yield in the case of ***t*-BD** and 54% with **BD** (Table 5, entries 6, 10). The higher conversions obtained in the presence of ***t*-BD** as substrate were probably due to the good affinity with the cavity by CH- π interactions. Notably, in the presence of **TEA** without the capsule all diazoacetate esters **ED**, ***t*-BD** and **BD** led to the formation of the corresponding product in 32, 40 and 20% yield respectively, indicating that the 1,3-dipolar cycloaddition reaction was actually catalyzed by the presence of ammonium salts. This observation was in agreement with other studies describing the catalytic effect of imidazolium-based ionic liquids⁹⁶ in the Diels-Alder reaction between cyclopentadiene and electron-poor alkenes. In ref. 96 the activation of the reaction was attributed to the interactions between the dienophile and the imidazolium moiety. The lower catalytic activity of the capsule filled with **TEA** (Table 5, entries 3, 7, 11) could be explained by considering the interactions between ammonium and substrate molecules. In fact the encapsulation within the cavity severely limited the contact of the ammonium with substrate molecules while the external **TEA** molecules interact with the external surface of the supramolecular hexamer.

In order to exclude a possible catalytic effect due to interactions between the hydroxyl groups of the capsule and the substrate molecules, the reactions were carried out in the presence of 24 equivalent of resorcinol with respect to the capsule under the same experimental conditions (Table 5, entries 4, 8, 12). In no case a catalytic effect of resorcinol was found, even if it is reported in the literature that this reaction is sensitive to H-bond. These data showed that the catalytic effect of the resorcin[4]arene capsule was mainly due to the availability of a supramolecular cavity capable to interact with the substrate molecules.

#	Diazoacetate	Capsule	TEA	Product	Yield ^a (%)
1	ED	-	-	P _{AcED}	12
2	ED	+	-	P _{AcED}	47
3	ED	+	+	P _{AcED}	8
4 ^b	ED	-	-	P _{AcED}	12
5	<i>t</i> -BD	-	-	P _{Act-BD}	25
6	<i>t</i> -BD	+	-	P _{Act-BD}	97
7	<i>t</i> -BD	+	+	P _{Act-BD}	6
8 ^b	<i>t</i> -BD	-	-	P _{Act-BD}	30
9	BD	-	-	P _{AcBD}	18
10	BD	+	-	P _{AcBD}	54
11	BD	+	+	P _{AcBD}	5
12 ^b	BD	-	-	P _{AcBD}	29

Table 5. Catalytic tests for the 1,3-dipolar cycloaddition of diazoacetate esters **ED**, ***t***-**BD** and **BD** with acrolein **Ac** mediated by the capsule and control experiments. Reaction conditions: [Resorcinarene] = 36 mM; [diazoacetate ester] = 60 mM; [**Ac**] = 60 mM; [**TEA**] = 60mM; water-saturated CDCl₃ (0.5 mL), T = Room Temperature; 20 h. + : Present; - : absent. a) Determined by integration of the signals 1H-NMR spectrum. b) [Resorcinol] = 144 mM (24 eq. with respect to resorcin[4]arene).

After proving the catalytic activity of the capsule in the presence acrolein **Ac**, we decided to extend the employment of this supramolecular system to reactions between diazoacetate esters and other kinds of dienophiles. For this purpose ***t***-**BD** as the most reactive diazoacetate was tested with acrylonitrile (**An**), *trans*-crotonaldehyde (**C4**), and *trans*-2-hexenal (**C6**) as electron-poor alkenes (Table 6). The reactions were carried out at 50°C because of the intrinsic lower reactivity of these alkenes. Under these conditions the reaction between **An** and ***t***-**BD** did not provide a significant catalytic effect of the supramolecular capsule. In fact just a 13% higher yield to the corresponding 4,5-dihydro-1*H*-pyrazole **P_{An-t-BD}** was obtained in the presence of the capsule after 20 hours (Table 6, entries 1,2). However, the reaction carried out in the presence of **TEA** as competitive guest for the capsule significantly slowed down the reaction (Table 6, entry 3). When the α,β -unsaturated aldehydes **C4** and **C6** reacted with ***t***-**BD**, the 1,3-dipolar cycloaddition was quite slower compared with that with **An** as all reactions required 48 h reaction time. With these substrates no conversion was observed without the capsule or in the presence of **TEA** as competitive guest (Table 6, entries

4,6 and 7,9), while when the capsule was in the reaction medium yields of 95 and 79% for the 4,5-dihydro-*IH*-pyrazoles **P_{C4t-BD}** and **P_{C6t-BD}** respectively were observed at 50°C.

Given the excellent results obtained with the α,β -unsaturated aldehydes we decided to study the catalytic activity of the capsule with acrylate esters such as methyl-acrylate (**MA**) and butyl-acrylate (**BA**). In the absence of the supramolecular structure the 1,3-dipolar cycloaddition product obtained with **MA** decomposed, while the capsule allowed to achieve the 4,5-dihydro-*IH*-pyrazole **P_{MAt-BD}** in 79% yield after 48h (Table 6, entry 11). Similar results were obtained with the longer acrylate **BA** but in this case the catalytic activity of the capsule was evidently lower and the expected product **P_{BAt-BD}** was obtained in only 18% yield after 48 h (Figure 19). The latter results clearly show an interesting preference for shorter substrates (substrate selectivity); in fact the higher yield achieved with shorter **MA** could not be attributed to electronic effects but was actually ascribable to better packing of such a smaller substrate. Since the space within the capsule is quite large, the substrate molecules were not so bulky to completely fill the cavity. Therefore we supposed that solvent molecules and substrates reside together within the cavity in order to occupy an amount of space as close as possible to 55% of the volume, accounting for a packing coefficient of 0.55, typical of most solvents.

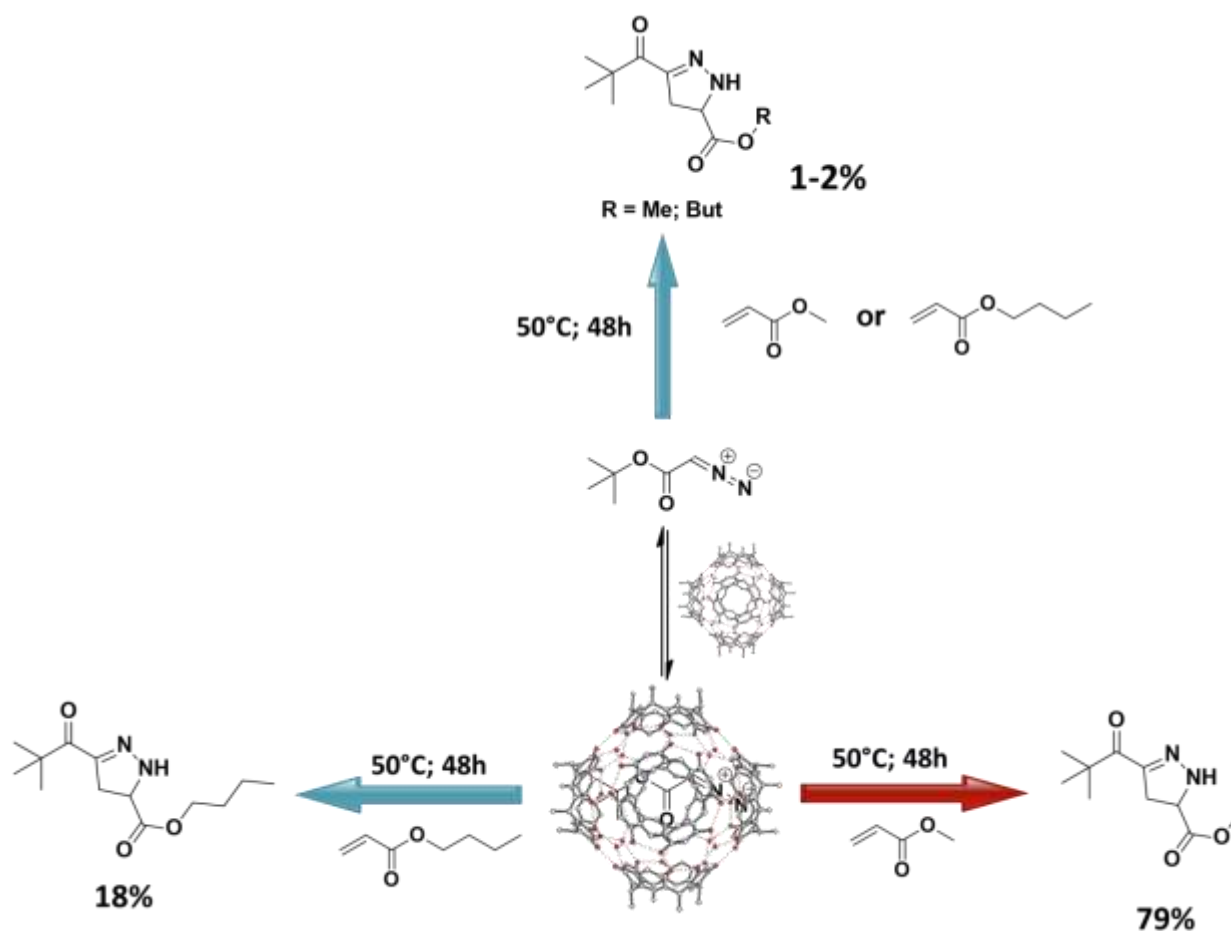


Figure 19. 1,3-Dipolar cycloaddition of *t*-BD with MA or BA catalyzed by supramolecular hexameric capsule and deriving substrate selectivity.

Finally, we decided to study the reactivity towards more activated alkenes. For this reason methyl propiolate (MP) was chosen as substrate, observing the formation of the corresponding 4,5-dihydro-1*H*-pyrazole product $P_{MP-t-BD}$ with 30% of yield in the absence of the capsule (Table 6, entry 16). Unfortunately the presence of the capsule did not cause an increase in reactivity and the reaction product was obtained with a lower yield (Table 6, entry 17). This indicated that the intrinsic high reactivity of this alkyne towards *t*-BD was even inhibited by the affinity of diazoacetate compounds for the hexameric capsule.

#	Alkene	t (h)	Capsule	TEA	Product	Yield ^a (%)
1	An	20	-	-	P_{An<i>t</i>-BD}	44
2	An	20	+	-	P_{An<i>t</i>-BD}	58
3	An	20	+	+	P_{An<i>t</i>-BD}	9
4	C4	48	-	-	P_{C4<i>t</i>-BD}	0 ^b
5	C4	48	+	-	P_{C4<i>t</i>-BD}	95
6	C4	48	+	+	P_{C4<i>t</i>-BD}	0
7	C6	48	-	-	P_{C6<i>t</i>-BD}	0 ^b
8	C6	48	+	-	P_{C6<i>t</i>-BD}	79
9	C6	48	+	+	P_{C6<i>t</i>-BD}	0
10	MA	48	-	-	P_{MA<i>t</i>-BD}	1 ^b
11	MA	48	+	-	P_{MA<i>t</i>-BD}	79
12	MA	48	+	+	P_{MA<i>t</i>-BD}	0
13	BA	48	-	-	P_{BA<i>t</i>-BD}	2 ^b
14	BA	48	+	-	P_{BA<i>t</i>-BD}	18
15	BA	48	+	+	P_{BA<i>t</i>-BD}	5
16	MP	20	-	-	P_{MP<i>t</i>-BD}	30
17	MP	20	+	-	P_{MP<i>t</i>-BD}	22

Table 6. Catalytic tests for the 1,3-dipolar cycloaddition of diazoacetate ester *t*-BD with a series of electron-poor alkenes mediated by the resorcin[4]arene capsule and control experiments. Experimental Conditions: [Resorcinarene] = 36 mM; [*t*-BD] = 60 mM; [Alkene] = 60 mM; [TEA] = 60 mM; water-saturated CDCl₃ (0.5 mL); T = 50°C. + : present; - : absent. a) Determined by integration of the signals in the ¹H-NMR spectrum. b) Decomposition products were detected, but the formation of the desired 4,5-dihydro-1H-pyrazole was not observed.

3.2.1.7. Conclusions

In conclusion we described the property of the hexameric capsule to host neutral non-hydrogen bonding substrates such as isocyanides and diazoacetate esters due to the particular electronic properties of these organic compounds.

In the case of the isocyanides the capsule caused their conversion into the corresponding N-formylamides in the presence of water under mild experimental conditions. Notably the interaction

with isocyanides was not attributable solely to the acidity of the capsule, but the presence of a cavity with electron-rich aromatic surface proved necessary to stabilize the isocyanide addition intermediates and, thus, to obtain high conversions. In order to show a further confirmation of this assumption, TMSN_3 was introduced in the reaction mixture as competitive substrate for the water molecules. In the presence of this compound the hexameric capsule showed capable to catalyse its chemo-selective cycloaddition to several isocyanides causing the formation of the corresponding *IH*-tetrazoles. Therefore, by adjusting the reaction conditions and the amount of water in solution the capsule proved able to catalyze the addition of different nucleophiles to isocyanides with moderate substrate selectivity.

The particular electronic properties of diazoacetate esters were exploited to demonstrated the ability of the self-assembled resorcin[4]arene capsule to accommodate these organic compounds. The supramolecular system showed catalytic activity in 1,3-dipolar cycloaddition between the diazoacetate esters and electron-poor alkenes such as α,β -unsaturated aldehydes, acrylonitrile and acrylate esters when the reaction was carried out within the cavity. The weak interactions between the substrate molecules and the internal surface of the resorcin[4]arene capsule proved responsible for the observed catalytic effect.

3.2.2. Capsule and Dipolar Compounds

The six-months experience spent with Prof. Ballester research group at the Institut Català d'Investigació Química (ICIQ) in Tarragona was employed to investigate the interaction between resorcin[4]arene and N-oxides. This class of dipolar compounds has been extensively studied by the Ballester research group disclosing their employment as guest for supramolecular structures like cavitands.

3.2.2.1. N-oxides properties

The amine oxides (also known as amine-N-oxides or N-oxides) are chemical compounds obtained by oxidation of tertiary amines. In their structure three alkyl chains are attached to the N atom that is involved in an extremely polarized N–O bond that leads to a positive charge on the N atom and a negative charge on the O. In recent years the interest for these compounds has grown due to their possible uses as: (i) stoichiometric oxidants in synthetic processes;⁹⁷ (ii) ligands for

transition metal complexes;⁹⁸ (iii) Lewis base catalysts⁹⁹ also in the asymmetric version; (iv) guests for receptors like cavitands.¹⁰⁰

3.2.2.2. Interaction between N-oxides and the resorcin[4]arene capsule

The presence of a strongly polarized N-O bond provides a suitable hydrogen bond acceptor system that is likely to interact with the resorcin[4]arene hexameric capsule. In fact, the strongly negatively charged oxygen atom could interact with the hydroxyl groups of the resorcin[4]arene through H-bonding, while the positive charge on the N atom could develop π -cation interactions with the internal surfaces of the cavity within the capsule. In order to preliminarily study the capsule behaviour in the presence of N-oxides, a titration of the resorcin[4]arene hexamer (**Caps**) with different amounts of N-oxide was carried out by means of ¹H-NMR. We initially investigated the titration of the capsule with an N-oxide with a long alkyl chain such as N,N-dimethyldodecylamine N-oxide (**DDNO**) because its encapsulation could be easily observed because of the shielding effect by the inner surface of the capsule that caused intense signal shifts in the < 0 ppm region of the ¹H-NMR spectrum (Figure 20).

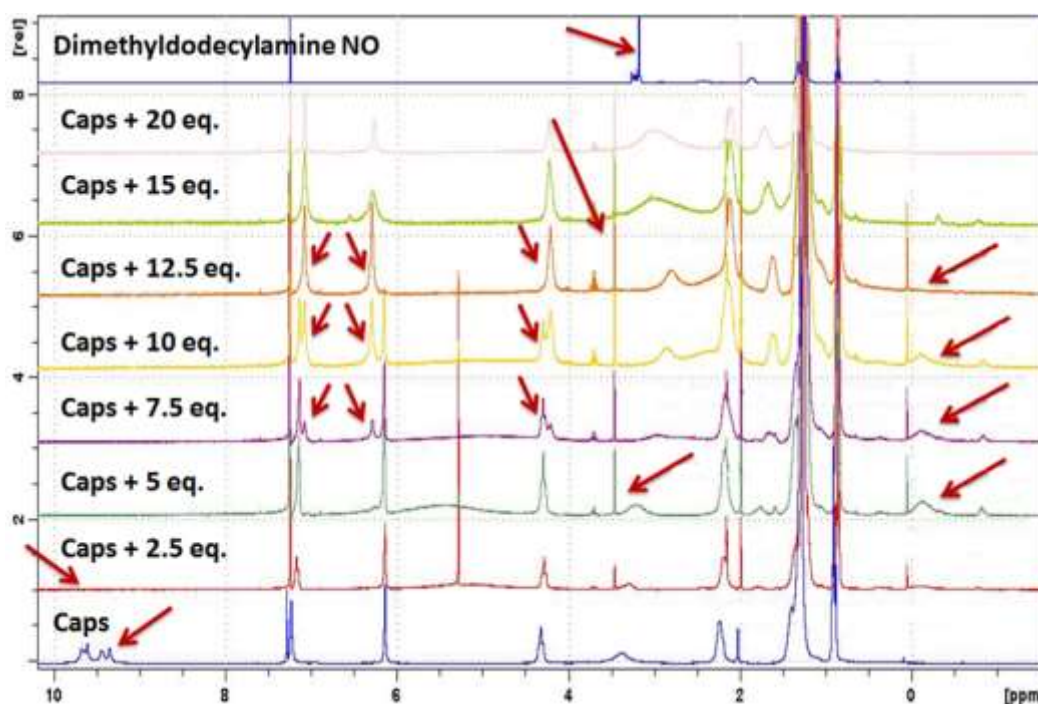
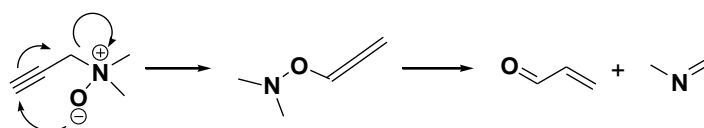


Figure 20. Titration of the resorcin[4]arene hexamer (**Caps**) with different amounts of dimethyldodecylamine N-oxide (NO)

The titration showed a strong interaction between the N-oxide and the resorcin[4]arene molecules. The shifting of the N-oxide methyl groups signal at 3.5 ppm and the disappearance of the hydroxyl

groups signals at 9.5 ppm even at low amounts of **DDNO** confirmed the formation of the H-bond between capsule and amine oxides. When the amount of N-oxide was increased up to 5 equivalents with respect to the capsule the appearance of broadened signals at -0.25 ppm proved the partial encapsulation of the **DDNO**. The observation of an host-guest complex between N-oxide and resorcin[4]arene was in agreement with what reported by Rissanen and co-workers while this investigation was in progress.¹⁰¹ Their study on the interactions between C₂-2-methylresorcinarene and pyridine N-oxide or quinolone N-oxide in the crystal state proved resorcinarenes as remarkable hosts for N-oxides that template the capsule formation by utilizing hydrogen bonding. A further increase beyond 7.5 equivalents of N-oxide amount in the solution caused a shift in the resorcin[4]arene signals at 6.2, 7.1 and 4.3 ppm, the signals of encapsulated species at -0.25 ppm slowly disappeared while the **DDNO** reappeared slightly shifted to lower magnetic fields. These results suggested that the N-oxide interacted with the surface of the capsule via hydrogen bonding with the OH of resorcin[4]arene causing the formation of new supramolecular species in equilibrium with the starting self-assembled hexamer. Therefore when the amount of **DDNO** exceeded 5 equivalents compared to the capsule it was sufficient to cause the disassembly of the capsule and the formation of new species in which the resorcin[4]arene and the amine oxide were linked through the H-bond between the OH groups and the N-oxide.

As an alternative N-oxide derivative, we investigated the titration of the capsule with N,N-dimethylprop-2-yn-1-amine oxide (**DPNO**). This particular compound bearing an alkyne moiety undergoes a thermal decomposition that causes an intramolecular rearrangement leading eventually to acrolein and the corresponding azomethine (Scheme 5). It was recently demonstrated that such substrate can be trapped within the cavity of an aryl-extended calix[4]pyrroles scaffold conferring kinetic stability to **DPNO**.¹⁰²



Scheme 5. Thermal decomposition of **DPNO** into acrolein and the corresponding Schiff base.

The study of the interaction between the **DPNO** and the hexameric capsule, as expected, showed a high increase in the N-oxide stability (Figure 21). We demonstrated that the cavity could bind the N-oxide group of **DPNO** via H-bonding increasing its stability and suppressing its

decomposition. In fact 4 days at room temperature were sufficient to cause an extensive **DPNO** decomposition, while in the presence of the capsule **DPNO** was stable even after 14 days and no decomposition products were observed (Figure 21). It was interesting to understand whether this stabilization was an effect of the capsule as a whole or was due to simple hydrogen bonding. To this end we found that the H-bond given by a simple resorcinol molecule was enough to make the **DPNO** stable as observed with the capsule (Figure 21). This experiment seems to suggest that H-bond to the O atom of the N-oxide is the key factor for stabilization rather the encapsulation of the whole molecule within the cavity of the capsule, as previously thought.¹⁰² However all these studies confirmed that the H-bond between N-oxide and hydroxyl groups of the capsule is a very strong interaction.

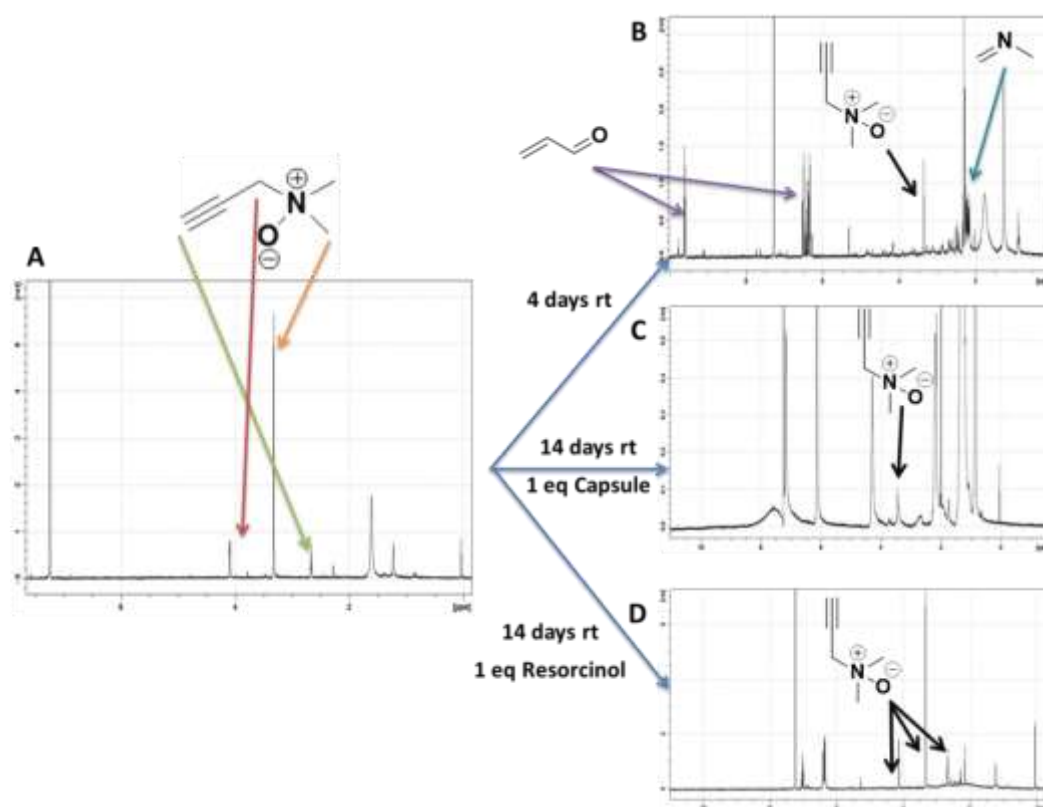


Figure 21. ¹H-NMR spectra of the **DPNO** (A) and its thermal decomposition reaction mixture B) after 4 days at room temperature; C) after 14 days at room temperature in the presence of 6 equivalents of resorcin[4]arene; D) after 14 days at room temperature in the presence of 1 equivalents of resorcinol

DOSY analyses (Figure 22) were carried out in the presence of the capsule either empty or occupied by tetraethyl ammonium bromide. This was done in order to verify if the **DPNO** could interact with the hydroxyl groups on the external surface of the self-assembled hexamer. Since the hexameric capsule and the N-oxide had very different size, the diffusion coefficients of the two

individual species were expected to be very different. Conversely, when the two species were present in the same system, the N-oxide should diffuse in the solution together with the capsule because of its interaction by H-bonding showing the same diffusion coefficient. Instead if the capsule was disassembled by the N-oxide, larger diffusion coefficients should be obtained. From the diffusion coefficients of the species it was possible to calculate the value of the hydrodynamic radius of the species, using the equation reported below.

$$R = \frac{K_b T}{6\pi\eta D}$$

K_b = Boltzman constant

T = temperature in K

η = viscosity

D = diffusion coefficient

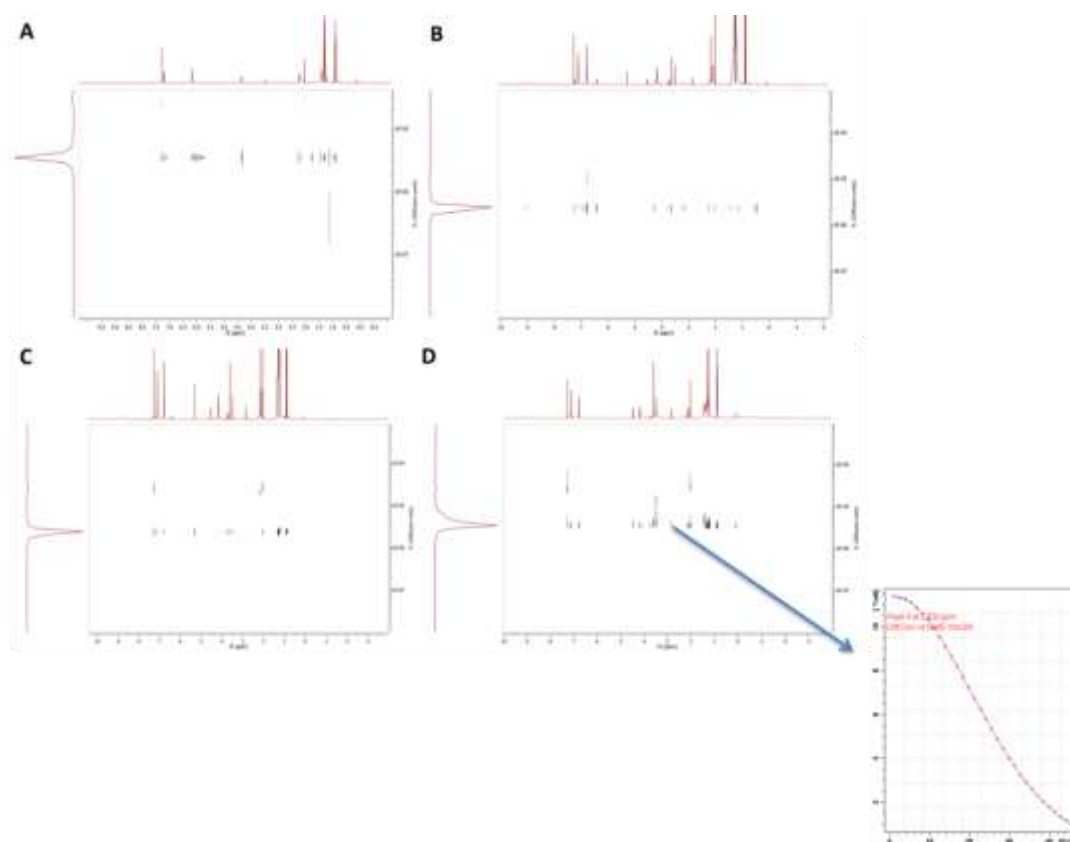


Figure 22. DOSY analyses of samples with 6 equivalents of resorcin[4]arene and A) 5 equivalents of DPNO ($D_{\text{resorcin[4]arene}} = 2.7 \cdot 10^{-10} \text{ m}^2/\text{s}$); B) 1 equivalent DPNO and 10 equivalents of tetraethyl ammonium bromide ($D_{\text{resorcin[4]arene}} = 2.6 \cdot 10^{-10} \text{ m}^2/\text{s}$; $D_{\text{DPNO}} = 2.5 \cdot 10^{-10} \text{ m}^2/\text{s}$); C) 2.5 equivalents DPNO and 10 equivalents of tetraethyl ammonium bromide ($D_{\text{resorcin[4]arene}} = 2.6 \cdot 10^{-10} \text{ m}^2/\text{s}$; $D_{\text{DPNO}} = 2.5 \cdot 10^{-10} \text{ m}^2/\text{s}$); D) 5 equivalents DPNO and 10 equivalents of tetraethyl ammonium bromide ($D_{\text{resorcin[4]arene}} = 3.5 \cdot 10^{-10} \text{ m}^2/\text{s}$; $D_{\text{DPNO}} = 4.1 \cdot 10^{-10} \text{ m}^2/\text{s}$)

The DOSY analysis of a solution with 5 equivalents of **DPNO** and 6 equivalent of resorcin[4]arene (1 equivalent of capsule) confirmed that the capsule remains intact under these experimental conditions, observing a diffusion coefficient of $2.7 \cdot 10^{-10} \text{ m}^2/\text{s}$ and a hydrodynamic radius of about 14.9 Å. Both these values were very similar to those known for the resorcin[4]arene hexamer¹⁰³ proving that an excess of **DPNO** can interact by H-bonding with the capsule without disassembling the supramolecular structure. Moreover, the shift of the **DPNO** signals and the disappearance of the resorcin[4]arene signals at 9.5 ppm confirmed that the N-oxide group of **DPNO** interacted with the hydroxyl groups in the capsule surface. This allowed to observe that **DPNO** in the presence of the empty capsule behaves like **DDNO** remaining attached to the resorcin[4]arene in equilibrium between the inside and the outside of the capsule. When tetraethyl ammonium bromide was added as a competitive guest different results were observed. In this case when the N-oxide amount remained below 2.5 equivalents with respect to the capsule, the same diffusion coefficient for the signals of both species was observed ($2.5 \cdot 10^{-10} \text{ m}^2/\text{s}$) confirming the integrity of the capsule. Unluckily a further increase of the amount of **DPNO** in solution led to the disassembly of the capsule and the formation of new smaller resorcin[4]arene-**DPNO** supramolecular adducts. In fact, in the presence of 5 equivalents of N-oxide a drastic change of the diffusion coefficient for both the resorcin[4]arene resonances ($3.5 \cdot 10^{-10} \text{ m}^2/\text{s}$, hydrodynamic radius = 11.5 Å) and **DPNO** ($4.1 \cdot 10^{-10} \text{ m}^2/\text{s}$, hydrodynamic radius = 9.6 Å) was observed. It can be assumed that these values were the result of an average of the diffusion coefficients of different adducts rapidly exchanging in solution. In fact the divergence of diffusion coefficient values of the two species could be attributed to a fast equilibrium between their free form and an unidentified number of possible adducts.

Therefore, when the amount of N-oxide is not high enough to cause the hexamer disassembly, the interaction between **DPNO** and capsule may be explained as in Figure 23. Indeed the H-bond between N-oxide and the hydroxyl groups caused a strong binding of the **DPNO** to the capsule surface. When the capsule was empty, the N-oxide was free to reside outside or inside of the capsule although the lower steric hindrance and the π -cation interaction that involved the positive charge of the nitrogen atom would mostly promote encapsulation inside the cavity. Instead the presence of tetraethylammonium as competitive guest prevented the N-oxide from entering the cavity forcing the **DPNO** to remain attached on the outer surface of the capsule (Figure 23). Obviously the presence of small **DPNO** on the outer surface of the capsule did not influence the diffusion coefficient due to the large difference in size between the partners.

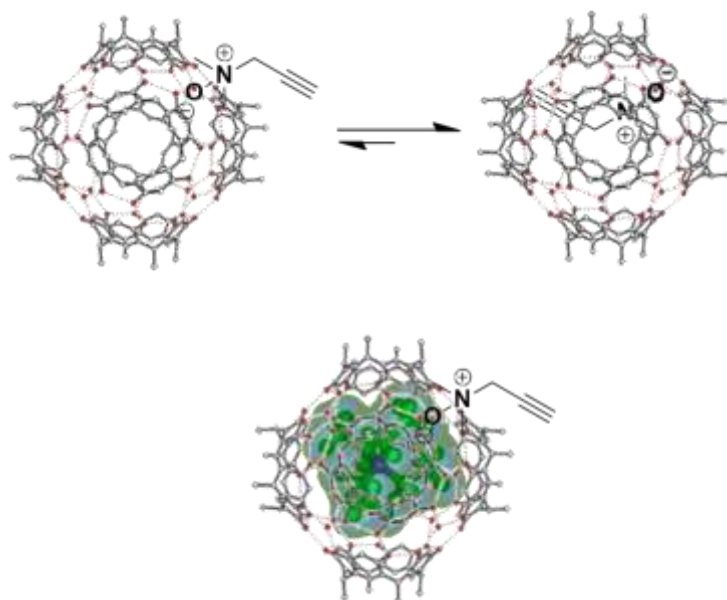


Figure 23. Interaction between DPNO and resorcin[4]arene hexamer when the capsule is empty (on the top) or filled (below).

3.2.2.3. Reaction between N-oxides and isocyanates

On the basis of the strong interactions observed between resorcin[4]arene and N-oxide and considering the numerous examples of reactions catalysed by the capsule we wondered whether similar supramolecular effects imparted by the capsule could be exploited in reactions involving N-oxides as substrates. With this in mind we tested a reaction between N-oxides as nucleophiles with isocyanates as electrophiles. Only very few examples of this interaction were found in the literature. In 1962 Monagle studying the catalytic properties of phosphine and arsine oxides in the synthesis of carbodiimides from isocyanates, speculated that amine oxides could lead to the same products.¹⁰⁴ In 1997 Coşkun reported the first examples of 1,3-dipolar cycloaddition of imidazoline N-oxides to isocyanates whose first step is the nucleophilic attack of the negatively charged oxygen atom of the N-oxide on the carbon atom of the isocyanate group.¹⁰⁵ More recently Chain and co-workers exploited the interaction between phenyl isocyanate and N,N-dimethylaniline-N-oxide to introduce a new C-N bond on the aromatic ring of the N-oxide by a structural rearrangement that causes a temporary increase in the oxidation level of N,N-dialkylanilines to N,N-dialkylaniline N-oxides and the excision of the weak N-O bond.¹⁰⁶

Initially p-methoxyphenyl isocyanate was used as substrate and its reactivity was tested in the presence of 1 equivalent of several N-oxides such as trimethylamine N-oxide (**TMNO**), dimethyldodecylamine N-oxide (**DDNO**) and N-methyl morpholine N-oxide (**MMNO**). The

reactions were carried out in CDCl_3 at room temperature with 27 mM substrates for 1 night monitoring the reaction by ^1H NMR (Figure 24).

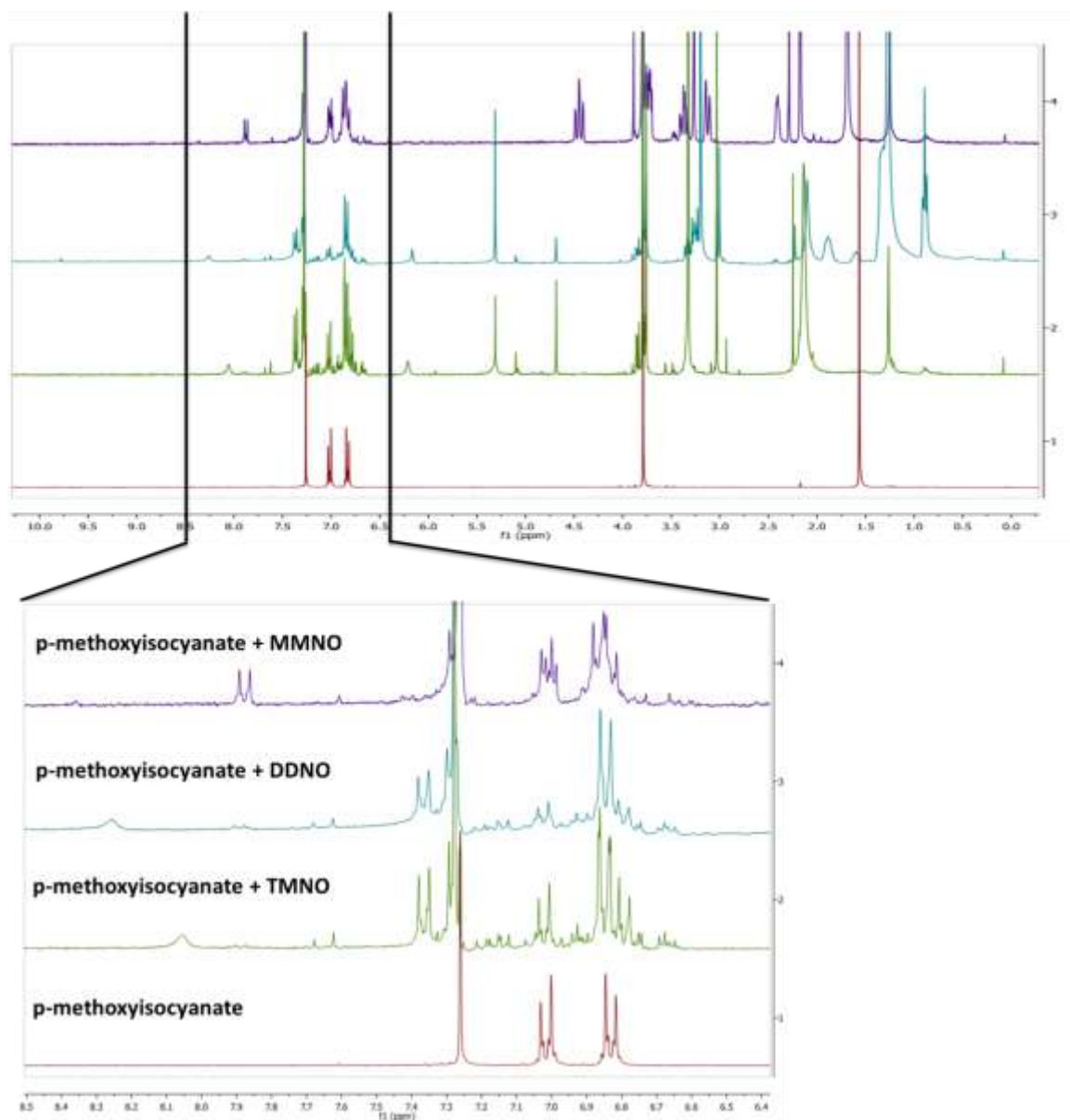
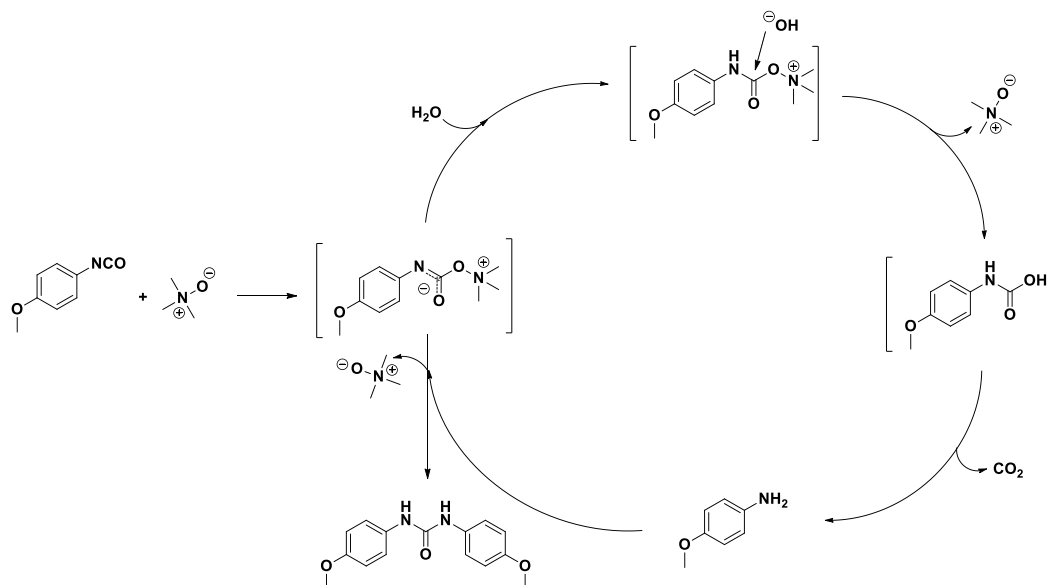


Figure 24. ^1H NMR analyzes in CDCl_3 of the N-oxides reactions with p-methoxyphenyl isocyanate. Reaction conditions: [Substrates] = 27mM; CDCl_3 = 1,5 mL; T = 25°C; t = 18 h.

Contrary to what reported in the literature the chemical shifts of the obtained ^1H -NMR analyses showed that the 1,3-di(p-methoxyphenyl)carbodiimide could not be the main product of the reaction. In fact the chemical shift values reported for the corresponding carbodiimide¹⁰⁷ did not match with those obtained. A careful inspection of the spectra led us to conclude that the main

product was actually p-methoxy-phenyl urea. The formation of this product was probably due to the interaction of the N-oxide as a Lewis base on the isocyanate moiety forming an activated species highly reactive towards the nucleophilic attack by traces of water present in the system. This caused the formation of the corresponding unstable phenylcarbamic acid that rapidly decomposed to p-methoxyaniline¹⁰⁸ that immediately attacked a second isocyanate molecule leading eventually to the symmetric aromatic urea derivative (Scheme 6).



Scheme 6. Hypothetic mechanism of the reaction between **TMNO** and p-methoxyphenyl isocyanate leading to the formation of p-methoxy-phenyl urea

As a control experiment, the reaction between one equivalent of p-methoxyphenyl isocyanate and one equivalent of p-methoxy aniline was carried out at room temperature in CDCl_3 comparing the results to those obtained with both substrates in the presence of 1 equivalent of **MMNO** in order to verify the possible catalytic effect imparted by the latter species. The presence of the N-oxide considerably increased the reaction rate providing quantitative conversion of the substrates within few minutes while the un-catalysed reaction required more than an hour to get to completion.

It was worth noting that, differently from all the other N-oxides tested, **MMNO** led to the formation of a secondary product in significant amount (Figure 24). By means of GC-MS analysis and literature data on $^1\text{H-NMR}$ chemical shifts, the new product was identified as p-methoxy azobenzene. Initially the formation of this compound was puzzling. The only reported azo compound obtained in the presence of **MMNO** and a chemical species present in our reaction mixture required the presence of CuBr as catalyst for the oxidative coupling of anilines.¹⁰⁹ In order to better quantify the amount of isocyanate converted to the azo-compound and to the related urea

derivative, the reaction was repeated and the analysis was carried out in $\text{dms}\text{-d}_6$ to ensure good solubility of all species. When the reaction was carried out for 18 hours at 60°C , complete conversion of the isocyanate substrate was observed together with the formation of 40% *bis*(4-methoxyphenyl)diazene derivative, 54% urea derivative and 6% *p*-methoxyaniline (Figure 25).

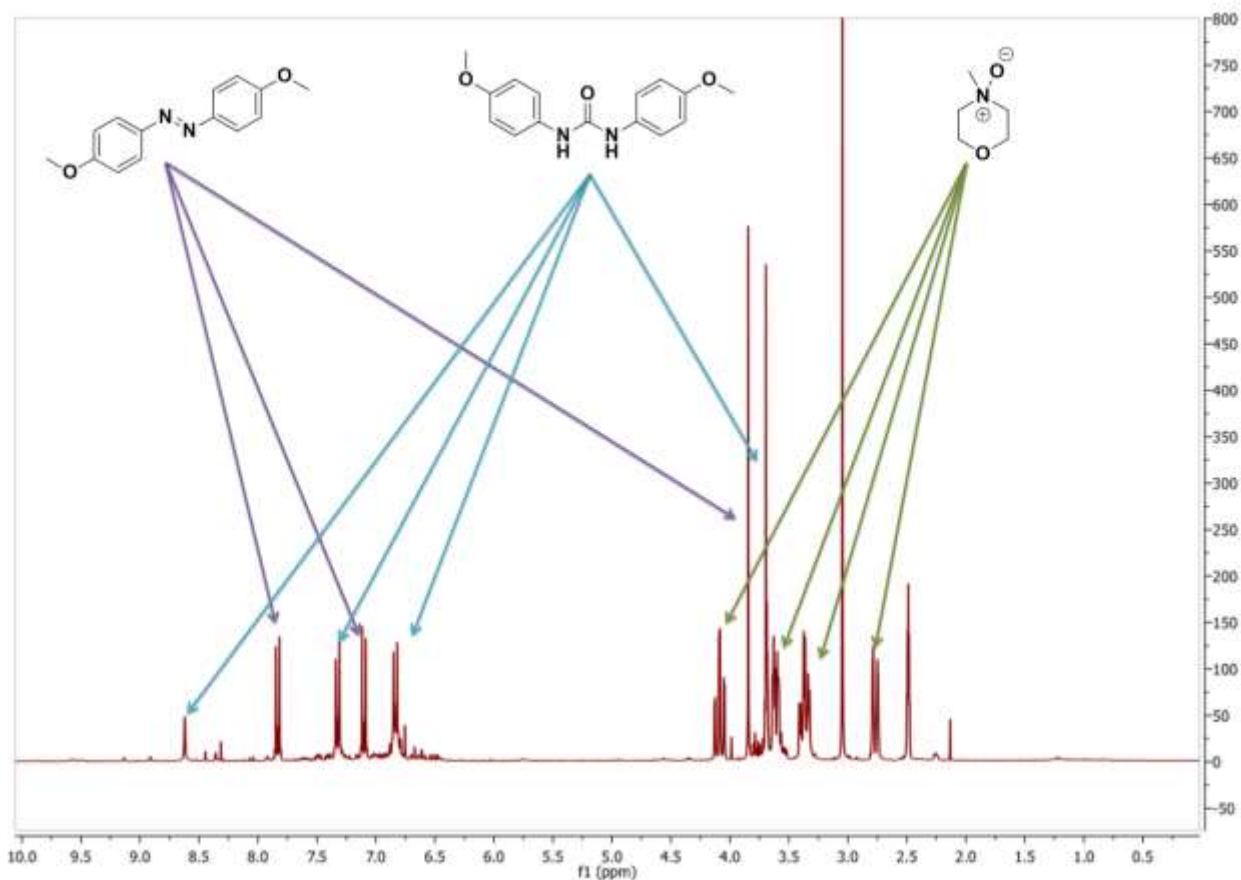


Figure 25. ^1H -NMR spectrum in $\text{dms}\text{-d}_6$ of the reaction between MMNO and *p*-methoxyphenyl isocyanate carried out in CDCl_3 at 60°C with 27 mM substrates for 18h.

The unexpected formation of the azo-compound spurred the study of the reaction of **MMNO** in the presence of several aromatic isocyanates characterized by different electronic properties. Substrates bearing electron-donating groups like *p*-tolyl isocyanate and *p*-dimethylaminophenyl isocyanate or electron-withdrawing groups as in the cases of *p*-nitrophenyl isocyanate and *p*-acetylphenyl isocyanate were investigated. The last two substrates turned out to be poorly soluble in chloroform and, because of this, the substrate concentration was decreased to 2.7 mM to ensure the presence of a homogeneous solution. Indeed *p*-nitrophenyl isocyanate showed much lower solubility and for this reason it was not further investigated. In Figure 26 are reported the ^1H -NMR spectra in $\text{dms}\text{-d}_6$ of the reactions between **MMNO** and differently substituted phenyl isocyanates highlighting the products present in solution. In order to observe the different phenylisocyanate

derivatives behaviour under identical conditions, the reactions were carried out at 60°C with a substrate concentration value lowered to 2.7 mM as required in the case of *p*-acetylphenyl isocyanate.

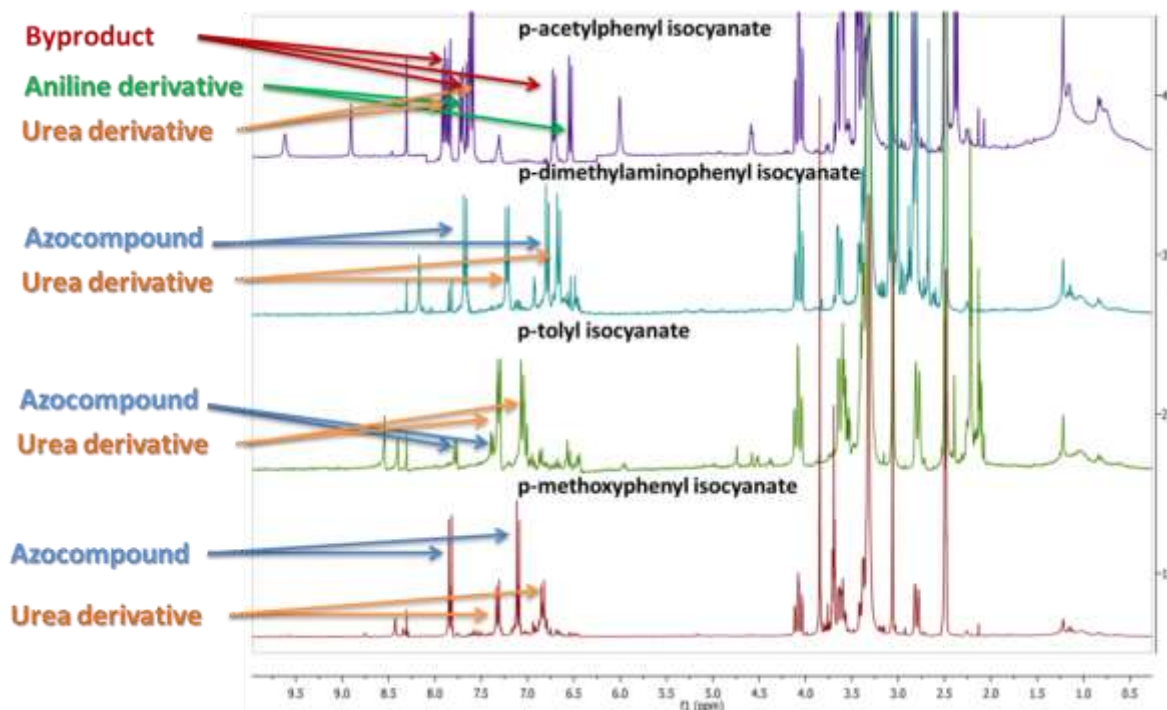


Figure 26. $^1\text{H-NMR}$ spectrum in $\text{dms}\text{-d}_6$ of the reaction between **MMNO** and differently substituted phenyl isocyanates carried out in CDCl_3 at 60°C with 2.7 mM substrates for 18h.

The data collected by $^1\text{H-NMR}$ analysis of the reactions between **MMNO** and differently substituted isocyanates (Table 7) lead to two important observations. First at all a completely different product-selectivity was obtained depending on the electronic nature of the substituents of the aromatic moieties. The conversion of isocyanates to azo-compounds was favoured by the electron donor character of substituent groups on the aromatic ring. Conversely the presence of electron withdrawing groups caused the formation of completely different unidentified by-products in large amount. These by-products were obtained by a reaction mechanism different from that under investigation and their instability hampered their identification. Therefore their characterization was impracticable for us.

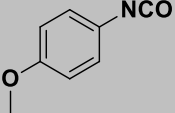
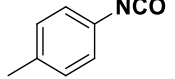
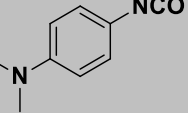
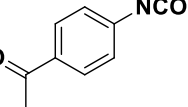
Phenyl Isocyanate	Urea (%)	Azo-compound (%)	Aniline (%)	By-products (%)
	32	62	6	<1
	70	13	17	<1
	43	44	13	<1
	22	-	49	41

Table 7. Product distribution of the reactions between MMNO and differently substituted isocyanates determined by $^1\text{H-NMR}$ in $\text{dms-}d_6$. Reaction conditions: [Substrate] = 2.7 mM; CDCl_3 1.5 mL; $T = 60^\circ\text{C}$; $t = 18\text{h}$; Conversion $\geq 98\%$.

Moreover comparing the results obtained with p-methoxyphenyl isocyanate in the 27 mM and in 2.7 mM reactions an increase in the *bis*(4-methoxyphenyl)diazene yield could be observed. In fact the azo-compound amount corresponded to 40% at the end of the reaction carried out under high concentration conditions, whereas it reached 62% when the isocyanate initial concentration value was 2.7 mM. This unusual phenomenon could be attributed to a slowdown in the rate of the urea derivative formation. In fact lowering the substrate concentration decreases the concentration of the activated intermediate obtained from the interaction of isocyanate and **MMNO**. Since the activated intermediate was involved in a bimolecular reaction with water, a lowering of its concentration caused a slowing down of the reaction rate that led to the urea derivative, favouring the formation of the azocompound. As the diazene synthesis was promoted by the slowdown of a bimolecular reaction we should suppose that this reaction was unimolecular. For this reason the activated intermediate unimolecular decomposition to nitrene has been hypothesized in the case of isocyanate substituted with electron-donor groups to explain the diazene derivative synthesis. Indeed it is well known that the nitrenes are molecular species with a monovalent neutral electron-deficient nitrogen atom that dimerize forming the azo species.¹¹⁰

The reaction of p-methoxyphenyl isocyanate (27 mM) was repeated at 60°C under nitrogen atmosphere using chloroform-d stored under molecular sieves to minimize the presence of water and verify its negative effect on the formation of the azo compound due to consumption of a common intermediate species. Under these conditions the reaction gave a product distribution very

similar to that obtained with concentration value of 2.7 mM (azo compound 60%; urea derivative 35%; *p*-methoxy aniline 5%) confirming the original assumption. Subsequently, the 2.7 mM reaction was followed over time (Figure 27) in order to monitor better the formation of the various species and possibly get more insight the mechanism of azobenzene formation and N-oxide consumption.

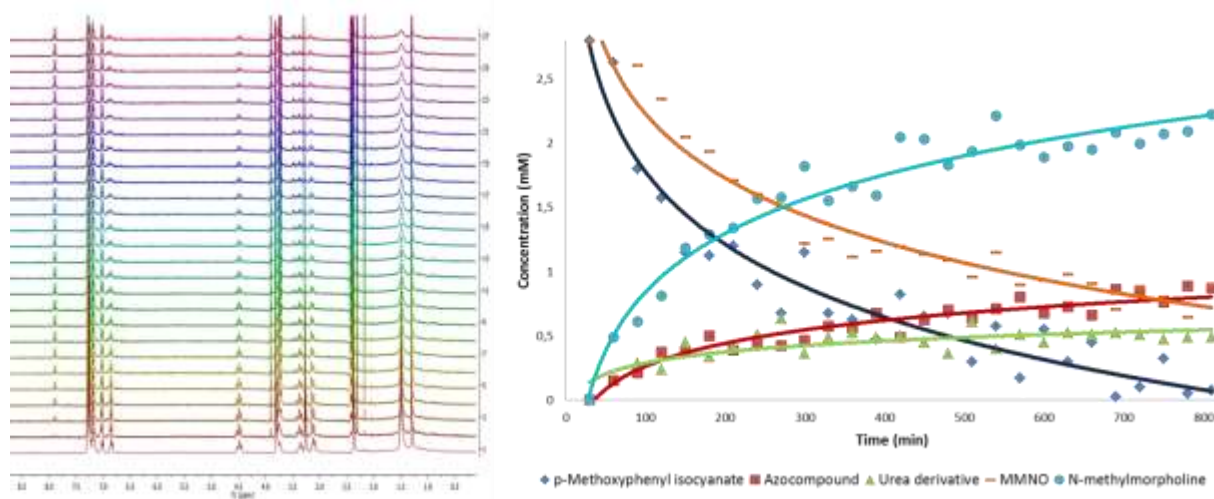


Figure 27. ¹H-NMR spectra (on the left) and variation in the concentration of the species in solution over time (on the right).
[Substrate] = 2.7 mM; CDCl₃ 1.5 mL; T = 60°C.

The variations in the concentrations of the species in solution clearly showed the correlation between the formation of the azobenzene derivative and the **MMNO** conversion to the relative tertiary amine N-methyl-morpholine. In fact the profile of concentration of the species confirmed a consumption of two **MMNO** molecules for each molecule of bis(4-methoxyphenyl)diazene formed.

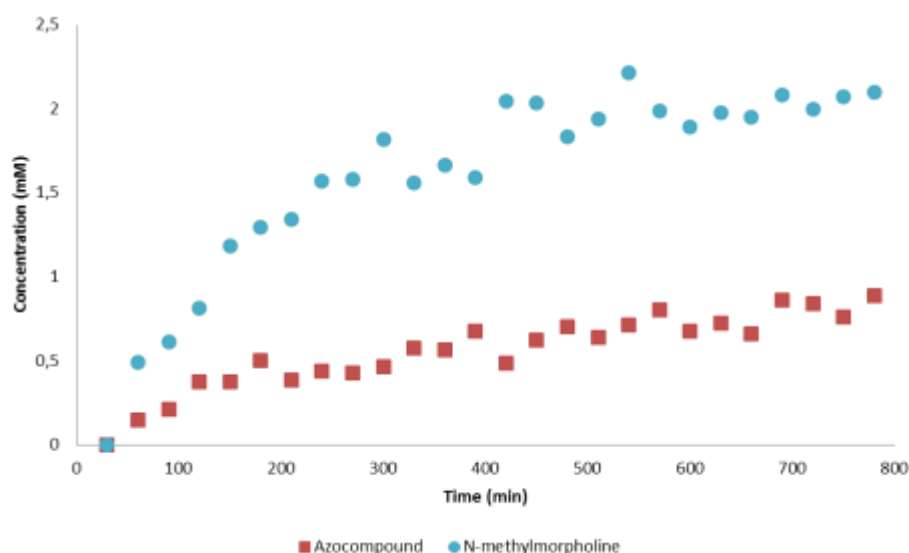


Figure 28. Profile of concentration of azo-compound and N-methyl-morpholine in solution over time.

This observation seemed to confirm that the urea derivatives formation was simply due to the Lewis base behaviour of the N-oxides while the azobenzene derivatives formed according to another reaction mechanism. In order to get support to this hypothesis, the reaction between *p*-methoxyphenyl isocyanate and **MMNO** was carried out changing the stoichiometric ratio of the two species and introducing an excess of isocyanate (Table 8).

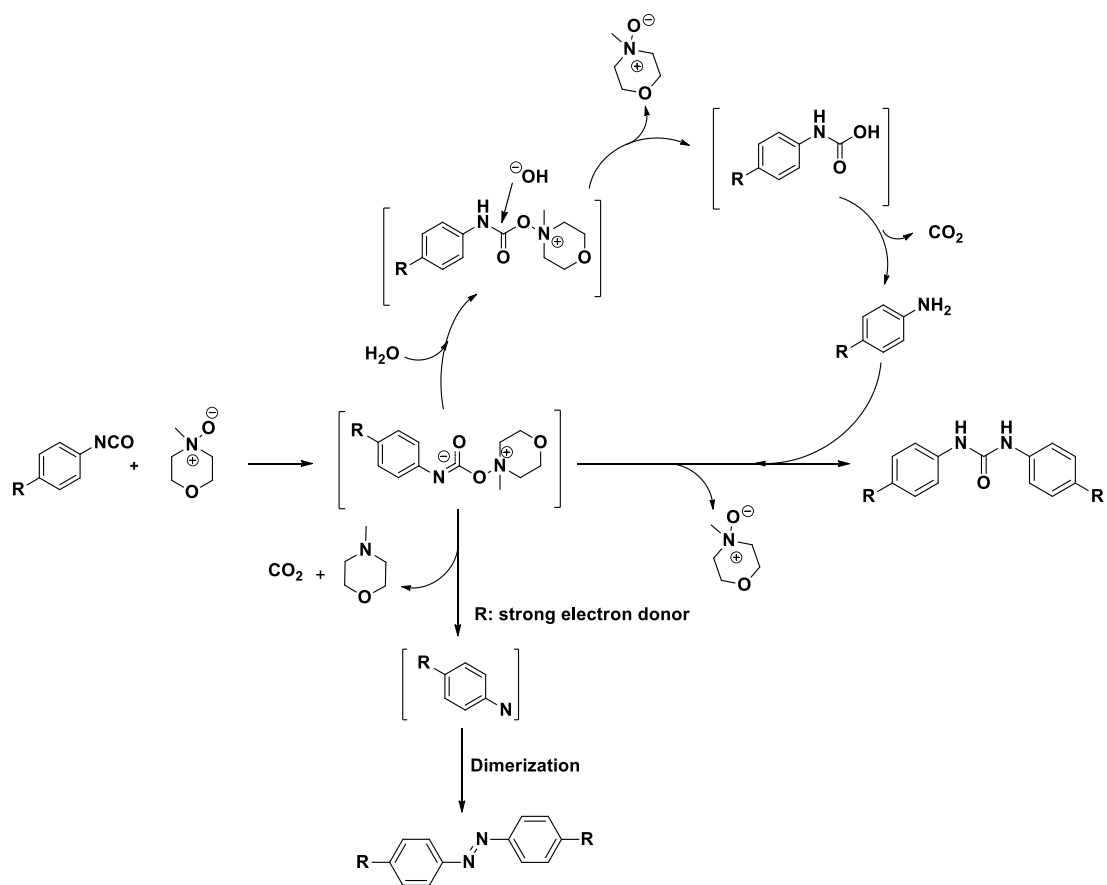
Isocyanate/MMNO	Isocyanate (%)	Urea (%)	Aniline (%)	Azobenzene (%)
1/1	0	54	6	40
2/1	0	68	1	30
4/1	0	70	3	27
6/1	12	76	3	9
8/1	15	76	2	7

Table 8. Reaction between **MMNO** and different amounts of *p*-methoxyphenyl isocyanate analyzed by $^1\text{H-NMR}$ in dmsO-d_6 .

[**MMNO**] = 27 mM; CDCl_3 = 1.5 mL; T = 60°C; t = 18h.

The data reported in Table 2 show no direct correlation between the *p*-methoxyphenyl isocyanate consumed and the **MMNO** to form the urea derivative. In fact, higher conversions and higher selectivities to the urea derivative were obtained when the amount of isocyanate was 8 times that of the N-oxide. Moreover it is possible to observe that upon increasing the isocyanate/**MMNO** ratio the azobenzene yield decreased due to the lower amount of N-oxide available.

All the experimental observations allowed to draw a possible reaction mechanism as outlined below in Scheme 7.



Scheme 7. Mechanism of the reaction between **MMNO** and p-methoxyphenyl isocyanate.

3.2.2.4. Effect of the hexameric capsule in the reaction between N-methylmorpholine and p-methoxyphenyl isocyanate

The innovative reaction between **MMNO** and phenylisocyanates with strongly electron-donating groups was chosen to study the effects of the resorcin[4]arene supramolecular hexamer on the product selectivity in reactions of amine oxides. Unfortunately p-(dimethylamino)phenyl isocyanate holds a substituent group that can be easily protonated forming the corresponding ammonium species which is a possible competitive guest for the cavity of the capsule. Therefore, only p-methoxyphenyl isocyanate was chosen as a reference substrate for the study.

Initially it was necessary to study the interaction between **MMNO** and capsule as done for the other N-oxides. For this purpose were carried out titration of both a 4.5 mM solution containing

only the capsule and the same solution in the presence of 10 equivalents of tetraethylammonium tetrafluoroborate (**TEA**) (Figure 29).

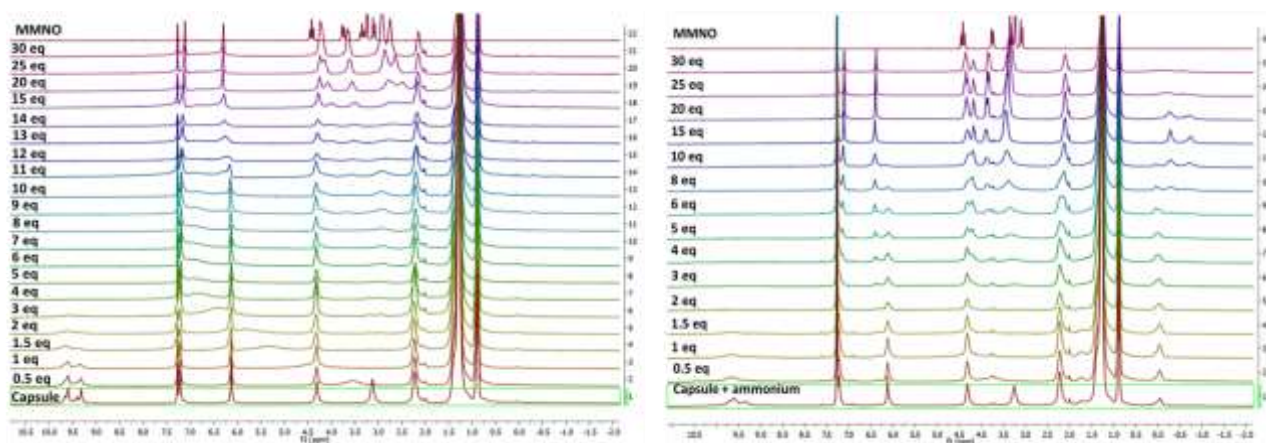


Figure 29. Titration of both the resorcin[4]arene hexamer (on the left) and the resorcin[4]arene hexamer with TEA (on the right) with different amounts of N-methylmorpholine N-oxide (MMNO).

The results observed during these titrations confirmed the data obtained in the presence of **DDNO**, **TMNO** and **DPNO**. In fact also in this case the $^1\text{H-NMR}$ spectra clearly showed the variations in the resonance signals of the capsule that were attributed to the interaction between N-oxide group and hydroxyl groups of the resorcin[4]arene molecules. Notably the titration performed in the presence of the capsule with high amounts of **MMNO** showed unexpected results. In fact the variations of the resorcin[4]arene signals were accompanied by the appearance of more and more visible broaden signals belonging to the N-oxide that were shifted to higher magnetic fields with respect to the N-oxide alone (Figure 29). These results could reveal the formation of new supramolecular species, still able to encapsulate N-oxide molecules with a slow-exchange on the NMR time scale equilibrium between outside and inside, remaining attached to the resorcin[4]arene moieties. A further confirmation of these assumptions was provided by the same titration carried out in the presence of **TEA**. In fact even under these conditions in the presence of high amount of **MMNO**, the resorcin[4]arene resonances were shifted as in the absence of ammonium species, while the N-oxide signals became increasingly cleaner with the formation of new molecular species and the encapsulated ammonium signals completely changed their shape shifting at slightly higher magnetic fields (from 0 ppm to -0.5/-1 ppm). Therefore it was possible to conclude that, even with **TEA** in solution, the presence of a high amount of N-oxide leads to the formation of new supramolecular species that could interact with **MMNO** only via hydrogen bond because of the

presence of ammonium molecules within its cavity. This assumption explained also the slight change of N-oxide chemical shifts that should be due to the H-bond interaction with the resorcin[4]arene monomers (Figure 29)

DOSY experiments were carried out in order to confirm the formation of the new supramolecular species (Figure 30). The results obtained showed that, in the case of the empty capsule, the addition of more than 7 equivalents of **MMNO** caused the formation of a new supramolecular species with a diffusion coefficient value equal to $5.8 \cdot 10^{-10} \text{ m}^2/\text{s}$ (Figure 28, B). In the presence of **TEA** molecules within the hexameric capsule, the formation of another supramolecular species with a diffusion coefficient value equal to $3.6 \cdot 10^{-10} \text{ m}^2/\text{s}$ was observed with just 5 equivalents of **MMNO** (Figure 28, D). Therefore the study of the effects of resorcin[4]arene was conducted in the presence of **MMNO** amount below to 5 equivalents with respect to the capsule in order to avoid the formation of supramolecular species different from the hexameric one.

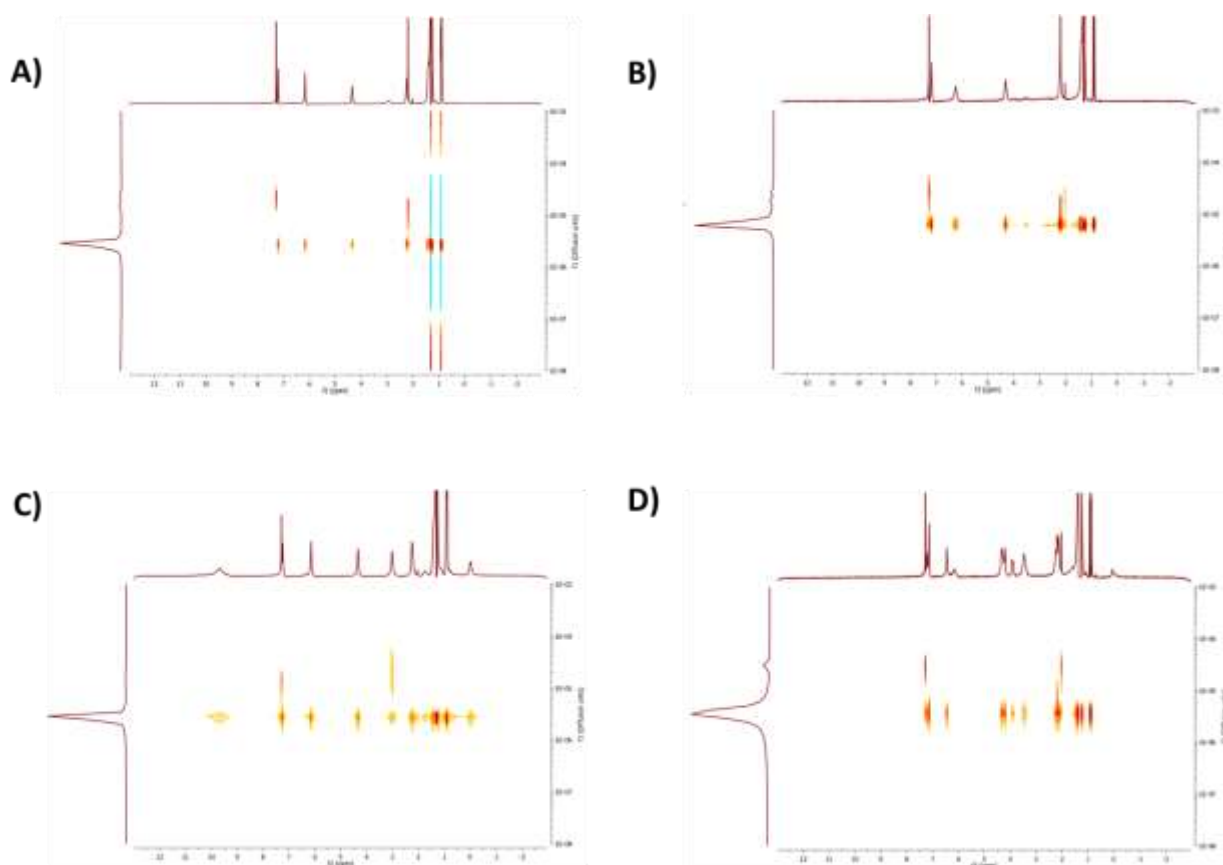


Figure 30. DOSY analyses of samples with 6 equivalents of resorcin[4]arene and A) 5 equivalents of **MMNO** ($D = 2.8 \cdot 10^{-10} \text{ m}^2/\text{s}$); B) 7 equivalent **MMNO** ($D = 5.8 \cdot 10^{-10} \text{ m}^2/\text{s}$) C) 3 equivalents **MMNO** and 10 equivalents of tetraethyl ammonium bromide ($D = 2.8 \cdot 10^{-10} \text{ m}^2/\text{s}$); D) 5 equivalents **MMNO** and 10 equivalents of tetraethyl ammonium bromide ($D = 3.6 \cdot 10^{-10} \text{ m}^2/\text{s}$)

The reaction between **MMNO** and p-methoxyphenyl isocyanate was studied in the presence of 1 equivalent of capsule with respect to the N-oxide in order to exclude the presence of the disassembled supramolecular hexamer. Under the same conditions used above (Figure 27) the reaction was carried out overnight at 60°C, solely observing the formation of the p-methoxyphenyl urea derivative and the p-methoxyaniline. In order to correctly estimate the amounts of the two products, ¹H-NMR analysis was carried out in the presence of DMSO as solvent after removing chloroform by rotary evaporator. The data collected in this way (Figure 31, A) showed that the p-methoxyphenyl urea derivative was the main product (67%) even if the obtained amount of p-methoxyaniline was relatively high (33%) (Table 3, entry 1). These results showed that the presence of the capsule prevented the azo-compound formation. However it was unclear if this effect was due to the H-bonding interaction between the OH groups of resorcin[4]arene and the N-oxide or to the capsule capability to add water molecules to particularly suitable compounds as in the previously discussed case of the isocyanides. Therefore the reaction was repeated under the same conditions with 10 equivalents of **TEA**. Even in this case (Figure 31, B) the p-methoxyphenyl urea derivative was the main product (87%) but the amount of p-methoxyaniline was reduced (12%) (Table 9, entry 2).

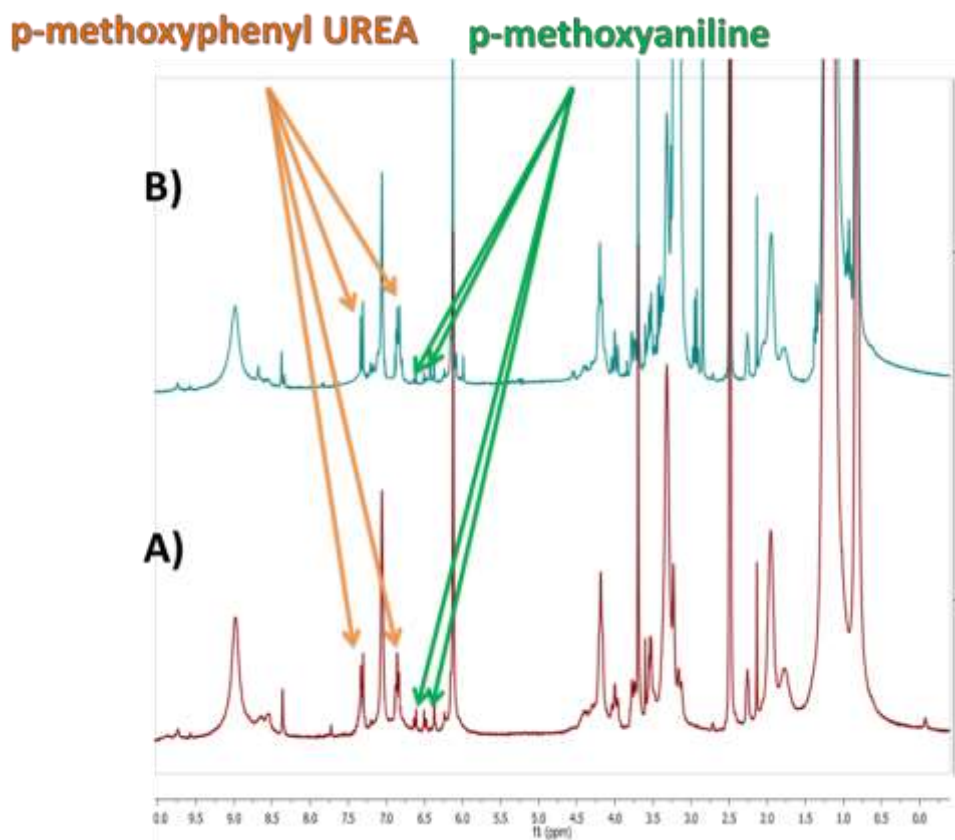


Figure 31. $^1\text{H-NMR}$ spectrum in $\text{dms}\text{-d}_6$ of the reaction between MMNO p-methoxyphenyl isocyanates carried out in CDCl_3 at 60°C with 2.7 mM substrates for 18h in the presence of A) resorcin[4]arene (1 equivalent with respect to MMNO); b) resorcin[4]arene (1 equivalent with respect to MMNO) and TEA (10 equivalents with respect to the capsule).

These results confirmed that the H-bonding interaction between the OH groups of resorcin[4]arene and the N-oxide on the outer part of the cavity was enough to modify the reactivity of the MMNO causing the formation of the urea derivative. In order to further demonstrate the responsibility of the H-bonding interaction in the variation of products distribution, the reaction was carried out by replacing the 6 equivalents of resorcin[4]arene with 24 equivalents of resorcinol. In fact it could still be possible that the MMNO anchored to the capsule surface through H-bonds could interact with p-methoxyphenyl isocyanate, move into the cavity and undergo to water attack causing the urea derivative formation. Resorcinol caused the selective formation of urea derivative (Table 9, entry 4) confirming that the strong interaction between the N-oxide group and the OH groups can modify the reactivity of MMNO.

#	Capsule	TEA	Resorcinol	Yield ^a (%) urea	Yield ^a (%) aniline	Yield ^a (%) azocompound
1	-	-	-	32	6	62
2	+	-	-	67	33	<<1
3	+	+	-	87	12	1
4	-	-	+	98	2	<<1

Table 9. Reaction between **MMNO** and p-methoxyphenyl isocyanate in the presence of different additives. Reaction conditions: [resorcinarene]= 16.2 mM, [**MMNO**]= 2.7 mM (1 eq. with respect to the capsule), [p-methoxyphenyl isocyanate] = 2.7 mM; [**TEA**] = 27 mM; [Resorcinol] = 65 mM. chloroform-d 1.5 mL, T= 60°C. +: presence; -: absence; a) Determined by ¹H-NMR in the presence of dmsd₆ as solvent.

3.2.2.5. Conclusions

The interaction between N-oxides and the capsule was thoroughly investigated. The N-oxide showed high affinity for the hydroxyl groups of the resorcin[4]arene monomers due to H-bonding interactions. When the amount of N-oxide was below 5 equivalents with respect to the capsule, its molecules remained attached to the supramolecular hexamer surface in equilibrium exchange between the internal cavity and the outer part. Even in the presence of a competitive guest the N-oxide was able to interact with the resorcin[4]arene capsule remaining anchored to the outer surface. However further increase of the N-oxide amounts caused the disassembly of the capsule. In order to demonstrate the capability of the N-oxide to interact with the capsule even in the presence of competitive guest DOSY analyses were carried out. Moreover the never previously studied reaction between phenylisocyanates and N-oxides allowed to give a further proof of this strong interaction. Indeed, despite the reaction between p-methoxyphenyl isocyanate and N-methylmorpholine N-oxide **MMNO** with a substrate concentration of 2.7 mM in chloroform gave the diazocompound derivative as the main product, the either empty or filled capsule modified the product selectivity causing the formation of the urea derivative due to the still present H-bonding between **MMNO** and resorcin[4]arene.

3.2.3. Capsule effect on the activation energy of reactions with encapsulable intermediates

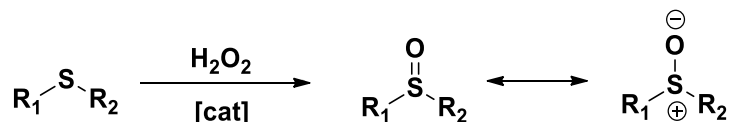
3.2.3.1. Sulfoxidation with hydrogen peroxide as oxidizing agent

In the last years organic sulfoxides have become useful intermediates in the synthesis of several biologically and chemically active compounds. Sulfoxides show important properties as antibacterial¹¹¹ and antifungal¹¹² agents and can have therapeutic effect as anti-ulcer,¹¹³ anti-atherosclerotic,¹¹⁴ anthelmintic,¹¹⁵ antihypertensive¹¹⁶ and cardiotoxic¹¹⁷ drugs. The easiest method to synthesize the sulfoxides is to oxidize the corresponding sulfide compounds. Unfortunately most of the reagents available for oxidation of sulfides can cause an over-oxidation to the corresponding sulfones. The use of cheap hydrogen peroxide (H₂O₂) as oxidant has recently shown interesting results in the selective formation of sulfoxides.¹¹⁸ The use of this reactant allows to oxidize sulfides to the corresponding sulfoxides with high yields under mild conditions giving water as by-product. Aliphatic sulfides are easily oxidized by H₂O₂ even in the absence of any catalyst, while the oxidation of diaryl sulfides needs to be catalyzed.¹¹⁹ For this purpose a series of transition metals such as Ru,¹²⁰ Ti,¹²¹ Mo,¹²² Fe¹²³ and V¹²⁴ were employed as soluble complexes. However the use of metal complexes is not always required and this affects the economic impact of the reaction. For this reason several research groups developed cheaper methodologies to obtain efficient and selective oxidation of sulfide compounds. Examples of Brønsted acid-catalysed sulfoxidation reaction have been reported.¹²⁵ Later it became clear that the use that H-bonding donor species can cause an electrophilic activation of hydrogen peroxide through hydrogen-bonding interactions. This allowed to develop a series of hydrogen-bonding donor organocatalysts for the sulfoxidation reaction in the presence of H₂O₂. For example ureas and thioureas,¹²⁶ sulfoxides,¹²⁷ surfactants¹²⁸ and many others¹²⁹ proved interesting organocatalyst in this reaction.

3.2.3.2. Sulfoxidation within the capsule cavity

The opportunity to employ H-bonding donor organocatalysts prompted us to use the hexameric capsule of resorcin[4]arene as a catalyst for the sulfoxidation reactions of aliphatic and aryl sulfides. In fact, the capsule is assembled through hydrogen bonds between the hydroxyl

groups of monomeric units and water molecules. If hydrogen peroxide molecules replace water in the hydrogen bond network, they could be activated for reaction. Moreover, the presence of a cavity capable of accommodating cationic species could promote the formation of a product that has at least a partially positively charged sulfur atom due to the resonance structures of the S=O bond (Scheme 8).



Scheme 8. Sulfoxidation reaction of a generic sulfide compound and resonance structures of the resulting sulfoxide.

Dibutyl sulfide (**dBS**) was employed as model substrate in order to investigate the catalytic properties of the resorcin[4]arene capsule in the sulfoxidation reaction in the presence of hydrogen peroxide as oxidant agent. The substrate conversion was monitored over time via 1H NMR analyses. Initially the interaction between **dBS** and hexameric capsule in chloroform-d was investigated observing the absence of encapsulated resonances. The addition of 1.2 eq. of a 30 w/w% aqueous solution of H_2O_2 caused the immediate formation of new sets of resonance signals in the <0 ppm region together with new resonances at 2.7 ppm attributed to the dibutyl sulfoxide (**dBSO**) (Figure 30). Under these conditions the quantitative oxidation of **dBS** was achieved in 65 minutes, while only 10% of **dBSO** was obtained after 90 minutes without the capsule (Table 10, entries 1, and 2). Several experiment with increasing amounts of **dBSO** were carried out to demonstrate the sulfoxide encapsulation. In this way the same type of up-field shifted resonance signals obtained during the **dBS** oxidation were observed. This highlighted that **dBSO** was a suitable guest for the capsule and therefore a few equivalents of sulfoxide stayed within the cavity of the supramolecular catalyst during the oxidation reaction of **dBS**.

#	Capsule	TEA	Time (min)	Yield ^a (%)
1	-	-	90	10
2	+	-	65	>98
3 ^b	-	-	90	21
4 ^c	-	-	90	28
5	+	+	65	46
6	-	+	90	15
7 ^d	-	+	50	69

Table 10. Sulfoxidation reaction of **dB**S to **dB**SO in the presence of 30 w/w% H₂O₂ under various conditions. Reaction conditions: [resorcinarene]= 36 mM, [dBS]= 30 mM (5 or 10 eq. with respect to the capsule), 30 w/w% H₂O₂ 1.2 eq.; [tetraethyl ammonium tetrafluoroborate (TEA)]= 60 mM (10 eq. with respect to the capsule), water saturated chloroform-d 1.5 mL, T= room temperature. +: presence; -: absence; a) Determined by ¹H-NMR; b) [acetic acid] = 6 mM (1 eq. with respect to capsule); c) [resorcinol] = 144 mM (24 eq. with respect to capsule); d) 200 μL of CD₃OD.

To prove that the catalytic activity of the capsule was not due to its Brønsted acid properties activating H₂O₂, we performed the oxidation reaction with one equivalent of acetic acid (pK_a 4.7) with respect to the capsule. Under these conditions 21% of **dB**SO was obtained after 90 minutes (Table 10, entry 3) confirming our hypothesis. Besides it must be considered that commercially available 35% w/w H₂O₂ solution shows an apparent pH < 2, giving further evidence of the insufficient effect of the acidity in hydrogen peroxide activation. If the high catalytic activity of the capsule was due simply to the entrapment of H₂O₂ in the network of H-bonds on the capsule surface the reaction should proceed either on the outside or in the inside of the cavity with the same rate.

To evaluate the contribution of hydrogen bonding to the sulfoxidation catalyzed by the resorcin[4]arene, this reaction was carried out replacing capsule with an equivalent amount of resorcinol molecules capable of developing H-bonds through the phenolic OH groups. Under these conditions no conversion was observed (Table 10, entry 4) but an unwanted reaction between resorcinol and the H₂O₂ was noticed. Therefore we tried to carry out the reaction in a solvent capable to inhibit the capsule assembling solubilizing effectively the resorcin[4]arene monomers. Unfortunately, solvents with these properties must provide hydrogen bonds that could activate the molecules of H₂O₂. When we introduced 200 μL of deuterated methanol the capsule disassembly

was achieved, but it also increased the reactivity of H_2O_2 and its solubility in organic medium causing a 69% conversion of substrate in 50 minutes (Table 10, entry 7). Finally we decided to investigate the catalytic activity of the supramolecular cavity repeating the oxidation reaction in the presence of ten equivalents of tetraethylammonium tetrafluoroborate (**TEA**) as a competitive cationic guest for the capsule.¹³⁰ The presence of a cationic species in the cavity caused an evident reduction of the catalytic activity (Table 10, entry 5), while **TEA** turned out to be inert in the reaction during control experiments (Table 10, entry 6) even though application of ammonium salts as catalysts for the sulfoxidation reactions have been recently reported.¹³¹ This demonstrated the central role of the capsule empty cavity in the high catalytic activity of resorcin[4]arene (Figure 32).

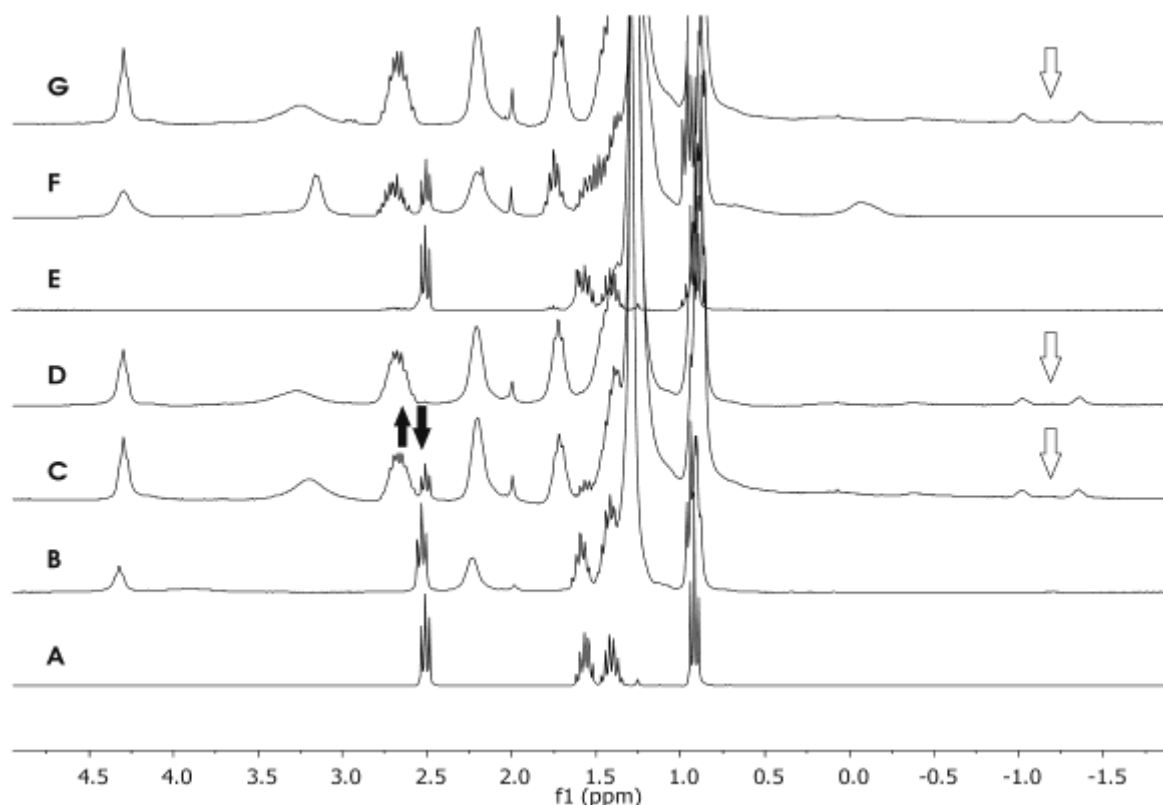
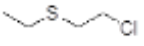

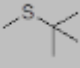
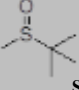
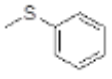
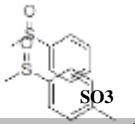
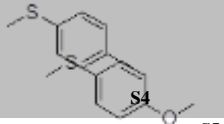

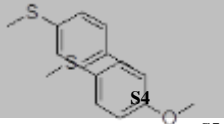


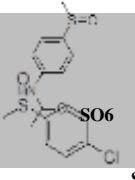
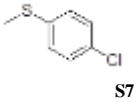
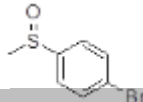
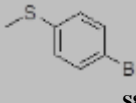
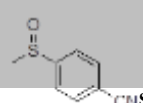
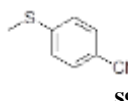

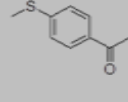
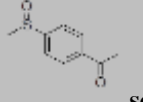
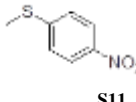
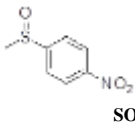
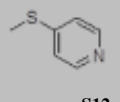
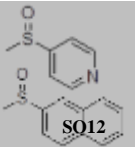




Figure 32. ^1H NMR spectra in water saturated chloroform- d : A) **dBS** (60 mM); B) **dBS** (60 mM) and capsule (6 mM); C) **dBS** (60 mM) with H_2O_2 (1.2 eq.) and capsule (6 mM) after 25 minutes; D) **dBS** (60 mM) with H_2O_2 (1.2 eq.) and capsule (6 mM) after 65 minutes; E) **dBS** (60 mM) with H_2O_2 (1.2 eq.) after 90 minutes; F) **dBS** (60 mM) with H_2O_2 (1.2 eq.), capsule (6 mM) and **TEA** (60 mM) after 90 minutes; G) **dBSO** (60 mM) with H_2O_2 (1.2 eq.) and capsule (6 mM) after 4 hours. \blacktriangledown free sulfoxide, \triangledown encapsulated sulfoxide.

We decided to investigate the catalytic activity of the supramolecular capsule in the sulfoxidation reaction of several thioethers using hydrogen peroxide as oxidant. With this purpose

aliphatic sulfides such as the analogue of the mustard gas **Sa** and t-butyl methyl sulfide **Sb** (Table 11, entries 1 and 2), alkyl aryl sulfides (Table 11, Entries 3-15) and di-aryl sulfide (Table 11, entries 16-18) were employed. As reported in the literature, aryl substrates are less reactive than aliphatic ones, although good to excellent sulfoxide yields were obtained as a function of the electronic properties of the substrates. Electron withdrawing groups demonstrated to further reduce the reactivity of the aryl substrates and longer reaction times were required to achieve good yields. Diaryl sulfides turned out to be the least reactive substrates, but even with these compounds the presence of electron donor groups allowed to obtain high conversions in relatively short time as in the case of **S16**. The presence of the dimethylamino moiety in the molecular structure of this molecule increased the electron density of the S atom and favoured its sulfoxidation (Table 11, entry 16). Finally the capsule demonstrated high chemo-selectivity in the sulfoxidation of *p*-tolyl disulfide **S18** causing the only formation of the mono-sulfoxide product in 51% yield after 18 hours in the presence of 5 eq. of H₂O₂ (Table 11, Entry 18).

The inhibitory effect of **TEA** due to competitive occupation of the capsule cavity was observed to various extent with all the investigated substrates showing the importance of the empty cavity in order to catalyse the sulfoxidation reaction. More specifically the collected data showed that the ammonium inhibition was more evident in the presence of substrates with higher steric hindrance. This indicated that the residual space left in the cavity by the competitive ammonium guest was enough to allow the entrance of substrates, if not particularly bulky, causing a co-encapsulation of the two species in order to fit the best packing coefficient of 0.45-0.55 typical of supramolecular encapsulation phenomena.¹³²

#	Substrate	Product	Time (min)	Yield (%) ^a
1	 S1	 SO1	120	95 22 ^b
2	 S2	 SO2	35	>98 >98 ^b
3	 S3	 SO3	110	>98 23 ^b
4	 S4	 SO4	60	>98 50 ^b
5	 S5	 SO5	100	>98 40 ^b
6	 S6	 SO6	20	>98 75 ^b
7	 S7	 SO7	150	76 13 ^b
8	 S8	 SO8	80	90 28 ^b
9	 S9	 SO9	130	68 15 ^b
10	 S10	 SO10	180	70 6 ^b
11	 S11	 SO11	375	80 6 ^b
12	 S12	 SO12	380	70 10 ^b
13	 S13	 SO13	180	80

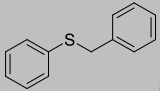
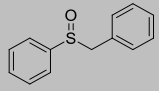
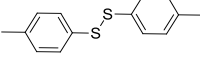
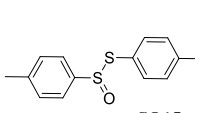
				10 ^b
14			20	94 ^d
				23 ^{b,d}
15			1100	51 ^{d,e}
				21 ^{b,d,e}

Table 11. Sulfoxidation reaction of several thioethers **S1-S15** with H₂O₂ catalysed by the capsule. Experimental conditions: [substrate]= 30 mM, 30% H₂O₂ 1.2 eq.; [resorcinarene]= 36 mM, water saturated chloroform-d 1.5 mL, T= room temperature, time 18h. a) Determined by ¹H NMR; b) [TEA] = 60 mM; d) determined by GC; e) H₂O₂ 5.0 eq.

In order to investigate the catalytic efficiency of the resorcin[4]arene capsule and the possible product inhibition in the sulfoxidation reaction, we used increasing amounts of 4-chlorophenyl methyl sulfide **S8** as substrate. This substrate was chosen because of its moderate reactivity under the selected experimental conditions. The obtained results (Figure 33) clearly showed that the capsule maintained its catalytic activity in the presence of 10, 25 and 50 equivalents of **S8** observing super impossible plots of the yield in **SO8** with time. Only a drastic increase in the substrate amount (200 eq.) caused a slowdown of sulfoxide formation after about 25% conversion. This loss of catalytic activity in the presence of very high amounts of substrate could be traced to the product inhibition effects due to the guest character of the sulfoxides. Indeed, as the progress of the reaction led to the formation of a guest competitive, the substrate conversion caused the development of a catalytic system inhibitor capable to occupy the capsule cavity. In the presence of so many equivalents of substrate with respect to the capsule, the amount of sulfoxide, capable to effectively occupy the cavity, rapidly became high enough to reduce the catalytic activity capsule. This gave further evidence of the cavity responsibility in the sulfoxidation reaction catalysis.

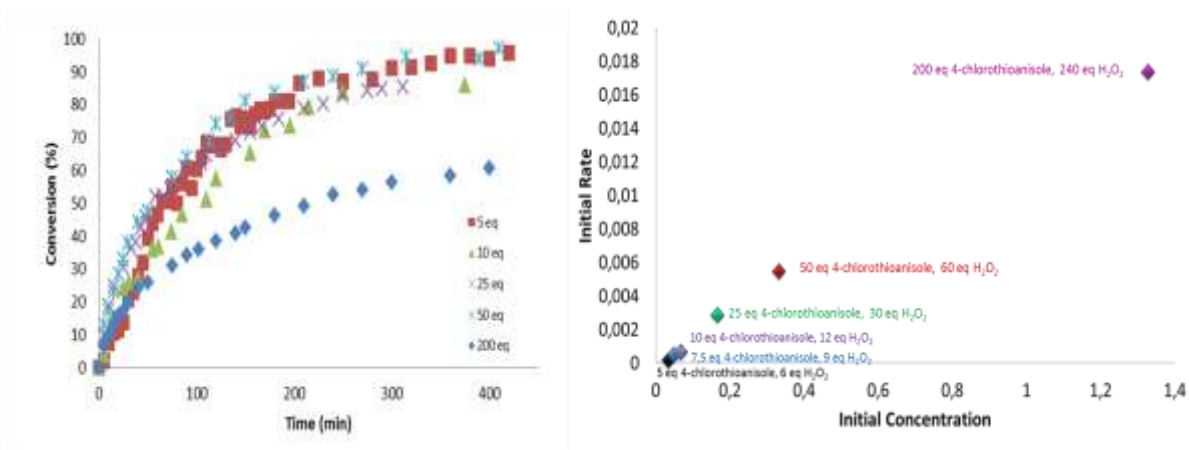
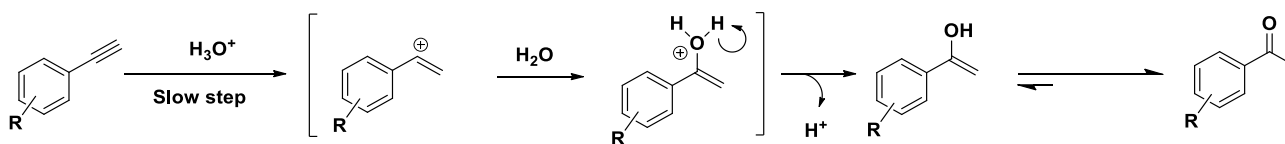


Figure 33. Percentage conversions of different equivalents of 4-chlorophenyl methyl sulfide **Sf** to the corresponding sulfoxide **Sof** over time (on the left) and correlation between initial rates of the reactions and initial concentrations of **Sf**. [Resorcinarene] = 36 mM, **Sf** equivalents with respect to the capsule are shown in figure, H₂O₂ = 1.2 equivalents with respect to the substrate, water saturated chloroform-d 1.5 mL, T= room temperature.

Finally we decided to verify the selectivity of the supramolecular catalytic system towards sulfoxides. Therefore **dbSO** was chosen as substrate and the oxidation reaction was carried out under the same conditions used during the sulfoxidation of **dbS** (Table 10, entry 1). This reaction caused no conversion to sulfone even after 24 hours, demonstrating that the capsule of resorcin[4]arene is a very chemoselective organocatalyst in the oxidation reaction of thioethers to sulfoxides using hydrogen peroxide as the oxidant (Figure 32, G).

3.2.3.3. Hydration of alkynes

The results obtained during the previous reaction showed that the capsule can exhibit catalytic properties even with substrates that are neither cationic nor electron poor species as in the case of the thioethers oxidation to sulfoxides. However, the weak interactions between capsule and sulfoxide led us to assume also a certain affinity of the supramolecular system for the activated state capable to decrease the activation energy of the reaction. Therefore we thought that reactions with cationic intermediates could be accelerated through the π -cation interactions within the capsule even in the absence of affinity for the substrates. In order to demonstrate this vision we decided to study reactions whose mechanism would cause the formation of cationic intermediates while substrate could not exhibit affinity for the capsule cavity. With this purpose we chose the acid catalyzed hydration reaction of aromatic alkynes (**C** \equiv **C**) to ketones (**ket**) in which a water molecule is added to the protonated alkyne (Scheme 9).



Scheme 9. Acid catalysed Markovnikov hydration of terminal aromatic alkynes to ketones.

The reaction is composed by the hydro-hydroxylation of the triple bond and the subsequent tautomerization of the intermediary enol to the corresponding ketone.¹³³ In the presence of terminal alkynes as substrates, the reaction could give either methyl-ketones (Markovnikov addition) or aldehydes (anti-Markovnikov addition).¹³⁴ Alkyne hydration is a particularly interesting reaction also because of its 100% atom efficiency. The synthesis of methyl ketone compounds via alkyne hydration historically has been carried out using high amounts of mineral acid and toxic co-catalysts such as Hg(II).¹³⁵ Although this method allowed very high yields, the employment of mercury compounds forced the search for other processes for industrial application. More recently less polluting but more expensive Co(III), Ru(II), Pt(II) or Au(I) and Au(III)¹³⁶ precursors were introduced in order to obtain hydration products. Conversely, large amounts of Brønsted acids and harsh reaction conditions are requested in order to achieve metal-free hydration of alkynes. In fact this reaction is usually carried out in the presence of concentrated sulfuric-, formic-, p-toluensulfonic-, trifluoromethanesulfonic acids at high temperatures for long times.¹³⁷ Very recently functionalized imidazole based Brønsted acid ionic liquids (BAILs) proved to be efficient and eco-friendly catalytic media for the alkyne hydration under mild conditions.¹³⁸ However, the synthesis of ionic liquids is a long process especially if compared with the synthesis of resorcin[4]arene.

Observing the trend of the reaction energy in relation to reaction progress (Figure 34), it is assumed that the rate determining step of the alkynes hydration is the attack of H_3O^+ on the triple bond leading to the formation of the corresponding vinyl carbocation.¹³⁹ Therefore we thought that the presence of a resorcin[4]arene capsule, capable of π -cation interactions, could facilitate the formation of this intermediate lowering the activation energy of the rate determining step thus catalyzing the reaction.

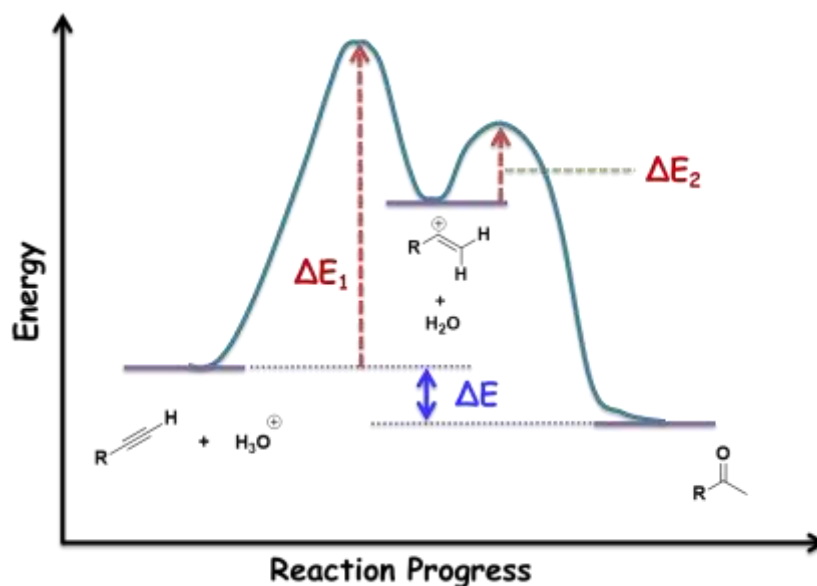


Figure 34. Plot of the reaction energy in relation to the reaction progress in the alkyne hydration reaction.

Phenylacetylene $\text{C}\equiv\text{C}_1$ was used as a model substrate in order to carry out an initial study on the catalytic properties of the self-assembled capsule while substrate conversion was monitored over time by means of ^1H NMR analyses. The reaction was initially investigated at 60°C for a few hours, observing the inefficacy of the capsule in catalyzing the reaction despite its slight acidity ($\text{pK}_a \approx 5.5 - 6$; Table 12, entry 1).⁶⁰ Similarly we tested the effect of strong inorganic Brønsted acids such as HBF_4 , HCl or HNO_3 but the reaction did not proceed under these conditions (Table 12, entries 2 – 4). When 0.5 equivalents of methanesulfonic acid with respect to $\text{C}\equiv\text{C}_1$ were added as strong organic Brønsted acid the partial formation of acetophenone **ket**₁ together with smaller amounts of acid addition product were observed as confirmed by GC-MS (Table 12, entry 5). Interestingly, the addition of catalytic amounts of the resorcin[4]arene capsule together with strong Brønsted acids caused the quantitative hydration of $\text{C}\equiv\text{C}_1$ to the corresponding ketone **ket**₁. In particular in the presence of 10 mol% of the capsule and 0.5 equivalents of HBF_4 with respect to the substrate $\text{C}\equiv\text{C}_1$ the hydration reaction gave quantitative phenylacetylene conversion after slightly more than one hour (Table 12, entry 7). In order to further demonstrate the efficiency of this catalytic system, the reaction was repeated under the same conditions decreasing the amount of acid (0.2 equivalents with respect to $\text{C}\equiv\text{C}_1$) and a quantitative conversion to **ket**₁ was achieved after 18 hours (Table 12, entry 8). When the 0.5 equivalents of HBF_4 were replaced with either HCl or methanesulfonic acid, the combination with the capsule efficiently promoted the reaction (Table 12, entries 9, 12). However, when the amount of these acids was decreased we obtained a clear loss in

the catalytic activity (Table 12, entries 10, 13), further confirming their importance in the reaction. The effect of nitric acid as catalyst was only slightly improved by the presence of the capsule (Table 12, entry 11).

#	Brønsted Acid	Acid/C≡C ₁	Time (h)	Capsule	Ammonium (TEA)	ket ₁ ^a (%)
1	-	-	24	+	-	0
2	HBF ₄	0.5	1	-	-	<2
3	HCl	0.5	1	-	-	<2
4	HNO ₃	0.5	1	-	-	<2
5	CH ₃ SO ₃ H	0.5	1	-	-	57 (19) ^e
6 ^b	CH ₃ SO ₃ H	0.2	18	-	-	13 (3) ^e
7	HBF ₄	0.5	1.2	+	-	>98
8 ^b	HBF ₄	0.2	18	+	-	>98
9	HCl	0.5	1.5	+	-	>98
10 ^b	HCl	0.2	18	+	-	15
11	HNO ₃	0.5	1	+	-	18
12	CH ₃ SO ₃ H	0.5	1	+	-	>98 (0) ^e
13 ^b	CH ₃ SO ₃ H	0.2	24	+	-	59 (17) ^e
14	HBF ₄	0.5	24	+	+	1
15	HBF ₄	0.5	24	-	+	1
16 ^c	HBF ₄	0.5	24	-	-	<1
17 ^d	HBF ₄	0.1	24	+	-	>98

Table 12. Catalytic tests for the acid-catalysed hydration reaction of the phenylacetylene C≡C₁ to the corresponding ketone ket₁. Reaction conditions: [Resorcinarene]= 36 mM, [C≡C₁] = 60 mM, [TEA] = 60 mM (10 eq. with respect to the capsule), water saturated chloroform-d 1.5 mL, T= 60°C. +: presence; -: absence; a) Determined by ¹H-NMR; b) [Brønsted acid]= 12 mM c) [resorcinol] = 140 mM (24 eq. with respect to capsule); d) [resorcinarene] = 18 mM [C≡C₁]= 120 mM, [Brønsted acid]= 12 mM; e) Percentage of the detected product obtained from the addition of the acid on the triple bond.

The data described above substantially confirmed our hypothesis about the catalytic activity of the capsule due to the ability of the nanometric cavity to stabilize the protonated form of the alkyne favoring the attack of the water molecule. In order to definitively ascertain this hypothesis a

series of control experiments were carried out. The hydration of $\text{C}\equiv\text{C}_1$ was repeated in the presence of 0.5 equivalents of HBF_4 , 10 mol% of capsule and 1 equivalent of tetraethylammonium tetrafluoroborate (**TEA**) with respect to the substrate. The presence of **TEA** as a competitive cationic guest for the capsule caused a complete inactivation of the catalytic activity due to ammonium encapsulation (Table 12, entry 14) as reported by the ^1H NMR spectra in Figure 35. Moreover the ^1H NMR investigation of the capsule in the presence of either phenylacetylene $\text{C}\equiv\text{C}_1$ or $\text{C}\equiv\text{C}_1$ and HBF_4 allowed to exclude the encapsulation of the alkyne within the cavity (Figure 36).

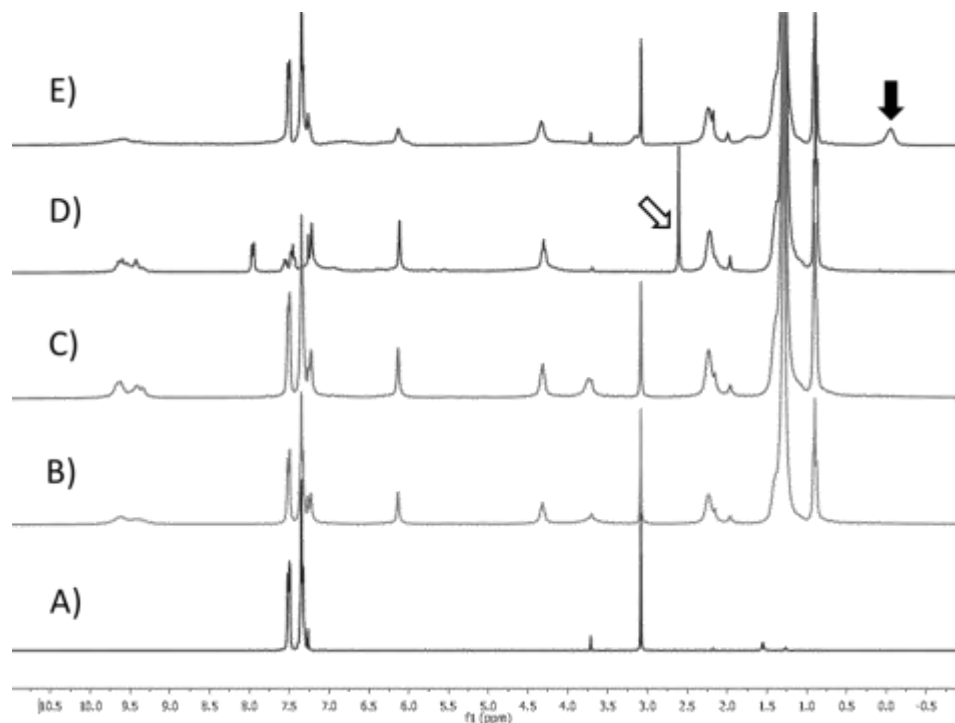


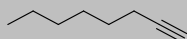
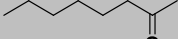
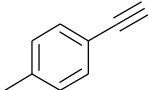
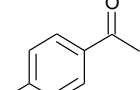
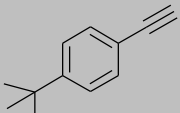
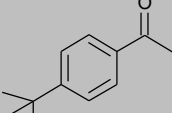
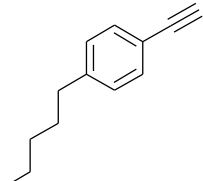
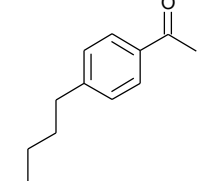
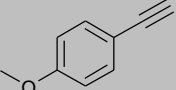
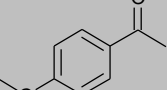
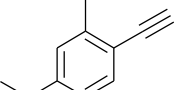
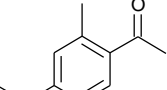
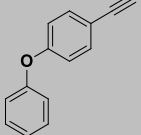
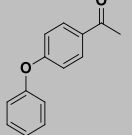
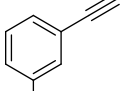
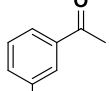
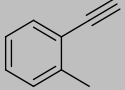
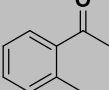
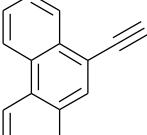
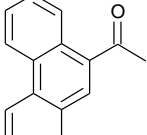
Figure 35. ^1H NMR spectra in water saturated chloroform- d : A) phenylacetylene $\text{C}\equiv\text{C}_1$ (60 mM); B) phenylacetylene $\text{C}\equiv\text{C}_1$ (60 mM) and capsule (6 mM); C) phenylacetylene $\text{C}\equiv\text{C}_1$ (60 mM) with HBF_4 (0.5 eq.) and capsule (6 mM); D) phenylacetylene $\text{C}\equiv\text{C}_1$ (60 mM) with HBF_4 (0.5 eq.) and capsule (6 mM) after 70 minutes at 60°C ; E) phenylacetylene $\text{C}\equiv\text{C}_1$ (60 mM) with HBF_4 (0.5 eq.), capsule (6 mM) and **TEA** (60 mM) after 18h at 24°C ; \blacktriangledown encapsulated ammonium, \blacktriangledown acetophenone.

The collected data allowed us to assume that the reaction was promoted by protonation of the alkyne by the strong Brønsted acid, followed by the encapsulation of such species and the rapid attack of water leading to the methyl ketone **ket**₁. Finally, to exclude the contribution of the resorcinol moieties of the capsule in the reaction, we carried out the reaction replacing the supramolecular hexamer with 24 equivalents of resorcinol with respect to the original amount of capsule. Even in this case the system did not show sufficient catalytic activity and no conversion was obtained (Table 12, entry 16). This provided a further demonstration of the key role of the

cavity to interact with the positively charged species formed by Brønsted acid activation of the alkyne in order to achieve catalytic effects.

To emphasize the efficiency of this catalytic system, both the amount of acid and supramolecular hexamer were further lowered adding just 0.1 equivalents of HBF_4 and 5 mol% of capsule with respect to the amount of $\text{C}\equiv\text{C}_1$ in the solution. The hydration reactions are usually carried out in the literature with low amounts of acid just in the presence of metal catalysts,¹⁴⁰ but the possibility of favoring the formation of the cationic intermediate within the cavity of the hexamer could allow to achieve interesting results even with very low amounts of acid. When the reaction was carried out under these conditions 24 hours were a sufficient time to obtain a complete conversion of $\text{C}\equiv\text{C}_1$ to the corresponding ketone **ket₁**, confirming the high catalytic activity of the capsule.

The catalytic system composed by resorcin[4]arene capsule and HBF_4 was employed with a series of alkynes in order to investigate its catalytic activity in the presence of substrates with different electronic as well as steric properties. The reactions were carried out both with 50 mol% of HBF_4 together with 10 mol% of capsule in order to observe the efficiency of the catalytic system in 1 hour and with 10 mol% of HBF_4 together with 5 mol% of capsule in 18 hours in order to emphasize the mild conditions under which the capsule can exhibit its full catalytic activity (Table 13). With all substrates, the reactions were repeated also in the presence of tetraethyl ammonium tetrafluoroborate (**TEA**) as a competitive guest in order to demonstrate the importance of the cavity of the capsule in the reaction (Table 13).

#	Substrate	Product	Yield ^a with available capsule (%)	Yield ^a with filled capsule ^b (%)
1	 C≡C ₂	 ket ₂	<1	<1
2	 C≡C ₃	 ket ₃	>98 >98 ^c	2 18 ^c
3	 C≡C ₄	 ket ₄	60 98 ^c	1 1 ^c
4	 C≡C ₅	 ket ₅	46 83 ^c	7 8 ^c
5	 C≡C ₆	 ket ₆	>98 >98 ^c	72 98 ^c
6	 C≡C ₇	 ket ₇	>98 >98 ^c	>98 >98 ^c
7	 C≡C ₈	 ket ₈	54 >98 ^c	17 >98 ^c
8	 C≡C ₉	 ket ₉	56 78 ^c	<1 <1 ^c
9	 C≡C ₁₀	 ket ₁₀	78 40 ^c	<1 <1 ^c
10	 C≡C ₁₁	 ket ₁₁	40 85 ^c	<1 3 ^c

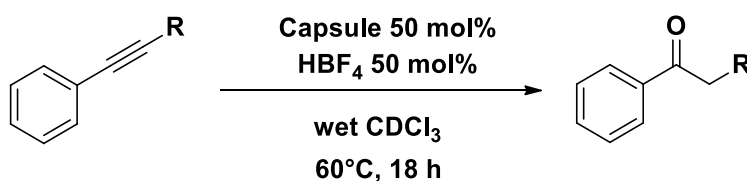
11			<1	<1
12			<1	<1
13			<1	<1

Table 13. Hydration reaction of several alkynes catalysed by the capsule with HBF_4 . Experimental conditions: [resorcinarene] = 36 mM; $\text{HBF}_4/\text{Substrate}$ = 0.5; [substrate] = 60 mM, water saturated chloroform-d 1.5 mL, $T = 60^\circ\text{C}$; time = 1 h; a) Determined by ^1H NMR; b) reaction in the presence of [TEA] = 60 mM, c) [resorcinarene] = 18 mM; $\text{HBF}_4/\text{Substrate}$ = 0.1; time = 18 h.

First we observed that the capsule showed no catalytic activity in the presence of aliphatic terminal alkynes as 1-octyne $\text{C}\equiv\text{C}_2$ (Table 13, entry 1), probably due to the low reactivity of this substrate. Conversely, with aromatic substrates under the same conditions interesting results were obtained. The presence of relatively small electron-donating substituents in *para*-position of the aromatic ring caused an increase in the terminal alkynes reactivity. In fact 4-ethynyltoluene $\text{C}\equiv\text{C}_3$ was converted to the corresponding ketone **ket₃** (Table 13, entry 2) with improved efficiency if compared to phenylacetylene $\text{C}\equiv\text{C}_1$ (Table 12, entries 7 and 17). When the *p*-methyl group was replaced either with *p*-tert butyl ($\text{C}\equiv\text{C}_4$) or *p*-pentyl ($\text{C}\equiv\text{C}_5$), the supramolecular capsule showed a gradually lower catalytic activity due to the increasing steric hindrance of the substituent group (Table 13, entries 3, 4). This effect could be explained considering the limited space within the cavity that disfavored the accommodation of bulky molecules compared to the smaller substrates causing a kind of substrate selectivity. Unfortunately the presence of even more electron donating substituents such as *p*-methoxy group over-activated the substrates and their complete conversion was achieved in a short time even when the capsule was occupied by **TEA** (Table 13, entries 5, 6). Although less effective in activating the substrate, also the *p*-phenoxy group showed a behavior similar to that of *p*-methoxy; in fact no substantial differences were detected in the catalytic activity comparing the reaction carried out either with the empty or **TEA** filled capsule (Table 13, entry 7). The effect of the position of substituents on the aromatic ring was investigated using 3-ethynyltoluene $\text{C}\equiv\text{C}_9$ and the 2-ethynyltoluene $\text{C}\equiv\text{C}_{10}$ as substrates comparing the results achieved with that obtained with $\text{C}\equiv\text{C}_3$. The methyl group in the meta position caused lower conversion even

if compared to that obtained with $C\equiv C_{10}$ bearing the methyl in the ortho position, even though the latter is characterized by higher steric hindrance close to the triple bond. Conversely, in the presence of lower amounts of both capsule and HBF_4 , the steric hindrance effect of the *o*-methyl group became prevalent and thus higher conversion were achieved with $C\equiv C_9$ as substrate (Table 13, entries 8, 9). The catalytic activity of the supramolecular capsule in the presence of bulky substrates was further investigated using 9-ethynylphenanthrene $C\equiv C_{11}$ as substrate. The results obtained under these conditions showed a clear decrease of the catalytic efficiency of the supramolecular system (Table 13, entries 10). This effect was attributed to the confined space within the capsule that hampered the access of particularly bulky substrates into the cavity as for $C\equiv C_5$. Unfortunately the capsule ability to catalyze the reaction by promoting the formation of the cation intermediate did not allow the hydration of substrates bearing electron-withdrawing group in their molecular structure. In fact, with 1-bromo-4-ethynylbenzene $C\equiv C_{12}$, methyl 4-ethynylbenzoate $C\equiv C_{13}$ and 3-ethynylpyridine $C\equiv C_{14}$ no conversion of the substrates to the corresponding acetophenones was observed (Table 13, entries 11-13).

After studying the catalytic activity of the supramolecular system in the presence of terminal alkynes, we decided to test its activity with aromatic substrates that presented internal triple bonds. With this purpose 1-phenyl-1-propyne $C\equiv C_{15}$, 1-phenyl-1-hexyne $C\equiv C_{16}$ and diphenylacetylene $C\equiv C_{17}$ were used as substrate with different steric hindrance in the presence of 50 mol% of both capsule and HBF_4 with respect to the alkyne for 18 hours, this because of the lower reactivity of this class of substrate (Scheme 10).



Scheme 10. Hydration reaction of aromatic internal alkynes catalysed by resorcin[4]arene capsule and HBF_4 .

Under the conditions described above, conversions of the substrates turned out to be strictly dependent on the steric hindrance of the substrates (Table 14). In particular the reaction carried out in the presence of $C\equiv C_{15}$ as substrate caused the formation of the corresponding ketone **ket₁₅** in 50% yield (Table 14, entry 1). When the steric hindrance was increased going from the methyl group of $C\equiv C_{15}$ to the hexyl group of $C\equiv C_{16}$, the catalytic activity of the capsule was nearly halved and only 25% yield of **ket₁₆** was obtained (Table 14, entry 2). Finally, the use of an even more

bulky substrate such as the $C\equiv C_{17}$ caused a complete deactivation of the supramolecular catalytic system (Table 14, entry 3). These results demonstrate that the capsule has a fair catalytic activity but the confined space within the cavity made the supramolecular system extremely sensitive to steric hindrance. For this reason substrate with high steric hindrance could not efficiently react.

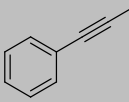
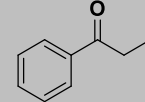
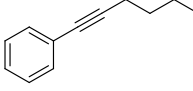
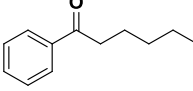
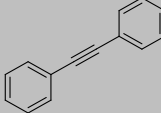
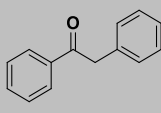
#	Substrate	Product	Yield ^a (%)
1	 $C\equiv C_{15}$	 ket₁₅	50 <1 ^b
2	 $C\equiv C_{16}$	 ket₁₆	25 <1 ^b
3	 $C\equiv C_{17}$	 ket₁₇	<1 <1 ^b

Table 14. Hydration reaction of differently bulky internal alkynes catalysed by resorcin[4]arene capsule and HBF_4 . Experimental conditions: [resorcinarene] = 36 mM; HBF_4 /Substrate = 0.5; [substrate] = 12 mM, water saturated chloroform-d 1.5 mL, T = 60°C; time = 1 h; a) Determined by 1H NMR; b) reaction in the presence of [TEA] = 60 mM.

3.2.3.4. Conclusions

In conclusion, we showed that the resorcin[4]arene capsule can exhibit catalytic properties even without any interaction with substrate molecules.

The supramolecular hexamer was an efficient organocatalyst for the selective oxidation of thioethers to sulfoxide (Figure 36). The catalytic activity of the capsule was probably due both to hydrogen bonds on the hexamer surface that activate the H_2O_2 and the cavity that stabilizes the partial positive charge of the sulfur atom in the sulfoxide molecule. Moreover, the affinity of the sulfoxide molecule for the capsule cavity confer the high product selectivity to this self-assembled organocatalyst.

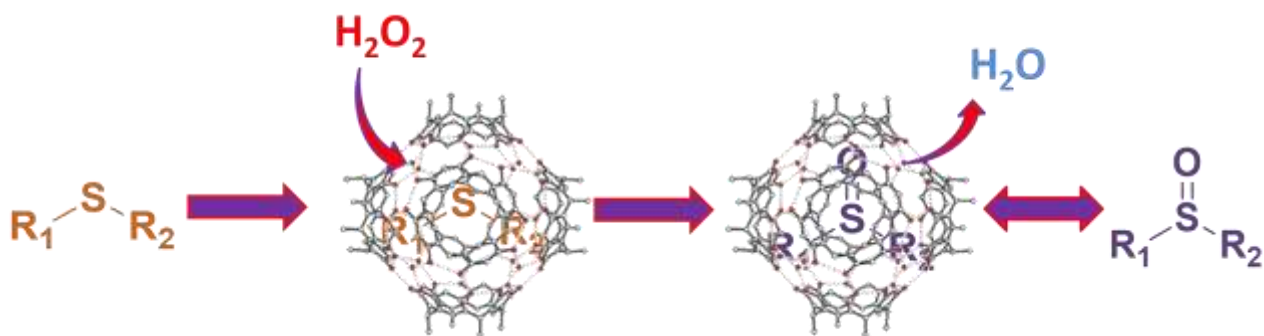


Figure 36. Mechanism of the selective oxidation of thioethers to sulfoxide catalyzed by resorcin[4]arene capsule in the presence of H₂O₂ as oxidizing agent.

The π -cation interactions between the capsule cavity and the cationic intermediate formed during the rate determining step of the reaction play a key role in the catalytic properties of the resorcin[4]arene capsule, even in the absence of any affinity with the substrate molecules. This assumption was demonstrated through the study of the hydration reaction of terminal alkynes to the corresponding methyl ketones (Figure 37). The application of this interaction allowed to obtain high conversion of non-deactivated aromatic alkynes in the presence of sub-stoichiometric amounts of HBF₄ at 60°C within hours. The role of the Brønsted acid was to promote the protonation of the substrate while at the same time the supramolecular capsule provided a suitable nano-environment to stabilize the positively charged intermediate species and thus favoring water addition. The inactivation of the reaction by the addition of a competitive guest for the supramolecular cavity clearly demonstrated the occurrence of the reaction within the capsule. An effect clearly caused by the confined space in which the reaction must take place was the sensitivity of the catalyst to the steric hindrance of the substrate both with terminal and internal alkynes.

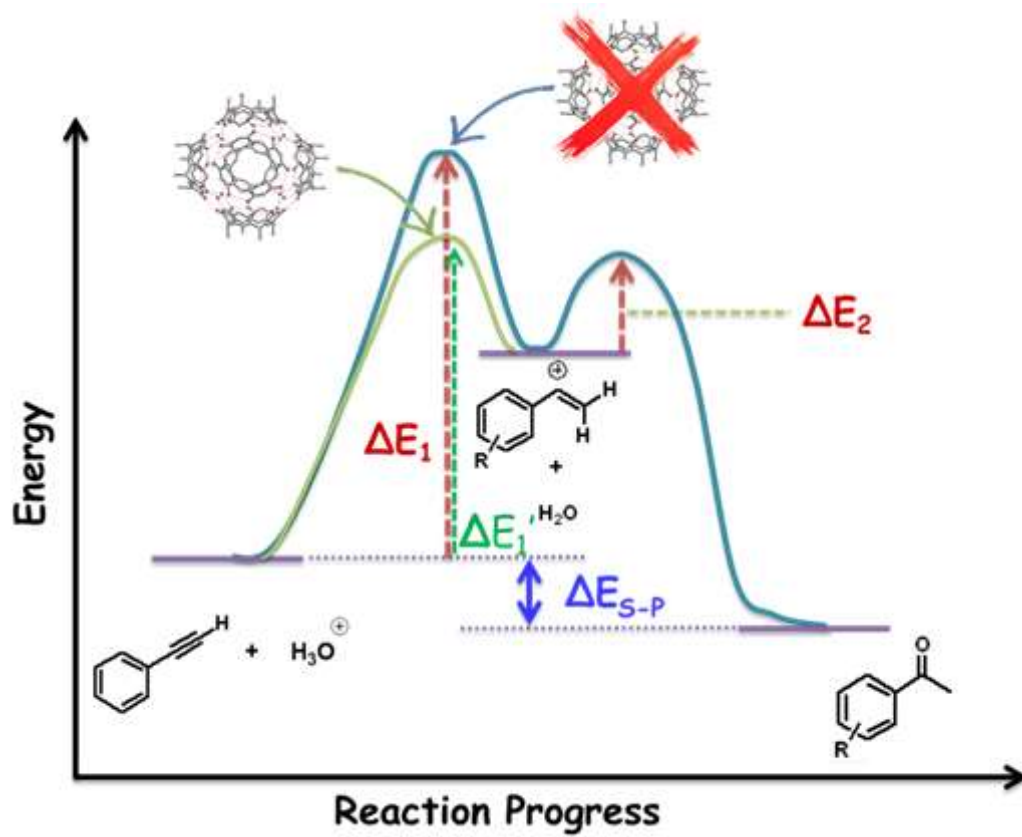


Figure 37. π -cation interactions within the capsule effect on the activation energy of the acid-catalyzed alkynes hydration.

4. CATALYSIS IN WATER BY MEANS OF MICELLAR MEDIA

4.1. State of the art

4.1.1. Green Chemistry

During the Nineties the introduction in the USA of the “Green Chemistry” philosophy completely changed the notion of chemical research and scientific progress. The new target was the achievement of a sustainable scientific development that caused the minimal possible environmental impact avoiding pollution. Indeed the chemical processes were no longer just a series of reactions optimized with the aim of obtaining the target molecules with high efficiency, but it became a system that must also consider the impact to the environment and human health.¹⁴¹ Twelve principles summarize the new interpretation of the chemical research and drive the behaviour of new researchers:

1. Prevent waste;
2. Use of synthetic methodologies that reduce the employment and formation of substances that possess toxicity to human health and the environment
3. Design of less hazardous chemical syntheses;
4. Maximization of the atom economy;
5. Avoid the use of solvents and auxiliary chemicals or employ solvents safe and non-toxic if necessary;
6. Use renewable sources;
7. Maximize energy efficiency;
8. Increase the use of catalytic systems to reduce the employ of stoichiometric reagents;
9. Avoid the use of protective groups and other derivatives that produce waste;
10. Design of reagents and products that are degradable after use;
11. Analysis in real time to prevent pollution;
12. Minimization of chemical risks to prevent accidents.

These twelve principles say that an ideal “green” synthesis allows the total selective formation of the desired product, in the presence of environmentally friendly solvents (if necessary) in substitution of the classic flammable, explosive and toxic volatile organic solvents. Furthermore this synthesis needs catalytic systems capable to work with high efficiency under mild conditions of pressure and temperature. Eventually the product must be easy to separate from the reaction medium and the catalyst that can thus be recycled.¹⁴²

The elimination of toxic, noxious or polluting compounds is fundamental in the development of a “green” chemical process. The environmental impact should be minimized, trying to use recyclable materials, obtaining energy from alternative and renewable sources and mandatorily avoiding the dispersion of chemicals in the environment. Several metrics have been proposed to encourage chemists and engineers to design processes that observe the principles of “green chemistry”.

One of the most used parameter is the *atom efficiency* that estimates the amount of the starting atoms included in the products:¹⁴³

$$\text{Atom Efficiency (\%)} = \frac{\text{Molecular Weight of the Required Product}}{\Sigma(\text{Molecular Weight of the Reagents})} \times 100$$

Another important metric is the Environmental Factor (E. Factor) that rates the amount of wastes developed per unit of desired product obtained. It is used to highlight the importance of employing the minimum necessary amount of reactive compounds and the requirement to recycle chemical species when possible, minimizing waste.¹⁴⁴

$$E. \text{ Factor} = \frac{\text{Waste (Kg)}}{\text{Required Product (Kg)}}$$

However not only the produced waste amount is important to estimate the real environmental impact of a chemical process, but their degrees of toxicity and environmental contamination are even more important. Therefore another parameter was introduced: the Environmental Quotient (EQ) that is calculated by multiplying the E Factor for a Q factor, that takes an arbitrary value proportional to the waste toxicity. For example, a harmless molecule such as sodium chloride has the EQ value equal to 1 while for a chromium salt this parameter could reach 100-1000 due to its toxicity and its difficult recycling or disposal.¹⁴³

$$EQ = E.Factor \times Q$$

In pharmaceutical syntheses, particular emphasis is placed on the control of waste production and specific parameters have been introduced. The most used of these parameters is the Process Mass Intensity (PMI) that is defined as the total mass of catalyst, reagents and solvents used to produce and purify a specified mass of product, starting from commonly available materials. In the absence of waste, when all materials are incorporated into the product this parameter assume the unitary value.¹⁴⁵

$$PMI = \frac{\text{Total mass in a process or process step (Kg)}}{\text{Mass of product (Kg)}}$$

4.1.2. Surfactants

Water is a very interesting solvent whose potentialities in organic synthesis were discovered only in the Eighties. The environmental compatibility is the fundamental property of this solvent that shows many other advantageous properties that make it a very attractive solvent:

- high polarity that allows an easy separation from apolar organic solvents;
- non-flammability;
- high availability at low cost;
- absence of color and odor that facilitates the detection of contaminants;
- density higher than most organic solvents;
- ability to dissolve gases easily;
- amphoteric behavior.

The main problems in the choice of water as a reaction solvent are the generally low solubility of most reagents and the incompatibility of several intermediate species traditionally found in homogeneous catalysts. Even if the catalysts can be modified adding polar groups to the ligands, via sometimes complex synthesis, in order to make them soluble in water, different

approaches are required to increase the solubility of the reagents in aqueous solution.^{146,147,148} New strategies have been devised to overcome this problem and one of the techniques that has proved most effective for this purpose is the use of surface active agents. A surface active agent (surfactant) is an amphiphilic compound characterized by the presence of a polar and a nonpolar portion. Surfactants are classified as cationic, anionic, zwitterionic and nonionic based on the electronic properties of the polar group. Most of the commercially available surfactants are obtained from petroleum feedstock but certain classes of bio-surfactants have recently emerged thanks to their biological functionalities.¹⁴⁹

In aqueous solvents polar groups (the so called “heads”) spontaneously orient towards water, while the non-polar groups (“tails”) behave as hydrophobic molecules minimizing the interactions with water molecules. When the concentration of these amphiphilic compound reaches a certain value (Critical Micelle Concentration, CMC), the surfactants self-assemble in a supramolecular structure called “micelle” (Figure 38). Indeed, micelles are water soluble aggregates of approximately 50 monomers with shapes ranging from pseudo-spherical to cylindrical, with the heads of the surfactants all positioned on the outer surface and the tails forming an hydrophobic core.¹⁵⁰ The globular structure of the micelle is not static but it is in a dynamic equilibrium between the aggregate and the free surfactant in solution.

The concentration of micelles (C_m) in solution can be obtained by a mathematical equation that correlates the concentration of the surfactant (C_t), the CMC and the number of surfactant in a micelle (also called “micelle aggregation number” - N):¹⁵¹

$$C_m = \frac{C_t - \text{CMC}}{N}$$

The micelle aggregation number is strictly dependent on several factors such as the nature¹⁵² and shape of the surfactant,¹⁵³ the temperature^{154,155} and the presence of organic additives.¹⁵⁶ The value of the aggregation number provides information on the micelle size and shape.¹⁵⁷

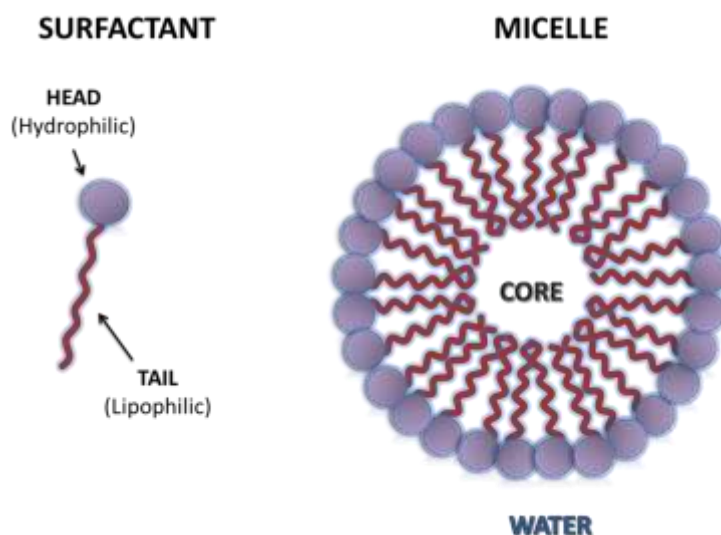


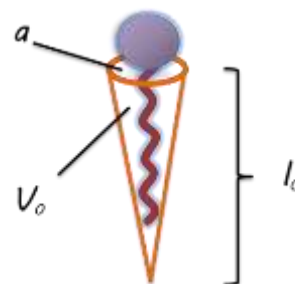
Figure 38. Surfactant and micelle.

The driving force leading to surfactants aggregation is the hydrophobic effect consisting in the repulsion exerted by water on the hydrocarbon chains of the surfactant molecules that self-assemble forming micelles when in concentration higher than the CMC value. The formation of an ordered structure causes a loss in the total Gibbs energy, but this effect is largely counterbalanced by the entropy gained by water molecules that can freely move in solution thanks to four hydrogen bonds.¹⁵⁸

The physical-chemical properties of micelles derive from the surfactant's structure. The heads control the charges present on the surface of the micelle while the tails impose the packing properties within the aggregate and the shape of the self-assembly.¹⁵⁹ For this reason surfactants with different molecular structures lead to micelles with different shapes and sizes. The connection between the molecular structure of the surfactant and its tendency to aggregation was widely investigated. More than 40 years ago, Tanford formulated a quantitative expression for the standard free energy change on aggregation to explain the surfactant aggregates form in aqueous solutions, their finite size and growth with a given shape.¹⁶⁰ Soon after, Israelachvili, Mitchell and Ninham found that the use of a molecular packing parameter could predict the size and the shape of the micellar aggregate at the equilibrium using general thermodynamic principles.¹⁶¹

The molecular packing parameter (P) is defined as:

$$P = \frac{V_0}{a \times l_0}$$



Where:

- V_0 is the volume of the surfactant tail;
- l_0 is the length of the surfactant tail;
- a is the surface area of the hydrophobic core of the aggregate (expressed per molecule in the aggregate).

Therefore the shape and the size of the equilibrium aggregate can be readily identified with the molecular packing parameter combined with simple geometric formulas:

- Spherical micelles are obtained when $0 \leq V_0/(a \times l_0) \leq \frac{1}{3}$;
- cylinder when $\frac{1}{3} \leq V_0/(a \times l_0) \leq \frac{1}{2}$;
- bilayer structure when $\frac{1}{2} \leq V_0/(a \times l_0) \leq 1$.

The ratio V_0/l_0 is a constant in common surfactants and its value is 21 \AA^2 for surfactants with single tail and 42 \AA^2 for double tail. For this reason, the factor that characterizes the packing parameter of every surfactant is the a area.¹⁶²

Micelles are able to solubilize hydrophobic compounds in water forming a thermodynamically stable solution. Surfactants are intrinsically capable to increase the solubility of organic compounds in water even below the CMC. When the CMC is achieved, the solubility increases dramatically and further addition of surfactant causes a linear increase of solubility due to formation of micelles able to accommodate organic compounds within the hydrophobic core.¹⁶³

The solubilization process in the presence of micelles can be described considering water and micelles as two different phases. In the micellar phase the amount of hydrophobic reactants increases with the length of the surfactant tail while the maximum concentration of organic compounds within the micelles reduces with increasing hydrophobicity of the reactant.¹⁶⁴

The capability to solubilize organic compounds in a limited space suggests micelles to be considered as micro- or nano- supramolecular reactors in which polar and nonpolar regions are

extremely close. Moreover the use of a micellar phase can have particular effects on the normal course of a reaction due to the following properties:

- The solvent effect due to the lower dielectric constant in the micelle than in water.
- The possibility to stabilize the transition state of the reaction via interaction with the surfactant's polar heads.
- The high concentration of the reactants within the micelle that might increase the rate of bimolecular reactions
- The acidity or basicity near the surface of the micelle that is significantly higher than in the bulk water phase.

Furthermore, the surfactant's properties establish several features of micelles, modifying the nano-environments where the reaction takes place. Therefore it is possible to obtain micellar catalytic systems¹⁶⁵ with various properties using different surfactants that can behave either as a simple medium capable to disperse water insoluble catalysts, or directly as reaction promoters themselves. A good deal of knowledge regarding this topic has been acquired during the contribution to the drafting of a review for Green Chemistry regarding the recent advances in catalysis in micellar media.¹⁶⁶

Prof. Bruce Lipshutz is one of the prominent figure in the surfactants field. His research group has designed and developed innovative surfactants to carry out several categories of reactions in water obtaining amazing results. In fact, many of the most important C-C, C-H, and C-heteroatom bond-forming reactions can show high performance under mild and environmentally friendly conditions.¹⁶⁷ Interesting results had already been obtained with first generation surfactant PTS, but more recently further advances were achieved when second generation surfactants TPGS-750-M were synthesized. This surfactants are diesters composed of lipophilic α -tocopherol moieties and a hydrophilic PEG-750-M chains, linked by succinic acid derivatives (Figure 39). The performances of these surfactants were so impressive that Sigma Aldrich decided to commercialize them.

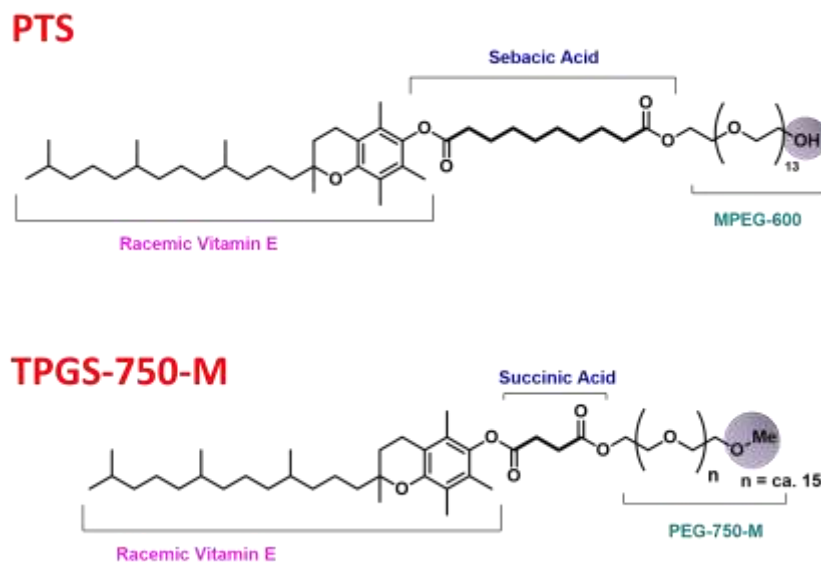
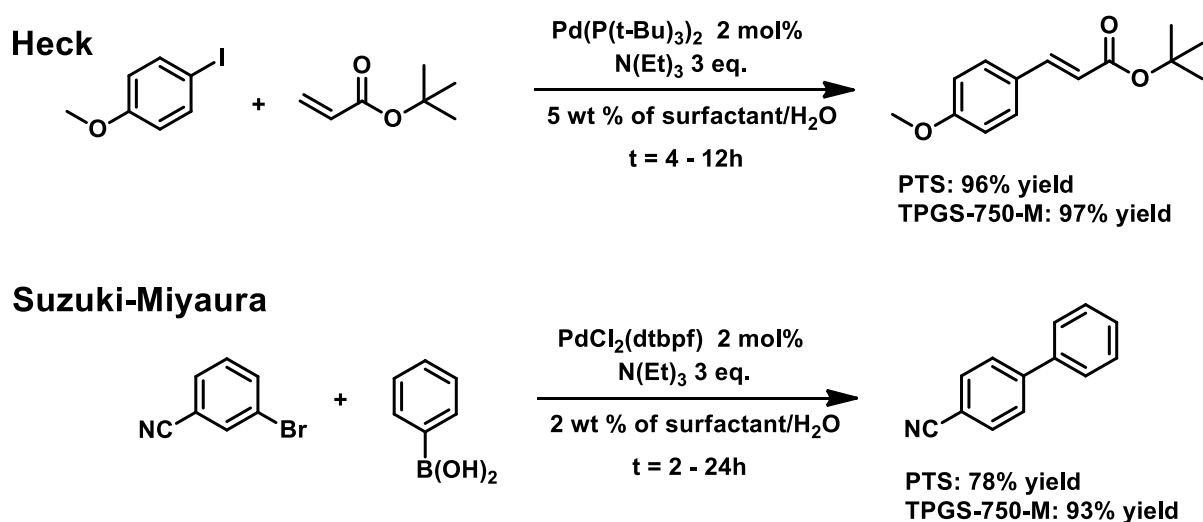


Figure 39. Surfactants developed by Lipshutz research group PTS (on top) and TPGS-750-M (below).

These surfactants generate micelles capable to accommodate several substrates and catalysts, allowing to the assembly of Pd- and Ru- systems that efficiently catalyse cross-coupling reactions at room temperature. The excellent results achieved in reactions such as Heck, Suzuki-Miyaura, Sonogashira and Negishi-like couplings and the physical measurements suggest that PTS and TPGS-750-M play a primary role in the synthesis of metal particles with proper size and shape to achieve high levels of conversion and good yields of products.¹⁶⁷



Scheme 11. Examples of results achieved during cross coupling Heck and Suzuki-Miyaura reactions in aqueous micellar media in the presence of either PTS or TPGS-750-M as surfactants.

4.2. Results and Discussion

4.2.1. Palladium Nanoparticles and Commercial Sulfonate Anionic Surfactants

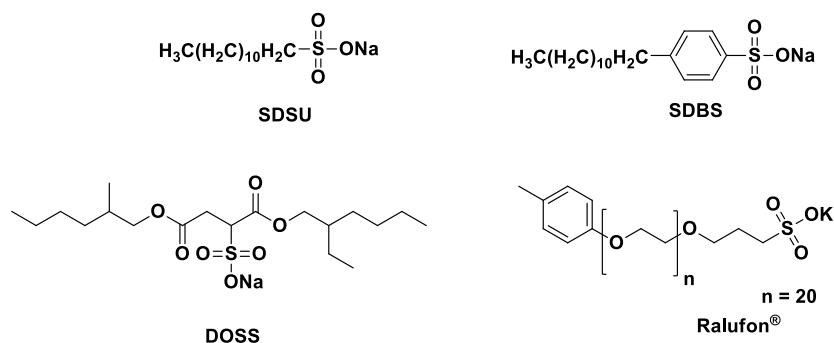
4.2.1.1. Metal nanoparticles and micelles

Nanoparticles are particles of any shape with dimensions in the 10^{-9} - 10^{-7} m range. When metal structures achieve these dimensions the metals show peculiar properties that attract the attention of several research fields.¹⁶⁸ Catalysis is one of the disciplines that most studied and exploited the advantages of using metal-nanoparticles (NPs). Metal NPs prepared for this purpose are usually obtained from the reaction of the proper metal salt and a suitable reducing agent. The presence of a stabilizer that prevents an uncontrolled growth of the nanoparticles is fundamental to reproducibly obtain active systems. The stabilizers can be of different kind, from solid supports such as carbon,¹⁶⁹ zeolites¹⁷⁰ and metal oxides¹⁷¹ to organic compounds like polymers,¹⁷² dendrimers¹⁷³ and many others.

As evidenced by the vast amount of literature on the subject, metal NPs are strongly attractive for catalysis due to their peculiar properties.¹⁷⁴ With the introduction of the “Green Chemistry” principles that promote the use of environmentally friendly solvents, the creation of systems able to stabilize metal NPs in water has become an attractive topic for research in catalysis. Nevertheless the use of water as a solvent is somewhat problematic as already mentioned. In fact, on the one hand it allows an easier product separation and catalyst recycling, but, on the other hand, most organic substrates are insoluble in water hampering the reaction. The use of surfactants proved to be an interesting solution to bridge these problems and stabilize metal NPs in water. In the literature there are several cases of micelles or larger assemblies employed for the stabilization of different metal species. Sometimes the presence of organic solvents is required and the surfactant allows the formation of microemulsions that stabilize the NPs. For example water/isooctane or hexane microemulsions in the presence of sodium di(ethylhexyl)sulfosuccinate and sodium tetraborohydride as reducing agent proved to stabilize Co-NPs in the size range 2-5 nm.¹⁷⁵ In other cases, in the presence of an appropriate aqueous systems, the employed surfactant can have other

additional functions. The spontaneous formation of Au NPs with an average diameter of 7-20 nm could be achieved when an hydrogen tetrachloroaurate(III) hydrate ($\text{HAuCl}_4 \cdot 3\text{H}_2\text{O}$) precursor was dissolved in air-saturated aqueous non ionic copolymers poly(ethylene oxide) – poly(propylene oxide) – poly(ethylene oxide) ($\text{PEO}_x\text{-PPO}_y\text{-PEO}_x$) solution without any reducing agent. The surfactant acts both as a reductant and as a stabilizer for the growth of Au NPs.¹⁷⁶ However the most used and most efficient surfactants that have been employed for the stabilization of NPs catalytic systems in water are usually either commercial or specifically synthesized cationic or zwitterionic ones.¹⁷⁷ In this context the most interesting and versatile example was the TPGS-750-M surfactant reported by Lipshutz and co-workers. The Pd NPs stabilized with this surfactant showed high activity in cross-coupling¹⁷⁸ and hydrogenation reactions.¹⁷⁹

The lack of examples in the literature on the use of anionic surfactants to stabilize metal NPs for catalytic systems operating in water prompted us to explore this area of research. In this respect commercial anionic sulfonated surfactants such as sodium dodecylbenzenesulfonate (**SDBS**), dioctyl sulfosuccinate sodium salt (**DOSS**), poly(ethylene glycol) 4-nonylphenyl-3-sulfopropyl ether potassium salt (**Ralufon**[®]) and sodium dodecyl sulfonate (**SDSU**) (Scheme 12) were used to study their properties as possible stabilizers of Pd-NPs based catalytic systems active in various hydrogenation reactions.



Scheme 12. Sulfonated anionic surfactants employed for the stabilization of Pd NPs in water.

4.2.1.2. Synthesis and characterization of the Pd NPs in the presence of surfactants

The purpose of “Green Chemistry” is not only to work with environmentally friendly systems but also to achieve them with simple, effective and economical methods. Therefore our

idea was to show the opportunity to synthesize Pd-NPs catalyst capable to work in water in the presence of commercially available surfactants following a facile and effective procedure.

We observed that when Pd(OAc)₂ was well dissolved in aqueous solution with SDSU under nitrogen atmosphere, a simple treatment with H₂ was sufficient to achieve the reduction of palladium. Therefore a standard procedure was tuned in order to make this reduction reproducible. The complete homogenization of the mixture containing Pd(OAc)₂ and SDSU was obtained by leaving the system under stirring for 1 h under nitrogen atmosphere. Subsequently, treatment with 1 bar of hydrogen for variable time caused the color change of the solution from orange to gray-black, indicative of the Pd reduction. Initially a study of the surfactant concentration was carried out in order to find the necessary amount requested to obtain a stable, reproducible and efficient catalytic system. Experiments at 20, 40, 60 and 80 mM SDSU in water were performed at room temperature using *trans*-2-hexenal (C₆) as a model substrate at a ratio of 50:1 with respect to the Pd(OAc)₂ introduced (Table 15).

[SDSU] (mM)	Yield (%)	
	After 10 min	After 30 min
20	30	70
40	21	71
60	35	92
80	29	>98

Table 15. Catalytic hydrogenation of *trans*-2-hexenal C₆ by Pd-NPs in SDSU micellar medium with different concentrations of surfactant in water. Experimental conditions: [Substrate] = 120 mM, [Pd(OAc)₂] = 2.4 mM (2%), p_{H₂} = 1 bar, water = 3 mL, t = room temperature.

The obtained results showed a correlation between both the stability of the catalytic system and the reduction time with the concentration of surfactant. In fact, a 5 minutes activation process with H₂ was necessary with 80 mM SDSU while lower concentrations of surfactant caused a gradual decrease of the reduction time. Nevertheless when a 20 mM SDSU catalytic system was employed the precipitation of Pd black (indicative of large Pd particles formation) was observed after approximately 30 minutes. Instead higher surfactant amounts conferred greater stability to the Pd-NPs allowing an increase in the catalytic activity and system stability and the best results were obtained with 80 mM SDSU. Because of its low CMC (0.9 mM)¹⁸⁰ and moderate water solubility, SDSU at the formal concentration of 80 mM is not completely dissolved in water causing the formation of an aqueous emulsion. Therefore the Pd catalytic system obtained with this surfactant does not operate under real micellar conditions but rather the Pd-NPs are likely to be stabilized by

interaction with the organic portion of the un-dissolved surfactant that avoids their aggregation into Pd black.

TEM analyses¹⁸¹ were carried out to understand the level of aggregation of Pd. The resulting images showed the presence of Pd-NPs with an average size of 4.6 nm and a size distribution between 2.0 and 7.5 nm (Figure 40).

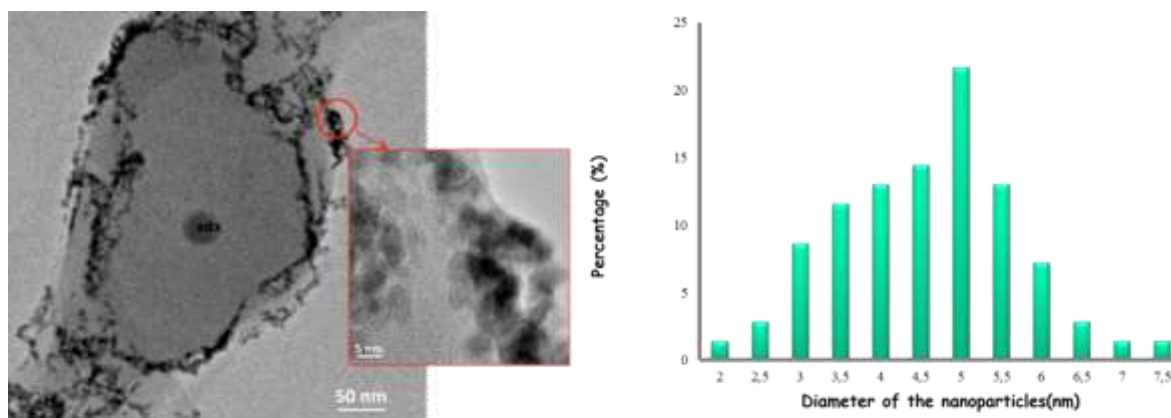


Figure 40. Tem image of Pd-NPs prepared at RT by H₂ flushing of a solution of Pd(OAc)₂ (2.4 mM) in the presence of **SDSU** (80 mM) as the surfactant in water (3 mL) (left) and size distribution determined for the Pd-NPs (right).

The round-shaped Pd-NPs are mainly confined as aggregates at the edge of a much larger organic aggregate formed by the surfactant. High resolution electron microscopy (HREM) evidenced that in most cases nanoparticles are pure Pd single crystals. Energy-dispersive X-ray analysis (EDX) of different areas of the sample evidenced the presence of Na and S atoms deriving from the surfactant, while the presence of palladium was further detected in the areas containing Pd-NPs.

The synthesis of catalytically active and stable Pd-NPs through a simple and inexpensive method prompted us to extend the procedure used with **SDSU** to other anionic sulfonated surfactants such as sodium dodecylbenzenesulfonate (**SDBS**), dioctyl sulfosuccinate sodium salt (**DOSS**), poly(ethylene glycol) 4-nonylphenyl-3-sulfopropyl ether potassium salt (**Ralufon**[®]) and sodium dodecyl sulfonate (**SDSU**). The concentration of surfactant employed was in all cases at least one order of magnitude higher than the corresponding C.M.C. and the concentration was further optimized in order to give to the system the highest stability using the lowest possible amount of surfactant. **SDBS** proved ineffective in stabilizing the Pd NPs at concentrations below 100 mM. **Ralufon**[®] and **DOSS** effectively stabilized nanoparticles at low concentrations but, soon after the addition of organic substrates, Pd black precipitated in both systems. 90 mM **DOSS** and 80 mM **Ralufon**[®] solutions proved necessary to obtain stable catalytic systems. The range of the

reduction times necessary to the Pd activation varied from a minimum of 2 minutes, as in the case of **Ralufon**[®], up to 10 minutes for **SDBS**.

After activation with H₂, the catalytic systems with the series of different anionic surfactants were analyzed by means of transmission electron microscope (TEM). Thanks to this technique, images of these samples were acquired showing the presence of differently dispersed pseudo-spherical nanoparticles with an average diameter of about 5 nm and a distribution between 2.0 and 7.5 nm (Figure 41). Even in these cases High Resolution Electron Microscopy (HREM) evidenced that the NPs were pure Pd single crystals.

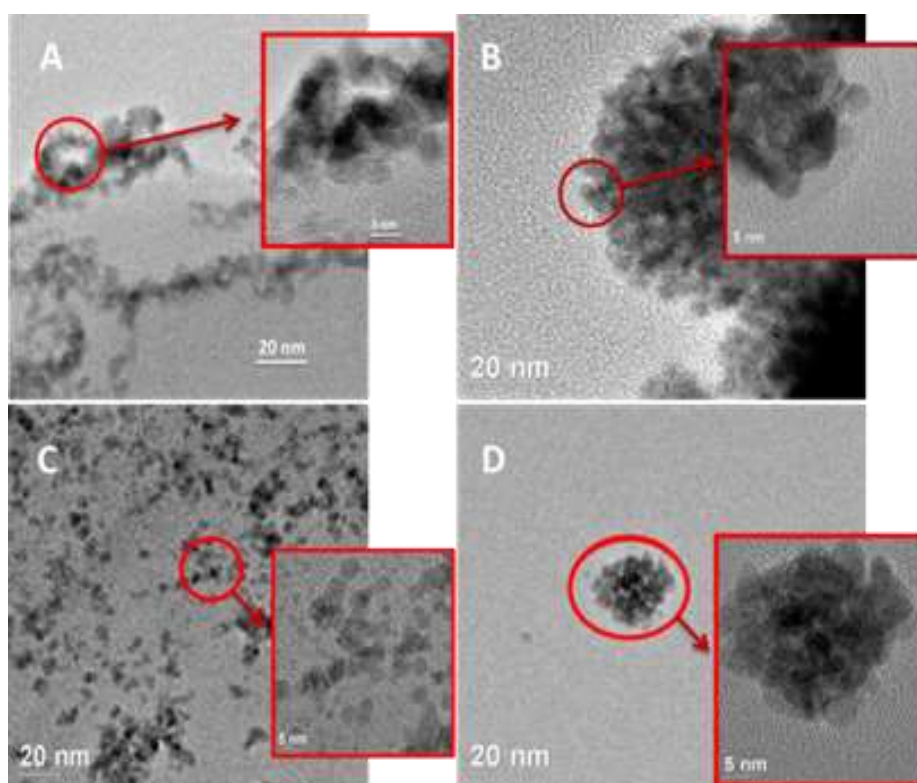


Figure 41 TEM images of the Pd-NPs stabilized by sulfonated anionic surfactant obtained stirring for 1 h and treating with hydrogen a solution of 3 mL of water with Pd(OAc)₂ 2.4 mM and A) **SDSU** 80 mM; B) **SDBS** 100mM; C) **DOSS** 90mM; D) **Ralufon**[®] 80mM.

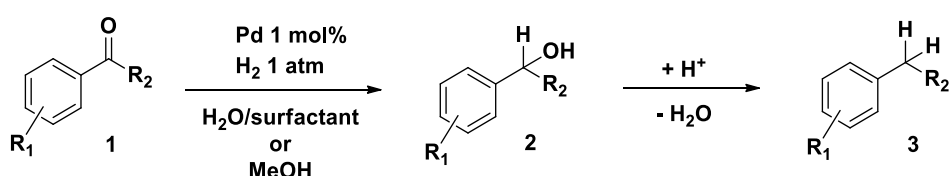
It must be said that samples for TEM analysis were obtained after drying to remove the solvent and for this reason TEM images may not be representative of the real nanoparticles morphology in solution, but they can be used to have an indication of the nature of the different samples. Therefore we could just say that the images showed well-dispersed and small-sized nanoparticles in the presence of **DOSS**, while slightly larger Pd-NPs, with **SDSU**, and more aggregated cluster nanoparticles, with **Ralufon**[®] and **SDBS**, were present.

4.2.1.3. Study of the Pd-NPs catalytic activity

The catalytic activity of the aqueous Pd-NPs solutions was tested in hydrogenation reactions with molecular hydrogen. In particular, the reactions that attracted our interest were i) the hydrogenation of aromatic ketones and aldehydes to alcohols and the subsequent aryl-alcohol reduction to toluene derivatives, ii) the selective semi-hydrogenation of alkynes to alkenes and the iii) hydrodehalogenation reaction of aromatic chlorinated compounds.

Hydrogenation of aromatic carbonyl and alcohol compounds

The hydrogenation of aromatic carbonyl compounds like ketones and aldehydes is usually carried out in the presence of hydrogen donors such as Polymethylhydrosiloxane (PMHS)¹⁸² or with molecular hydrogen. The reaction causes the formation of the corresponding benzyl alcohol, that can be further de-hydroxylated to the corresponding hydrocarbon (Scheme 13). In order to catalyze alcohol de-hydroxylation a source of acidity is normally required and for this purpose appropriate heterogeneous supports¹⁸³ or acid co-catalysts¹⁸⁴ could be used.



Scheme 13. Generic hydrogenation reaction of aromatic aldehydes and ketones catalysed by Pd at the experimental conditions tested in this work.

Preliminary tests showed that the catalytic systems with **SDSU**, **DOSS** and **Ralufon**[®] were suitable for this reaction, while the use of **SDBS** caused Pd black precipitation right after the addition of the substrate. The catalytic activity of **SDSU**, **DOSS** and **Ralufon**[®] systems in water was studied and compared with that in the presence of commercial heterogeneous Pd/C in methanol without adding sources of acidity (Table 16).

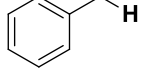
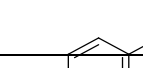
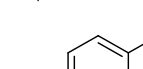

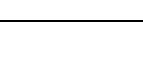
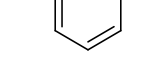
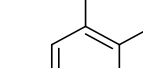

#	Substrate		Pd@SDSU ^a		Pd@DOSS ^b		Pd@Ralufon ^a		Pd/C	
1		Time (min)	50	350	60	500	60	350	10	50
		1a Conv. (%)	97	>99	97	>99	99	>99	94	>99
		2a (%)	88	1	92	1	96	80	73	-
		3a (%)	9	99	5	99	3	20	21	>99
2		Time (min)	40	120	60	120	70	500	10	60
		1b Conv. (%)	95	>99	97	>99	99	>99	91	>99
		2b (%)	62	-	76	-	96	3	68	-
		3b (%)	33	>99	21	>99	3	97	23	>99
3		Time (min)	40	150	60	250	120	500	10	30
		1c Conv. (%)	92	99	96	99	92	>99	97	>99
		2c (%)	77	2	78	4	74	2	55	-
		3c (%)	15	98	18	95	18	98	42	>99
4		Time (min)	50	350	70	500	90	350	10	50
		1d Conv. (%)	95	>99	98	>99	93	>99	98	>99
		2d (%)	90	-	91	1	92	85	71	-
		3d (%)	5	>99	7	99	1	15	27	>99
5		Time (min)	50	350	60	500	100		10	50
		1e Conv. (%)	96	>99	93	>99	98		99	>99
		2e (%)	81	-	90	1	95		68	-
		3e (%)	14	>99	3	99	3		31	>99
6		Time (min)	50	350	70	500	500		10	50
		1f Conv. (%)	97	>99	95	>99	95		98	>99
		2f (%)	89	-	90	1	90		75	-
		3f (%)	8	>99	5	99	5		23	>99
7		Time (min)	50	350	60	500	500		10	50
		1g Conv. (%)	98	>99	98	>99	98		97	>99
		2g (%)	84	-	94	1	96		70	-
		3g (%)	15	>99	4	99	2		27	>99
8		Time (min)	60	1440	1440		1440		60	1440
		1h Conv. (%)	94	99	90		45		97	98
		2h (%)	90	1	20		39		93	18
		3h (%)	4	98	70		7		4	80

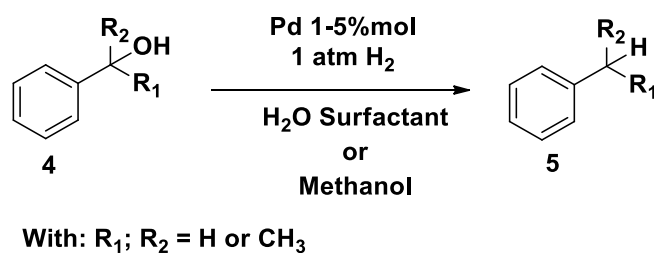
Table 16. Hydrogenation reaction of aromatic aldehydes **1a-d** and ketones **1e** with different Pd/surfactant combinations in water and with Pd/C in THF. Experimental conditions: [substrate] = 237 mM, [Pd] = 2.4 mM (1 mol%), p_{H₂} = 1 atm, water or THF 3 mL, t = room temperature. a) [SDSU] = [Ralufon[®]] = 80 mM; b) [DOSS] = 90 mM.

First of all the results reported in Table 16 showed the close dependence of the catalytic activity of Pd NPs systems in water with the nature of the surfactant. More specifically, comparing

the conversions over time in the hydrogenation reactions, the system with **SDSU** resulted the most catalytically active, while the use of **Ralufon**[®] caused the formation of the system with the lowest catalytic activity. Moreover, Pd/C in methanol seemed more active in the hydrogenation reaction of aromatic aldehydes if compared to micellar NPs systems in water. The high activity made the Pd/C much less effective toward the selective formation of alcohols from the corresponding aldehydes. This different selectivity was already evident when benzaldehyde **1a** was used as substrate. In fact Pd/C reached high conversions in 10 minutes but the amount of generated toluene **1c** was already very high (21%) without allowing to obtain the benzyl alcohol in good yields. Conversely, the micellar systems showed a much higher selectivity towards the benzyl alcohol and in the presence of **DOSS** and the **Ralufon**[®] the highest selectivities of 95% and 97% were obtained, respectively. To further investigate the selectivity of our catalytic systems we decided to use aromatic aldehydes as substrates endowed with activating groups such as 4-(tert-butyl)benzaldehyde **1b** and 4-methoxybenzaldehyde **1c**. The use of these substrates further highlighted the inefficiency of Pd/C in the selective formation of alcohols leading to increasing amount of toluene derivatives. The micellar catalytic systems still demonstrated a higher selectivity towards benzyl alcohol derivatives compared to Pd/C but their catalytic activities were much more affected by the electronic properties of the substituents present on the substrate. The catalytic systems with **SDSU** and **DOSS** suffered a sharp decrease in selectivity already in **1b** while **Ralufon**[®] caused the formation of toluene derivatives in small amounts. Unfortunately, in the presence of a particularly activated substrate like **1c**, **Ralufon**[®] showed a selectivity comparable to that obtained with the other surfactants. The use of variously methyl-substituted aromatic aldehydes **1d-1g** as substrates evidenced the different sensitivity to steric hindrance of the micellar catalytic systems. In the presence of **SDSU** and **DOSS** the catalytic activities of the Pd NPs were not affected by the steric hindrance of the methyl groups near the reaction site, just as for Pd/C. In fact the steric hindrance of such small groups was not very significant and this explains their low influence on the catalytic activity. In contrast, the Pd NPs with **Ralufon**[®] were much more affected by the presence of these mild steric hindrance effects causing a quite evident lowering in the catalytic activity. Nevertheless, the selectivity of this catalytic system still remained the highest.

When we began to investigate the catalytic activity of the micellar catalytic systems in the hydrogenation of aromatic ketones in water an unexpected result was observed. As can be seen in Table 16, entry 8, Pd NPs with **SDSU** converted acetophenone **1h** to the corresponding alcohol **2h** after 1 h with conversions very similar to those of the Pd/C in methanol. Moreover the micellar catalytic system caused the formation of higher amounts of **3h** with respect to Pd/C after 24 hours despite the absence of acidity sources. In the presence of **DOSS** conversions comparable to those

obtained with Pd/C were achieved while the low catalytic activity caused much worse results when **Ralufon**[®] was employed as surfactant. Therefore the micellar systems with **SDSU** and **DOSS** in water showed a catalytic activity at least comparable with that of Pd/C in methanol during the de-oxygenation reaction of **2h** to **3h**. In order to investigate better this aspect, we decided to compare Pd NPs in micellar media systems and Pd/C catalytic activities directly in the de-hydroxylation reaction of primary, secondary and tertiary benzyl alcohols using the already optimized conditions of the hydrogenation reaction of carbonyl groups (Scheme 14).



Scheme 14. De-oxygenation reaction of benzyl alcohols **4** to the corresponding alkylbenzene derivatives **5**.

The de-hydroxylation reactions of benzyl alcohol **2a**, 1-phenylethanol **2h** and 2-phenylpropan-2-ol **4** were first carried out in methanol under 1 atmosphere of H₂ in the presence of Pd/C (Pd = 1mol%) as catalyst in order to observe the different reactivity of these alcohols. In these conditions **2a** reacted quite rapidly and a quantitative conversion of the substrate was achieved after only 1.5 h while **2h** proved to be less reactive resulting in 70% conversion after 24 h. Even worse, an increase of the amount of Pd to 5 mol% was necessary to obtain only 40% conversion of **4** after 24h.

When we decided to perform these reactions with the Pd NPs in micellar media, the order of reactivity of **2a**, **2h** and **4** was confirmed and the use of **SDSU** and **DOSS** as surfactants proved to be very effective in the de-hydroxylation reaction of secondary and tertiary benzyl alcohols (Table 17).

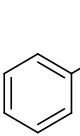
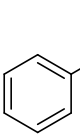
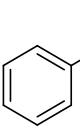
#	Substrate	Catalyst	Time (h)	Conversion (%)
1		Pd NPs with SDSU	6	>99
		Pd NPs with DOSS	10	>99
		Pd NPs with Ralufon [®]	24	50
		Pd/C	1,5	>99
2		Pd NPs with SDSU	20	>99
		Pd NPs with DOSS	24	>99
		Pd NPs with Ralufon [®]	24	10
		Pd/C	24	70
3 ^a		Pd NPs with SDSU	24	>99
		Pd NPs with DOSS	24	>99
		Pd NPs with Ralufon [®]	24	8
		Pd/C	24	40

Table 17. De-hydroxylation reaction of benzyl alcohols **4a-c** with Pd NPs with surfactants in water and Pd/C in THF. Experimental conditions: [substrate] = 237 mM, [Pd] = 2.4 mM (1 mol%), p_{H₂} = 1 atm, water 3 mL, t = room temperature., [SDSU] = [Ralufon[®]] = 80 mM, [DOSS] = 90 mM, a) [Pd] = 12mM.

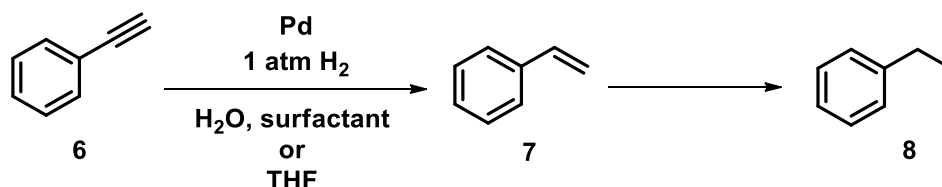
During the de-hydroxylation reactions of **2h** and **4** the aqueous micellar catalytic systems with **SDSU** and **DOSS** as surfactant showed a quite similar catalytic activity, higher than that of Pd/C in methanol. In fact, at the same conditions these catalysts led to a quantitative conversion of the substrates while the Pd/C did not guarantee the same good results. As expected Pd NPs with **Ralufon**[®] as surfactant turned out to be completely unsuitable for this type of reaction due to its low catalytic activity.

The high catalytic activity of systems with **DOSS** and **SDSU** in this de-hydroxylation reaction, in the absence of any external acid source could be explained considering the structures of the surfactants. In fact, these surfactants generate supramolecular aggregates with a negatively charged outer surface and the presence of negative charges could favor the presence of protons that could co-catalyze the de-oxygenation reaction of the benzyl alcohols. Obviously, the Pd/C did not present these features and also because of this in the absence of acidity sources its catalytic activity was much lower compared to systems with **SDSU** and **DOSS**. As long as the low catalytic activity of the aqueous micellar system with **Ralufon**[®] as surfactant was concern, this could be due to the

long PEG chains present in the molecular structures of the surfactants that probably keeps the catalytic site away from the anionic surface of the aggregates rather than favoring the interaction with the anionic surface made by sulfonate groups.

Catalytic semi-hydrogenation of alkynes to alkenes

The possibility of modulating the Pd NPs catalytic activity simply modifying the surfactant of the aqueous micellar medium is well suited for reactive substrates that undergo more than one catalytic step in sequence, especially when the intermediate species is desired. This is the case of the semi-hydrogenation of alkynes to the corresponding alkenes. This reaction is an extremely important chemical transformation since the production of *Z*-alkenes starting from internal alkynes allows to obtain important molecular building blocks for the synthesis of several fine chemicals.¹⁸⁵ The conventional heterogeneous approaches, including the traditional Lindlar catalyst¹⁸⁶ that makes use of toxic Pb salts, are based on metal catalysts like Pd on supports. The surface of their supports plays a key role in the pre-orientation of the substrates that lead the selective formation of the *Z* products,¹⁸⁷ even though sometimes possible isomerization of the product to the *E* isomer was observed. In recent years, most of the homogeneous catalytic systems developed for this reaction are mainly based on transition metal complexes (Ni,¹⁸⁸ Pd,¹⁸⁹ Pt,¹⁹⁰ etc.) in most cases operating in organic solvents. Recently Lipshutz and co-workers reported a new and efficient methodology to obtain a highly selective semi-hydrogenation of alkynes to *Z* alkenes using Pd NPs stabilized by TPGS-750-M as surfactant and NaBH₄ as catalyst activator and reducing agent.¹⁹¹ Considering the low atom efficiency of NaBH₄ and the interest to develop other “green” catalytic systems for this reaction, we decided to test the activity of our Pd NPs micellar systems in the semi-hydrogenation reaction of alkynes to alkenes in water with H₂ as reducing agent with higher atom efficiency. However, the employment of molecular hydrogen did not allow to selectively obtain the semi-hydrogenation product without stopping the reaction at the alkene level. This made necessary to follow the substrate conversion over time in order to get the moment when the greater conversion was obtained while preserving the high selectivity to the alkene.



Scheme 15. Hydrogenation reaction of phenylacetylene **6** to styrene **7** and further hydrogenation to ethylbenzene **8**.

First of all phenylacetylene **6** (Scheme 15) was selected as a model substrate to optimize the reaction conditions. Pd/C in tetrahydrofuran (THF) was used as a reference in order to investigate the normal course of the reaction in the presence of a commercial catalyst in the appropriate organic solvent. The reaction was repeated with different amounts of catalyst to maximize the selectivity to styrene **7**, achieving 96% conversion in 90 minutes with good selectivity (95%) in the presence of 0.04 mol% of Pd compared to **6**. Subsequently we decided to optimize the conditions to carry out the semi-hydrogenation reaction in water. Cetyl trimethylammonium bromide (CTAB) was also tested along with a series of anionic sulfonated surfactants. In the presence of CTAB a long activation with H₂ was required to achieve the change of the solution colour using the same procedure reported above for **SDSU**. This catalytic system allowed to achieve better results than Pd/C obtaining a 93% conversion with high selectivity (99%) in 80 minutes. However the presence of CTAB fairly deactivated the Pd NPs and a large increase in the amount of Pd was necessary (Table 18). Then we studied the catalytic efficiency of the systems with the anionic sulfonated surfactants under the same conditions. Unfortunately the micellar systems obtained with **Ralufon**[®] and **DOSS** proved unsuitable for this selective reaction. In fact when the conversion of **6** reached values in a range of 80-90%, the hydrogenation reaction of styrene became very fast and high yields of ethylbenzene **8** were obtained. Differently, the application of **SDSU** and **SDBS** gave Pd NPs micellar systems with both high catalytic activity and high selectivity. The results obtained with these surfactants are shown in Table 18.

#	Catalyst	[Surfactant] (mM)	Cat./Sub.	Solvent	Time (min)	Conversion (%)	Selectivity to 7 (%)
1	Pd/C ^a	-	0.01	THF	10	94	93
2	Pd/C ^b	-	0.001	THF	50	88	97
3	Pd/C ^c	-	0.0004	THF	90	96	95
4	Pd NPs with CTAB	80	0.01	H ₂ O	80	93	99
5	Pd NPs with SDSU	80	0.01	H ₂ O	50	94	97
6	Pd NPs with SDBS	100	0.01	H ₂ O	25	96	98
7	Pd NPs with SDBS ^d	100	0.005	H ₂ O	27	99	98
8	Pd NPs with SDBS ^e	100	0.0033	H ₂ O	120	96	97
9	Pd NPs with SDBS ^d	120	0.005	H ₂ O	75	85	98

Table 18. Semi-hydrogenation reaction of phenylacetylene **6** with Pd NPs and surfactant (CTAB, **SDSU** and **SDBS**) in water and with Pd/C in THF. Experimental conditions: Reaction volume = 3mL, p_{H₂} = 1 atm, t = room temperature. In THF: a) phenylacetylene (1.5mmol), 16 mg Pd/C ($1.5 \cdot 10^{-2}$ mmol); b) phenylacetylene (1.5 mmol), 1.6mg Pd/C ($1.5 \cdot 10^{-3}$ mmol); c) phenylacetylene (3.5 mmol), 1.6mg Pd/C ($1.5 \cdot 10^{-3}$ mmol). In H₂O: 1.6 mg Pd(OAc)₂ ($7.1 \cdot 10^{-3}$ mmol), phenylacetylene (0.7mmol), d) phenylacetylene (1.4 mmol), e) phenylacetylene (2.1 mmol).

The results reported in Table 18 showed that the Pd NPs aqueous micellar systems with **SDSU** and **SDBS** gave selectivity values comparable to those obtained with CTAB but with a higher catalytic activity. In particular the system with **SDBS** showed particular high activity and selectivity reaching 96% conversion in 25 minutes with a 98% selectivity to **7** and with the extra advantage with respect to Pd/C to operate in water instead of THF. Therefore we focused our attention on the study of the catalytic properties of the latter surfactant system and additional tests were carried out to optimize the amounts of **SDSU** and Pd(OAc)₂ in the reaction. From these tests we could observe that a 100mM solution of **SDSU** in water with 0.5 mol% Pd with respect to the substrate **6** allowed to obtain a highly active catalytic system characterized by high selectivity (Table 18, Entry 7). With the best catalytic system at hand, we applied this experimental conditions to a series of different alkynes, comparing the results observed with the traditional Pd/C catalyst (Table 19).

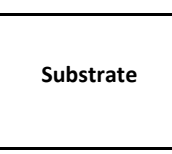
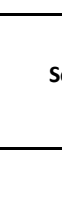
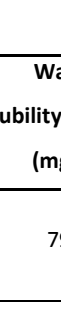
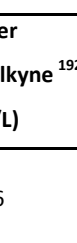

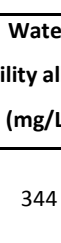




#	Substrate	Water	Water	Catalyst	Time (min)	Conversion (%)	Selectivity to alkene (%)
		Solubility alkyne ¹⁹² (mg/L)	Solubility alkene ¹⁹² (mg/L)				
1		796	344	Pd/C ^a	90	96	95
				Pd NPs with SDBS ^b	27	99	98
2		415	117	Pd/C ^a	70	98.5	95
				Pd NPs with SDBS ^b	45	>99	95
3		5	1	Pd/C ^a	60	88	93
				Pd NPs with SDBS ^b	20	93	95
4		19	5	Pd/C ^a	70	90	93
				Pd NPs with SDBS ^b	70	94	95
5		904	255	Pd/C ^a	40	95	84
				Pd NPs with SDBS ^b	80	99	95
6		10	3	Pd/C ^a	40	85	95
				Pd NPs with SDBS ^b	30	85	94
7		n.a.	n.a.	Pd/C ^a	60	80	97
				Pd NPs with SDBS ^b	50	77.5	97
8		n.a.	n.a.	Pd/C ^a	80	98	94
				Pd NPs with SDBS ^b	60	>99	97
9		n.a.	n.a.	Pd/C ^a	90	68	95
				Pd NPs with SDBS ^b	80	62	93
10		n.a.	n.a.	Pd/C ^a	80	97	90
				Pd NPs with SDBS ^b	90	98.5	88

Table 19. Semi-hydrogenation of alkynes **6-17** catalyzed by Pd NPs with **SDBS** in water and Pd/C in THF. Experimental conditions: Reaction volume = 3mL, p_{H_2} = 1 atm, rt. a) 1.6 mg Pd/C ($1.5 \cdot 10^{-3}$ mmol), [substrate] = 116.7 mM; b) 1.6 mg Pd(OAc)₂ ($7.1 \cdot 10^{-3}$ mmol), [substrate] = 46.7 mM, solvent = THF; [SDBS] = 100 mM, solvent = H₂O. n.a. not available.

No improvement in selectivity was obtained using Pd NPs in water with SDBS when the semi-hydrogenation reaction was carried out on aliphatic alkynes (Table 19, entries 7-10). However a generally better performances of Pd NPs in water with SDBS compared to the Pd/C in THF were observed in the presence of aromatic substrates, showing higher activity and selectivity. This

became more evident in the presence of substrates with electron donating substituents bound to the aromatic ring. Pd/C in THF proved less and less selective to the alkenes in the presence of substrates with electron donor substituents on the aromatic ring. Instead Pd NPs in water with **SDBS** were much less sensitive to the effect of the electronic properties of the substituents and the selectivity to alkene remained relatively elevated even at higher conversions (Table 19, entries 1-5). The reason of the selectivity loss in the presence of electron donor substituents was probably due to the higher capacity of the corresponding alkenes to coordinate the Pd. In fact triple bonds usually coordinate to the Pd metal center easier than double bonds due to their higher electron density. This allows alkynes to react with high conversions before producing alkanes. However, the presence of electron donating groups increases the electron density on the double bond and reduces the gap between alkynes and the corresponding alkenes in the coordination to Pd. As a consequence the double bond is faster converted, reducing the selectivity to the alkene for the semi-hydrogenation reaction. The presence of micellar aggregates, that forced the reaction to occur in its hydrophobic core, reduced this effect increasing the alkyne concentration close to the metal center. Only in the presence of 1-ethynyl-4-phenoxybenzene **13** as substrate the use of the catalytic system in water with **SDBS** did not bring any improvement in selectivity compared to Pd/C in THF. Overall, the obtained results clearly show that the semi-hydrogenation reaction of aryl alkynes catalyzed by Pd NPs in water with **SDBS** provided better selectivity with respect to the same reaction carried out in organic solvent. We further decided to apply this catalytic system to semi-hydrogenation reactions of internal triple bonds of aromatic alkynes. Unfortunately many substrates of this family were excluded because they are solid at room temperature hence hardly soluble in aqueous micellar solution. For this reason we decided to use 1-phenyl-1-propyne **18** and the 1-phenyl-1-hexyne **19** as liquid substrates to test this aspect (Table 20).

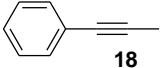
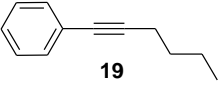
#	Substrate	Catalyst	Time (min)	Conversion (%)	Alkene (%)	Alkane (%)	Z:E
1		Pd/C ^a	35	>99	27	72	92.5 : 7.5
		Pd NPs with SDBS ^b	40	>99	57	42	94.5 : 5.5
2		Pd/C ^a	165	84	79	5	97 : 3
		Pd NPs with SDBS ^b	360	85	77	8	86 : 14

Table 20. Semi-hydrogenation reaction of internal alkynes **18** and **19** catalysed by Pd NPs in water with **SDBS** and Pd/C in THF.

Experimental conditions: Reaction volume = 3mL, H₂ pressure = 1 atm, rt. a) 1.6 mg Pd/C ($1.5 \cdot 10^{-3}$ mmol), [substrates] = 116.7 mM; b) 1.6 mg Pd(OAc)₂ ($7.1 \cdot 10^{-3}$ mmol), [substrate] = 46.7mM, solvent = THF; [**SDBS**] = 100 mM, solvent = H₂O.

Different results were observed for the two substrates. **18** demonstrated very high reactivity and the corresponding alkene was obtained in low yields. However the use of micellar medium somehow improved the semi-hydrogenation reaction yielding 57% of alkene. Substrate **19** was less reactive but the use of the micellar system did not afford any improvement. Moreover the hydrogenation of these internal triple bonds yields both *Z* and *E* isomers. Even if the hydrogenation reaction of **18** caused the formation of the corresponding alkane in large amount, in the presence of the aqueous micellar catalyst a Z:E ratio (94.5:5.5) was observed, slightly better than that obtained with Pd/C (92.5:7.5).

In conclusion, interesting results were obtained in the semi-hydrogenation reaction of aromatic terminal alkynes using the aqueous micellar catalytic system with Pd-NPs in the presence of **SDBS** as surfactant. Moreover working in the aqueous solvent this system achieved more significant values of selectivity to alkenes if compared to commercial catalyst such as Pd/C in organic media even in the presence of particularly reactive substrates.

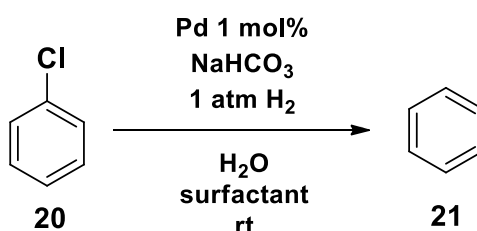
Catalytic hydrodechlorination of aromatic substrates

Many halogenated hydrocarbons are hazardous compounds that are quite persistent and difficult to eliminate by biological degradation. High amounts of these compounds are found in ground water of some industrial areas and they tend to bio-accumulate in the environment. Nevertheless, their biological degradation can be considerably improved by prior de-halogenation. For this reason several methods for the hydrogenolysis of chloroarenes using either stoichiometric and/or catalytic reagents have been developed. Unfortunately most of the devised systems suffer from incomplete dechlorination, low catalytic activity, low substrate/catalyst ratio or extreme

conditions.¹⁹³ Catalytic hydrodehalogenation is still a convenient and promising method for the decontamination of water from this kind of waste¹⁹⁴ and Pd-based catalysts proved highly active in this reaction.

Since our catalytic systems showed a good versatility in different reactions, we decided to test their catalytic activity in the hydrodehalogenation reaction of chlorinated aromatic compounds in water. The employment of surfactants increases the hydrophobic compounds solubility in water improving the efficiency of the catalysts due to an easier interaction with the substrates. This effect made Pd-NPs in micellar media particularly attractive for the disposal of pollutants from water.

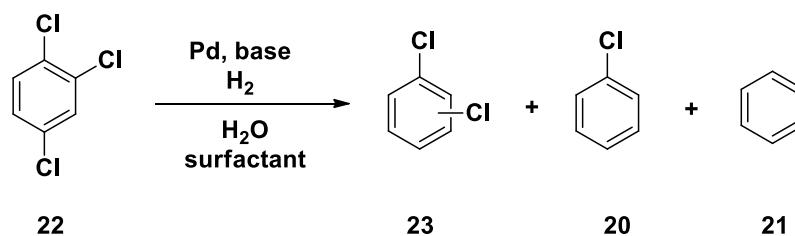
Chlorobenzene **20** was employed as a reference substrate and all Pd-NPs in water systems were tested at room temperature and 1 atm of H₂ in the presence of 1 equivalent of sodium bicarbonate as the base¹⁹⁵ (Scheme 16).



Scheme 16. Hydrodechlorination reaction of chlorobenzene **20** leading to benzene **21**.

When the Pd-NPs aqueous micellar systems with **SDSU**, **SDBS** and **DOSS** were employed in the hydrodechlorination reaction, the rapid precipitation of Pd black was observed after a short time without any conversion of the substrate. This is not surprising since liquid-phase hydro-dehalogenation reactions of chlorinated aromatic compounds with H₂ over palladium-supported catalysts are usually strongly deactivated by the HCl formed during the reaction.¹⁹⁶

The presence of **Ralufon**[®] as surfactant gave sufficient stability to the catalytic system in water and a quantitative conversion of the substrate **20** into benzene **21** was achieved under the conditions described above. The efficiency of this catalytic system could be attributed to the polyethyleneglycol groups (PEG) in the molecular structure of the surfactant that are particularly effective in the stabilization of Pd NPs.¹⁹⁷ Accordingly, the latter catalytic system was further tested in the hydrodechlorination of a polychlorinated aromatic substrate such as 1,2,4-trichlorobenzene **22** (Scheme 17). Since the reaction does not take place in a single step and each C-Cl bond reacts individually, the aim was to achieve a complete substrate dechlorination in order to reduce as much as possible its environmental impact.



Scheme 17. Hydro-de-chlorination reaction of the 1,2,4-trichloro-substituted benzene derivative **22** leading to several possible products.

The hydro-de-chlorination reaction of **22** was optimized in order to obtain a quantitative conversion to benzene **21**. As reported in Table 21 this result was achieved after a gradual change of some reaction parameters such as the amount of Pd(OAc)₂ and the equivalents of base (Entries 1-5). The quantitative formation of **21** was obtained under mild conditions (room temperature and 1 atm of H₂) in 24 hours increasing the amount of Pd (5 mol%) in the presence of an excess of base (Table 21, entry 7). In order to reduce the Pd amount required to achieve the quantitative formation of **21**, the H₂ pressure could alternatively be increased to 5 atm. Impressively, the Pd NPs system was stable under these conditions and excellent results in terms of catalytic activity were achieved even in the presence of only Pd 2 mol% with respect to **22** (Table 21, entry 6).

#	Cat/Sub	Sub/Base	H ₂ (atm)	Conversion (%)	Yield 23 (%)	Yield 20 (%)	Yield 21 (%)
1	1/100	1/3	1	83	30	7	46
2	1/100	1/3 ^a	1	71	36	5	30
3	2/100	1/3	1	90	33	7	50
4	2/100	1/6	1	90	24	6	60
5	2/100	1/9	1	95	17	3	75
6	2/100	1/6	5	>99	-	-	>99
7	5/100	1/6	1	>99	>1	-	99
8 ^b	5/100	1/3	1	>99	-	-	>99

Table 21. Hydrodechlorination reaction of **22** catalyzed by Pd NPs in aqueous micellar medium with as surfactant. Experimental conditions: [Pd(OAc)₂] 2.4 mM; water 3 mL; base = NaHCO₃; [Ralufo[®]] = 80 mM; room temperature. a) base = K₂CO₃; b) = Recycling, after products extraction with 3 aliquots of 15 ml of pentane.

The effective abatement of pollutants under mild conditions prompted us to investigate the possibility to recycle the catalytic system. The facile reuse of the catalyst lowers the cost of a

possible process, making the catalytic system more attractive for “Green Chemistry”. Hence when pentane was chosen to extract product **21**, the micellar system maintained a moderate stability. For this reason we decided to recycle the catalytic system after removal of the residual amount of pentane from the solution via rotary evaporator. When the micellar phase was recycled, the quantitative conversion of **22** to **21** was still achieved simply by introducing an equivalent amount of base. Therefore Pd-NPs in micellar medium with Ralufon[®] as surfactant showed high activity allowing quantitative dechlorination even in the presence of polychlorinated compounds as substrates under mild conditions or under higher H₂ pressures as well as high stability allowing the possibility to recycle the catalyst while maintaining the activity quite high.

4.2.1.4. Conclusions

We reported the facile, inexpensive and environmentally friendly preparation of Pd-NPs stabilized by commercial anionic sulfonated surfactants in aqueous medium. These NPs were simply obtained by leaving an aqueous solutions of Pd(OAc)₂ with an appropriate surfactant under stirring for 1 h under nitrogen atmosphere and afterwards flowing H₂ for variable times into the system. The Pd-NPs showed different size range, distribution and catalytic activity that could be modulated by the surfactant employed. Because of this property, these surfactant stabilized Pd-NPs proved to be more efficient with respect to commercial Pd/C in various hydrogenation and semi-hydrogenation reactions. The selective formation of the corresponding benzyl alcohols was achieved during the hydrogenation reactions of benzaldehyde derivatives in the presence of Ralufon[®] as surfactant. The catalytic systems with SDS and DOSS showed higher activity in the de-hydroxylation reactions of benzyl alcohols at room temperature and 1 atm of H₂ without any acid co-catalyst. The semi-hydrogenation reactions of aryl-alkynes to alkenes gave better results when SDBS was used as stabilizer for the Pd-NPS and higher selectivity was observed with respect to Pd/C in THF. To demonstrate a possible application of these systems we investigated also the decomposition of hazardous compounds in water via hydro-de-chlorination reaction. In this way we demonstrated that Pd NPs obtained in the presence of Ralufon[®] could convert quantitatively 1,2,4-trichlorobenzene under mild conditions in water. Moreover, the possibility to recycle the micellar phase was achieved without detrimental effects on the catalytic activity.

4.2.2. Multi-component synthesis of 1,2,3-triazoles promoted by micelles

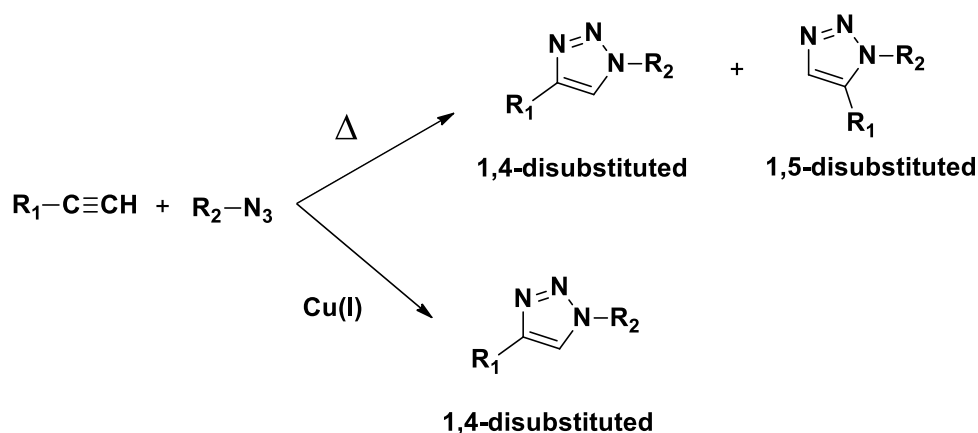
The results presented in this chapter were published in: E. Tasca, G. La Sorella, L. Sperti, G. Strukul, A. Scarso, "Micellar promoted multi-component synthesis of 1,2,3-triazoles in water at room temperature", *Green Chem.*, 2015, **17**, 1414-1422.

4.2.2.1. Two steps in one through micelles

After having demonstrated the possibility of obtaining simple, economic and efficient catalytic systems for hydrogenation reactions in aqueous media simply using commercial surfactant to stabilize Pd-NPs, we continued the search of peculiar applications of micellar systems in catalysis. In particular our interest focused on the hydrophobic nano-environments generated by micelles in water to carry out two-step syntheses in a single reaction mixture. The development of simplified catalytic systems able to work in environmentally friendly media (water) and easier to obtain, as made up of components that are commercial and characterized by low cost, is one of the fundamental objectives of green chemistry. Moreover, to emphasize how the use of these systems might be advantageous we looked for a reaction that would give important products for fine chemistry and needing improvement.

In recent years, organic compounds containing 1,2,3-triazoles as heterocyclic structures have showed interesting biological¹⁹⁸ and pharmaceutical properties.¹⁹⁹ In fact they exhibit high activity as anti-allergic,²⁰⁰ anti-viral,²⁰¹ anti-bacterial,²⁰² anti-cancer²⁰³ and anti-HIV²⁰⁴ agents, as selective β 3-adrenergic receptor agonists²⁰⁵ and as fungicides and herbicides.²⁰⁶ Moreover, 1,2,3-triazoles are finding attractive applications in supramolecular chemistry²⁰⁷ and in polymer science.²⁰⁸ Certainly the most efficient method to synthesize the 1,2,3-triazoles is the Huisgen 1,3-dipolar cycloaddition between alkynes and organic azides.²⁰⁹ The Huisgen reaction can be thermally activated, giving an approximate 1:1 mixture of 1,4- and 1,5-disubstituted 1,2,3-triazoles isomers,²¹⁰ and it is favoured by the use of particular substrates like strained cyclo-octynes,²¹¹ activated²¹² and electron deficient²¹³ alkynes under microemulsion conditions (Scheme 18).²¹⁴ Recently Sharpless²¹⁵ and Medal²¹⁶ demonstrated that the reaction becomes regioselective under mild conditions in the presence of Cu(I) catalyst obtaining the exclusive formation of the 1,4-regioisomer in high yields within a relative short time. Conversely 1,5-disubstituted 1,2,3 triazoles can be selectively obtained

with ruthenium catalysts²¹⁷ or with iridium complexes²¹⁸ when applied to electron rich internal alkynes (Scheme 18).



Scheme 18. Huisgen 1,3-dipolar cycloaddition between alkynes and organic azides giving approximate 1:1 mixture of 1,4- and 1,5-disubstituted 1,2,3-triazoles isomers in the case of thermally activation and the selective formation of 1,4-regioisomer in the presence of Cu(I).

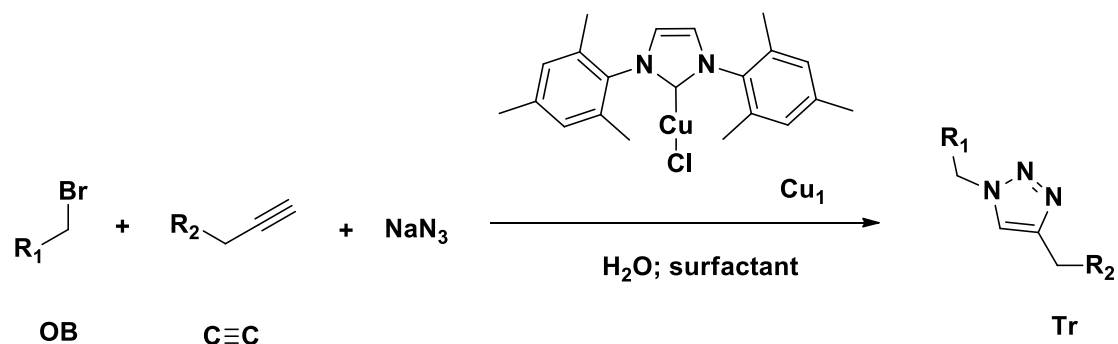
The Cu(I)-catalyzed azide-alkyne cycloaddition has become a key reaction for “click chemistry” a concept born to express the efficiency of these reactions. The simplest Cu(I) catalytic system is usually generated *in situ* from CuSO₄ in the presence of an excess of sodium ascorbate. However this system suffers from high metal loading, thus alternative methods were devised to catalyse the cycloaddition reaction. For example, preformed stable Cu(I) complex with phosphines like Cu(PPh₃)NO₃²¹⁹ or with PTA-iminophosphorane (PTA = 1,3,5-triaza-7-phosphaadamantane)²²⁰ or with nitrogen ligands like polytriazoles and tris(2-aminoethyl)amine derivatives (tren) could be employed. In order to obtain more efficient catalytic systems, Nolan recently developed a particular Cu(I) complex of the type [(NHC)CuX] (NHC = N-heterocyclic carbene, X = halogen),²²¹ while Cazin and collaborators²²² generated *bis*-carbenic complexes like the heteroleptic bis(N-heterocyclic carbene)copper(I) complexes and Whittlesey and co-worker produced ring-expanded carbene ligands.²²³ The catalytic properties of these systems are rather attractive as they showed high activity and selectivity working well under neat conditions at room temperature with high yields in the presence of Cu loadings lower than 1 mol%. Despite the solvent-free conditions are desirable in terms of green chemistry, they are not always optimal for this type of reactions because of the presence of potentially unstable small organic azides,²²⁴ the high exothermicity of the cycloaddition reaction and the possible presence of solid substrates that are difficult to solubilize in

the reaction mixture. Therefore multicomponent one-pot reactions between terminal alkynes and *in situ* formed organic azides from organic halides and NaN_3 were designed in order to avoid the pre-isolation of organic azides. Lately, alternative multicomponent syntheses from anilines and sodium nitrite under acid catalysis²²⁵ or from epoxides with sodium azide and alkynes avoiding the presence of organic bromides²²⁶ were developed. Most examples of multicomponent 1,2,3-triazole syntheses are carried out in water or under neat conditions using heterogeneously supported catalysts like $\text{Cu}(\text{OAc})_2$ on MCM-41,²²⁷ NHC–Cu(I) complexes on silica²²⁸ as well as magnetically recoverable heterogeneous Cu catalysts²²⁹ or copper nanoparticles on silica coated magnetic nanoparticles (5–30 nm).²³⁰ Usually these synthetic methods are carried out at 70–120 °C in order to achieve high yields in a few hours. Other alternative catalytic systems take advantage of mechano-chemical conditions in a ball milling apparatus using a copper vial at high temperature for at least 16 hours or they are based on insoluble in the reaction medium structurally well-defined Cu(I) isonitrile complexes²³¹ that can be recycled for at least five runs without significant loss of activity through a ready recover by precipitation and filtration. Completely homogeneous catalytic system that can be applied to the multicomponent reactions for the synthesis of triazoles are not many. Some of them require the presence of CuSO_4 at 100 °C in water with an excess of azide that acts as a reducing agent²³² while others work at room temperature exploiting complexes like the original $[\text{Cu}(\text{NHC})\text{X}]$ system developed by Nolan²²¹ or the PTA-iminophosphorane Cu(I) complex²²⁰ both in water in the presence of terminal aromatic alkynes as substrates. Only very recently, a supramolecular catalytic approach for this reaction was reported by Astruc who used dendrimers as nanoreactors for the solubilization of preformed Cu(I) species or *in situ* generated Cu(I) species from Cu(II) and ascorbate. This system is able to operate in water under mild conditions, requiring very low catalyst loading and it can be easily recycled.²³³

Exploiting the supramolecular properties of readily available and economical micellar systems to promote the one-pot multicomponent click reactions in water at room temperature was a fascinating opportunity. In fact, the employment of micellar media in triazoles synthesis has been rarely investigated and even less the direct formation from organic bromide (**OB**), alkynes (**C≡C**) and sodium azide, but always starting from organic azides.²³⁴ For this reason we decided to use a lipophilic Cu-complex such as the highly catalytically active²²¹ $[\text{Cu}(\text{IMes})\text{Cl}]$ (**Cu₁**) (IMes = 1,3-bis(2,4,6-trimethylphenyl)imidazol-2-ylidene) instead of the traditional Cu(II)/ascorbate system.

The employment of a micellar media allowed an effective dissolution of all the components of the reaction. The aqueous phase enabled the effective solubilization of the inorganic azide (NaN_3), while the micellar cores provided hydrophobic nano-environments capable to

accommodate apolar organic substrates like organic bromides, alkynes and the catalyst Cu_1 , increasing the reciprocal contact among these species. Therefore this system seems ideal to test the one-pot synthesis of 1,4- disubstituted 1,2,3-triazoles (**Tr**) with low catalyst loading (Scheme 19).



Scheme 19. Multicomponent cycloaddition reactions between organic bromides (**OB**), sodium azide and alkynes ($\text{C}\equiv\text{C}$) to 1,4-disubstituted 1,2,3-triazoles (**Tr**) mediated by $[\text{Cu}(\text{IMes})\text{Cl}] \text{Cu}_1$ in water at room temperature under micellar conditions.

The multicomponent synthesis of triazoles consists in two consecutive steps:

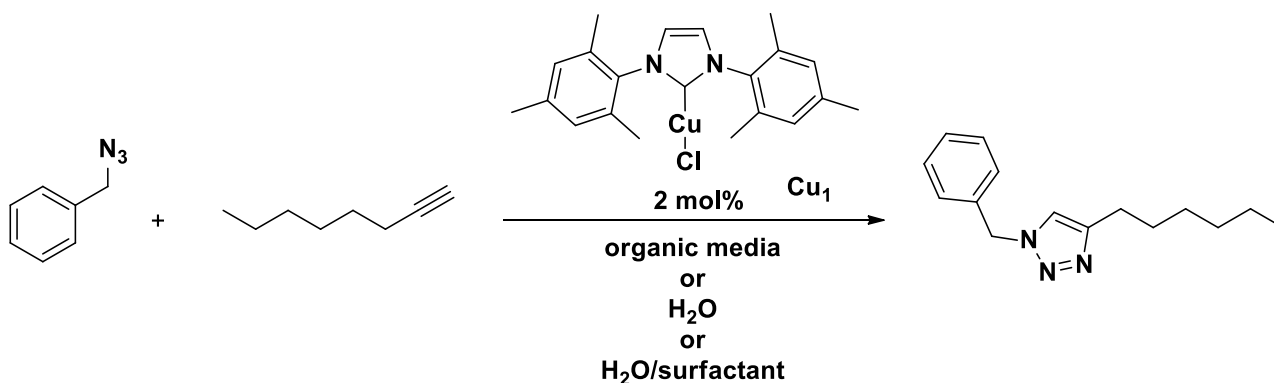
- the in situ reaction between sodium azide and organic bromide to give the organic azide;
- the triazole formation through the click reaction between the organic azide and the alkyne catalysed by the Cu(I) complex.

In order to find the best micellar system for this multicomponent reaction we investigated separately each step, screening several micellar media.

4.2.2.2. Micellar media for each step

Reaction between organic azides and alkynes

Initially we decided to investigate the metal mediated reaction between organic azides and alkynes in different media ranging from organic solvents to water with the addition of a wide range of surfactants searching for the best medium to dissolve all species and favour the cycloaddition reaction catalysed by $[\text{Cu}(\text{IMes})\text{Cl}] \text{Cu}_1$. For this purpose we used the pre-synthesized benzyl azide and the 1-octyne as referring substrates (Scheme 20, Table 22).



Scheme 20. Cycloaddition reactions between benzyl azide and 1-octyne to the corresponding 1,4- disubstituted 1,2,3-triazole catalysed by [Cu(IMes)Cl] **Cu₁** in different media.

#	Medium	Yield ^a (%)
1	CH ₂ Cl ₂	5
2	CH ₃ OH	2
3	H ₂ O	54
4	H ₂ O/CTAB	2
5	H ₂ O/SDS	23
6	H ₂ O/DDAPS	6
7	H ₂ O/Triton X-100	3
8	H ₂ O/TPGS-750-M	>98
9	H ₂ O/SLS	63

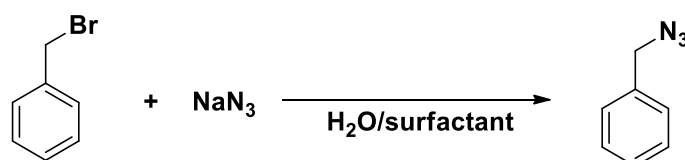
Table 22. Triazole synthesis from benzyl azide and 1-octyne catalysed by [(NHC)CuCl] **Cu₁** in several media. Experimental conditions: [benzyl azide] = 250 mM; [1-octyne] = 250 mM; [**Cu₁**] = 5 mM (2 mol%); [surfactant] = 180 mM, for TPGS-750-M 2% (w/w); solvent (1 mL), room temperature, 1 h. a) Determined by ¹H NMR.

As **Cu₁** operates efficiently under neat conditions, the reactions carried out both in apolar and protic organic solvent were very sluggish (Table 22, entries 1, 2). Conversely the presence of pure water as solvent caused an interesting increase in the activity of the catalyst **Cu₁**. This result was easily explained considering the poor solubility of both substrates and catalyst in water that provide pseudo-neat conditions and because of this promoted the **Cu₁** activity (Table 22, entry 3). When surfactants were added, the catalytic systems showed very different activity with regard to the properties of the micellar media. Ionic surfactants like SDS and CTAB, zwitterionic surfactant N-dodecyl-N,Ndimethyl-3-ammonium-1-propan sulfonate (DDAPS) and the non-ionic Triton X-

100 caused a clear decrease of the yield of triazole. The non-ionic TPGS-750-M proved to be the most performing surfactant for this reaction enabling the formation of the tetrazole product in high yields (>98%, Table 22, entry 8). Interestingly, the only exception to this trend was the anionic surfactant sodium lauryl sulfosuccinate (SLS) that improved the results obtained with just water at variance with what observed by other non-ionic surfactants, leading to 63% yield in the cycloaddition test reaction (Table 22, entry 9).

Reaction between sodium azide and organic bromides

An effective study on the effects of surfactants in the reaction between sodium azide and alkyl bromides for the synthesis of organic azides in water has never been done. Only a few examples of applications of systems such as cationic phase transfer species²³⁵ or surfactant pillared clays operating exclusively on α -tosyloxyketones under sonochemistry conditions and at high temperature²³⁶ have been reported in the literature. Therefore, also for this reaction we decided to compare the results obtained carrying out the reaction between sodium azide and benzyl bromide at room temperature for 1 h in different aqueous micellar media (Scheme 21, Table 23).



Scheme 21. Reaction between sodium azide and benzyl bromide leading to benzyl azide in different micellar media.

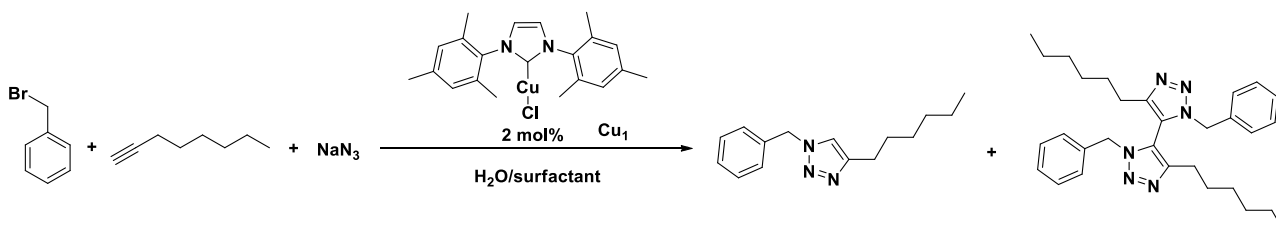
#	Medium	Yield ^a (%)
1	H ₂ O	36
2	H ₂ O/SDS	74
3	H ₂ O/CTAB	>98
4	H ₂ O/DDAPS	>98
5	H ₂ O/Triton X-100	>98
6	H ₂ O/TPGS-750-M	62
7	H ₂ O/SLS	79

Table 23. Benzyl azide synthesis from benzyl bromide and sodium azide in different aqueous media. Experimental conditions: [benzyl bromide] = 250 mM; [NaN₃] = 370 mM; [surfactant] = 180 mM, for TPGS-750-M 2% (w/w); water (1 mL), room temperature, 1 h. a) Determined by ¹H NMR.

As can be observed from the data reported in Table 23, the reaction between sodium azide and benzyl bromide was not favoured by the presence of pure water as solvent (entry 1). The reason of this effect was the poor contact between the two substrates since benzyl bromide is an organic compound slightly soluble in water, while sodium azide is completely soluble in water. For this reason the use of surfactants showed a general improvement in the yield of the triazole allowing a better solubilisation of benzyl bromide in the aqueous medium. In particular anionic SDS and SLS as well as non-ionic TPGS-750-M surfactants (Table 23, entries 2, 6 and 7) exhibited a good increase in the reaction rate and product formation, while excellent results were obtained in the presence of cationic CTAB, zwitterionic DDAPS and non-ionic Triton X-100 surfactants (Table 23, entries 3–5).

Direct multicomponent metal mediated synthesis of triazole from sodium azide, organic bromides and alkynes

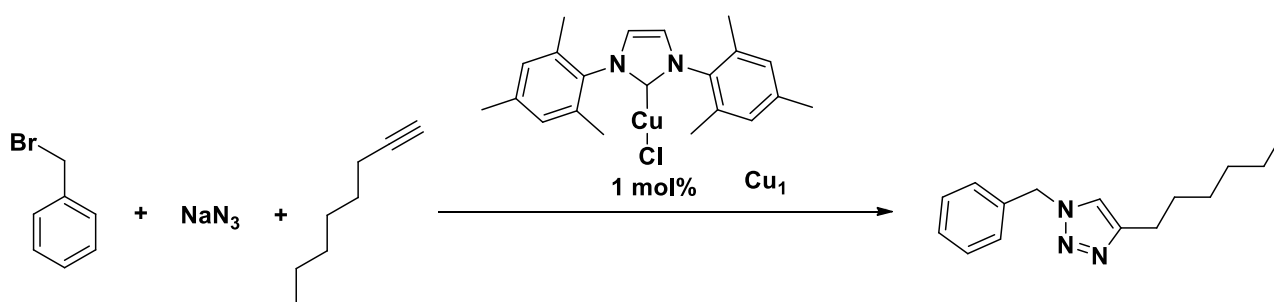
On the basis of the influence of surfactants on both steps of the reaction we investigated the direct three component reaction between benzyl bromide, sodium azide and 1-octyne catalysed by Cu_1 in different micellar media. When the catalyst was added to the reaction mixture since the very beginning, the formation of different amounts of a dimeric by-product 3,3'-dibenzyl-5,5'-di-n-hexyl-3H,3'H-4,4'-bis-1,2,3-triazole was observed together with the desired triazole product (Scheme 22).



Scheme 22. Formation of dimeric by-product 3,3'-dibenzyl-5,5'-di-n-hexyl-3H,3'H-4,4'-bis-1,2,3-triazole when the Cu-catalyst is added since the beginning of the reaction.

More specifically, 11% yield of this atropisomeric dimer was obtained in the presence of CTAB and DDAPS as surfactants, while the value decreased to 6% in pure water and to 4% with SDS. The formation of this product can be rationalized considering the initial 1-alkyne dimerization

catalysed by Cu_1^{237} and the subsequent double click reaction with benzyl azide on the two conjugated internal triple bonds. The formation of this by-product occurred in the early stage of the reaction when the catalyst interacted with the alkynes molecules in the presence of small amounts of the newly formed organic azide. To avoid this undesired effect, we modified the experimental procedure leaving 1-octyne, benzyl bromide and sodium azide to react for 1 hour and then adding the Cu_1 catalyst. With this expedient the amount of by-product was drastically decreased in all the micellar media considered (Scheme 23, Table 24).



Scheme 23. Direct reaction between benzyl bromide, sodium azide and 1-octyne catalysed by $[\text{Cu}(\text{IMes})\text{Cl}] \text{Cu}_1$ to the corresponding triazole in different aqueous media.

#	Medium	Azide Yield ^a (%)	Triazole Yield ^a (%)
1	H ₂ O	44	22
2	H ₂ O	54 ^b	37 ^b
3	H ₂ O	56 ^c	17 ^c
4	H ₂ O/SDS	86	1
5	H ₂ O/CTAB	93	7
6	H ₂ O/DDAPS	88	12
7	H ₂ O/Triton X-100	87	3
8	H ₂ O/TPGS-750-M	25	68
9	H ₂ O/TPGS-750-M	27 ^b	71 ^b
10	H ₂ O/TPGS-750-M	56 ^c	25 ^c
11	H ₂ O/SLS	18	73
12	H ₂ O/SLS	10 ^b	88 ^b
13	H ₂ O/SLS	46 ^c	26 ^c

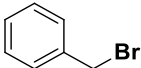
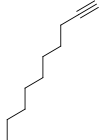
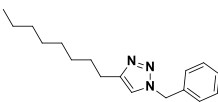
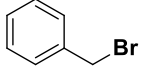
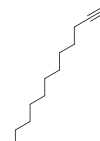
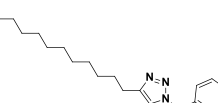
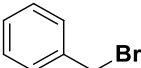
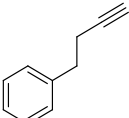
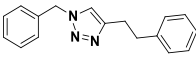
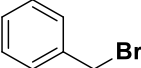
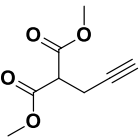
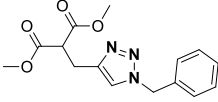
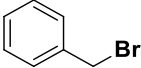
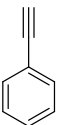
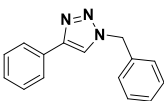
Table 24. Triazole direct synthesis from benzyl bromide, sodium azide and 1-octyne mediated by [Cu(IMes)Cl] **Cu₁** in different aqueous media. Experimental conditions: [benzyl bromide] = 250 mM; [NaN₃] = 370 mM; [1-octyne] = 370 mM; [**Cu₁**] = 2.5 mM (1 mol%); [surfactant] = 180 mM, for TPGS-750-M 2% (w/w); water (1 mL), room temperature. **Cu₁** added after 1 h; total reaction time 2 h. a) Determined by ¹H NMR. b) **Cu₁** added after 1 h; total reaction time 3 h. c) CuSO₄ (1 mol%) and sodium ascorbate (2%) added after 1 h; total reaction time 3 h.

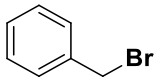
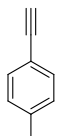
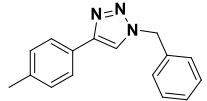
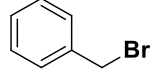
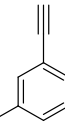
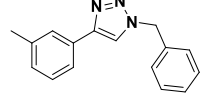
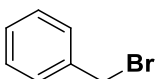
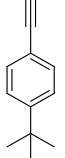
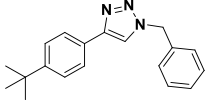
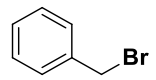
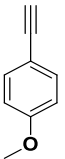
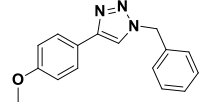
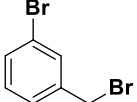
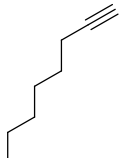
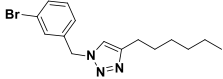
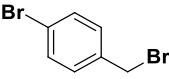
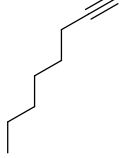
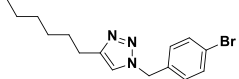
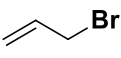
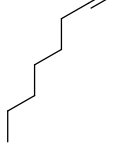
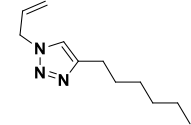
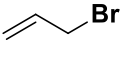
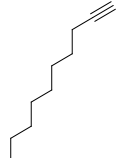
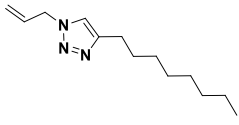
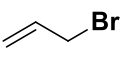
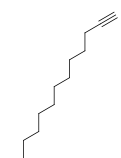
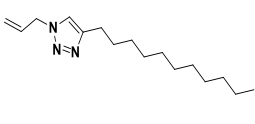
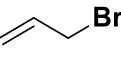
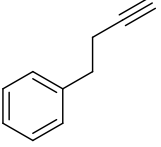
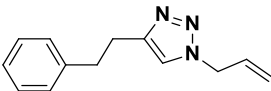
The data obtained during the direct multicomponent reaction approximately confirmed the trend observed in the preliminary investigations carried out on the two individual steps. The use of pure water as solvent showed only partial triazole formation (Table 24, entries 1-3) probably due to inefficient azide formation (Table 23, entry 1). SDS, CTAB, Triton X-100 and DDAPS surfactants proved inadequate for the direct synthesis of triazoles causing the formation of the product in very low yields (Table 24, entries 4–7) probably because of low efficiency in the click reaction (Table 22, entries 4 - 7). Conversely the neutral surfactant TPGS-750-M and the bis-anionic SLS caused respectively 68 and 73% yield of the corresponding triazole (Table 24, entries 8-13). These surfactants showed to be the best compromise promoting both the organic azide formation, the solubilisation of **Cu₁** and the click reaction. In order to increase the overall yield, the reaction was repeated running the click reaction for 2 hours instead of 1 hour in pure water or in the presence of

either TPGS-750-M or SLS. Under these conditions we observed a small increase in both the organic azide and triazole formation. Since SLS and TPGS-750-M proved to be the most efficient surfactants with **Cu₁**, we investigated their behaviour in the presence of *in situ* formed Cu(I) species from CuSO₄/ascorbate as a traditional catalyst for the click triazole synthesis (Table 24, entries 10, 13) comparing results with the same system in water (Table 24, entry 1). Using this catalytic system a general drop in the overall yield was observed compared to the results obtained with **Cu₁** achieving just a 26% yield at the best. A possible reason of this effect could be the poor lipophilicity of the *in situ* formed catalytic system that was insufficient to cause an effective dissolution in the micelles where substrates are hosted.

4.2.2.3. Scope of the reaction

In order to verify the possibility to apply the catalytic systems composed of **Cu₁** and either TPGS-750-M or SLS as surfactants in water, we investigated the use of a wide combination of organic bromides and alkynes with sodium azide (Table 25).

#	Organic Bromide	Alkyne	Triazole product	Medium	Azide Yield ^a (%)	Triazole Yield ^a (%)
1				H ₂ O	45	45
				H ₂ O/SLS	0	>98
				H ₂ O/TPGS-750-M	58	39
2				H ₂ O	56	31
				H ₂ O/SLS	17	77
				H ₂ O/TPGS-750-M	26	62
3				H ₂ O	65	16
				H ₂ O/SLS	9	87
4				H ₂ O	80	1
				H ₂ O/SLS	14	86
				H ₂ O/TPGS-750-M	26	67
5				H ₂ O	41 ^b	17 ^b
				H ₂ O/SLS	16 ^b	51 ^b
				H ₂ O/TPGS-750-M	19 ^b	46 ^b

6				H ₂ O	10 ^b	61 ^b
				H ₂ O/SLS	2 ^b	76 ^b
				H ₂ O/TPGS-750-M	21 ^b	42 ^b
7				H ₂ O	46 ^b	32 ^b
				H ₂ O/SLS	5 ^b	79 ^b
				H ₂ O/TPGS-750-M	15 ^b	65 ^b
8				H ₂ O	36 ^b	42 ^b
				H ₂ O/SLS	3 ^b	83 ^b
				H ₂ O/TPGS-750-M	34 ^b	42 ^b
9				H ₂ O	52 ^b	19 ^b
				H ₂ O/SLS	13 ^b	54 ^b
				H ₂ O/TPGS-750-M	50 ^b	25 ^b
10				H ₂ O	32	20
				H ₂ O/SLS	4	55
				H ₂ O/TPGS-750-M	18	25
11				H ₂ O	21	24
				H ₂ O/SLS	11	72
				H ₂ O/TPGS-750-M	13	18
12				H ₂ O	25	68
				H ₂ O/SLS	4	93
				H ₂ O/TPGS-750-M	2	98
13				H ₂ O	18	77
				H ₂ O/SLS	0	>98
				H ₂ O/TPGS-750-M	0	>98
14				H ₂ O	15	77
				H ₂ O/SLS	0	>98
				H ₂ O/TPGS-750-M	0	>98
15				H ₂ O	0	66
				H ₂ O/SLS	0	>98
				H ₂ O/TPGS-750-M	0	88

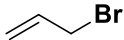
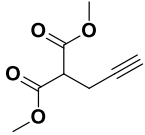
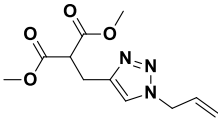
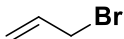
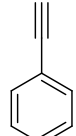
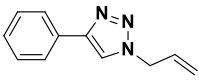
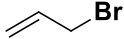
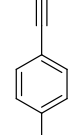
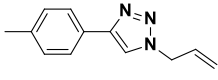
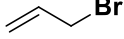
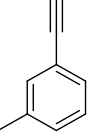
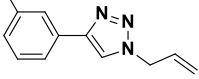
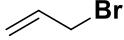
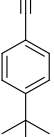
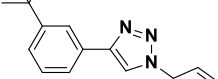
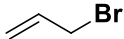
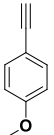
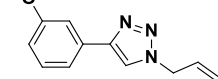
16				H ₂ O	44	56
				H ₂ O/SLS	8	92
17				H ₂ O	9 ^b	52 ^b
				H ₂ O/SLS	15 ^b	64 ^b
18				H ₂ O	3 ^b	56 ^b
				H ₂ O/SLS	0 ^b	>98 ^b
19				H ₂ O	0 ^b	53 ^b
				H ₂ O/SLS	0 ^b	>98 ^b
20				H ₂ O	0 ^c	53 ^c
				H ₂ O/SLS	0 ^c	>98 ^c
21				H ₂ O	0 ^c	0 ^c
				H ₂ O/SLS	14 ^c	>86 ^c
				H ₂ O/TPGS-750-M	35 ^c	>65 ^c

Table 25. Triazole direct synthesis from different organic bromides, sodium azide and alkynes mediated by [Cu(IMes)Cl] **Cu₁** in different aqueous media. Experimental conditions: [organic bromide] = 250 mM; [NaN₃] = 370 mM; [alkyne] = 370 mM; [**Cu₁**] = 2.5 mM (1 mol%); [surfactant] = 180 mM, for TPGS-750-M 2% (w/w); water (1 mL), room temperature, **Cu₁** added after 1 h; total reaction time 3 h. a) Determined by ¹H NMR. b) **Cu₁** added after 1 h; total reaction time 1.5 h. c) **Cu₁** (0.5 mol%) added after 1 h; total reaction time 1.25 h.

The reaction between a series of different terminal aliphatic alkynes with benzyl bromide and sodium azide was positively affected by the presence of SLS or TPGS-750-M as surfactants with respect to the same reaction in pure water. Particularly good yields for the corresponding triazoles were obtained in the presence of 1-decyne, 1-dodecyne, and 4-phenyl-1-butyne as substrates, reaching values in the range 77 to >98% (Table 25, entries 1-3). Moreover, it should be emphasized that even when the reaction in pure water gave negligible yields, the presence of surfactants TPGS-750-M and SLS allowed good results (Table 25, entry 4). When aromatic alkynes were used as substrates the reaction was highly favoured and in the presence of micellar media we observed a good reactivity of these compounds achieving interesting yields of triazole in 30 minutes (Table 25, entries 5-9). In particular, SLS in all cases ensured much higher yields compared to the use of pure water as the reaction medium. Observing the data collected using different benzyl

bromides such as 3-bromobenzyl bromide and 4-bromo-benzyl bromide in the multicomponent reaction, a three-fold increase of the catalytic activity in the presence of surfactants compared with pure water could be achieved (Table 25, entries 10, 11), even though the solid bromides tested dissolved with difficulty in the micellar medium.

Interesting results were obtained with allyl bromide that in the presence of aliphatic alkynes caused the quantitative formation of the corresponding triazoles in micellar media, while in pure water the yields were in the range 66–77% (Table 25, entries 12–15). Even the multicomponent reaction in the presence of propargyl dimethyl malonate was more effective with SLS and TPGS-750-M with respect to pure water (Table 25, entry 16). Moreover, allyl bromide proved quite reactive with aromatic alkynes in the presence of SLS as well as TPGS-750-M and the corresponding triazoles were quantitatively obtained in 30 minutes. The use of pure water as reaction medium caused a decrease in the reactivity mostly in the presence of less substituted alkynes (Table 25, entries 17–19). The high reactivity of the allyl bromide in micellar media with the electron rich aromatic alkynes reported in Table 25, entries 20 and 21, allowed to obtain the corresponding triazoles with very good yields in just 15 minutes and with a reduced catalyst loading down to 0.5 mol%, half of the value used in the previous reactions.

Unfortunately the reaction did not proceed using purely aliphatic halogenated substrates like butyl bromide or iodide because of the difficult formation of the corresponding organic azide. In fact the latter compounds are usually prepared either in polar non-protic solvents like DMSO or DMF²³⁸ at low temperature or in water with acetone under reflux.²³⁹ Moreover the multicomponent reaction was sluggish with terminal sterically hindered alkynes bearing substituents close to the triple bond like in the case of 3,3-dimethyl-1-butyne, ethynyl cyclopentene, ethynyl cyclohexane or with internal alkynes like 1-phenyl-1-propyne.

In almost all the cases reported, SLS proved to be the most effective surfactant for the reaction under investigation. For this reason it was chosen for the scale-up of the multicomponent reaction between sodium azide, benzyl bromide and 1-octyne catalysed by **Cu₁**. We increased to 2 mmoles the amount of organic bromide that was used as limiting reagent, the reaction was carried out under the same experimental conditions as those in Table 25 and the corresponding triazole was obtained in 82% isolated yield. These good results spurred us to carry out recycling tests of the Cu-catalyst. For this purpose we decided to investigate the reaction between benzyl bromide, sodium azide and dimethyl propargyl malonate in H₂O/SLS. After the extraction of the products with ethyl acetate, fresh substrates were added, obtaining at the end of the second cycle the corresponding triazole in just 27% yield together with 61% of the benzyl azide, showing the inability to effectively recycle the catalytic system.

4.2.2.4. Conclusions

In conclusion, we reported an extremely simple and efficient regioselective multicomponent synthesis of 1,4-disubstituted 1,2,3-triazoles from organic bromides, sodium azide and alkynes mediated by 1 mol% of [Cu(IMes)Cl] **Cu₁** catalyst in aqueous micellar media. The use of commercially available SLS or TPG-750-M surfactants was critical for the catalytic system as they generate apolar nano-environments favouring the *in situ* formation of the organic azide, avoiding its separate synthesis and storage. The micellar media were also responsible for the consecutive interaction between the organic azide and the alkyne catalysed by **Cu₁**. A wide variety of substrates could be employed with this catalytic system, achieving good yields in relatively short time and at room temperature. Moreover the triazole products could be easily isolated by means of simple extraction with ethyl acetate. All these characteristics make the one-pot reaction carried out with this catalytic system in water a very interesting and attractive innovation for green chemistry.

5. SUBSTRATE SELECTIVITY

5.1. State of the art

5.1.1. Learning from enzymes

Substrate selectivity is a typical property of the natural enzymes and describes their ability to choose among the possible available substrates the only one to be transformed. In a first approximation this selectivity can be justified by the formation of an intermediate complex between substrate molecule and the enzyme that was hypothesized for the first time by Svante Arrhenius in 1888.²⁴⁰ More recently the induced-fit theory was introduced to explain better the interactions between enzymes and substrate molecules. According to this theory the enzyme first pre-oriens the reagent through weak interactions. Then a precise spatial arrangement of the substrate molecules into the reaction site brings appreciable changes in the three-dimensional structure of the enzyme. This causes a new positioning of the functional groups within the active site that fit the guest molecule in a better way. This series of weak supramolecular interactions are essential in order to achieve substrate selectivity.²⁴¹

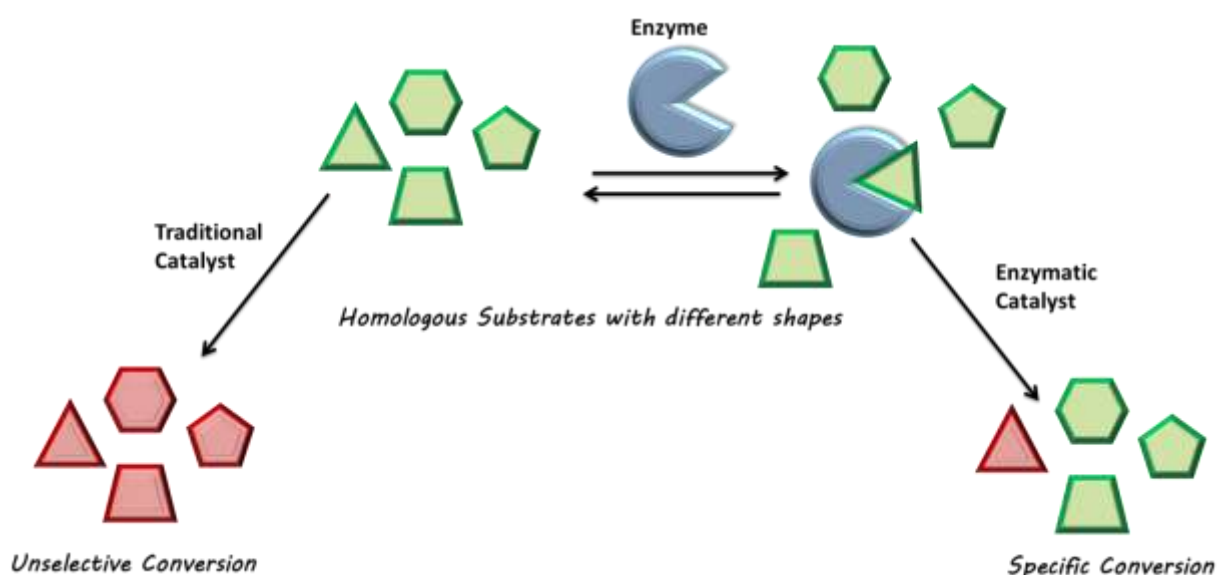


Figure 42. Differences between the unselective conversion in the presence of traditional catalyst and the Substrate selectivity typical of enzymes

More specifically an enzyme can exhibit four modes of selectivity of substrate:

- *Complete selectivity.* The enzyme catalyzes only one reaction with a specific substrate. This is the case of the succinate de-hydrogenase, that is specific for succinate.²⁴²
- *Group selectivity.* Only molecules with a specific functional group can react with the enzyme. A clear example of this category of enzyme is the Trypsin that can hydrolyze central peptide bonds in which the amino group belongs to basic amino acids such as arginine, lysine and histidine.²⁴³
- *Bond selectivity.* The enzyme can interact with a specific functional group regardless of the rest of the substrate molecule structure. This type of selectivity is typical of enzymes such as lipase that hydrolyzes ester bonds of different triglycerides.²⁴⁴
- *Stereochemical selectivity.* Only specific steric or optical isomers can interact with the enzyme. For example, D-amino acid Oxidase, catalyze the oxidation of several D-amino acid, but not the oxidation of L-amino acids.²⁴⁵

5.1.2. Artificial substrate selectivity

Examples of substrate selectivity in artificial catalysts are rare. As demonstrated by the catalytic activity of the enzymes, a three-dimensional structure and a large surface area to establish the proper interaction are required to observe this feature. For this reason the few categories of artificial catalysts characterized by substrate selectivity refer almost exclusively to heterogeneous catalysts and exploit the support porosity.

Zeolites are crystalline aluminosilicate derivatives with a huge variety of applications both as acid catalysts and as catalyst supports for nanometer-sized metal clusters, due to the presence of micropores with adjustable shape and dimension.²⁴⁶ The positioning of the active site in a confined space makes these catalysts shape selective with respect to substrates (molecular sieving), products and the reaction transition state resulting in unusual product distributions in many reactions.²⁴⁷ For example in a study of the Baeyer-Villiger oxidation reaction of cyclic ketones with hydrogen peroxide catalyzed by Sn supported on zeolites β , Corma and co-workers recently reported the

oxidation of 4-tert-butylcyclohexanone to the corresponding ϵ -caprolactone with 91% conversion while no conversion was observed when 2-tert-butylcyclohexanone was used.²⁴⁸

Montmorillonite is a mineral of the family of phyllosilicate whose structure contains aluminum and magnesium. Several cases of substrate selective catalysts obtained from metal-complexes supported on montmorillonite have been reported.²⁴⁹ An interesting application of this support was demonstrated by Choudary and co-workers who showed the existence of substrate selectivity in the competitive hydrogenation of a mixture of acrylates and cyclic olefins using montmorillonite-diphenylphosphinepalladium(II) chloride catalyst. The catalytic system provided good selectivity towards the methylacrylate when this was placed in competition with longer substrates, while no particular selectivity could be observed in the competitive hydrogenation of long acrylates. Comparable results in substrate selectivity were obtained in the competitive hydrogenation between cyclopentene and cyclohexene, cyclooctene or cyclododecene.²⁵⁰

In the absence of a matrix, like in ordinary homogeneous catalysts, substrate selectivity is quite unusual because of the low contact area capable to interact with reagent molecules. To increase selective substrate recognition two strategies have been followed: a) the selected reagent molecules contain additional functional groups that cause secondary interactions with the catalyst and increase their affinity;²⁵¹ b) the catalytic system is associated with a three dimensional structure capable to increase the contact area of the catalyst conferring steric hindrance effects in the interactions with the substrate molecules. Obviously the first option is not always possible and desirable, while creating catalytic sites surrounded by a three-dimensional supramolecular structure is a more general approach allowing to develop homogeneous catalysts with an enzyme-like behaviour. Initial attempts to combine homogeneous catalysis and three-dimensional structures was carried out using catalytic systems based on polymers.

Particularly interesting results in substrate selectivity were obtained by applying molecular imprinting technology to catalysis. The molecular imprinting technology is based on the synthesis of polymeric matrices possessing recognition sites obtained using a template molecule and monomers with appropriate functional groups. Template molecules spontaneously develop weak interactions with the monomers causing the formation of self-assembled structures that can be trapped in the two or three dimensional network obtained through a subsequent polymerization. The extraction of the template molecule generates the recognition site.²⁵² The very high selectivity of these materials was applied to catalysis observing in several cases intriguing substrate selectivity effects with different kinds of imprinted matrices. For example the radical co-polymerization of 4-(5)-vinylimidazole with divinylbenzene in the presence of derivatives of N-protected amino acids as imprinting molecules and Co(II) ions caused the formation of a matrix with cavities that exhibited

esterolytic activity.²⁵³ The hydrolysis reaction was carried out in the presence of various substrates such as N-t-boc-l-alanine p-nitrophenyl ester, N-t-boc-l phenylalanine p-nitrophenyl ester, N-t-boc-l-leucine p-nitrophenyl ester and p-nitrophenyl acetate in order to study the specific activity of this imprinted polymer. The highest activity was achieved in the presence of the first substrate whose molecular structure was very similar to that of the imprinted molecule, while a gradually lower catalytic activity was observed as the molecular structure became different.²⁵⁴ The substrate selectivity values were not so high, but interestingly depending on the nature of the imprinting molecule different selectivities could be achieved (Figure 43).

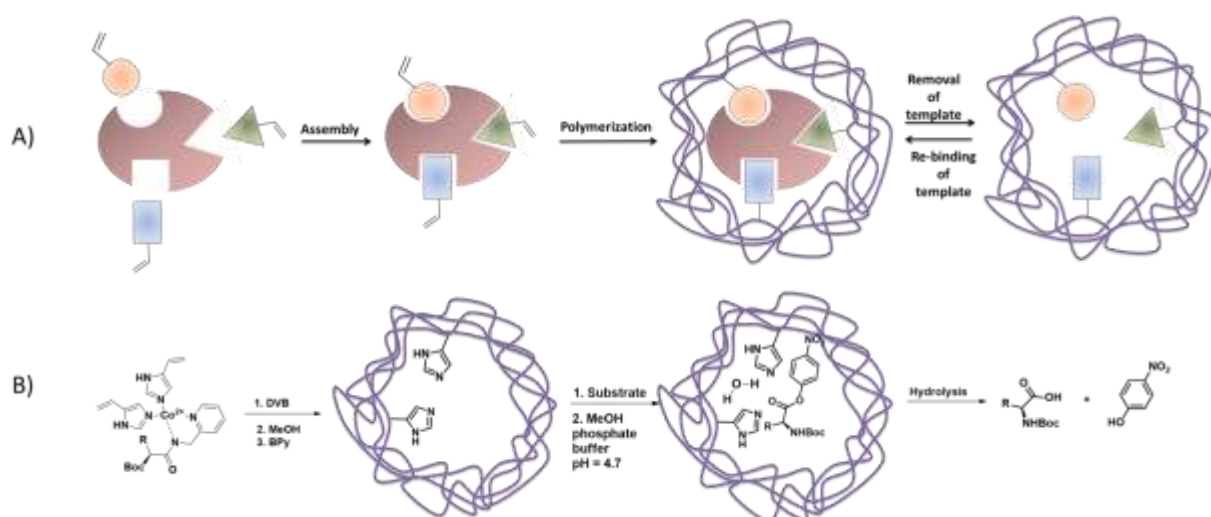


Figure 43. (A) General procedure for the synthesis of molecularly imprinted polymer that shows enzymatic activity and (B) synthesis of imprinted polymer for the substrate selective hydrolysis reaction of esters.

Dendrimers are another class of polymers that can be applied to catalysis as functionalized well-defined hyper-branched macromolecules. An enzyme-mimic catalyst can be obtained when transition metals are bound into the dendrimer's core.²⁵⁵ Crooks and co-workers described dendrimers behavior like nanoreactors that, stabilizing Pd nanoparticles within their nanoporous core, are capable to distinguish between substrates differing only slightly in their chemical structure. In fact, the steric hindrance on the dendrimer peripheral part is like a sizable grid that allows to control the approach of substrate molecules to the enclosed metal nanoparticles. The resulting effect was employed to achieve an elevated substrate selectivity during the competitive hydrogenation of allyl alcohol derivatives, observing the faster conversion of the smallest substrate.²⁵⁶

A second way to increase the contact area between the substrate and the catalytic system is to use a macromolecule possessing host cavities as a micro-reactor to perform chemical reactions.

The environment within the cavity is different from the external bulk solvent causing possible changes in the reaction pathway.²⁵⁷

The selective interaction of cyclodextrins can be properly used to achieve substrate selectivity in competitive reactions both when cyclodextrins are the catalysts²⁵⁸ and when an organometallic catalyst is accommodated within the cavity. Monflier and co-workers reported an interesting example of substrate selectivity in the Pd catalyzed Tsuji-Trost reaction with different pairs of structural isomers of water-insoluble alkylallylcarbonates and alkylallylurethanes through metal complexes encapsulation in cyclodextrines. α - and β -cyclodextrins derivatives caused a remarkable substrate selectivities towards linear structures with respect to branched ones.²⁵⁹

The idea of exploiting a cavity to obtain substrate selective catalysts has also been applied to self-assembling supramolecular capsules. Raymond and co-workers reported size- and shape-specific substrate selectivity in the catalytic isomerization of allylic alcohols when a Rh catalyst was encapsulated in a Ga_4L_6 tetrahedral capsule. The empty space within the cavity conferred high substrate selectivity to the encapsulated Rh-complexes and the competitive reaction between the easy to encapsulate allyl alcohol and the sterically bulky crotyl alcohol led to the selective conversion of the former (Figure 44).²⁶⁰

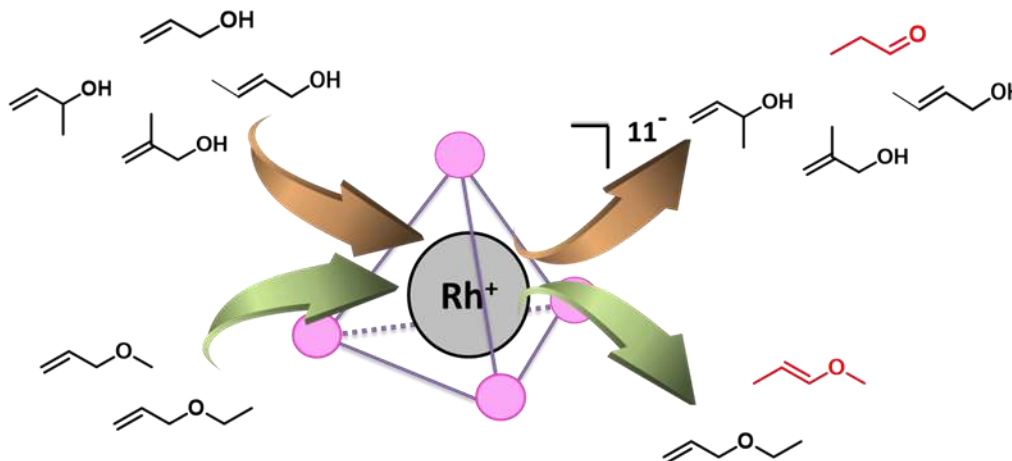


Figure 44. Substrate selectivity conferred by Raymond capsule to the Rh-catalyst in the competitive isomerization reaction of allyl alcohols and ethers.

Scarso and co-workers demonstrated the regio-selective catalytic activity of (NHC)-Au complexes within a resorcin[4]arene capsule in the hydration of terminal alkynes. The competitive hydration of a series of terminal alkynes showed interesting results also in terms of substrate selectivity. The restricted space available for substrate molecules in the cavity after encapsulation of the Au-complex caused the preferential conversion of aliphatic cyclic compounds in competition

with linear ones because the latter are forced to assume a more compact shape through several conformation torsions. With rigid aromatic substrates the host-guest system exhibited an inverse selectivity compared to the free Au-complex in solution leading to the faster conversion of rigid aromatic alkynes even if less electron rich and intrinsically less reactive.⁶²

Another method allowing high substrate selectivity is the use of organometallic complexes whose ligands provide a steric hindrance that regulates the access of the substrate molecules to the catalytically active metal center. An example of these systems was reported by Mandolini and co-workers on specific salophen-uranyl complexes. These metal catalysts showed different catalytic activity in the addition of benzenethiols to methyl substituted 2-cyclohexen-1-one derivatives. When combined with tertiary amines the system was highly active due to base activation of the thiol nucleophile and the metal activation of the enone. The steric hindrance around the free coordination site of the metal could be modified generating a pocket with a limited interior space through the presence of two parallel phenyl groups in the salophen ligand structure. The resulting controlled access to the catalytic site provided a high degree of substrate selectivity (Figure 44).²⁶¹

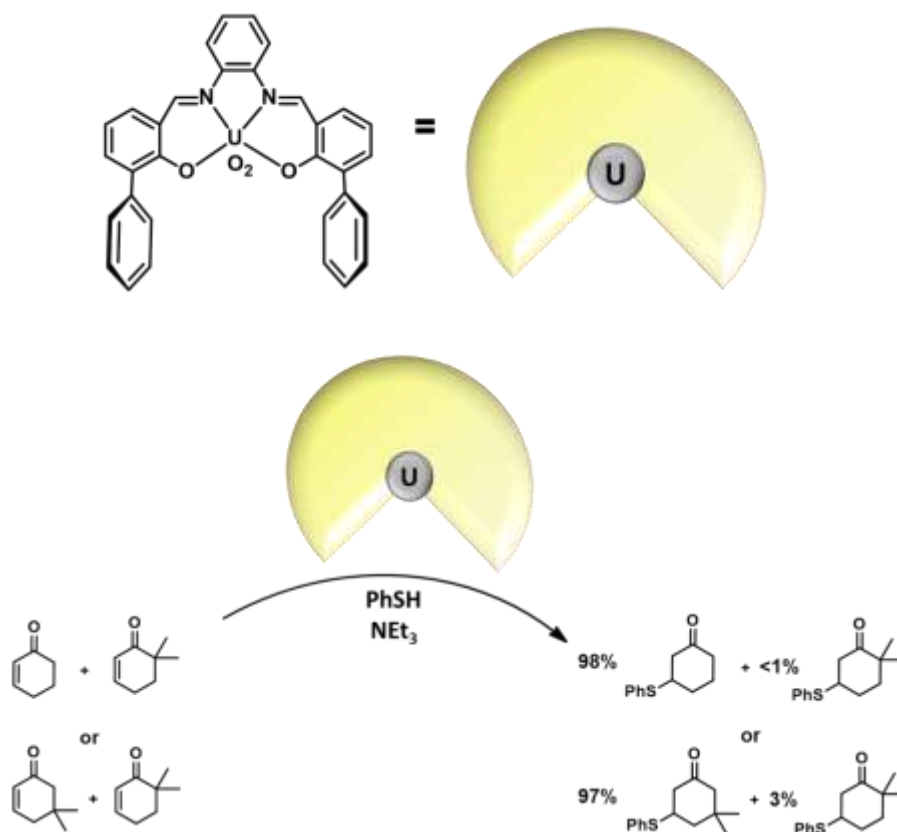


Figure 45. Modified salophen-uranyl complexes showed substrate selectivity in the competitive addition reaction of thiophenol to 2-cyclohexen-1-one derivatives variously substituted with methyl groups.

Micellar media have already proved to confer peculiar product selectivity²⁶² with particularly interesting results in diastereo- and enantio-selectivity.²⁶³ The presence of a catalytic system in an hydrophobic microenvironment solubilized in water can be used to achieve the faster conversion of hydrophobic substrates compared to hydrophilic ones that are not susceptible to enter the micelles. Cases in which this effect is used to obtain of substrate selectivity in competitive reactions are rarely described. Kobayashi and co-workers reported a catalytic acid-surfactant-combined system applicable to various reactions including esterification. This reaction was carried out in water in the presence of dodecylbenzenesulfonic acid (DBSA) as surfactant that can act as a Brønsted acid-surfactant-combined catalyst (BASC) showing the importance of the dual function of this molecule in order to catalyze the esterification reaction with high conversion at 40°C. Moreover when the competitive esterification of a 1:1 mixture of lauric acid and acetic acid was carried out using this catalytic system a faster conversion of the more hydrophobic substrate was obtained (Figure 44).²⁶⁴

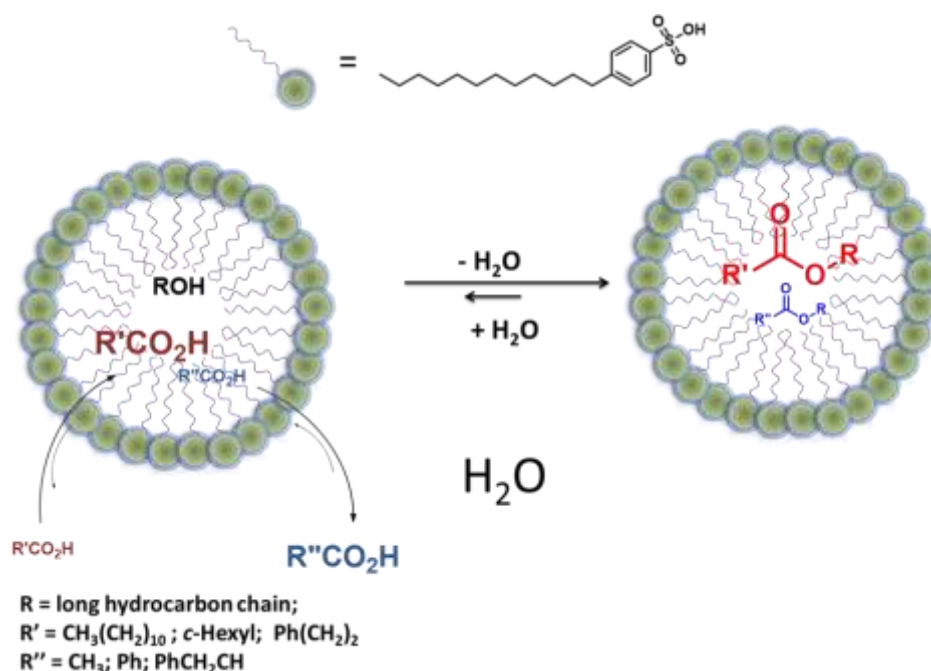


Figure 46. Catalytic effect of dodecylbenzenesulfonic acid (DBSA) in the substrate selective esterification reaction in water

Finally, Scarso and co-workers reported another interesting example of hydrophobic effect driven substrate selectivity in micellar media. The competitive Diels Alder reaction between cyclopentadiene and C₄-C₁₀ α,β-unsaturated aldehydes catalyzed by Cr(III)(salen)Cl showed a 3.5 fold increase in activity in favor of longer substrates compared to shorter ones simply by the presence of a micellar media. Indeed the same catalytic system operating in chloroform did not give any particular selectivity.²⁶⁵

5.2. Results and Discussion

The results presented in this chapter were published in:

- S. Giust, G. La Sorella, L. Sporni, G. Strukul, A. Scarso, “*Substrate Selective Amide Coupling Driven by Encapsulation of a Coupling Agent within a Self-Assembled Hexameric Capsule*”, *Chem. Commun.*, 2015, **51**,1658-1661;
- G. La Sorella, M. Bazan, A. Scarso, G. Strukul, “*Competitive micellar induced substrate selectivity in the Pd mediated heck coupling between iodoaryl substrates and linear acrylic esters in water*”, *J. Mol. Catal. A: Chem.*, 2013, **379**, 192-196;
- G. La Sorella, P. Canton, G. Strukul, A. Scarso, “*Surfactant-Induced Substrate Selectivity in the Palladium-Nanoparticle-Mediated Chemoselective Hydrogenation of Unsaturated Aldehydes in Water*”, *ChemCatChem*, 2014, **6**,1575-1578.

5.2.1. Substrate selective amide coupling driven by self-assembled resorcin[4]arene capsule

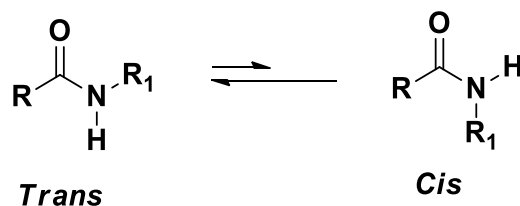
The 3D structure of the resorcin[4]arene capsule causes the formation of a confined space inside the cavity. The walls of the capsule determine a steric restriction that limits the size and the shape of the molecules that can be hosted within the cavity. This effect can be used to obtain catalytic systems exhibiting peculiar properties compared to traditional homogeneous catalysts. The most interesting of these properties is substrate selectivity.

In order to demonstrate an innovative and effective application of the supramolecular capsule to achieve substrate selective catalytic systems, 1-ethyl-3-(3-dimethylaminopropyl) carbodiimide hydrochloride (EDAPC) was used as amide coupling agent. We inferred that EDAPC could be a good guest for the resorcin[4]arene capsule and could force the coupling reaction to take place within the supramolecular cavity.

5.2.1.1. Carbodiimides as amide coupling agents

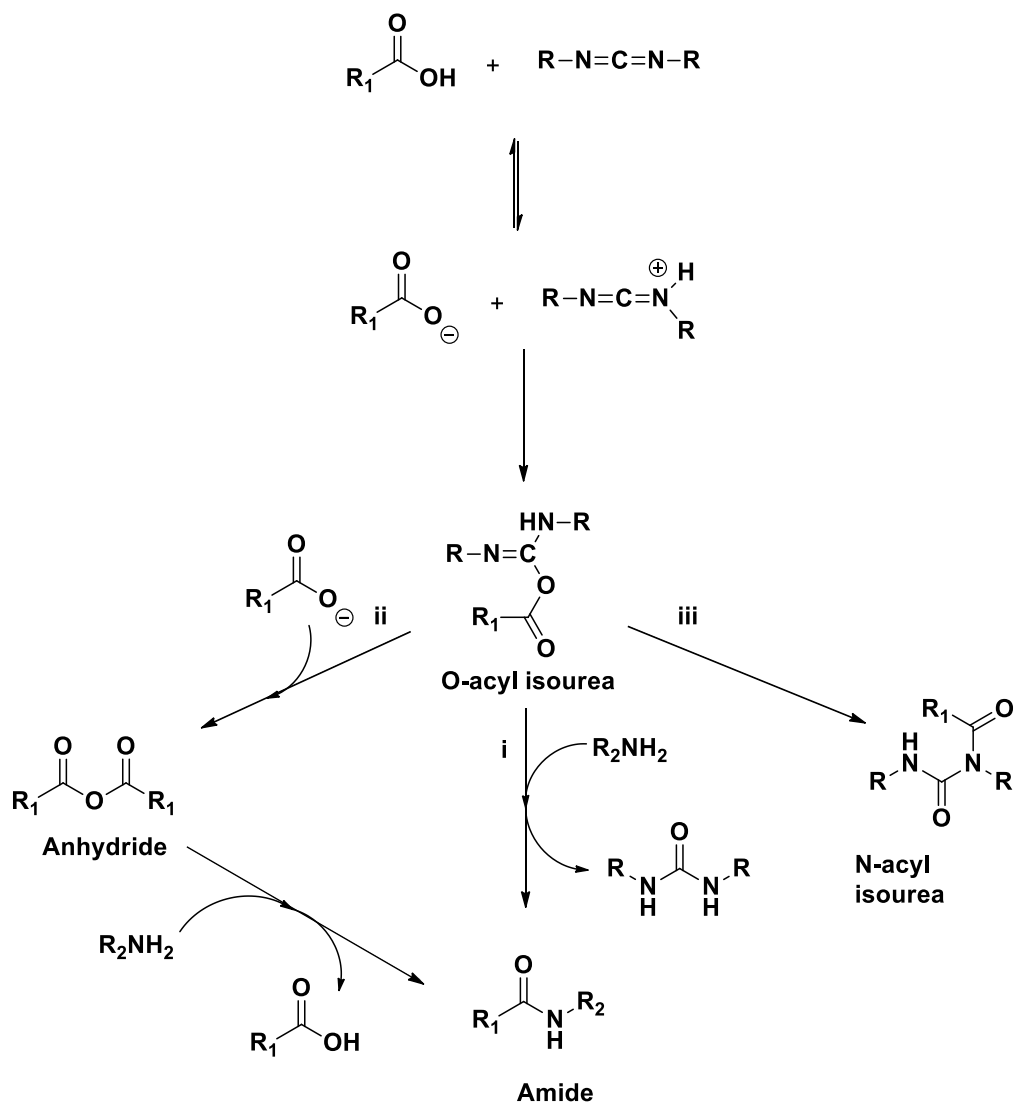
The amide bond play a pivotal role in biological processes being the functional group present in proteins but it is also extremely common in medicinal chemistry being present in more than 25% of known drugs²⁶⁶ as well as in the industrial synthesis of polymers such as nylon. The delocalisation of electrons over the N-C-O bond causes an almost completely rigid structure that

can assume both cis and trans configuration. However the cis configuration is quite uncommon due to the much higher stability of the trans isomer (Scheme 24).²⁶⁷



Scheme 24. Cis and Trans conformations of a generic amide bond.

Acyl halides, acyl azides, acylimidazoles, anhydrides, esters and similar compounds are often used as substrates to prepare amides.²⁶⁸ Alternatively, the amide bond can be obtained through a direct condensation reaction between a carboxylic acid and an amine. The use of these substrates is highly desirable due to their ready availability, the good atom economy and the low environmental impact of the reaction, being water the only side product. Unfortunately, the direct condensation has to overcome the thermodynamic barrier of the salt formation due to the spontaneous acid-base reaction.²⁶⁹ Therefore high temperature (160-180°C) should be reached in order to synthesize amides from amines and carboxylic acids, but these conditions are often incompatible with other functional groups. Accordingly either coupling agents capable to activate the carboxylic acid towards nucleophilic attack of the amine or metal and non-metal²⁷⁰ catalytic systems are used to favour the reaction. As yet the most common agents used for this purpose are carbodiimides. The mechanism of carboxylic acid activation by a generic carbodiimide is reported in scheme 25. At first, carboxylic acid interact with carbodiimide to form O-acylurea as an intermediate. Subsequently this intermediate can undergo several processes causing the formation of different products: i) the direct reaction with amine causes the formation of the desired amide and the corresponding urea of the carbodiimide employed; ii) the attack of another carboxylic acid molecule gives the corresponding anhydride that can react with the amine leading to the desired amide; iii) the acyl transfer from oxygen to nitrogen atom provides the N-acylurea as an undesired by-product.²⁷¹

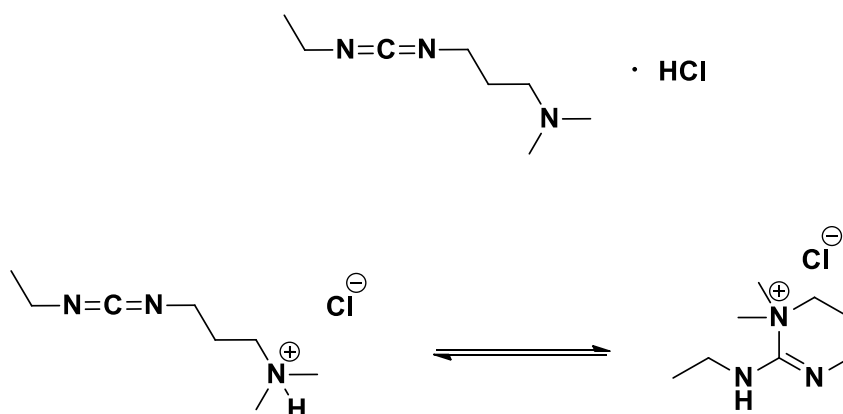


Scheme 25. Mechanism of the amide synthesis in the presence of a generic carbodiimide as coupling agent. i) Direct reaction with amine causes the formation of the desired amide and the corresponding urea of the carbodiimide employed; ii) the attack of another carboxylic acid molecule gives the corresponding anhydride that can react with the amine leading to the desired amide; iii) the acyl transfer from oxygen to nitrogen atom provides the N-acylurea as an undesired by-product.

Despite the stoichiometric consumption, carbodiimides are extremely efficient auxiliaries and they can mediate the amide coupling reaction without interacting with the functional groups distant from the acid and amine groups.

5.2.1.2. Interactions with the capsule

The opportunity to work with a coupling agent inside a nanoreactor providing a limited space for the reaction could be exploited to obtain a supramolecular catalytic system displaying substrate selectivity. With this purpose we decided to investigate the ability of the resorcin[4]arene capsule to accommodate the positively charged 1-ethyl-3-(3-dimethylaminopropyl) carbodiimide hydrochloride (**EDAPC**) within its cavity (Scheme 26).



Scheme 26. 1-Ethyl-3-(3-dimethylaminopropyl) carbodiimide hydrochloride (**EDAPC**) molecular structure (upward) and its equilibrium between open and six-membered closed form (below).

Initially we observed that **EDAPC** was soluble in water saturated chloroform-d and it existed in chloroform-d solution as a \approx 5:1 mixture of both the open and six-membered closed form deriving by intramolecular attack by the dimethylamino terminal moiety on the carbodiimide C atom (Scheme 26). By means of ¹H-NMR analyses it was observed that **EDAPC** afforded quantitative encapsulation when added in stoichiometric amounts with respect to the hexameric capsule (Figure 47). All resonances of **EDAPC** completely disappeared after the addition of 1.1 equivalents of the hexameric supramolecular capsule due to the shielding effect imparted by the aromatic surfaces of the cavity.

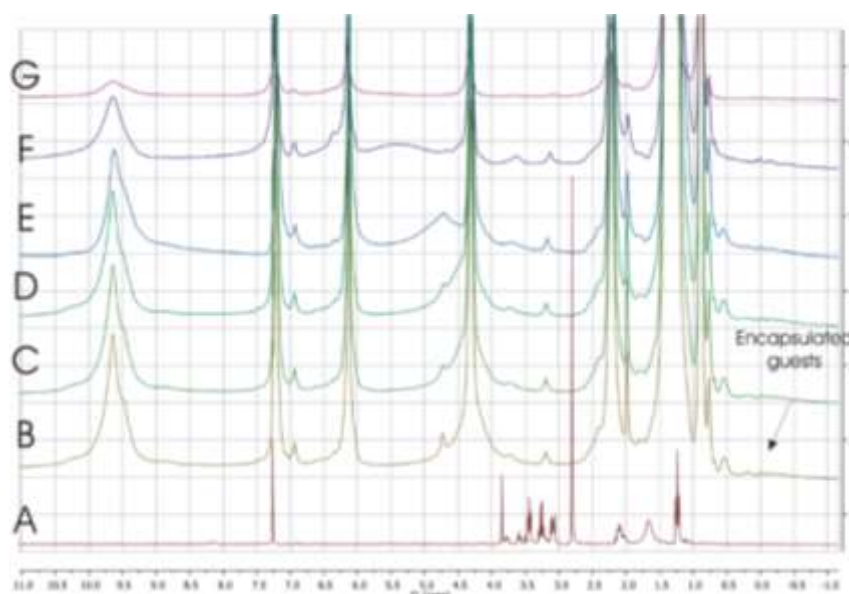


Figure 47. ^1H NMR spectra in water saturated chloroform-d: A) 1-ethyl-3-(3-dimethylaminopropyl) carbodiimide hydrochloride **EDAPC** (26.5 mM), B) **EDAPC** (26.5 mM) and hexameric capsule (26.5 mM) after mixing; C) **EDAPC** (26.5 mM) and hexameric capsule (26.5 mM) after 15 min; D) **EDAPC** (26.5 mM) and hexameric capsule (26.5 mM) after 30 min; E) **EDAPC** (26.5 mM) and hexameric capsule (26.5 mM) after 2 h; F) **EDAPC** (26.5 mM) and hexameric capsule (26.5 mM) after 3 days; G) **EDAPC** (26.5 mM) and hexameric capsule (26.5 mM) after 11 days.

EDAPC proved stable for several days when encapsulated and no trace of the corresponding urea resulting from water attack was observed. However, the addition of 10 equivalents of tetraethylammonium tetrafluoroborate (**TEA**) as a competitive cationic guest caused the release of **EDAPC** from the capsule (Figure 48).

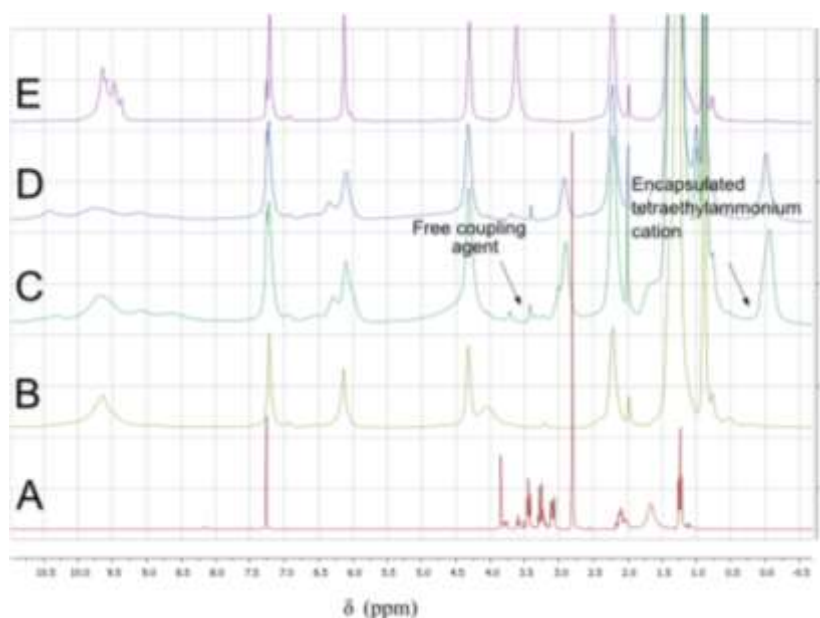


Figure 48. ^1H NMR spectra in water saturated chloroform- d : A) 1-ethyl-3-(3-dimethylaminopropyl) carbodiimide hydrochloride **EDAPC** (26.5 mM), B) **EDAPC** (26.5 mM) and hexameric capsule (26.5 mM) C) **EDAPC** (26.5 mM) and hexameric capsule (26.5 mM) and tetraethylammonium tetrafluoroborate **TEA** (265.3 mM); D) **EDAPC** (26.5 mM), hexameric capsule (26.5 mM) and **TEA** (265.3 mM) after 3 days; E) Hexameric capsule (13.5 mM).

Similarly, in order to check the existence of interactions between carboxylic acids and the resorcin[4]arene capsule, several ^1H -NMR spectra of different samples with amounts of hexanoic acid (**HA**) up to 2 equivalents with respect to the capsule were acquired. These analyses showed no particular affinity between carboxylic acids and capsule despite the possible formation of hydrogen bonds (Figure 49).

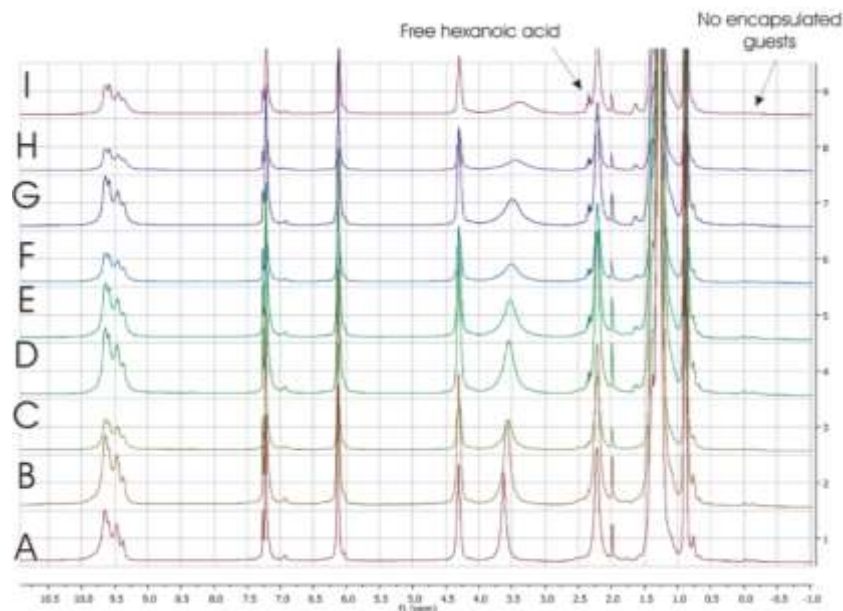


Figure 49. ^1H NMR spectra in water saturated chloroform-d: A) hexameric capsule (13.5 mM); B) hexameric capsule (13.5 mM) with 0.2 eq. of hexanoic acid (**HA**); C) hexameric capsule (13.5 mM) with 0.4 eq. of **HA**; D) hexameric capsule (13.5 mM) with 0.6 eq. of HA; E) hexameric capsule (13.5 mM) with 0.8 eq. of **HA**; F) hexameric capsule (13.5 mM) with 1.0 eq. of **HA**; G) hexameric capsule (13.5 mM) with 1.2 eq. of **HA**; H) hexameric capsule (13.5 mM) with 1.6 eq. of **HA**; I) hexameric capsule (13.5 mM) with 2.0 eq. of **HA**.

The same control experiments were carried out to observe the possible interactions between the hexameric capsule and amines. With this purpose butylamine (**BAm**) was chosen as the reference substrate. In this case the partially acidic capsule⁶⁰ caused the protonation of the amine and the formation of an encapsulated ammonium species was observed (Figure 50).

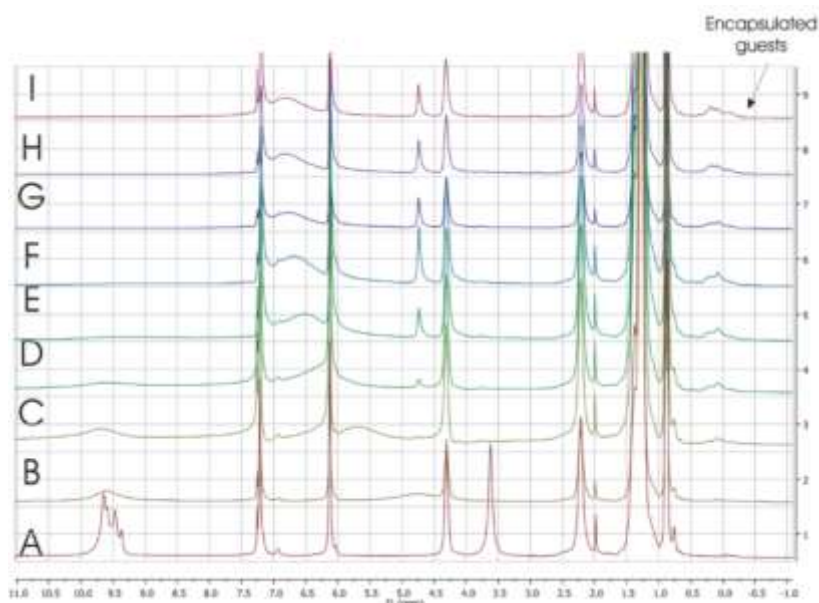


Figure 50. ^1H NMR spectra in water saturated chloroform-d: A) Hexameric capsule (13.5 mM); B) Hexameric capsule (13.5 mM) and 0.2 eq. of butylamine (**BAm**); C) Hexameric capsule (13.5 mM) and 0.4 eq. of **BAm**; D) Hexameric capsule (13.5 mM) and 0.6 eq. of **BAm**; E) Hexameric capsule (13.5 mM) and 0.8 eq. of **BAm**; F) Hexameric capsule (13.5 mM) and 1.0 eq. of **BAm**; G) Hexameric capsule (13.5 mM) and 1.2 eq. of **BAm**; H) Hexameric capsule (13.5 mM) and 1.6 eq. of **BAm**; I) Hexameric capsule (13.5 mM) and 2.0 eq. of **BAm**. ↓ encapsulated n-butylammonium cation.

Finally, titration of the capsule with increasing amounts of a 1:1 mixture of **BAm** and **HA** showed the presence of new resonances in the region <0 ppm differing from those observed in the titration with **BAm** and relative to encapsulated butylammonium cation. These signals were attributed to possible co-encapsulation of the two species (Figure 51).

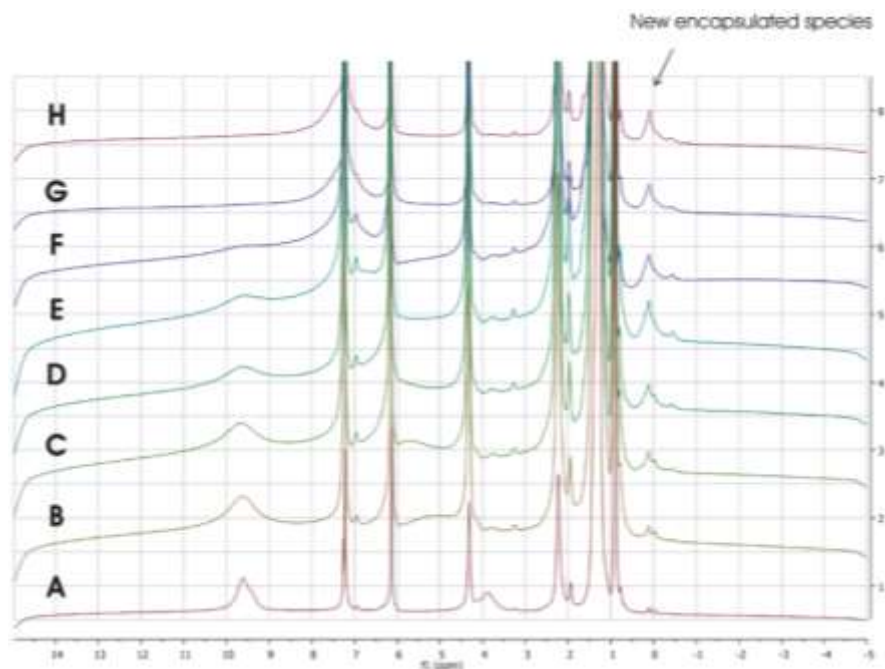


Figure 51. ^1H NMR spectra in water saturated chloroform-d: A) hexameric capsule (13.5 mM) and 0.1 eq. of **BA**m and 0.1 eq. of **HA**; B) hexameric capsule (13.5 mM) and 0.2 eq. of **BA**m and 0.2 eq. of **HA**; C) Hexameric capsule (13.5 mM) and 0.4 eq. of **BA**m and 0.4 eq. of **HA**; D) hexameric capsule (13.5 mM) and 0.6 eq. of **BA**m and 0.6 eq. of **HA**; E) hexameric capsule 16·8H₂O (13.5 mM) and 0.8 eq. of **BA**m and 0.8 eq. of **HA**; F) Hexameric capsule 16·8H₂O (13.5 mM) and 1.0 eq. of **BA**m and 1.0 eq. of **HA**; G) hexameric capsule (13.5 mM) and 1.5 eq. of **BA**m and 1.5 eq. of **HA**; H) hexameric capsule (13.5 mM) and 2.0 eq. of **BA**m and 2.0 eq. of **HA**. ↓ new encapsulated species.

5.2.1.3. Amide coupling within the cavity

After observing the interaction of the substrates with the capsule, we investigated the competitive condensation reactions between acids and amines to amides comparing the substrate selectivity imparted by the **EDAPC** encapsulated in the hexameric capsule with that obtained in the absence of the supramolecular capsule. Initially we investigated the competitive condensation reaction between two aliphatic amines such as **BA**m and octylamine (**OAm**) with butyric acid (**BAc**). With this purpose 0.5 equivalents of each amine and the carboxylic acid (0.5 equivalents) were introduced in a solution with 1 equivalent of **EDAPC** in the presence and in the absence of 1.1 equivalents of capsule. The reactions were carried out at 60°C for 18 hours (Table 26).

#	Acid	Amine	Capsule	Amide (%) ^a	Short/Long Amide ratio
1	BAC (C ₄)	BAm (C ₄)	-	Ad _{BAC-BAm} (C ₄ + C ₄) 25	1.7
		OAm (C ₈)		Ad _{BAC-OAm} (C ₄ + C ₈) 15	
2	BAC (C ₄)	BAm (C ₄)	+	Ad _{BAC-BAm} (C ₄ + C ₄) 32	2.2
		OAm (C ₈)		Ad _{BAC-OAm} (C ₄ + C ₈) 15	
3	HA (C ₆)	BAm (C ₄)	-	Ad _{HA-BAm} (C ₆ + C ₄) 50	2.5
		OAm (C ₈)		Ad _{HA-OAm} (C ₆ + C ₈) 20	
4	HA (C ₆)	BAm (C ₄)	+	Ad _{HA-BAm} (C ₆ + C ₄) 57	5.1
		OAm (C ₈)		Ad _{HA-OAm} (C ₆ + C ₈) 11	
5	DAc (C ₁₂)	BAm (C ₄)	-	Ad _{DAc-BAm} (C ₁₂ + C ₄) 27	1.2
		OAm (C ₈)		Ad _{DAc-OAm} (C ₁₂ + C ₈) 23	
6	DAc (C ₁₂)	BAm (C ₄)	+	Ad _{DAc-BAm} (C ₁₂ + C ₄) 19	2.0
		OAm (C ₈)		Ad _{DAc-OAm} (C ₁₂ + C ₈) 10	

Table 26. Catalytic tests for the competitive coupling of amines BAm and OAm with carboxylic acids (BAC, HA or DAc) in the presence of cationic EDAPC with or without the resorcin[a]arene capsule. [Resorcin[4]arene] = 81.4mM, [EDAPC] = 13.2mM, [Carboxylic acids] = 6.7mM, [Amines] = 6.7mM, water saturated chloroform-d 1 mL, 60°C, time 18 h. +: presence; -: absence. a) Determined by GC-MS analysis with an alkane standard.

Under these conditions the substrate selectivity imparted by the capsule was not so high and the presence of the supramolecular system caused only a slight improvement in the ratio between the shorter **Ad_{BAm-BAC}** with respect to the longer **Ad_{OAm-BAC}** amide product. The same general result was observed during the competitive reactions between **BAm** and **OAm** with **HA** or dodecanoic acid (**DAc**). Indeed the mechanism of the carbodiimide coupling provides an easy explanation for the low substrate selectivity obtained during the competitive reactions. In fact, it is known that the rate determining step of the coupling reaction is the acid attack on the carbodiimide to form the O-acylurea intermediate.²⁷² Therefore it was more sensible to carry out the experiment introducing two aliphatic carboxylic acid such as **HA** and **DAc** and to study their competitive reactivity towards one aliphatic amine either with or without the capsule (Table 24). This led to a more evident substrate selectivity effect imparted by the capsule with a much higher preference towards the shorter acid substrate. While free EDAPC showed no selectivity in the formation of short and long amides, after encapsulation shorter/longer amide ratios between 8 and 28 in the case of hexadecylamine (**HDAm**) were observed (Table 27, entries 5,6).

#	Amine	Acid	Capsule	Amide (%) ^a	Short/Long amide ratio
1	BAm (C ₄)	HA (C ₆)	-	Ad _{HA-BAm} (C ₆ + C ₄) 15	0.5
		DAC (C ₁₂)		Ad _{DAC-BAm} (C ₁₂ + C ₄) 30	
2	BAm (C ₄)	HA (C ₆)	+	Ad _{HA-BAm} (C ₆ + C ₄) 22	8.1
		DAC (C ₁₂)		Ad _{DAC-BAm} (C ₁₂ + C ₄) 3	
3	OAm (C ₈)	HA (C ₆)	-	Ad _{HA-OAm} (C ₆ + C ₈) 28	1.1
		DAC (C ₁₂)		Ad _{DAC-OAm} (C ₁₂ + C ₈) 25	
4	OAm (C ₈)	HA (C ₆)	+	Ad _{HA-OAm} (C ₆ + C ₈) 39	7.9
		DAC (C ₁₂)		Ad _{DAC-OAm} (C ₁₂ + C ₈) 5	
5	HDAm (C ₁₆)	HA (C ₆)	-	Ad _{HDAC-HAm} (C ₁₆ + C ₆) 24	1.2
		DAC (C ₁₂)		Ad _{HDAC-DAm} (C ₁₆ + C ₁₂) 19	
6	HDAm (C ₁₆)	HA (C ₆)	+	Ad _{HDAC-HAm} (C ₁₆ + C ₆) 22	28
		DAC (C ₁₂)		Ad _{HDAC-DAm} (C ₁₆ + C ₁₂) 0.8	

Table 27. Catalytic tests for the competitive coupling of hexanoic acid **HA** and dodecanoic acid **DAC** with several amines catalyzed by **EDAPC** in the presence or absence of the hexameric capsule. Reaction conditions: [Resorcinarene] = 81.4mM, [EDAPC] = 13.2mM, [Carboxylic acid] = 6.7mM, [Amine] = 6.7mM, water-saturated chloroform-d 1 mL, 60°C, time 18 h. +: presence; -: absence. a) Determined by GC-MS analysis with an alkane standard.

The study was extended to the reaction of **OAm** with pairs of acids such as **BAC**, **HA**, **DAC** and tridecanoic acid **TDAC** in the presence and absence of the capsule (Table 28). From the data obtained it was possible to observe that in the presence of the **EDAPC** alone, the substrate maintained the same reactivity regardless of the length of the acids. Conversely, the reaction carried out inside the cavity could discriminate between acids with different length. Although this effect was negligible with acids differing by only one C atom, the selectivity greatly increased when the molecules length changed from two, to six and to eight methylene units (Figure 52). Particularly interesting was the comparison between **BAC** and **DAC**. The presence of the capsule caused an increase of the selectivity higher than 10 times in favour of the shorter substrate (Table 28, entry 4, Figure 52).

#	Acid	Capsule	Amide (%) ^a	Short/Long amide ratio
1	BAC (C ₄)	-	Ad _{BAC-OAm} (C ₄ + C ₈) 32	1.1
	HA (C ₆)		Ad _{HA-OAm} (C ₆ + C ₈) 29	
2	BAC (C ₄)	+	Ad _{BAC-OAm} (C ₄ + C ₈) 30	2.0
	HA (C ₆)		Ad _{HA-OAm} (C ₆ + C ₈) 15	
3	BAC (C ₄)	-	Ad _{BAC-OAm} (C ₄ + C ₈) 30	1.2
	DAC (C ₁₂)		Ad _{DAC-OAm} (C ₁₂ + C ₈) 26	
4	BAC (C ₄)	+	Ad _{BAC-OAm} (C ₄ + C ₈) 45	11.1
	DAC (C ₁₂)		Ad _{DAC-OAm} (C ₁₂ + C ₈) 4	
5	HA (C ₆)	-	Ad _{HA-OAm} (C ₆ + C ₈) 28	1.1
	DAC (C ₁₂)		Ad _{DAC-OAm} (C ₁₂ + C ₈) 25	
6	HA (C ₆)	+	Ad _{HA-OAm} (C ₆ + C ₈) 38	4.4
	DAC (C ₁₂)		Ad _{DAC-OAm} (C ₁₂ + C ₈) 9	
7	DAC (C ₁₂)	-	Ad _{DAC-OAm} (C ₁₂ + C ₈) 17	0.9
	TDAC (C ₁₃)		Ad _{TDAC-OAm} (C ₁₃ + C ₈) 18	
8	DAC (C ₁₂)	+	Ad _{DAC-OAm} (C ₁₂ + C ₈) 9	0.8
	TDAC (C ₁₃)		Ad _{TDAC-OAm} (C ₁₃ + C ₈) 11	

Table 28. Catalytic tests for the competitive coupling of couple of carboxylic acids with octyl amine **OAm** catalyze by **EDAPC** in the presence or absence of the hexameric capsule. Reaction conditions: [Resorcinarene] = 81.4mM, [EDAPC] = 13.2mM, [Carboxylic acid] = 6.7mM, [OAm] = 6.7mM, water-saturated chloroform-d 1 mL, 60°C, time 18 h. +: presence; -: absence. a) Determined by GC-MS analysis with an alkane standard

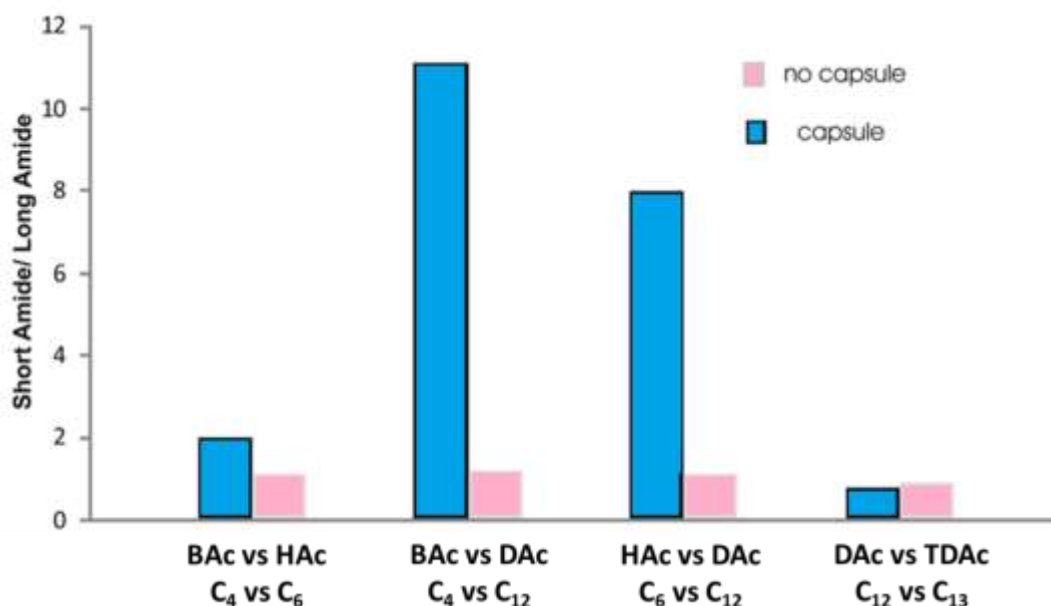


Figure 52. Selectivity in the competitive coupling reaction between couples of acids with octyl amine **OAm** in the presence (in blue) or absence (in pink) of the hexameric capsule.

The results could be more clearly compared by plotting the ratio between the obtained amounts of short and long amides with respect to the ratio between the C atoms number that were present in the molecular structure of short and long carboxylic acids used as substrates (Figure 53). From this graph a linear trend with approximately zero slope was obtained using the data collected in the absence of the capsule showing the inability of **EDAPC** to select on the basis of the substrates length. Conversely, the results achieved in the presence of the capsule showed an approximately sigmoidal trend indicating a substrate selectivity that increased with the difference between the length of the competitive acids.

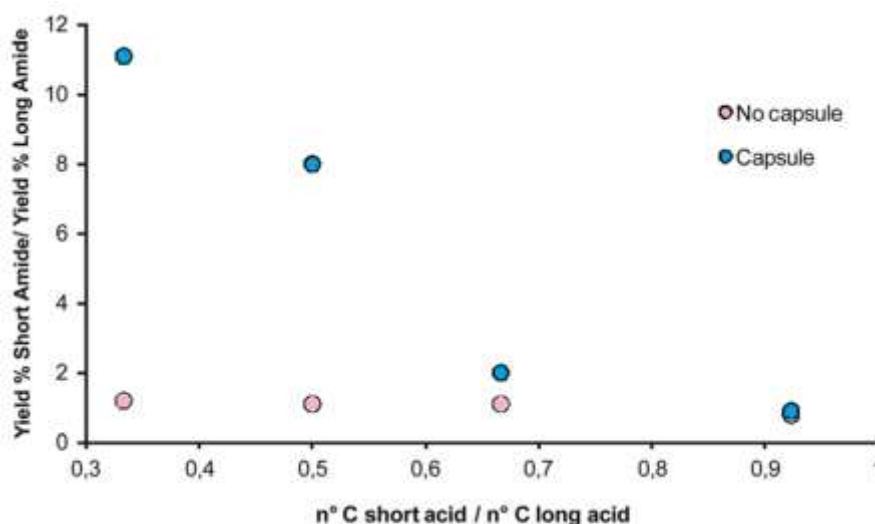


Figure 53. Plot of the ratio between the yields of the short and long amides for the reaction of **OAm** and couples of acids vs. the ratio between the number of C atoms of the competing carboxylic acids

Finally we decided to carry out a competitive reaction between two acids (**HA** and **DAC**) and two amines (**BAm** and **OAm**) in order to observe the substrate selectivity of the supramolecular system when four different products were possible (Figure 54). As in the previous experiments, **EDAPC** alone showed no selectivity and the four possible product were obtained in similar amounts (yields 28-12%). Conversely, the presence of the capsule caused the preferential formation of the amide obtained from the combination of the shorter acid **HA** with the shorter amine **BAm** with 50% yield. Moreover the longer amide **Ad_{DAC-OAm}** obtained from the combination of the longer acid **DAC** and the longer amine **OAm** was formed with only 4% yield. Surprisingly, the condensing agent within the capsule allowed high selectivity also for the two intermediate length amides that have very similar overall size but are obtained from a different combination of substrates. In particular the **Ad_{HA-OAm}** obtained from the shorter acid was formed in almost double amount with respect to the **Ad_{BAm-DAC}**, while the same products were obtained in 17 and 18% yield, respectively, in the absence of the capsule.

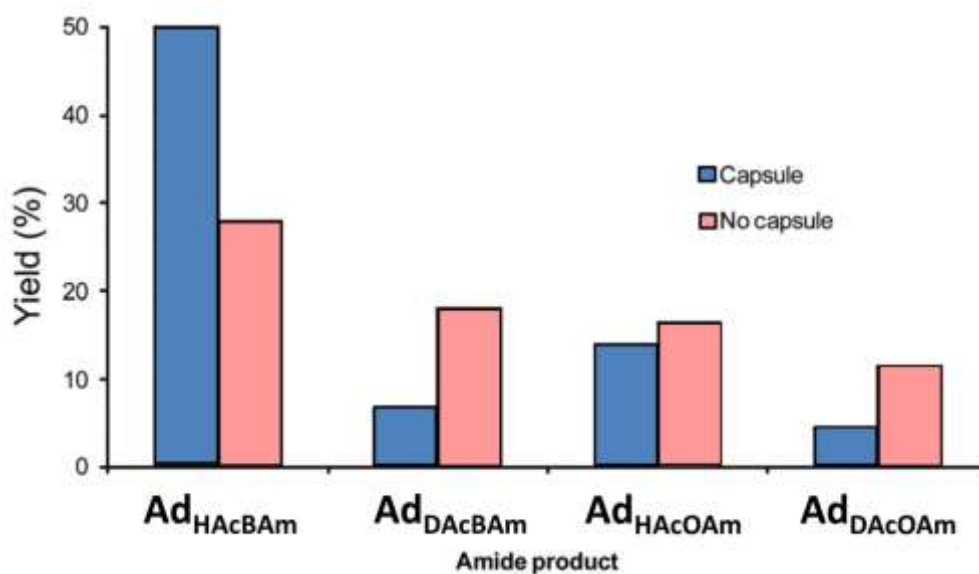


Figure 54. Catalytic tests for the competitive coupling of pairs of carboxylic acids **HA** and **DAc** with pairs of amine **BAm** and **OAm** mediated **EDAPC** either in the presence or in the absence of the resorcinarene capsule. Experimental conditions: [Resorcinarene] = 81.4 mM, [EDAPC] = 13.2 mM, [Carboxylic acid] = 6.7 mM, [Amine] = 6.7 mM, 60°C, 18 h.

5.2.1.4. Conclusions

In conclusion, the cationic carbodiimide **EDAPC** hosted within the hexameric resorcin[4]arene capsule showed different selectivity when operating as a condensing agent in the presence of a series of carboxylic acids and amines characterized by different lengths. In fact a better co-encapsulation of smaller substrates resulted in a high selectivity leading to the formation of the shorter amides, while in the absence of the self-assembled capsule, the coupling reaction was much less substrate selective leading to very similar amides distribution. The results obtained during the competitive reaction demonstrated the main role of the selective binding of the carboxylic acid as the driving force for substrate selectivity because the substrate selectivity achieved during the competitive condensation of two acids in the presence of one amine was much higher than viceversa. Nevertheless the competitive reaction in the presence of two pairs of competitive substrates leading to four possible products allowed to obtain good results in terms of selectivity, showing best values for shorter products (Figure 55).

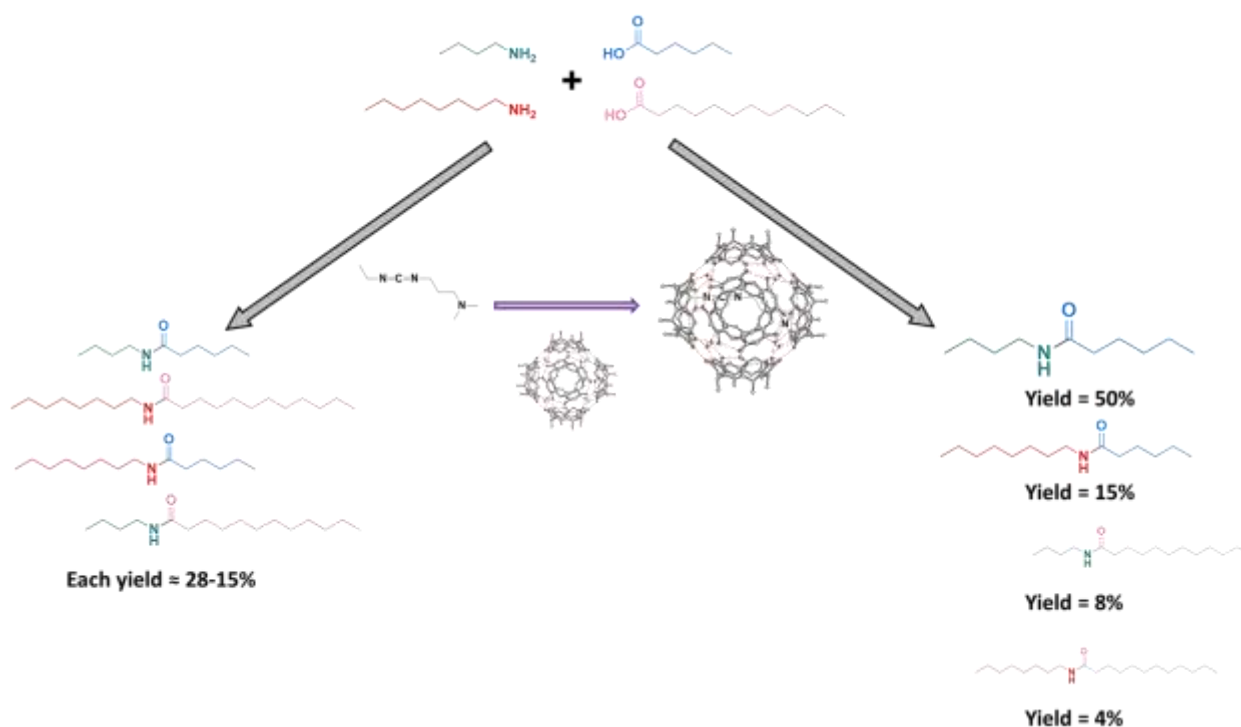


Figure 55. Competitive coupling of pairs of carboxylic acids **HA** and **DAc** with pairs of amine **BAm** and **OAm** mediated by **EDAPC** either in the presence or in the absence of the resorcinarene capsule. Experimental conditions: [Resorcinarene] = 81.4 mM, [EDAPC] = 13.2 mM, [Carboxylic acid] = 6.7 mM, [Amine] = 6.7 mM, 60°C, 18 h.

5.2.2. Substrate selectivity due to hydrophobic effect in micellar media

Micelles high ability to dissolve apolar substrates and catalysts in water can be employed in order to obtain substrate selective catalytic systems. The presence of a lipophilic nano-environment in aqueous solution allows to exploit the organic compounds hydrophobicity as driving force to achieve substrate selectivity. Hence a catalytic system within the micelle core will interact preferentially with hydrophobic substrates because of their higher affinity. The application of micellar media to obtain substrate selective homogeneous catalysts has been an highly attractive field of research with very few works present in the literature.^{264, 265, 273}

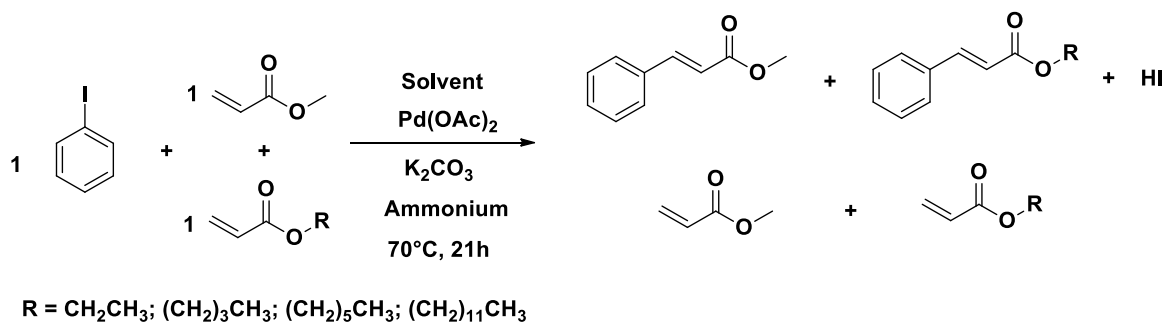
5.2.2.1. Substrate selective Cross-Coupling Heck reactions in water

Initially the effect of micellar media in the competitive Heck coupling reactions between acrylate esters from methyl to lauryl and iodobenzene derivatives catalyzed by Pd(OAc)₂ was

investigated. The Heck reaction (also known as Mizoroki-Heck reaction) is a Palladium catalysed cross-coupling reaction between an aryl, benzyl or vinyl halides and an electron poor alkenes in the presence of a base.²⁷⁴ Heck reactions are well known and the procedure in organic solvents has been improved several times. The literature emphasizes the importance of using quaternary ammonium cations like tetrabutyl ammonium chloride (TBAC) and bromide (TBAB) in combination with an alkaline carbonate base to favour the reaction.²⁷⁵ Only recently the use of water as a solvent for this reaction has been established and the employment of micellar media began to be investigated. As expected cetyl trimethyl ammonium bromide (CTAB) surfactant imparted better activity and selectivity to this reaction because of its cationic character.²⁷⁶ This surfactant reduces the formation of large palladium aggregates avoiding their precipitation and extending the catalyst lifetime. Recently an interesting example of Mizoroki–Heck cross-coupling reaction between aryl iodides and bromides with terminal olefins under aerobic conditions showed the possibility to use palladium acetate in the absence of any kind of ligand just employing K_2CO_3 and a mixture of (2:1) $H_2O/DMSO$ as optimal base and coordinating solvent, respectively.²⁷⁷

Unselective Heck reaction in organic media

In order to understand the intrinsic relative activity of the series of acrylate esters with iodobenzene, the competitive Heck reaction was first carried out in DMF as organic solvent. Competitive experiments were carried out using 2 mol% of $Pd(OAc)_2$, 150 mM (50 equiv.) of iodobenzene, pairs of acrylates each 163 mM (55 equiv.) and K_2CO_3 (110 equiv.) for each reaction. To each reaction, 5 equivalents of tetrabutyl ammonium bromide (TBAB) were added in order to increase the stability of the catalytic system minimizing Pd aggregation in organic solvent.²⁷⁸ The reactions were carried out for 21 h at 70 °C to avoid the evaporation of methyl acrylate that is the smaller substrate employed. In each reaction a competitive experiment between methyl acrylate (**MA**) and another substrate chosen among ethyl (**EA**), butyl (**BA**), hexyl (**HeA**) and lauryl (**LA**) acrylate was performed (scheme 27). A competitive reaction containing a mixture of all acrylates was not performed due to extensive overlap between reagents and products occurring in GC analysis. Thus the reaction was followed by 1H NMR and the determination of the yields for each substrate came from the integration of the corresponding resonances. Therefore four competitive experiments were carried out studying the conversion rate of the individual acrylates in relation to **MA** used as a reference in each test.



Scheme 27. Competitive cross-coupling reactions between iodobenzene (**PhI**), methylacrylate (**MA**) and one among ethylacrylate (**EA**), butylacrylate (**BA**), hexylacrylate (**HeA**) and laurylacrylate (**LA**).

In Figure 56 are reported the iodobenzene conversions for each competitive reaction and the substrate selectivity was calculated as the ratio between the yield of a given acrylate ester product with respect to the yield of the shorter methyl acrylate product.

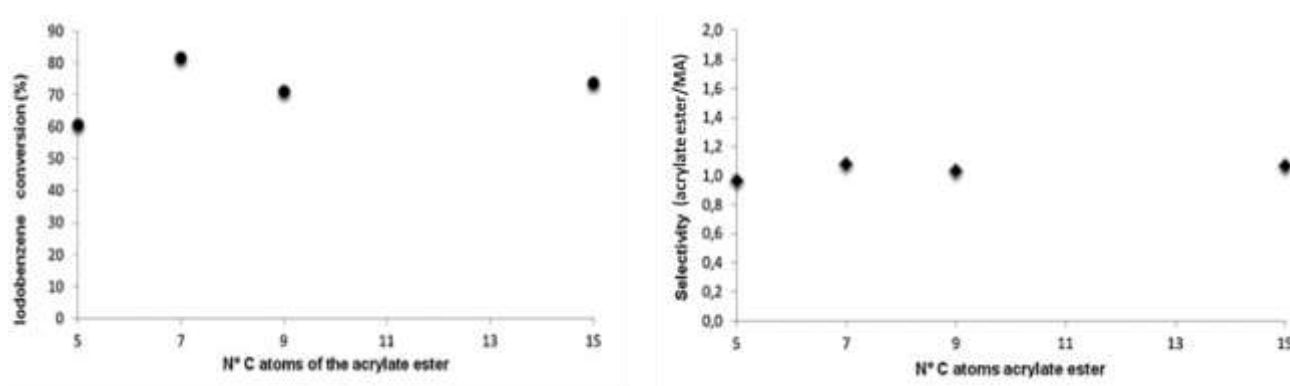


Figure 56. Iodobenzene (**PhI**) conversions (on the left) and relative substrate selectivity (on the right) for each competitive experiment carried out in DMF. Experimental conditions: $[\text{Pd}(\text{OAc})_2] = 3.0 \text{ mM}$, $[\text{acrylate ester}] = 163 \text{ mM}$ each, $[\text{PhI}] = 150 \text{ mM}$, $[\text{K}_2\text{CO}_3] = 300 \text{ mM}$, solvent 3 mL DMF, 70 °C, 21 h.

The results showed iodobenzene (**PhI**) conversions in the 60-80% range for all the competitive reactions. Moreover no substrate selectivity was observed when the reaction was carried out in DMF as shown in Fig. 56 where the ratio between the products yields with respect to **MA** always assumes values in the 0.95-1.08 range. These results were expected in the absence of a discriminating device.

Substrate selective Heck reaction in micellar media

Before dealing with micellar medium effects on the reaction selectivity a series of $^1\text{H-NMR}$ experiments were carried out on each substrate in D_2O in the presence and absence of the cationic CTAB surfactant (80mM) (Figure 57).

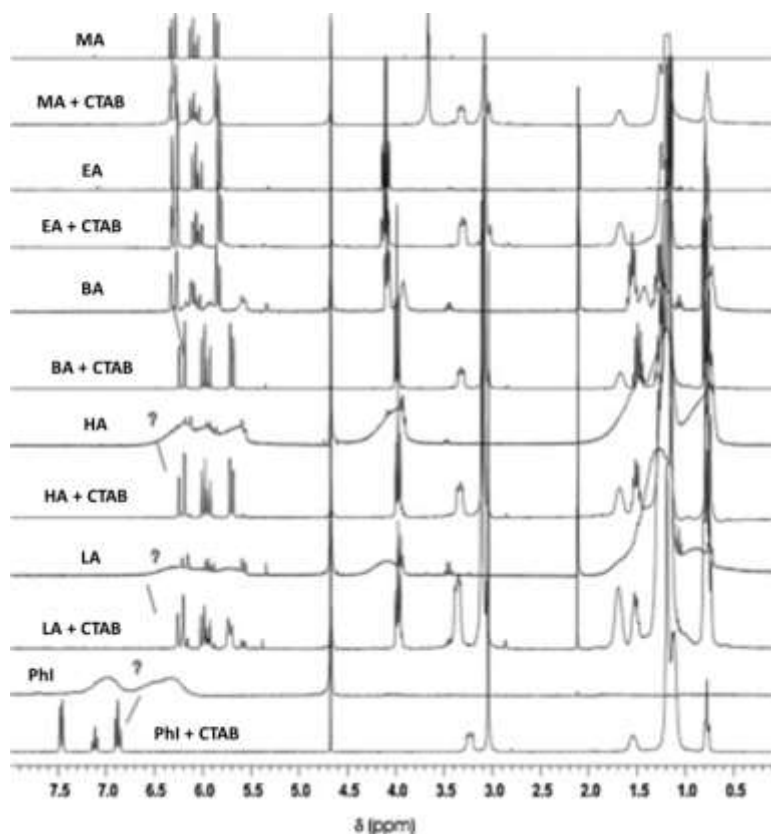


Figure 57 ^1H NMR spectra of substrates **MA**, **EA**, **BA**, **HA**, **LA** and iodobenzene (**Phi**) (150 mM) in the absence and in the presence of CTAB (80 mM) in D_2O

As shown by the $^1\text{H-NMR}$ spectra in Figure 55 the smaller **MA** and **EA** were completely soluble in water and no change in chemical shifts was observed by CTAB addition. The **BA** signals were partially shielded and sharp after the addition of CTAB indicating a better solubilization in the micellar medium. The more hydrophobic longer acrylates were not soluble in D_2O causing the presence of extremely broad signals in their $^1\text{H-NMR}$ spectra. However CTAB addition in solution allowed their solubilization as shown by the clear sharpening of their NMR signals. Similar results were obtained with **Phi** that was insoluble in water but it was brought into solution by CTAB. Even the poorly water soluble $\text{Pd}(\text{OAc})_2$ was completely solubilized by CTAB.

In testing the competitive Heck reaction in aqueous micellar medium the optimum concentration of CTAB in solution was identified carrying out a series of reaction between **BA** and **PhI** in water with 60, 80 and 100 mM CTAB (c.m.c. of surfactant 0.9 mM) under the experimental conditions used with DMF. These reactions showed an increase in yield to the corresponding cinnamyl ester from 51% to 63% when the CTAB concentration was brought from 60 to 80 mM while a drop in conversion was found when the surfactant amount was further increased. These effects were ascribable to an increase of substrates solubility in the micelles up to a 80 mM CTAB concentration after which the dilution effect became predominant and the yield decreased.

Hence the competitive Heck reactions involving each acrylate **EA**, **BA**, **HeA** and **LA** associated with **MA** as reference were carried out in CTAB 80 mM micellar medium. In Figure 58 are reported the **PhI** conversions and the relative substrate selectivity of each competitive reaction calculated as previously. Iodobenzene conversions in the 69-87% range testified for the efficiency of this reaction in the micellar medium. As to substrate selectivity a more complex interpretation was necessary. **MA** and **EA** were intrinsically soluble in water and they did not need to interact with the micellar hydrophobic core where the catalytic site was situated. Therefore the discrimination effect of the micellar aggregate did not significantly influence the substrate selectivity of the competitive reaction between **MA** and **EA**. Conversely, longer acrylate esters **BA**, **HeA** and **LA** were poorly soluble in water and their solubilisation in the reaction medium was closely related to interaction with the hydrophobic core of the micelle. This explained their 3.5 times faster reactivity with respect to **MA**.

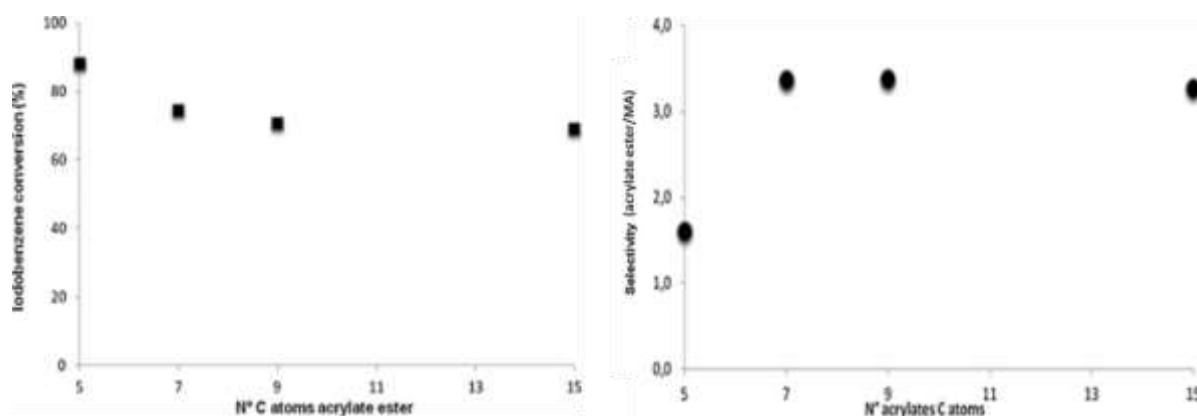
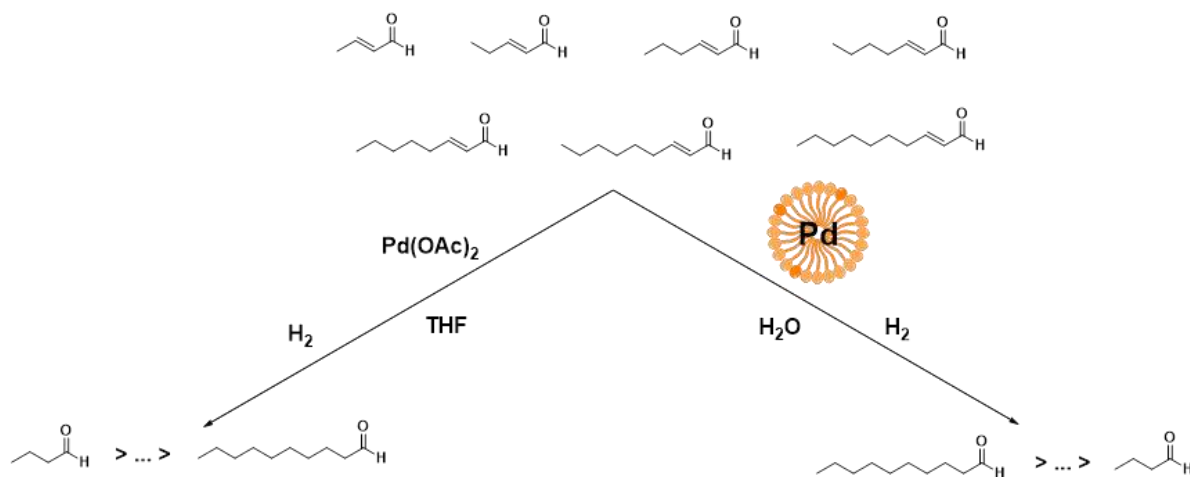


Figure 58. Iodobenzene conversion (on the left) and substrate selectivity (on the right) of each competitive experiment carried out in water with CTAB (80 mM). Experimental conditions: $[Pd(OAc)_2] = 3.0$ mM, $[acrylate\ ester] = 163$ mM each, $[PhI] = 150$ mM, $[K_2CO_3] = 300$ mM, solvent 3 mL water, $[CTAB] = 80$ mM, 70 °C, 21 h.

The same reactions were carried out replacing **PhI** with other iodinated aromatic compounds such as 1-iodo-naphthalene and 2-chloro-iodobenzene in order to check the generality of the observed results. These compounds were chosen because they are liquid and easily miscible in an aqueous micellar medium. Both the iodoaryl derivatives showed a behavior analogous to iodobenzene. No substrate selectivity was observed when the competitive reactions were carried out in DMF as organic solvent, while in water with CTAB an increasing preference for longer substrates up to a **LA/MA** yield ratio of 7.9 was achieved.

5.2.2.2. Substrate selective hydrogenation of α,β -unsaturated aldehydes

After demonstrating that the hydrophobic effect is a suitable driving force to steer substrate selectivity in Pd catalyzed Heck cross-coupling reaction carried out in cationic micellar medium, we decided to investigate the same phenomenon in hydrogenation reactions. For this purpose the palladium catalyzed competitive hydrogenation of a series of α,β -unsaturated aldehydes of different length was taken into consideration (Scheme 28).



Scheme 28. Opposite substrate selectivity of the competitive hydrogenation reaction of α,β -unsaturated aldehydes conducted in organic solvent or in aqueous micellar medium.

Competitive hydrogenation in organic media

In order to observe the relative intrinsic reactivity of the substrates the competitive reaction was initially carried out in tetrahydrofuran (THF). The reaction was performed with 0.6 mol% Pd(OAc)₂ in the presence of 59.4 mM individual aldehyde from trans-2-butenal (C₄) to trans-2-decenale (C₁₀) at room temperature under 1 bar of H₂. All the substrates were selectively converted to the corresponding saturated aldehydes and following the decrease of concentration of each substrate over time it was possible to determinate the initial rate of the reaction for each substrate. Since such initial reaction rates were rather different for each substrate, they were normalized with respect to the longer and slower substrate giving an indication of the substrate selectivity (in some cases the initial rate of the reaction was calculated with one single point). As shown in Figure 59 a moderate increase of selectivity in favour of C₄, that reacts 3.6 times faster than the C₁₀ can be observed.

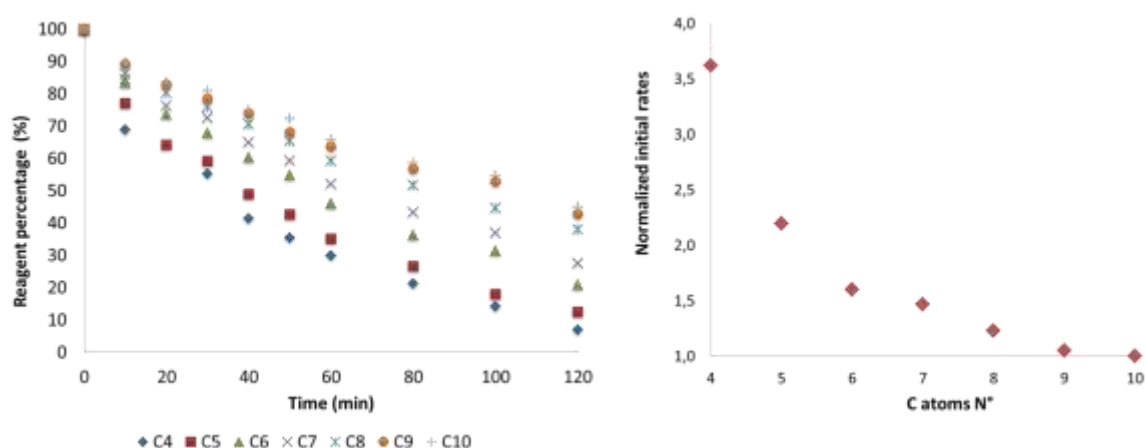


Figure 59. Plot of the percentage of each α,β -unsaturated aldehydes with respect to the time of the reaction (on the left) and the initial reaction rate of each aldehyde normalized with respect to the longer substrate (on the right) in the competitive hydrogenation reaction catalysed by Pd(OAc)₂ in THF. Reaction conditions: [Substrate] = 59.4 mM, Pd(OAc)₂ = 0.6 mol%, T = room temperature, p_{H₂} = 1 bar, 6 mL THF.

The slightly lower reactivity of longer aldehydes could be attributed to possible folds of the alkyl chain that cause a steric hindrance sufficient to slow the interaction of the metal catalyst with the C=C bond. Interestingly the introduction of H₂ in the reaction caused a colour change of the solution from a pale orange to grey indicative of Pd metal formation. This did not cause the precipitation of Pd as a black solid probably thanks to the solubilizing interaction of the large excess of substrate molecules present in the system.

Competitive hydrogenation in micellar media

Subsequently a series of experiments was carried out in order to find the most suitable surfactant for replacing THF with an aqueous micellar medium. In this respect surfactants differing in charge, lipophilicity and critical micellar concentration (CMC) were tested. A series of experiments was carried out dissolving Pd(OAc)₂ (0.6 mol%) in water in the presence of each surfactant for 1 h followed by reduction of the metal under 1 bar of H₂ until the solution turned from orange to black, indicative of Pd-NPs formation as observed during the synthesis of Pd nanoparticles with sulfonated anionic surfactants. Initially, we investigated the use of cationic surfactant CTAB (80 mM) as previously done for the competitive cross-coupling Heck reactions. Under these experimental conditions the competitive hydrogenation carried out *in situ* gave only 0.5-9% conversion of the mixture of unsaturated aldehydes after 1h confirming the low catalytic activity of Pd-NPs stabilized by CTAB in hydrogenation reactions as previously observed during the semi-hydrogenation of alkynes to alkenes.

Thereafter we decided to replace cationic surfactants with Triton-X100 and Triton-X114 as neutral surfactants (8mM) but after the reduction with H₂ the subsequent addition of the substrate caused Pd metal precipitation. When the concentration of both Triton surfactants was increased to 80mM a stable black suspension was obtained after a 20 min reduction with H₂, but a phase separation between water and surfactant containing Pd metal was observed. Even if this behavior is typical for an aqueous biphasic system rather than a micellar medium, we investigated the catalytic activity of the system with apolar surfactants observing the formation of the corresponding saturated aldehydes obtained in a quantitative yield after about 40 and 50 minutes using Triton X-114 and Triton X-100, respectively (Figure 60). Analyzing the initial rates it can be noticed an increasing activity from the smaller substrate up trans-2-heptenal (C₇) followed by a slight decrease for longer substrates. This particular trend may be probably justified by the existence of two different phenomena related to the biphasic nature of the system. On the one hand the reactivity of water-soluble shorter aldehydes increased with increasing lipophilicity because they become more soluble in the organic phase where the catalyst resided, on the other hand substrates longer than C₇, that were probably completely soluble in the polyetheral organic phase, suffered from a phenomenon similar to what observed in THF where the activity decreased with increasing the substrate size.

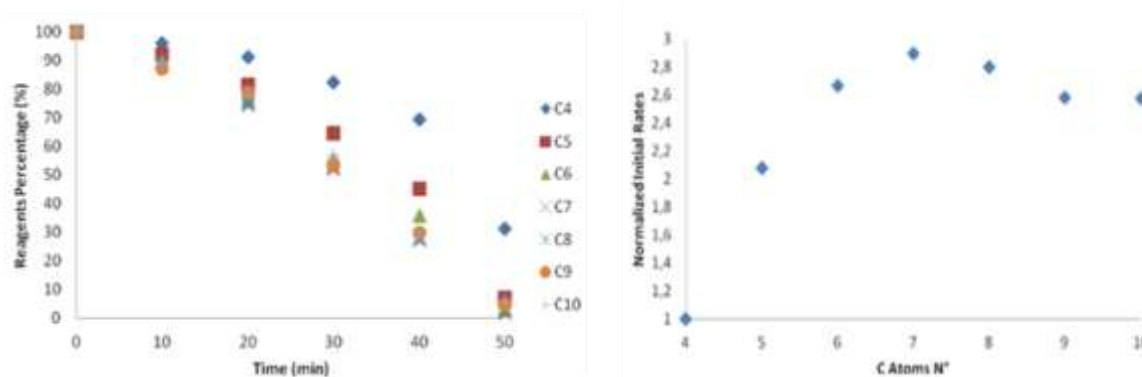


Figure 60. Plot of the percentage of each α,β -unsaturated aldehydes with respect to the time of the reaction (on the left) and the initial reaction rate of each aldehyde normalized with respect to the longer substrate (on the right) in the competitive hydrogenation reaction catalysed by $\text{Pd}(\text{OAc})_2$ in Triton X-100. Reaction conditions: $[\text{Substrate}] = 59.4 \text{ mM}$, $\text{Pd}(\text{OAc})_2 = 0.6 \text{ mol}\%$, $T = \text{room temperature}$, $p\text{H}_2 = 1 \text{ bar}$, 3 mL water , $[\text{Triton X-100}] = 80 \text{ mM}$.

Extremely substrate selective hydrogenation catalysed by Pd-NPs stabilized by sodium dodecyl sulfate

Finally anionic surfactants were tested to check for a stable and substrate selective catalytic system. When sodium dodecyl sulfate (**SDS**, 80 mM) was employed as surfactant the formation of Pd-NPs under H_2 required only 5 minutes. The competitive hydrogenation of the unsaturated aldehydes exhibited a moderate substrate selectivity in favour of more hydrophobic compounds conferring to C_{10} an initial rate 3.7 times higher than that of the shorter C_4 . Therefore we moved to sodium dodecyl sulfonate (**SDSU**) that was already found to produce highly active Pd-NPs (chapter 4.2.1.1.). Extremely interesting results were obtained under these conditions. In fact the shorter C_4 and C_5 substrates were characterized by a very low conversion rate, while a strong increase in reactivity was observed with longer and more hydrophobic substrates causing the complete conversion of C_{10} in 40 minutes (Figure 61). Notably, the most and the least active substrate differ by a rate factor of more than 330. This impressive result was mainly due to the hydrophobic effect that caused substrate partition between bulk water and the apolar phase provided by the surfactant that stabilized the Pd-NPs.

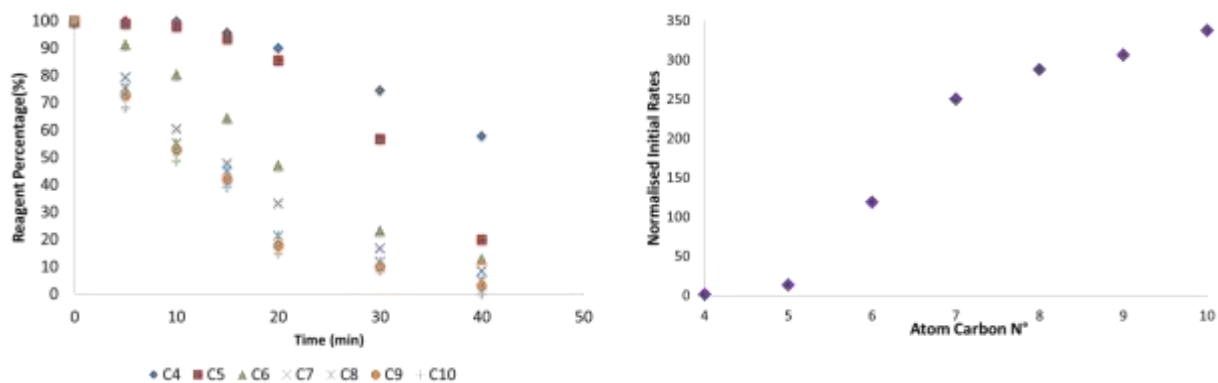


Figure 61. Plot of the percentage of each α,β -unsaturated aldehydes with respect to the time of the reaction (on the left) and the initial reaction rate of each aldehyde normalized with respect to the longer substrate (on the right) in the competitive hydrogenation reaction catalysed by $\text{Pd}(\text{OAc})_2$ in **SDSU**. Reaction conditions: [Substrate] = 59.4 mM, $\text{Pd}(\text{OAc})_2$ = 0.6 mol%, T = room temperature, pH_2 = 1 bar, 3 mL water, [SDSU] = 80 mM.

5.2.2.3. Conclusions

In conclusion we reported the possibility to achieve substrate selective catalytic systems simply through the hydrophobic effect imparted by the surfactants that make the systems capable to operate in aqueous media.

A moderate substrate selectivity was observed during the study of cross-coupling Heck reactions between acrylate esters with different length and iodoaryl derivatives, simply by the use of an aqueous micellar medium with the right concentration of the cationic surfactant. Instead a hundred-fold hydrophobicity induced substrate selectivity was obtained in the competitive chemoselective hydrogenation of a series of α,β -unsaturated aldehydes from **C**₄ to **C**₁₀ in water catalyzed by Pd-NPs that were stabilized by **SDSU**. Indeed the latter were very easily synthesized and their high catalytic activity allowed to achieve impressive substrate selectivity just by means of the hydrophobic effect.

6. GENERAL CONCLUSIONS

The research activity of the past three years began with the idea of obtaining catalytic systems capable of mimicking enzymes through the use of supramolecular structures. Enzymes are biological catalysts whose properties are still unrivalled by traditional homogeneous catalysts. One reason for this unique efficiency is attributed to the large dimensions of enzymes and their ability to pre-orient the substrate molecules to reach the active site. Here, functional groups specifically interact with the substrate causing changes in the three-dimensional structure of both the enzyme and the guest molecule thereby favouring the catalytic phenomenon. Therefore the development of especially designed supramolecular three-dimensional structures surrounding homogeneous catalysts was the easier way conceived to organize systems behaving similarly to enzymes. For this reason the research activity of these three years covered the study of the catalytic applications of both the resorcin[4]arene hexameric self-assembly in organic solvent and micelles self-assembly in water using commercial surfactants.

In Chapter 3.2 it has been proven that the hexameric capsule of resorcin[4]arene is much more than a simple supramolecular host capable of accommodating cationic compounds providing steric hindrance. In fact, it can behave as an efficient supramolecular organo-catalyst capable of both interacting with formally neutral substrates increasing their reactivity and generating reactive nano-environments in solution where cation- π interactions favour the formation of cationic activated intermediates accelerating certain reactions.

Although isocyanides are neutral molecules with minimal hydrogen bonding properties, the supramolecular hexameric capsule proved capable to encapsulate them. The reason of this phenomenon was attributed to the particular electronic distribution of the isonitrile functional group that has to be considered predominantly carbenic with substantial nitrogen lone pair donation. Their encapsulation catalysed the addition of water leading to the effective formation of the corresponding N-formylamides under mild experimental conditions.

The cation- π interactions and the partial acidity of the capsule lead us to exploit the nucleophilic attack of species other than water. With this purpose trimethylsilyl azide was used as a source of nucleophilic species to drive the formation of *1H*-tetrazoles via the [3+2] cycloaddition with isocyanides. The supramolecular capsule effectively catalysed this reaction, proving sensitive to the size and nature of the substrate (Figure 62).

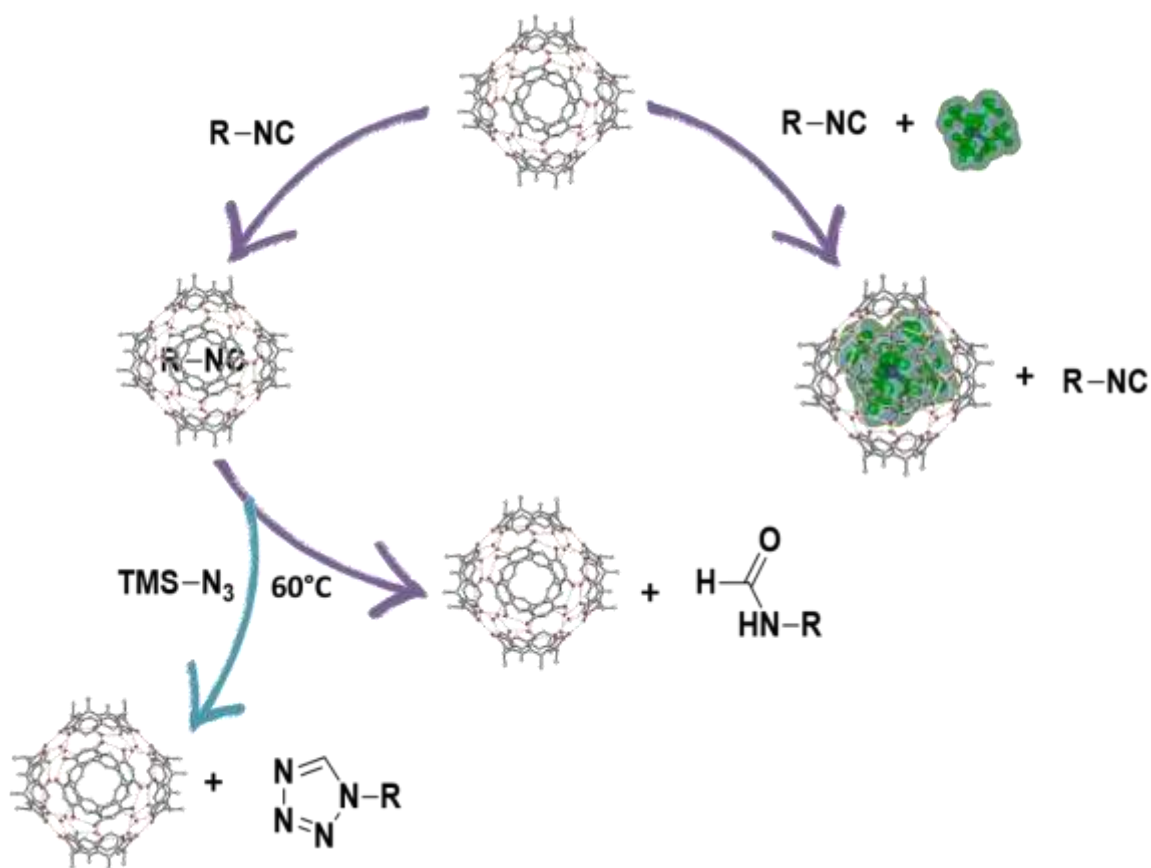


Figure 62. Nucleophile attack either of water or trimethylsilyl azide mediated by resorcin[4]arene capsule (chapter 3.2.1)

The interaction of isocyanides within the resorcin[4]arene capsule suggested to demonstrate the possible encapsulation of other formally neutral compounds with partial carbene-like electron poor character like diazoacetate esters. Hence the 1,3-dipolar cycloaddition between the diazoacetate esters and electron-poor alkenes such as α,β -unsaturated aldehydes, acrylonitrile and acrylate esters was successfully proven, with the internal surface of the resorcin[4]arene capsule being responsible for the observed catalytic effect (Figure 63).

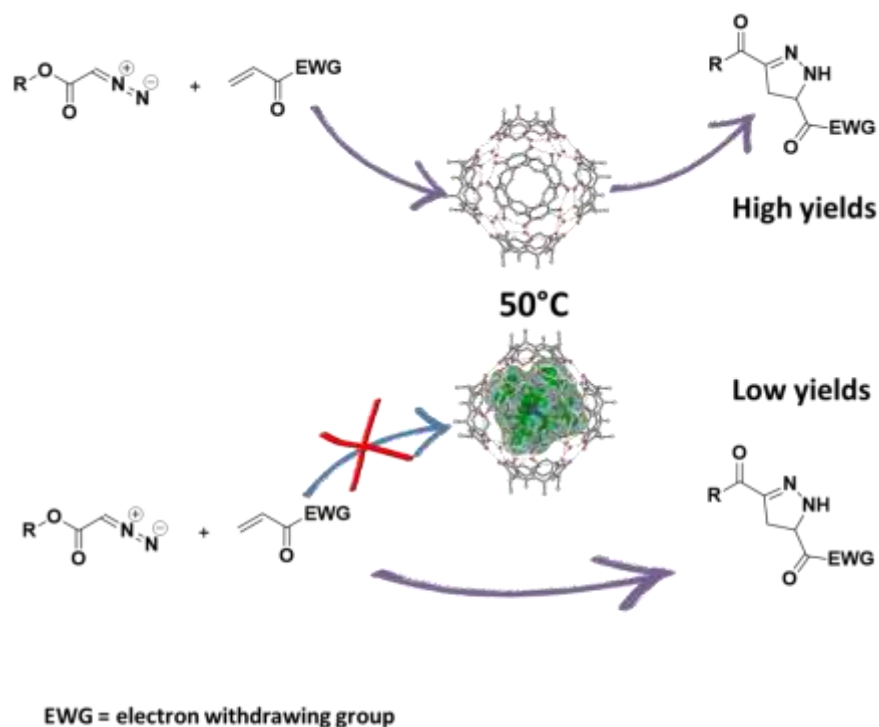


Figure 63. 1,3-dipolar cycloaddition between the diazoacetate esters and electron-poor alkenes mediated by the capsule (Chapter 3.2.1.)

The six-month collaboration with prof. Ballester research group at the ICIQ in Tarragona was employed to investigate the interaction between the hexameric capsule and N-oxides as highly polar formally neutral molecules. This study allowed to observe the behavior of the supramolecular system in the presence of a guest capable to interact with the capsule through hydrogen bonds. N-oxides exhibit the presence of both a positively charged nitrogen atom conferring a guest character to these compounds and also a strongly negatively charged oxygen atom capable of hydrogen bonding with the hydroxyl groups of resorcin[4]arene. The latter effect proved quite interesting since it connected the N-oxide also with the outer surface of the supramolecular structure when the cavity was occupied by a competitive guest (Figure 64). Unfortunately when an excess of N-oxide molecules with respect to the capsule were introduced in solution, the capsule was disassembled in other supramolecular structures.

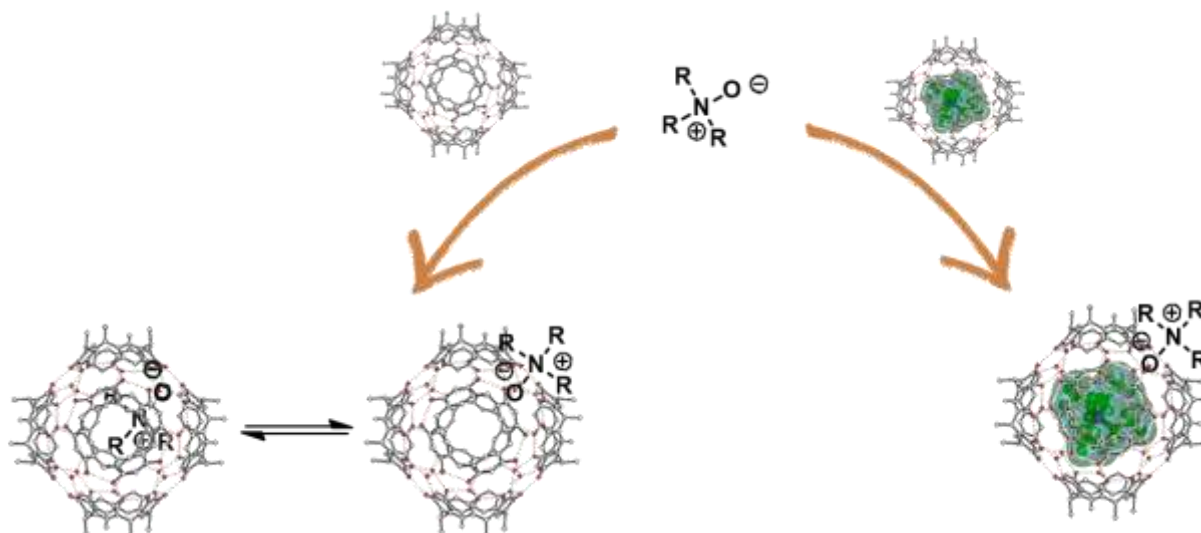


Figure 64. Interaction between N-oxides and resorcin[4]arene capsule (chapter 3.2.2.).

The N-oxides ability to maintain the connection with the capsule even in the presence of a competitive guest was employed to demonstrate the importance of hydrogen bonds in stabilizing N,N-dimethylprop-2-yn-1-amine oxide (**DPNO**) rather than encapsulating it in the supramolecular host. The strong interaction with the capsule was exploited to modify the product selectivity in the reaction between isocyanates and N-oxides that was never investigated before. This reaction proved sensitive to both the electronic features of isocyanates and the specific N-oxide employed. Under appropriate conditions the reaction between N-methylmorpholine N-oxide (**MMNO**) and phenyl isocyanate substituted with electron withdrawing groups led to the formation of diazo compound derivatives in yields depending on the phenyl isocyanate nature. The supramolecular system, even in the presence of a competitive guest, completely changed the product selectivity due to H-bonds interaction with **MMNO** and the reaction gave the corresponding urea derivative as the main product even in the presence of a competitive guest (Figure 65).

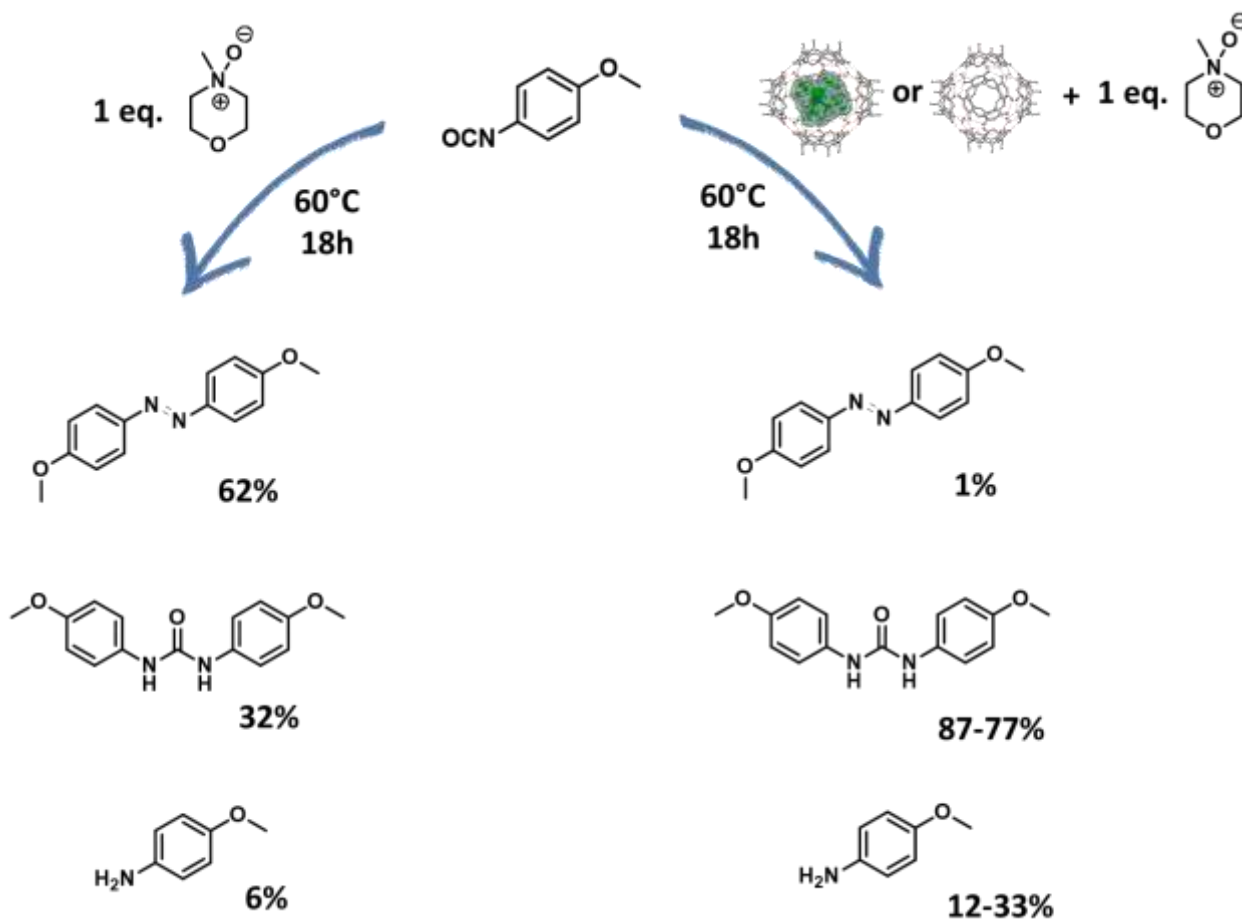


Figure 65. Product selectivity of the reaction between p-methoxyphenyl isocyanate and N-methylmorpholine N-oxide either in the presence and in the absence of the supramolecular capsule (Chapter 3.2.2.).

The proven potentialities of the cation- π interactions within the supramolecular cavity were pushed a step forward towards catalysis and were exploited to facilitate the formation of reaction intermediates, achieving catalytic effects. This was the case of the selective oxidation of thioethers to sulfoxide in the presence of hydrogen peroxide as oxidant where the capsule acted as an effective and selective organocatalyst in the presence of both aliphatic and aromatic sulfides (Figure 66). Although the H-bonding donor character of the hexameric capsule might not be considered sufficient to activate hydrogen peroxide to achieve this result, catalytic tests confirmed that the supramolecular cavity could indeed promote the formation of sulfoxides because of the partially positively charged S atom in this class of molecules.

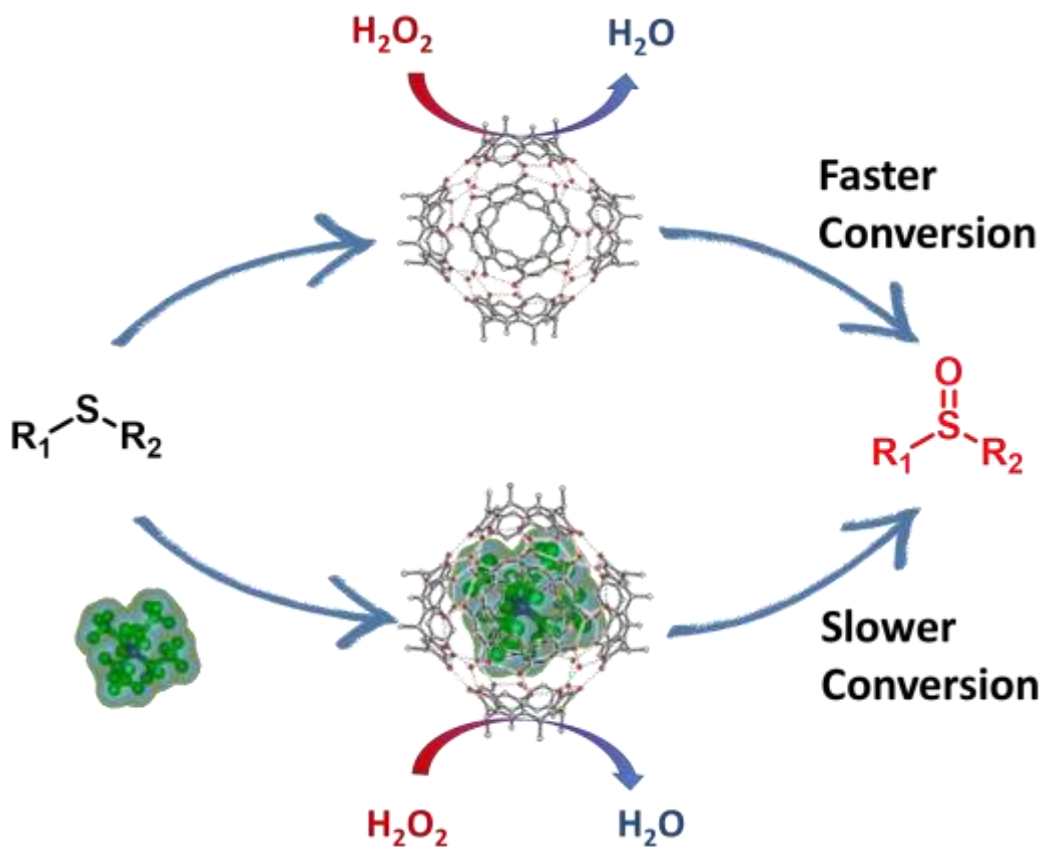


Figure 66. Sulfoxidation mediated by the capsule in the presence of H_2O_2 as oxidizing agent (Chapter 3.2.3.).

The promoting properties of the hexameric capsule were further studied during the acid-catalyzed alkynes hydration. Even in this case the resorcin[4]arene capsule did not show interactions with substrates molecules however the hydration reaction of terminal alkynes to the corresponding methyl ketones was actually speeded up by the supramolecular system. We inferred that the cation- π interactions within the cavity caused affinity of the capsule for the cationic intermediate obtained after the protonation of the alkyne during the rate determining step. Therefore the presence of the empty capsule allowed the hydration of non-deactivated aromatic alkynes with sub-stoichiometric amounts of HBF_4 at $60^\circ C$ within hours, while the introduction of a competitive guest caused the clear deactivation of the supramolecular system (Figure 67). The confined space within the cavity conferred substrate selectivity to the supramolecular system due to the steric hindrance of the substrate both with terminal and internal alkynes.

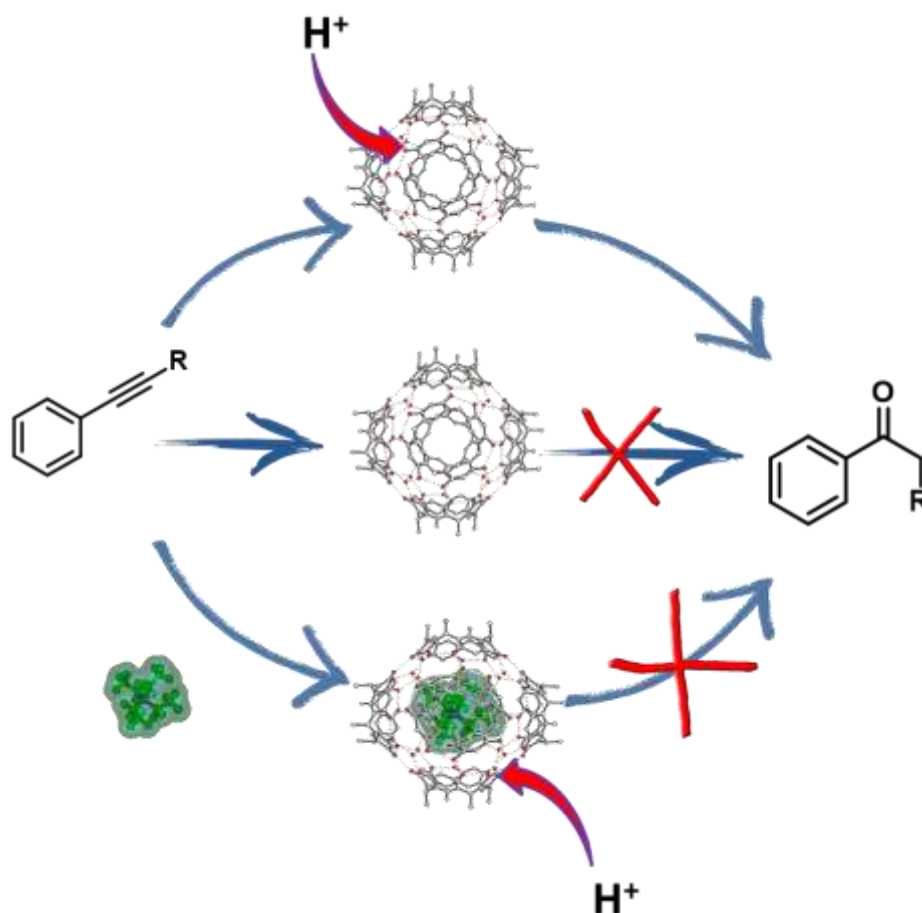


Figure 67. Acid-catalysed hydration of alkynes mediated by the hexameric capsule in the presence of few amounts of Brønsted acid (Chapter 3.2.3.).

In Chapter 4.2 innovative applications of micellar media in the field of “green chemistry” have been reported. In particular, very interesting results were achieved when we tried to develop catalytic systems for hydrogenation reactions in water through a facile, economical and environmentally friendly procedure. The use of sodium dodecylbenzenesulfonate (SDBS), dioctyl sulfosuccinate sodium salt (**DOSS**), poly(ethylene glycol) 4-nonylphenyl-3-sulfopropyl ether potassium salt (**Ralufon**[®]) and sodium dodecyl sulfonate (**SDSU**) as sulfonated anionic surfactants proved pivotal to reach this result. With these surfactants, stable Pd nanoparticles systems were formed simply by treating a solution of Pd(OAc)₂ and a surfactant in water with 1 atmosphere of H₂ at room temperature. These Pd-NPs systems proved versatile catalytic activity by simply changing the sulfonated anionic surfactant employed during their synthesis. This allowed to achieve catalytic systems that proved more effective under mild conditions compared to commercial Pd/C both in reactions requiring high activity and in semi-hydrogenation reactions (Figure 68). Moreover the use

of **Ralufon**[®] allowed to obtain a recyclable system capable to catalyze the hydrodechlorination reaction in water showing stability even at high pressures.

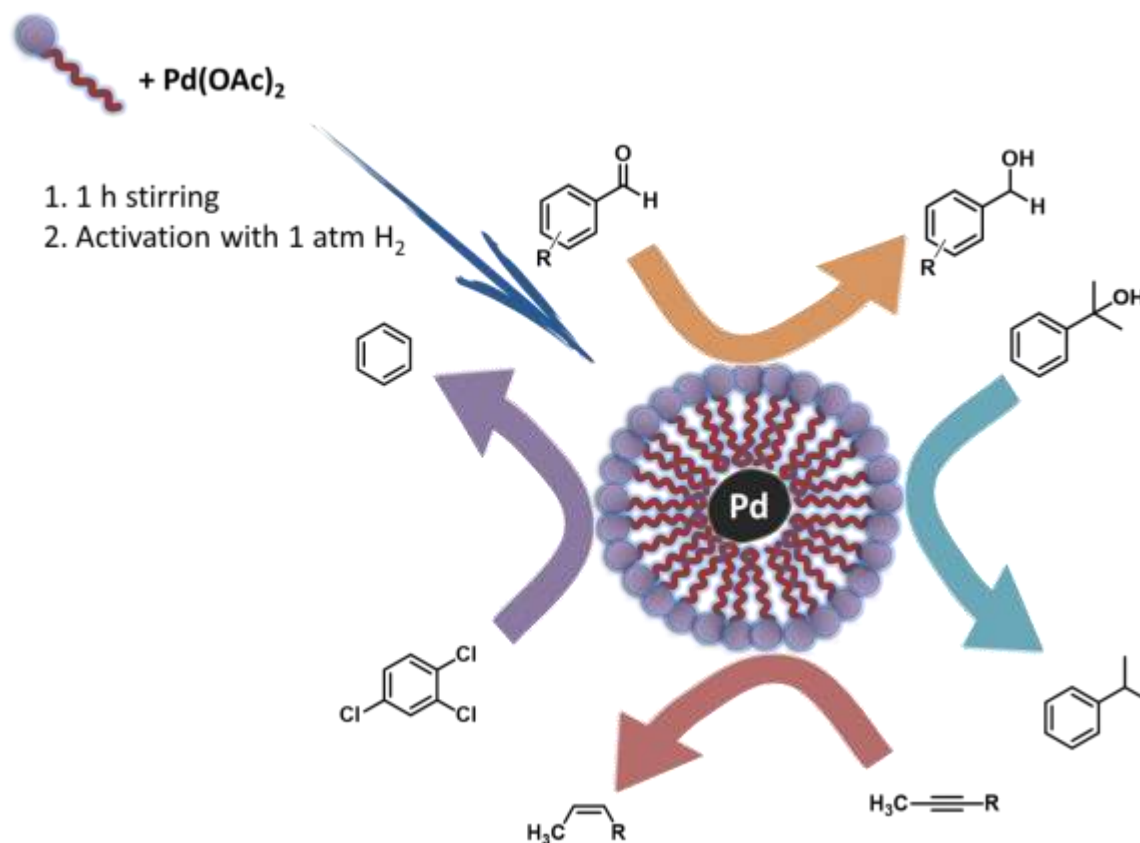


Figure 68. Hydrogenation reactions catalysed by Pd-NPs in micellar media with sulfonated anionic surfactants in water under mild conditions (chapter 4.2.1.)

Another impressive application of the micellar media was showed during the study of the multi-component synthesis of 1,4-disubstituted 1,2,3-triazoles from organic bromides, sodium azide and alkynes catalysed by [Cu(IMes)Cl] (IMes 1,3-bis(2,4,6-trimethylphenyl)imidazol-2-ylidene). The reaction is usually carried out in two steps. In the first step a highly polar solvent is required to solubilize the NaN₃ salt and obtain the formation of the organic azide with high yields, while in the second step an apolar organic medium is necessary to solubilize substrates and catalyst. A suitable surfactant in water could be exploited to obtain an environmentally friendly reaction medium capable of accommodating both the steps in one shot. Water dissolved NaN₃ while the apolar nano-environment inside the micelles dissolved both the organic substrate and the Cu-catalyst. In the attempt to use only commercially available surfactants we proved that SLS and TPG-750-M gave the best results, achieving good yields in a relatively short time, at room temperature with several substrates. Moreover, the micellar media allowed triazole products isolation by a simple extraction

with ethyl acetate. Therefore we demonstrated that the employment of micellar media could allow the one-pot synthesis of 1,4-disubstituted 1,2,3-triazoles in water, avoiding the purification of intermediate products through a very economic expedient (Figure 69).

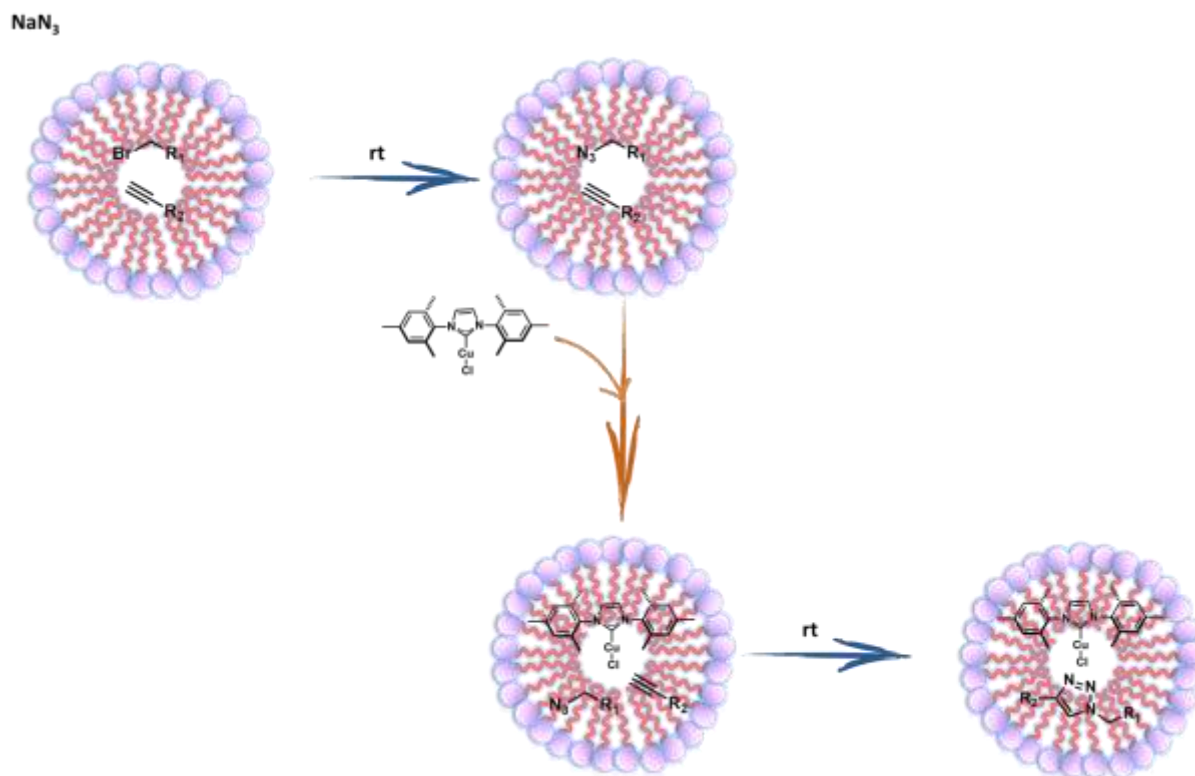


Figure 69. One-pot synthesis of 1,4-disubstituted 1,2,3-triazoles aqueous micellar media (Chapter 4.2.2.)

Then supramolecular structures were used to achieve substrate selectivity mimicking one of the most important properties of enzymes.

The resorcin[4]arene capsule could allow to obtain catalytic systems with substrate selectivity exploiting the steric hindrance caused by the walls of the supramolecular scaffold. The presence of a catalyst within the cavity forces the reaction to take place in a limited space accessible only to substrates with suitable size and shape. In the first example the cationic carbodiimide 1-ethyl-3-(3-dimethylaminopropyl) carbodiimide hydrochloride (**EDAPC**) was employed as coupling agent during the competitive condensation between acids and amines to amides. The reaction was carried out both in the presence and in the absence of the hexameric capsule checking the different selectivities imparted by the catalytic system with a series of carboxylic acids and amines characterized by different lengths. In the absence of the self-assembled capsule the coupling reaction caused the formation of all possible amides in very similar amounts. Conversely the small empty space remaining within the hexameric capsule caused the better co-encapsulation of smaller

substrates leading to the preferential formation of shorter amides. The collected data demonstrated the main role of the selective binding of the carboxylic acid as the driving force for substrate selectivity. Good results in terms of substrate selectivity were achieved during the competitive reaction of pairs of competitive substrates showing higher selectivity for the shorter products (Figure 70).

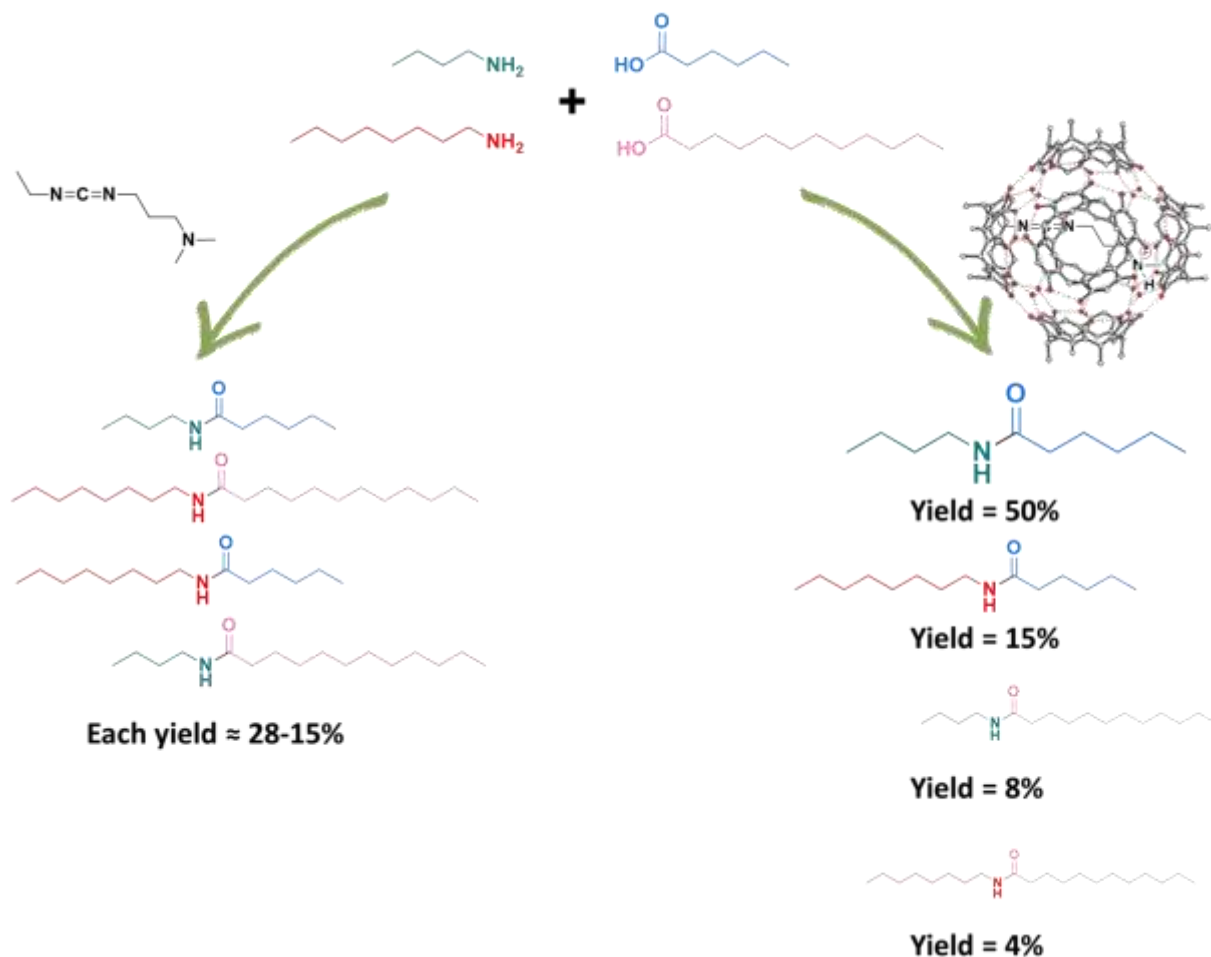


Figure 70. Substrate selective amide coupling catalyzed by 1-ethyl-3-(3-dimethylaminopropyl) carbodiimide hydrochloride within the hexameric capsule (Chapter 5.2.2.).

The presence of apolar nano-environments within aqueous micellar media was employed to achieve catalytic systems capable to give the selective conversion of more hydrophobic substrates during competitive reactions. An interesting example of this kind of selectivity was reported carrying out the competitive cross-coupling Heck reaction in water in the presence of cetyl trimethyl ammonium bromide (CTAB) as cationic surfactant. CTAB imparted better activity to the catalytic system avoiding the precipitation of palladium aggregates. Moreover the presence of this

surfactant and the employment of acrylate esters with different length as competitive substrates allowed to reach a good substrate selectivity in cross-coupling reactions with iodoaryl derivatives (Figure 71). The same reaction carried out in organic solvent did not exhibit any preferential conversion, showing the importance of the hydrophobic effect to achieve substrate selectivity.

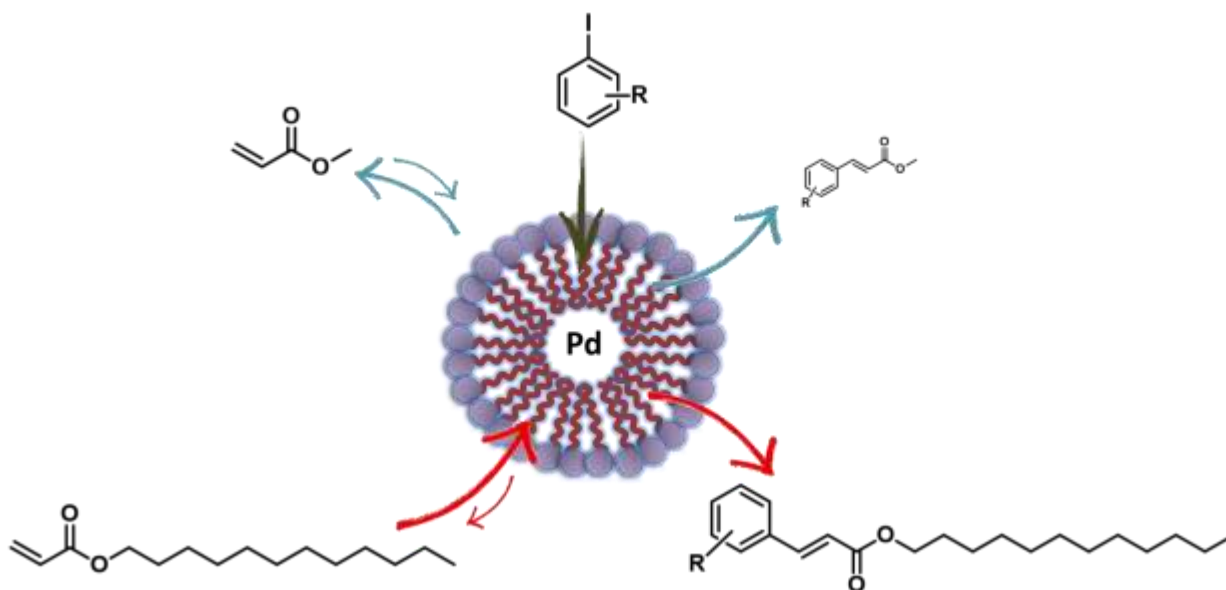


Figure 71. Substrate selective Cross-Coupling Heck reaction mediated by Pd in cationic micellar medium (Chapter 5.2.2.)

The use of micellar media to achieve the faster conversion of more hydrophobic compounds in competitive reactions was further investigated during the competitive chemo-selective hydrogenation of α,β -unsaturated aldehydes. The reaction carried out in an organic solvent showed that shorter substrates reacted faster probably due to their lower steric hindrance, while in the presence of micellar media we obtained catalytic systems with different properties depending on the surfactant employed. Cationic surfactants proved unsuitable to obtain active catalytic system for this reaction because they were unable to avoid the aggregation of the involved Pd-NPs. Neutral surfactants caused the formation of a biphasic system with maximum selectivity for intermediate sized substrates like *trans*-2-heptenal. Finally, anionic surfactants enabled the achievement of a catalytic system with effective substrate selectivity. In particular, sodium dodecyl sulfate exhibited an increasing substrate selectivity for more hydrophobic compounds conferring to the longer substrate *trans*-2-decenal an initial rate 3.7 times higher than that of the shorter crotonaldehyde. The replacement of sodium dodecyl sulfate with sodium dodecyl sulfonate proved very successful showing very high substrate selectivity in favour of the more hydrophobic aldehydes. In fact, a 330 times higher initial hydrogenation rate was observed in the presence of longest substrate in

comparison with the shortest one (Figure 72). This result proved very impressive considering that the substrate selectivity is simply due to the hydrophobic effect.

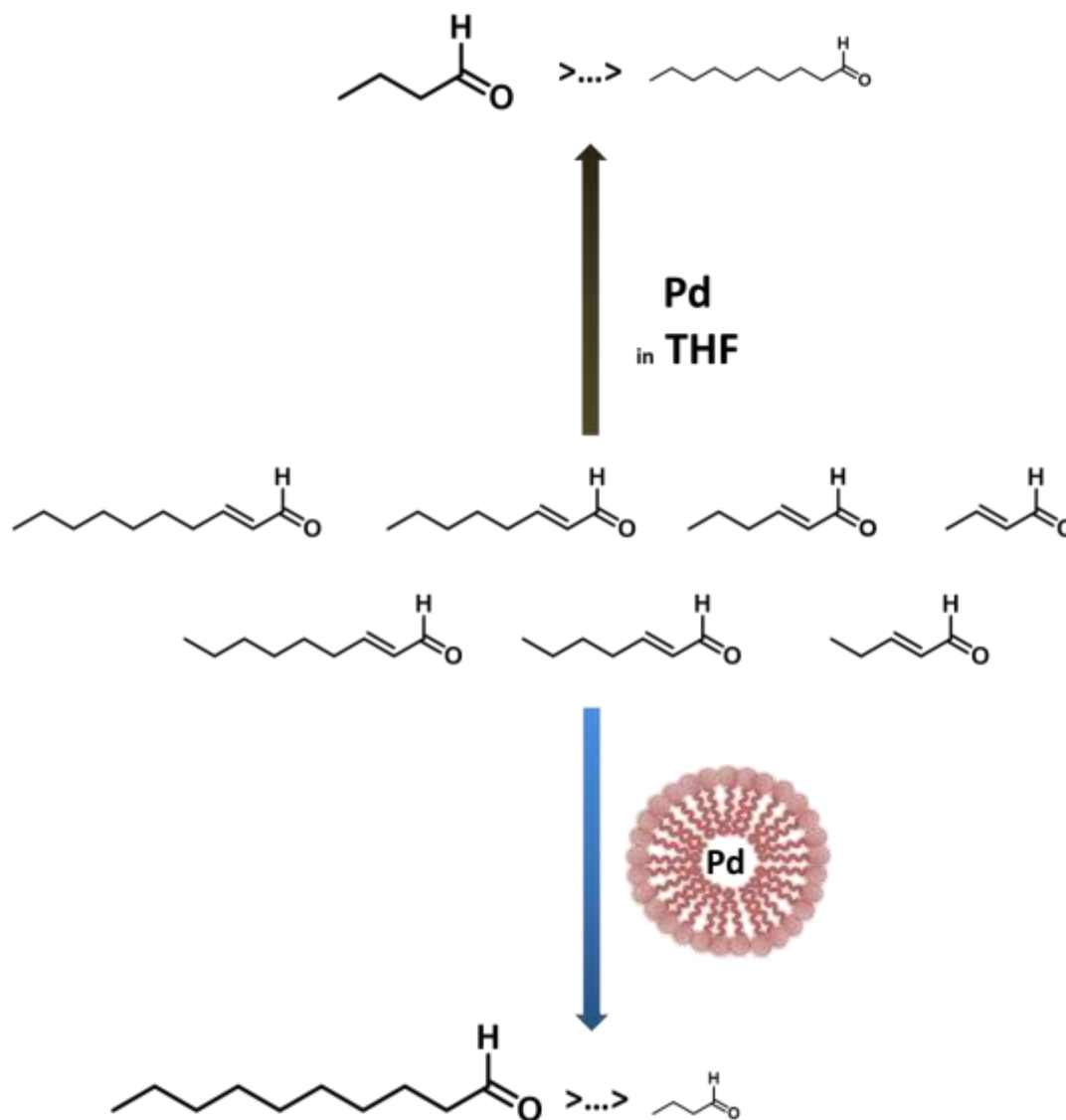


Figure 72. Substrate selective hydrogenation reaction of α,β -unsaturated aldehydes in micellar media (Chapter 5.2.2.)

The aim of this work was to show the advantages that supramolecular structures could confer to homogeneous catalysts through simple and effective methodologies. The use of supramolecular scaffolds around the reaction sites allowed to reach systems capable to mimic some enzyme features, avoiding further complications during the synthesis of the catalysts. In fact, we demonstrated that the confined space within a supramolecular structures could behave like the active site of an enzyme. In the case of the hexameric capsule, the weak interactions developed within the cavity play a pivotal role both in the recognition, in the activation of substrates and in the formation of reaction intermediates like enzymes do. Micellar assemblies cause the formation of

apolar nano-environments that enable to carry out reactions in water even in the presence of strongly hydrophobic organic compounds. Moreover several other interesting properties can be implemented. The use of the proper micelles allows to synthesize very active metal nanoparticles in water achieving highly active catalytic systems capable to work in eco-friendly media. The formation of apolar nano-environments in water enables multi-step reactions between substrates with very different solubility properties in one-pot processes. Finally the presence of a confined space with well-defined size and shape like in capsules, or with polarity properties completely different from the external solution like in micelles, can allow to achieve substrate selectivity.

Therefore the scientific endeavour required for artificial catalysts to reach the amazing properties of enzymes will certainly need the contribution of supramolecular chemistry and I sincerely hope that this work will be helpful in this process.

7. EXPERIMENTAL

7.1. Compounds and Analyses

SOLVENTS

Solvents were used as received; otherwise they were purified as reported in the literature.²⁷⁹

SUBSTRATES AND CATALYSTS

- Crotonaldehyde, trans-2-pentenal, trans-2-hexenal, trans-2-heptenal, trans-2-octenal, trans-2-nonenal, trans-2-decenal, benzaldehyde, 4-(tert-butyl)-benzaldehyde, 4-methoxy-benzaldehyde, o-tolualdehyde, 2,4-dimethylbenzaldehyde, 2,6-dimethylbenzaldehyde, 2,4,6-trimethylbenzaldehyde, acetophenone, benzyl alcohol, 1-phenylethanol, 2-phenylpropan-2-ol, phenylacetylene, 4-ethynyl-toluene, 1-ethynyl-4-pentylbenzene, 1-(tert-butyl)-4-ethynylbenzene, 1-ethynyl-4-methoxybenzene, 1-ethynyl-4-phenoxybenzene, 1-decyne, 4-phenyl-1-butyne, Dimethyl propargylmalonate, 5-hexyn-1-ol, 1-phenyl-1-propyne, 1-phenyl-1-hexyne, chlorobenzene, 1,2,4-trichlorobenzene, sodium ascorbate, 1-octyne, sodium azide, benzyl bromide, 1-tetradecyne, 3-ethynyltoluene, 3-bromobenzyl bromide, 4-bromobenzyl bromide, allyl bromide, 3,3-dimethyl-1-butyne, ethynyl cyclopentene, ethynyl cyclohexane, isopropyl isonitrile, iodobenzene, 1-iodo-naphthalene, 2-chloriodobenzene, methyl acrylate, ethyl acrylate, butyl acrylate, hexyl acrylate, lauryl acrylate, t-butyl isonitrile, cyclohexyl isonitrile, benzyl isonitrile, 2,6-dimethyl-phenyl isonitrile, 2-naphthyl isonitrile, (S)-(-)- α -methylbenzyl isonitrile, 1,1,3,3-tetramethylbutyl isonitrile, trimethylsilyl azide, ethyl-diazoacetate, *tert*-butyl-diazoacetate, benzyl-diazoacetate, acrolein, methyl propiolate, 1-ethyl-3-(3-dimethylaminopropyl) carbodiimide hydrochloride, tetraethylammonium tetrafluoroborate, hexanoic acid, butyric acid, dodecanoic acid, tridecanoic acid, butylamine, octylamine, hexadecylamine, butyl sulfide, 2-chloroethyl ethyl sulfide, *tert*-butyl methyl sulfide, thioanisole, 4-methoxythioanisole, 4-chlorothioanisole, 4-bromothioanisole, 4-(methylthio)benzonitrile, 1-(4-(methylsulfinyl)phenyl)ethanone, 4-nitrothioanisole, benzyl phenyl sulfide, 2-(methylthio)naphthalene, 4-mercaptopyridine, *p*-Tolyl disulfide, 4-(methylthio)aniline, 1-ethynyl-4-methoxy-2-methylbenzene, 2-ethynyltoluene, 9-ethynylphenanthrene, methyl 4-

ethynylbenzoate, 3-ethynylpyridine, $\text{HBF}_4 \sim 55 \text{ wt.}\%$ in H_2O , methanesulfonic acid, trimethylamine N-oxide, N,N-Dimethyldodecylamine N-oxide N-methylmorpholine N-oxide, p-methoxyphenyl isocyanate, p-dimethylaminephenyl isocyanate, p-tolyl isocyanate, p-acetylphenyl isocyanate, p-nitrophenylisocyanate, p-methoxyaniline are all commercially available products (Aldrich) and were used as received without any further purification.

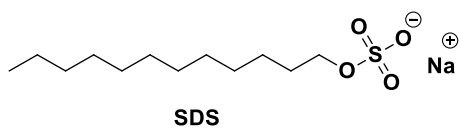
- $\text{Pd}(\text{OAc})_2$, Pd/C 10 wt.%, CuSO_4 , $[\text{Cu}(\text{IMes})\text{Cl}]$ (IMes = 1,3-bis(2,4,6-trimethylphenyl)imidazol-2-ylidene), are all commercially available products (Aldrich) and were used as received without any further purification.

- $\text{HCl} \geq 37 \text{ wt}\%$, $\text{HNO}_3 \geq 69 \text{ wt}\%$ are commercially available products (Fluka) and were used as received without any further purification,

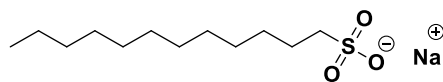
- Resorcin[4]arene²⁸⁰ was prepared as reported in the literature. All the cycloaddition products were identified by GC-MS and $^1\text{H-NMR}$ analysis.

SURFACTANTS

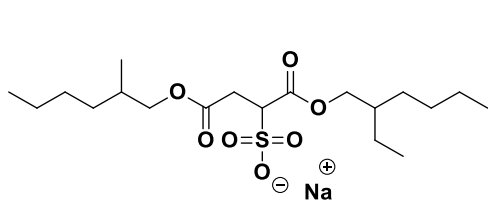
Sodium dodecyl sulfate (SDS), sodium dodecyl sulfonate (SDSU), dioctyl sulfosuccinate sodium salt (DOSS), sodium dodecylbenzene sulfonate (SDBS), poly(ethylene glycol) 4-nonylphenyl-3-sulfopropyl ether potassium salt (Ralufon[®]), sodium lauryl sulfosuccinate (SLS), Triton-X114, Triton-X100, cetyl trimethylammonium bromide (CTAB), TPGS-750-M, and N-dodecyl-N,Ndimethyl-3-ammonium-1-propan sulfonate (DDAPS) are all commercially available products (Aldrich) and were used as received without any further purification.



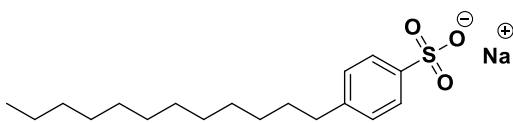
SDS



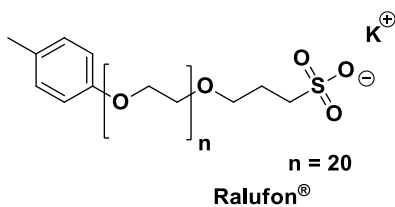
SDSU



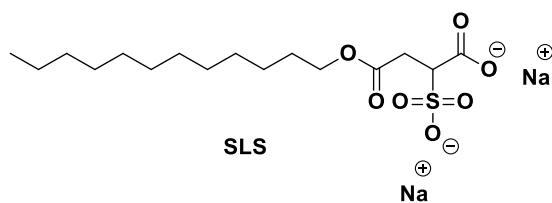
DOSS



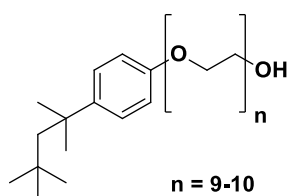
SDBS



Ralufon[®]

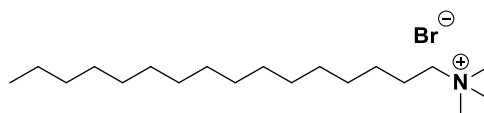


SLS

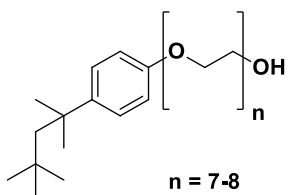


n = 9-10

Triton-X 100

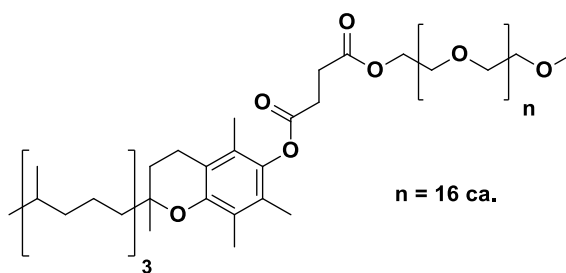


CTAB



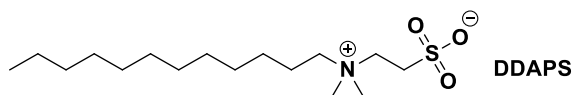
n = 7-8

Triton-X 114



n = 16 ca.

TPGS-750-M



DDAPS

SAMPLES ANALYSIS

- General ¹H NMR were recorded at 298 K, unless otherwise stated, on a Bruker AVANCE 300 spectrometer operating at 300.15 MHz. δ values in ppm are relative to SiMe₄.

- TLC analysis were performed on TLC Polygram[®] Sil G/UV254 of 0.25 mm thickness and flash-chromatography separations were performed on silica gel Merk 60, 230-400 mesh.²⁸¹

- GC-MS analyses were performed on a GC Trace GC 2000 coupled with a quadrupole MS Thermo Finnigan Trace MS with Full Scan method. Experimental conditions are reported in the following table.

Experimental conditions for GC-MS analyses

Capillary column:	HP5-MS 30 m, 0.25 mm x 0.25 μ m
Initial T (°C):	80°C for 5 min
Rate (°C/min.):	30°C/min.
Final T (°C):	280°C for 30 min.
Injector T, split (°C):	280°C
Gas carrieri flow (mL/min.):	0.8 mL/min.
Injected volume (μL):	0.8-1 μ L
Solvent delay (min.):	4 min.
Mass range (amu):	35-500 amu
Detector voltage (V):	350 V
Interface T (°C)	280°C
Source T (°C)	200°C

- Samples of the Pd-NPs obtained in water in the presence of SDSU as surfactant were analysed by means of TEM methods. Size and morphology of the nanoparticles were studied through a JEOL JEM 3010 transmission electron microscope (TEM) operating at 300 kV; the powder specimens were suspended in isopropyl alcohol and then sonicated, 5 μ l of this suspension were deposited on a copper grid (300 mesh) coated with holey carbon film. The copper grids were allowed to dry in air.

7.2. Reactions

7.2.1. Hydration reaction of isocyanides capsule-catalysed

EXPERIMENTAL CONDITIONS

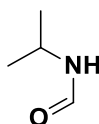
Water saturated solvent was prepared by shaking chloroform-d with bidistilled water at room temperature in a separation funnel. Resorcin[4]arene (6 equivalents, 79.6 mM) was placed in a 1.5 mL screw-capped vial equipped with silicone septum and dissolved in the water saturated chloroform-d (0.5 mL) stirring for a few minutes. To this solution, the chosen isocyanide (10 equivalents, 132.6 mM) was added. The system was then left at 60 °C and the reaction progress was monitored by ¹H NMR and GC analysis by periodically sampling directly from the reaction mixtures. Conversion, product assignment and product distribution were determined by direct GC, GC-MS and ¹H NMR analysis of the reaction mixture as the average of three experiments.

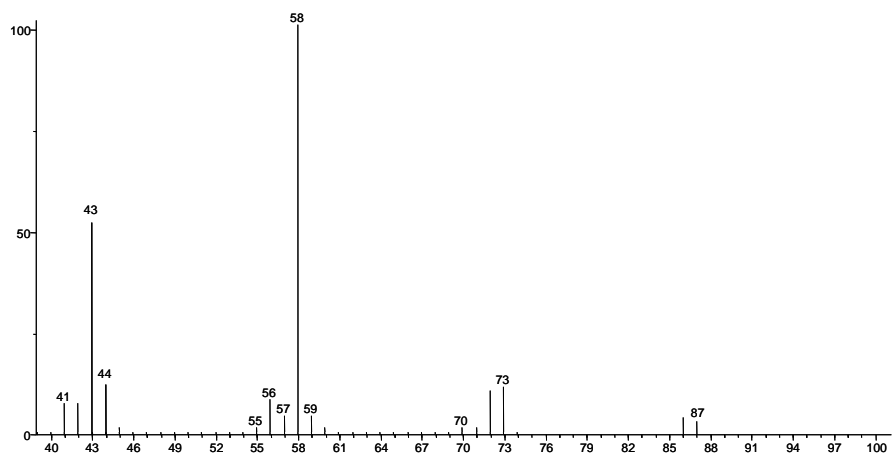
Experimental procedure as above reported was employed adding tetraethyl ammonium trifluoromethanesulfonate (10 equivalents, 132.6 mM) together with the substrates in order to carry out control tests of the catalytic activity of the activity within the capsule.

The reaction was carried out replacing resorcin[4]arene (79.6 mM) with resorcinol (318.4 mM) under the same conditions.

FORMYLAMIDES CHARACTERIZATION

- **N-isopropylformamide F2**





- **Figure 73.** Mass spectrum of N-isopropylformamide **F2**

- **N-tert-butylformamide F3**

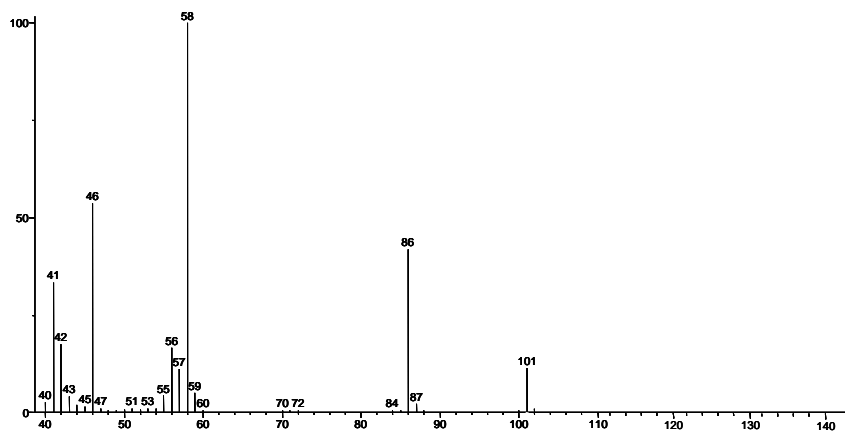
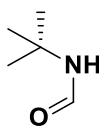
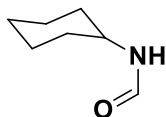


Figure 74. Mass spectrum of N-tert-butylformamide **F3**

- **N-cyclohexylformamide F1**



The observed $^1\text{H-NMR}$ chemical shifts corresponded to those reported by Lebleu and co-workers.²⁸²

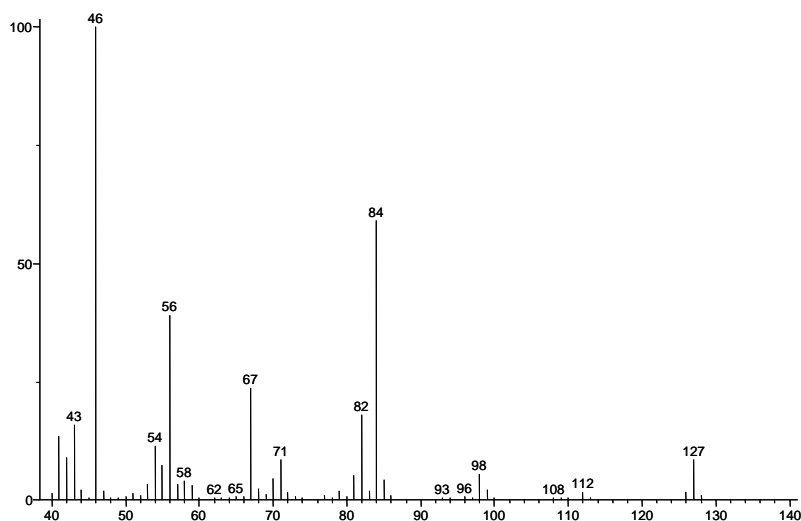
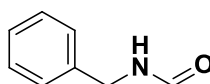
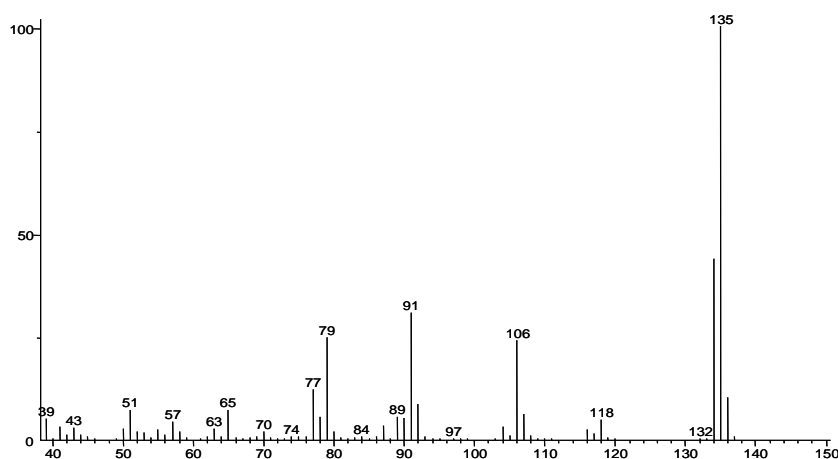


Figure 75. Mass spectrum of N-cyclohexylformamide F1

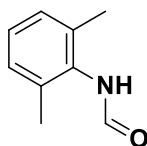
- N-benzylformamide F4



The observed $^1\text{H-NMR}$ chemical shifts corresponded to those reported by Lebleu and co-workers.²⁸²



- N-(2,6-dimethylphenyl)formamide F5



The observed $^1\text{H-NMR}$ chemical shifts corresponded to those reported by Deetz and co-workers.²⁸³

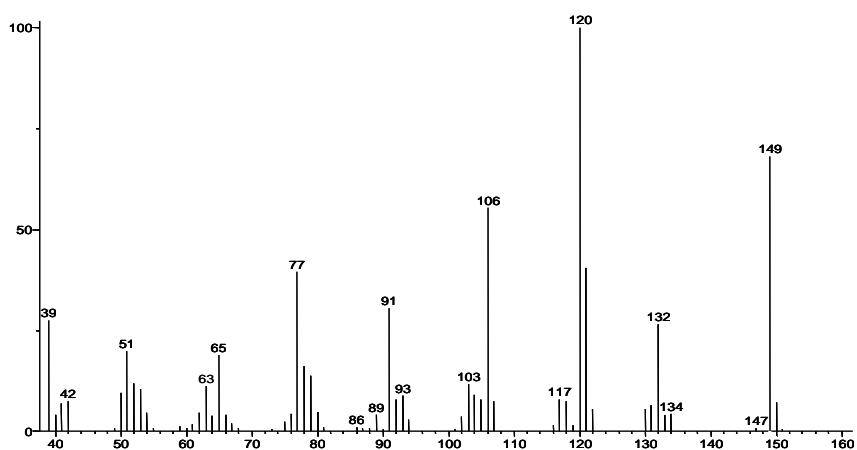


Figure 76. Mass spectrum of N-(2,6-dimethylphenyl)formamide **F5**

7.2.2. Addition of trimethylsilyl azide on isocyanides

EXPERIMENTAL CONDITIONS

Water saturated solvent was prepared by shaking chloroform-d with bidistilled water at room temperature in a separation funnel. Resorcin[4]arene (6 equivalents, 79.6 mM) was placed in a screw-capped vial equipped with silicone septum and dissolved in the water saturated chloroform-d (0.5 mL) stirring for a few minutes. To this solution, the chosen isonitrile (10 equivalents, 132.6 mM) and trimethylsilyl azide (10 equivalents, 132.6 mM) were added. The reaction was then thermostatted at 60 °C and the reaction progress was monitored by ^1H NMR and GC analysis by periodically sampling directly from the reaction mixtures. Conversion, product assignment and product distribution were determined by direct GC, GC-MS and ^1H NMR analysis of the reaction mixture as the average of three experiments.

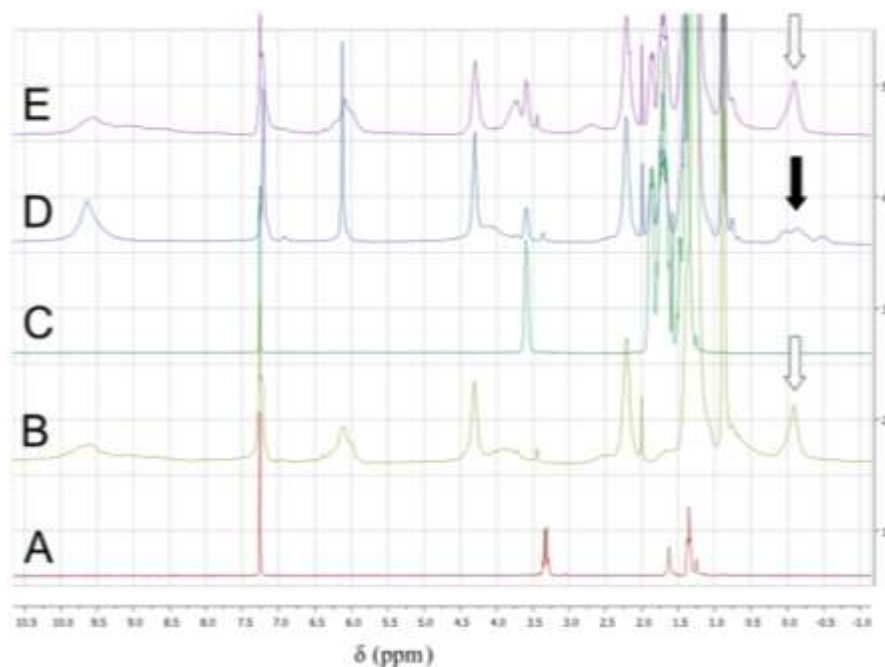
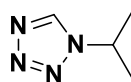


Figure 77. ^1H NMR spectra in water saturated chloroform-d: A) $\text{N}(\text{CH}_2\text{CH}_3)_4(\text{BF}_4)$ (132.6 mM), B) $\text{N}(\text{CH}_2\text{CH}_3)_4(\text{BF}_4)$ (132.6 mM) and capsule (13.3 mM) C) cyclohexyl isonitrile **II** (132.6 mM); D) cyclohexyl isonitrile **II** (132.6 mM) and capsule (13.3 mM); E) cyclohexyl isonitrile **II** (132.6 mM) and $\text{N}(\text{CH}_2\text{CH}_3)_4(\text{BF}_4)$ (132.6 mM) and capsule (13.3 mM); \blacktriangledown encapsulated isonitrile, \blacktriangledown encapsulated $\text{N}(\text{CH}_2\text{CH}_3)_4(\text{BF}_4)$.

PRODUCTS SYNTHESIS AND CHARACTERIZATION

- 1-isopropyl-1H-tetrazole **T2**



^1H NMR (300.15 MHz, CDCl_3): δ 8.59 (s, 1H); 4.85 (hept, $J = 6.4$ Hz, 1H); 1.38 (d, $J = 6.4$ Hz, 6H).

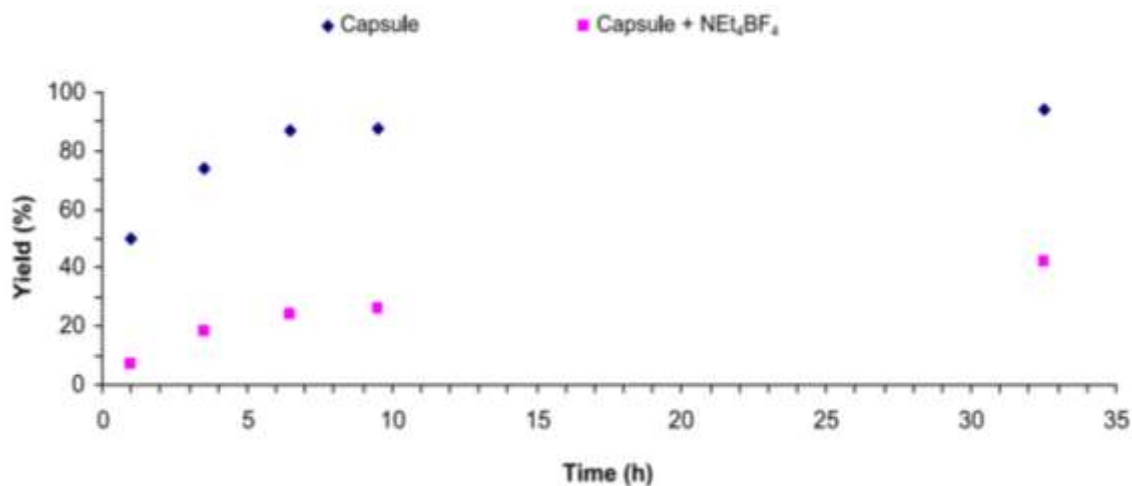


Figure 78. Product **T2** formation during the reaction between isocyanide **I2** and trimethylsilyl azide mediated by either by the empty (Blu) or filled (Pink) capsule in chloroform-d. Reaction conditions: [substrate] = 132.6 mM; [N(CH₂CH₃)₄(BF₄)] = 132.6 mM; [capsule] = 13.3 mM; 60°C; CDCl₃ = 0.5 mL

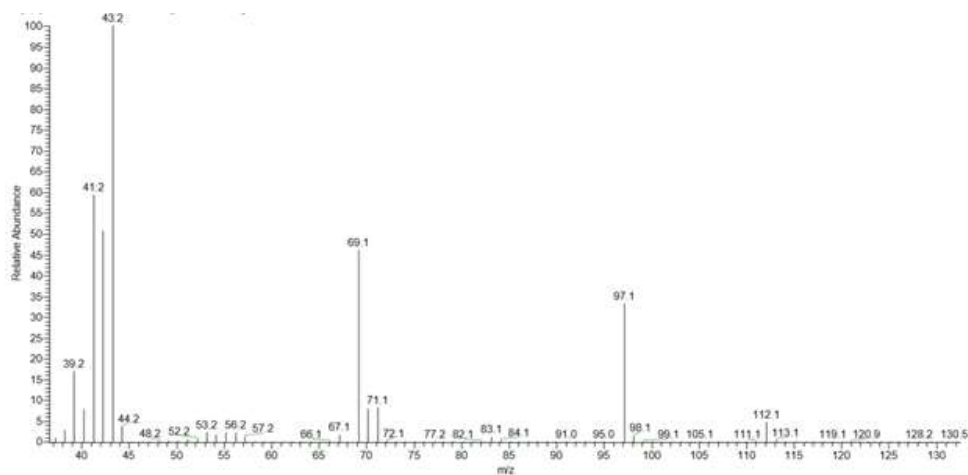
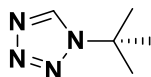


Figure 79. Mass spectrum of 1-isopropyl-1H-tetrazole **T2**.

- **1-tert-butyl-1H-tetrazole T3**



¹H NMR (300.15 MHz, CDCl₃): δ 8.61 (s, 1H); 1.71 (s, 9H).

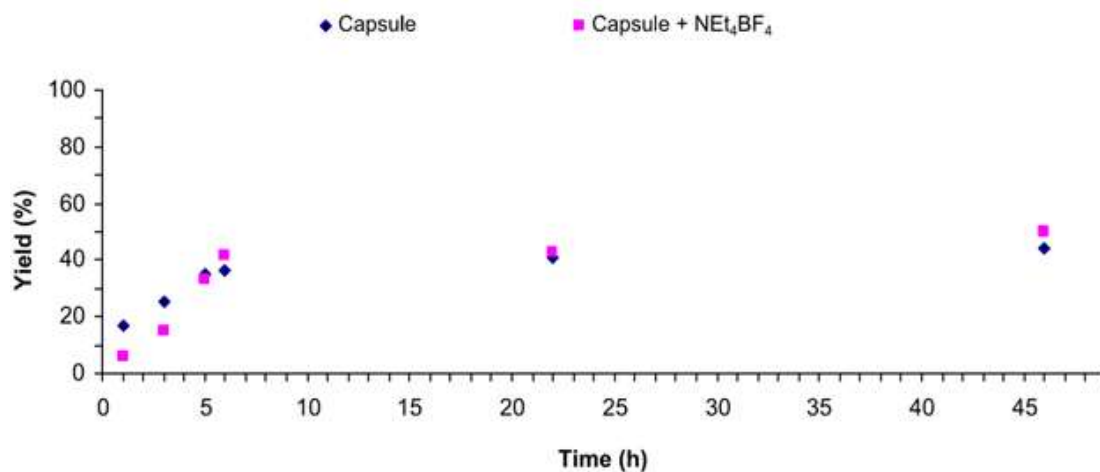


Figure 80. Product **T3** formation during the reaction between isocyanide **I3** and trimethylsilyl azide mediated by either by the empty (Blu) or filled (Pink) capsule in chloroform-d. Reaction conditions: [substrate] = 132.6 mM; [N(CH₂CH₃)₄(BF₄)] = 132.6 mM; [capsule] = 13.3 mM; 60°C; CDCl₃ = 0.5 mL.

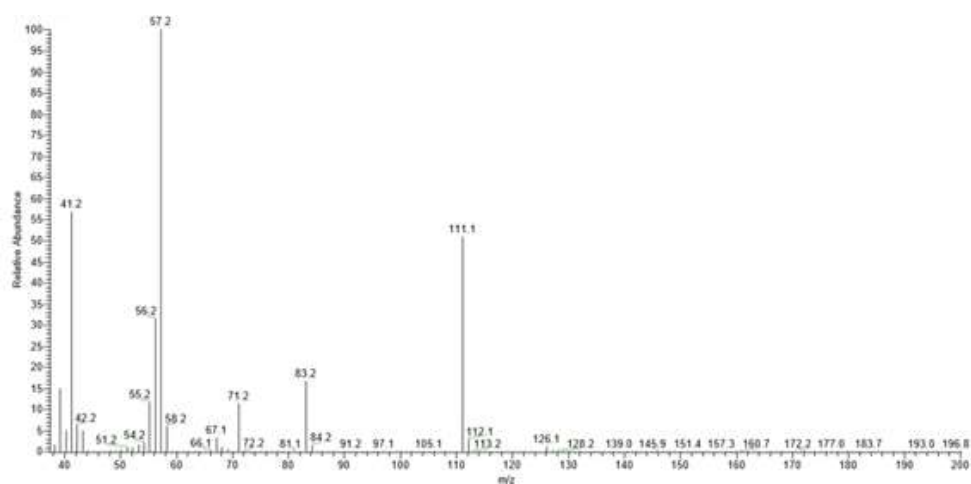
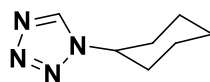


Figure 81. Mass spectrum of 1-tert-butyl-1H-tetrazole **T3**

- **1-cyclohexyl-1H-tetrazole T1**



¹H NMR (300.15 MHz, CDCl₃): δ 8.61 (s, 1H); 4.48 (tt, J = 11.4, 3.8 Hz, 1H); 1.95 (m, 2H); 1.78 (m, 4H) ; 1.47 (m, 4H).

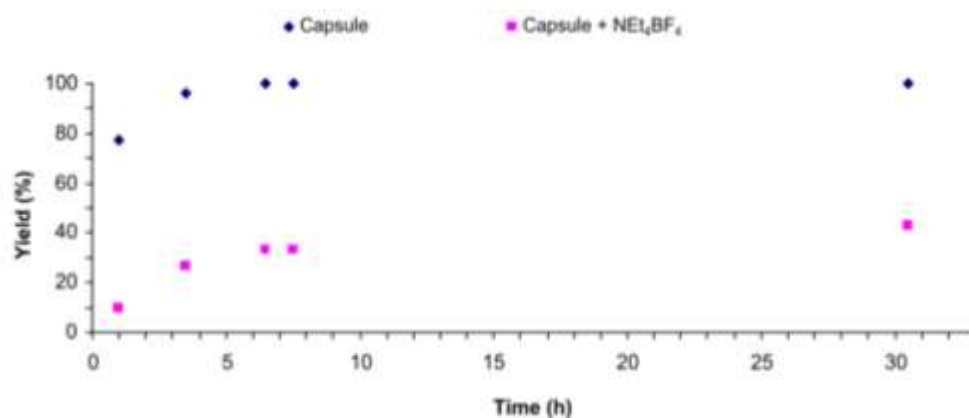


Figure 82. Product **T1** formation during the reaction between isocyanide **II** and trimethylsilyl azide mediated by either by the empty (Blu) or filled (Pink) capsule in chloroform-d. Reaction conditions: [substrate] = 132.6 mM; [N(CH₂CH₃)₄(BF₄)] = 132.6 mM; [capsule] = 13.3 mM; 60°C; CDCl₃ = 0.5 mL.

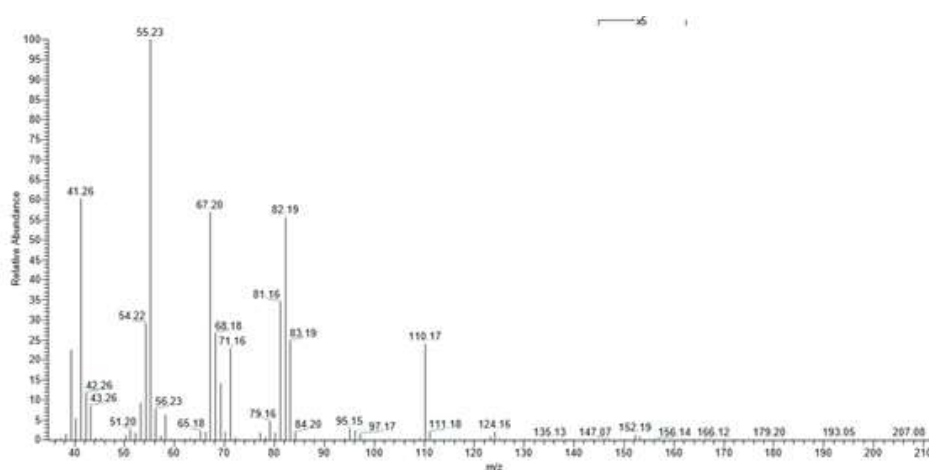
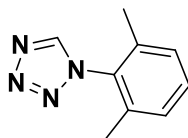


Figure 83. Mass spectrum of 1-cyclohexyl-1H-tetrazole **T1**

- **1-(2,6-dimethylphenyl)-1H-tetrazole T5**



¹H NMR (300.15 MHz, CDCl₃): δ 8.70(s, 1H); 7.37 (t, J = 7.6 Hz, 1H); 7.23 (d, J = 7.6 Hz, 2H); 1.97 (s, 6H).

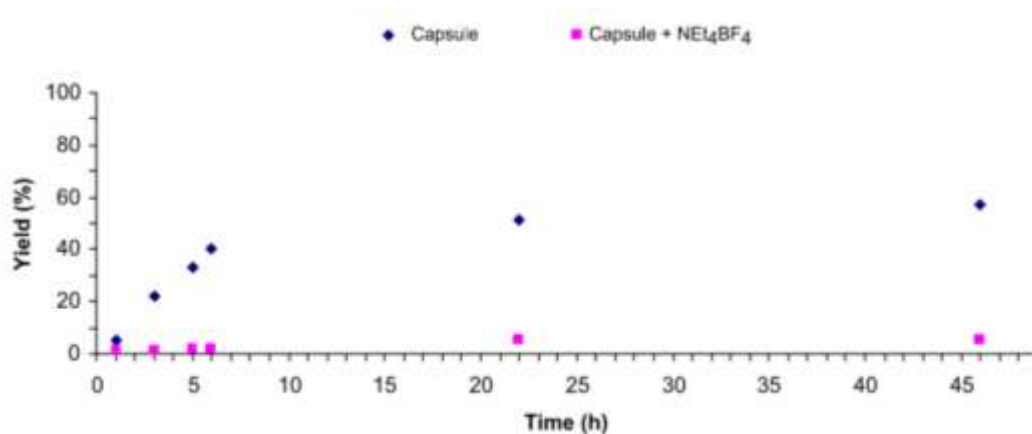


Figure 84. Product **T5** formation during the reaction between isocyanide **I5** and trimethylsilyl azide mediated by either by the empty (Blu) or filled (Pink) capsule in chloroform-d. Reaction conditions: [substrate] = 132.6 mM; [N(CH₂CH₃)₄(BF₄)] = 132.6 mM; [capsule] = 13.3 mM; 60°C; CDCl₃ = 0.5 mL.

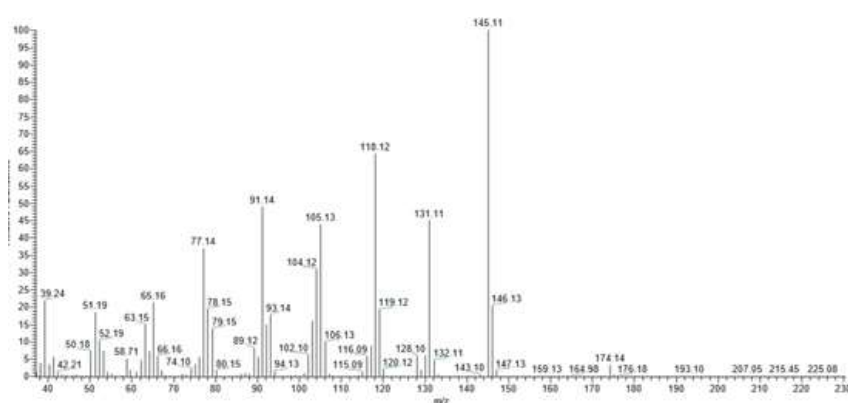


Figure 85. Mass spectrum of 1-(2,6-dimethylphenyl)-1H-tetrazole **T5**

The GC-MS analysis of this tetrazole led to partial thermal decomposition of the species showing overall two species, the original tetrazole and the corresponding cyanamide below reported.

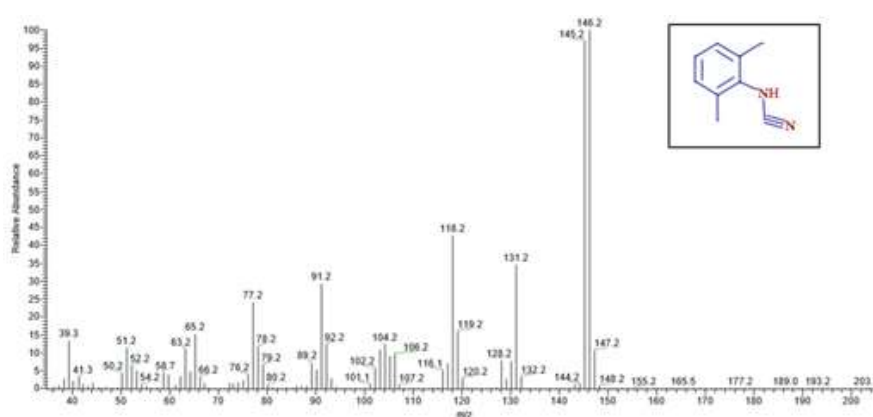
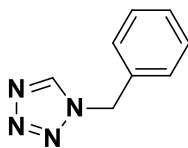


Figure 86. Mass spectrum of the cyanamide obtained by the thermal decomposition of the corresponding tetrazole **T5**.

- 1-benzyl-1H-tetrazole **T4**



$^1\text{H NMR}$ (300.15 MHz, CDCl_3): δ 8.49 (s, 1H), 7.41 (m, 3H); 7.29 (m, 2H); 5.59 (s, 2H).

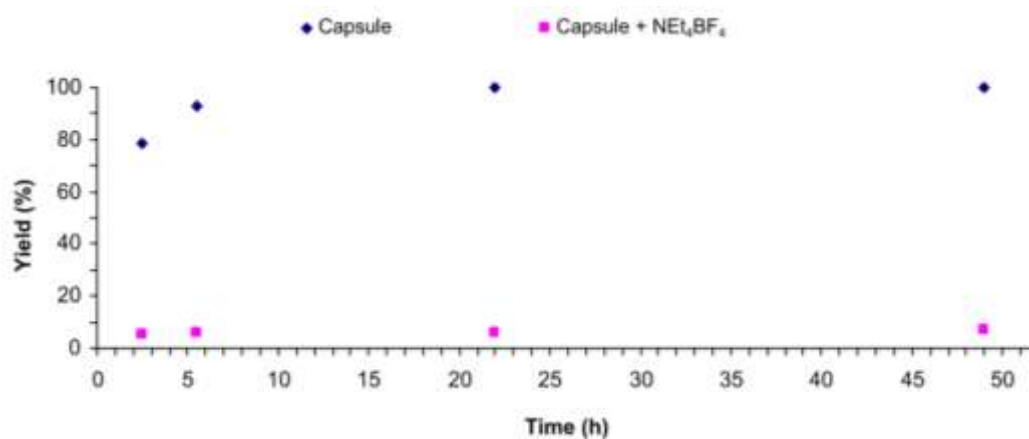


Figure 87. Product **T4** formation during the reaction between isocyanide **I4** and trimethylsilyl azide mediated by either by the empty (Blu) or filled (Pink) capsule in chloroform-d. Reaction conditions: [substrate] = 132.6 mM; $[\text{N}(\text{CH}_2\text{CH}_3)_4(\text{BF}_4)] = 132.6$ mM; [capsule] = 13.3 mM; 60°C ; $\text{CDCl}_3 = 0.5$ mL.

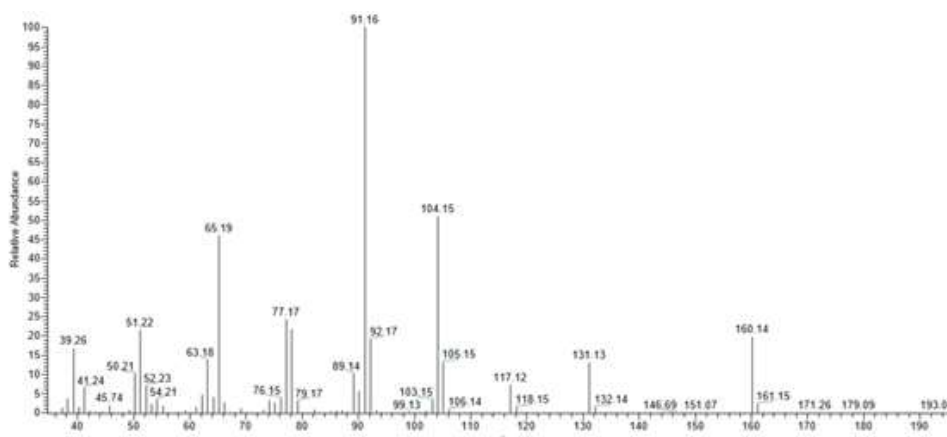
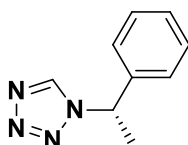


Figure 88. Mass spectrum of 1-benzyl-1H-tetrazole **T4**

- (S)-1-(1-phenylethyl)-1H-tetrazole **T7**



^1H NMR (300.15 MHz, CDCl_3): δ 8.44 (s, 1H), 7.28 (m, 5H), 5.81 (q, $J = 6.9$ Hz, 1H), 2.02 (d, $J = 7.1$ Hz, 3H).

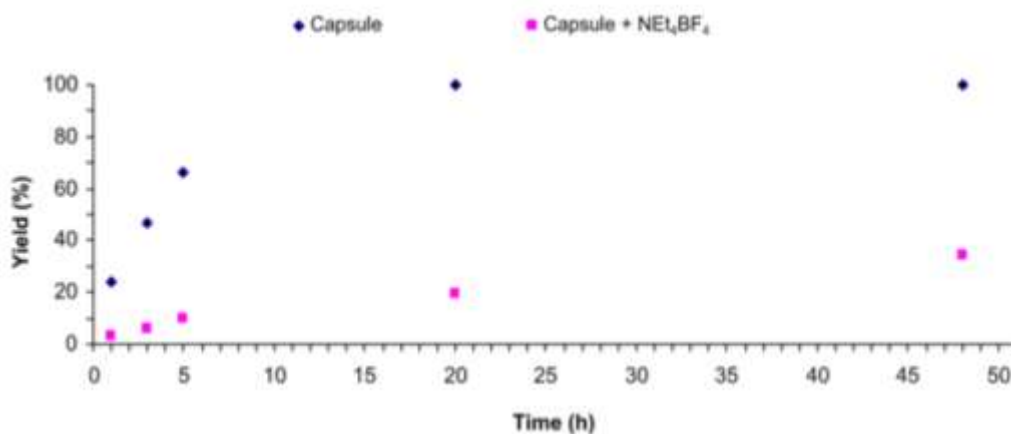


Figure 89. Product **T7** formation during the reaction between isocyanide **I7** and trimethylsilyl azide mediated by either by the empty (Blu) or filled (Pink) capsule in chloroform-d. Reaction conditions: [substrate] = 132.6 mM; $[\text{N}(\text{CH}_2\text{CH}_3)_4(\text{BF}_4)] = 132.6$ mM; [capsule] = 13.3 mM; 60°C ; $\text{CDCl}_3 = 0.5$ mL.

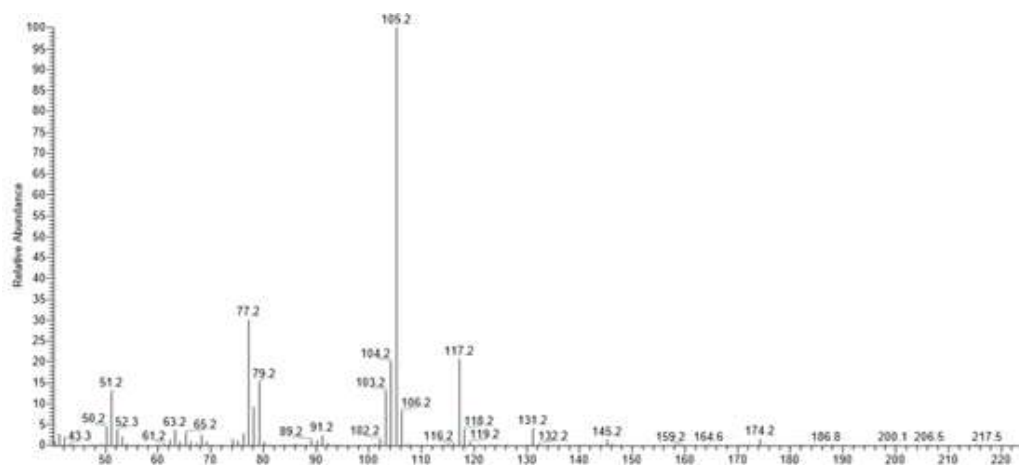
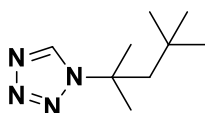


Figure 90. Mass spectrum of (S)-1-(1-phenylethyl)-1H-tetrazole **T7**

- **1-(2,4,4-trimethylpentan-2-yl)-1H-tetrazole T6**



^1H NMR (300.15 MHz, CDCl_3): δ 8.61 (s, 1H), 2.04 (s, 2H), 1.74 (s, 6H), 0.77 (s, 9H).

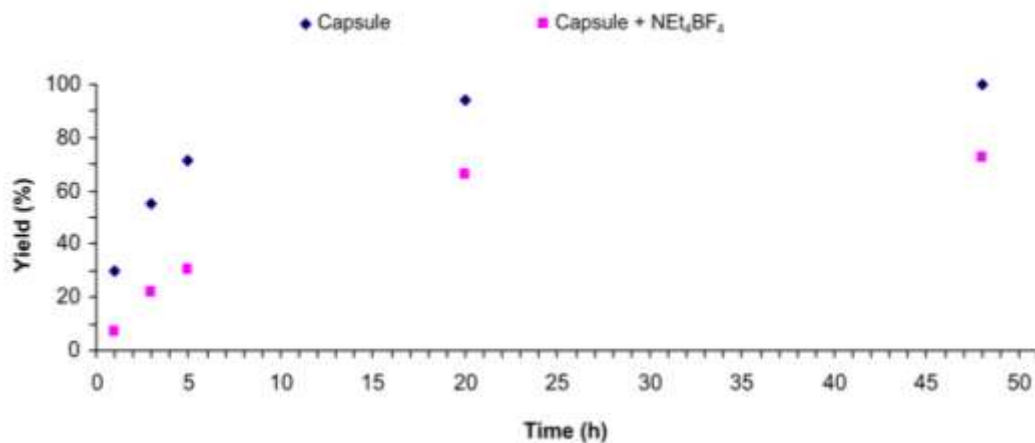


Figure 91. Product **T6** formation during the reaction between isocyanide **I6** and trimethylsilyl azide mediated by either by the empty (Blu) or filled (Pink) capsule in chloroform-d. Reaction conditions: [substrate] = 132.6 mM; [N(CH₂CH₃)₄(BF₄)] = 132.6 mM; [capsule] = 13.3 mM; 60°C; CDCl₃ = 0.5 mL.

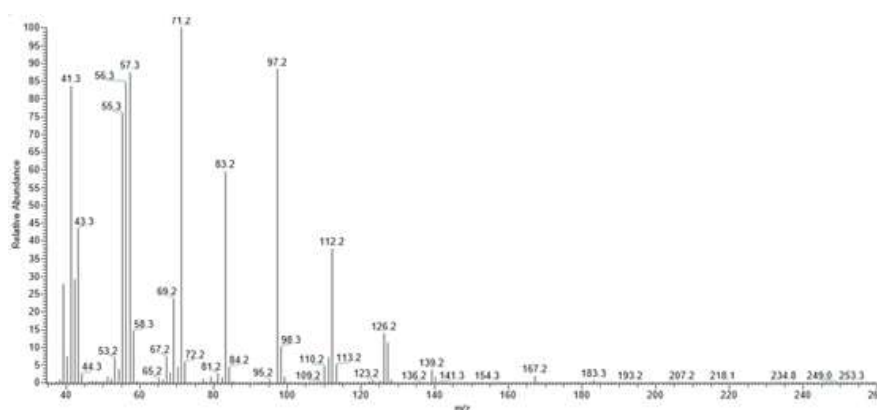
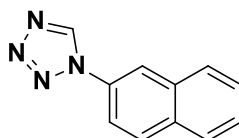


Figure 92. Mass spectrum of 1-(2,4,4-trimethylpentan-2-yl)-1H-tetrazole **T6**

- **1-(naphthalen-2-yl)-1H-tetrazole T8**²⁸⁴



¹H NMR (300.15 MHz, CDCl₃): δ 9.11 (s, 1H), 8.19 (d, J = 2.1 Hz, 1H), 8.08 (d, J = 8.9 Hz, 1H), 7.96 (dd, J = 9.4, 3.2 Hz, 2H), 7.82 (dd, J = 8.9, 2.1 Hz, 1H), 7.68-7.60 (m, 2H).

The GC-MS spectrum of **T8** does not correspond to the tetrazole but to the corresponding cyanamide that is formed by thermal decomposition of the original tetrazole molecule.

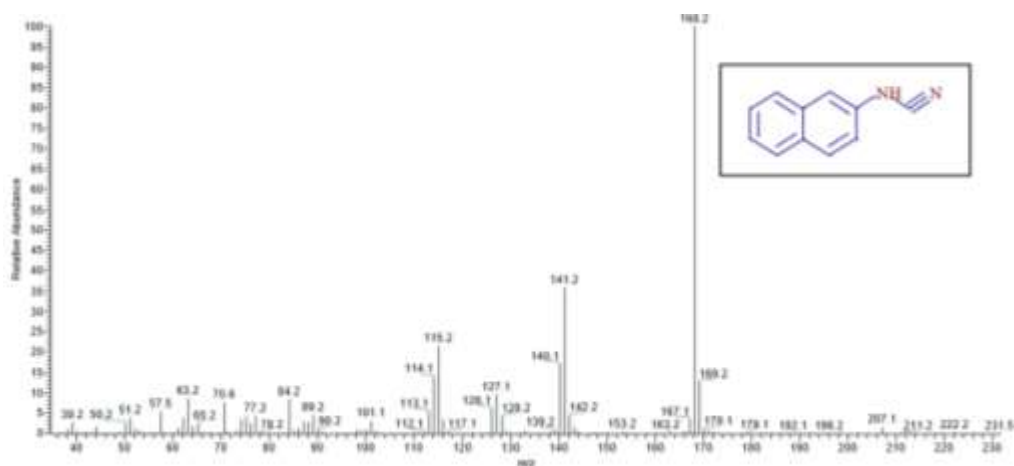


Figure 93. Mass spectrum of the cyanamide obtained by the thermal decomposition of the corresponding tetrazole **T8**.

7.2.3. Diazoacetate esters and Resorcin[4]arene capsule

TITRATIONS

In a NMR tube was introduced a water saturated chloroform solution of resorcin[4]arene (36 mM, 0.5 mL). Specific amounts of the chosen diazoacetate were added to the solution at room temperature in order to obtain samples with 2, 5, 10, 15 and 20 equivalents of diazoacetate with respect to the capsule. $^1\text{H-NMR}$ analyses were carried out after each addition.

$^1\text{H-NMR}$ spectra of the titration are reported below.

- Ethyl diazoacetate ED

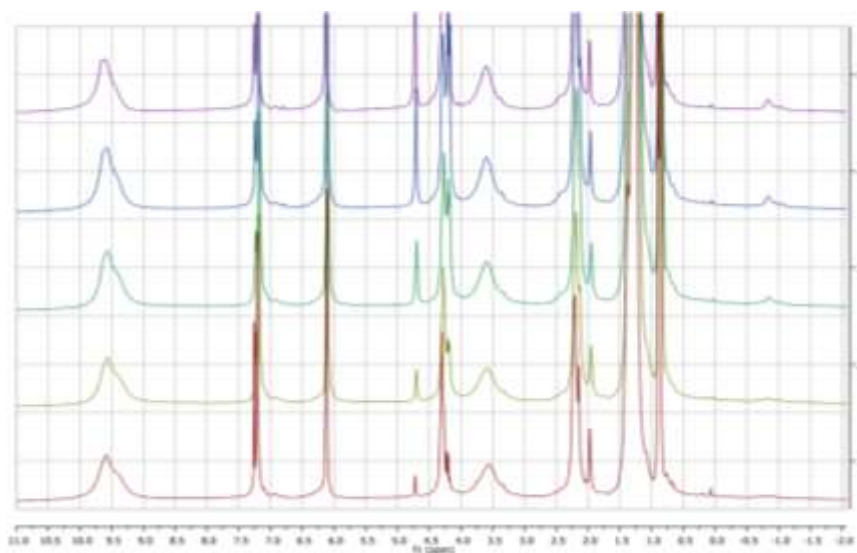


Figure 94. ¹H NMR spectra of capsule with 2, 5, 10, 15 and 20 equivalents of ethyl diazoacetate ED (from bottom to top) in chloroform-d.

- *tert*-butyl diazoacetate *t*-BD

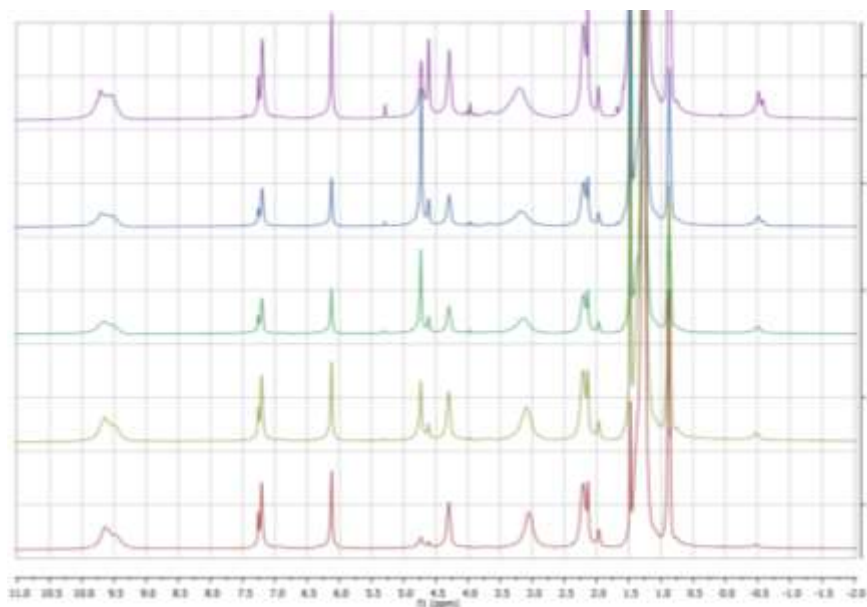


Figure 95. ¹H NMR spectra of capsule with 2, 5, 10, 15 and 20 equivalents of *tert*-butyl diazoacetate *t*-BD (from bottom to top) in chloroform-d.

- **benzyl diazoacetate BD**

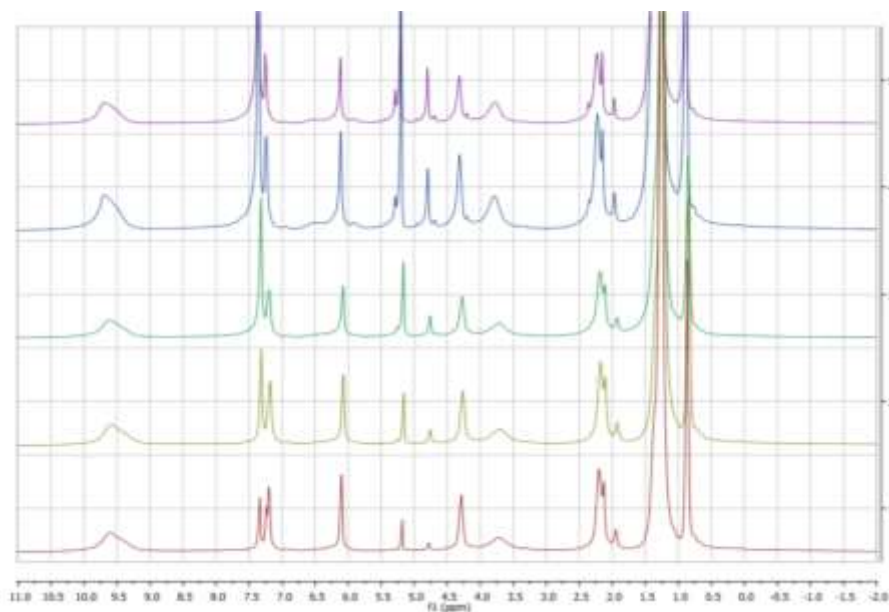


Figure 96. ¹H NMR spectra of capsule with 2, 5, 10, 15 and 20 equivalents of benzyl diazoacetate BD (from bottom to top) in chloroform-d.

Experimental procedure as above reported for diazoacetate titration was employed in the presence of acrolein and methyl acrylate in order to demonstrate the absence of interaction.

- **Acrolein Ac**

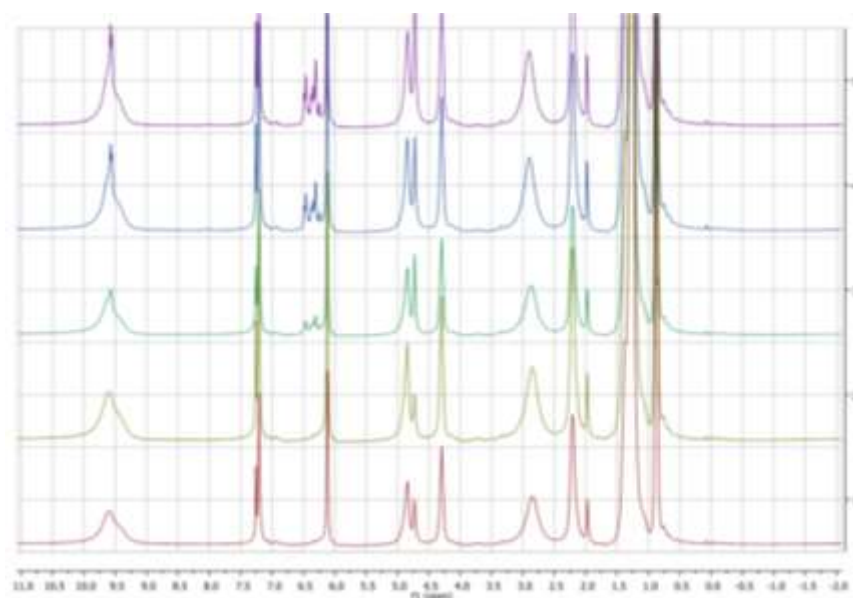


Figure 97. ¹H NMR spectra of capsule with 2, 5, 10, 15 and 20 equivalents of acrolein Ac (from bottom to top) in chloroform-d.

- **Methyl acrylate MA**

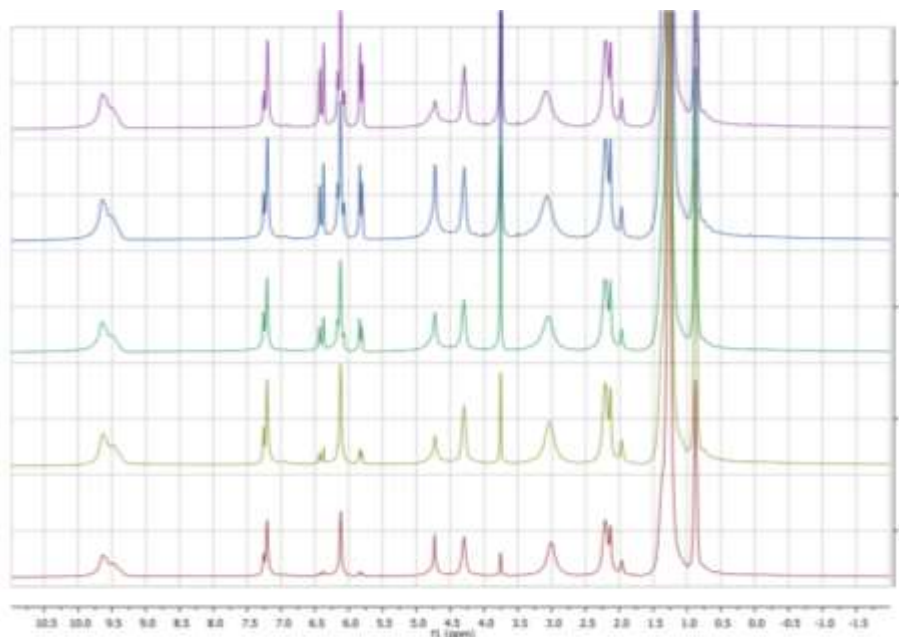


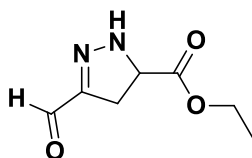
Figure 98. ¹H NMR spectra of capsule with 2, 5, 10, 15 and 20 equivalents of methyl acrylate MA (from bottom to top) in chloroform-d.

EXPERIMENTAL CONDITIONS

In a 1.5 mL vial were introduced a water saturated chloroform solution of resorcin[4]arene (36 mM, 0.5 mL) followed by the proper diazoacetate ester (10 eq. with respect to resorcin[4]arene capsule, 60 mM) and the resulted mixture stirred at 750 rpm until completely homogeneous. Subsequently the desired electron poor alkene was added (10 eq. with respect to resorcin[4]arene capsule, 60 mM), the vial sealed and thermostatted at room temperature or at 50°C. The reaction progress was followed by GC or ¹H NMR analyses sampling the reaction mixture at different times and diluting the sample with water saturated chloroform. The cycloaddition products were confirmed by GC-MS and ¹H NMR. GC-MS analyses demonstrated that 4,5-dihydro-1H-pyrazole derivatives are partially thermally labile since in several cases significant amounts of the corresponding cyclopropyl products obtained by dinitrogen loss was observed. Nevertheless, no evidence was found of the formation of such cyclopropyl derivatives in solution.

PRODUCTS CHARACTERIZATION

- Ethyl 3-formyl-4,5-dihydro-1H-pyrazole-5-carboxylate P_{AcED}



^1H NMR (300.15 MHz, CDCl_3): δ 9.72 (s, 1H), 6.02 (s, 1H), 4.51 (dd, $J = 12.7, 5.8$ Hz, 1H), 4.21 (q, $J = 7.1$ Hz, 2H), 3.24 (dd, $J = 17.5, 5.8$ Hz, 1H), 3.10 (dd, $J = 17.5, 12.7$ Hz, 1H), 1.29 (t, $J = 7.1$ Hz, 3H).

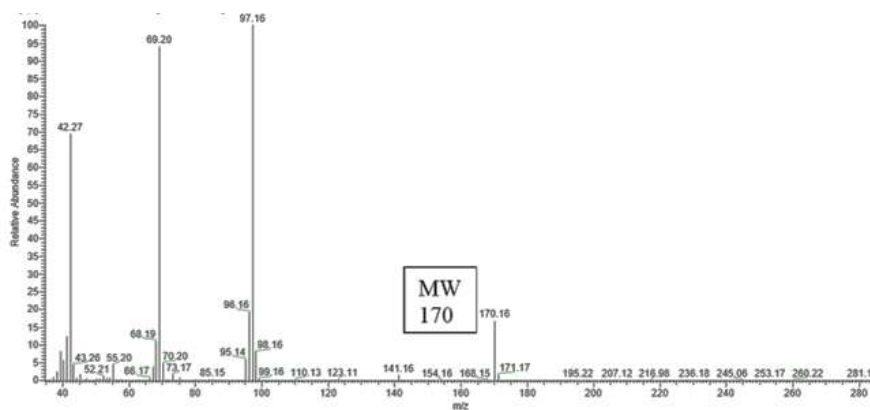
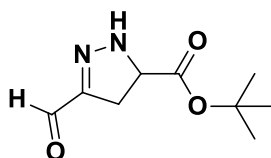


Figure 99. Mass spectrum of ethyl 3-formyl-4,5-dihydro-1H-pyrazole-5-carboxylate P_{AcED}

- *tert*-Butyl 3-formyl-4,5-dihydro-1H-pyrazole-5-carboxylate P_{Act-BD}



^1H NMR (300.15 MHz, CDCl_3): δ 9.72 (s, 1H), 6.28 (s, 1H), 4.41 (dd, $J = 12.7, 5.9$ Hz, 1H), 3.19 (dd, $J = 17.6, 5.9$ Hz, 1H), 3.06 (dd, $J = 17.6, 12.7$ Hz, 1H), 1.47 (s, 9H).

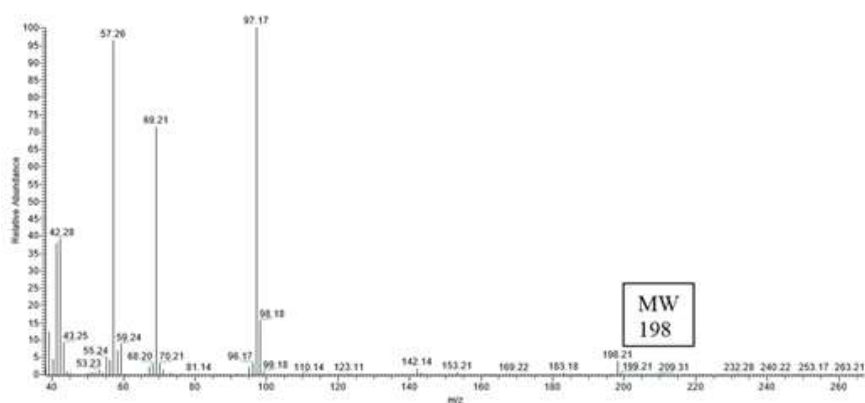
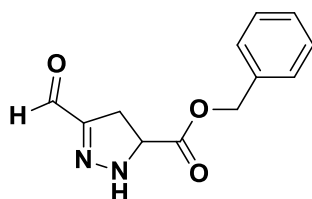


Figure 100. Mass spectrum of the *tert*-Butyl 3-formyl-4,5-dihydro-1H-pyrazole-5-carboxylate P_{AcT-BD}.

- **Benzyl 3-formyl-4,5-dihydro-1H-pyrazole-5-carboxylate P_{AcBD}**



¹H NMR (300.15 MHz, CDCl₃): δ 9.72 (s, 1H), 7.36 (br, 5H), 6.52 (s, 1H), 5.20 (s, 2H), 4.56 (dd, J = 12.8, 5.8 Hz, 1H), 3.26 (dd, J = 17.6, 5.8 Hz, 1H), 3.11 (dd, J = 17.6, 12.8 Hz, 1H).

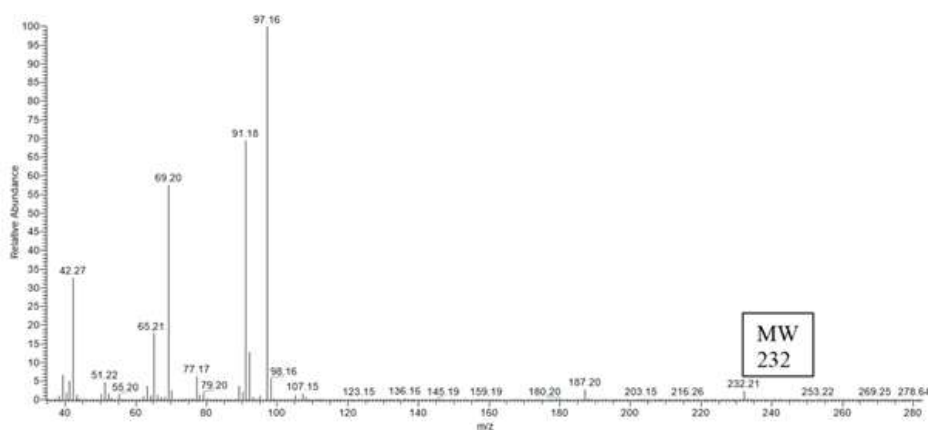
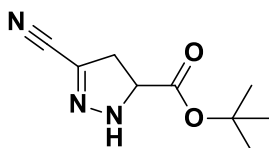


Figure 101. Mass spectrum of benzyl 3-formyl-4,5-dihydro-1H-pyrazole-5-carboxylate P_{AcBD}

- ***tert*-butyl 3-cyano-4,5-dihydro-1H-pyrazole-5-carboxylate P_{Am-BD}**



^1H NMR (300.15 MHz, CDCl_3): δ 6.52 (s, 1H), 4.37 (dd, $J = 12.0, 5.8$ Hz, 1H), 3.21 (dd, $J = 17.3, 5.8$ Hz, 1H), 3.11 (dd, $J = 17.3, 12.0$ Hz, 1H), 1.54 (s, 9H).

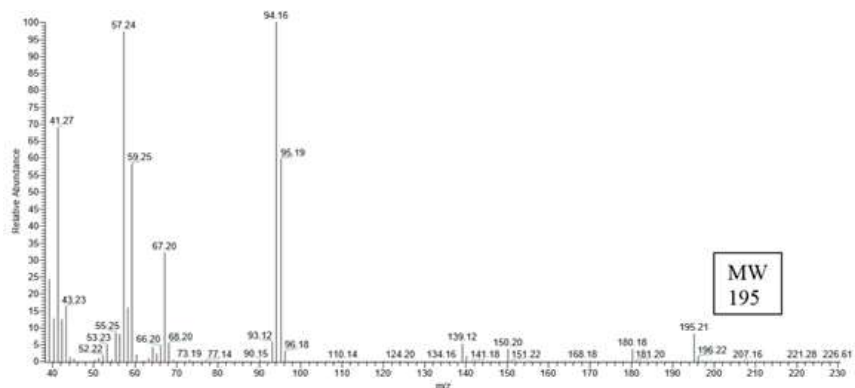
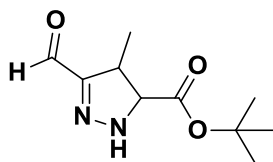


Figure 102. Mass spectrum of *tert*-butyl 3-cyano-4,5-dihydro-1H-pyrazole-5-carboxylate $\text{P}_{\text{Ant-BD}}$

tert-butyl 3-formyl-4-methyl-4,5-dihydro-1H-pyrazole-5-carboxylate $\text{P}_{\text{C4t-BD}}$



^1H NMR (300.15 MHz, CDCl_3): δ 9.66 (s, 1H), 6.78 (s, 1H), 3.97 (d, $J = 1.3$ Hz, 1H), 3.50 (m, 1H), 1.48 (d, $J = 3.3$ Hz, 3H), 1.48 (s, 9H).

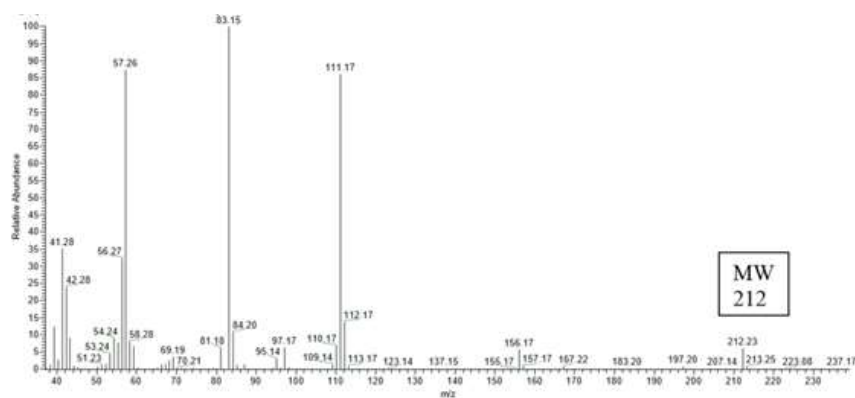
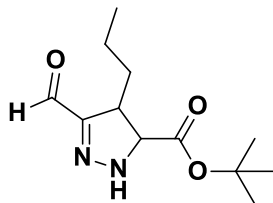


Figure 103. Mass spectrum of *tert*-butyl 3-formyl-4-methyl-4,5-dihydro-1H-pyrazole-5-carboxylate $\text{P}_{\text{C4t-BD}}$.

- *tert*-butyl 3-formyl-4-propyl-4,5-dihydro-1H-pyrazole-5-carboxylate P_{C6t-BD}



¹H NMR (300.15 MHz, CDCl₃): δ 9.68 (s, 1H), 6.78 (s, 1H), 4.08 (d, J = 4.3 Hz, 1H), 3.57 – 3.39 (m, 1H), 1.84 – 1.69 (m, 4H), 1.48 (s, 9H), 0.97 (t, 7.2 Hz, 3H).

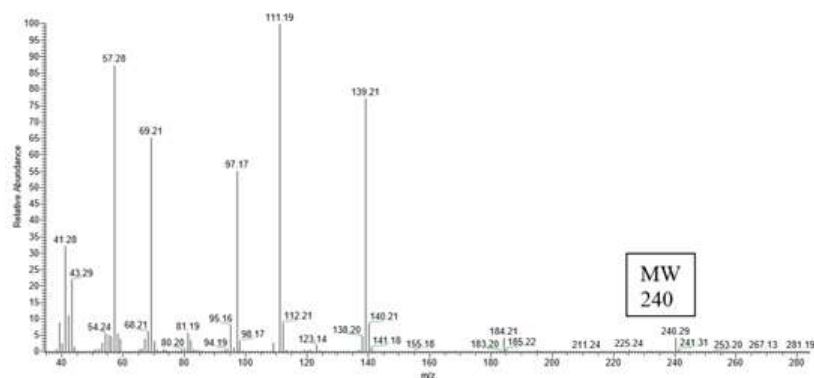
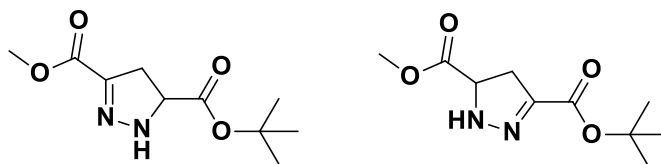


Figure 104. Mass spectrum of *tert*-butyl 3-formyl-4-propyl-4,5-dihydro-1H-pyrazole-5-carboxylate P_{C6t-BD}.

- 3-*tert*-butyl 5-methyl 4,5-dihydro-1H-pyrazole-3,5-dicarboxylate P_{MAt-BD}



¹H NMR (300.15 MHz, CDCl₃): δ 5.98 (s, 1H), 4.42 (dd, J = 12.2, 5.2 Hz, 1H), 4.34 (dd, J = 12.4, 5.4 Hz, 1H), 3.85 (s, 3H), 3.26 (m, 1H), 3.13 (m, 1H), 1.49 (s, 9H).

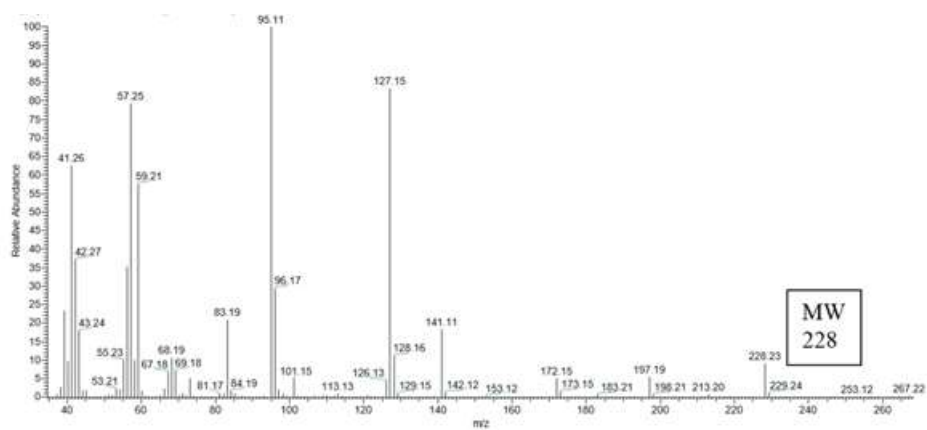
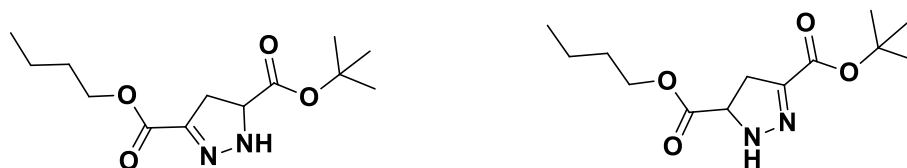


Figure 105. Mass spectrum of 3-*tert*-butyl 5-methyl 4,5-dihydro-1H-pyrazole-3,5-dicarboxylate P_{MA}-BD.

- **5-butyl 3-*tert*-butyl 4,5-dihydro-1H-pyrazole-3,5-dicarboxylate P_{BA}-BD.**



¹H NMR (300.15 MHz, CDCl₃): δ 6.41 (s, 1H), 4.40 (dd, J = 12.4, 5.5 Hz, 1H), 4.33 (dd, J = 12.3, 5.6 Hz, 1H), 4.26 – 4.20 (t, J = 6.6 Hz, 2H), 3.25 (ddd, J = 10.9, 6.3, 4.7 Hz, 1H), 3.13 (dd, J = 17.7, 12.4 Hz, 1H), 1.72 – 1.59 (m, 4H), 1.49 (s, 9H), 0.94 (t, J = 7.4 Hz, 3H).

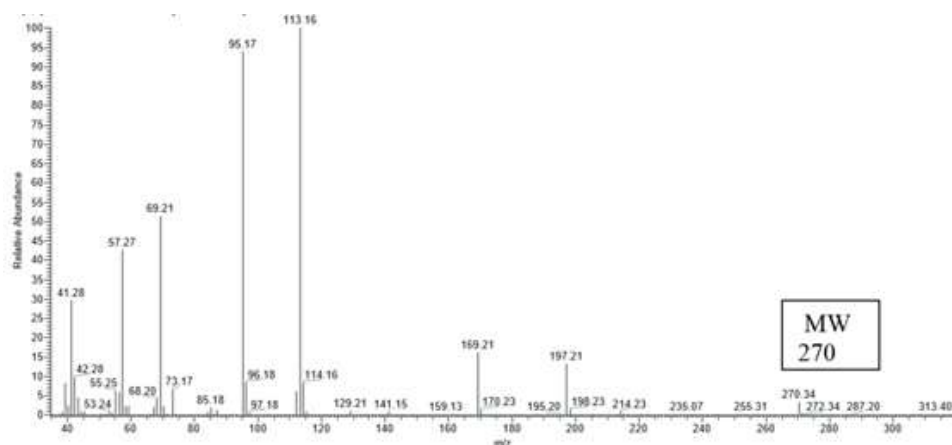
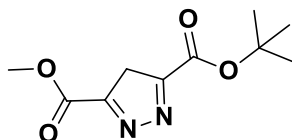


Figure 106. Mass spectrum of 5-butyl 3-*tert*-butyl 4,5-dihydro-1H-pyrazole-3,5-dicarboxylate P_{BA}-BD.

- **3-*tert*-butyl 5-methyl 1H-pyrazole-3,5-dicarboxylate P_{MP_T-BD}**



¹H NMR (300.15 MHz, CDCl₃): δ 6.78 (s, 1H), 3.95 (s, 3H), 2.88 (s, 1H), 1.60 (s, 9H).

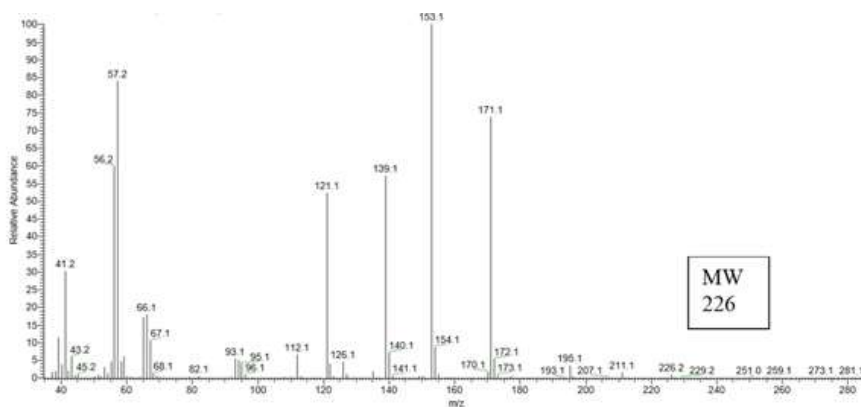
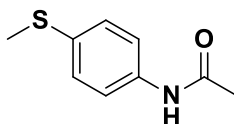


Figure 107. Mass spectrum of 3-*tert*-butyl 5-methyl 1H-pyrazole-3,5-dicarboxylate P_{MP_T-BD}.

7.2.4. Sulfoxidation

SYNTHESIS OF N-(4-(METHYLTHIO)PHENYL)ACETAMIDE **S7**



The synthesis of **S7** was performed following the procedure reported by Zinzalla and co-workers.²⁸⁵

Acetyl chloride (1.01 eq) was added dropwise to a stirred solution of 4-(methylthio)aniline (1.0 eq) and triethylamine (2.0 eq) in THF (25 ml) at room temperature. After total consumption of the starting material (~1 h) the solution was diluted with EtOAc (100 ml) and washed with water (3 × 100 ml), dried with MgSO₄ and concentrated in vacuum to afford the products as colourless solids.

¹H-NMR (CDCl₃, 400 MHz): δ 2.15 (s, 3 H, CH₃), 2.45 (s, 3 H, SCH₃), 7.22 (d, 2 H, J = 8.6 Hz, H_{3'} and H_{5'}), 7.37 (br s, 1 H, NH), 7.42 (d, 2 H, J = 8.6 Hz, H_{2'} and H_{6'}).

EXPERIMENTAL CONDITIONS

- Catalytic oxidation with resorcin[4]arene: General procedure

Water saturated solvent was prepared by shaking chloroform-d with bidistilled water at room temperature in a separation funnel. Resorcin[4]arene (6 equivalents, 36 mM) was placed in a screw-capped vial equipped with silicone septum and dissolved in the water saturated chloroform-d (1.5 mL) stirring at 750 rpm for few minutes. To this solution, the chosen sulfide (5 equivalents, 30 mM) and H₂O₂ (6 equivalents, 36 mM) were added. The reaction was left at room temperature and the reaction progress was monitored by ¹H-NMR and GC analysis by periodically sampling directly from the reaction mixtures.

As an example of the reaction followed over time it is shown below 1-(4-(methylsulfinyl)phenyl)ethanone **SO10** during the formation of the oxidation reaction of 1-(4-(methylthio)phenyl)ethanone **S10** mediated by the capsule in the presence of H₂O₂.

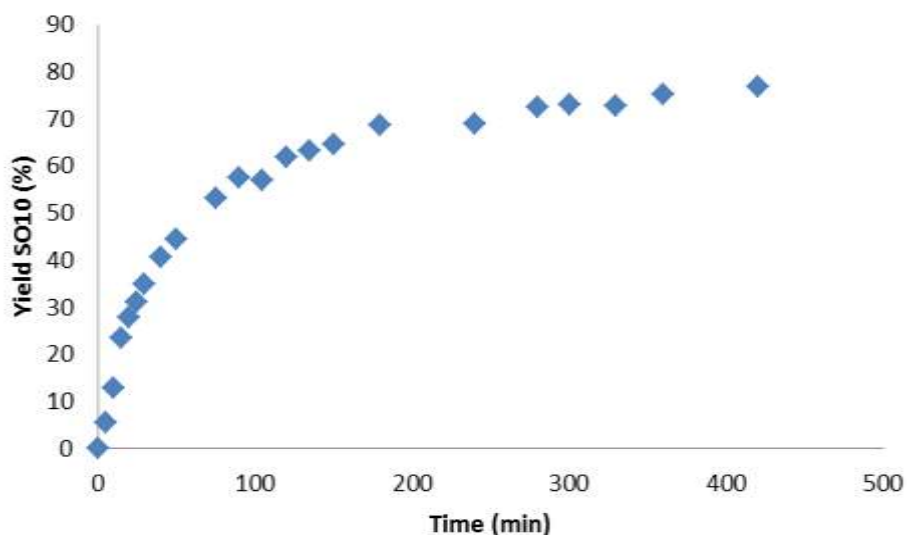


Figure 108. Percentage yield of 1-(4-(methylsulfinyl)phenyl)ethanone **SO10** during the selective oxidation of 1-(4-(methylthio)phenyl)ethanone **S10** mediated by the hexameric capsule in the presence of H₂O₂. Experimental conditions: [resorcinarene] = 36 mM; [**S10**] = 30 mM; [H₂O₂] = 36 mM.

- Catalytic oxidation reactions of butyl sulfide with Resorcinol

The procedure is the same but Resorcinol (4 equivalents, 24 mM) was added in place of resorcin[4]arene.

- **Catalytic oxidation reactions of butyl sulfide with Acetic Acid**

The procedure is the same but acid acetic (1 equivalent, 6 mM) was added in place of resorcin[4]arene.

- **Catalytic oxidation reactions with different amounts of 4-Chlorothioanisole S7**

Water saturated solvent was prepared by shaking chloroform-d with bidistilled water at room temperature in a separation funnel. Resorcin[4]arene **1** (6 equivalents, 36 mM) was placed in a screw-capped vial equipped with silicone septum and dissolved in the water saturated chloroform-d (1.5 mL) stirring for few minutes. To this solution, 4-Chlorothioanisole **S7** (5, 10, 20 50 or 200 equivalents with respect to the hexamer) and H₂O₂ (1.2 equivalents with respect to **S7**) were added. The reaction was left at room temperature and the reaction progress was monitored by 1H-NMR and GC analysis by periodically sampling directly from the reaction mixtures. Conversion, product assignment and distribution were determined by direct GC, GC-MS and 1H-NMR analysis of the reaction mixture as the average of three experiments.

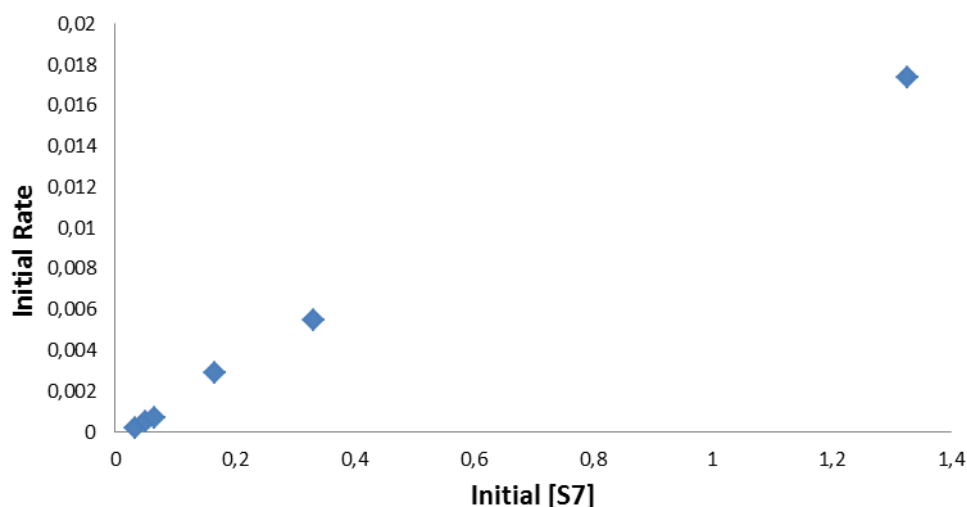
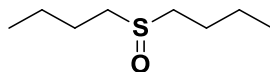


Figure 109. Initial rate dependent on the **S7** concentration with a constant amount of capsule in water saturated chloroform-d. Experimental conditions: [Resorcinarene] = 36 mM; **S7** = 5, 10, 25, 50 and 200 equivalents with respect to resorcin[4]arene capsule; H₂O₂ = 1.2 equivalents with respect to **S7**; V = 1.5 mL; T = rt.

SULFOXIDES CHARACTERIZATION

- 1-(butylsulfinyl)butane



The observed $^1\text{H-NMR}$ chemical shifts corresponded to those reported by He and co-workers.²⁸⁶

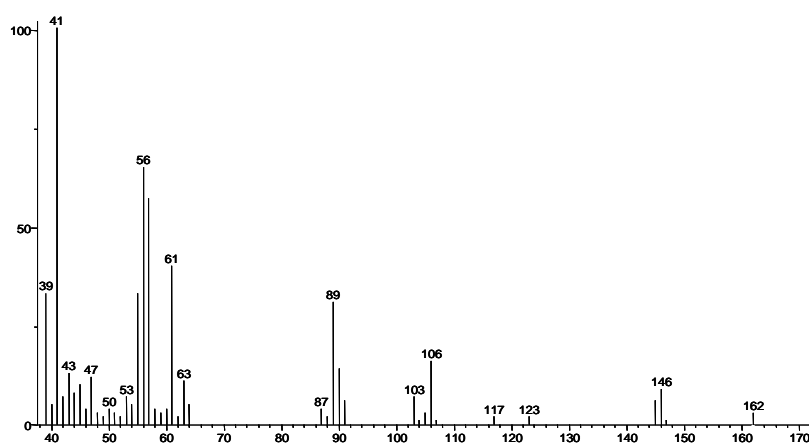
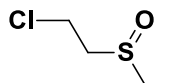


Figure 110. Mass spectrum of 1-(butylsulfinyl)butane

- 1-chloro-2-(ethylsulfinyl)ethane SO1



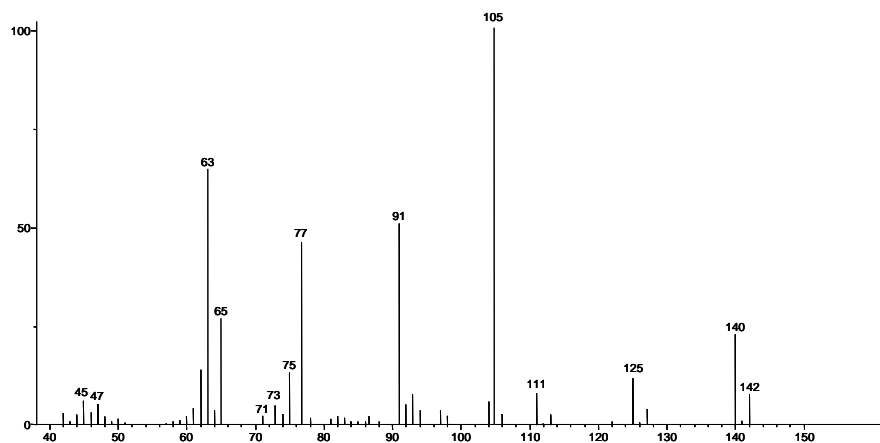
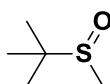


Figure 111. Mass spectrum of 1-chloro-2-(ethylsulfinyl)ethane SO1

- 2-methyl-2-(methylsulfinyl)propane SO2



The observed $^1\text{H-NMR}$ chemical shifts corresponded to those reported by Doherty and co-workers.²⁸⁷

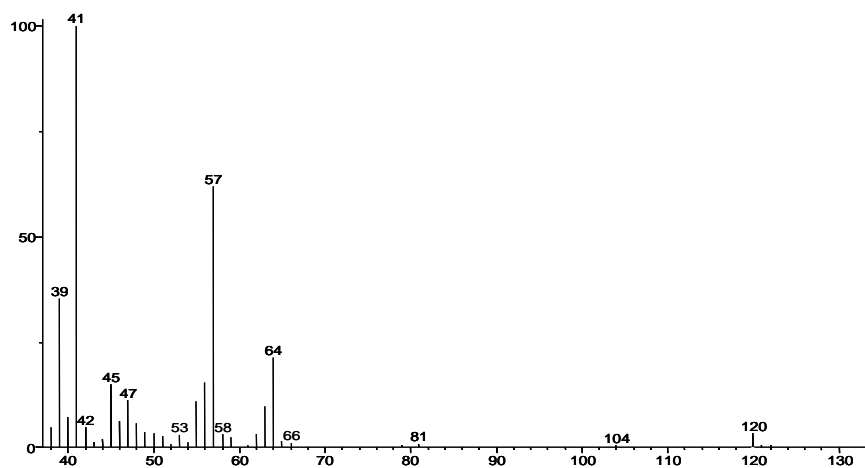
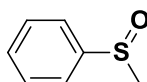


Figure 112. Mass spectrum of 2-methyl-2-(methylsulfinyl)propane SO2

- (methylsulfinyl)benzene SO3



The observed $^1\text{H-NMR}$ chemical shifts corresponded to those reported by Doherty and co-workers.²⁸⁷

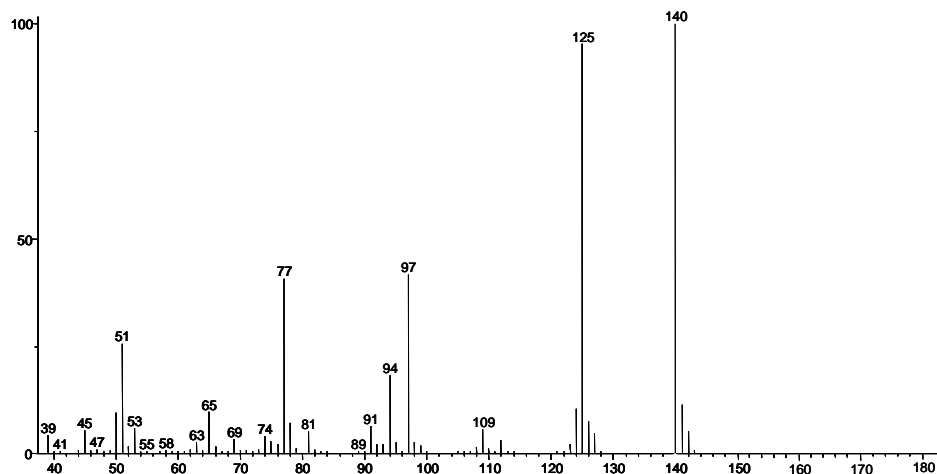
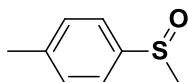


Figure 113. Mass spectrum of (methylsulfinyl)benzene SO3

- **1-methyl-4-(methylsulfinyl)benzene SO4**



The observed $^1\text{H-NMR}$ chemical shifts corresponded to those reported by He and co-workers.²⁸⁶

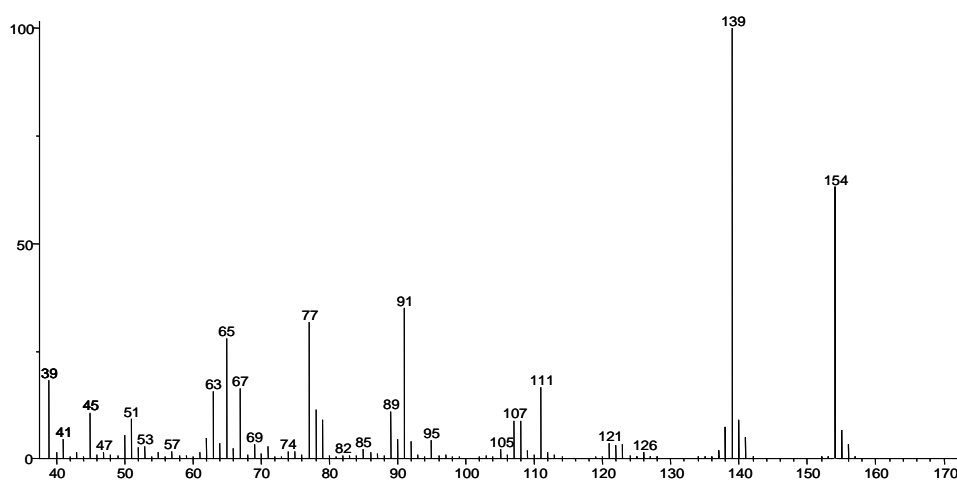
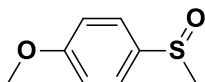


Figure 114. Mass spectrum of 1-methyl-4-(methylsulfinyl)benzene SO4

- **1-methoxy-4-(methylsulfinyl)benzene SO5**



The observed $^1\text{H-NMR}$ chemical shifts corresponded to those reported by He and co-workers.²⁸⁶

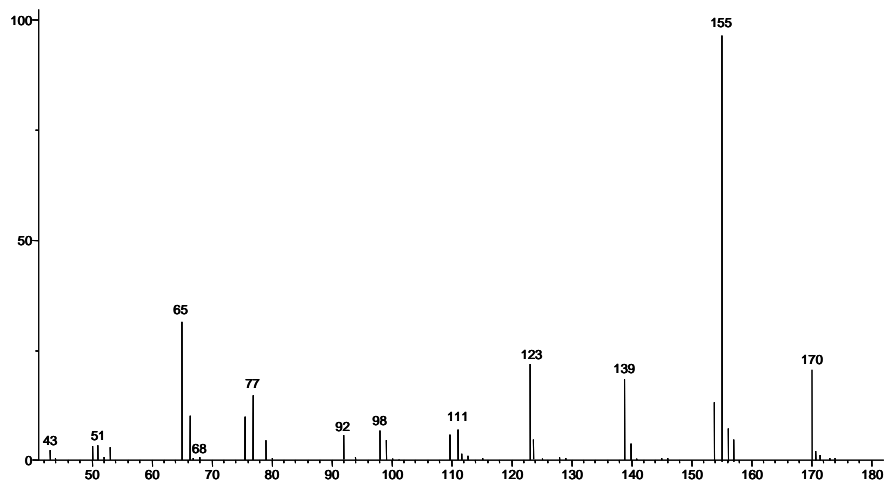
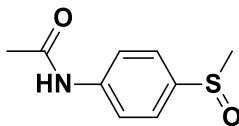


Figure 115. Mass spectrum of 1-methoxy-4-(methylsulfinyl)benzene **SO5**

- **N-(4-(methylsulfinyl)phenyl)acetamide SO6**



The observed $^1\text{H-NMR}$ chemical shifts corresponded to those reported by Murahashi and co-workers.²⁸⁸

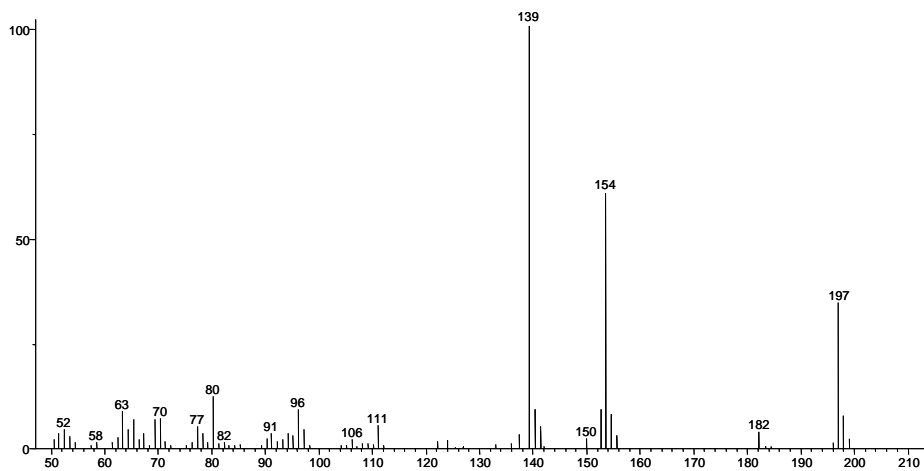
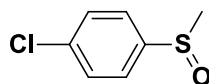


Figure 116. Mass spectrum of N-(4-(methylsulfinyl)phenyl)acetamide **SO6**

- **1-chloro-4-(methylsulfinyl)benzene SO7**



The observed $^1\text{H-NMR}$ chemical shifts corresponded to those reported by Murahashi and co-workers.²⁸⁸

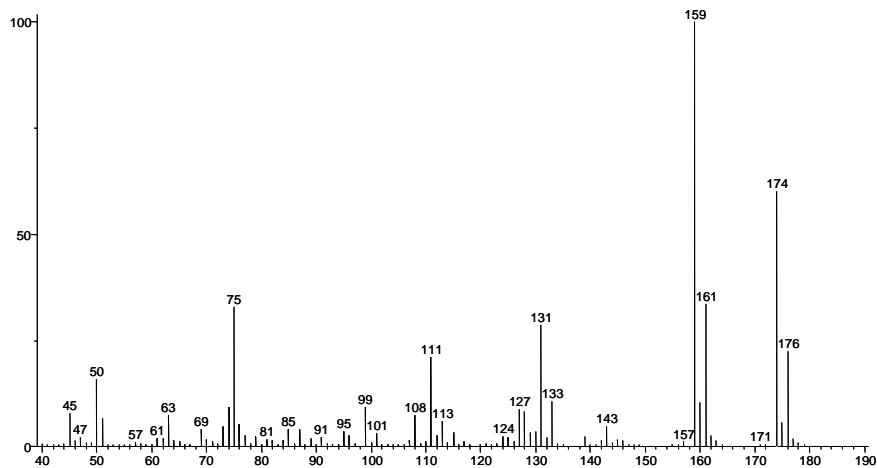
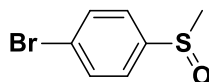


Figure 117. Mass spectrum of 1-chloro-4-(methylsulfinyl)benzene SO7

- **1-bromo-4-(methylsulfinyl)benzene SO8**



The observed $^1\text{H-NMR}$ chemical shifts corresponded to those reported by Sato and co-workers.²⁸⁹

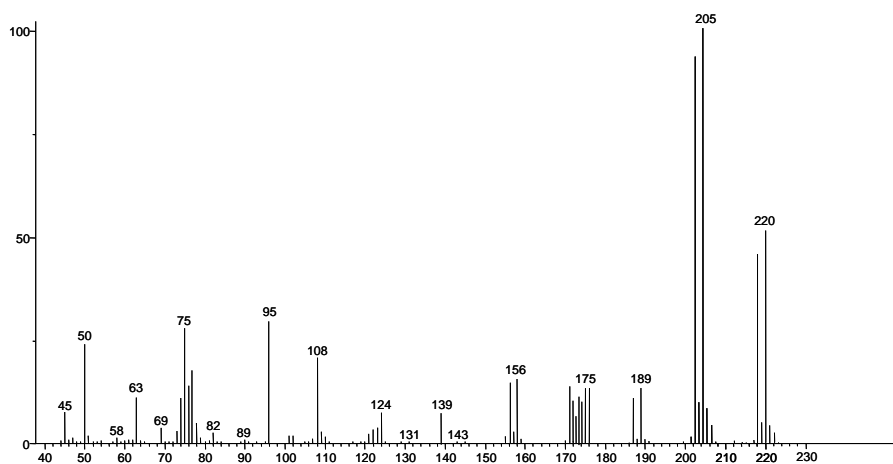
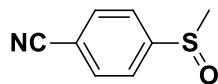


Figure 118. Mass spectrum of 1-bromo-4-(methylsulfinyl)benzene SO8

- **4-(methylsulfinyl)benzointrile SO9**



The observed ¹H-NMR chemical shifts corresponded to those reported by He and co-workers.²⁸⁶

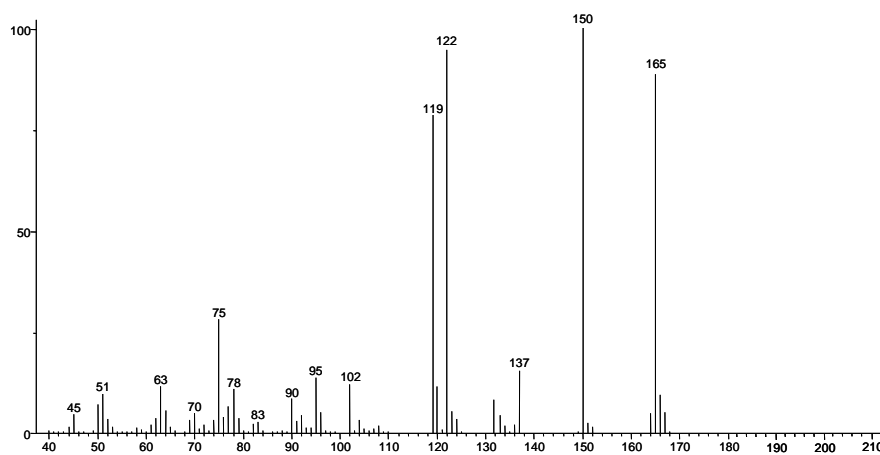
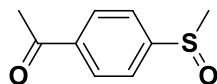


Figure 119. Mass spectrum of 4-(methylsulfinyl)benzointrile **SO9**

- **1-(4-(methylsulfinyl)phenyl)ethanone SO10**



The observed ¹H-NMR chemical shifts corresponded to those reported by Jeon and co-workers.²⁹⁰

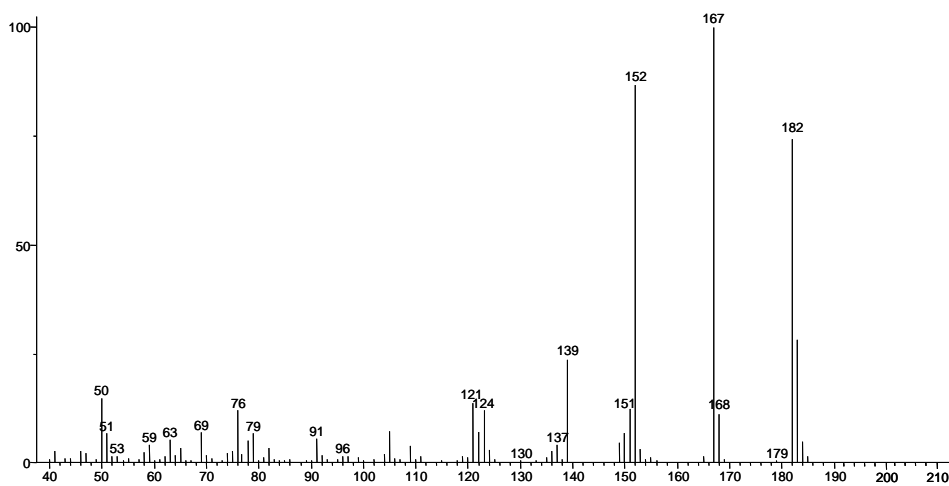
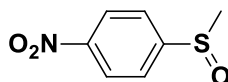


Figure 120. Mass spectrum of 1-(4-(methylsulfinyl)phenyl)ethanone SO10

- **1-(methylsulfinyl)-4-nitrobenzene SO11**



The observed $^1\text{H-NMR}$ chemical shifts corresponded to those reported by Jeon and co-workers.²⁹⁰

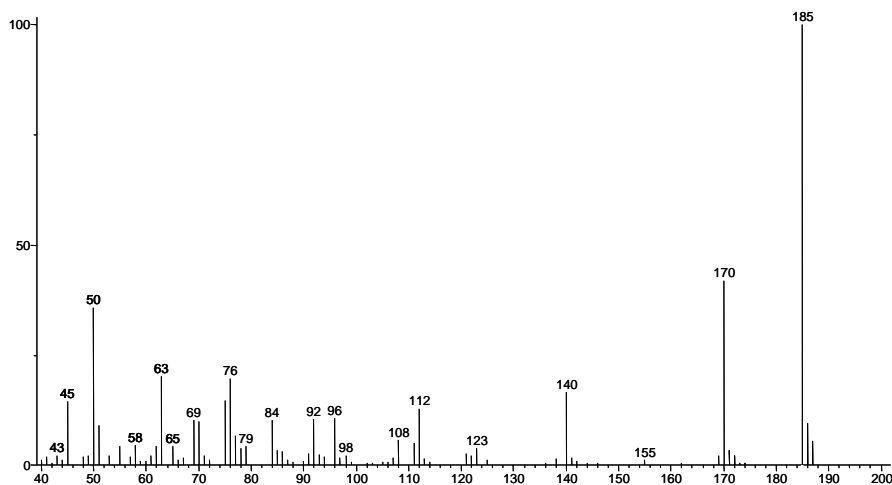
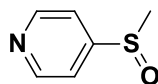


Figure 121. Mass spectrum of 1-(methylsulfinyl)-4-nitrobenzene SO11

- **4-(methylsulfinyl)pyridine SO12**



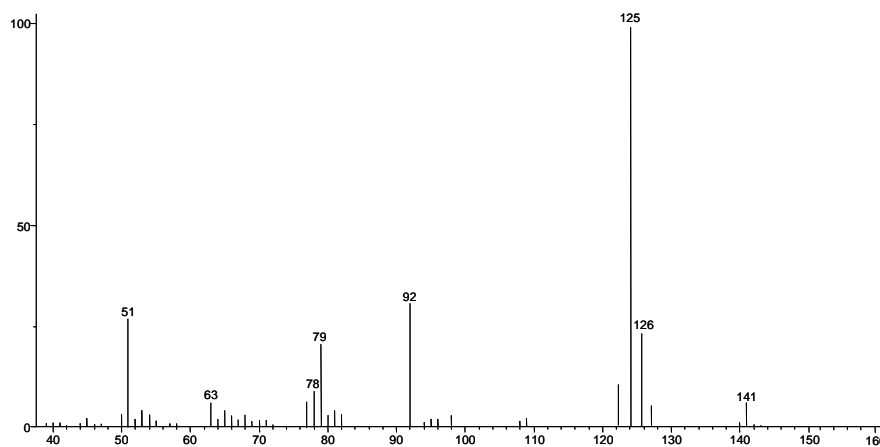
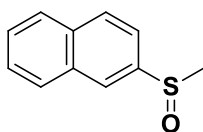


Figure 122. Mass spectrum of 4-(methylsulfinyl)pyridine SO12

2-(methylsulfinyl)naphthalene SO13



The observed $^1\text{H-NMR}$ chemical shifts corresponded to those reported by Imada and co-workers.²⁹¹

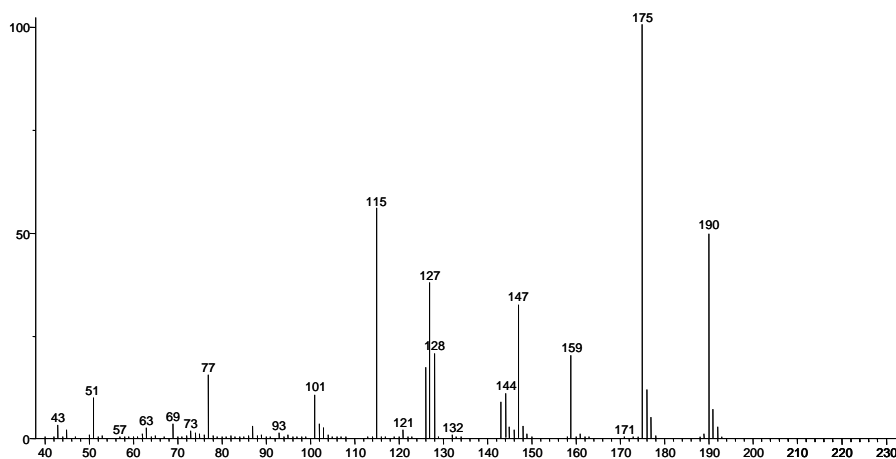
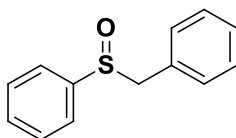


Figure 123. Mass spectrum of 2-(methylsulfinyl)naphthalene SO13

(Benzylsulfinyl)benzene SO14



The observed $^1\text{H-NMR}$ chemical shifts corresponded to those reported by Doherty and co-workers.²⁸⁷

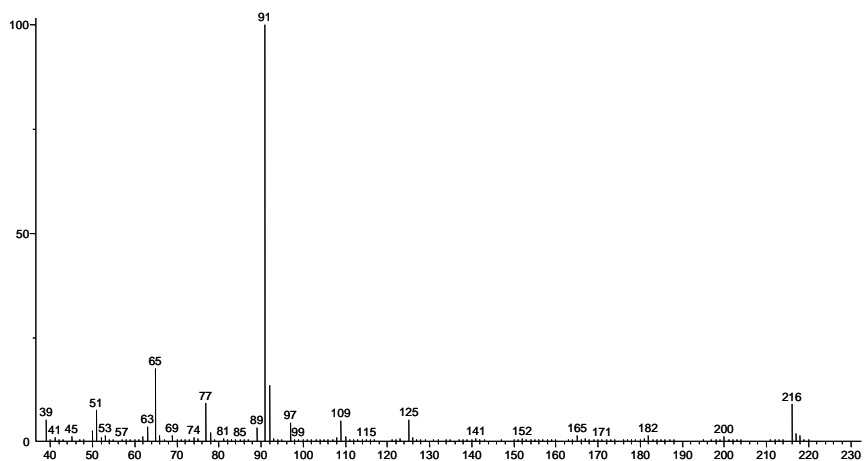
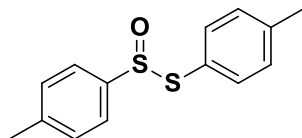


Figure 124. Mass spectrum of (benzylsulfinyl)benzene **SO14**

- **S-phenyl benzenesulfinothioate SO15**



The observed $^1\text{H-NMR}$ chemical shifts corresponded to those reported by Back and co-workers.²⁹²

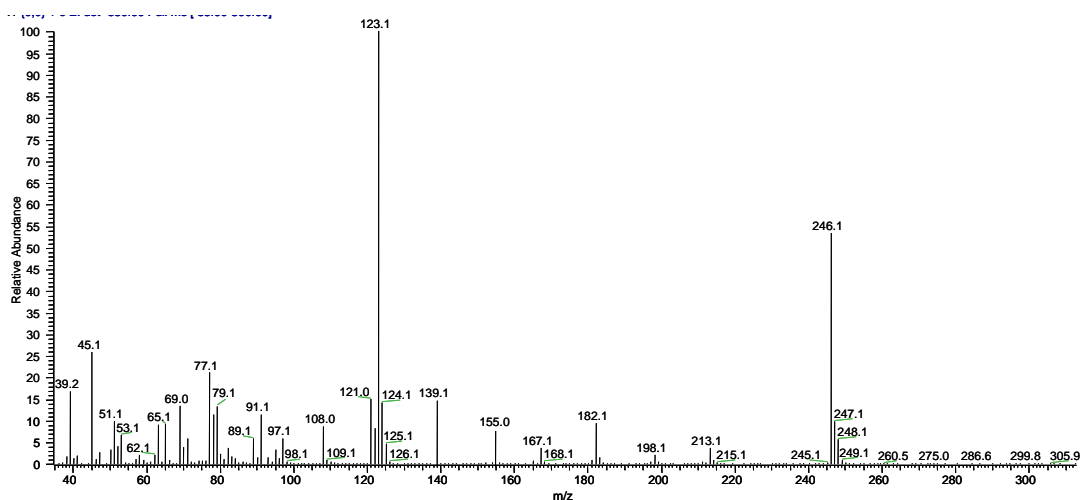


Figure 125. Mass spectrum of S-phenyl benzenesulfinothioate SO15

7.2.5. Alkynes hydration mediated by the capsule

EXPERIMENTAL CONDITIONS

- **Terminal Alkynes**

In a 3 mL vial were introduced a water saturated chloroform solution of resorcin[4]arene (36 mM, 1.5 mL) followed by the proper terminal alkyne (10 eq. or 20 eq. with respect to resorcin[4]arene capsule, 60 mM or 120 mM) and the resulted mixture was stirred at 750 rpm until completely homogeneous. Subsequently the HBF_4 (0.5, 0.2 or 0.1 eq. with respect to the alkyne) was added, the vial sealed and thermostatted at room temperature or at 60°C . The reaction progress was followed by GC or $^1\text{HNMR}$ analyses sampling the reaction mixture at different times and

diluting the sample with water saturated chloroform. The hydration products were confirmed by GC-MS and ^1H NMR.

Experimental procedure as above reported was repeated adding tetraethyl ammonium trifluoromethanesulfonate (10 equivalents with respect to the capsule, 132.6 mM) together with the substrates in order to carry out control tests of the catalytic activity of the activity within the capsule.

- **Catalytic hydration reaction of phenylacetylene with other acid**

The procedure is the same but HCl, HNO_3 or methanesulfonic acid (0.5 or 0.2 equivalents) were added in place of HBF_4 .

- **Catalytic hydration reaction of phenylacetylene with Acetic Acid**

The procedure is the same but resorcinol (24 equivalents with respect to the capsule, 140 mM) was added in place of resorcin[4]arene.

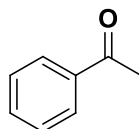
- **Internal Alkynes**

In a 3 mL vial were introduced a water saturated chloroform solution of resorcin[4]arene (36 mM, 1.5 mL) followed by the proper internal alkyne (2 eq. with respect to resorcin[4]arene capsule, 12 mM) and the resulted mixture was stirred at 750 rpm until completely homogeneous. Subsequently the $\text{HBF}_4 \sim 55$ wt. % in H_2O (0.5 with respect to the alkyne) was added, the vial sealed and thermostatted at room temperature or at 60°C . The reaction was left under these condition overnight. The hydration products were confirmed by GC-MS and ^1H NMR.

Experimental procedure as above reported was repeated adding tetraethyl ammonium trifluoromethanesulfonate (10 equivalents with respect to the capsule, 132.6 mM) together with the substrates in order to carry out control tests of the catalytic activity of the activity within the capsule.

KETONES CHARACTERIZATION

- **Acetophenone**



^1H NMR (300.15 MHz, CDCl_3): 7.98-7.3 (m, 4H), 2.60 (s, 3H).

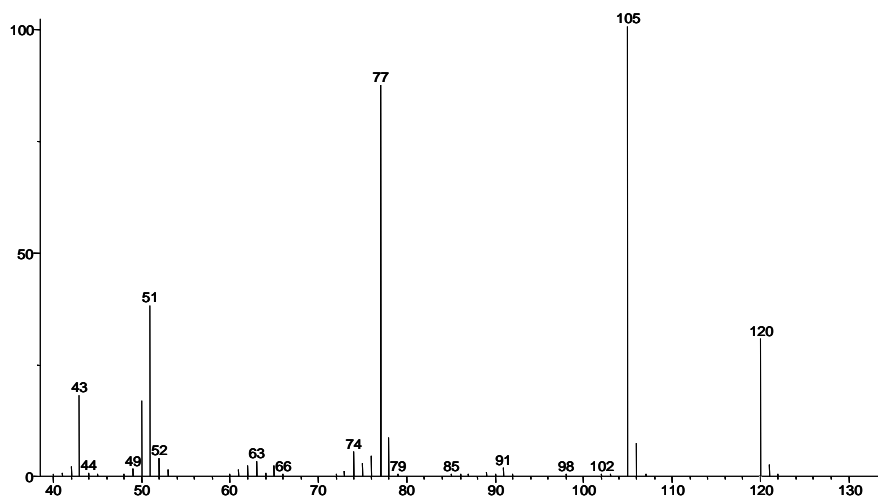
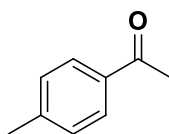


Figure 126. Mass spectrum of acetophenone

- 1-(p-tolyl)ethanone



¹H NMR (300.15 MHz, CDCl₃): 7.84 (d, J=8.2 Hz, 2H), 7.25 (d, J=8.1 Hz, 2H), 2.59 (s, 3H), 2.45 (s, 3H).

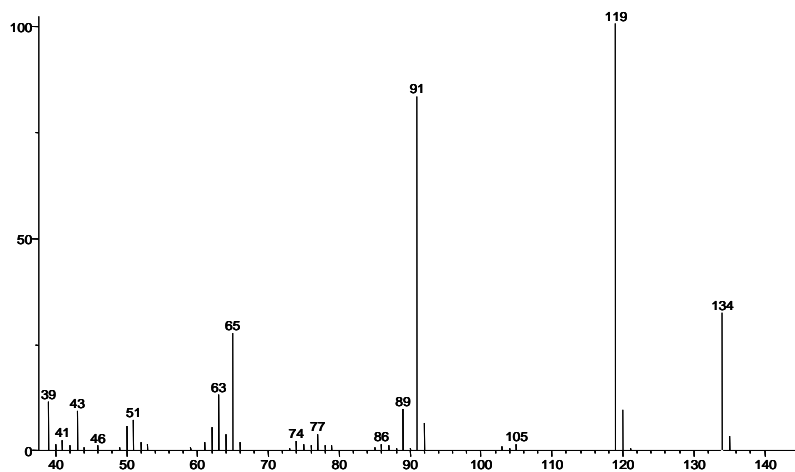
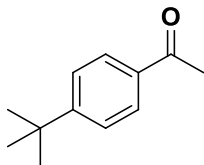


Figure 127. Mass spectrum of 1-(p-tolyl)ethanone

- **1-(4-(tert-butyl)phenyl)ethanone**



¹H NMR (300.15 MHz, CDCl₃): 7.90 (d, J=8.5 Hz, 2H), 7.48 (d, J=8.5 Hz, 2H), 2.57 (s, 3H), 1.34 (s, 9H).

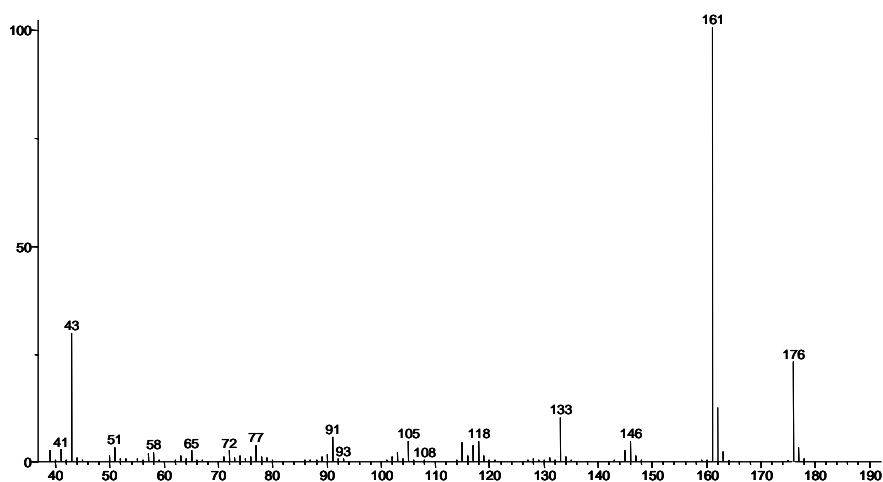
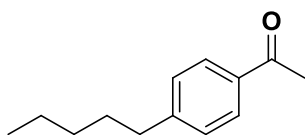


Figure 128. Mass spectrum of 1-(4-(tert-butyl)phenyl)ethanone

- **1-(4-pentylphenyl)ethanone**



¹H NMR (300.15 MHz, CDCl₃): 7.90 (d, J = 8.1 Hz, 2 H), 7.26 (d, J = 8.1 Hz, 2 H), 2.68 (t, J = 7.6 Hz, 2 H), 2.58 (s, 3 H), 1.69-1.57 (m, 2 H), 1.40-1.27 (m, 4 H), 0.89 (t, J = 6.8 Hz, 3 H).

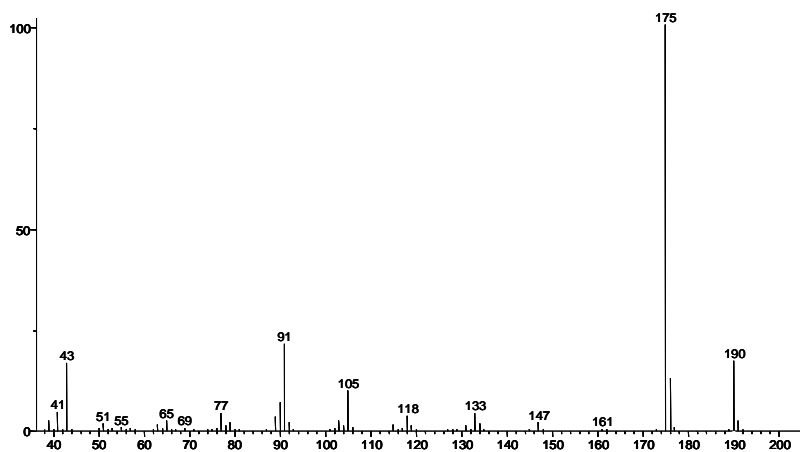
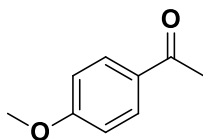


Figure 129. Mass spectrum of 1-(4-pentylphenyl)ethanone

- 1-(4-methoxyphenyl)ethanone



$^1\text{H NMR}$ (300.15 MHz, CDCl_3): 7.91 (m, 2H), 6.91 (m, 2H), 3.83 (s, 3H), 2.53 (s, 3H).

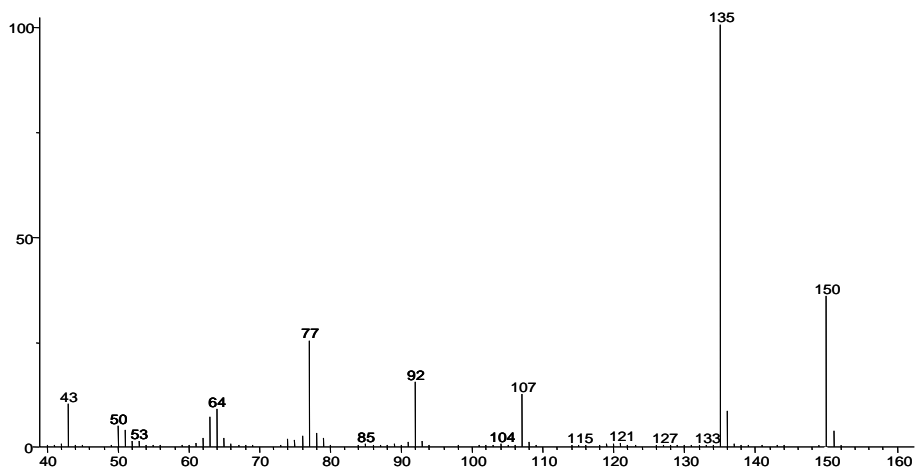
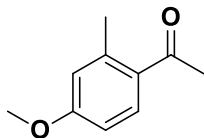


Figure 130. Mass spectrum of 1-(4-methoxyphenyl)ethanone

- **1-(4-methoxy-2-methylphenyl)ethanone**



¹H NMR (300.15 MHz, CDCl₃): 8.15 (d, J=8.5, 2H), 7.15 (s, 1H), 6.91 (d, J=8.5, 2H), 3.85 (s, 3H), 2.56 (s, 3H), 2.45 (s, 3H).

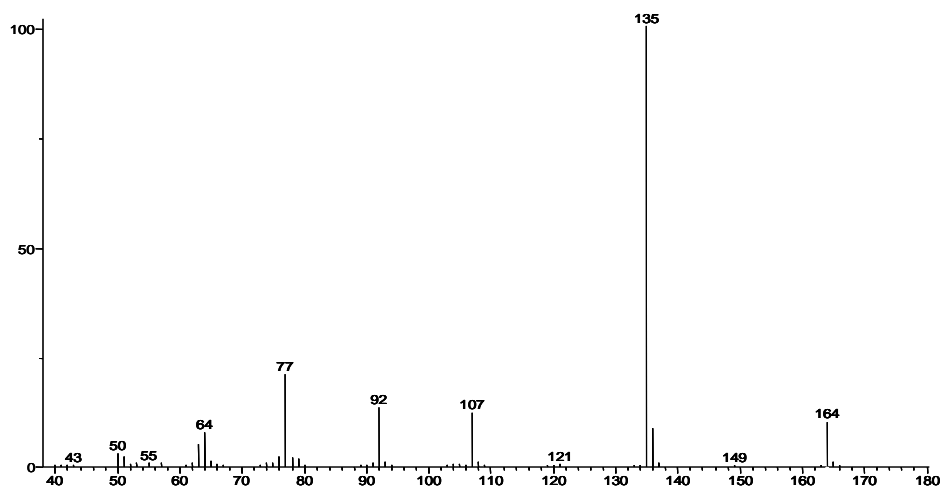
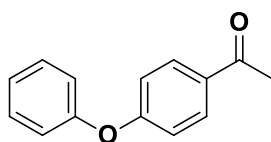


Figure 131. Mass spectrum of 1-(4-methoxy-2-methylphenyl)ethanone

- **1-(4-phenoxyphenyl)ethanone**



¹H NMR (300.15 MHz, CDCl₃): 7.94 (d, J=8.7 Hz, 2H), 7.39 (t, J=7.4 Hz, 2H), 7.20 (t, J=7.4 Hz, 1H), 7.07 (d, J=7.8 Hz, 2H), 6.95 (d, J=8.8 Hz, 2H), 2.57 (s, 3H).

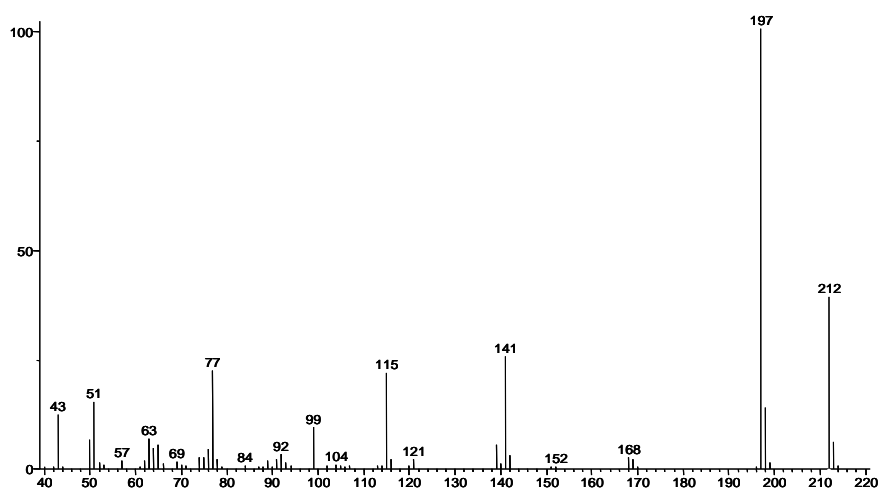
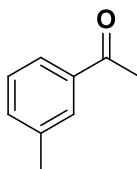


Figure 132. Mass spectrum of 1-(4-phenoxyphenyl)ethanone

- 1-(m-tolyl)ethanone



$^1\text{H NMR}$ (300.15 MHz, CDCl_3): 7.79-7.71 (m, 2 H), 7.40-7.29 (m, 2 H), 2.59 (s, 3 H), 2.41 (s, 3 H).

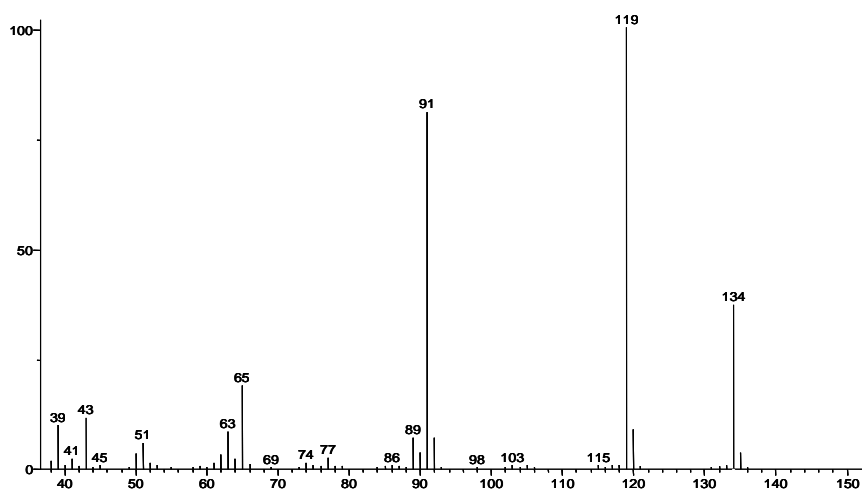
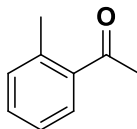


Figure 133. Mass spectrum of 1-(m-tolyl)ethanone

- **1-(o-tolyl)ethanone**



¹H NMR (300.15 MHz, CDCl₃): 7.94 (d, J = 7.4 Hz, 2 H), 7.45-7.35 (m, 1 H), 7.30-7.24 (m, 2 H), 2.58 (s, 3 H), 2.53 (s, 3 H).

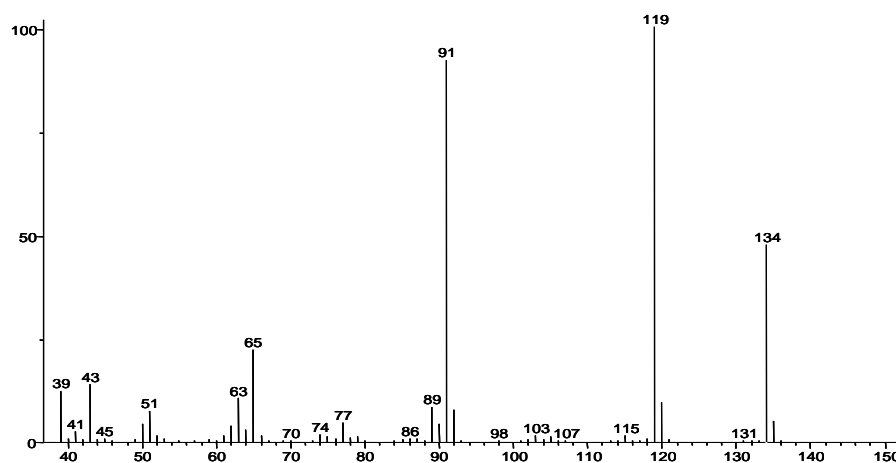
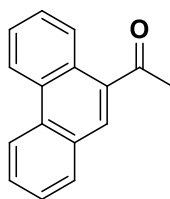


Figure 134. Mass spectrum of 1-(o-tolyl)ethanone

- **1-(phenanthren-9-yl)ethanone**



¹H NMR (300.15 MHz, CDCl₃): 8.77-8.67 (m, 3H), 8.21 (s, 1 H), 8.00-7.95 (m, 1H), 7.80-7.63 (m, 4H), 2.84 (s, 3H).

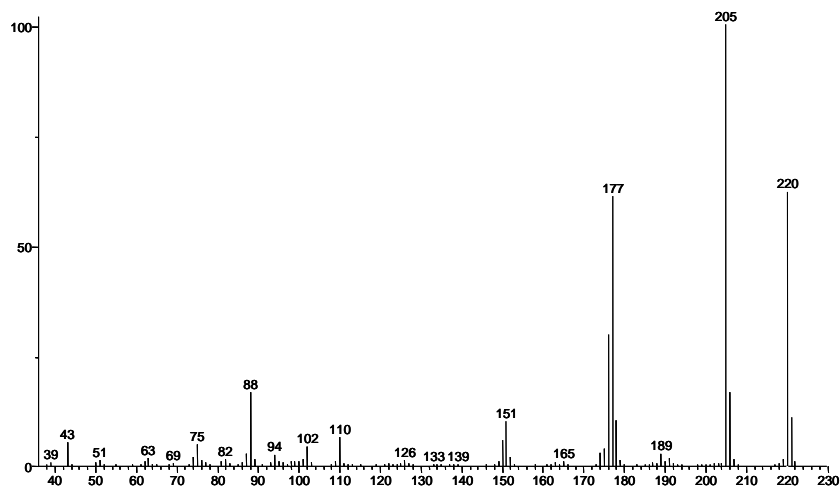


Figure 135. Mass spectrum of 1-(o-tolyl)ethanone

- Propiophenone

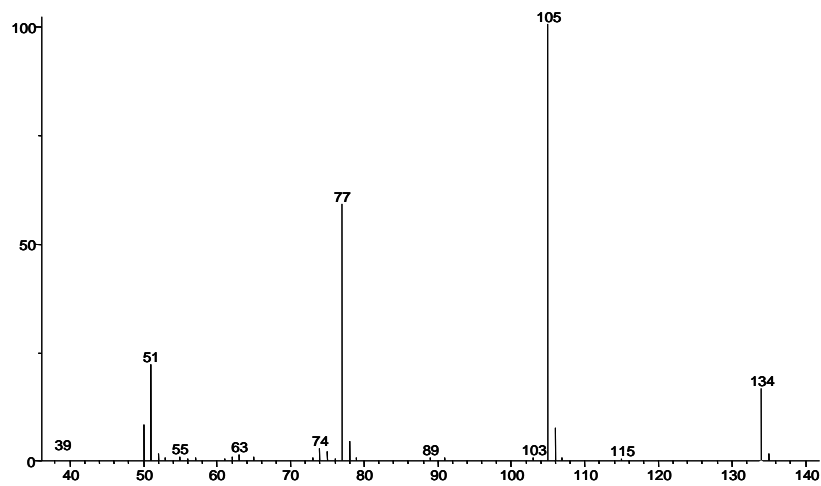
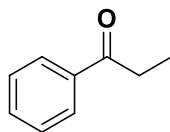


Figure 136. Mass spectrum of propiophenone

- 1-phenylhexan-1-one

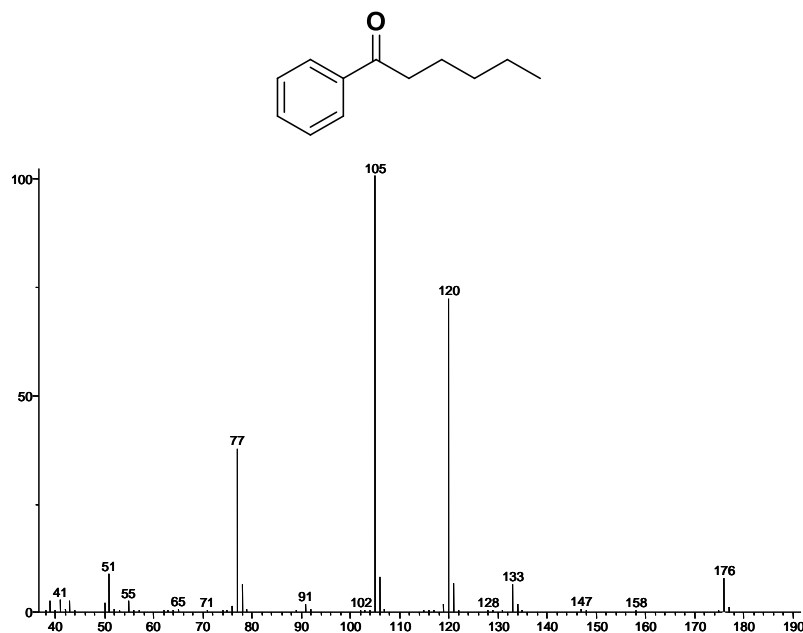


Figure 137. Mass spectrum of 1-phenylhexan-1-one

7.2.6. N-oxides and capsule

TITRATION BETWEEN CAPSULE AND N-OXIDE

In a NMR tube was introduced a chloroform solution of resorcin[4]arene (36 mM, 0.5 mL). Specific amounts of the N,N-dimethyldodecylamine N-oxide **DDNO** were added to the solution at room temperature in order to obtain samples with 2.5, 5, 7.5, 10, 12.5, 15 and 20 equivalents of amino-oxide with respect to the capsule. $^1\text{H-NMR}$ analyses were carried out after each addition.

$^1\text{H-NMR}$ spectra of the titration between the hexameric capsule (36 mM) and several amounts of trimethylamine N-oxide **TMNO** (1, 2.5, 5, 7.5, 10, 12.5, 15 equivalents with respect to the capsule) are reported below.

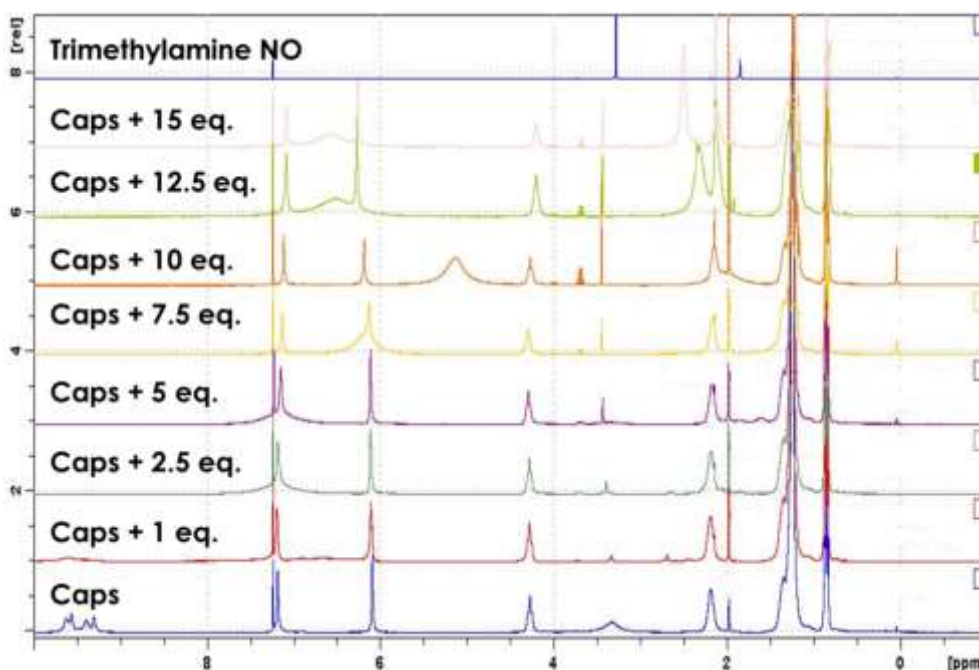


Figure 138 Titration of the resorcin[4]arene hexamer (Caps) with different amounts of trimethylamine N-oxide.

INTERACTION BETWEEN CAPSULE AND N,N-DIMETHYLPROP-2-YN-1-AMINE OXIDE

In a 3 mL vial were introduced chloroform-d solution of resorcin[4]arene (72 mM, 0.5 mL) followed by the N,N-dimethylprop-2-yn-1-amine oxide (1 eq. with respect to resorcin[4]arene capsule, 12 mM). The resulted mixture was stirred until completely homogeneous and left at room temperature for several days. The possible rearrangement products were confirmed by ¹H-NMR.

- **Interaction with resorcinol**

The procedure is the same but resorcinol (30 mM) was added in place of resorcin[4]arene.

- **DOSY analysis**

In a NMR tube were introduced chloroform-d solution of resorcin[4]arene (36 mM, 0.5 mL) followed by the N,N-dimethylprop-2-yn-1-amine oxide (1, 2.5 or 5 eq. with respect to resorcin[4]arene capsule).

The same procedure was employed in the presence of tetraethylammonium tetrafluoroborate (10 equivalents with respect to the capsule, 60 mM).

REACTION BETWEEN N-OXIDES AND ISOCYANIDES

In a 1.5 mL vial were placed 1 mL of chloroform-d, the desired phenyl isocyanate (27 mM) and the chosen amino-oxide (1.1 equivalents with respect to the phenyl isocyanate). The reaction was thermostatted at room temperature or at 60°C and the system was left under these condition overnight. The products were confirmed by ¹H NMR and GC-MS in the cases of azocompounds and p-methoxyaniline.

- **Reaction at lower concentration of substrate**

The procedure is the same but stock solutions of the substrates (37 mM) in 0.5 mL of chloroform-d were prepared and the reactants were introduced into the reaction by means of them.

- **Reaction in partially dried chloroform-d**

In a 10 mL flask were placed 3mL of chloroform-d previously treated to remove water simply adding molecular sieves kept at 120°C until shortly before. Keeping the reaction under N₂ flux were added the p-methoxyisocyanate (27 mM) and the N-methylmorpholyne N-oxide (1.1 equivalents with respect to the phenyl isocyanate). The reaction was thermostatted at 60°C under N₂ atmosphere overnight. The products were confirmed by ¹H NMR and GC-MS in the cases of azo-compounds and p-methoxyaniline.

KINETIC STUDY

In a NMR tube were placed 0.5 mL of chloroform-d, the p-methoxyphenyl isocyanate (2.7 mM) and the N-methylmorpholine N-oxide (1.1 equivalents with respect to the p-methoxyphenyl isocyanate). The reaction was thermostatted at 60°C and the system was left under these condition overnight and analysed every 30 minutes through ¹H-NMR.

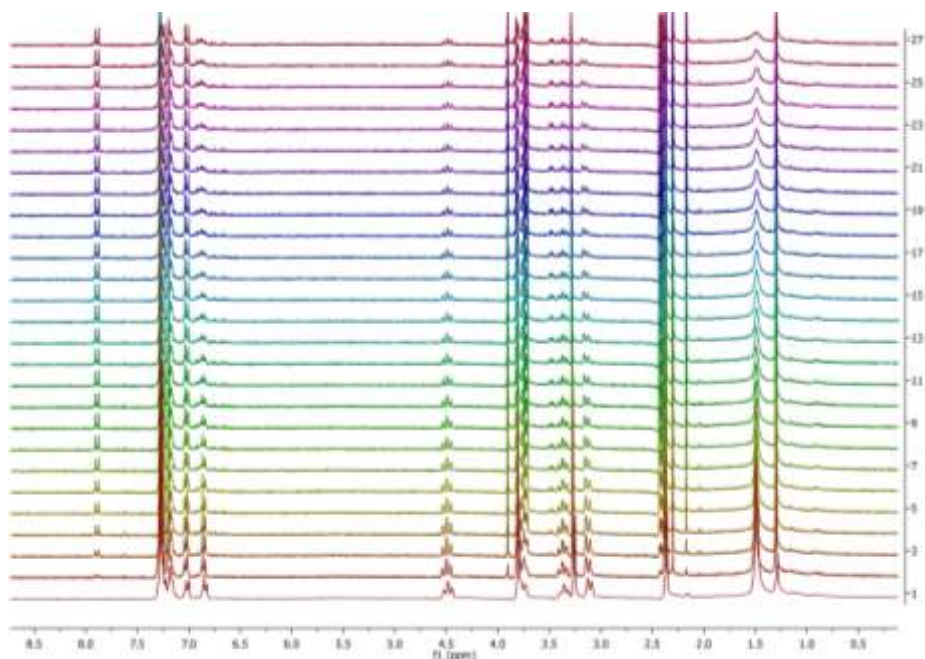


Figure 139. Reaction between p-methoxyphenyl and N-methylmorpholine N-oxide analysed every 30 minutes (from bottom to up). Experimental conditions: [p-methoxyphenyl isocyanate] = 2.7 mM; N-methylmorpholine N-oxide = 1.1 equivalents with respect to the isocyanate; T = 60°C; Chloroform-d = 0.5 mL.

REACTION BETWEEN P-METHOXYPHENYL ISOCYANATE AND P-METHOXYANILINE MEDIATED BY MMNO

In a 1.5 mL vial were placed 1 mL of chloroform-d, the p-methoxyphenyl isocyanate (27 mM), the p-methoxyaniline (1 equivalent with respect to the isocyanate 27 mM) and the N-methylmorpholine N-oxide **MMNO** (1.1 equivalents with respect to the isocyanate, 29.7 mM). The reactions were thermostatted at 60°C and the system was left under these condition overnight. The products were confirmed by ^1H NMR.

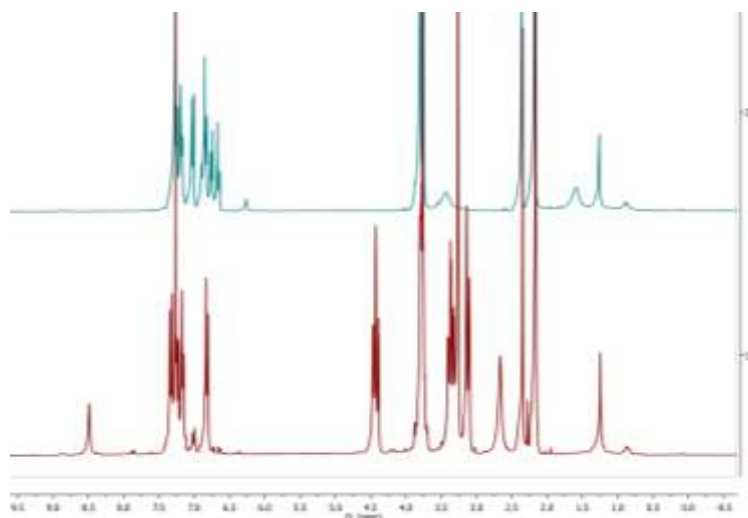


Figure 140. ^1H -NMR spectra of the reaction between p-methoxyphenyl isocyanate and p-methoxyaniline both in the presence (in red) and in the absence (in blue) of MMNO. Experimental conditions: [p-methoxyphenyl isocyanate] = 27 mM; [p-methoxyaniline] = 27 mM; [MMNO] = 29.7 mM; chloroform-d = 1 mL; room temperature, 30 minutes.

REACTION BETWEEN P-METHOXYPHENYL ISOCYANATE AND DIFFERENT AMOUNTS OF MMNO

In a 1.5 mL vial were placed 1 mL of chloroform-d, the p-methoxyphenyl isocyanate (27 mM) and the N-methylmorpholine N-oxide (1, 2, 4, 6 or 8 equivalents with respect to the phenyl isocyanate). The reactions were thermostatted at 60°C and the system was left under these condition overnight. The products were confirmed by ^1H NMR.

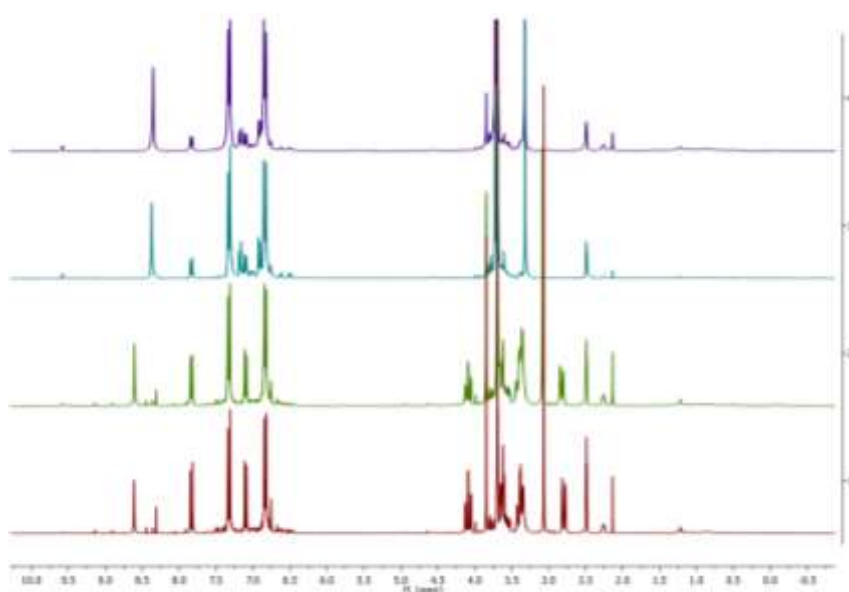


Figure 141. ^1H -NMR spectra in dmsO-d_6 of the reaction between p-methoxyphenyl isocyanate and 2, 4, 6 and 8 amounts of MMNO (from bottom to up). Experimental conditions: [p-methoxyphenyl isocyanate] = 27 mM; chloroform-d = 1 mL; $T = 60^\circ\text{C}$.

- **Capsule**

In a NMR tube were placed 1 mL of chloroform-d, the N-methylmorpholine N-oxide (3 mM) and the resorcin[4]arene (6 equivalents with respect to the N-methylmorpholine N-oxide). The mixture was stirred few minute in order to achieve an homogeneous solution. The p-methoxyphenyl isocyanate (2.7 mM) was added to the solution and the reaction was thermostatted at 60°C and the system was left under these condition overnight and analysed every 30 minutes through ¹H-NMR.

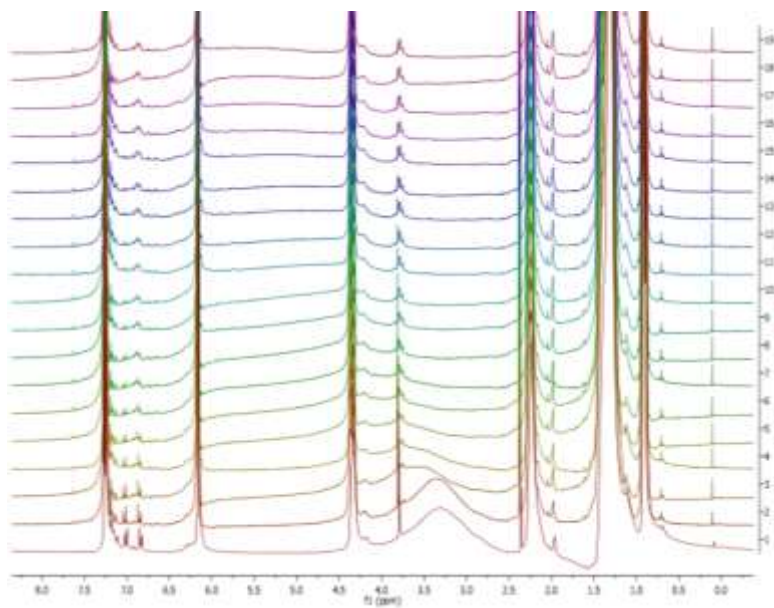


Figure 142 Reaction between p-methoxyphenyl and N-methylmorpholine N-oxide in the presence of the capsule analysed every 30 minutes (from bottom to up). Experimental conditions: [p-methoxyphenyl isocyanate] = 2.7 mM; N-methylmorpholine N-oxide = 1.1 equivalents with respect to the isocyanate; resorcin[4]arene = 6 equivalents with respect to the capsule; T = 60°C; Chloroform-d = 1 mL.

- **Capsule and ammonium**

In a NMR tube were placed 1 mL of chloroform-d, the N-methylmorpholine N-oxide (3 mM), the resorcin[4]arene (6 equivalents with respect to the N-methylmorpholine N-oxide) and tetraethylammonium tetrafluoroborate (10 equivalents with respect to the capsule). The mixture was stirred few minute in order to achieve an homogeneous solution. The p-methoxyphenyl isocyanate

(2.7 mM) was added to the solution and the reaction was thermostatted at 60°C and the system was left under these condition overnight and analysed every 30 minutes through $^1\text{H-NMR}$.

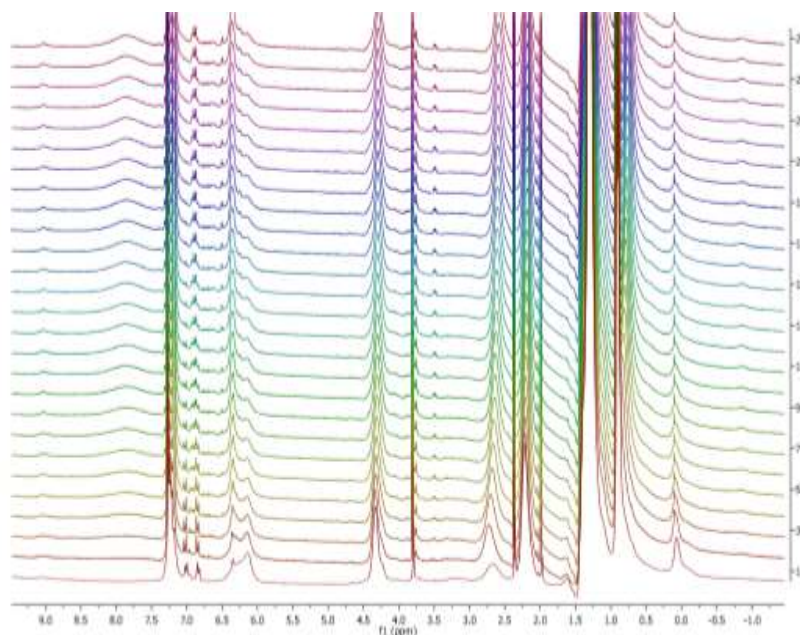


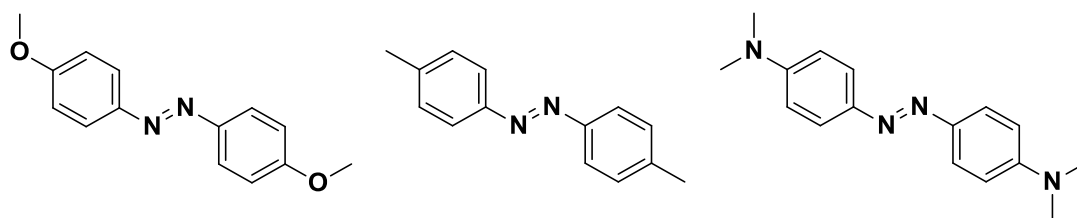
Figure 143. Reaction between p-methoxyphenyl and N-methylmorpholine N-oxide in the presence of the capsule filled by tetraethylammonium analysed every 30 minutes (from bottom to up). Experimental conditions: [p-methoxyphenyl isocyanate] = 2.7 mM; N-methylmorpholine N-oxide = 1.1 equivalents with respect to the isocyanate; resorcin[4]arene = 6 equivalents with respect to the capsule; tetraethylammonium tetrafluoroborate = 10 equivalents with respect to the capsule; T = 60°C; Chloroform-d = 1 mL.

- Resorcinol

In a 1.5 mL vial were placed 1 mL of chloroform-d, the N-methylmorpholine N-oxide (3 mM), the resorcinol (24 equivalents with respect to the N-methylmorpholine N-oxide) and the p-methoxyphenyl isocyanate (2.7 mM). The reaction was thermostatted at 60°C and the system was left under these condition overnight. The products were confirmed by $^1\text{H NMR}$.

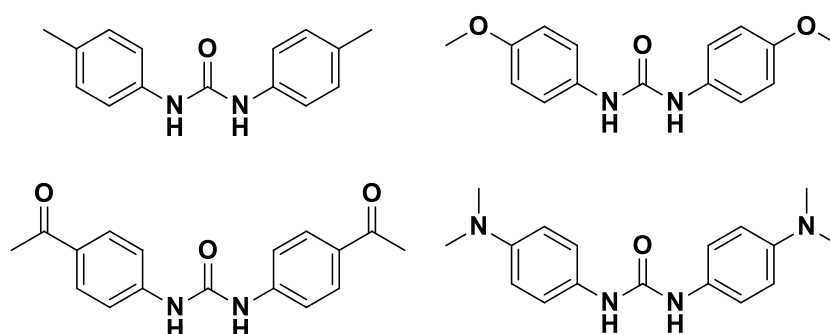
PRODUCTS CHARACTERIZATION

- Azobenzene derivatives



The observed $^1\text{H-NMR}$ chemical shifts in CDCl_3 corresponded to those reported by Gu and co-workers.²⁹³

- **Aromatic Urea derivatives**



The observed $^1\text{H-NMR}$ chemical shifts in DMSO-d_6 corresponded to those reported by Guan and co-workers.²⁹⁴

7.2.7. Hydrogenation mediated by Pd-NPs in aqueous anionic micellar media

SYNTHESIS OF Pd-NPs IN MICELLAR MEDIA

- **Micellar medium (CTAB)**

In a 25 mL flask equipped with magnetic stirrer were placed 3 mL of distilled water followed by $\text{Pd}(\text{OAc})_2$ (2.4 mM) and cetyltrimethylammonium bromide (CTAB) (80 mM). The solution was stirred at 750 rpm for 1 h and then treated with 1 bar of H_2 under stirring for 1 hour until the colour changed from pale orange to dark grey.

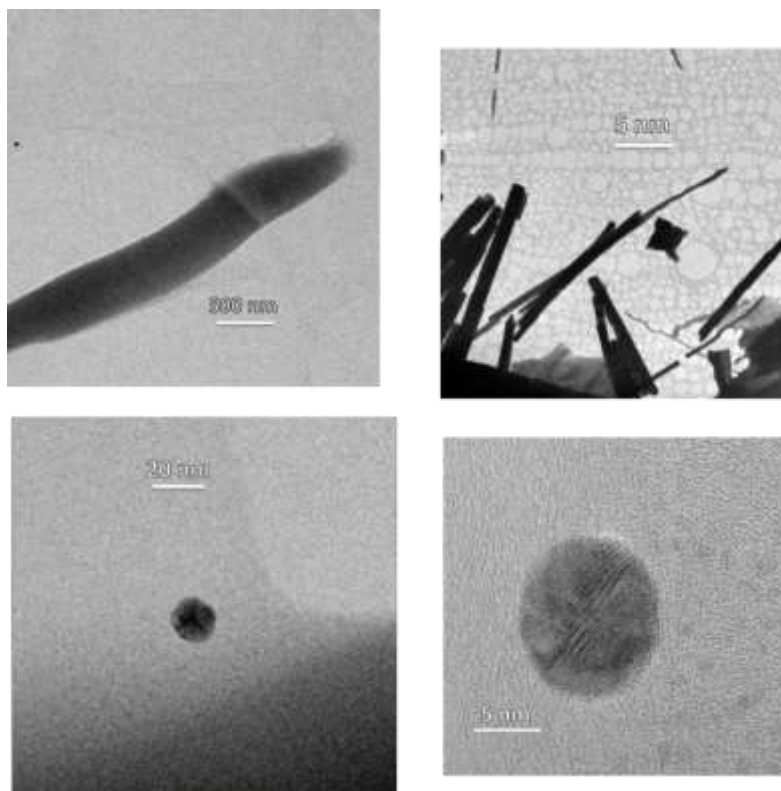


Figure 144. TEM image of the Pd-NPs activated in water in the presence of CTAB.

- **Micellar medium (Triton-X100 and Triton X-114)**

Experimental procedure as above reported for CTAB. H₂ activation time 20 minutes.

- **Micellar medium (SDS and SDSU)**

Experimental procedure as above reported for CTAB. H₂ activation time 5 minutes.

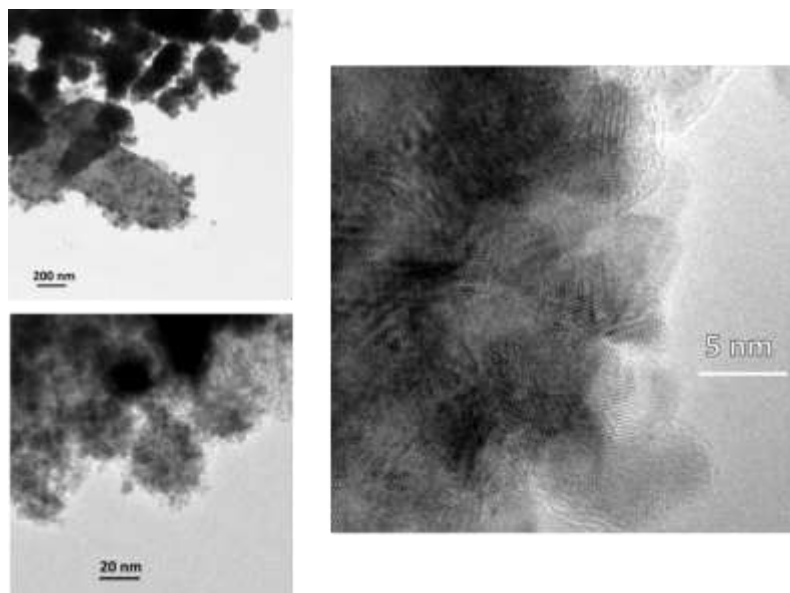


Figure 145. TEM image of the Pd-NPs activated in water in the presence of SDS.

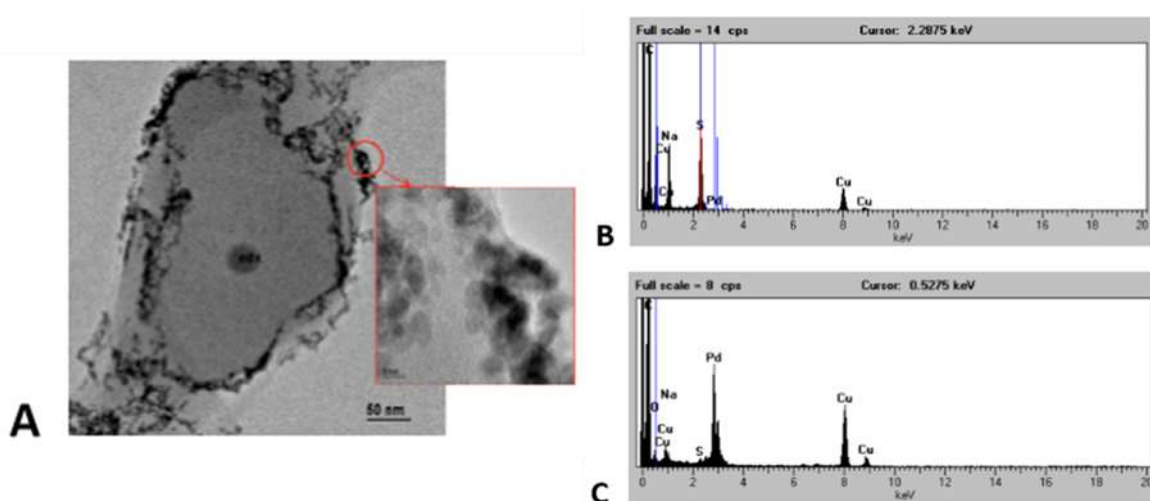


Figure 146. A) TEM image of palladium nanoparticles prepared at room temperature by H_2 flushing on an solution of $Pd(OAc)_2$ (2.4 mM) in the presence of SDSU (80 mM) as surfactant in water (3 mL). B) EDX measurements on the PdNPs prepared in the presence of SDSU in the middle grey spot. C) EDX measurements on the PdNPs prepared in the presence of SDSU in the red spot.

- **Micellar medium (SDBS)**

Experimental procedure as above reported for CTAB. [SDBS] = 100 mM; H_2 activation time up to 10 minutes.

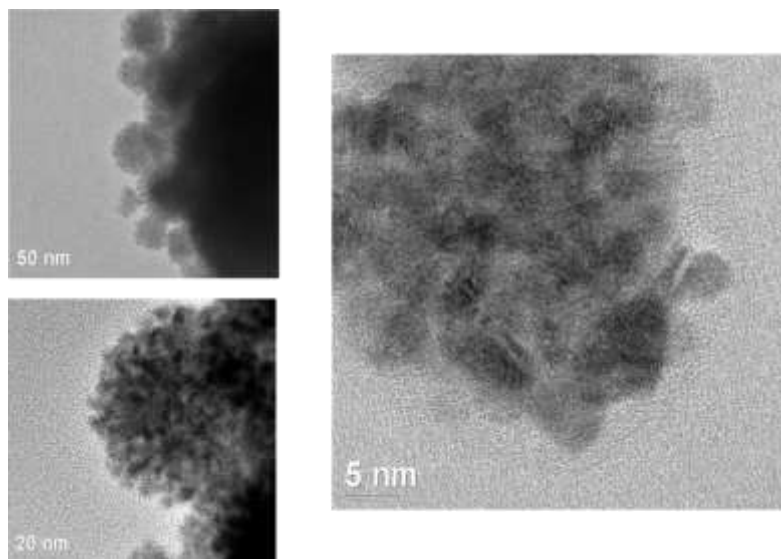


Figure 147. TEM image of the Pd-NPs activated in water in the presence of SDBS.

- **Micellar medium (DOSS)**

Experimental procedure as above reported for CTAB. [DOSS] = 90 mM; H₂ activation time 5 minutes.

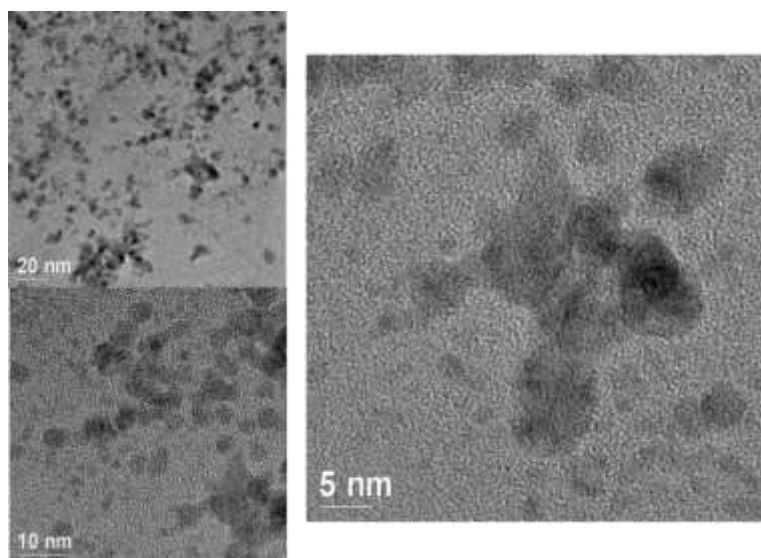


Figure 148. TEM image of the Pd-NPs activated in water in the presence of DOSS.

- **Micellar medium (Ralufon[®])**

Experimental procedure as above reported for CTAB. H₂ activation time 2 minutes.

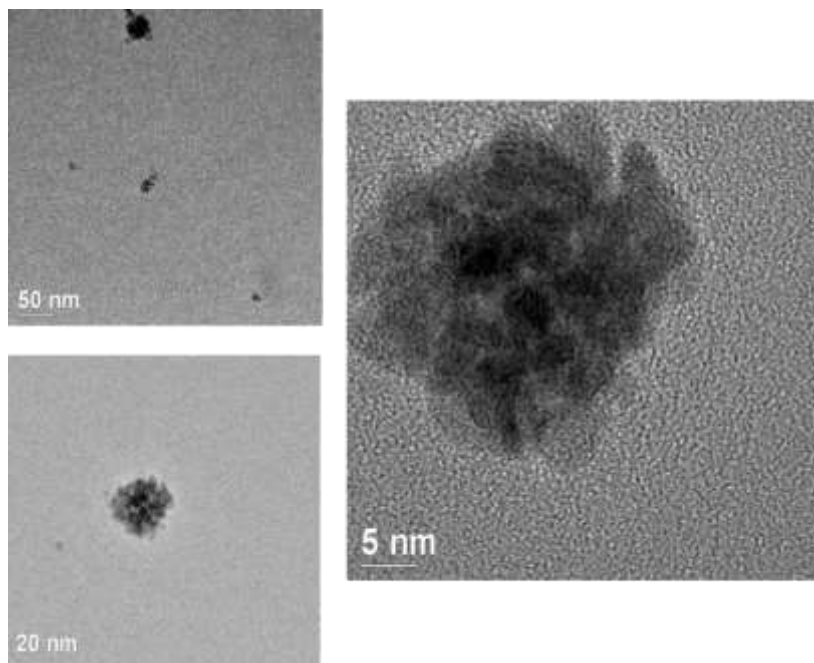
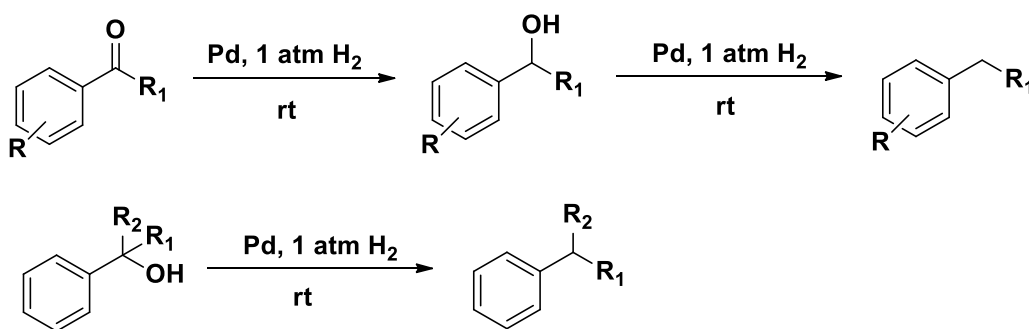


Figure 149. TEM image of the Pd-NPs activated in water in the presence of Ralufon®.

HYDROGENATION OF AROMATIC CARBONYL AND ALCOHOL COMPOUNDS IN METHANOL



R₁; R₂ = CH₃ or H

Scheme 29. Hydrogenation reaction of aromatic carbonyl compounds and alcohol catalysed by Pd with H₂.

In a 25 mL flask equipped with magnetic stirrer were placed 3 mL of methanol and 7.6 mg of Pd/C 10 wt.% ($7.2 \cdot 10^{-3}$ mmol, 2.4 mM). The solution was treated with 1 bar of H₂ for 5 minutes after which benzaldehyde **1a** (0.72 mmol) was added at room temperature maintaining the system stirring at 750 rpm under hydrogen atmosphere. The substrate conversion over time was followed

through 50 μL periodical sampling of the mixture. The samples were analysed by GC in order to determine the conversion degree. The catalytic experiment was repeated three times determining the benzaldehyde conversion through the average of the three results was used. All the hydrogenation products were identified by GC-MS analysis.

The same procedure was applied to the aromatic aldehydes **1b-1g**, acetophenone **1h** and benzyl alcohols **4a** and **4b**. Instead the amount of Pd/C was increased to 38 mg ($3.6 \cdot 10^{-2}$ mmol, 12 mM) in the presence of 2-phenylpropan-2-ol **4c**.

HYDROGENATION OF AROMATIC CARBONYL AND ALCOHOL COMPOUNDS IN WATER WITH SURFACTANTS

In the 25 mL flask containing the Pd-NPs (Pd = $7.2 \cdot 10^{-3}$ mmol, 2.4 mM) in aqueous micellar medium benzaldehyde **1a** (0.72 mmol, 240 mM) was added at room temperature maintaining the system stirring at 750 rpm under hydrogen atmosphere. The substrate conversion over time was followed through 50 μL periodical sampling of the mixture, extracting the aqueous micellar solution with 150 μL of ethyl acetate. The organic phase was then analysed by GC in order to determine the conversion degree. The catalytic experiment was repeated three times determining the benzaldehyde conversion through the average of the three results was used. All the hydrogenation products were identified by GC-MS analysis.

The same procedure was applied to the aromatic aldehydes **1b-1g**, acetophenone **1h** and benzyl alcohols **4a** and **4b**. Instead the amount of Pd(OAc)₂ was increased to 8.2 mg ($3.6 \cdot 10^{-2}$ mmol, 12 mM) in the presence of 2-phenylpropan-2-ol **4c**.

BENZYL ALCOHOLS AND DEOXYGENATION PRODUCTS CHARACTERIZATION

- **Benzyl alcohol 2a**

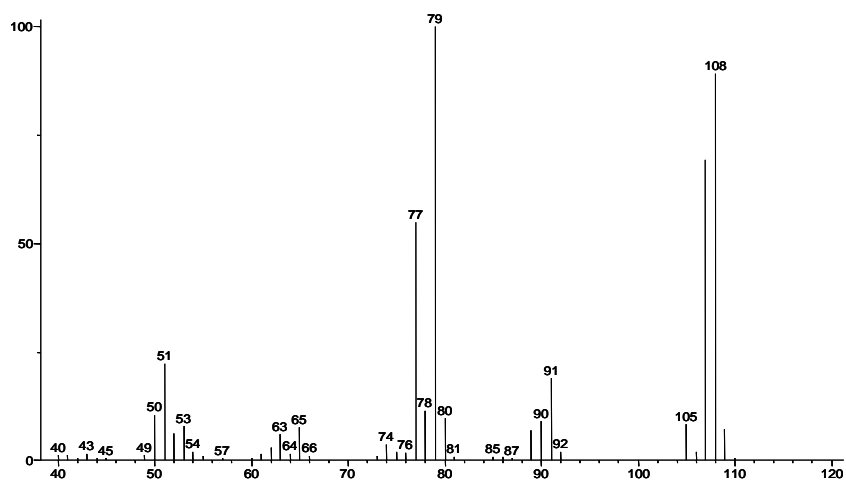
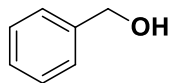
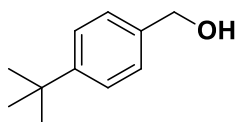


Figure 150. Mass spectrum of benzyl alcohol 2a

- **(4-(tert-butyl)phenyl)methanol 2b**



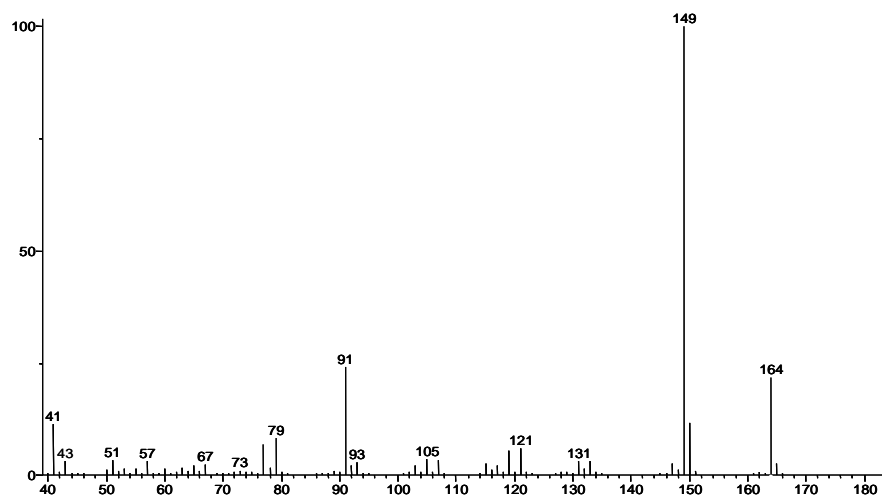


Figure 151. Mass spectrum of (4-(tert-butyl)phenyl)methanol **2b**

- (4-methoxyphenyl)methanol **2c**

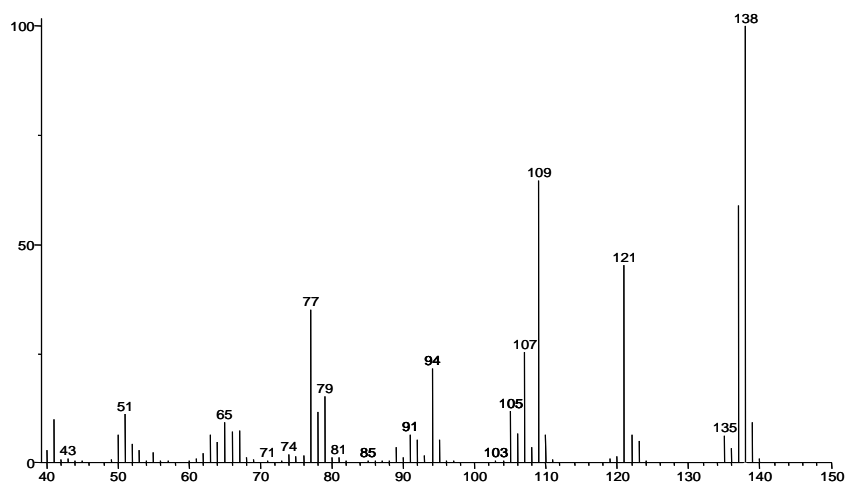
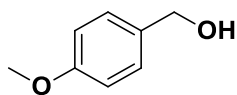
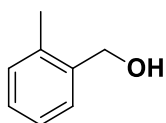


Figure 152. Mass spectrum of (4-methoxyphenyl)methanol **2c**

- *o*-tolylmethanol **2d**



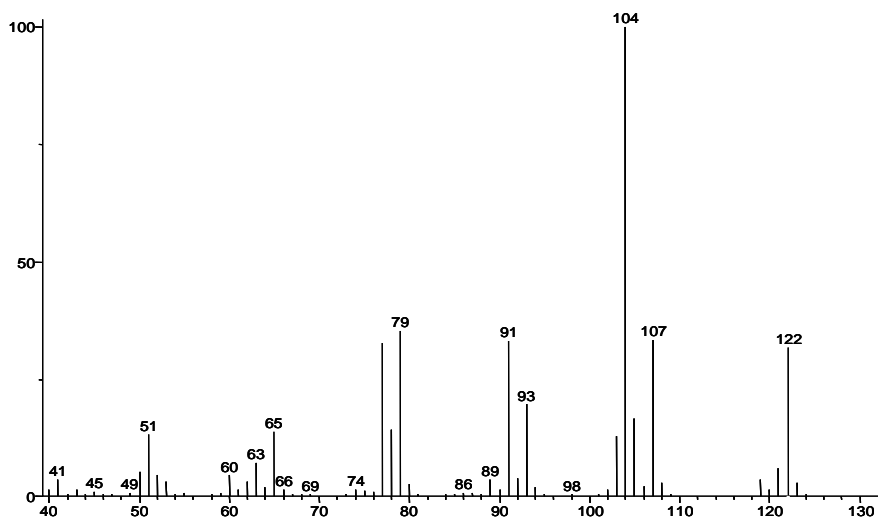


Figure 153. Mass spectrum of o-tolymethanol 2d

- (2,4-dimethylphenyl)methanol 2e

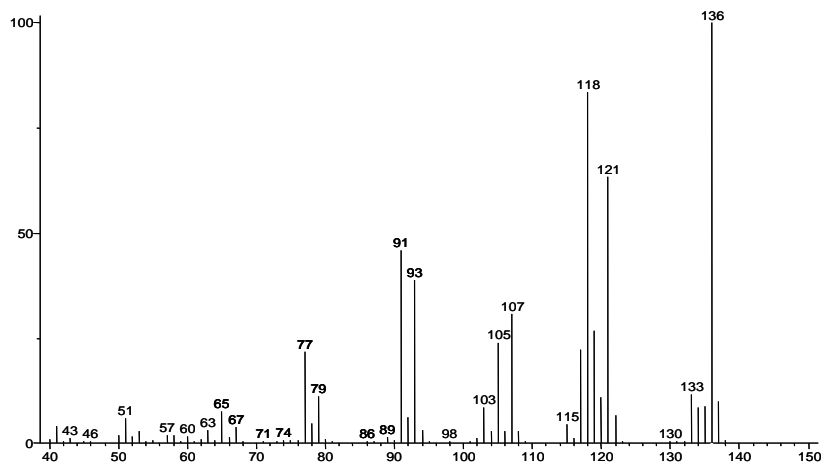
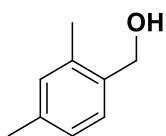
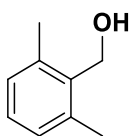


Figure 154. Mass spectrum of (2,4-dimethylphenyl)methanol 2e

- (2,6-dimethylphenyl)methanol 2f



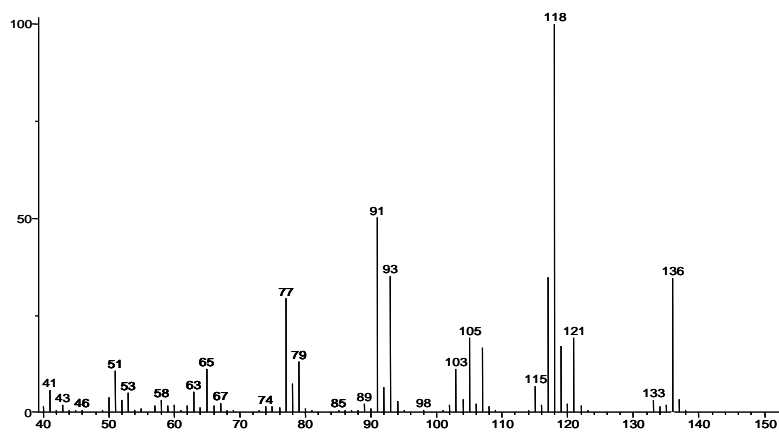
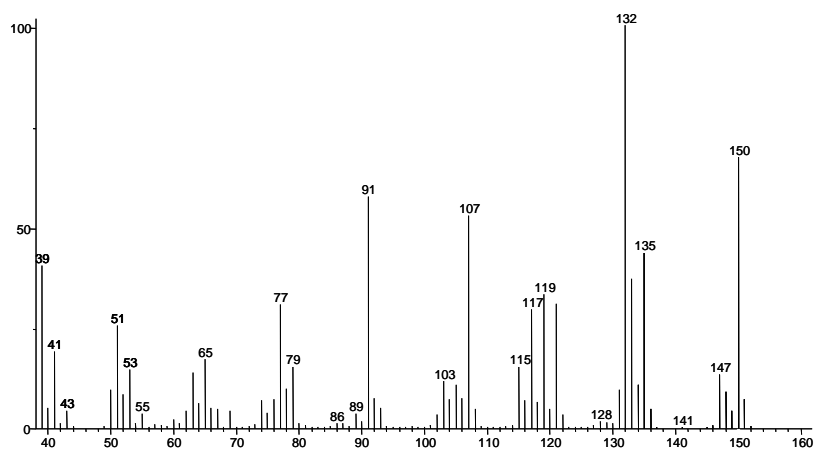
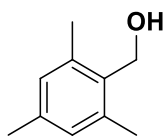


Figure 155. Mass spectrum of (2,6-dimethylphenyl)methanol **2f**

- Mesitylmethanol 2g



- Toluene 3a

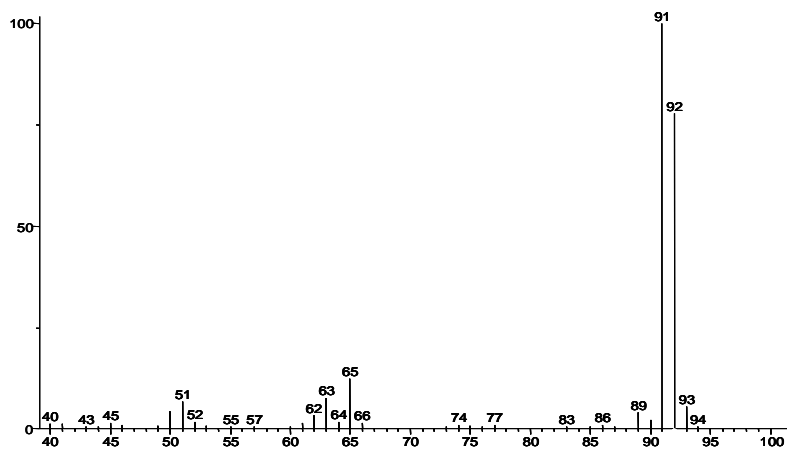
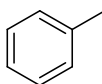
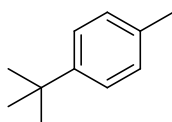


Figure 156. Mass spectrum of toluene 3a

- 1-(tert-butyl)-4-methylbenzene 3b



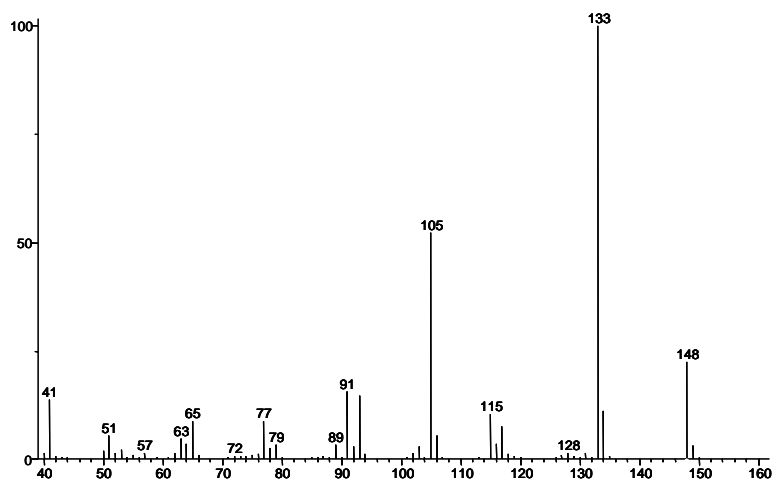


Figure 157. Mass spectrum of 1-(tert-butyl)-4-methylbenzene **3b**

- 1-methoxy-4-methylbenzene **3c**

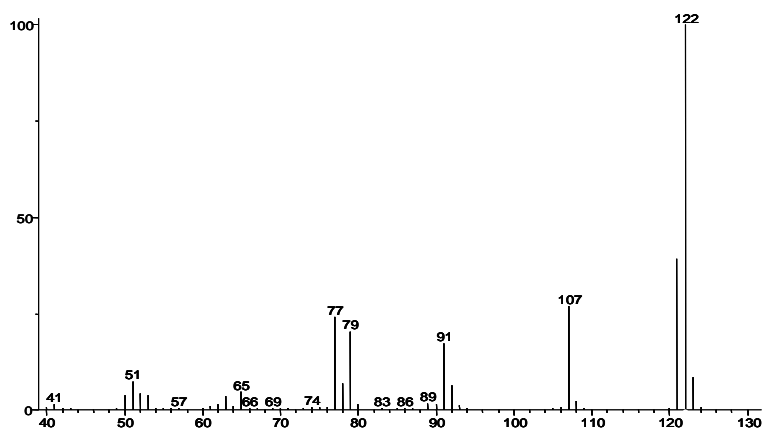
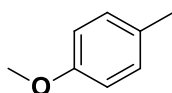
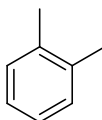


Figure 158. Mass spectrum of 1-methoxy-4-methylbenzene **3c**

- o-xylene **3d**



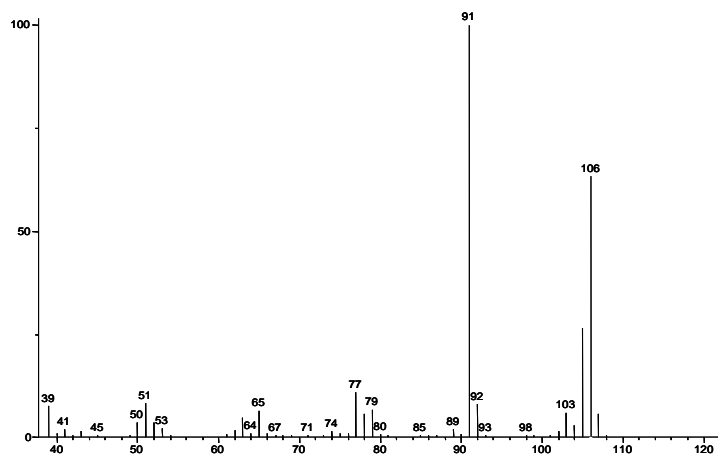


Figure 159. Mass spectrum of o-xylene 3d

- 1,2,4-trimethylbenzene 3e

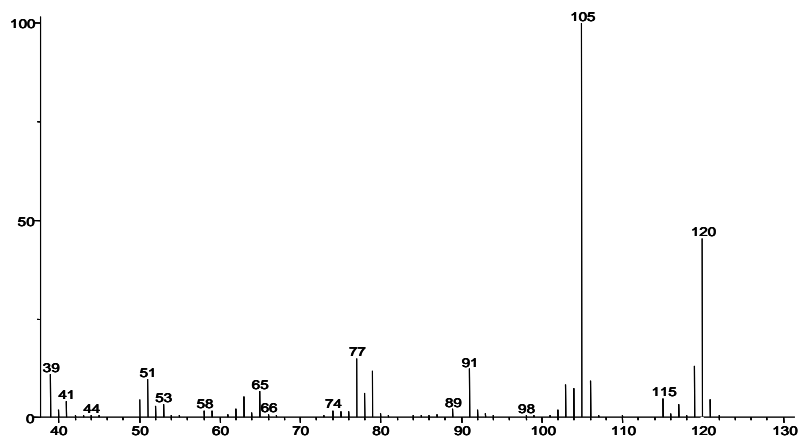
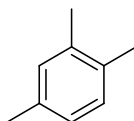


Figure 160. Mass spectrum of 1,2,4-trimethylbenzene 3e

- 1,2,3-trimethylbenzene **3f**

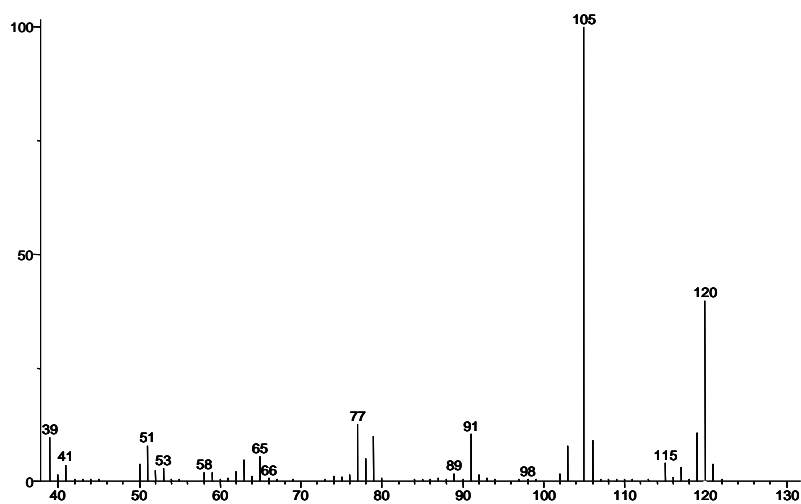
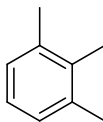
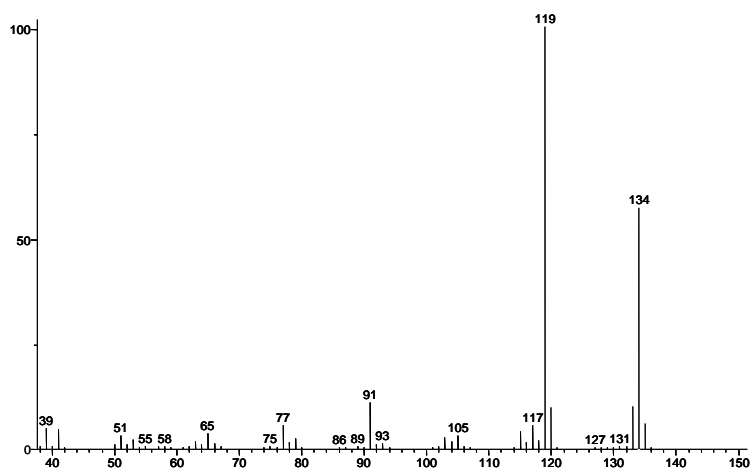
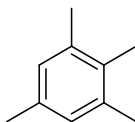


Figure 161. Mass spectrum of 1,2,3-trimethylbenzene **3f**

- 1,2,3,5-tetramethylbenzene **3g**



- 1-phenylethanol 2h

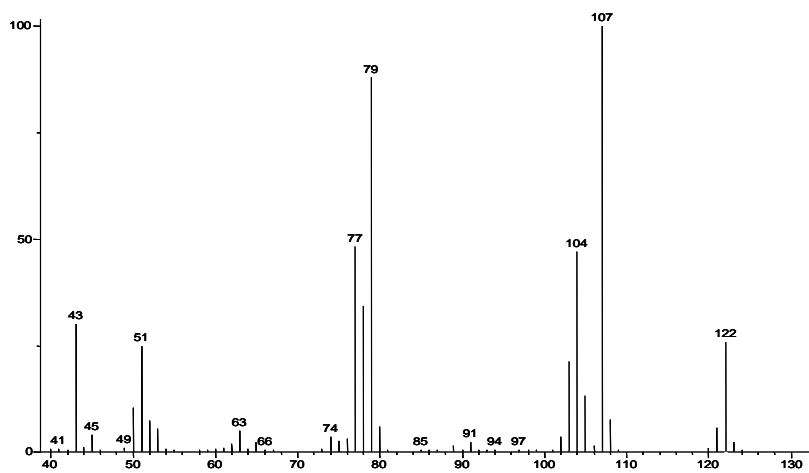
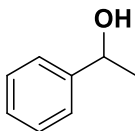


Figure 162. Mass spectrum of 1-phenylethanol 2h

- Ethylbenzene 3h

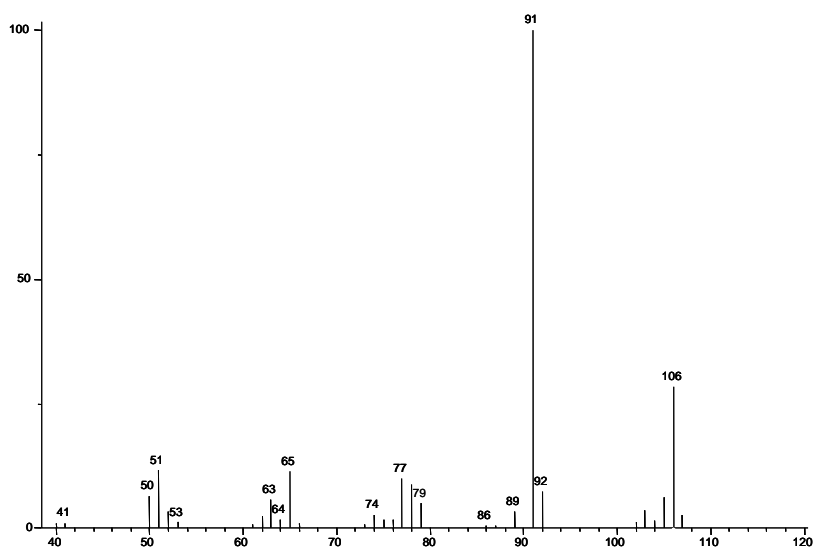
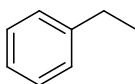


Figure 163. Mass spectrum of ethylbenzene 3h

- Cumene

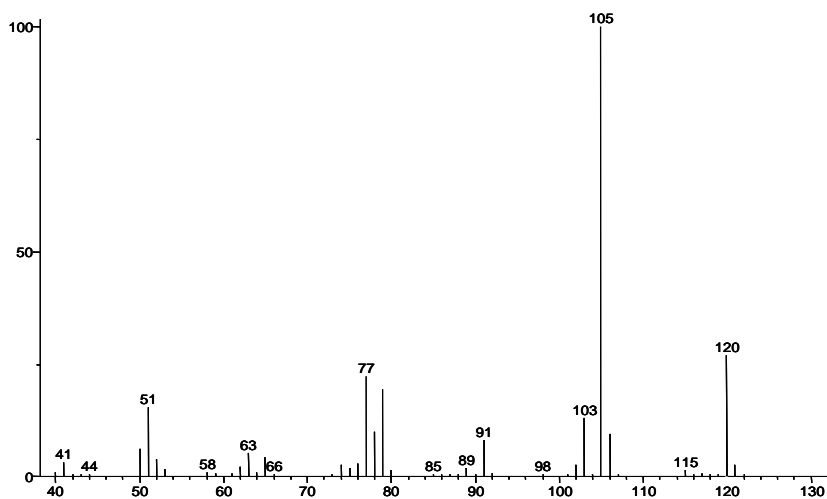
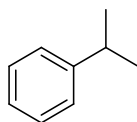
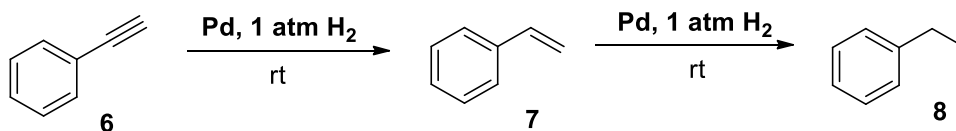


Figure 164. Mass spectrum of cumene

SEMI-HYDROGENATION OF PHENYLACETYLENE TO STYRENE IN THF



Scheme 30. Semi-hydrogenation reaction of phenylacetylene catalysed by Pd with H₂.

In a 25 mL flask equipped with magnetic stirrer were placed 3 mL of THF and 16 mg of Pd/C 10 wt.% (Pd = $1.5 \cdot 10^{-2}$ mmol). The solution was treated with 1 bar of H₂ for 5 minutes after which phenylacetylene **6** (1.5 mmol, 480 mM) was added at room temperature maintaining the system stirring at 750 rpm under hydrogen atmosphere. The conversion was determined through GC analyses obtaining 94% conversion and 93% selectivity to the corresponding alkene after only 10 minutes. The catalytic experiment was repeated three times determining the conversion of **6** through

the average of the three results was used. All the hydrogenation products were identified by GC-MS and $^1\text{H-NMR}$ analysis.

The reaction was repeated decreasing the amount of catalyst and 1.6 mg Pd/C ($\text{Pd} = 1.5 \cdot 10^{-3}$ mmol) were introduced in the reactor obtaining 88% conversion and 97% selectivity to the corresponding alkene after 50 minutes. Therefore the amount of substrate was slightly increased to reduce the ratio between the catalyst and the substrate and 3.5 mmol of **6** (1,1 M) with 1.6 mg Pd/C ($1.5 \cdot 10^{-3}$ mmol). The substrate conversion over time was followed through 50 μL periodical sampling of the mixture. The samples were analysed by GC in order to determine the conversion degree. The catalytic experiment was repeated three times determining the benzaldehyde conversion through the average of the three results was used. Under these conditions 96% conversion and 95% selectivity to the corresponding alkene were achieved after 90 minutes.

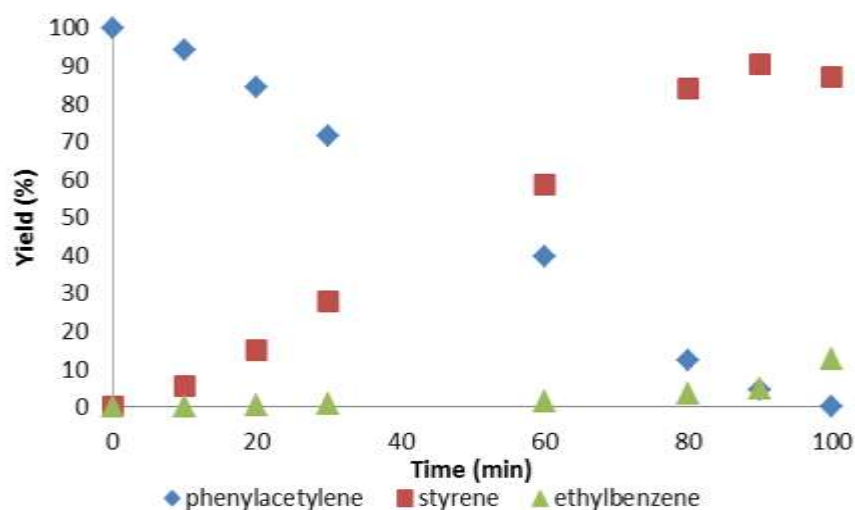


Figure 165. Percentage concentration of phenylacetylene **6**, styrene **7** and ethylbenzene **8** during the semi-hydrogenation reaction catalysed by Pd/C in THF. Reaction conditions: Pd = $1.5 \cdot 10^{-3}$ mmol; [**6**] = 1,1 M; $\text{pH}_2 = 1$ atm; room temperature, THF = 3 mL.

SEMI-HYDROGENATION OF PHENYLACETYLENE TO STYRENE IN AQUEOUS MICELLAR MEDIA

In the 25 mL flask containing the Pd-NPs ($\text{Pd} = 7.2 \cdot 10^{-3}$ mmol, 2.4 mM) in aqueous micellar medium with CTAB as surfactant phenylacetylene **6** (0.72 mmol, 240 mM) was added at room temperature maintaining the system stirring at 750 rpm under hydrogen atmosphere. The substrate conversion over time was followed through 25 μL periodical sampling of the mixture, extracting the aqueous micellar solution with 100 μL of ethyl acetate. The organic phase was then analysed by GC in order to determine the conversion degree. The catalytic experiment was repeated three times determining the conversion of **6** through the average of the three results was used. All the

hydrogenation products were identified by GC-MS and $^1\text{H-NMR}$ analysis. Under these conditions 93% conversion and 99% selectivity to the corresponding alkene were achieved after 80 minutes.

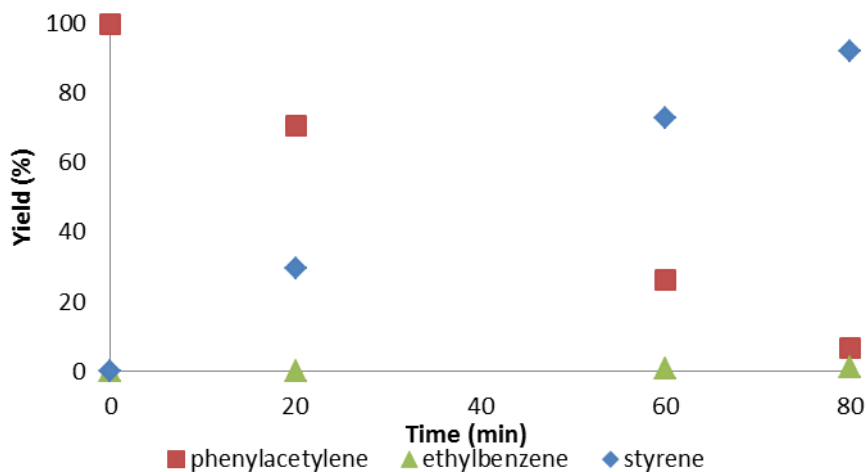


Figure 166. Percentage concentration of phenylacetylene **6**, styrene **7** and ethylbenzene **8** during the semi-hydrogenation reaction catalysed by Pd-NPs in water with CTAB. Reaction conditions: $[\text{Pd}] = 2.4 \text{ mM}$; $[\mathbf{6}] = 240 \text{ mM}$; $[\text{CTAB}] = 80 \text{ mM}$; $\text{pH}_2 = 1 \text{ atm}$; room temperature, water = 3 mL.

Experimental procedure as above reported for CTAB was employed in the presence of SDSU. Under these conditions 94% conversion and 97% selectivity to the corresponding alkene were achieved after 50 minutes.

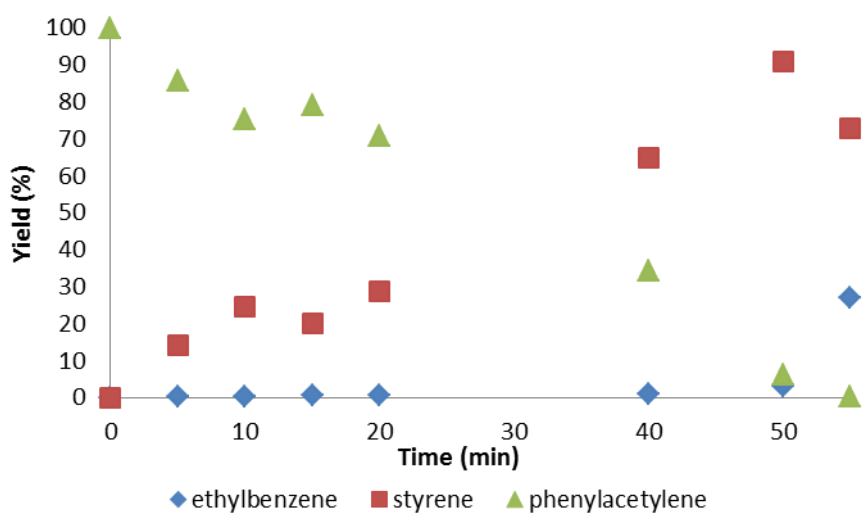


Figure 167. Percentage concentration of phenylacetylene **6**, styrene **7** and ethylbenzene **8** during the semi-hydrogenation reaction catalysed by Pd-NPs in water with CTAB. Reaction conditions: $[\text{Pd}] = 2.4 \text{ mM}$; $[\mathbf{6}] = 240 \text{ mM}$; $[\text{SDSU}] = 80 \text{ mM}$; $\text{pH}_2 = 1 \text{ atm}$; room temperature, water = 3 mL.

Experimental procedure as above reported for CTAB was employed in the presence of SDBS (100 mM). Under these conditions 96% conversion and 98% selectivity to the corresponding alkene were achieved after only 25 minutes. Therefore the reaction was repeated in the presence of 1.4 mmol of **6** in order to reduce the ratio between the catalyst and the substrate amounts.

The same procedure was applied further increasing the amount of **6** (2.1 mmol).

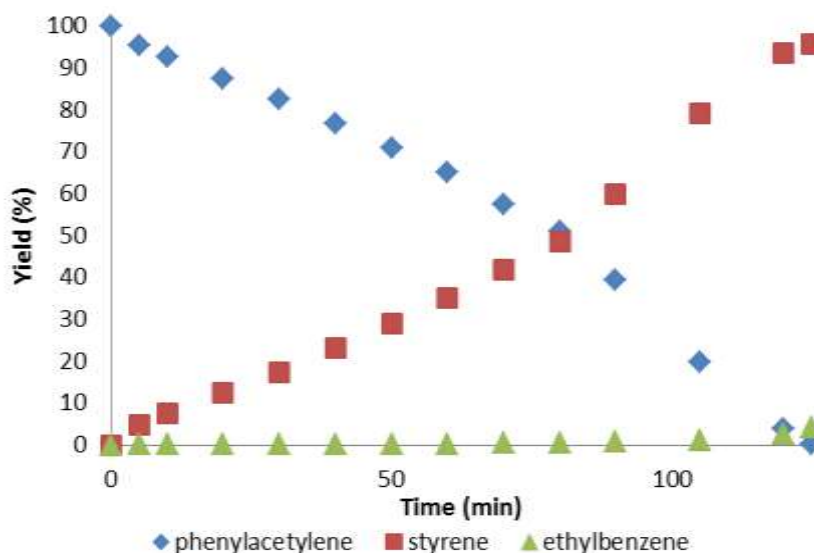


Figure 168. Percentage concentration of phenylacetylene **6**, styrene **7** and ethylbenzene **8** during the semi-hydrogenation reaction catalysed by Pd-NPs in water with SDBS. Reaction conditions: [Pd] = 2.4 mM; [**6**] = 700 mM; [SDBS] = 100 mM; p_{H_2} = 1 atm; room temperature, water = 3 mL.

SEMI-HYDROGENATION OF TERMINAL ALKYNES TO CORRESPONDING ALKENES IN THF

In a 25 mL flask equipped with magnetic stirrer were placed 3 mL of THF and 1.6 mg of Pd/C 10 wt.% (Pd = $1.5 \cdot 10^{-3}$ mmol). The solution was treated with 1 bar of H_2 for 5 minutes after which 4-ethynyl-toluene **9** (3.5 mmol, 1.1 M) was added at room temperature maintaining the system stirring at 750 rpm under hydrogen atmosphere. The substrate conversion over time was followed through 10 μ L periodical sampling of the mixture. The samples were analysed by GC in order to determine the conversion degree. The catalytic experiment was repeated three times determining the conversion of **9** through the average of the three results was used. All the hydrogenation products were identified by GC-MS and 1H -NMR analysis.

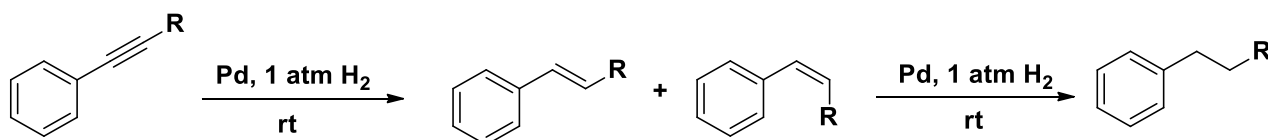
The same procedure was applied to the terminal alkynes **10-17**.

SEMI-HYDROGENATION OF TERMINAL ALKYNES TO CORRESPONDING ALKENES IN WATER WITH SDBS

In the 25 mL flask containing the Pd-NPs ($\text{Pd} = 7.2 \cdot 10^{-3}$ mmol, 2.4 mM) in aqueous micellar medium with SDBS as surfactant 4-ethynyl-toluene **9** (2.1 mmol, 720 mM) was added at room temperature maintaining the system stirring at 750 rpm under hydrogen atmosphere. The substrate conversion over time was followed through 25 μL periodical sampling of the mixture, extracting the aqueous micellar solution with 100 μL of ethyl acetate. The organic phase was then analysed by GC in order to determine the conversion degree. The catalytic experiment was repeated three times determining the conversion of **9** through the average of the three results was used. All the hydrogenation products were identified by GC-MS and ^1H -NMR analysis.

The same procedure was applied to the terminal alkynes **10-17**.

SEMI-HYDROGENATION OF INTERNAL ALKYNES TO CORRESPONDING ALKENES IN THF



Scheme 31. Semi-hydrogenation reaction of aromatic internal alkynes catalysed by Pd with H₂.

In a 25 mL flask equipped with magnetic stirrer were placed 3 mL of THF and 1.6 mg of Pd/C 10 wt.% ($\text{Pd} = 1.5 \cdot 10^{-3}$ mmol). The solution was treated with 1 bar of H₂ for 5 minutes after which the internal alkyne (3.5 mmol, 1.1 M) was added at room temperature maintaining the system strring at 750 rpm under hydrogen atmosphere. The substrate conversion over time was followed through 10 μL periodical sampling of the mixture. The samples were analysed by GC in order to determine the conversion degree and the Z:E ratio of the corresponding alkene. The catalytic experiment was repeated three times determining the conversion and Z:E ratio through the average of the three results was used. All the hydrogenation products were identified by GC-MS and ^1H -NMR analysis.

SEMI-HYDROGENATION OF INTERNAL ALKYNES TO CORRESPONDING ALKENES IN WATER WITH SDBS

In the 25 mL flask containing the Pd-NPs ($\text{Pd} = 7.2 \cdot 10^{-3}$ mmol, 2.4 mM) in aqueous micellar medium with SDBS as surfactant, the internal alkyne (2.1 mmol, 720 mM) was added at room temperature maintaining the system stirring at 750 rpm under hydrogen atmosphere. The substrate conversion over time was followed through 25 μL periodical sampling of the mixture, extracting the aqueous micellar solution with 100 μL of ethyl acetate. The organic phase was then analysed by GC in order to determine the conversion degree and the Z:E ratio of the corresponding alkene. The catalytic experiment was repeated three times determining the conversion and Z:E ratio through the average of the three results was used. All the hydrogenation products were identified by GC-MS analysis.

SEMI-HYDROGENATION PRODUCTS CHARACTERIZATION

- Styrene 7

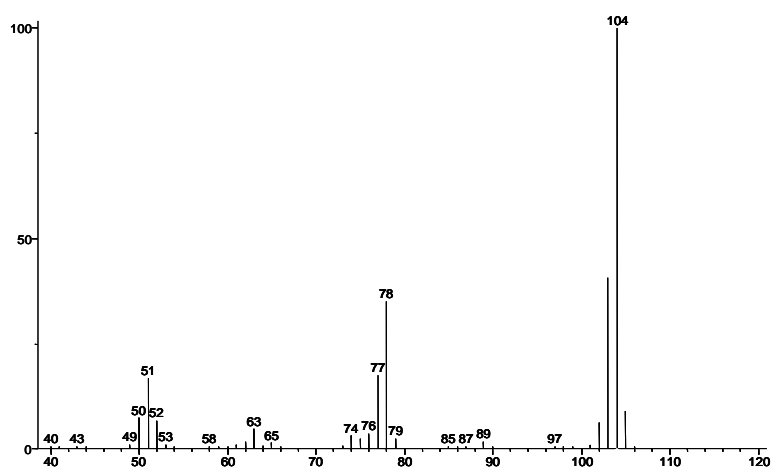
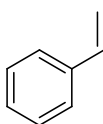


Figure 169. Mass spectrum of styrene 7

- **1-methyl-4-vinylbenzene**

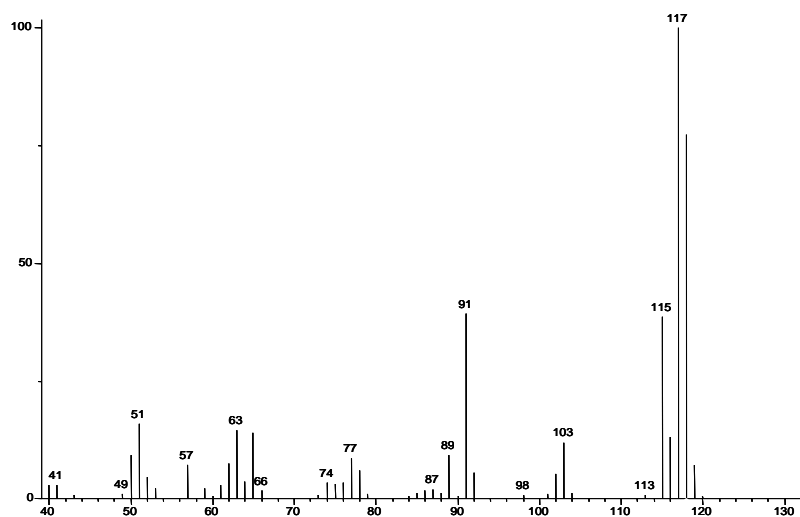
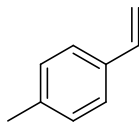


Figure 170. Mass spectrum of 1-methyl-4-vinylbenzene

- **1-pentyl-4-vinylbenzene**

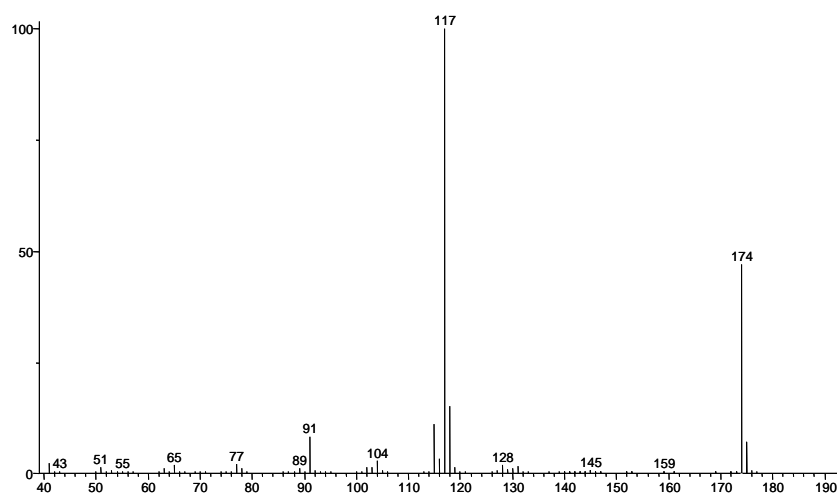
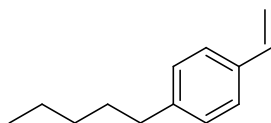


Figure 171. Mass spectrum of 1-pentyl-4-vinylbenzene

- **1-(tert-butyl)-4-vinylbenzene**

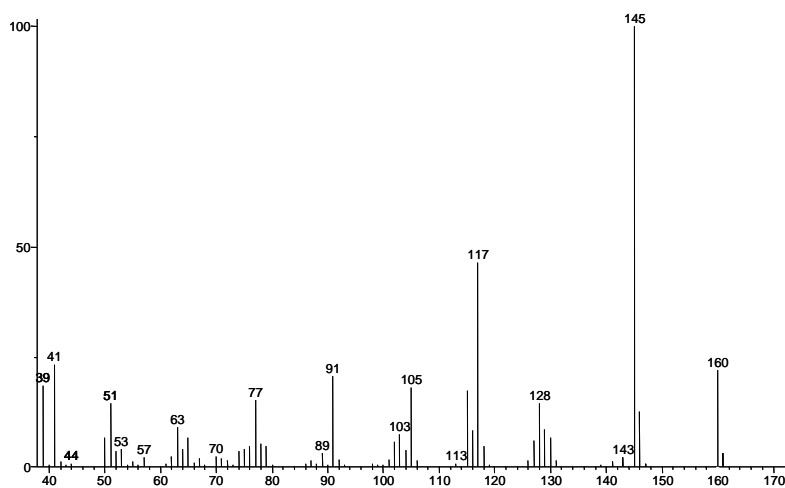
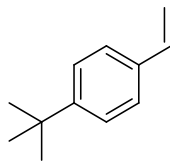


Figure 172. Mass spectrum of 1-(tert-butyl)-4-vinylbenzene

- **1-methoxy-4-vinylbenzene**

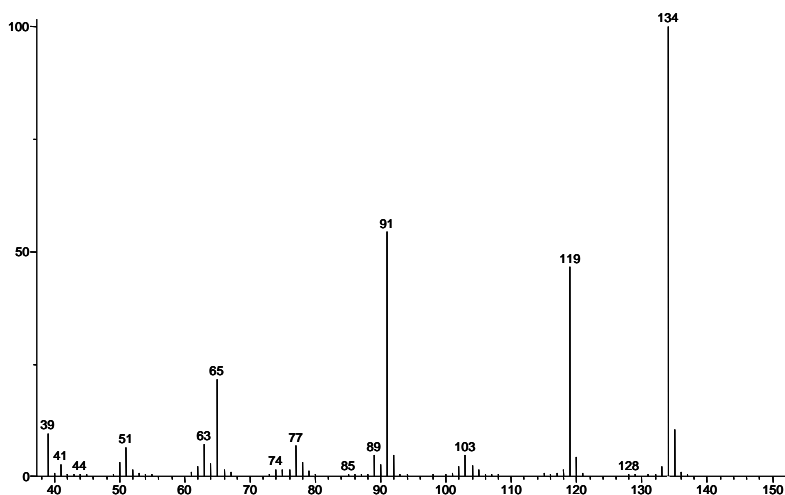
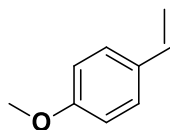


Figure 173. Mass spectrum of 1-methoxy-4-vinylbenzene

- **1-phenoxy-4-vinylbenzene**

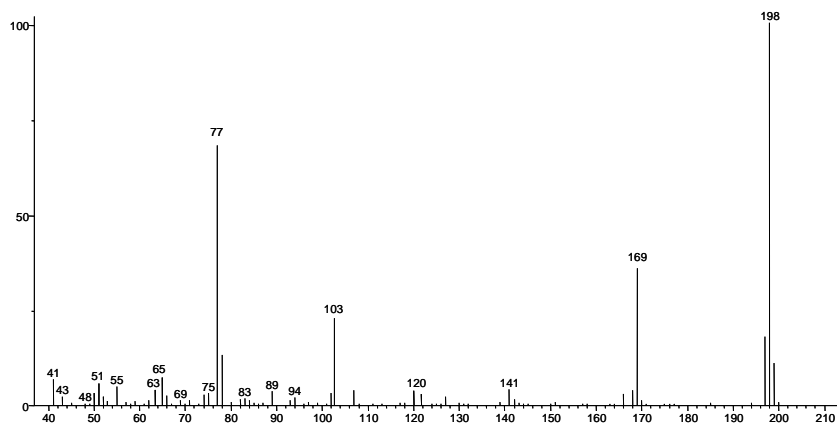
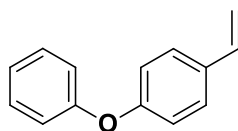


Figure 174. Mass spectrum of 1-phenoxy-4-vinylbenzene

- **1-decene**

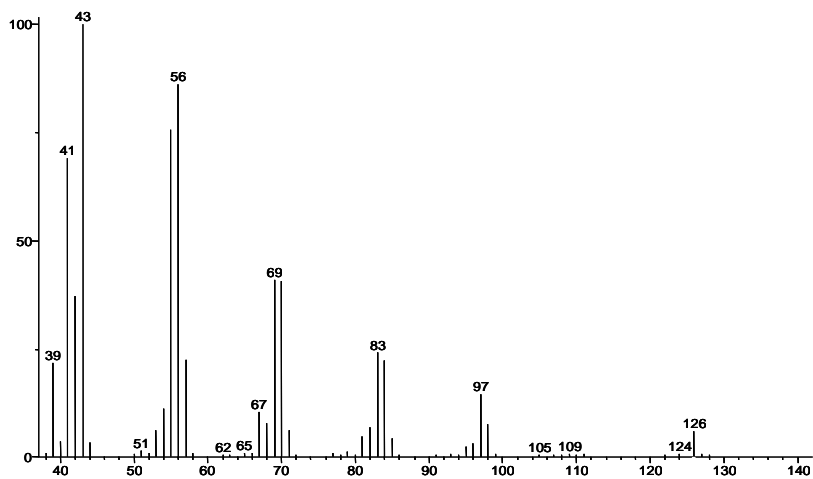
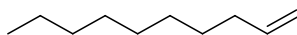


Figure 175. Mass spectrum of 1-decene

- **But-3-en-1-ylbenzene**

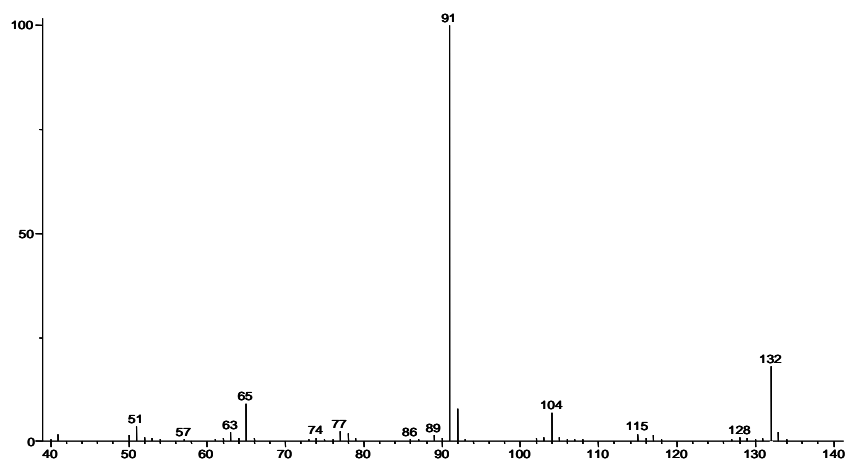
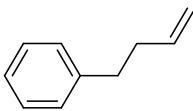


Figure 176. Mass spectrum of but-3-en-1-ylbenzene

- **Hex-5-en-1-ol**

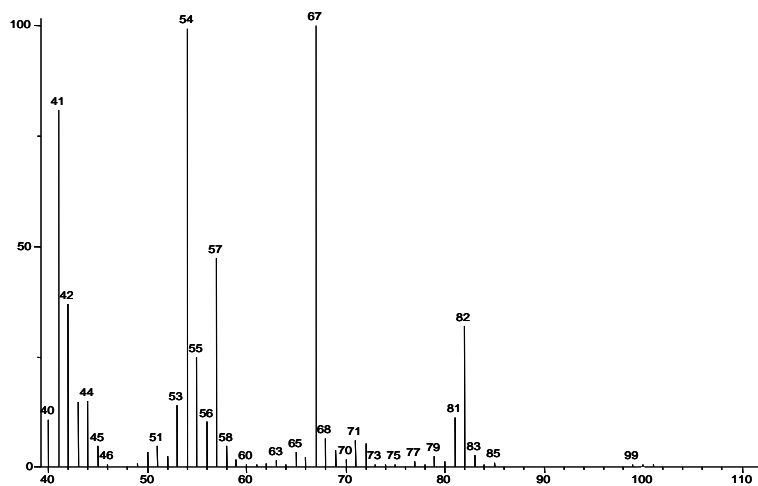
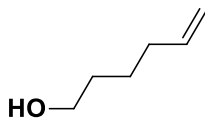


Figure 177. Mass spectrum of hex-5-en-1-ol

- dimethyl 2-allylmalonate

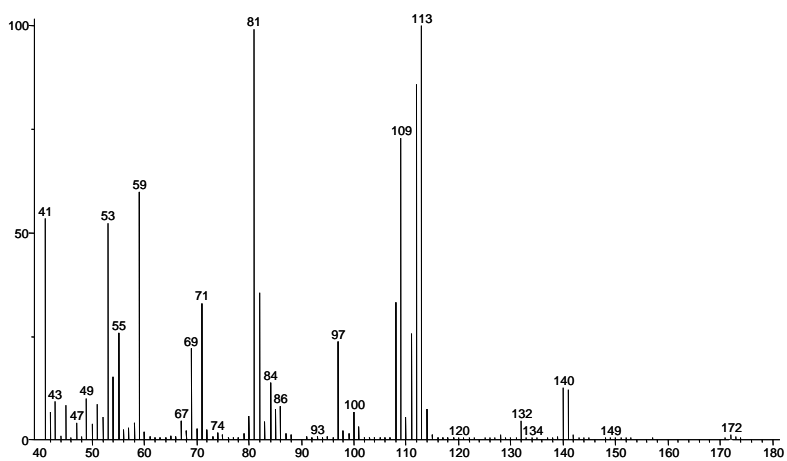
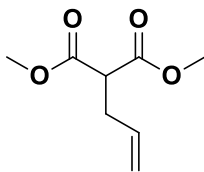


Figure 178. Mass spectrum of dimethyl 2-allylmalonate

- (E)-prop-1-en-1-ylbenzene and (Z)-prop-1-en-1-ylbenzene

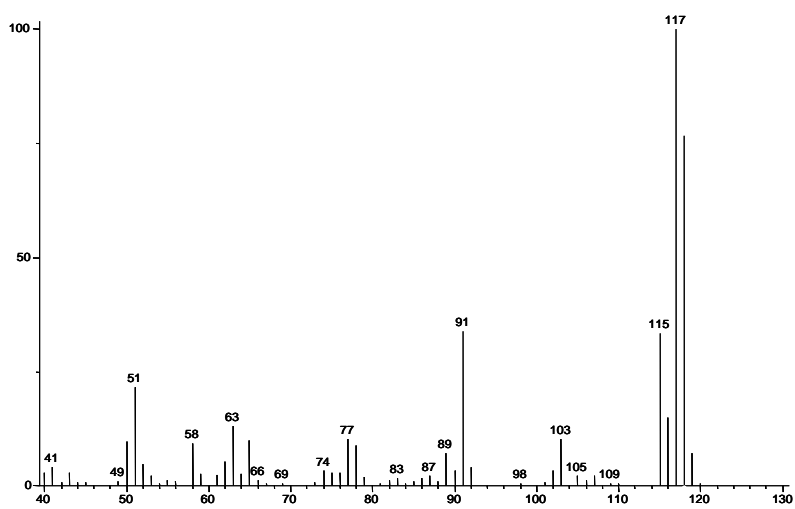
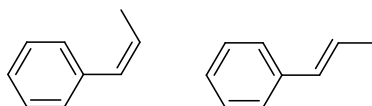


Figure 179. Mass spectrum of (E)-prop-1-en-1-ylbenzene and (Z)-prop-1-en-1-ylbenzene

- (E)-hex-1-en-1-ylbenzene and (Z)-hex-1-en-1-ylbenzene

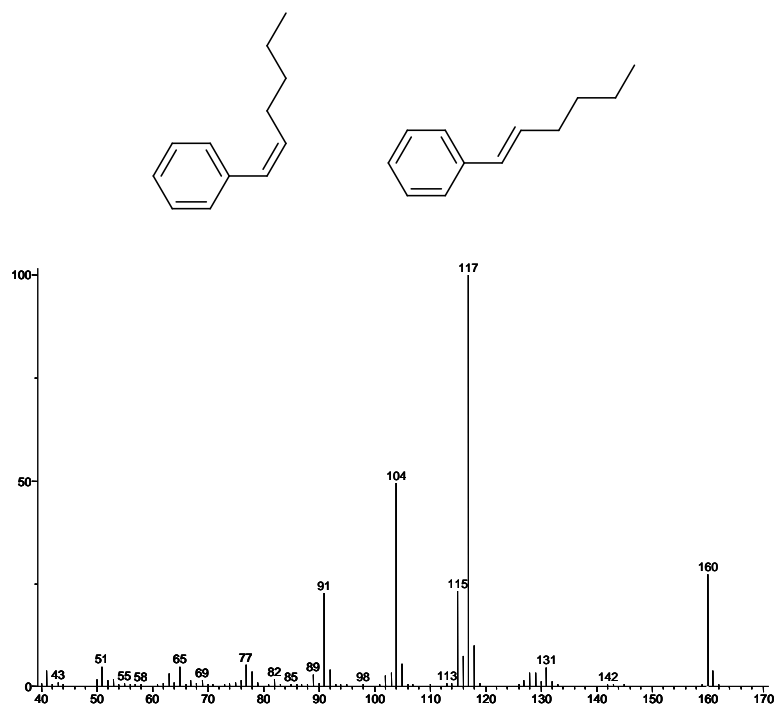
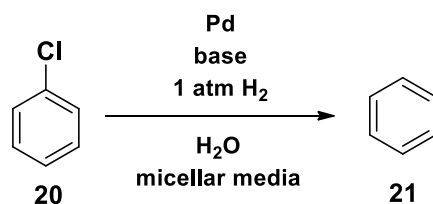


Figure 180. Mass spectrum of (E)-hex-1-en-1-ylbenzene and (Z)-hex-1-en-1-ylbenzene

HYDRODECHLORINATION OF CHLOROBENZENE IN WATER WITH SURFACTANTS



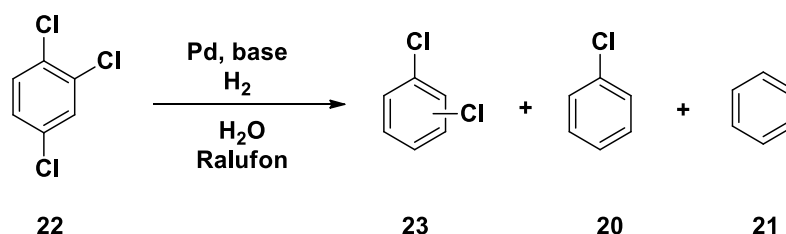
Scheme 32. Hydrodechlorination reaction of chlorobenzene **20** leading to benzene **21** catalysed by Pd in water with surfactant in the presence of a base under H₂ atmosphere.

In the 25 mL flask containing the Pd-NPs (Pd = $7.2 \cdot 10^{-3}$ mmol, 2.4 mM) in aqueous micellar medium with Ralufon[®] as surfactant chlorobenzene **20** (0,72 mmol, 240 mM) and sodium bicarbonate NaHCO₃ as base (0,72 mmol) were added at room temperature maintaining the system stirring at 750 rpm under hydrogen atmosphere. Under these condition a quantitative conversion of **20** to benzene **21** was observed in 18 hours. The reaction mixture was analysed by GC in order to determine the conversion of **20**. The reaction was repeated three times determining the conversion

of **20** through the average of the three results was used. All the hydrogenation products were identified by GC-MS and $^1\text{H-NMR}$ analysis.

Experimental procedure as above reported for Ralufon[®] was employed in the presence of SDSU, DOSS and SDBS as surfactant observing the precipitation of the catalyst.

HYDRODECHLORINATION OF CHLOROBENZENE IN WATER WITH SURFACTANTS (1 ATM H₂)



Scheme 33. Hydrodechlorination reaction of the 1,2,4-trichlorobenzene **22** leading to several possible products catalysed by Pd-NPs in water with Ralufon[®] in the presence of a base under H₂ atmosphere.

In the 25 mL flask containing the Pd-NPs ($\text{Pd} = 7.2 \cdot 10^{-3}$ mmol, 2.4 mM) in aqueous micellar medium with Ralufon[®] as surfactant 1,2,4-trichlorobenzene **22** (0,14 mmol, 47 mM) and sodium bicarbonate NaHCO₃ as base (0,84 mmol) were added at room temperature maintaining the system stirring at 750 rpm under hydrogen atmosphere. Under these condition a quantitative conversion of **22** to benzene **21** was observed in 24 hours. The reaction mixture was analysed by GC in order to determine the conversion of **22**. The reaction was repeated three times determining the conversion of **22** through the average of the three results was used. All the hydrogenation products were identified by GC-MS and $^1\text{H-NMR}$ analysis.

Experimental procedure as above reported was employed in all the reaction carried out under 1 atmosphere of H₂, changing from time to time the amounts of substrate **22** and NaHCO₃ in the reaction mixture. In the presence of K₂CO₃ (0.21 mmol) this base was introduced instead of NaHCO₃ under the same conditions.

HYDRODECHLORINATION OF CHLOROBENZENE IN WATER WITH SURFACTANTS (5 ATM H₂)

In a 20 mL reaction tube equipped with magnetic stirrer were added at room temperature the solution containing the Pd-NPs ($\text{Pd} = 7.2 \cdot 10^{-3}$ mmol, 2.4 mM) in aqueous micellar medium with Ralufon[®] as surfactant 1,2,4-trichlorobenzene **22** (0,36 mmol, 121 mM) and sodium bicarbonate NaHCO_3 (2.2 mmol) as base maintaining the system stirring at 750 rpm under inert atmosphere. The reaction tube was transferred in an autoclave that was loaded with 5 atm of H_2 . Under these condition a quantitative conversion of **22** to benzene **21** was observed in 24 hours. The reaction mixture was analysed by GC in order to determine the conversion of **22**. The reaction was repeated three times determining the conversion of **22** through the average of the three results was used. All the hydrogenation products were identified by GC-MS analysis.

HYDRODECHLORINATION PRODUCTS CHARACTERIZATION

- Dichlorobenzene **23**

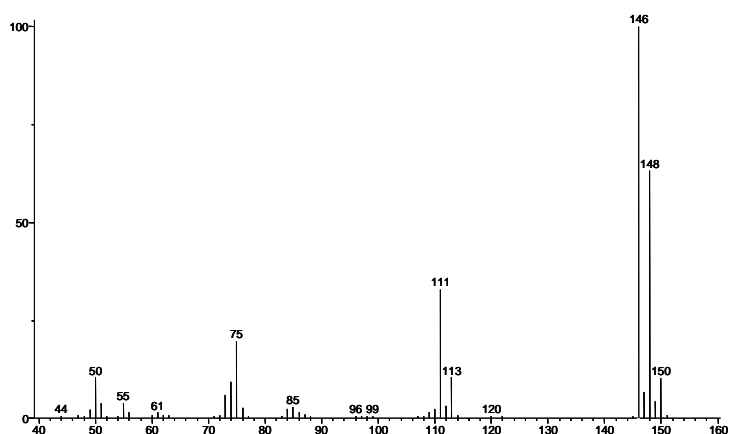
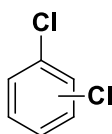
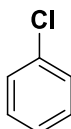


Figure 181. Mass spectrum of dichlorobenzene **23**

- Chlorobenzene **20**



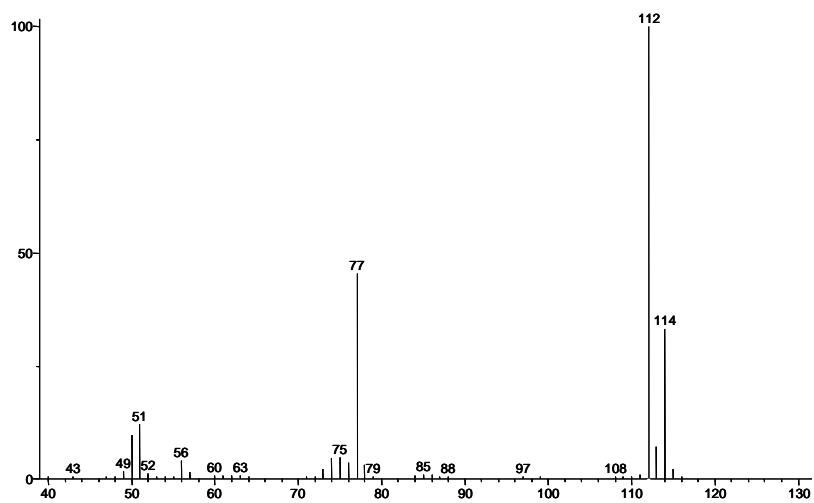


Figure 182. Mass spectrum of Chlorobenzene 20

- Benzene 21

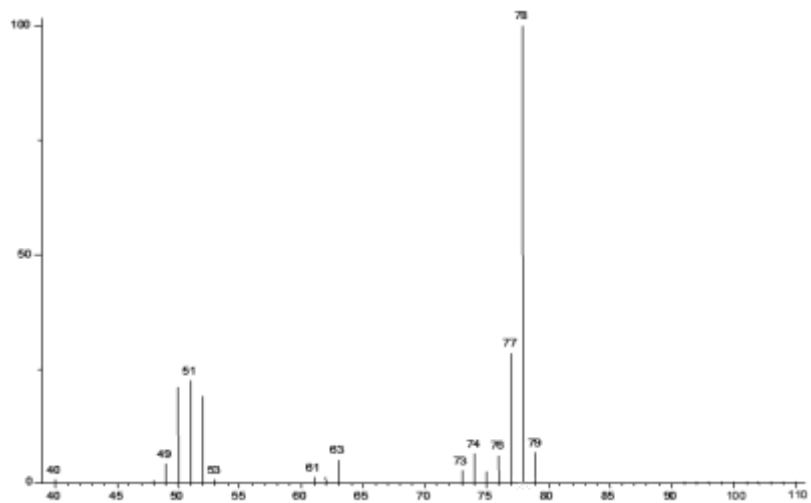
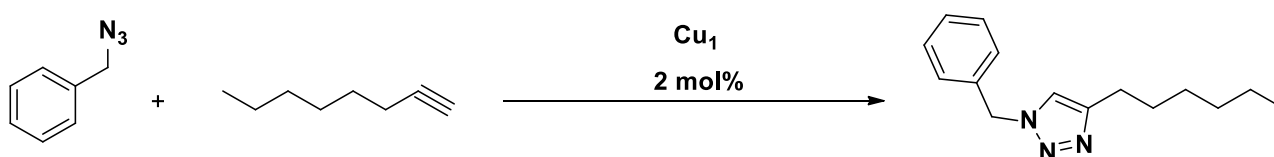


Figure 183, Mass spectrum of benzene 20.

7.2.8. Multi-component synthesis of 1,2,3-triazoles promoted by micelles

REACTION BETWEEN ORGANIC AZIDES AND ALKYNES



Scheme 34. Cycloaddition reactions between benzyl azide and 1-octyne to the corresponding 1,4- disubstituted 1,2,3-triazole catalysed by [Cu(IMes)Cl] **Cu₁**.

- **Organic media and water**

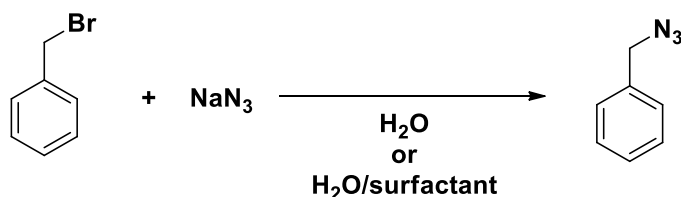
In a 3 mL vial equipped with a screw capped septum and magnetic stirrer benzyl bromide (0.25 mmol), 1-octyne (0.37 mmol) and the catalyst **Cu₁** ($2.5 \cdot 10^{-3}$ mmol) were dissolved in CH₂Cl₂ (1 mL). The reaction mixture was stirred at 750 rpm at room temperature for 1h. ¹H NMR and GC-MS analysis were employed to determine product yield.

Experimental procedure as above reported for CH₂Cl₂ was employed for CH₃OH and H₂O.

- **Micellar media**

In a 3 mL vial equipped with a screw capped septum and magnetic stirrer benzyl bromide (0.25 mmol), 1-octyne (0.37 mmol) and the catalyst **Cu₁** ($2.5 \cdot 10^{-3}$ mmol) were dissolved in water (1 mL) with the aid of the proper amount of surfactant (180 mM). The reaction mixture was stirred at 750 rpm at room temperature for 1h. Subsequently, 2 mL of AcOEt or Et₂O were added to the vial, the mixture was stirred for 10' and the organic phase was separated and concentrated under vacuum. ¹H NMR and GC-MS analysis were employed to determine product yield.

REACTION BETWEEN SODIUM AZIDE AND ORGANIC BROMIDES

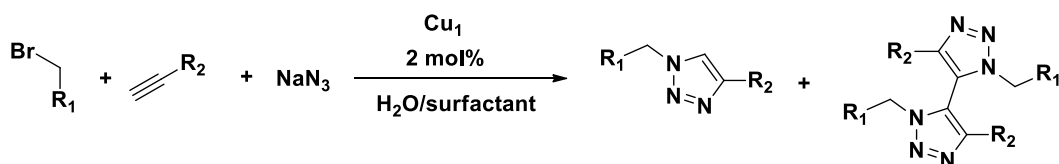


Scheme 35. Reaction between sodium azide and benzyl bromide to give the benzyl azide either in water or in different micellar media.

In a 3 mL vial equipped with a screw capped septum and magnetic stirrer benzyl bromide (0.25 mmol) and sodium azide (0.37 mmol) were dissolved in water (1 mL). The reaction mixture was stirred at 750 rpm at room temperature for 1h. Subsequently, 2 mL of AcOEt or Et₂O were added to the vial, the mixture was stirred for 10' and the organic phase was separated and concentrated under vacuum. ¹H NMR and GC-MS analysis were employed to determine product yield.

Experimental procedure as above reported for H₂O was employed in the presence of proper amount of each surfactant (180 mM).

DIRECT SYNTHESIS OF TRIAZOLE FROM SODIUM AZIDE, ORGANIC BROMIDES AND ALKYNES



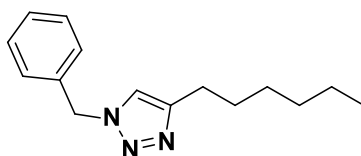
Scheme 36. Direct reaction between organic bromide, sodium azide and terminal alkynes catalysed by [Cu(IMes)Cl] Cu₁ to the corresponding triazole in different aqueous media

In a 3 mL vial equipped with a screw capped septum and magnetic stirrer the alkyl bromide (0.25 mmol), the alkyne (0.37 mmol) and sodium azide (0.37 mmol) were dissolved in water (1 mL) with the aid of the proper amount of surfactant (180 mM). The reaction mixture was stirred at 750

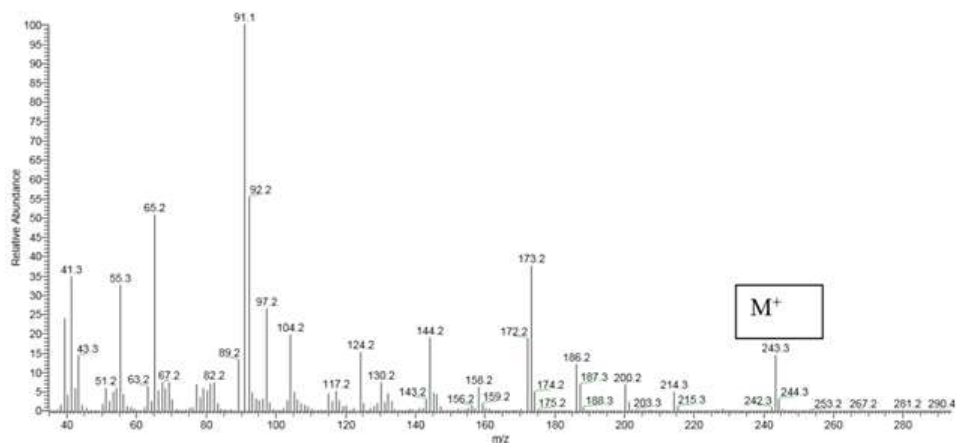
rpm at room temperature for 1h. A methanol solution of the catalyst **Cu₁** ($2.5 \cdot 10^{-3}$ mmol) was added to this solution and the vial was stirred at room temperature for 15, 30 minutes, 1h or 2h as a function of the substrates considered. Subsequently, 2 mL of AcOEt or Et₂O were added to the vial, the mixture was stirred for 10' and the organic phase was separated and concentrated under vacuum. ¹H NMR and GC-MS analysis were employed to determine product yield.

TRIAZOLES CHARACTERIZATIONS

- 1-benzyl-4-hexyl-1,2,3-triazole

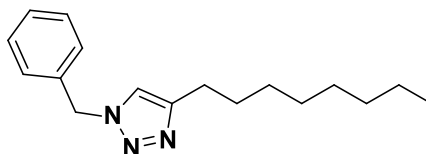


¹H NMR 300 MHz δ (ppm), 7.35 (m, 3H), 7.25 (m, 2H), 7.17 (s, 1H), 5.49 (s, 2H), 2.68 (t, J = 7.7 Hz, 2H), 1.63 (q, J = 7.4 Hz, 2H), 1.29 (m, 4H), 0.85 (t, J = 6.7 Hz, 3H).

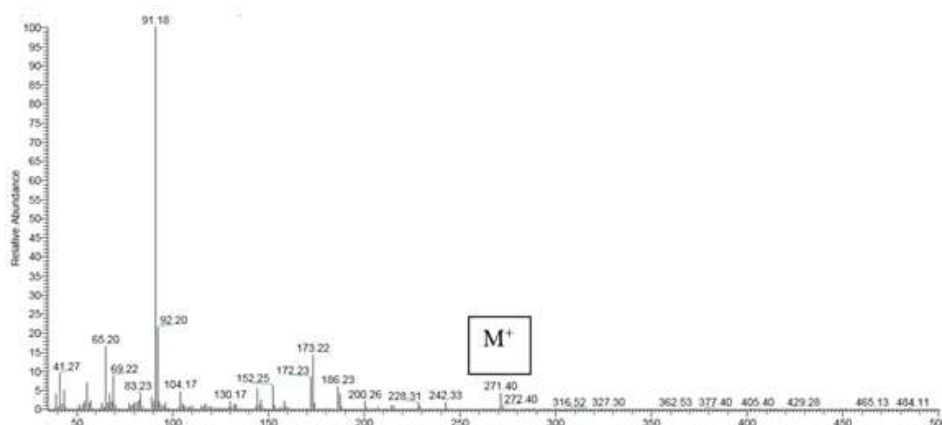


- Figure 184. Mass spectrum of 1-benzyl-4-hexyl-1,2,3-triazole

- 1-benzyl-4-octyl-1,2,3-triazole

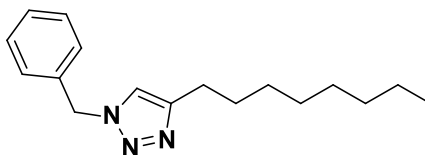


^1H NMR 300 MHz δ (ppm), 7.41-7.32 (m, 3H), 7.27-7.24 (m, 2H), 7.17 (s, 1H), 5.49 (s, 2H), 2.68 (t, $J = 7.7$ Hz, 2H), 1.62 (dd, $J = 14.3, 7.0$ Hz, 2H), 1.27 (m, 10 H), 0.87 (t, $J = 6.8$ Hz, 3H).



- **Figure 185.** Mass spectrum of 1-benzyl-4-octyl-1,2,3-triazole

- **1-benzyl-4-tridecyl-1,2,3-triazole**



^1H NMR 300 MHz δ (ppm), 7.43 – 7.28 (m, 3H), 7.23 (m, 2H), 7.17 (s, 1H), 5.49 (s, 2H), 2.72 – 2.62 (m, 2H), 1.71 – 1.57 (m, 2H) 1.26 (m, 20 H), 0.88 (t, $J = 6.6$ Hz, 3H).

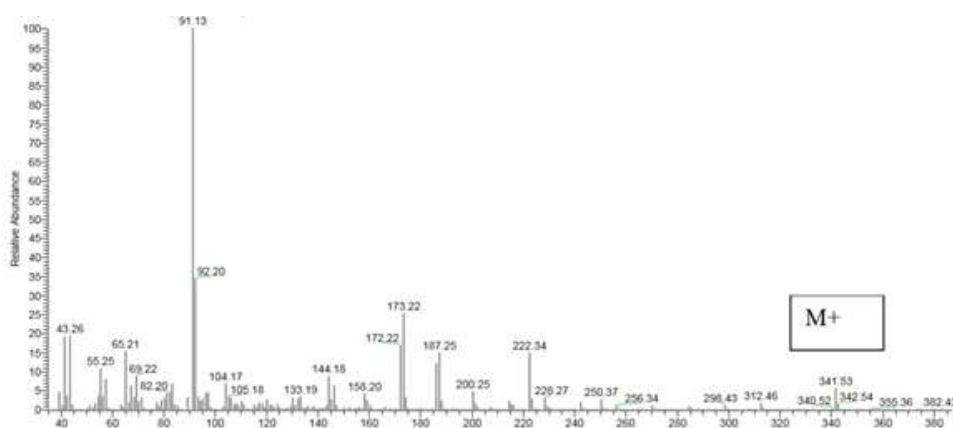
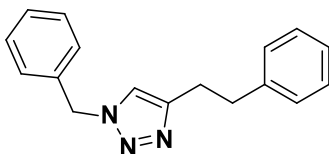
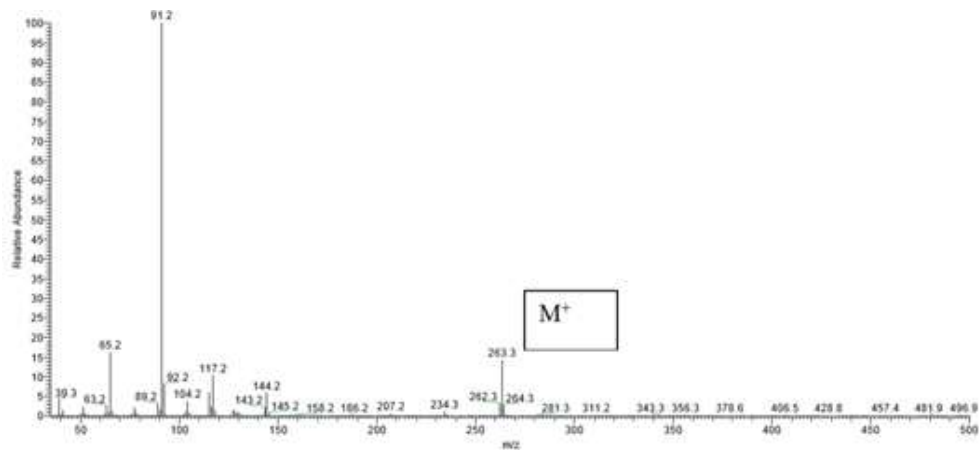


Figure 186. Mass spectrum of 1-benzyl-4-tridecyl-1,2,3-triazole

- 1-benzyl-4-phenyl-1,2,3-triazole

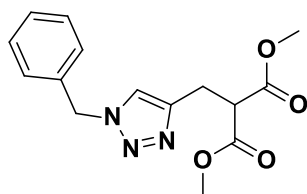


$^1\text{H NMR}$ 300 MHz δ (ppm), 7.40–7.10 (m, 10 H), 7.02 (s, 1 H), 5.47 (s, 2H), 3.01 (m, 4 H).



- **Figure 187.** Mass spectrum of 1-benzyl-4-phenyl-1,2,3-triazole

- 1-benzyl-1H-[1,2,3]triazolo-4-ylmethyl)-malonate dimethyl ester



$^1\text{H NMR}$ 300 MHz δ (ppm), 7.41 – 7.15 (m, 6H), 5.48 (s, 2H), 3.89 (t, $J = 7.5$ Hz, 1H), 3.69 (s, 6H), 3.29 (d, $J = 7.5$ Hz, 2H).

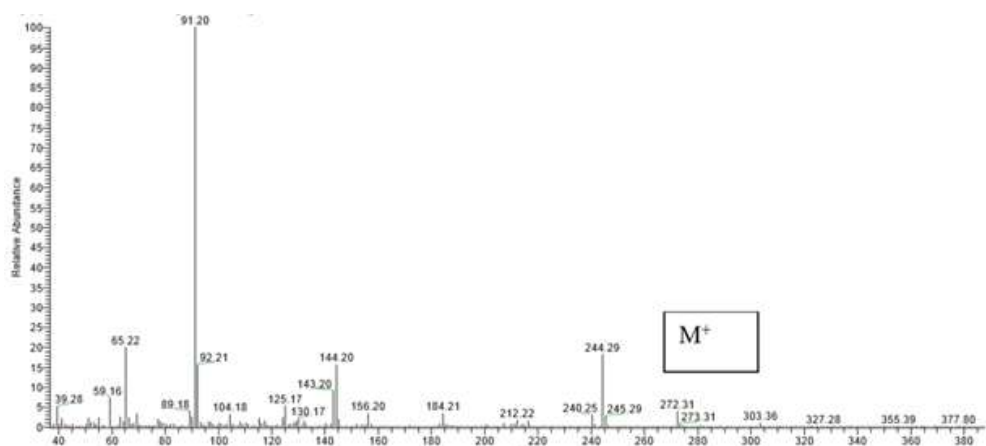
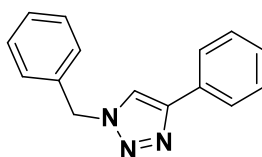


Figure 188. Mass spectrum of 1-benzyl-1H-[1,2,3]triazolo-4-ylmethyl)-malonate dimethyl ester

- 1-benzyl-4-phenyl-1,2,3-triazole



$^1\text{H NMR}$ 300 MHz δ (ppm), 7.81-7.83 (d, 2H); 7.69 (s, 1H), 7.29-7.42 (m, 8H), 5.60 (s, 2H).

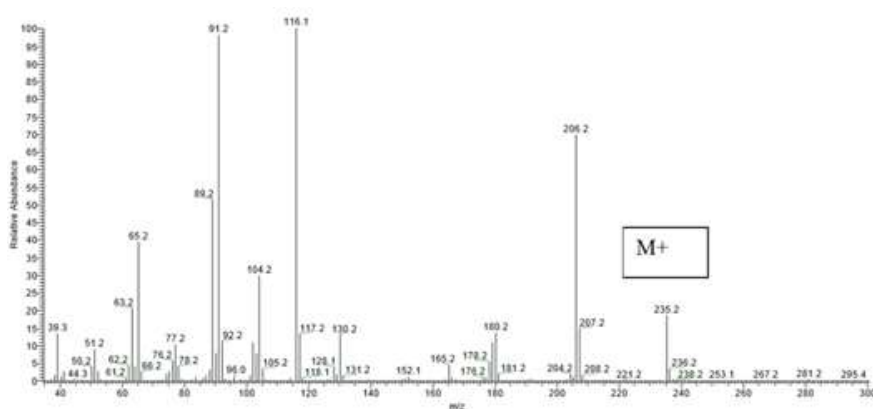
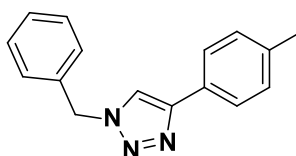


Figure 189. Mass spectrum of 1-benzyl-4-phenyl-1,2,3-triazole

- 1-benzyl-4-p-tolyl-1,2,3-triazole



^1H NMR 300 MHz δ (ppm), 7.69 (d, J = 8.0 Hz, 2H), 7.62 (s, 1H), 7.43 – 7.28 (m, 5H), 7.21 (d, J = 8.0 Hz, 2H), 5.57 (s, 2H), 2.33 (s, 3H).

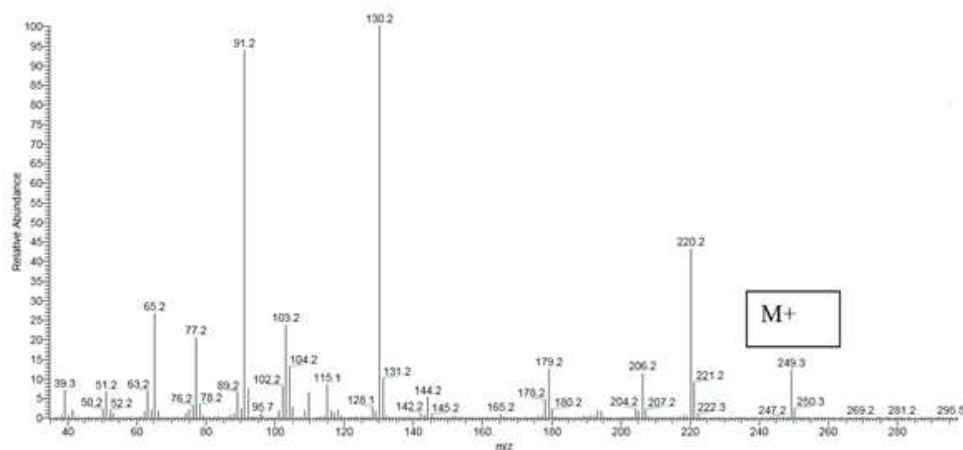
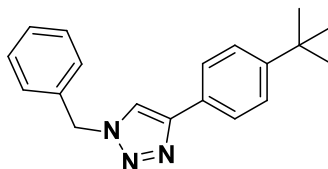


Figure 190. Mass spectrum of 1-benzyl-4-p-tolyl-1,2,3-triazole

- **1-benzyl-4-(4-(tert-butyl)phenyl)-1,2,3-triazole**



^1H NMR 300 MHz δ (ppm), 7.69 (d, J = 7.8 Hz, 2H), 7.63 (s, 1H), 7.42 – 7.20 (m, 7H), 5.51 (s, 2H), 1.32 (s, 9H).

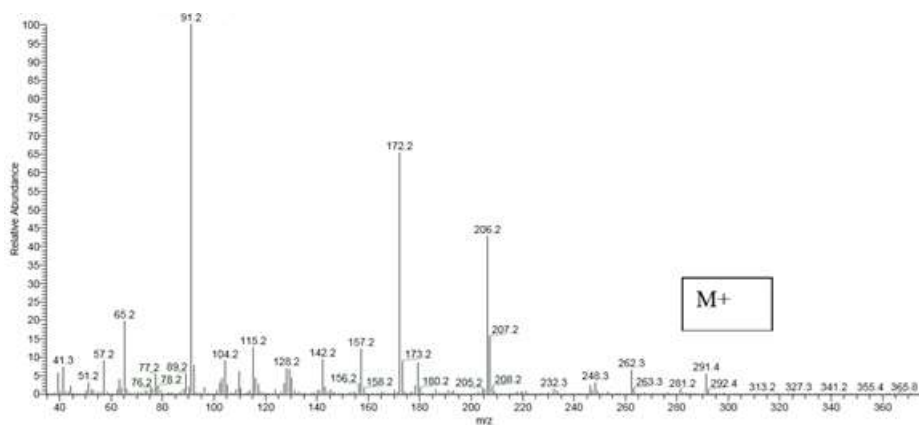
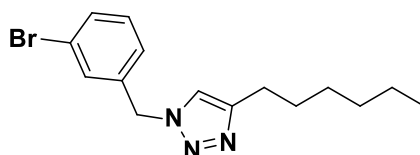


Figure 191. Mass spectrum of 1-benzyl-4-(4-(tert-butyl)phenyl)-1,2,3-triazole

- 1-(3-bromobenzyl)-4-hexyl-1,2,3-triazole



$^1\text{H NMR}$ 300 MHz δ (ppm), 7.50 -7.15 (m, 5H), 5.46 (s, 2H), 2.69 (t, $J = 7.7$ Hz, 2H), 1.76 – 1.55 (m, 2H), 1.43 – 1.17 (m, 6H), 0.87 (t, $J = 6.6$ Hz, 3H).

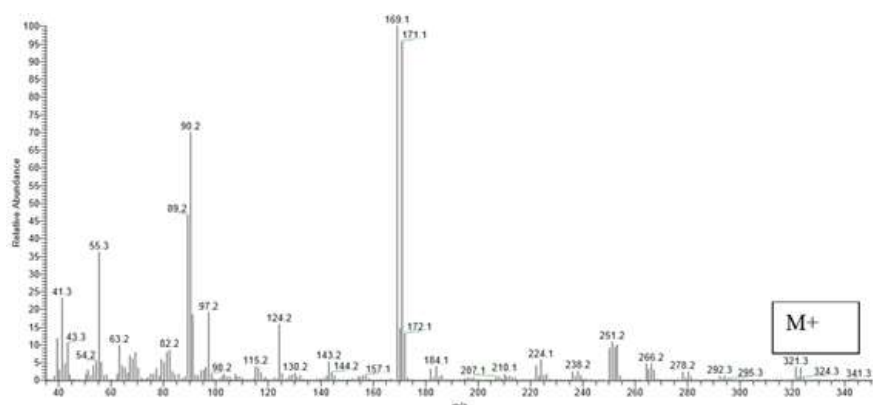
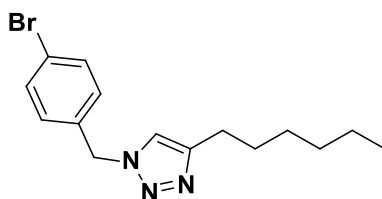


Figure 192. Mass spectrum of 1-(3-bromobenzyl)-4-hexyl-1,2,3-triazole

- 1-(4-bromobenzyl)-4-hexyl-1,2,3-triazole



$^1\text{H NMR}$ 300 MHz δ (ppm), 7.50 -7.15 (m, 5H), 5.44 (s, 2H), 2.68 (t, $J = 7.7$ Hz, 2H), 1.62 (bs, 2H), 1.29 (M 6H), 0.85 (T, $J = 6.8$ Hz, 3H).

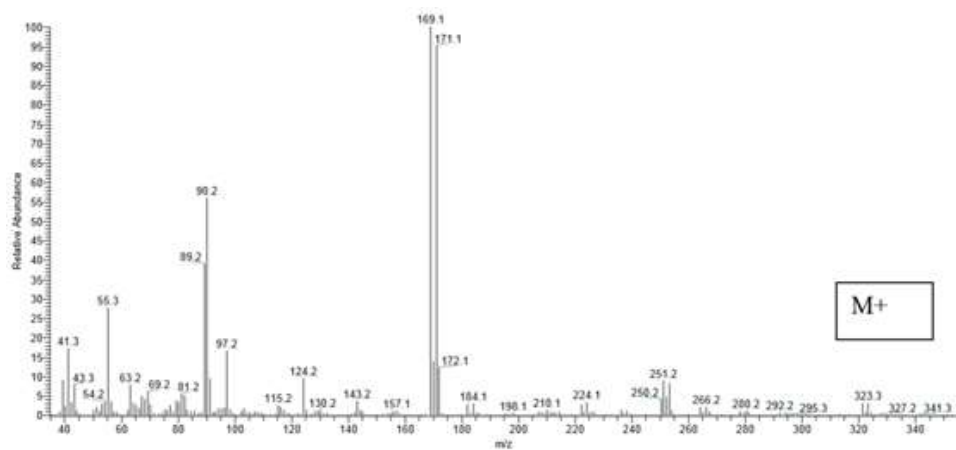
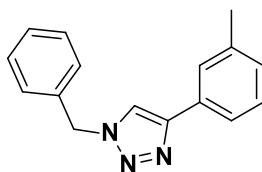


Figure 193. Mass spectrum of 1-(4-bromobenzyl)-4-hexyl-1,2,3-triazole

- 1-benzyl-4-(m-tolyl)-1H-1,2,3-triazole



^1H NMR 300 MHz δ (ppm) 7.69 – 7.53 (m, 3H), 7.65 (s, 1H), 7.27 – 7.08 (m, 6H), 5.57 (s, 2H), 2.38 (s, 3H).

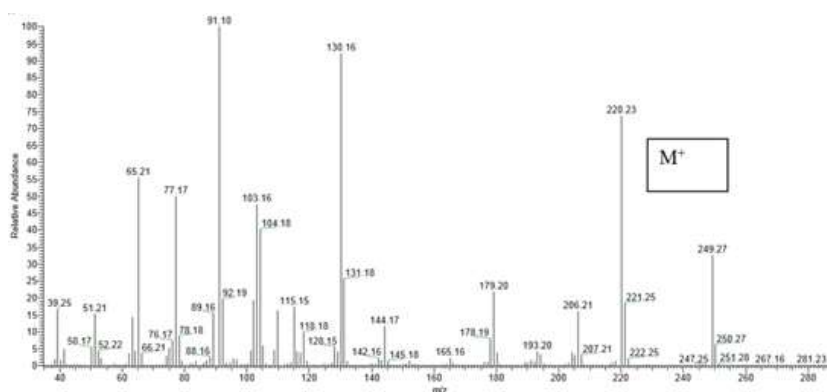
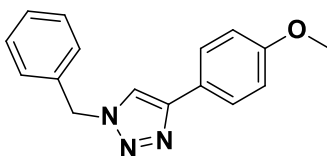


Figure 194. Mass spectrum of 1-benzyl-4-(m-tolyl)-1H-1,2,3-triazole

- 1-benzyl-4-(4-methoxyphenyl)-1,2,3-triazole



^1H NMR 300 MHz δ (ppm) 7.72 (d, $J = 8.5$ Hz, 2H), 7.57 (s, 1H), 7.46 – 7.27 (m, 5H), 6.93 (d, $J = 8.5$ Hz, 2H), 5.56 (s, 2H), 3.83 (s, 3H).

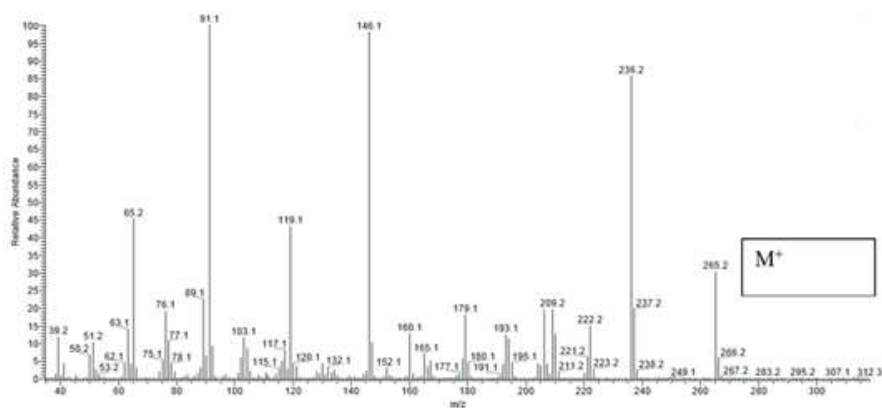
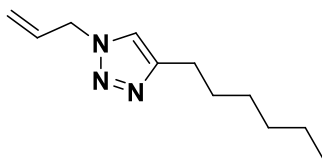


Figure 195. Mass spectrum of 1-benzyl-4-(4-methoxyphenyl)-1,2,3-triazole

- **1-allyl-4-hexyl-1,2,3-triazole**



^1H NMR 300 MHz δ (ppm), 7.26 (s, 1H), 6.00 (ddt, $J = 16.3, 10.3, 6.1$ Hz, 1H), 5.30 (m, 2H), 4.93 (dd, $J = 6.1, 1.1$ Hz, 1H), 2.70 (t, $J = 7.7$ Hz, 2H), 1.65 (dt, $J = 15.2, 7.5$ Hz, 2H), 1.30 (m, 6H), 0.87 (t, $J = 6.5$ Hz, 3H).

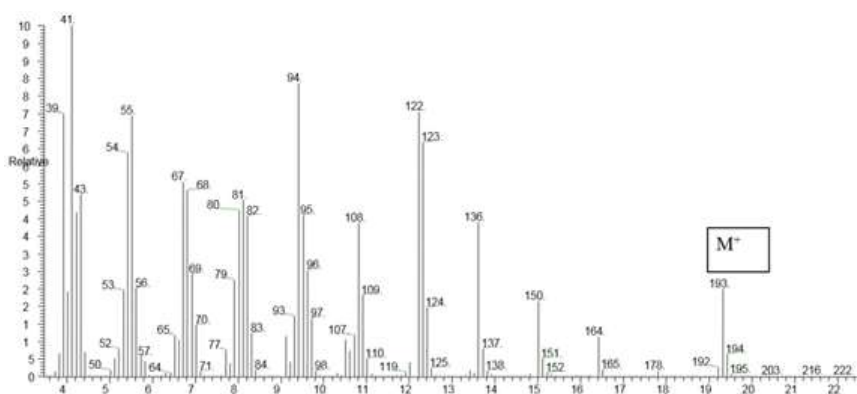
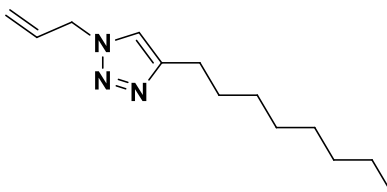


Figure 196. Mass spectrum of 1-allyl-4-hexyl-1,2,3-triazole

- **1-allyl-4-octyl-1,2,3-triazole**



^1H NMR 300 MHz δ (ppm), 7.26 (s, 1H), 6.00 (ddt, $J = 16.7, 10.8, 6.0$ Hz, 1H), 5.29 (m, 2H), 4.93 (dd, $J = 6.1, 1.0$ Hz, 2H), 2.69 (t, $J = 7.7$ Hz, 2H), 1.63 (m, 2H), 1.23 (m, 10H), 0.86 (t, $J = 6.4$ Hz, 3H).

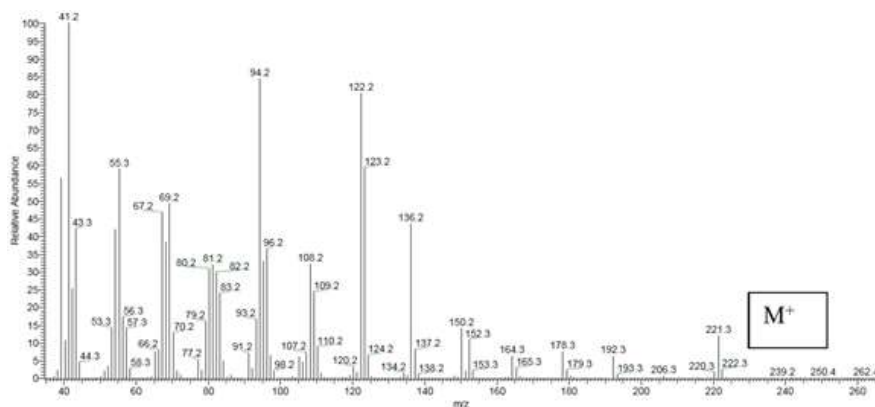
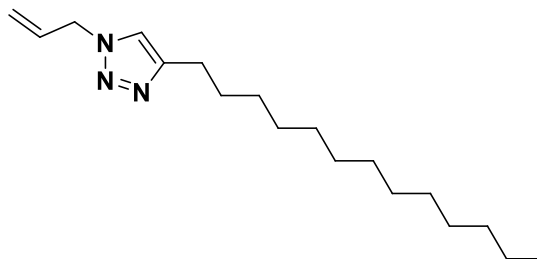


Figure 197. Mass spectrum of 1-allyl-4-octyl-1,2,3-triazole

- 1-allyl-4-tridecyl-1,2,3-triazole



^1H NMR 300 MHz δ (ppm), 7.26 (s, 1H), 6.00 (ddt, $J = 16.7, 10.8, 6.0$ Hz, 1H), 5.36 – 5.20 (m, 2H), 4.92 (dd, $J = 6.1, 1.0$ Hz, 2H), 2.69 (t, $J = 7.7$ Hz, 2H), 1.63 (m, 2H), 1.24 (s, 20H), 0.86 (t, $J = 6.5$ Hz, 3H).

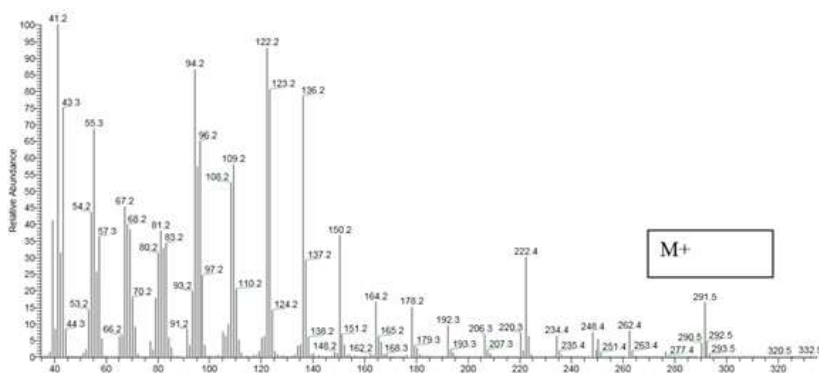
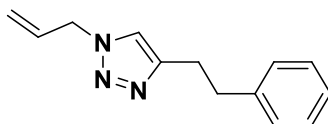


Figure 198. Mass spectrum of 1-allyl-4-tridecyl-1,2,3-triazole

- 1-allyl-4-phenethyl-1,2,3-triazole



^1H NMR 300 MHz δ (ppm), 7.32 – 7.15 (m, 5H), 7.13 (s, 1H), 5.97 (ddt, $J = 16.3, 10.2, 6.0$ Hz, 1H), 5.26 (ddd, $J = 17.9, 13.6, 1.1$ Hz, 2H), 4.91 (dt, $J = 6.0, 1.1$ Hz, 2H), 3.09 – 2.94 (m, 4H).

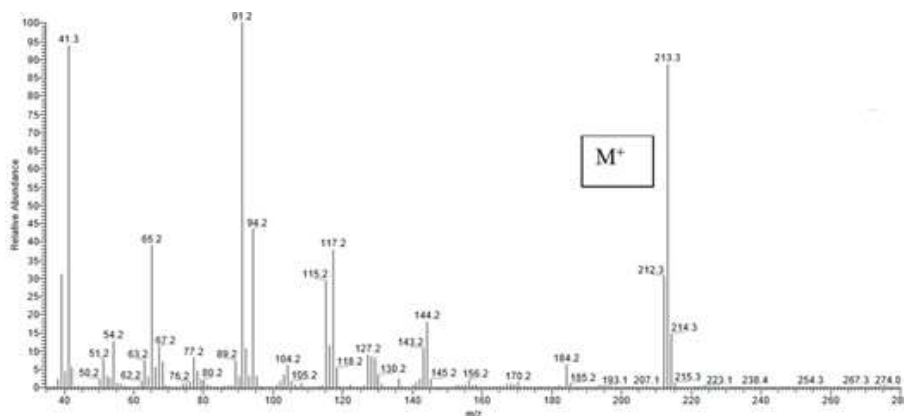
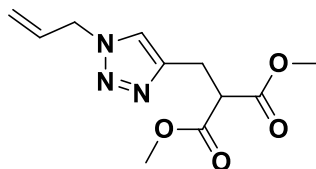


Figure 199. Mass spectrum of 1-allyl-4-phenethyl-1,2,3-triazole

- Dimethyl-2-((1-allyl-1H-1,2,3-triazo-4-yl)methyl)malonate



^1H NMR 300 MHz δ (ppm), 7.37 (s, 1H), 5.98 (ddt, $J = 16.3, 10.3, 6.1$ Hz, 1H), 5.41 – 5.19 (m, 2H), 4.91 (d, $J = 6.1$ Hz, 2H), 3.89 (t, $J = 7.4$ Hz, 1H), 3.72 (s, 6H), 3.30 (d, $J = 7.4$ Hz, 2H).

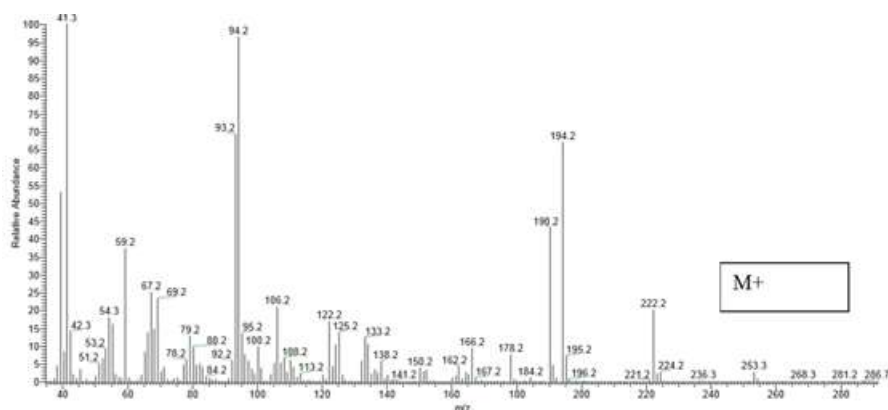
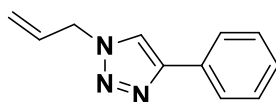


Figure 200. Mass spectrum of Dimethyl-2-((1-allyl-1H-1,2,3-triazo-4-yl)methyl)malonate

- 1-Allyl-4-phenyl-1,2,3-triazole



^1H NMR 300 MHz δ (ppm), 7.76 (s, 1H), 7.52 – 7.46 (m, 2H), 7.36 – 7.29 (m, 3H), 6.06 (ddd, $J = 16.4, 10.4, 5.8$ Hz, 1H), 5.41 – 5.30 (m, 2H), 5.03 (d, $J = 6.1$ Hz, 2H).

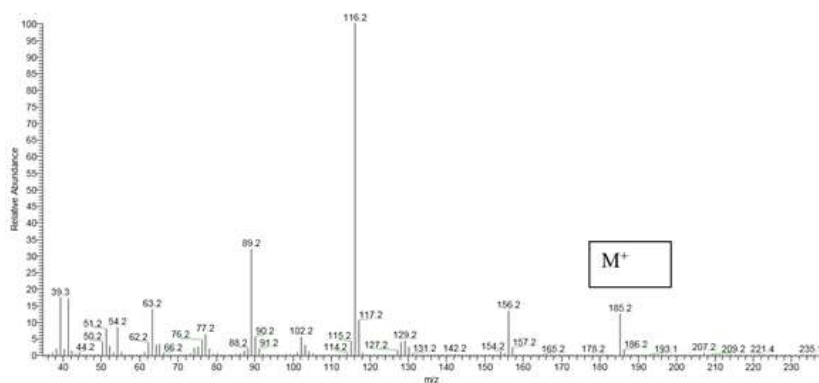
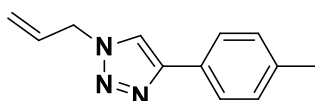


Figure 201. Mass spectrum of 1-Allyl-4-phenyl-1,2,3-triazole

- **4-(p-tolyl)-1-allyl-1,2,3-triazole**



^1H NMR 300 MHz δ (ppm), 7.72 (d, $J = 8.2$ Hz, 2H), 7.71 (s, 1H), 7.23 (d, $J = 8.2$ Hz, 2H), 6.06 (ddt, $J = 16.6, 10.4, 6.1$ Hz, 1H), 5.41 – 5.29 (m, 2H), 5.01 (d, $J = 6.1$ Hz, 2H), 2.37 (d, $J = 4.2$ Hz, 2H).

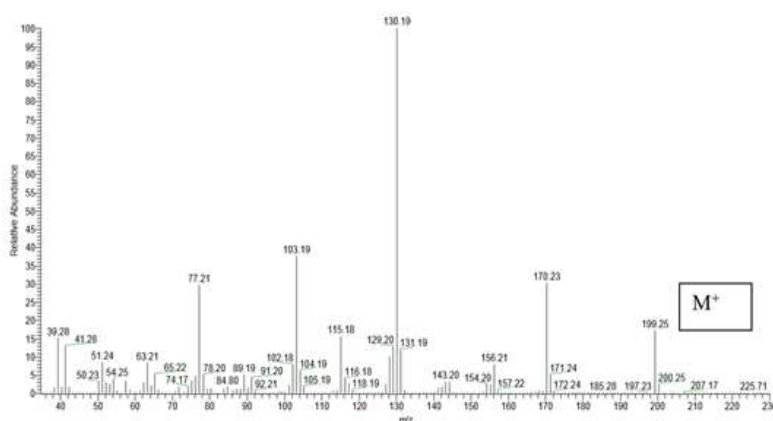
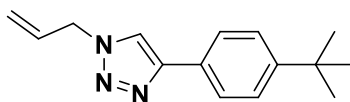


Figure 202. Mass spectrum of 4-(p-tolyl)-1-allyl-1,2,3-triazole

- **4-(t-butyl-phenyl)-1-allyl-1,2,3-triazole**



$^1\text{H NMR}$ 300 MHz δ (ppm), 7.76 (d, $J = 8.3$ Hz, 2H), 7.73 (s, 1H), 7.30-7.40 (m, 2H), 6.06 (ddt, $J = 16.4, 10.3, 6.1$ Hz, 1H), 5.33 (m, 2H), 5.01 (d, $J = 6.1$ Hz, 1H), 1.35 (s, 9H).

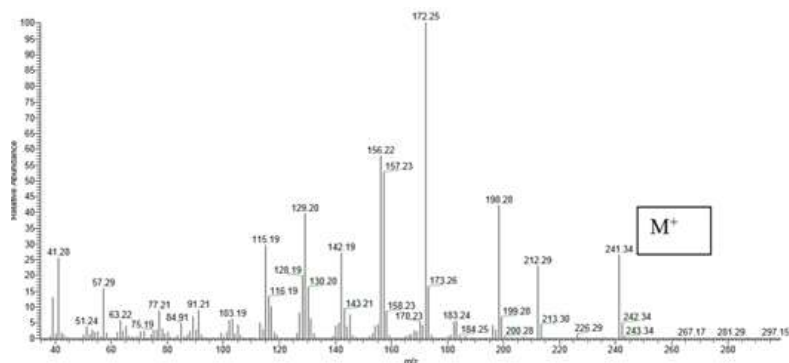
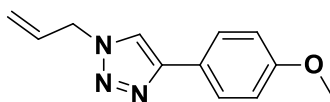


Figure 203. Mass spectrum of 4-(t-butyl-phenyl)-1-allyl-1,2,3-triazole

- **1-allyl-4-(4-methoxyphenyl)-1,2,3-triazole**



$^1\text{H NMR}$ 300 MHz δ (ppm) 7.74 (d, $J = 8.9$ Hz, 2H), 7.67 (s, 1H), 6.95 (d, $J = 8.9$ Hz, 2H), 6.14 – 5.95 (m, 1H), 5.42 – 5.28 (m, 2H), 5.00 (dt, $J = 6.1, 1.4$ Hz, 1H), 3.83 (s, 3H).

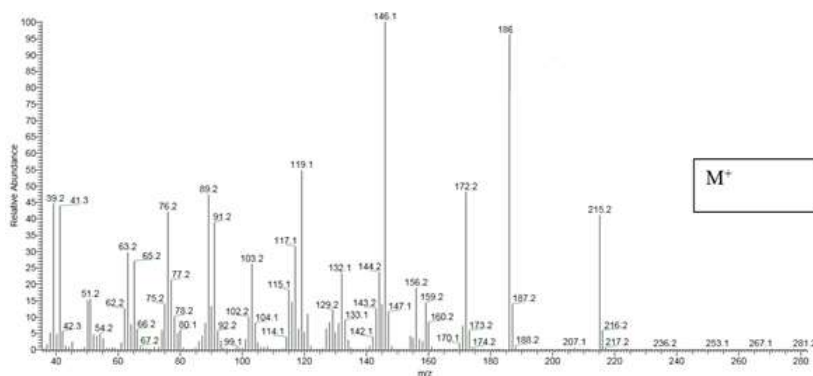
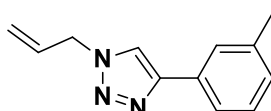


Figure 204. Mass spectrum of 1-allyl-4-(4-methoxyphenyl)-1,2,3-triazole

- **1-allyl-4-(m-tolyl)-1,2,3-triazole**



^1H NMR 300 MHz δ (ppm) 7.74 (s, 1H), 7.72 – 7.53 (m, 2H), 7.34 – 7.09 (m, 2H), 6.14 – 5.94 (m, 1H), 5.42 – 5.25 (m, 2H), 5.05 – 4.93 (m, 2H), 2.39 (s, 3H).

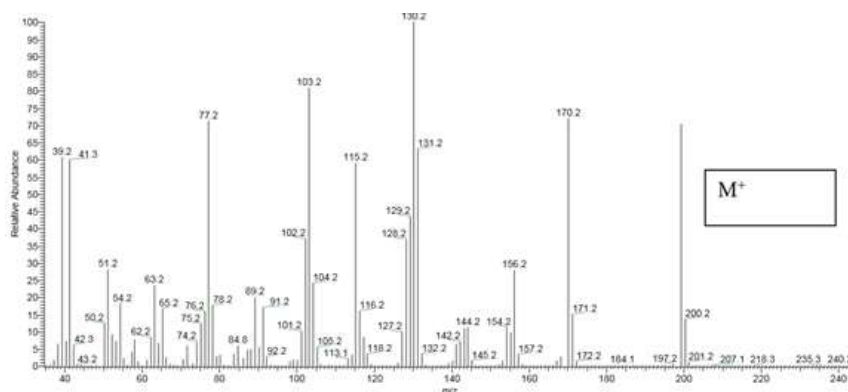


Figure 205. Mass spectrum of 1-allyl-4-(m-tolyl)-1,2,3-triazole

7.2.9. Substrate selective amide coupling

EXPERIMENTAL CONDITIONS

Water saturated solvent was prepared by shaking chloroform-d with bidistilled water at room temperature in a separation funnel. Resorcin[4]arene (6.6 equivalents, 81.4 mM) was placed in a screw-capped vial equipped with silicone septum and dissolved in the water saturated chloroform-d (1 mL) stirring at 750 rpm for few minutes. To this solution, 1-ethyl-3-(3-dimethylaminopropyl) carbodiimide hydrochloride (**EDAPC**) (1 equivalent, 13.2 mM) was added, followed after few minutes stirring, by octane, decane, dodecane, tetradecane, or docosane as GC-MS standard (3.3 mM), a series of carboxylic acids (0.5 equivalents each, 6.7 mM) and a series of amines (0.5 equivalents each, 6.7 mM). The reaction was then left at 60°C under vigorous stirring for 2 days and the reaction progress was monitored by GC-MS analysis by periodically sampling directly from the reaction mixtures. Conversion, product assignment and distribution were determined by direct GC-MS analysis of the reaction mixture as the average of three experiments.

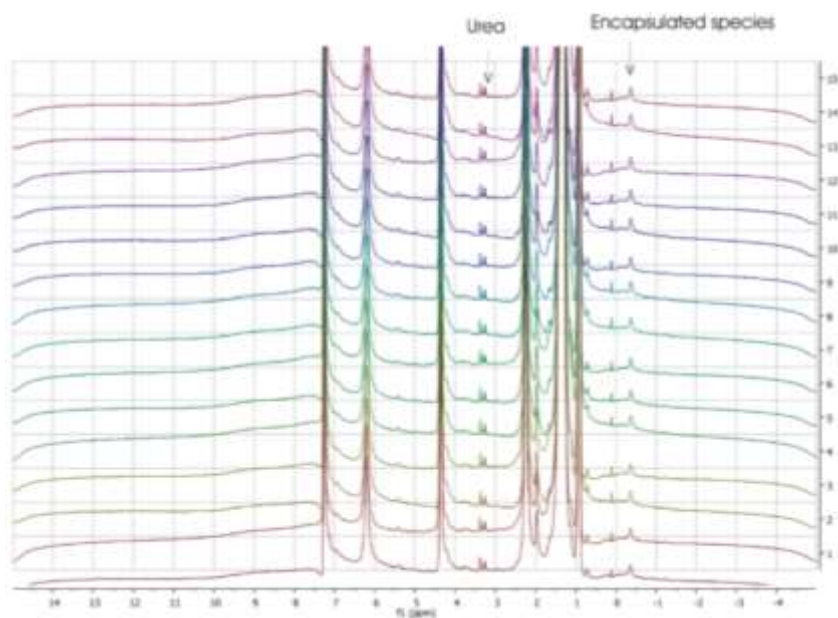


Figure 206. ^1H NMR spectra in water saturated chloroform-d for the reaction at 50°C monitored every 1h (from bottom to top) for the hexameric capsule (13.5 mM) octylamine (6.7 mM) hexanoic acid (6.7 mM) and **EDAPC** (13.2 mM).

PRODUCTS CHARACTERIZATION

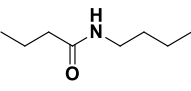
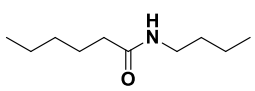
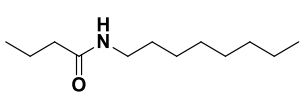
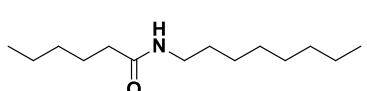
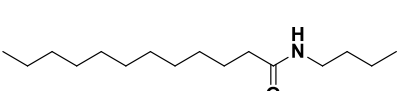
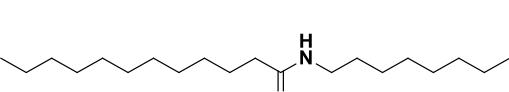
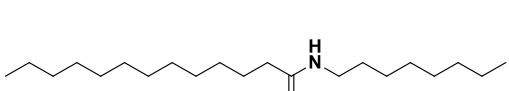
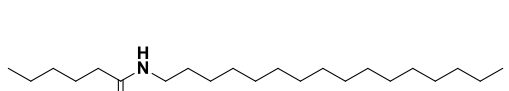
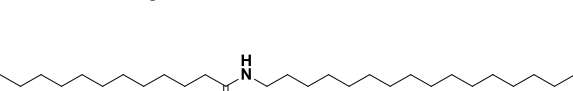
Reagents	RT	Product	PM	Internal standard
BAc (C ₄) + BAm (C ₄)	9.57		143	Octane (C ₈)
HAc (C ₆) + BAm (C ₄)	10.63		171	Decane (C ₁₀)
BAc (C ₄) + OAm (C ₈)	11.51		199	Dodecane (C ₁₂)
HAc (C ₆) + OAm (C ₈)	12.27		227	Tetradecane (C ₁₄)
DAc (C ₁₂) + BAm (C ₄)	12.99		255	Octane (C ₈)
DAc (C ₁₂) + OAm (C ₈)	14.31		311	Docosane (C ₂₀)
TDAc (C ₁₃) + OAm (C ₈)	14.72		325	Docosane (C ₂₀)
HAc (C ₆) + HDAm (C ₁₆)	15.21		339	Docosane (C ₂₀)
DAc (C ₁₂) + HDAm (C ₁₆)	20.66		423	Tetradecane (C ₁₄)

Table 29. Retention time and internal standard in the GS-MS analyses of each reaction.

- N-butylbutyramide Ad_BAcBA_m

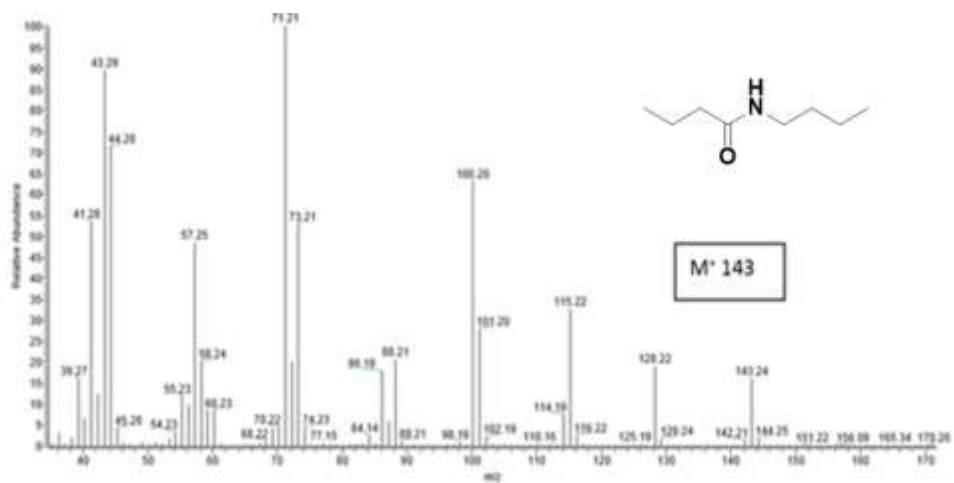


Figure 207. Mass spectrum of N-butylbutyramide Ad_BAcBA_m

- N-butylhexanamide Ad_HAcBA_m

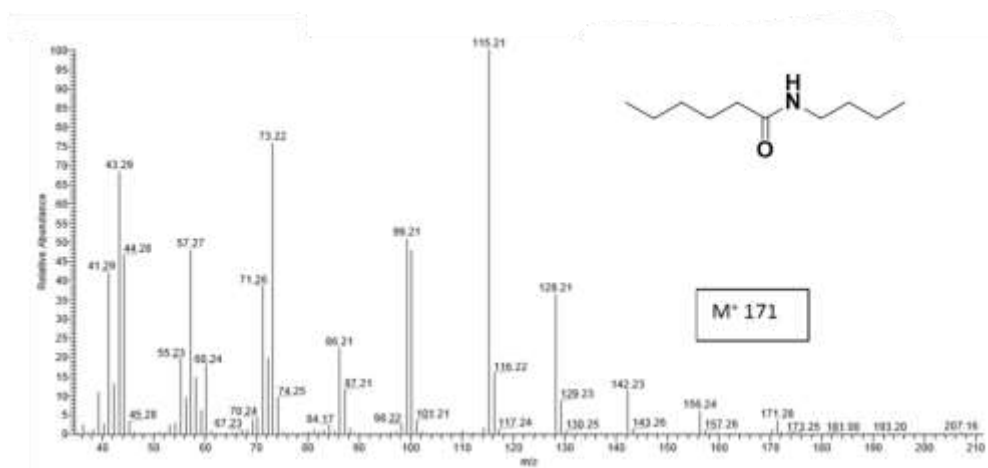


Figure 208. Mass spectrum of N-butylhexanamide Ad_HAcBA_m

- N-octylbutyramide Ad_{BAcOAm}

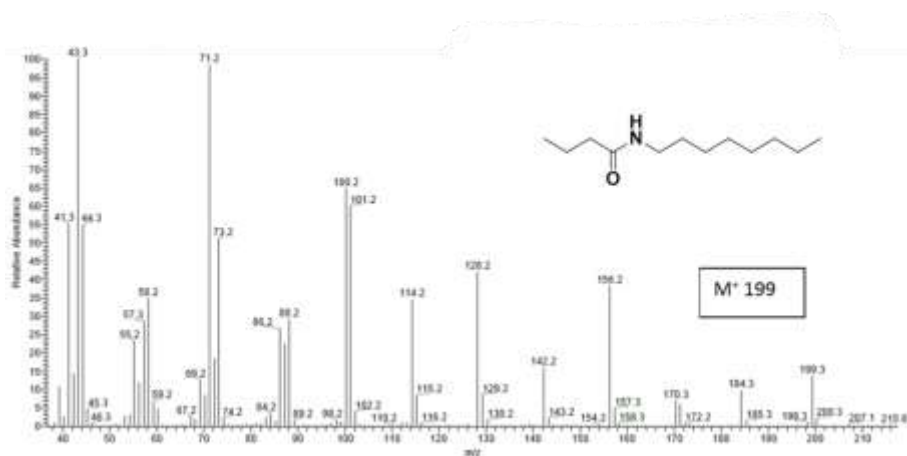


Figure 209. Mass spectrum of N-octylbutyramide Ad_{BAcOAm}

- N-octylhexanamide Ad_{HAcOAm}

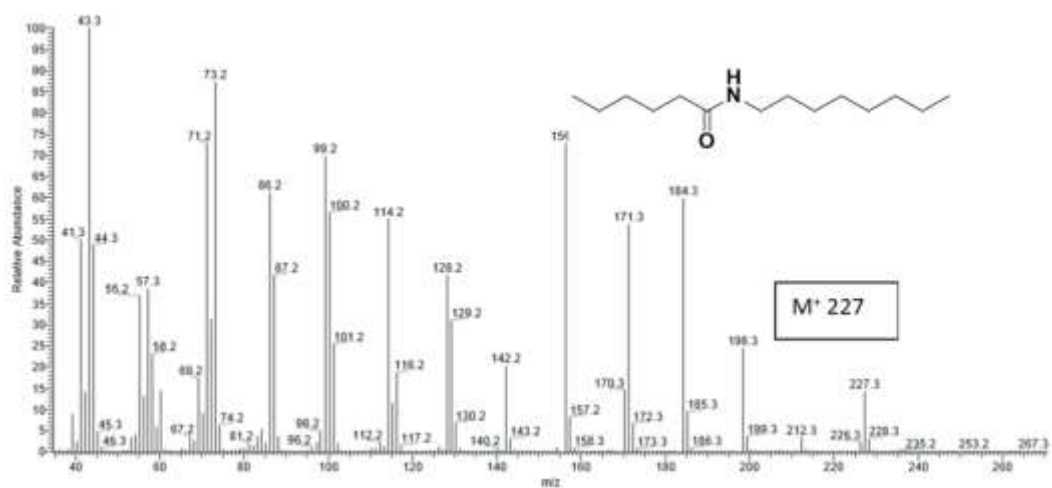


Figure 210. Mass spectrum of N-octylhexanamide Ad_{HAcOAm}

N-butyl-dodecanamide Ad_DAcBAm

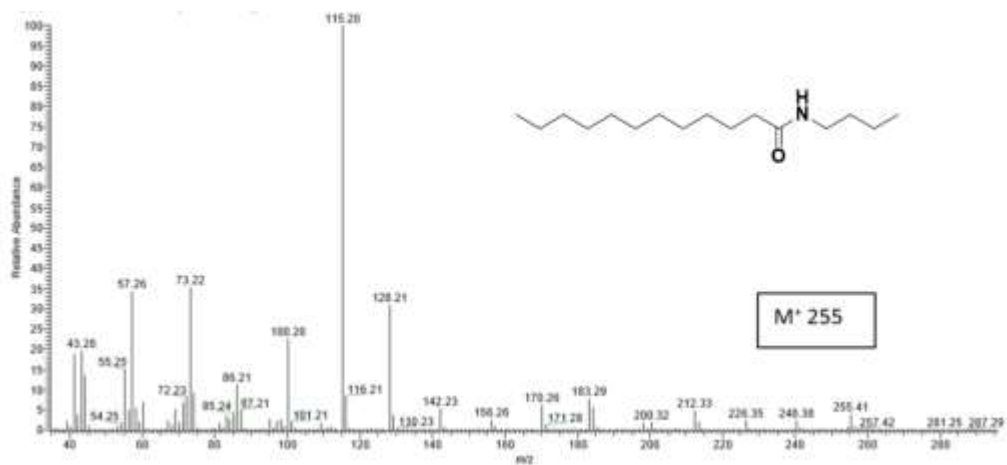


Figure 211. Mass spectrum of N-butyl-dodecanamide Ad_DAcBAm

N-octyl-dodecanamide Ad_DAcOAm

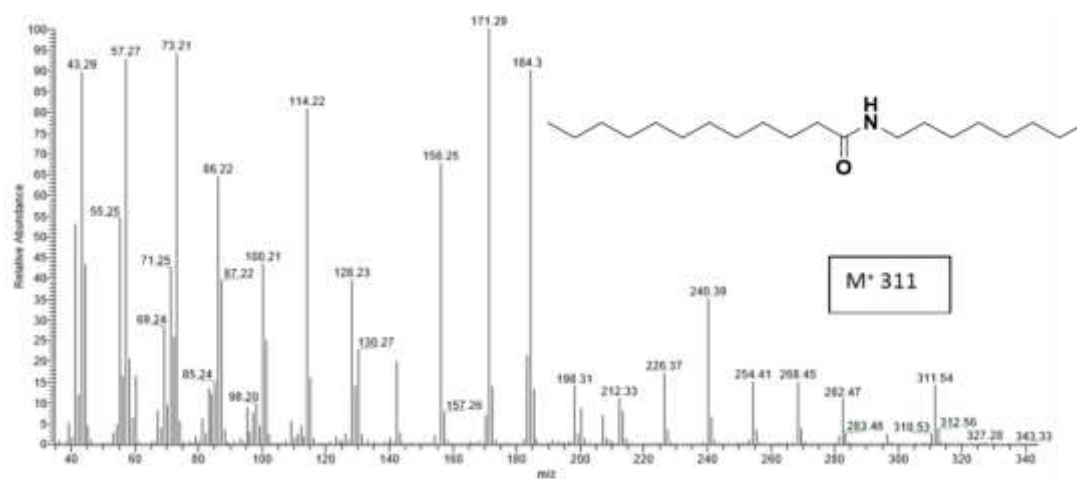


Figure 212. Mass spectrum of N-octyl-dodecanamide Ad_DAcOAm

- **N-octyltridecanamide Ad_{TDAcOAm}**

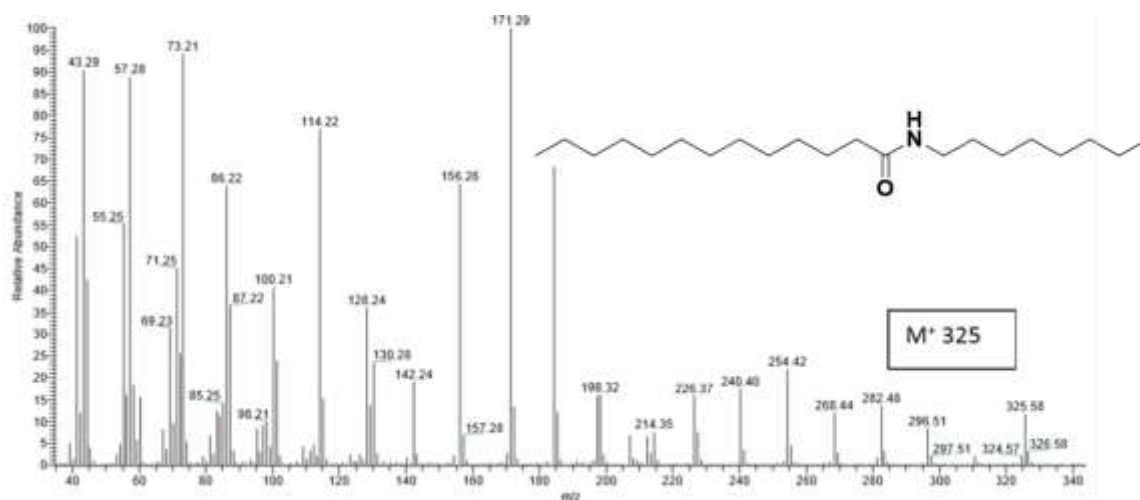


Figure 213. Mass spectrum of N-octyltridecanamide Ad_{TDAcOAm}

- **N-hexadecylhexanamide Ad_{HAcHDAm}**

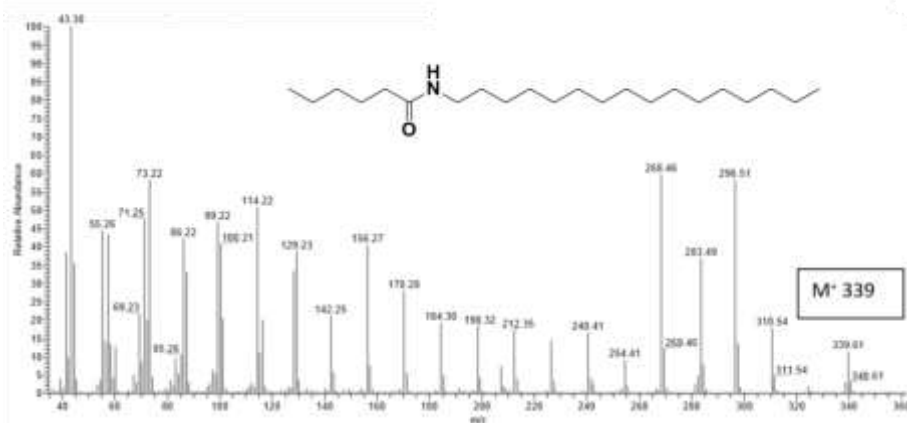


Figure 214. Mass spectrum of N-hexadecylhexanamide Ad_{HAcHDAm}

- **N-hexadecylidodecanamide Ad_DAcHAM**

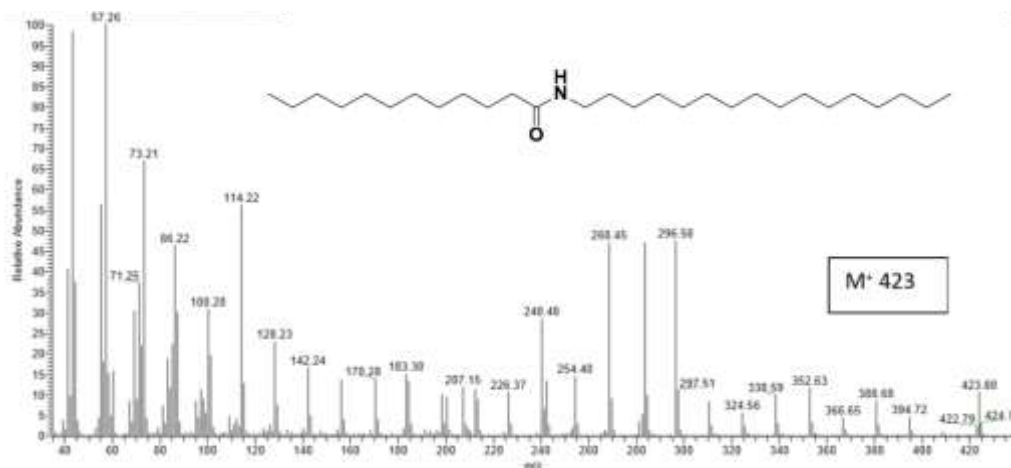


Figure 215. Mass spectrum of N-hexadecylidodecanamide Ad_DAcHAM

7.2.10. Substrate selective Cross-Coupling Heck reactions

EXPERIMENTAL CONDITIONS

- **Heck coupling reaction in organic solvent DMF**

In a vial containing a stirring bar Pd(OAc)₂ (2mg, 8.9·10⁻³ mmol), K₂CO₃ (123mg, 8.9·10⁻¹ mmol, 100 eq.) iodobenzene (50.5 μL, 4.5·10⁻¹ mmol, 50 eq.) methyl acrylate (55 eq.) and another acrylate ester as competitive substrate (55 eq.) were added, followed by 3mL of DMF. The vial was then thermostatted under stirring at 70°C for 21h. At the end, the reaction mixture was diluted with 3 mL di H₂O and extracted three times with 5 mL of diethyl ether. The organic phase was dried with Na₂SO₄ and filtered. Each experiment was repeated three times, conversion and selectivity were determined through the average of the three results. All the products were identified by GC-MS and ¹H-NMR analysis. The ¹H NMR of the sample was recorded and integration of the ester moieties for both substrates and products allowed to calculate the conversion for each substrate.

Experimental procedure as above reported for iodobenzene was employed in the presence of either 1-iodonaphthalene or 2-Cl-I-benzene as substrate. The substrate selectivity obtained under these conditions are reported below.

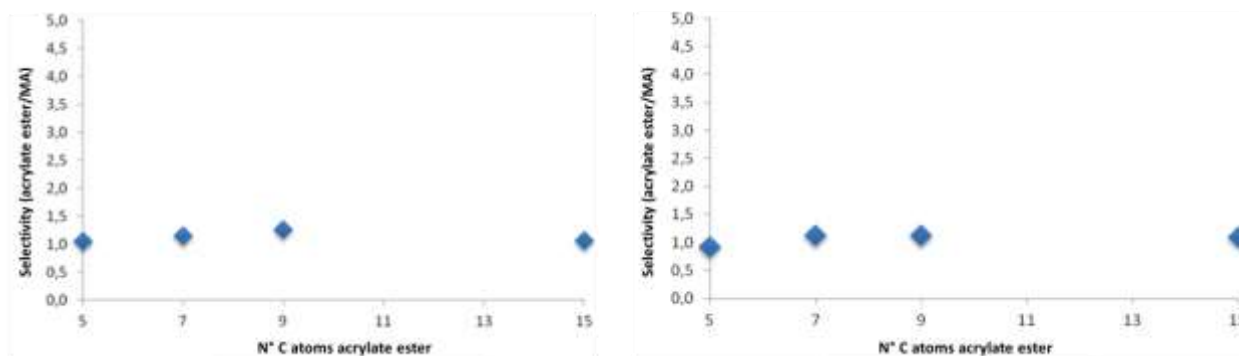


Figure 216. Substrate selectivity in pairwise competitive experiments in the Heck coupling reaction of 1-iodonaphthalene (on left) and 2-Cl-I-benzene (on right) carried out in DMF as organic solvent. Experimental conditions: [Pd(OAc)₂]= 3.0 mM, [acrylate ester]= 163 mM each, [iodo-aryl derivative]= 150 mM, [K₂CO₃] 300 mM, solvent 3 mL DMF, 70°C, 21h.

- Heck coupling reaction in water with cationic surfactant CTAB

In a vial containing a stirring bar Pd(OAc)₂ (2mg, 8.9·10⁻³ mmol), K₂CO₃ (123mg, 8.9·10⁻¹ mmol, 100 eq.) iodobenzene (50.5 μL, 4.5·10⁻¹ mmol, 50 eq.) methyl acrylate (55 eq.) and another acrylate ester as competitive substrate (55 eq.) were added, followed by 3mL of H₂O and cetyl trimethylammonium bromide (CTAB, 80 mM). The vial was then thermostatted under stirring at 70°C for 21h. At the end, the reaction mixture was diluted with 3 mL di H₂O and extracted three times with 5 mL of diethyl ether. The organic phase was dried with Na₂SO₄ and filtered. Each experiment was repeated three times, conversion and selectivity were determined through the average of the three results. All the products were identified by GC-MS and ¹H-NMR analysis. The ¹H NMR of the sample was recorded and integration of the ester moieties for both substrates and products allowed to calculate the conversion for each substrate.

Experimental procedure as above reported for iodobenzene was employed in the presence of either 1-iodonaphthalene or 2-Cl-I-benzene as substrate. The substrate selectivity obtained under these conditions are reported below.

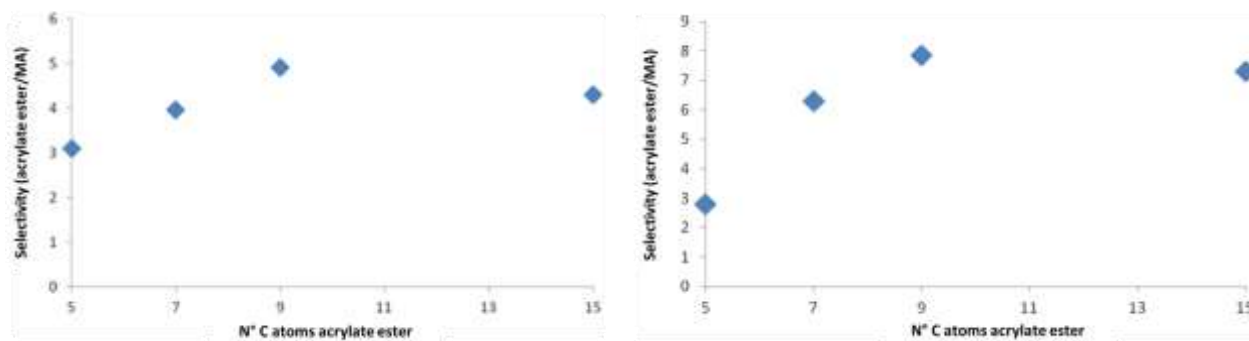


Figure 217. Substrate selectivity in pairwise competitive experiments in the Heck coupling reaction of 1-iodonaphthalene (on left) and 2-Cl-I-benzene (on right) carried out in water with CTAB (80 mM) after 21h. Experimental conditions: $[\text{Pd}(\text{OAc})_2] = 3.0 \text{ mM}$, $[\text{acrylate ester}] = 163 \text{ mM}$ each, $[1\text{-I-naphthalene}] = 150 \text{ mM}$, $[\text{K}_2\text{CO}_3] = 300 \text{ mM}$, solvent water 3 mL, $[\text{CTAB}] = 80 \text{ mM}$, 70°C , 21h.

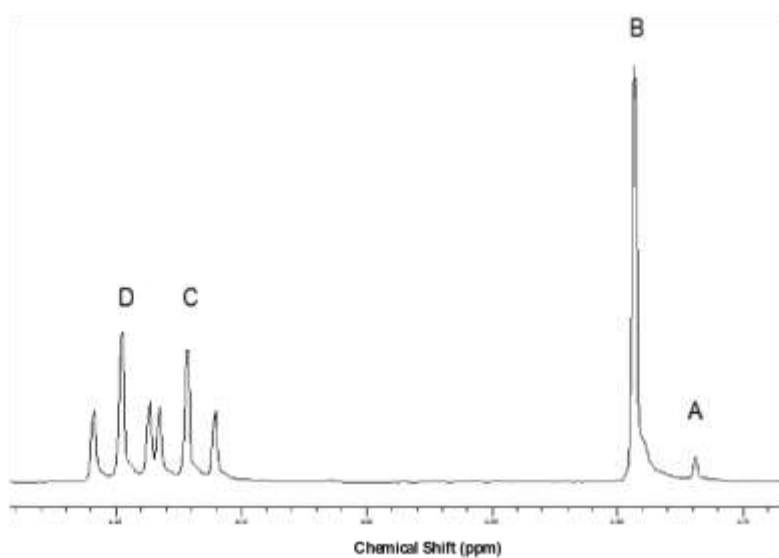


Figure 218. ^1H NMR spectrum reporting the resonances for acrylate ester substrates and Heck coupling ester products in chloroform-d. In the order from left: D) butyl cinnamate product, C) butyl acrylate reagent, B) methyl cinnamate product and A) methyl acrylate reagent.

HECK PRODUCTS CHARACTERIZATION

- Methyl cinnamate

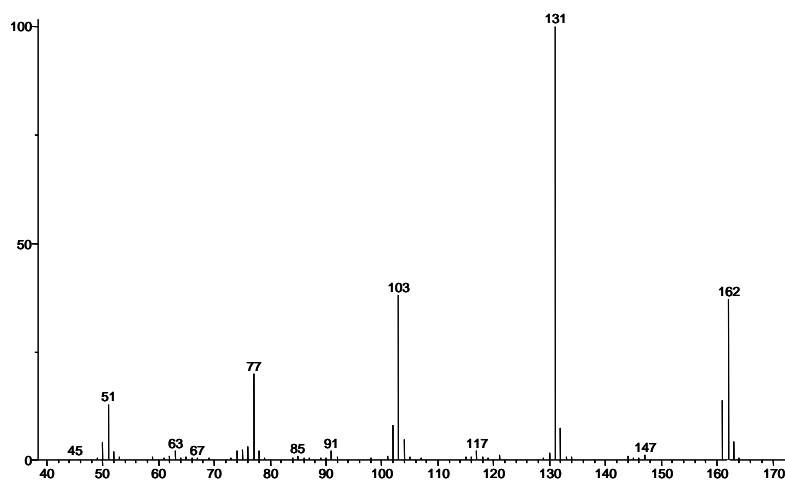
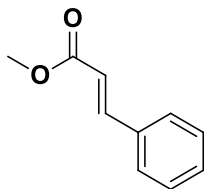


Figure 219. Mass spectrum of methyl cinnamate

- Ethyl cinnamate

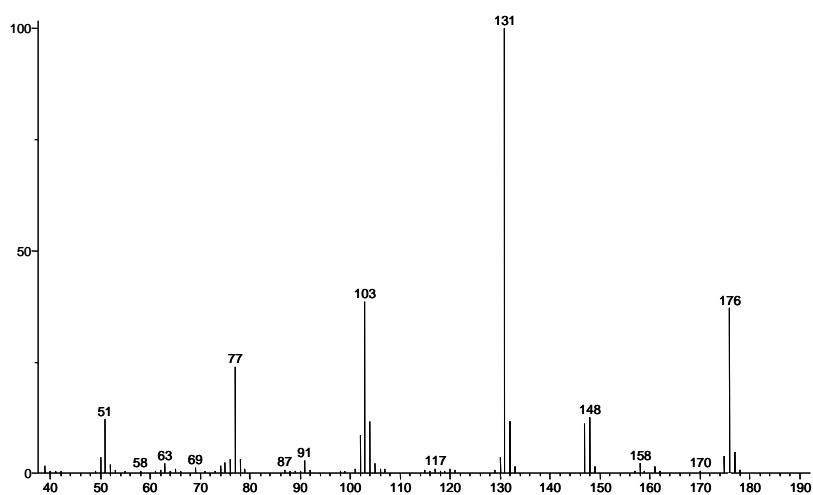
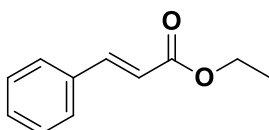


Figure 220. Mass spectrum of ethyl cinnamate

- Butyl cinnamate

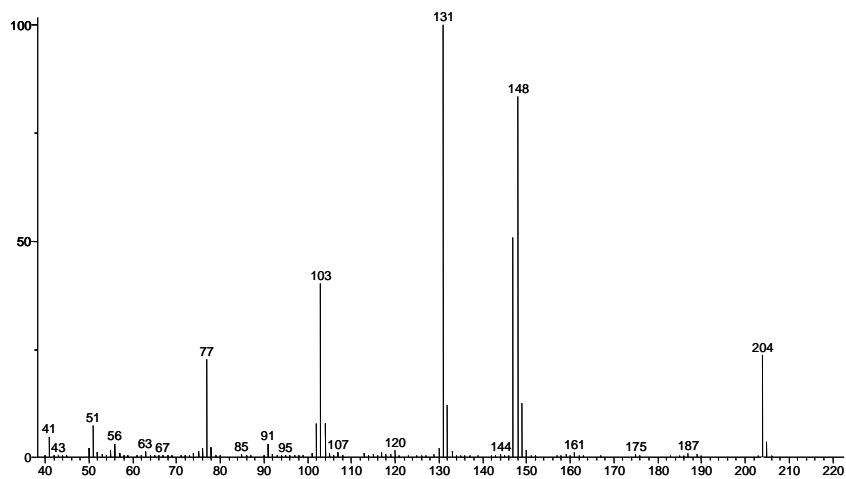
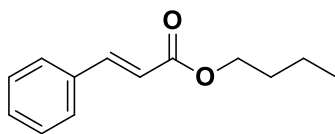


Figure 221. Mass spectrum of butyl cinnamate

- Hexyl cinnamate

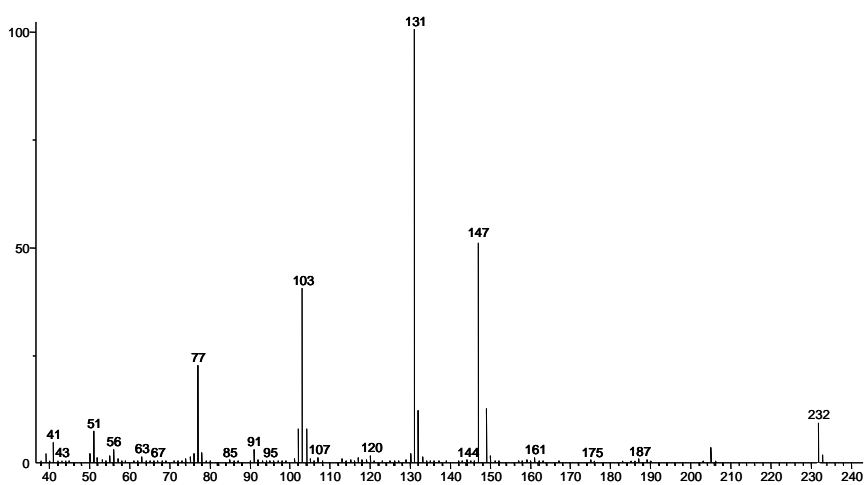
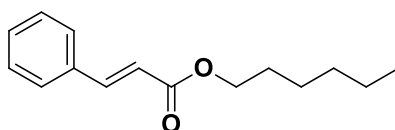


Figure 222. Mass spectrum of hexyl cinnamate

- Lauryl cinnamate

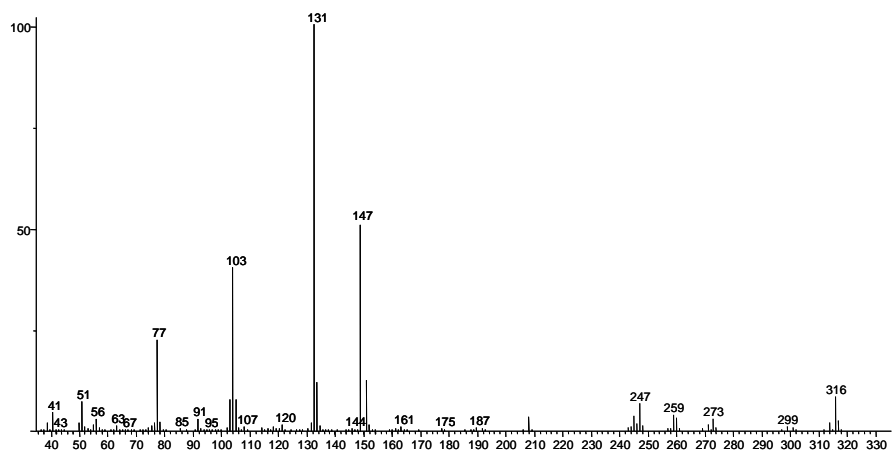
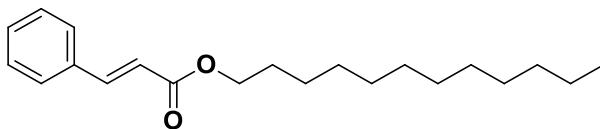


Figure 223. Mass spectrum of lauryl cinnamate

- Methyl 3-(naphthalen-1-yl)acrylate

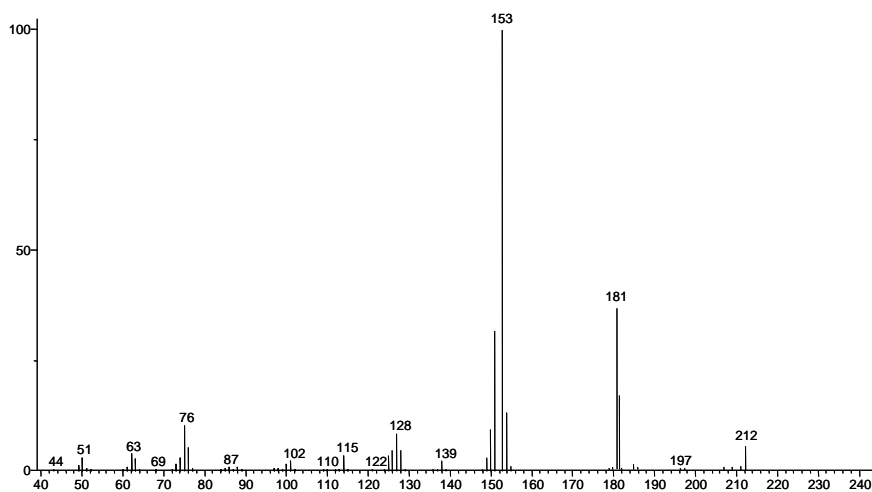
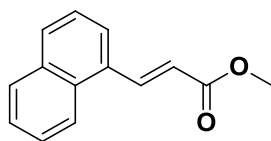


Figure 224. Mass spectrum of methyl 3-(naphthalen-1-yl)acrylate

- Ethyl 3-(naphthalen-1-yl)acrylate

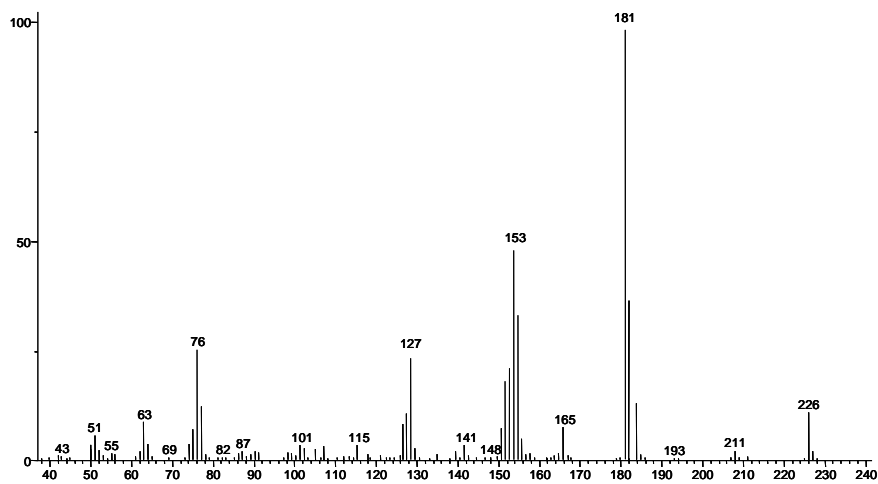
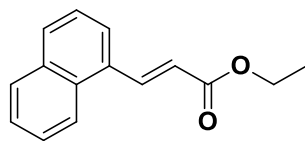
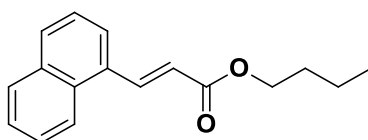


Figure 225. Mass spectrum of ethyl 3-(naphthalen-1-yl)acrylate

- Butyl 3-(naphthalen-1-yl)acrylate



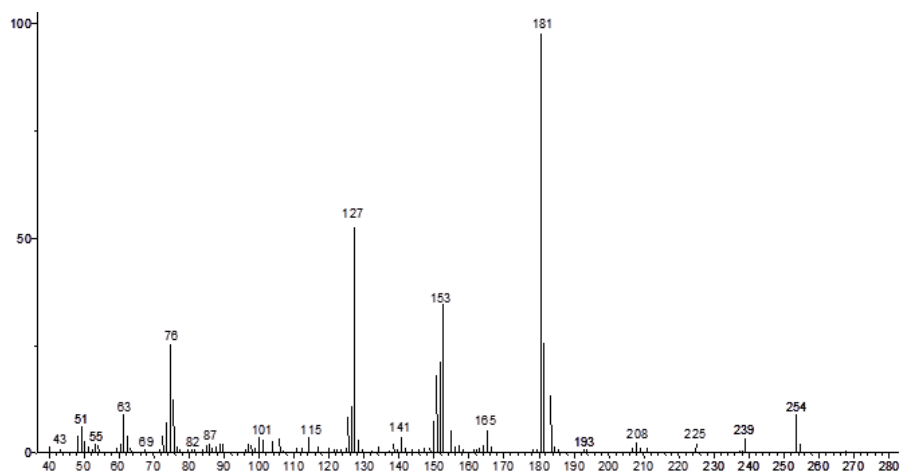


Figure 226. Mass spectrum of butyl 3-(naphthalen-1-yl)acrylate

- Hexyl 3-(naphthalen-1-yl)acrylate

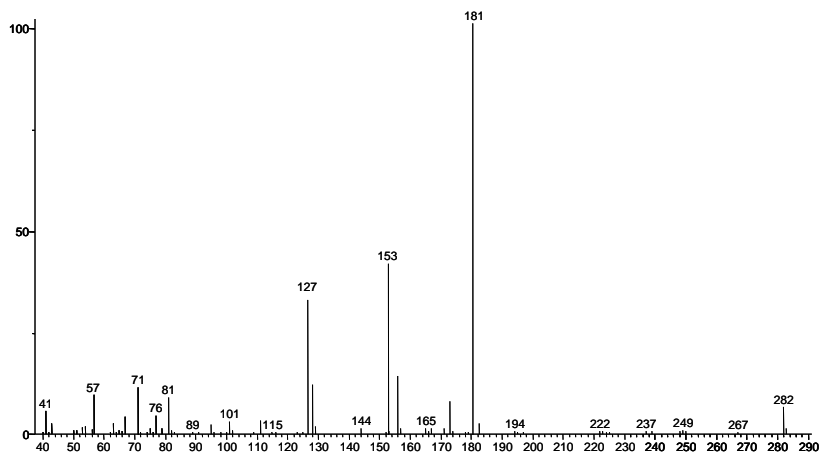
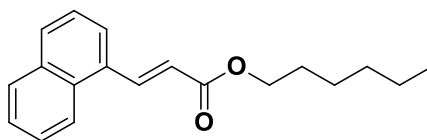
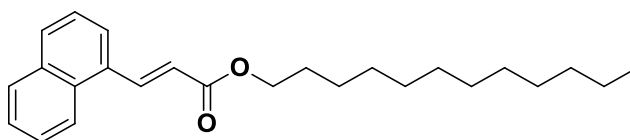


Figure 227. Mass spectrum of hexyl 3-(naphthalen-1-yl)acrylate

- Dodecyl 3-(naphthalen-1-yl)acrylate



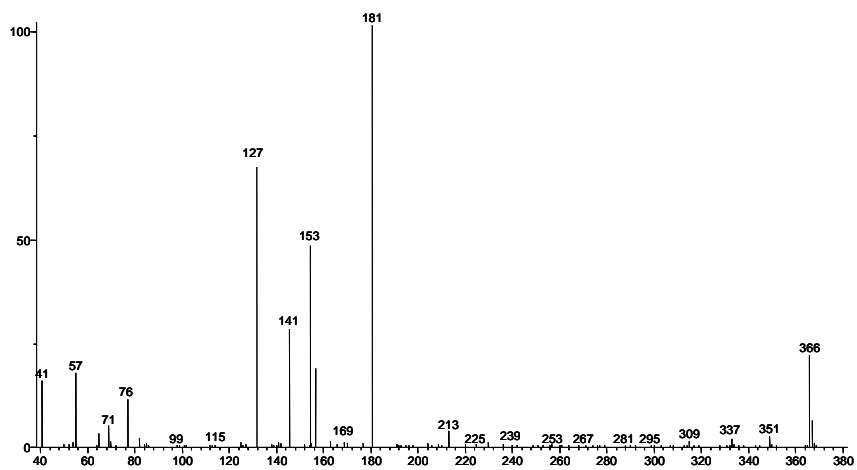


Figure 228. Mass spectrum of dodecyl 3-(naphthalen-1-yl)acrylate

- Methyl 3-(2-chlorophenyl)acrylate

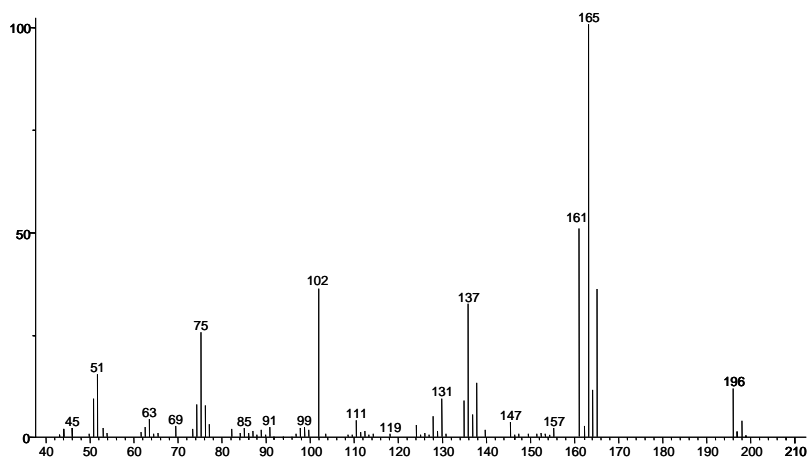
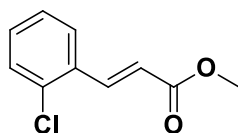
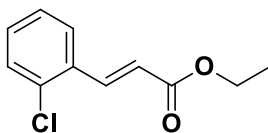


Figure 229. Mass spectrum of methyl 3-(2-chlorophenyl)acrylate

- Ethyl 3-(2-chlorophenyl)acrylate



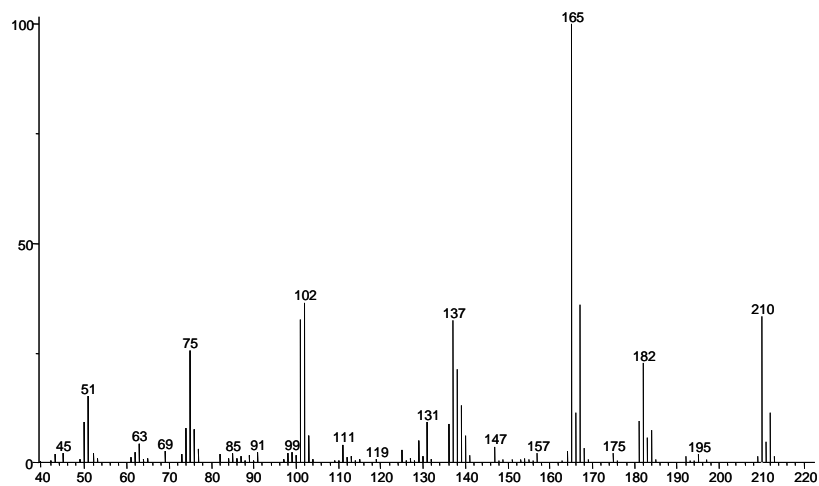


Figure 230. Mass spectrum of ethyl 3-(2-chlorophenyl)acrylate

- **Butyl 3-(2-chlorophenyl)acrylate**

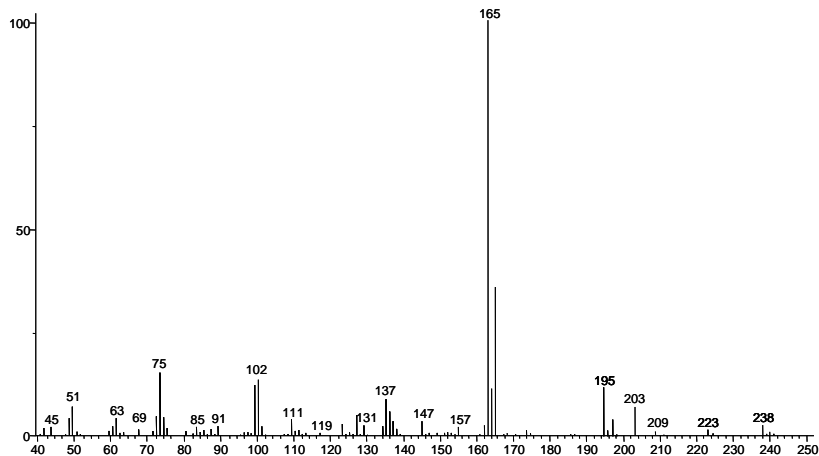
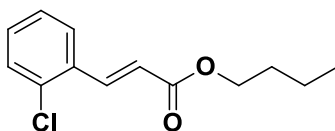
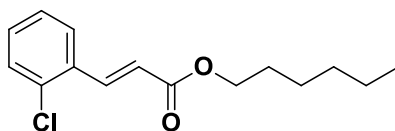


Figure 231. Mass spectrum of butyl 3-(2-chlorophenyl)acrylate

- **Hexyl 3-(2-chlorophenyl)acrylate**



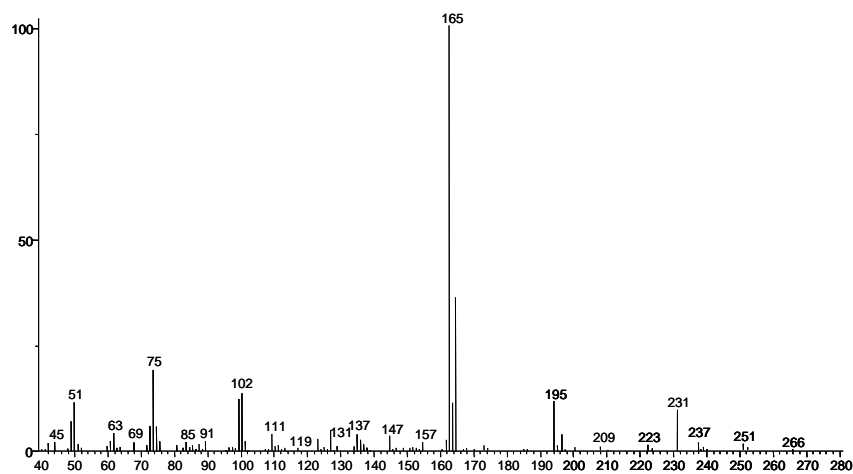


Figure 232. Mass spectrum of hexyl 3-(2-chlorophenyl)acrylate

- **Dodecyl 3-(2-chlorophenyl)acrylate**

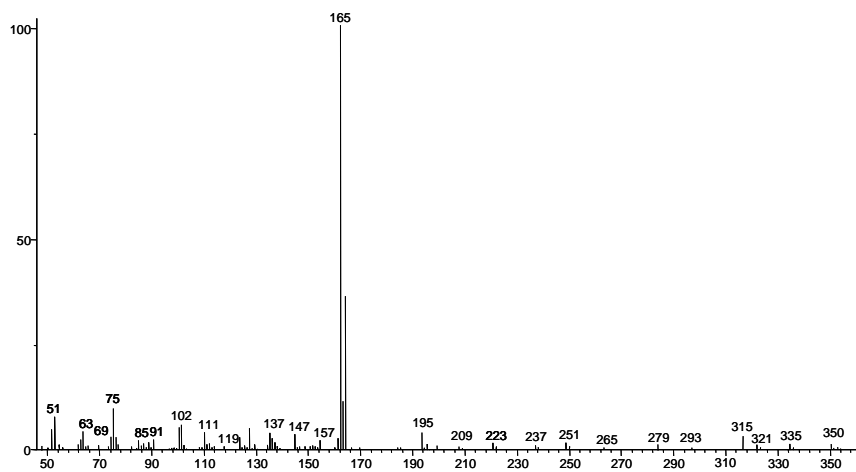
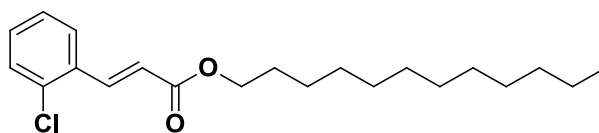
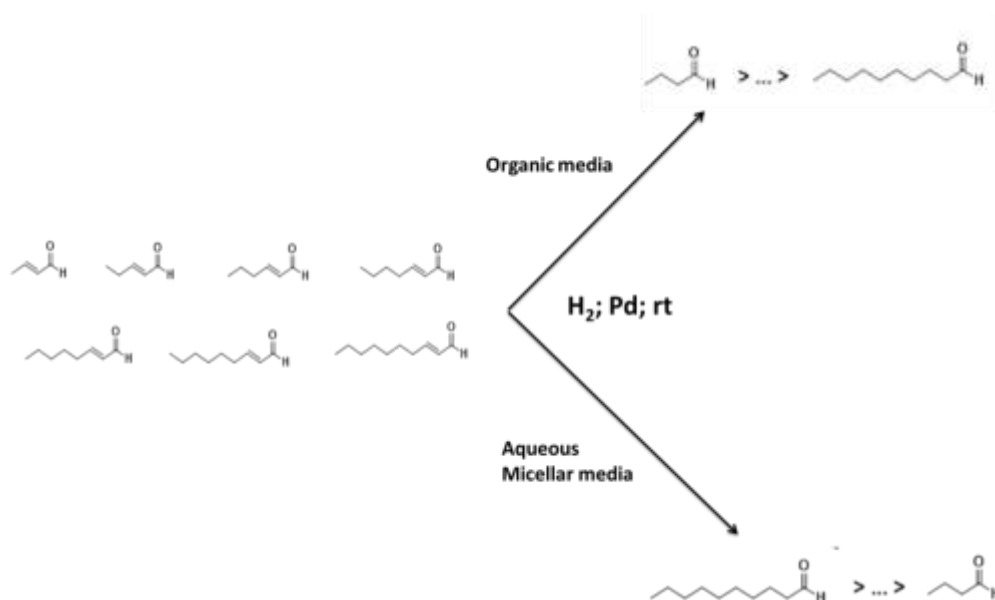


Figure 233. Mass spectrum of dodecyl 3-(2-chlorophenyl)acrylate

7.2.11. Competitive hydrogenation reaction of α,β -unsaturated aldehydes



Scheme 37. Competitive hydrogenation reaction of α,β -unsaturated aldehydes in organic and aqueous micellar media.

IN ORGANIC SOLVENT (THF)

In a 25 mL flask equipped with magnetic stirrer were placed 3 mL of tetrahydrofuran (THF) and $\text{Pd}(\text{OAc})_2$ (2.4 mM). The solution was stirred for 1 h and then treated with 1 bar of H_2 for 5 minutes until the colour changed from pale orange to grey. To the resulting system, a THF solution (3 mL) containing all the substrates from trans-2-butenal C_4 to trans-2-decenal C_{10} (1.8 mmol each) was added at room temperature maintaining the system stirring at 750 rpm under hydrogen atmosphere. The substrate conversion over time was followed through 100 μL periodical sampling of the mixture. The samples were analysed by GC in order to determine the degree of hydrogenation of each substrate. The catalytic experiment was repeated three times, for each experiment the initial rate of reaction for C_4 - C_{10} were determined and the average of the three results was used. All the hydrogenation products were identified by GC-MS analysis.

IN WATER WITH SURFACTANTS

To each aqueous micellar system with activated Pd, all substrates from trans-2-butenal C_4 to trans-2-decenal C_{10} (1.8 mmol each) were added at room temperature maintaining the system stirring at 750 rpm under hydrogen atmosphere. The substrate conversion over time was followed through 100 μL periodical sampling of the mixture, extracting the aqueous micellar solution with 300 μL of ethyl acetate. The organic phase was then analysed by GC in order to determine the

degree of hydrogenation of each substrate. The catalytic experiment was repeated three times, for each experiment the initial rate of reaction for **C₄-C₁₀** were determined and the average of the three results was used. All the hydrogenation products were identified by GC-MS analysis.

Below we reported the concentration profiles of the α,β -unsaturated aldehydes in relation to time in the presence of different surfactants not shown in the results discussion

- CTAB

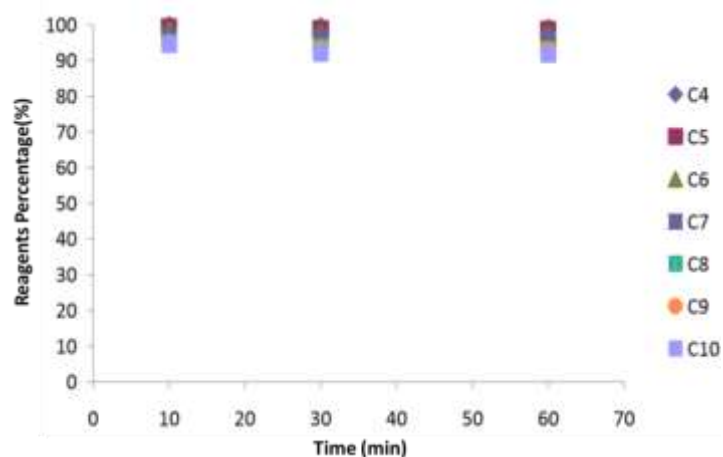


Figure 234. Competitive hydrogenation of C₄-C₁₀ with Pd(OAc)₂ in water in the presence of CTAB.

- Triton-X114

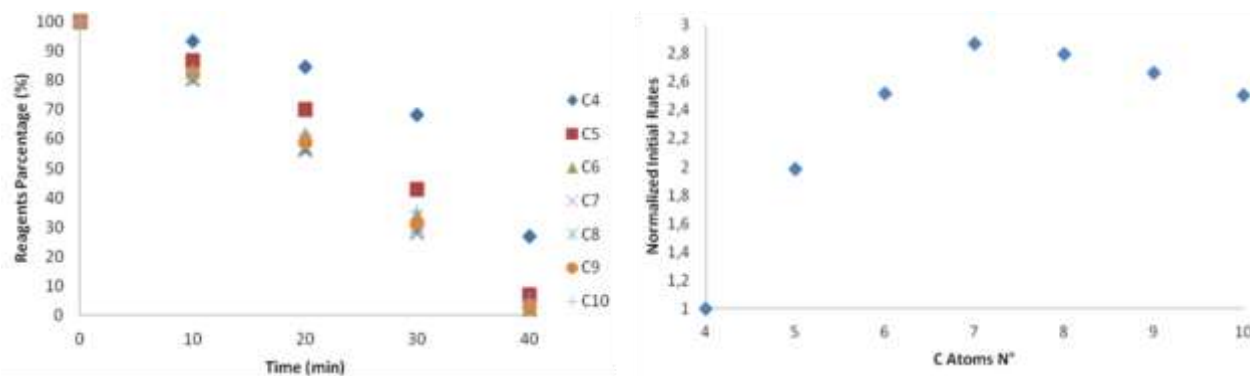


Figure 235. Decrease of the percentage concentration of each α,β -unsaturated aldehydes C₄-C₁₀ (on the left) and the initial reaction rate of each aldehyde normalized with respect to the longer substrate (on the right) in the competitive hydrogenation reaction catalysed by Pd(OAc)₂ in Triton X-100.

- SDS

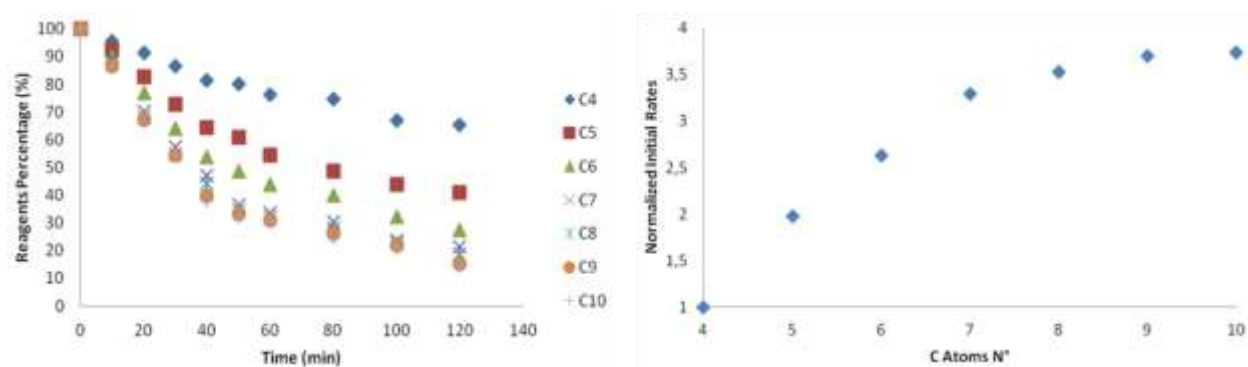


Figure 236. Decrease of the percentage concentration of each α,β -unsaturated aldehydes C_4 - C_{10} (on the left) and the initial reaction rate of each aldehyde normalized with respect to the longer substrate (on the right) in the competitive hydrogenation reaction catalysed by $Pd(OAc)_2$ in SDS.

- SDBS

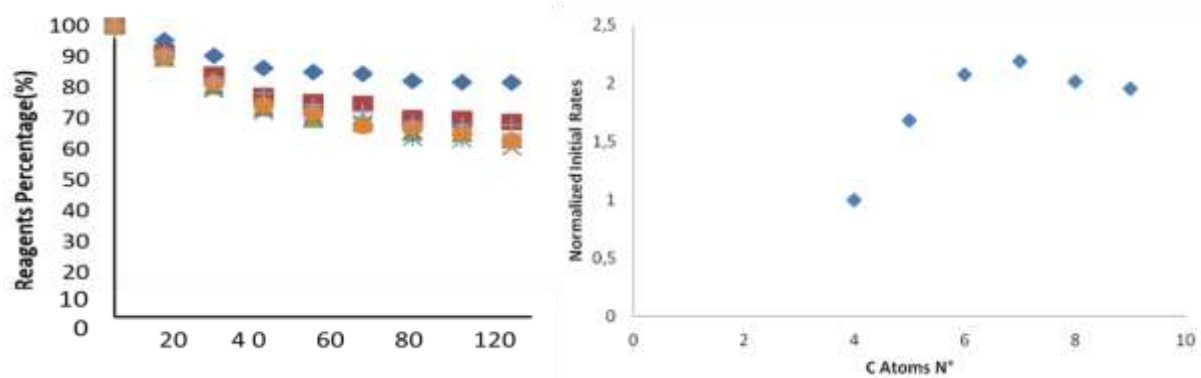


Figure 237. Decrease of the percentage concentration of each α,β -unsaturated aldehydes C_4 - C_{10} (on the left) and the initial reaction rate of each aldehyde normalized with respect to the longer substrate (on the right) in the competitive hydrogenation reaction catalysed by $Pd(OAc)_2$ in SDBS.

SATURATED ALDEHYDE CHARACTERIZATION

- Butyraldehyde

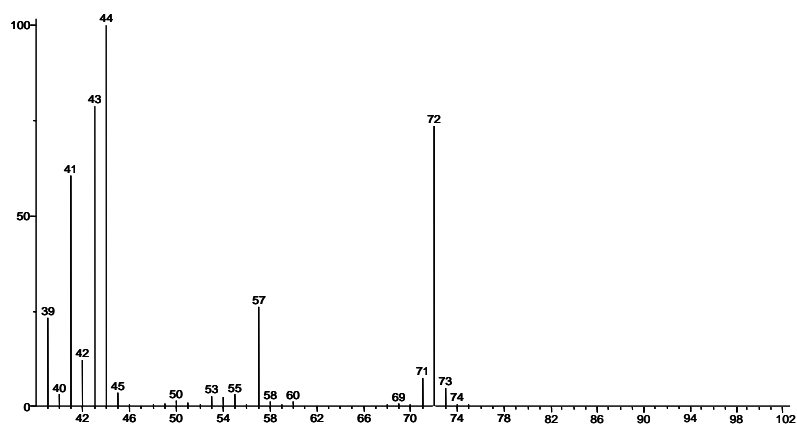
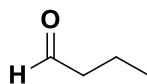


Figure 238. Mass spectrum of butyraldehyde

- Pentanal

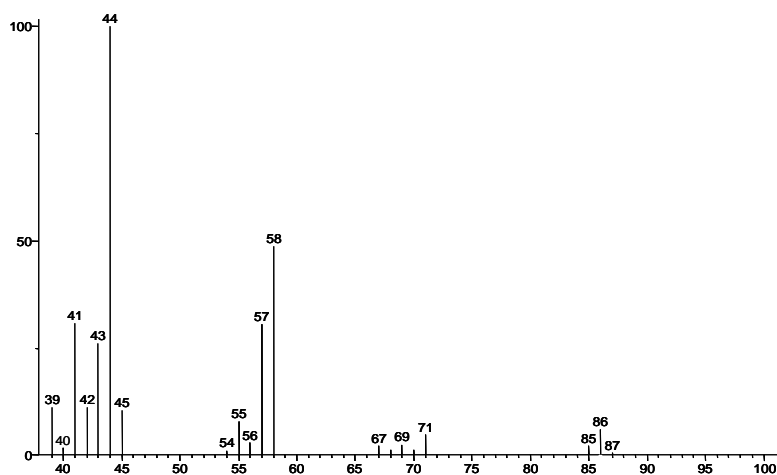
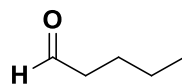


Figure 239. Mass spectrum of pentanal

- Hexanal

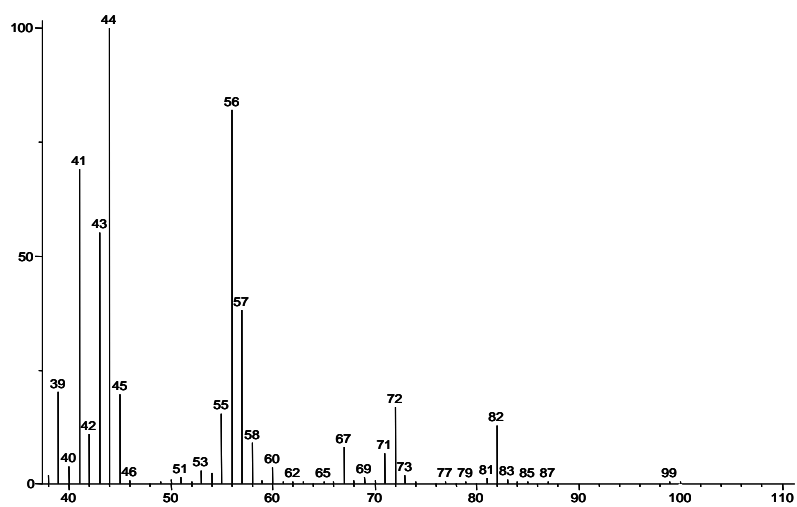
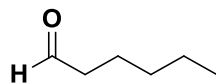


Figure 240. Mass spectrum of hexanal

- Heptanal

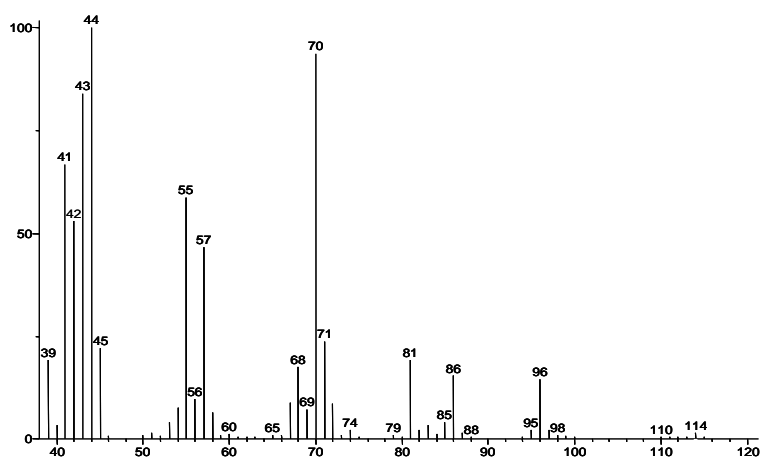
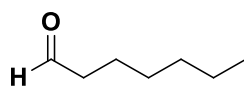


Figure 241. Mass spectrum of heptanal

- Octanal

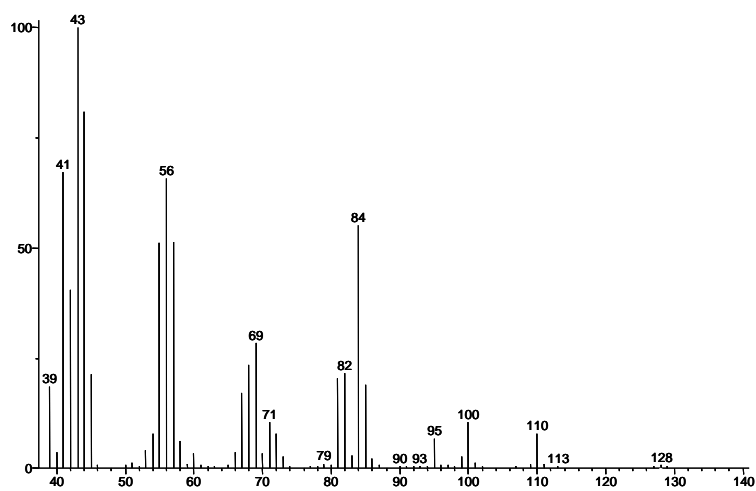
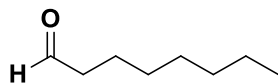


Figure 242. Mass spectrum of octanal

- Nonanal

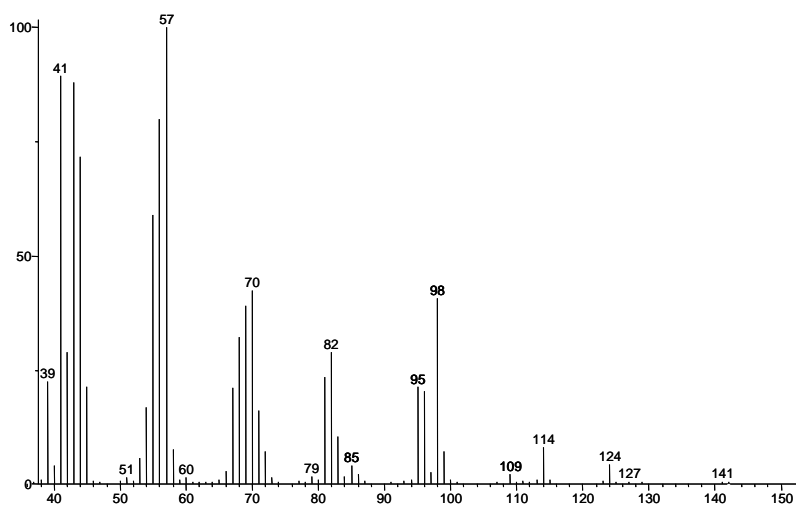
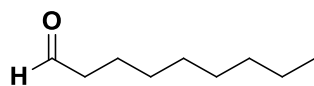


Figure 243. Mass spectrum of nonanal

- Decanal

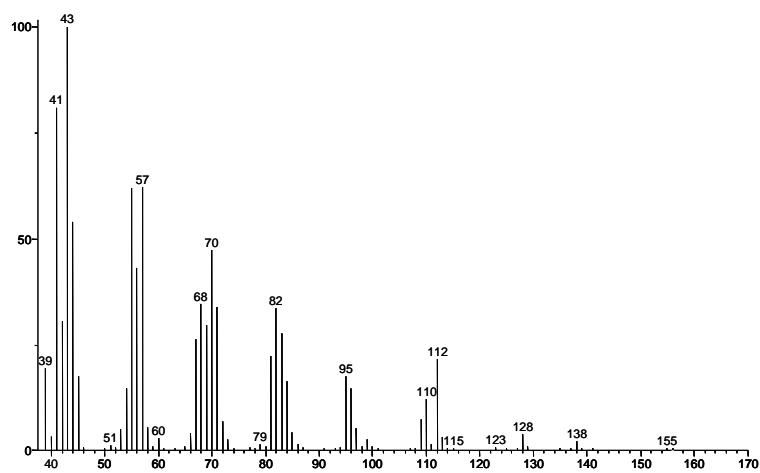
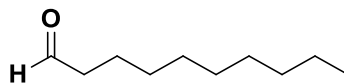


Figure 244. Mass spectrum of decanal

8. ACKNOWLEDGEMENTS

Special thanks go to Prof. Strukul for hosting me in his research group and to Dr. Scarso for his precious teachings, help and clever supervision. My heartfelt gratitude goes to L. Sporni for GC-MS analyses and her collaboration.

I thank Prof. P. Ballester group (Institut Català d'Investigació Química, ICIQ, Tarragona) for accepting me from March until September 2014 and for his courtesy and availability.

General thanks are expressed to all those who contributed to the achievement of the results here reported and particularly to the undergraduate students who worked hard with me.

9. BIBLIOGRAPHY

- 1 J. M. Thomas, R. J. P. Williams, *Phil. Trans. R. Soc. A*, 2005, **363**, 765-791.
- 2 O. Deutschmann, H. Knözinger, K. Kochloefl, T. Turek, *Heterogeneous Catalysis and Solid Catalysts, Ullmann's Encyclopedia of Industrial Chemistry*, 2009, Wiley-VCH, Weinheim, Germany.
- 3 J. M. Thomas, W. J. Thomas, *Principles and Practice of Heterogeneous Catalysis*, 2014, Wiley-VCH, Weinheim, Germany.
- 4 P. W. N. M. van Leeuwen, *Homogeneous Catalysis: Understanding the Art*, 2006, Springer Science & Business Media, NY, USA.
- 5 B. Cornilis, W. A. Herrmann, *Applied Homogeneous Catalysis with Organometallic Compounds*, 1996, Wiley-VCH, Weinheim, Germany.
- 6 G. G. Hlatky, *Chem. Rev.*, 2000, **100**, 1347-1376.
- 7 C.-H. Wong, G. M. Whitesides, *Enzymes in synthetic organic chemistry*, Pergamon Press, Oxford, UK.
- 8 D. E. Koshland Jr, K. E. Neet, *Annual Review of Biochemistry*, 1968, **37**, 359-411.
- 9 J. Gao, S. Ma, D. T. Major, K. Nam, J. Pu and D. G. Truhlar, *Chem. Rev.*, 2006, **106**, 3188-3209.
- 10 T. S. Koblenz, J. Wassenaar, J. N. H. Reek, *Chem. Soc. Rev.*, 2008, **37**, 247-262.
- 11 J.W. Steed, D. R. Turner, Karl J. Wallace, *Core Concepts in Supramolecular Chemistry and Nanochemistry*, 2007, John Wiley & Sons, Chichester, UK.
- 12 Number derived using Scopus as search engine.
- 13 a) S. Gladiali, A. Dore, D. Fabbri, O. De Lucchi and M. Manassero, *Tetrahedron: Asymmetry.*, 1995, **6**, 1453-1474; b) P. Espinet, K. Soulantica, *Coord. Chem. Rev.*, 1999, **499**, 193-195; c) V. F. Slagt, J. N. H. Reek, P. C. J. Kramer, P. W. N. M. van Leeuwen, *Angew. Chem. Int. Ed.*, 2001, **40**, 4271-4274; d) M. L. Merlau, M. d. P. Mejia, S. T. Nguyen, J. T. Hupp, *Angew. Chem. Int. Ed.*, 2001, **40**, 4239-4242; e) G. A. Morris, S. T. Nguyen, J. T. Hupp, *J. Mol. Catal. A: Chem.*, 2001, **174**, 15-20; f) V. F. Slagt, P. W. N. M. van Leeuwen, J. N. H. Reek, *Angew. Chem. Int. Ed.*, 2003, **42**, 5619-5623.
- 14 H Amouri, C Desmarets, J Moussa, *Chemical Reviews*, 2012, **112**, 2015-2041.

-
- 15 a) A. Cavarza, A. Scarso, P. Sgarbossa, G. Strukul, and J. N. H. Reek, *J. Am. Chem. Soc.*, 2011, **133**, 2848-2851; b) T. Besset, D. W. Norman, J. N. H. Reek, *Adv. Synth. Catal.*, 2013, **355**, 348-352.
- 16 P. Dydio, J. N. H. Reek, *Chem. Sci.*, 2014, **5**, 2135-2145.
- 17 M. Raynal, P. Ballester, A. Vidal-Ferran, P. W. N. M. van Leeuwen, *Chem. Soc. Rev.*, 2014, **43**, 1734-1787.
- 18 E. Lindbäck, S. Dawaigher, K. Wärnmark, *Chem. Eur. J.*, 2014, **20**, 13432-13481.
- 19 E. Schneiderman, A. M. Stalcup, *J. Chromatogr. B*, 2000, **745**, 83-102.
- 20 a) R. Ueoka, Y. Matsumoto, K. Harada, H. Akahoshi, Y. Ihara, Y. Kato, *J. Am. Chem. Soc.*, 1992, **114**, 8339-8340; b) A. G. Meyer, C. J. Easton, S. F. Lincoln, G. W. Simpson, *J. Org. Chem.*, 1998, **63**, 9069-9075.
- 21 R. Breslow, P. Campbell, *Tetrahedron Lett.*, 1976, **17**, 1645-1646.
- 22 C. J. Pedersen, *J. Am. Chem. Soc.*, 1967, **89**, 2495-2496.
- 23 D. J. Cram, *Angew. Chem. Int. Ed.*, 1988, **27**, 1009-1020.
- 24 a) J. W. Zubrick, B. I. Ounbar, H. DuPont Durst, *Tetrahedron Lett.*, 1975, **1**, 71-74; b) D. Landini, A. Maia, F. Montanari, P. Tundo, *J. Am. Chem. Soc.*, 1979, **101**, 2526-2530.
- 25 M.-Z. Asfari, Volker Böhmer, J. Harrowfield, Jacques Vicens, *Calixarenes 2001*, Springer Science & Business Media, Berlin, Germany.
- 26 a) S. Shinkai, *Tetrahedron*, 1993, **49**, 8933-8968; b) V. Böhmer, *Angew. Chem. Int. Ed.*, 1995, **34**, 713-745.
- 27 A. L. Maksimov, T. S. Buchneva, E. A. Karakhanov, *J. Mol. Catal. A: Chem.*, 2004, **217**, 59-67.
- 28 R. J. Hooley, S. M. Biro, J. Rebek Jr., *Angew. Chem. Int. Ed.*, 2006, **45**, 3517-3519.
- 29 D. M. Vriezema, M. C. Aragonès, J. A. A. W. Elemans, J. J. L. M. Cornelissen, A. E. Rowan, R. J. M. Nolte, *Chem. Rev.*, 2005, **105**, 1445-1489.
- 30 J. de Mendoza, *Chem. Eur. J.*, 1998, **4**, 1373-1377.
- 31 a) R. Wyler, J. De Mendoza, J. Rebek Jr., *Angew. Chem. Int. Ed.*, 1993, **32**, 1699-1701; b) N. Branda, R. Wyler, J. Rebek Jr., *Science*, 1994, **263**, 1267-1268.
- 32 J. Kang, J. Rebek Jr., *Nature*, 1997, **385**, 50-52.
- 33 J. Kang, J. Santamaría, G. Hilmersson, J. Rebek Jr., *J. Am. Chem. Soc.*, 1998, **120**, 7389-7390.
- 34 F. Hof, S. L. Craig, C. Nuckolls, J. Rebek Jr., *Angew. Chem. Int. Ed.*, 2002, **41**, 1488-1508.
- 35 D. L. Caulder, K. N. Raymond, *Acc. Chem. Res.*, 1999, **32**, 975-982.
- 36 D. L. Caulder, C. Brückner, R. E. Powers, S. König, T. N. Parac, J. A. Leary, K. N. Raymond, *J. Am. Chem. Soc.*, 2001, **123**, 8923-8938.

-
- 37 D. Fiedler, D. H. Leung, R. G. Bergman, K. N. Raymond, *Acc. Chem. Res.* 2005, **38**, 349-358.
- 38 M. Ziegler, J. L. Brumaghim, K. N. Raymond, *Angew. Chem.* 2000, **112**, 4285-4287.
- 39 A. J. Terpin, M. Ziegler, D. W. Johnson, K. N. Raymond, *Angew. Chem.*, 2001, **113**, 161-164.
- 40 J. L. Brumaghim, M. Michels, K. N. Raymond, *Eur. J. Org. Chem.*, 2004, **22**, 4552-4559.
- 41 J. L. Brumaghim, M. Michels, D. Pagliero, K. N. Raymond, *Eur. J. Org. Chem.*, 2004, **24**, 5115-5118.
- 42 A. V. Davis, K. N. Raymond, *J. Am. Chem. Soc.*, 2005, **127**, 7912-7919.
- 43 C. J. Hastings, M. D. Pluth, R. G. Bergman, K. N. Raymond, *J. Am. Chem. Soc.*, 2010, **132**, 6938-6940.
- 44 D. Fiedler, D. Pagliero, J. L. Brumaghim, R. G. Bergman, K. N. Raymond, *Inorg. Chem.*, 2004, **43**, 846-848.
- 45 D. H. Leung, D. Fiedler, R. G. Bergman, K. N. Raymond, *Angew. Chem. Int. Ed.*, 2004, **43**, 963-966.
- 46 D. Fiedler, D. H. Leung, R. G. Bergman, K. N. Raymond, *Acc. Chem. Res.*, 2005, **38**, 351-360.
- 47 C. J. Brown, G. M. Miller, M. W. Johnson, R. G. Bergman, K. N. Raymond, *J. Am. Chem. Soc.*, 2011, **133**, 11964-11966.
- 48 Z. J. Wang, K. N. Clary, R. G. Bergman, K. N. Raymond, F. D. Toste, *Nature Chemistry*, 2013, **5**, 100-103.
- 49 T. Kusakawa, M. Yoshizawa, M. Fujita, *Angew. Chem. Int. Ed.*, 2001, **40**, 1879-1884.
- 50 M. Fujita, D. Oguro, M. Miyazawa, H. Oka, K. Yamaguchi, K. Ogura, *Nature*, 1995, **378**, 469-471.
- 51 M. Yoshizawa, M. Tamura, M. Fujita, *J. Am. Chem. Soc.*, 2004, **126**, 6846-6847.
- 52 M. Yoshizawa, S. Miyagi, M. Kawano, K. Ishiguro, M. Fujita, *J. Am. Chem. Soc.*, 2004, **126**, 9172-9173.
- 53 M. Yoshizawa, Y. Takeyama, T. Okano, M. Fujita, *J. Am. Chem. Soc.*, 2003, **125**, 3243-3247.
- 54 Takashi Murase, Yuki Nishijima, and Makoto Fujita, *J. Am. Chem. Soc.* 2012, **134**, 162-164.
- 55 L. R. MacGillivray, J. L. Atwood, *Nature*, 1997, **389**, 469-471.
- 56 L. Avram, Y. Cohen, *J. Am. Chem. Soc.*, 2002, **124**, 15148-15149.
- 57 A. Shivanyuk, J. Rebek Jr., *Proc. Natl. Acad. Sci. U. S. A.*, 2001, **98**, 7662-7665.
- 58 D. A. Dougherty, *Acc. Chem. Res.*, 2013, **46**, 885-893.
- 59 Y. Aoyama, Y. Tanaka, Y. H. Toi, H. Ogoshi, *J. Am. Chem. Soc.*, 1988, **110**, 634-635.
- 60 Q. Zhang, K. Tiefenbacher, *J. Am. Chem. Soc.*, 2013, **135**, 16213-16219.

-
- 61 A. Cavarzan, A. Scarso, P. Sgarbossa, G. Strukul, J. N. H. Reek, *J. Am. Chem. Soc.*, 2011, **133**, 2848–2851.
- 62 A. Cavarzan, J. N. H. Reek, F. Trentin, A. Scarso, G. Strukul, *Catal. Sci. Technol.*, 2013, **3**, 2898-2901.
- 63 G. Bianchini, A. Scarso, G. La Sorella, G. Strukul, *Chem. Commun.*, 2012, **48**, 12082-12084.
- 64 I. Ugi, B. Werner, A. Dömling, *Molecules*, 2003, **8**, 53-66.
- 65 R. Ramozzi, N. Chéron, B. Braïda, P. C. Hiberty, P. Fleurat-Lessard, *New J. Chem.*, 2012, **36**, 1137-1140.
- 66 Y. Li, X. Xu, C. Xia, L. Zhang, L. Pana, Q. Liu, *Chem. Commun.*, 2012, **48**, 12228-12230.
- 67 L. A. Paquette, G. R. Allen Jr., M. J. Broadhurst, *J. Am. Chem. Soc.*, 1971, **93**, 4503-4508.
- 68 V. Nenajdenko, *Isocyanide Chemistry: Applications in Synthesis and Material Science*, 2012, John Wiley & Sons, Hoboken, NJ, USA.
- 69 H.-J. Knolker, T. Braxmeier, G. Schlechtingen, *Angew. Chem. Int. Ed.*, 1995, **34**, 2497-2502.
- 70 A. Porcheddu, G. Giacomelli, M. Salaris, *J. Org. Chem.*, 2005, **70**, 2361–2363.
- 71 Y. Kitano, K. Chiba, M. Tada, *Tetrahedron Lett.*, 1998, **39**, 1911-1912.
- 72 a) M. Lakshminarasimhan, P. Madzellan, R. Nan, N. M. Milkovic and M. A. Wilson, *J. Biol. Chem.*, 2010, **285**, 29651-29661; b) K. Hashimoto, H. Suzuki, K. Taniguchi, T. Noguchi, M. Yohda and M. Odaka, *J. Biol. Chem.*, 2008, **283**, 36617-26623.
- 73 I. Ugi, *Isonitrile Chemistry*, 2012, Elsevier, Amsterdam, Netherlands.
- 74 H. Prawat, C. Mahidol, S. Wittayalai, P. Intachote, T. Kanchanapoom, S. Ruchirawat, *Tetrahedron*, 2011, **67**, 5651-5655.
- 75 D. Zhang, X. Xu, J. Tan, Q. Liu, *Synlett*, 2010, **6**, 917-920.
- 76 A. Alimardanov, A. Nikitenko, T. J. Connolly, G. Feigelson, A. W. Chan, Z. Ding, M. Ghosh, X. Shi, J. Ren, E. Hansen, R. Farr, M. MacEwan, S. Tadayon, D. M. Springer, A. F. Kreft, D. M. Ho, J. R. Potoski, *Org. Process Res. Dev.*, 2009, **13**, 1161-1168.
- 77 J. Azuaje, A. Coelho, A. El Maatougui, J. M. Blanco, E. Sotelo, *ACS Comb. Sci.*, 2011, **13**, 89-95.
- 78 J. G. Polisar, J. R. Norton, *Tetrahedron*, 2012, **68**, 10236-10240.
- 79 S. Vorona, T. Artamonova, Y. Zevatskii, L. Myznikov, *Synthesis*, 2014, **46**, 781-786.
- 80 W. G. Finnegan, R. A. Henry, R. Lofquist, *J. Am. Chem. Soc.*, 1958, **80**, 3908-3911.
- 81 J. Roh, K. Vavrova, A. Hrabalek, *Eur. J. Org. Chem.*, 2012, **31**, 6101-6118.
- 82 T. Jin, S. Kamijo, Y. Yamamoto, *Tetrahedron Lett.*, 2004, **45**, 9435-9437.

-
- 83 D. J. P. Pinto, J. R. Pruitt, J. Cacciola, J. M. Favig, Q. Han, M. J. Orwat, M. L. Quan, K. A. Rossi, (1998) PCT Int Appl WO 98 28,269 (Cl. C07D207/34), CA (1998) 129:109090n.
- 84 M. Regitz, *Diazo Compounds: Properties and Synthesis*, **1986**, ACADEMIC PRESS INC., Elsevier Inc., Amsterdam, Netherlands.
- 85 a) A. Padwa, K. E. Krumpe, *Tetrahedron*, 1992, **48**, 5385-5453; b) G. Maas, *Angew. Chem. Int. Ed.*, 2009, **48**, 8186-8195.
- 86 J. D. Clark, A. S. Shah, J. C. Peterson, L. Patelis, R. J. A. Kerten, A. H. Heemskerk, M. Grogan, S. Camden, *Termochim. Acta*, 2002, **386**, 65-72.
- 87 J. Yao, Z. Yan, J. Ji, W. Wu, C. Yang, M. Nishijima, G. Fukuhara, T. Mori, Y. Inoue, *J. Am. Chem. Soc.*, 2014, **136**, 6916-6919.
- 88 a) J. Kang, J. Rebek Jr., *Nature*, 1997, **385**, 50-52; b) J. Kang, J. Santamaria, G. Hilmersson, J. Rebek Jr., *J. Am. Chem. Soc.*, 1998, **120**, 7389-7390; c) Y. Inokuma, S. Yoshioka, M. Fujita, *Angew. Chem. Int. Ed.*, 2010, **49**, 8912-8914; d) M. M. J. Smulders, J. R. Nitschke, *Chem. Sci.*, 2012, **3**, 785-788.
- 89 a) A. Bojilova, I. Videnova, C. Ivanov, *Tetrahedron*, 1994, **50**, 13023-13036; b) A. R. Tuktarova, A. R. Akhmetova, R. F. Kamalova, L. M. Khalilova, M. Pudasb, A. G. Ibragimova, U. M. Dzhemileva, *Russ. J. Org. Chem.*, 2009, **45**, 1168-117.
- 90 a) A. F. Noels, J. N. Btaham, A. J. Hubert, Ph. Teyssié, *Tetrahedron*, 1978, **34**, 3495-3497; b) A. Lévai, *Chem. Heterocycl. Comp.*, 1997, **33**, 647-659.
- 91 W. M. Jones, P. O. Sanderfer, D. G. Baarda, *J. Org. Chem.*, 1967, **32**, 1367-1372.
- 92 B. Branstetter, M. Mahmum Hossain, *Tetrahedron Lett.*, 2006, **47**, 221-223.
- 93 R. A. Novikov, D. N. Platonov, V. A. Dokichev, Y. V. Tomilov, O. M. Nefedov, *Russ. Chem. Bull.*, 2010, **59**, 984-990.
- 94 a) P. Radha Krishna, E. Raja Sekhar, F. Mongin, *Tetrahedron Lett.*, 2008, **49**, 6768-6772; b) P. Radha Krishna, Y. L. Prapura, *Tetrahedron Lett.*, 2010, **51**, 6507-6510.
- 95 T. Kano, T. Hashimoto, K. Maruoka, *J. Am. Chem. Soc.*, 2006, **128**, 2174-2175.
- 96 a) R. Bini, C. Chiappe, V. L. Mestre, C. S. Pomelli, T. Welton, *Theor. Chem. Acc.*, 2009, **123**, 347-352; b) R. Bini, C. Chiappe, V. L. Mestre, C. S. Pomelli, T. Welton, *Org. Biomol. Chem.*, 2008, **6**, 2522-2529.
- 97 B. Hinzen, S. V. Ley, *J. Chem. Soc., Perkin Trans. 1*, 1997, 1907-1908.
- 98 a) M. Carmeli, S. Rozen, *J. Org. Chem.*, 2005, **70**, 2131-2134; b) G. Dyker, B. Hölzer, G. Henkel, *Tetrahedron Asymm.* 1999, **10**, 3297-3307.

-
- 99 a) F. X. Chen, H. Zhou, X. Liu, B. Qin, X. Feng, G. Zhang, Y. Jiang, *Chem. Eur. J.* 2004, **10**, 4790-4797; b) F. Chen, X. Feng, B. Qin, G. Zhang, Y. Jiang, *Org. Lett.*, 2003, **5**, 949-952; c) Y. – S. Lin, C. – W. Liu, T. Y. R. Tsai, *Tetrahedron Lett.* 2005, **46**, 1859-1861.
- 100 B. Verdejo, G. Gil-Ramírez, P. Ballester, *J. Am. Chem. Soc.* 2009, **131**, 3178–3179.
- 101 N. K. Beyeh, R. Puttreddy, K. Rissanen, *RCS Adv.*, 2015, **5**, 30222-30226.
- 102 A. Galàn, G. Gil-Ramírez, P. Ballester, *Org. Lett.* 2013, **15**, 4976-4979.
- 103 L. Avram, Y. Cohen, *J. Am. Chem. Soc.* 2004, **126**, 11556-11563.
- 104 J. J. Monagle, *J. Org. Chem.* 1962, **27**, 3851–3855.
- 105 N. Coşkun, *Tetrahedron Lett.* 1997, **38**, 2299–2302.
- 106 R. S. Lewis, M. F. Wisthoff, J. Grissmerson, W. J. Chain, *Org. Lett.* 2014, **16**, 3832-3835.
- 107 a) C. Zhu, D. Xu, Y. Wei, *Synthesis*, 2011, **5**, 711-714; B. P. Zavesky, N. R. Babij, J. A. Fritz, J. Wolfe, *Org. Lett.* 2013, **15**, 5420-5423.
- 108 S. L. Johnson, D. L. Morrison, *J. Am. Chem. Soc.* 1971, **94**, 1323-1334.
- 109 S. Singh, P. Chauhan, M. Ravi, I. Taneja, Wahajuddin, Prem. P. Yadav, *RSC Adv.*, 2015, **5**, 61876-61880.
- 110 A. Schulz, A. Villinger, *Angew. Chem. Int. Ed.* 2013, **125**, 3146–3148.
- 111 H. C. Ansel, W. P. Norred, I. L. Rothi, *J. Pharm. Sci.*, 2006, **58**, 836-839.
- 112 A. W. Fothergill, C. Sanders, N. P. Wiederhold, *J. Clin. Microbiol.*, 2013, **51**, 1955-1957.
- 113 a) S. Okabe, K. Shimosako, *J. Physiol. Pharmacol.*, 2001, **52**, 639–656; b) D.E. Baker, *Rev. Gastroenterol. Disord.*, 2001, **1**, 32-41.
- 114 K. Fani, A. F. Debons, F. A. Jimenez, E. L. Hoover, *J. Pharmacol. Exp. Ther.*, 1988, **244**, 1145-1149.
- 115 B. P. Capece, S. Calsamiglia, G. Castells, M. Arboix, C. Cristòfol, *J. Anim. Sci.*, 2001, **79**, 1288-1294.
- 116 M. C. Carreño, G. Hernández-Torres, A. Urbano, F. Colobert, *Eur. J. Org. Chem.*, 2008, **12**, 2035-2038.
- 117 R. H. Hook, H. Boxenbaum, G. A. Thompson, R. A. Okerholm, *J. Pharm. Sci.*, 1988, **77**, 1012-1017.
- 118 K. Kaczorowska, Z. Kolarskaa, K. Mitkab, P. Kowalskia, *Tetrahedron*, 2005, **61**, I 8315–8327.
- 119 V. Hulea, P. Moreau, F. Di Renzo, *J. Mol. Catal.*, 1996, **111**, 325–332.
- 120 G. Bianchini, A. Scarso, G. La Sorella, G. Strukul, *Chem. Commun.*, 2012, **48**, 12082–12084.
- 121 B. Saito, T. Katsuki, *Tetrahedron Lett.*, 2001, **42**, 3873–3876.
- 122 P. S. Raghavan, V. Ramaswamy, T. T. Upadhya, A. Sudalai, A. V. Ramaswamy, S. Sivasanker, *J. Mol. Catal. A: Chem.*, 1997, **122**, 75-80.

-
- 123 H. Egami, T. Katsuki, *J. Am. Chem. Soc.*, 2007, **129**, 8940-8941.
- 124 A. H. Vetter, A. Berkessel, *Tetrahedron Lett.*, 1998, **39**, 1741-1744.
- 125 S. Liao, I. Čorić, Q. Wang, B. List, *J. Am. Chem. Soc.*, 2012, **134**, 10765-10768.
- 126 A. Russo, A. Lattanzi, *Adv. Synth. Catal.*, 2009, **351**, 521-524.
- 127 F. Shi, M. K. Tse, H. M. Kaiser, M. Beller, *Adv. Synth. Catal.*, 2007, **349**, 2425-2430.
- 128 H. Firouzabadi, N. Iranpoor, A. A. Jafari, E. Riazymontazer, *Adv. Synth. Catal.*, 2006, **348**, 434-438.
- 129 K. S. Ravikumar, J.-P. Begue, D. Bonnet-Delpon, *Tetrahedron Lett.*, 1998, **39**, 3141-3144; b) K. S. Ravikumar, Y. M. Zhang, J.-P. Begue, D. Bonnet-Delpon, *Eur. J. Org. Chem.*, 1998, 2937-2940; c) Ravikumar, K. S.; Barbier, F.; J.-P. Begue, D. Bonnet-Delpon, *J. Fluorine Chem.*, 1999, **95**, 123-125; d) W. L. Xu, Y. Z. Li, Q. S. Zhang, H. S. Zhu, *Synthesis*, 2004, **2**, 227-232; e) H. Golchoubian, F. Hosseinpour, *Molecules* 2007, **12**, 304-311.
- 130 It is known that up to three molecules of tetraethylammonium tetrafluoroborate are accommodated in the cavity of the resorcin[4]arene hexamer: L.C. Palmer, A. Shivanyuk, M. Yamanaka, J. Rebek Jr. *Chem. Commun.*, 2005, **21**, 857-858.
- 131 F. Secci, A. Frongia, P.P. Piras, *Tetrahedron Lett.*, 2014, **55**, 603-605.
- 132 S. Mecozzi, J. Rebek Jr., *Chem. Eur. J.*, 1998, **4**, 1016-1022.
- 133 Y.J. Kim, R.S Varma, *J. Org. Chem.*, 2005, **70**, 7882-7891.
- 134 A. Labonne, T. Kribber, L. Hintermann, *Org. Lett.*, 2006, **8**, 5853-5856.
- 135 R. J. Thomas, K. N. Campbell, G. F. Hennion, *J. Am. Chem. Soc.*, 1938, **60**, 718-720.
- 136 E. Mizushima, K. Sato, T. Hayashi, M. Tanaka, *Angew. Chem. Int. Ed.*, 2002, **114**, 4745-4747.
- 137 T. Tsuchimoto, T. Joya, E. Shirakawa, Y. Kawakami, *Synlett*, 2000, **12**, 1777-1778.
- 138 R. Kore, T. J. D. Kumar, R. Srivastava, *J. Mol. Catal. A: Chem.*, 2012, **360**, 61-70.
- 139 a) A. D. Allen, Y. Chiang, A. J. Kresge, T. T. Tidwell, *J. Org. Chem.*, 1982, **47**, 775-779; b) V. Lucchini, G. Modena, *J. Am. Chem. Soc.*, 1990, **112**, 6291-6296.
- 140 P. Nun, R. S. Ramón, S. Gaillard, S. P. Nolan, *J. Org. Chem.*, 2011, **696**, 7-11.
- 141 P.T. Anastas, J.C. Warnar, *Green Chemistry. Theory and Practice*, 1998, Oxford University press., UK.
- 142 a) P. Anastas, N. Eghbali, *Chem. Soc. Rev.*, 2010, **39**, 301-312.
- 143 R. A. Sheldon, *Pure Appl. Chem.*, 2000, **72**, 1233-1246.
- 144 A. Lapkin, D.J.C. Constable, *Green Chemistry Metrics-Measuring and Monitoring Sustainable Processes*, Wiley, New York, 2008.

-
- 145 C. Jimenez-Gonzalez, C. S. Ponder, Q. B. Broxterman, J. B. Manley, *Org. Process Res. Dev.*, 2011, **15**, 912-917.
- 146 F. Jo , *Aqueous Organometallic Catalysis*, 2012, Kluwer Acad. Publ., Dordrecht, Netherlands
- 147 B. Cornils, W. A. Herrman, I. T. Horv th, W. Leitern, S. Mecking, H. Oliver-Bourbigou, D. Vogt, *Multiphase Homogeneous Catalysis Vol. 1*, 2005, Wiley-VCH, Weinheim, Germany.
- 148 B. Cornils, W.A. Herrman, *Aqueous-Phase Organometallic Catalysis, 2nd ed.*, 2004, Wiley-VCH, Weinheim, Germany.
- 149 J. R. Lu, X. B. Zhao and M. Yaseen, *Curr. Opin. Colloid Interface Sci.*, 2007, **12**, 60-67.
- 150 L. S. Romsted, *Supramolecular Chemistry: From Molecules to Nanomaterials*; John Wiley & Sons, 2012, Hoboken, NJ, USA.
- 151 R. G. Alargova, I. I. Kochijashky, M. L. Sierra, R. Zana, *Langmuir* 1998, **14**, 5412-5418.
- 152 M. Ishikawa, K.-I. Matsumura, K. Esumi, K. Meguro, W. Binana-Limb l , R. Zana, *J. Colloid Interface Sci.*, 1992, **151**, 70-78.
- 153 A. M. Tedeschi, L. Franco, M. Ruzzi, L. Paduano, C. Corvaja, G. D'Errico, *Phys. Chem. Chem. Phys.*, 2003, **5**, 4204-4209.
- 154 A. Malliaris , J. Le Moigne , J. Sturm , R. Zana, *J. Phys. Chem.*, 1985, **89**, 2709-2713.
- 155 W. Binana-Limb l , R. Zana, *J. Colloid Interface Sci.*, 1988, **121**, 81-84.
- 156 Y. Chen, Y. Zhao, J. Chen, K. Zhuo, J. Wang, *J. Colloid Interface Sci.*, 2011, **364**, 388-394.
- 157 R. Alargova, J. Petkov, D. Petsev, I. B. Ivanov, G. Broze, A. Mehreteab, *Langmuir*, 1995, **11**, 1530-1536.
- 158 L. Maibaum, A. R. Dinner, D. Chandler, *J. Phys. Chem. B*, 2004, **108**, 6778-6781.
- 159 F. M. Menge, *Acc. Chem. Res.*, 1979, **12**, 111-117.
- 160 C. Tanford, *The Hydrophobic Effect*, Wiley-Interscience, New York, 1973.
- 161 J. Israelachvili, D. J. Mitchell, B. W. Ninham, *J. Chem. Soc., Faraday Trans. 2*, 1976, **72**, 1525-1568.
- 162 R. Nagarajan, *Langmuir*, 2002, **18**, 31-38
- 163 J. H. Fendler, *Catalysis in Micellar and Macromolecular Systems*, Accademic Press Inc., 1975, New York, USA.
- 164 S. D. Christian, J. E. Scamehorn, *Solubilization in Surfactant Aggregates*, Marcel Dekker Inc., 1995, New York, USA.
- 165 T. Dwar, E. Paetzold, G. Oehme, *Angew. Chem. Int. Ed.*, 2005, **44**, 7174-7199
- 166 G. La Sorella, G. Strukul, A. Scarso, *Green Chem.*, 2015, **17**, 644-683.

-
- 167 B. H. Lipshutz, S. Ghorai, A. R. Abela, R. Moser, T. Nishikata, C. Duplais, A. Krasovskiy, R. D. Gaston, R. C. Gadwood, *J. Org. Chem.*, 2011, **76**, 4379-4391.
- 168 a) R. G. Chaudhuri, S. Paria, *Chem. Rev.*, 2012, **112**, 2373-2433; b) M. C. Daniel and D. Astruc, *Chem. Rev.*, 2004, **104**, 293-346; c) Q. Zhang, E. Uchaker, S.L. Candelaria, G. Cao, *Chem. Soc. Rev.* 2013, **42**, 3127-3171; d) A. Balanta, C. Godard, C. Claver, *Chem. Soc. Rev.* 2011, **40**, 4973-4985; e) Y. Sun, *Chem. Soc. Rev.*, 2013, **42**, 2497-2511; f) F. Caruso, T. Hyeon, V.M. Rotello, *Chem. Soc. Rev.* 2012, **41**, 2537-2538; g) T.L. Doane, C. Burda, *Chem. Soc. Rev.* 2012, **41**, 2885-2911; P. K. Stoimenov, R. L. Klinger, G. L. Marchin, K. J. Klabunde, *Langmuir*, 2002, **18**, 6679-6686
- 169 a) S. H. Joo, S. J. Choi, I. Oh, J. Kwak, Z. Liu, O. Terasaki, R. Ryoo, *Nature*, **412**, 169-172; b) K. H. Park, K. Jang, H. J. Kim, S. U. Son, *Angew. Chem. Int. Ed.* 2007, **46**, 1152-1155.
- 170 a) S. Mandal, D. Roy, R. V. Chaudhari, M. Sastry, *Chem. Mater.*, 2004, **16**, 3714-3724; b) C. Sun, M. J. Peltre, M. Briend, J. Blanchard, K. Fajerweg, J.-M. Krafft, M. Breysse, M. Cattenot, M. Lacroix, *Appl. Catal. A*, 2000, **245**, 245-255; c) A. Brito, F. J. Garcia, M. C. Alvarez-Galvan, M. E. Borges, C. Diaz, V.A. de la Pena O'Shea, *Cat. Commun.* 2007, **8**, 2081-2086
- 171 a) A.A. Herzing, C.J. Kiely, A.F. Carley, P. Landon, G.J. Hutchings, *Science*, 2008, **321**, 1331-1335; b) T. Akita, M. Kohyama, M. Haruta, *Acc. Chem. Res.* 2013, **46**, 1773-1782.
- 172 a) A. B. Lowe, B. S. Sumerlin, M. S. Donovan, C. L. McCormick, *J. Am. Chem. Soc.*, 2002, **124**, 11562-11563; b) M. Králik, A. Biffis, *J. Mol. Catal. A: Chem.*, 2001, **177**, 113-138; c) T. Teranishi, M. Miyake, *Chem. Mater.*, 1998, **10**, 594-600; d) R. Narayanan, M. A. El-Sayed, *J. Am. Chem. Soc.*, 2003, **125**, 8340-8347.
- 173 a) R. M. Crooks, M. Zhao, L. Sun, V. Chechik, L. K. Yeung, *Acc. Chem. Res.*, 2001, **34**, 181-190.
- 174 a) Q. Zhang, E. Uchaker, S.L. Candelaria, G. Cao, *Chem. Soc. Rev.*, 2013, **42**, 3127-3171; b) A. Balanta, C. Godard, C. Claver, *Chem. Soc. Rev.*, 2011, **40**, 4973-4985; c) Y. Sun, *Chem. Soc. Rev.*, 2013, **42**, 2497-2511; d) F. Caruso, T. Hyeon, V.M. Rotello, *Chem. Soc. Rev.* 2012, **41**, 2537-2538; e) T.L. Doane, C. Burda, *Chem. Soc. Rev.* 2012, **41**, 2885-2911.
- 175 I. Lisiecki, M.P. Pileni, *Langmuir*, 2003, **19**, 9486-9489.
- 176 T. Sakai, P. Alexandridis, *J. Phys. Chem. B*, 2005, **109**, 7766-7772.
- 177 a) S. Bhattacharya, A. Srivastava and S. Sengupta, *Tetrahedron Lett.*, 2005, **46**, 3557-3560; b) G. La Sorella, M. Bazan, A. Scarso, G. Strukul, *J. Mol. Catal. A* 2013, **379**, 192-196; c) E.E. Drinkel, R.R. Campedelli, A.M. Manfredi, H.D. Fiedler, F. Nome, *J. Org. Chem.* 2014, **79**, 2574-2579.

-
- 178 B. H. Lipshutz, S. Ghorai, A. R. Abela, R. Moser, T. Nishikata, C. Duplais, A. Krasovskiy, *J. Org. Chem.*, 2011, **76**, 4379-4391.
- 179 E.D. Slack, C.M. Gabriel, B.H. Lipshutz, *Angew. Chem. Int. Ed.*, 2014, **53**, 14051-14054.
- 180 X. Y. Yang, H. C. Gao, X. I. Tan, H. Z. Yuan, G. Z. Cheng, S. Z. Mao, S. Zhao, L. Zhang, J. Y. Yu, Y. R. Du, *Colloid Polym. Sci.*, 2004, **282**, 280-286.
- 181 a) H. Friedrich, P. M. Frederik, G. de With, N. A. J. M. Sommerdijk, *Angew. Chem. Int. Ed.*, 2010, **49**, 7850-7858; *Angew. Chem.*, 2010, **122**, 8022-8031; b) Y. I. González, E. W. Kaler, *Curr. Opin. Colloid. Interface Sci.*, 2005, **10**, 256-260.
- 182 H. Wang, L. Li, X.-F. Bai, J.-Y. Shang, K.-F. Yang, L.-W. Xua, *Adv. Synth. Catal.* 2013, **355**, 341-347.
- 183 J. Huang, Y. Jianga, N. van Vegtena, M. Hunger, A. Baiker, *J. Catal.* 2011, **281**, 352-360.
- 184 R. A. Pascal Jr, S. Mischke, *J. Org. Chem.* 1991, **56**, 6954-6957.
- 185 T. Mitsudome, Y. Takanashi, S. Ichikawa, T. Mizugaki, K. Jitsukawa, K. Kaneda, *Angew. Chem. Int. Ed.*, 2012, **51**, 1-6.
- 186 H. Lindlar, R. Dubuis, *Org. Synth.* 1966, **46**, 89-91.
- 187 J. E. Germain, *Catalytic Conversion of Hydrocarbons*, 1969, Academic Press, New York, USA.
- 188 F. Alonso, I. Osante, M- Yus, *Adv. Synth. Catal.*, 2006, **348**, 305-308.
- 189 R. Nishio, M. Sugiura, S. Kobayashi, *Org. Biomol. Chem.*, 2006, **4**, 992-995.
- 190 B. A. Wilhite, M. J. McCready, A. Varma, *Ind. Eng. Chem. Res.*, 2002, **41**, 3345-3350.
- 191 E. D. Slack, C. M. Gabriel, B. H. Lipshutz, *Angew. Chem. Int. Ed.*, 2014, **53**, 14051-14054.
- 192 Data from <http://www.chemspider.com/>
- 193 M. E. Cucullu, S. P. Nolan, T. R. Belderrain, R.H. Grubbs, *Organometallics*, 1999, **18**, 1299-1304.
- 194 D. Fritsch, K. Kuhr, K. Mackenzie, F.-D. Kopinke, *Catalysis Today*, 2003, **82**, 105-118.
- 195 M. A. Aramendía, V. Boráu, I. M. García, C. Jiménez, A. Marinas, J. M. Marinas, F. J. Urbano, *Appl. Catal. B*, 2003, **43**, 71-79.
- 196 M.A Aramendía, V Boráu, I.M García, C Jiménez, F Lafont, A Marinas, J.M Marinas, F.J Urbano, *J. Mol. Cat. A*, 2002, **184**, 237-245.
- 197 F. A. Harraza, S. E. El-Houta, H. M. Killab, I. A. Ibrahima, *J. Catal.*, 2012, **286**, 184-192.
- 198 S. G. Agalave, S. R. Maujan, V. S. Pore, *Chem. Asian J.*, 2011, **6**, 2696-2718.
- 199 C. D. Hein, X.-M. Liu, D. Wang, *Pharm. Res.*, 2008, **25**, 2216-2230.
- 200 D. R. Buckle, C. J. M. Rockell, H. Smith, B. A. Spicer, *J. Med. Chem.*, 1986, **29**, 2269-2277.

-
- 201 A. D. Moorhouse, J. E. Moses, *Chem. Med. Chem.*, 2008, **3**, 715-723.
- 202 M. J. Genin, D. A. Allwine, D. J. Anderson, M. R. Barbachyn, D. E. Emmert, S. A. Garmon, D. R. Graber, K. C. Grega, J. B. Hester, D. K. Hutchinson, J. Morris, R. J. Reischer, C. W. Ford, G. E. Zurenko, J. C. Hamel, R. D. Schaadt, D. Stapert, B. H. Yagi, *J. Med. Chem.*, 2000, **43**, 953-970.
- 203 A. K. Jordão, V. F. Ferreira, E. S. Lima, M. C. B. V. de Souza, E. C. L. Carlos, H. C. Castro, R. B. Geraldo, C. R. Rodrigues, M. C. B. Almeida, A. C. Cunha, *Bioorg. Med. Chem.*, 2009, **17**, 3713-3719.
- 204 R. Alvarez, S. Velazquez, A. San-Felix, S. Aquaro, E. De Clercq, C. F. Perno, A. Karlsson, J. Balzariniand, M. J. Camarasa, *J. Med. Chem.*, 1994, **37**, 4185-4194.
- 205 L. L. Brockunier, E. R. Parmee, H. O. Ok, M. R. Candelore, M. A. Cascieri, L. F. Colwell, L. Deng, W. P. Feeney, M. J. Forrest, G. J. Hom, D. E. MacIntyre, L. Tota, M. J. Wyvrat, M. H. Fisher, A. E. Weber, *Bioorg. Med. Chem. Lett.*, 2000, **10**, 2111-2116.
- 206 S. B. Ötvös, Á. Georgiádes, I. M. Mándity, L. Kiss, F. Fülöp, *Beilstein J. Org. Chem.*, 2013, **9**, 1508-1516.
- 207 B. Schulzeab, U. S. Schubert, *Chem. Soc. Rev.*, 2014, **43**, 2522-2571.
- 208 G. Nagarjuna, S. Yurt, K. G. Jadhav, D. Venkataraman, *Macromolecules*, 2010, **43**, 8045-8050.
- 209 S. Ding, G. Jia, J. Sun, *Angew. Chem., Int. Ed.*, 2014, **53**, 1877-1880.
- 210 R. Huisgen, G. Szeimis, L. Möbius, *Chem. Ber.*, 1967, **100**, 2494-2507.
- 211 a) C. R. Becer, R. Hoogenboom, U. S. Schubert, *Angew. Chem., Int. Ed.*, 2009, **48**, 4900-4908;
b) N. J. Agard, J. A. Prescher, C. R. Bertozzi, *J. Am. Chem. Soc.*, 2004, **126**, 15046-15048.
- 212 S. Sawoo, P. Dutta, A. Chakraborty, R. Mukhopadhyay, O. Bouloussa, A. Sarkar, *Chem. Commun.*, 2008, **23**, 5957-5959.
- 213 a) H. Li, J. Wang, J. Z. Sun, R. Hu, A. Qin, B. Z. Tang, *Polym. Chem.*, 2012, **3**, 1075-1083; b) S. S. van Berkel, A. J. Dirks, S. A. Meeuwissen, D. L. L. Pingen, O. C. Boerman, P. Laverman, F. L. van Delft, J. J. L. M. Cornelissen, F. P. J. T. Rutjes, *Chem. Bio. Chem.*, 2008, **9**, 1805-1815.
- 214 E. M. Alexandrino, P. Buchold, M. Wagner, A. Fuchs, A. Kreyes, C. K. Weiss, K. Landfester, F. R. Wurm, *Chem. Commun.*, 2014, **50**, 10495-10498.
- 215 V. V. Rostovtsev, L. G. Green, V. V. Fokin, K. B. Sharpless, *Angew. Chem., Int. Ed.*, 2002, **41**, 2596-2599.
- 216 C. W. Tornoe, C. Christensen, M. Meldal, *J. Org. Chem.*, 2002, **67**, 3057-3064.
- 217 L. Zhang, X. Chen, P. Xue, H. H. Y. Sun, I. D. Williams, K. B. Sharpless, V. V. Fokin, G. Jia, *J. Am. Chem. Soc.*, 2005, **127**, 15998-15999.

-
- 218 S. Ding, G. Jia and J. Sun, *Angew. Chem., Int. Ed.*, 2014, **53**, 1877-1880.
- 219 D. Wang, N. Li, M. Zhao, W. Shi, C. Ma, B. Chen, *Green Chem.*, 2010, **12**, 2120-2123.
- 220 J. García-Álvarez, J. Díez and J. Gimeno, *Green Chem.*, 2010, **12**, 2127-2130.
- 221 a) S. Díez-González, A. Correa, L. Cavallo, S. P. Nolan, *Chem.-A Eur. J.*, 2006, **12**, 7558-7564;
b) S. Díez-González, E. C. Escudero-Adán, J. Benet-Buchholz, E. D. Stevens, A. M. Z. Slawin, S. P. Nolan, *Dalton Trans.*, 2010, **39**, 7595-7606.
- 222 F. Lazreg, A. M. Z. Slawin, C. S. J. Cazin, *Organometallics*, 2012, **31**, 7969-7975.
- 223 L. R. Collins, T. M. Rookes, M. F. Mahon, I. M. Riddlestone, M. K. Whittlesey, *Organometallics*, 2014, **33**, 5882-5887.
- 224 E. F. V. Scriven, K. Turnbull, *Chem. Rev.*, 1988, **88**, 297-368.
- 225 S. Roy, T. Chatterjee and S. M. Islam, *Green Chem.*, 2013, **15**, 2532-2539.
- 226 F. Alonso, Y. Moglie, G. Radivoy, M. Yus, *J. Org. Chem.*, 2011, **76**, 8394-8405.
- 227 R. Hosseinzadeh, H. Sepehrian, F. Shahrokhi, *Heteroat. Chem.*, 2012, **23**, 415-421.
- 228 L. Wan, C. Cai, *Catal. Lett.*, 2012, **142**, 1134-1140.
- 229 R. B. N. Baig, R. S. Varma, *Green Chem.*, 2012, **14**, 625-632.
- 230 F. Nador, M. A. Volpe, F. Alonso, A. Feldhoff, A. Kirschning, G. Radivoy, *Appl. Catal. A*, 2013, **455**, 39-45.
- 231 M. Liu, O. Reiser, *Org. Lett.*, 2011, **13**, 1102-1105.
- 232 Y. Jiang, D. Kong, J. Zhao, W. Zhang, W. Xu, W. Li, G. Xu, *Tetrahedron Lett.*, 2014, **55**, 2410-2414.
- 233 C. Deraedt, N. Pinaud, D. Astruc, *J. Am. Chem. Soc.*, 2014, **136**, 12092-12098.
- 234 a) R. A. Youcef, M. Dos Santos, S. Roussel, J.-P. Baltaze, N. Lubin-Germain, J. Uziel, *J. Org. Chem.*, 2009, **74**, 4318-4323; b) B. H. Lipshutz, Z. Bošković, C. S. Crowe, V. K. Davis, H. C. Whittimore, D. A. Vosburg, A. G. Wenzel, *J. Chem. Educ.*, 2013, **90**, 1514-1517.
- 235 S. Gutfelt, J. Kizling, K. Holmberg, *Colloids Surf. A*, 1997, **128**, 265-271.
- 236 a) R. S. Varma, D. Kumar, *Catal. Lett.*, 1998, **53**, 225-227; b) R. S. Varma, K. P. Naicker, D. Kumar, *J. Mol. Catal. A: Chem.*, 1999, **149**, 153-160.
- 237 a) Y. Liu, C. Wang, X. Wang, J. P. Wan, *Tetrahedron Lett.*, 2013, **54**, 3953-3955; b) S. L. Zhang, X. Y. Liu, T. Q. Wang, *Adv. Synth. Catal.*, 2011, **353**, 1463-1466; c) S. Adimurthy, C. C. Malakar, U. Beifuss, *J. Org. Chem.*, 2009, **74**, 5648-5651; d) K. Kamata, S. Yamaguchi, M. Kotani, K. Yamaguchi, N. Mizuno, *Angew. Chem., Int. Ed.*, 2008, **47**, 2407-2410; e) D. F. Li, K. Yin, J. Li, X. Jia, *Tetrahedron Lett.*, 2008, **49**, 5918-5919.

-
- 238 Y. Sayed, A. Bayat, M. Kondratenko, Y. Leroux, P. Hapiot, R. L. McCreery, *J. Am. Chem. Soc.*, 2013, **135**, 12972-12975.
- 239 L. Sahoo, A. Singhamahapatra, D. Loganathan, *Org. Biomol. Chem.*, 2014, **12**, 2615-2625.
- 240 D. L. Purich, R. D. Allison, *Handbook of Biochemical Kinetics: A Guide to Dynamic Processes in the Molecular Life Sciences*, 1999, Academic Press., Waltham, Massachusetts, USA.
- 241 J. L. Atwood, J. W. Steed, *Encyclopedia of Supramolecular Chemistry, Volume 1*, 2004, CRC Press, Boca Raton, Florida, USA.
- 242 K. A. Davis, Y. Hatefiz, *Biochemistry*, 1971, **10**, 2509-2516
- 243 G. A. Hornandberg, J. A. Mattis, M. Laskowski Jr, *Biochemistry*, 1978, **17**, 5220-5227.
- 244 G. Bucolo, H. David, *Clin. Chem.*, 1973, **19**, 476-482.
- 245 A. D'Aniello, A. Veterea, L. Petrucelli, *Comp. Biochem. Physiol. B: Biochem. Mol. Biol.*, 1993, **105**, 731-734
- 246 R. J. Davis, *J. Catal.*, 2003, **216**, 396-405.
- 247 N. Herron, *J. Coord. Chem.*, 1988, **19**, 25-38.
- 248 M. Renz, T. Blasco, A. Corma, V. Forne, R. Jensen, L. Nemeth, *Chem. Eur. J.*, 2002, **8**, 4708-4717.
- 249 a) B. M. Choudary, M. Ravichandra Sarma, K. Koteswara Rao, *Tetrahedron Lett.*, 1999, **31**, 5781-5784; b) P. Laszlo, M. Montaufier, *Tetrahedron Lett.*, 1991, **32**, 1561-1564.
- 250 B. M. Choudary, K. K. Rao, *Tetrahedron Lett.*, 1992, **33**, 121-124.
- 251 a) H. K. A. C. Coolen, J. A. M. Meeuwis, P. W. N. M. Leeuwen, R. J. M. Nolte, *J. Am. Chem. Soc.*, 1995, **117**, 11906-11913; b) S. Das, G. W. Brudvig, R. H. Crabtree, *J. Am. Chem. Soc.*, 2008, **130**, 1628-1637; c) R. Cacciapaglia, S. Di Stefano, L. Mandolini, *J. Org. Chem.*, 2001, **66**, 5926-5928; c) G. Ozturk, E. U. Akkaya, *Org. Lett.*, 2004, **6**, 241-243; d) R. Cacciapaglia, A. Casnati, L. Mandolinim D. N. Reinhoudt, R. Salvio, A. Sartori, R. Ungaro, *Inorg. Chem. Acta*, 2007, **360**, 981-986.
- 252 O. Ramström, K. Mosbach, *Curr. Opin. Chem. Biol.*, 1999, **3**, 759-764.
- 253 A. Leonhardt, K. Mosbach, *React. Polym.*, 1987, **6**, 285-290.
- 254 E. Toorisakaa, K. Uezua, M. Gotoa, S. Furusaki, *Biochem. Eng. J.*, 2003, **14**, 85-91.
- 255 G. E. Oosterom, J. N. H. Reek, P. C. J. Kamer, P. W. N. M. van Leeuwen, *Angew. Chem., Int. Ed.*, **40**, 1828-1849.
- 256 S.-K. Oh, Y. Niu, R. M. Crooks, *Langmuir.*, 2005, **22**, 10209-10213.
- 257 a) K. Takahashi, *Chem. Rev.*, 1998, **98**, 2013-2033 ; b) R. Breslow, *Acc. Chem. Res.*, 1991, **24**, 317-324.

-
- 258 R. Brelow, *Artificial Enzymes*, 2006, John Wiley & Sons, Hoboken, NJ, USA.
- 259 C. Torque, H. Bricout, F. Hapiot, E. Monflier, *Tetrahedron*, 2004, **60**, 6487-6493.
- 260 D. H. Leung, R. G. Bergman, K. N. Raymond, *J. Am. Chem. Soc.*, 2007, **129**, 2746-2747.
- 261 V. van Axel Castelli, A. Dalla Cort, L. Mandolini, D. N. Reinhoudt, L. Schiaffino, *Chem. Eur. J.*, 2000, **6**, 1193-1198.
- 262 a) T. Dwars, E. Paetzold, G. Oehme, *Angew. Chem. Int. Ed.*, 2005, **44**, 7174-7199; b) U.M. Lindström, *Angew. Chem. Int. Ed.*, 2006, **45**, 548-551; c) G. La Sorella, G. Strukul, A. Scarso, *Green Chem.*, 2015, **17**, 644-683.
- 263 a) F. Wang, H. Liu, L. Cun, J. Zhu, J. Deng, Y. Jiang, *J. Org. Chem.*, 2005, **70**, 9424-9429; b) M. Colladon, A. Scarso, G. Strukul, *Adv. Synth. Catal.*, 2007, **349**, 797-801; c) M. Gottardo, A. Scarso, S. Paganelli, G. Strukul, *Adv. Synth. Catal.*, 2010, **352**, 2251-2262.
- 264 K. Manabe, S. Iimura, X.-M. Sun, S. Kobayashi, *J. Am. Chem. Soc.*, 2002, **124**, 11971-11978.
- 265 F. Trentin, A. Scarso, G. Strukul, *Tetrahedron Lett.*, 2011, **52**, 6978-6981.
- 266 A. K. Ghose, V. N. Viswanadhan, J. J. Wendoloski, *J. Comb. Chem.*, 1999, **1**, 55-68.
- 267 A. Greenberg, C. M. Breneman, J. F. Liebman, *The Amide Linkage: Selected Structural Aspects in Chemistry, Biochemistry and Materials Science*, **2000**, Wiley Interscience, N Y.
- 268 C. A. G. N. Montalbetti, V. Falque, *Tetrahedron*, 2005, **61**, 10827-10852
- 269 R. V. Ulijn, B. D. Moore, A. E. M. Janssen, P. J. Halling, *J. Chem. Soc., Perkin Trans. 2*, 2002, 1024-1028.
- 270 K. Arnold, A. S. Batsanov, B. Davies, A. Whiting, *Green Chem.*, 2008, **10**, 124-134.
- 271 T. I. Al-Warhia, H. M. A. Al-Hazimib, A. El-Fahamb, *J. Saudi Chem. Soc.*, 2012, **16**, 97-116.
- 272 A. Williams, I. T. Ibrahim, *Chem. Rev.*, 1981, **81**, 589-636.
- 273 M. Kunishima, K. Kikuchi, Y. Kawai, K. Hioki, *Angew. Chem. Int. Ed.*, 2012, **51**, 2080-2083.
- 274 R. F. Heck, J. P. Nolley, *J. Org. Chem.*, 1972, **37**, 2320-2322.
- 275 T. Jeffery, *Tetrahedron Lett.*, 1994, **35**, 3051-3054.
- 276 S. Bhattacharya, A. Srivastava, S. Sengupta, *Tetrahedron Lett.*, 2005, **46**, 3557-3560.
- 277 M. Amini, M. Bagherzadeh, Z. Moradi-Shoeili, D.M. Boghaei, *RSC Adv.*, 2012, **2**, 12091-12095.
- 278 a) T. Jeffery, J.-C. Galland, *Tetrahedron Lett.*, 1994, **35**, 4103-4106; b) T. Jeffery, M. David, *Tetrahedron Lett.*, 1998, **39**, 5751-5754.
- 279 D.D. Perrin, W.L.F. Armarego, *Purification of laboratory chemicals*, 3rd edition, 1993, Pergamon Press, U.K., Oxford.
- 280 Y. Aoyama, Y. Tanaka, S. Sugahara, *J. Am. Chem. Soc.*, 1989, **111**, 5397-5404.

-
- 281 W. C. Still, M. Khan, A. Mitra, *J. Org. Chem.*, 1978, **43**, 2923-2925.
- 282 T. Lebleu, H. Kotsukib, J. Maddalunoa, J. Legros, *Tetrahedron Lett.*, 2014, **55**, 362-364.
- 283 M. J. Deetz, J. E. Fahey, B. D. Smith, *J. Phys. Org. Chem.*, 2001, **14**, 463-467.
- 284 C.M. Grunerta, P. Weinberger, J. Schweifer, C Hampel, A.F. Stassen, K. Mereiter, W Linert, *J. Mol. Struct.*, 2005, **733**, 41-52.
- 285 D. Antonow, T. Marrafa, I. Dawood, T. Ahmed, M. R. Haque, D. E. Thurston, G. Zinzalla, *Chem. Commun.*, 2010, **46**, 2289-2291.
- 286 B. Li, A.-H. Liu, L.-N. He, Z.-Z. Yang, J. Gao, K.-H. Chen, *Green Chem.*, 2012, **14**, 130-135.
- 287 S. Doherty, J. G. Knight, M. A. Carroll, J. R. Ellison, S. J. Hobson, S. Stevens, C. Hardacre, P. Goodrich, *Green Chem.*, 2015, **17**, 1559-1571.
- 288 S.-I. Murahashi, D. Zhang, H. Iida, T. Miyawaki, M. Uenaka, K. Murano, K. Meguro, *Chem. Commun.*, 2014, **50**, 10295-10298.
- 289 Y. Kon, T. Yokoi, M. Yoshioka, Y. Uesaka, H. Kujira, K. Sato, T. Tatsumi, *Tetrahedron Lett.*, 2015, **56**, 4721-4848.
- 290 H. B. Jeon, K. T. Kim, S. H. Kim, *Tetrahedron Lett.*, 2014, **55**, 3905-3908.
- 291 Y. Imada, I. Tonomura, N. Komiya, T. Naota, *Synlett*, 2013, **24**, 1679-1682.
- 292 N. M. R. McNeil, C. McDonnell, M. Hambrook, T.G. Back, *Molecules*, 2015, **20**, 10748-10762.
- 293 L. Hu, X- Cao, L. Shi, F. Qi, Z. Guo, J. Lu, H. Gu, *Org. Lett.*, 2011, **13**, 5640-5643.
- 294 Z.-H. Guan, H. Lei, M. Chen, Z.-H. Ren, Y. Bai, Y.-Y. Wang, *Adv. Synth. Catal.*, 2012, **354**, 489-496.